COMPLEMENT AND IMMUNOTHERAPEUTICS

EDITED BY: Marcin Okrój, Paolo Macor and Elena Volokhina
PUBLISHED IN: Frontiers in Immunology

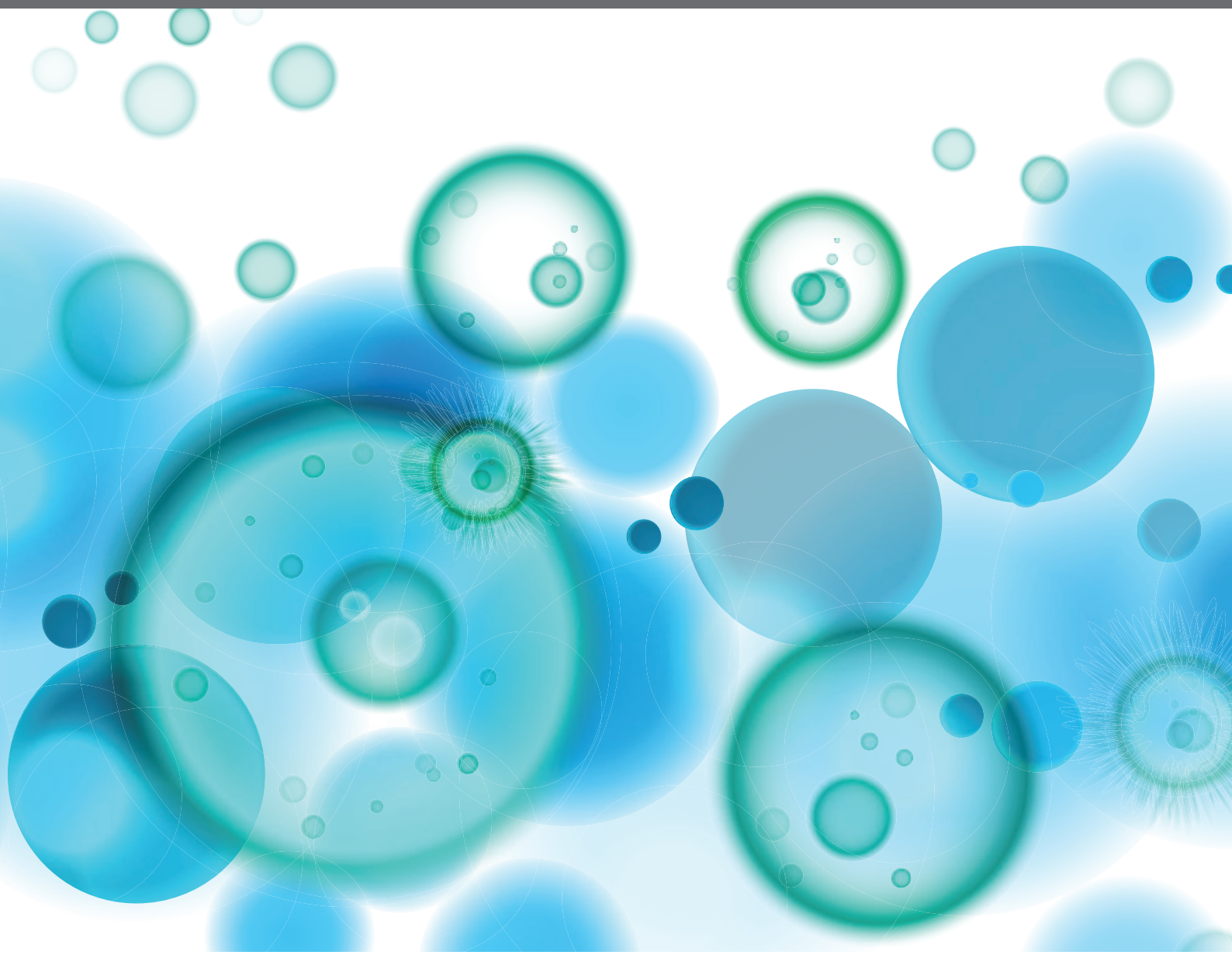

frontiers Research Topics

frontiers

ISSN 1664-8714
ISBN 978-2-88966-663-8
DOI 10.3389/978-2-88966-663-8

About Frontiers

Frontiers is more than just an open-access publisher of scholarly articles: it is a pioneering approach to the world of academia, radically improving the way scholarly research is managed. The grand vision of Frontiers is a world where all people have an equal opportunity to seek, share and generate knowledge. Frontiers provides immediate and permanent online open access to all its publications, but this alone is not enough to realize our grand goals.

Frontiers Journal Series

The Frontiers Journal Series is a multi-tier and interdisciplinary set of open-access, online journals, promising a paradigm shift from the current review, selection and dissemination processes in academic publishing. All Frontiers journals are driven by researchers for researchers; therefore, they constitute a service to the scholarly community. At the same time, the Frontiers Journal Series operates on a revolutionary invention, the tiered publishing system, initially addressing specific communities of scholars, and gradually climbing up to broader public understanding, thus serving the interests of the lay society, too.

Dedication to Quality

Each Frontiers article is a landmark of the highest quality, thanks to genuinely collaborative interactions between authors and review editors, who include some of the world's best academicians. Research must be certified by peers before entering a stream of knowledge that may eventually reach the public - and shape society; therefore, Frontiers only applies the most rigorous and unbiased reviews.
Frontiers revolutionizes research publishing by freely delivering the most outstanding research, evaluated with no bias from both the academic and social point of view. By applying the most advanced information technologies, Frontiers is catapulting scholarly publishing into a new generation.

What are Frontiers Research Topics?

Frontiers Research Topics are very popular trademarks of the Frontiers Journals Series: they are collections of at least ten articles, all centered on a particular subject. With their unique mix of varied contributions from Original Research to Review Articles, Frontiers Research Topics unify the most influential researchers, the latest key findings and historical advances in a hot research area! Find out more on how to host your own Frontiers Research Topic or contribute to one as an author by contacting the Frontiers Editorial Office: frontiersin.org/about/contact

COMPLEMENT AND IMMUNOTHERAPEUTICS

Topic Editors:
Marcin Okrój, Intercollegiate Faculty of Biotechnology of University of Gdańsk and Medical University of Gdańsk, Poland
Paolo Macor, University of Trieste, Italy
Elena Volokhina, Radboud University Nijmegen Medical Centre, Netherlands

Citation: Okrój, M., Macor, P., Volokhina, E., eds. (2021). Complement and Immunotherapeutics. Lausanne: Frontiers Media SA.
doi: 10.3389/978-2-88966-663-8

Table of Contents

frontiers in Immunology

EDITORIAL
published: 24 February 2021
doi: 10.3389/fimmu.2021.663459

Editorial: Complement and Immunotherapeutics

Marcin Okrój[1]* *and Elena Volokhina*[2,3]*

[1] Intercollegiate Faculty of Biotechnology, University of Gdańsk and Medical University of Gdańsk, Gdańsk, Poland, [2] Department of Pediatric Nephrology, Amalia Children's Hospital, Radboud Institute for Molecular Life Sciences, Nijmegen, Netherlands, [3] Department of Laboratory Medicine, Radboud University Medical Center, Nijmegen, Netherlands

Keywords: complement, immunotherapy, rituximab, eculizumab, factor H, antibodies

Editorial on the Research Topic

Complement and Immunotherapeutics

The complement system was discovered more than 100 years ago as an ancient defense system that prevents pathogens' invasion. For a long time, the complement was considered a scientifically interesting system with limited physiological relevance. However, it regained interest in the last decades when thousands of publications on its new role in health and disease appeared. The loss of proper control on complement activity became an acknowledged etiological factor in numerous autoimmune/inflammatory diseases. The discovery of complement receptors revealed that this system is not only an implement to kill microbes but an essential modulator of the immune responses, metabolism, angiogenesis, tissue repair and development, and many other processes influencing the overall body homeostasis (1–3). Additional interest in complement as an effector mechanism of therapeutic antibodies appeared when rituximab, the first antitumor antibody, was introduced into the clinics in 1997 (4) and a decade later when the first complement-specific drug, eculizumab was approved (5). Engagement of more than 40 proteins either as structural elements of the complement cascade or its regulators as well as crosstalk with other pathways creates a sophisticated network of interactions that keep a delicate balance between the deleterious and protective nature of the complement. Therefore, it is not surprising that on one hand markers of complement activation emerge as diagnostic and prognostic tools (6), and on the other hand increasing number of complement targets for potential therapeutic intervention appears, which are currently being exploited by registered drugs or compounds that are under evaluation in clinical trials (7).

This Research Topic entitled "Complement and Immunotherapeutics" presents a collection of articles describing a broad range of developments in the field of complement-targeting drugs.

The article by Urwyler et al. presents the results of an uncontrolled series of cases, where patients suffering from SARS-CoV-2 infection were treated with conestat alpha—the recombinant C1 inhibitor. Out of five patients with severe COVID-19 pneumonia enrolled into the therapeutic scheme, four patients achieved immediate recovery, and one needed mechanical ventilation, however, all patients finally recovered. Conestat showed good tolerability. Despite certain limitations of this study, the results encourage to perform of a controlled clinical trial.

The article by Zelek and Morgan introduces a novel monoclonal antibody targeting C7 and C5b-7 complex. Such antibody was successfully tested in both *in vitro* systems and *in vivo* models of C7-deficient mouse reconstituted with human C7 or rat model. Such an innovative therapeutic approach allows targeting of a membrane attack complex formation, a very late step of the cascade, leaving all upstream steps intact to protect the host from pathogens and clean up cell debris.

OPEN ACCESS

Edited and reviewed by:
Francesca Granucci,
University of Milano-Bicocca, Italy

***Correspondence:**
Marcin Okrój
marcin.okroj@gumed.edu.pl
Elena Volokhina
elena.volokhina@radboudumc.nl

Specialty section:
This article was submitted to Molecular Innate Immunity, a section of the journal Frontiers in Immunology

Received: *02 February 2021*
Accepted: *04 February 2021*
Published: *24 February 2021*

Citation:
Okrój M and Volokhina E (2021) Editorial: Complement and Immunotherapeutics. Front. Immunol. 12:663459. doi: 10.3389/fimmu.2021.663459

A novel therapeutically useful concept was presented by Banda et al. and involves natural IgM antibodies (NAbs). These antibodies are known to recognize injury-associated epitopes and may contribute to autoimmunity. However, when engineered, they may be employed to deliver complement regulators to the site of injury. In this study fusion protein consisting of NAb-derived fragment and mouse complement inhibitor Crry was shown to decrease clinical disease activity in a mouse model of arthritis. Another fusion construct of factor H (FH) CCP domains 18–20 with Fc fragment of human IgG1 applicable in combating *Neisseria gonorrhoeae* infection was described by. *Shaughnessy et al.* Point mutation introduced in CCP19 disabled lysis of human erythrocytes but left bactericidal potential. Production of recombinant protein in a high-yield plant system was described and the efficacy of the product was proven in a mouse model. Staying in the field of complement inhibitors, de Boer et al. have reviewed the role of complement regulation in oncological, anemic, renal, eye, and neurologic pathologies. The authors also discussed the potential of either full-length or engineered inhibitors and antibodies targeting complement regulatory proteins in the context of the abovementioned diseases and unmet clinical needs. Not only disruption of complement regulation but also deficiency of essential complement components may lead to autoimmunity. An example is C1q deficiency, which plays an important role in the development of systemic lupus erythematosus (SLE). The comprehensive review by *Hosszu et al.* discusses the impact of the C1q/C1qR axis in monocyte-to-dendritic cell differentiation and how the distortion of this axis leads to disease. Moreover, the authors deliberate on possible therapeutic strategies to attenuate pro-inflammatory response in SLE patients.

Two articles in the collection are dedicated to anti-CD20 antibodies. Bondza et al. dissected the mechanistic details of the interaction between clinically approved anti-CD20 mAbs (rituximab, ofatumumab, and obinutuzumab) and their target. The authors analyzed the kinetics of interactions and discussed them in the context of complement activation and complement-dependent cytotoxicity. Felberg et al. analyzed the cytotoxic potential of sera as well as the levels of complement activation markers and retention of rituximab in patients treated for lymphoproliferative disorders. The publication concludes that monitoring of the complement system status and measurement of cell-free rituximab during therapy may be valuable for clinicians and become the step forward to personalized treatment for the patient. The additional potentially relevant parameter in the course of immunotherapy is chronic, low-level complement activation. Naseraldeen et al. described complement-activating IgG hexamers in sera from chronic lymphocytic leukemia (CLL) patients and the pivotal role of alpha-2 microglobulin in their formation.

A lot of attention is given to the alternative complement pathway (AP) in the context of kidney diseases, as uncontrolled propagation of AP often leads to severe damage and eventually loss of kidney function. Eculizumab was the first complement medication approved for the treatment of atypical hemolytic uremic syndrome (aHUS). The two case-reports illustrate the heterogeneity of this disease and challenge for clinicians to establish a correct diagnosis and treatment scheme and the necessity of monitoring disease progression and complement status. Lumbreras et al. describe a patient with a very mild manifestation of aHUS. The aHUS diagnosis was established when low C3 levels and C3 genetic variant was detected. The mild phenotype may be explained by the absence of MCP risk polymorphisms in this patient. While in good health during publication, the patient should be closely monitored for signs of aHUS relapse to initiate complement therapy on time. Bouwmeester et al. described a case of a severely affected patient with aHUS that under eculizumab treatment has shown high intra-patient variability in the serum drug levels and CH50, and decline of renal function. This case underscores the need for continuous monitoring of patients under treatment for drug levels and complement status.

Lammerts et al. studied the nature of properdin binding to proximal tubular endothelial cells and found that this process and subsequent AP activation can be blocked by the recombinant tick protein Salp20. Intravascular hemolysis and release of heme may lead to acute kidney injury. *Merle et al.* assessed the role of the main fluid-phase inhibitor of AP, FH, in kidney protection from hemolysis-mediated damage. Authors postulate that FH-based approaches can be exploited as promising therapeutic strategies. The work by *Koopman et al.* focuses on C5b-9 deposition in the kidney. Nowadays, therapies of renal diseases include blockers of the terminal complement pathway (e.g., eculizumab), but it is not entirely clear how C5b-9 contributes to pathological processes since such staining is not routinely performed. Comparison between healthy and diseased kidneys, correlation with other histological lesions and clinical data, and potential prognostic value of C5b-9 deposits are discussed.

Chronic inflammation is observed in women suffering from endometriosis. Such inflammatory status may stem from pathological complement activation fueled by aberrant regulation of the cascade. *Agostinis et al.* discussed the prospect of complement inhibition as a novel therapeutic approach in endometriosis.

La-Beck et al. reviewed the link between adverse effects of nanoparticle-based drugs and activation of the complement system. Complement activation on nanoparticles generates either opsonins and their cleavage products or release of anaphylatoxins. Both processes can diminish the efficacy of nano-encapsulated anticancer therapeutics by uptake of nanoparticles by immune cells and creation of pro-tumor microenvironment via C5aR-dependent signaling. Understanding a complex network of nanoparticles, complement, and drug pharmacology will aid the improvement of cancer nanomedicines.

In summary, the current Research Topic is a collection of 16 original and review articles, which describe novel candidates for complement-related drugs, mechanistic insights of drug-target interaction, target cell sensitivity, nanoparticles-based complement medications, diagnostics, complement genetic screening, as well as complement

involvement in the course and treatment of diseases such as systemic lupus erythematosus (SLE), endometriosis, and a wide spectrum of kidney diseases. The articles highlight novelty and future perspectives of recent developments in these fields.

AUTHOR CONTRIBUTIONS

MO and EV wrote the manuscript and agreed on its final version. Both authors contributed to the article and approved the submitted version.

REFERENCES

1. Ricklin D, Hajishengallis G, Yang K, Lambris JD. Complement: a key system for immune surveillance and homeostasis. *Nat Immunol.* (2010) 11:785–97. doi: 10.1038/ni.1923
2. Reis ES, Mastellos DC, Yancopoulou D, Risitano AM, Ricklin D, Lambris JD. Applying complement therapeutics to rare diseases. *Clin Immunol.* (2015) 161:225–40. doi: 10.1016/j.clim.2015.08.009
3. Gavriilaki E, Brodsky RA. Complementopathies and precision medicine. *J Clin Invest*. (2020) 130:2152–63. doi: 10.1172/JCI136094
4. Maloney DG, Grillo-Lopez AJ, White CA, Bodkin D, Schilder RJ, Neidhart JA, et al. IDEC-C2B8 (Rituximab) anti-CD20 monoclonal antibody therapy in patients with relapsed low-grade non-Hodgkin's lymphoma. *Blood*. (1997) 90:2188–95.
5. Rother RP, Rollins SA, Mojcik CF, Brodsky RA, Bell L. Discovery and development of the complement inhibitor eculizumab for the treatment of paroxysmal nocturnal hemoglobinuria. *Nat Biotechnol.* (2007) 25:1256–64. doi: 10.1038/nbt1344
6. Reis ES, Mastellos DC, Ricklin D, Mantovani A, Lambris JD. Complement in cancer: untangling an intricate relationship. *Nat Rev Immunol.* (2018) 18:5–18. doi: 10.1038/nri.2017.97
7. Ricklin D, Mastellos DC, Reis ES, Lambris JD. The renaissance of complement therapeutics. *Nat Rev Nephrol.* (2018) 14:26–47. doi: 10.1038/nrneph.2017.156

Conflict of Interest: The authors declare that the research was conducted in the absence of any commercial or financial relationships that could be construed as a potential conflict of interest.

frontiers in Immunology

CASE REPORT
published: 16 July 2020
doi: 10.3389/fimmu.2020.01348

The Relevance of the MCP Risk Polymorphism to the Outcome of aHUS Associated With C3 Mutations. A Case Report

Javier Lumbreras[1†], Marta Subias[2*†], Natalia Espinosa[1], Juana María Ferrer[3], Emilia Arjona[2] and Santiago Rodríguez de Córdoba[2]*

[1] Unidad de Nefrología Infantil, Servicio de Pediatría, Hospital Universitari Son Espases–Instituto de Investigación Sanitaria Illes Balears (IdISBa), Palma de Mallorca, Spain, [2] Centro de Investigaciones Biológicas Margarita Salas and Ciber de Enfermedades Raras, Madrid, Spain, [3] Servicio de Inmunología, Hospital Universitari Son Espases–Instituto de Investigación Sanitaria Illes Balears (IdISBa), Palma de Mallorca, Spain

Thrombotic microangiopathy (TMA) has different etiological causes, and not all of them are well understood. In atypical hemolytic uremic syndrome (aHUS), the TMA is caused by the complement dysregulation associated with pathogenic mutations in complement components and its regulators. Here, we describe a pediatric patient with aHUS in whom the relatively benign course of the disease confused the initial diagnosis. A previously healthy 8-year-old boy developed jaundice, hematuria, hemolytic anemia, thrombopenia, and mild acute kidney injury (AKI) in the context of a diarrhea without hypertension nor oliguria. Spontaneous and complete recovery was observed from the third day of admission. Persistent low C3 plasma levels after recovery raised the suspicion for aHUS, which prompted clinicians to discard the initial diagnosis of Shigatoxin-associated HUS (STEC-HUS). A thorough genetic and molecular study of the complement revealed the presence of an isolated novel pathogenic C3 mutation. The relatively benign clinical course of the disease as well as the finding of a *de novo* pathogenic C3 mutation are remarkable aspects of this case. The data are discussed to illustrate the benefits of identifying the TMA etiological factor and the relevant contribution of the MCP aHUS risk polymorphism to the disease severity.

Keywords: C3, MCP risk polymorphism, atypical hemolytic uremic syndrome, *de novo* mutation, case report

OPEN ACCESS

Edited by:
Paolo Macor,
University of Trieste, Italy

Reviewed by:
Viviana P. Ferreira,
University of Toledo, United States
Zoltan Prohaszka,
Semmelweis University, Hungary

***Correspondence:**
Javier Lumbreras
javier.lumbreras@ssib.es
Marta Subias
m.subias@cib.csic.es

† These authors share first authorship

Specialty section:
This article was submitted to Molecular Innate Immunity, a section of the journal Frontiers in Immunology

Received: *05 April 2020*
Accepted: *27 May 2020*
Published: *16 July 2020*

Citation:
Lumbreras J, Subias M, Espinosa N, Ferrer JM, Arjona E and Rodríguez de Córdoba S (2020) The Relevance of the MCP Risk Polymorphism to the Outcome of aHUS Associated With C3 Mutations. A Case Report. Front. Immunol. 11:1348. doi: 10.3389/fimmu.2020.01348

INTRODUCTION

Atypical hemolytic uremic syndrome (aHUS) is an ultra-rare disease characterized by acute kidney injury, thrombocytopenia, and microangiopathic hemolytic anemia, which results from an impaired protection of host endothelial cells from complement damage (1). The complement system is a key element of innate immunity with crucial roles in the elimination of pathogens, immune complexes, or cell remains. The complement activates by three pathways, classical (CP), lectin (LP), and alternative (AP), which generates protease complexes, named C3 convertases that cleave C3 to generate C3b. Convertase-generated C3b can form more AP C3 convertase, providing exponential amplification of the initial activation. Clustering of C3b around the surface-bound C3 convertase generates the C5 convertase, which cleaves C5 and initiates formation of the lytic membrane attack complex (MAC) (2). In health, the activation of C3 in plasma is kept

at a very low level, and the deposition of C3b and further activation of complement are limited to the surface of pathogens by multiple regulatory proteins. The loss of complement regulation leads to the generation of proinflammatory components and/or tissue damage. Both situations have pathological consequences (3). Loss-of-function mutations in genes encoding the regulatory proteins factor H (FH), MCP, and factor I (FI), as well as gain-of-function mutations in the complement activating components factor B (FB) and C3, have been associated with aHUS (4–11). Criteria have been established to facilitate the clinical diagnosis of aHUS, but it is often difficult to exclude STEC-HUS and secondary HUS forms (12). Since 50–70% of aHUS patients have an underlying inherited and/or acquired complement abnormality (13, 14), genetic analyses are recommended to characterize the etiological factor, reinforce diagnosis, and assist patient management. We present a case that was initially classified as STEC-HUS but was reclassified to aHUS based on the complement follow-up and genetic analyses. We discuss the implications of the identification of a *de novo* gain-of-function C3 mutation in this case and the relevance of genotyping for the MCPggaac aHUS risk polymorphism.

Clinical Case

In October 2014, a previously healthy 8-year-old boy was evaluated at the pediatric emergency room (ER) in a tertiary care hospital for hematuria, asthenia, and mild jaundice observed in previous hours. Nonbloody diarrhea had been present for 3 days. Physical examination was unremarkable apart from mild jaundice. Nonfocal or generalized edema was found. He had no relevant personal or family past history. Initial blood test showed hemoglobin of 12.2 g/dl (>11.5 g/dl), platelets of 35,000/μl (>150,000/μl), creatinine of 84 μmol/L (<61 μmol/L), and normal transaminases, sodium, and potassium. Eight hours later, hemoglobin decreased to 10 g/dl and platelets to 28,900/μl; lactate dehydrogenase (LDH) was determined to be 1,657 U/L (<220 U/L) (**Figure 1**). Blood test was extended with haptoglobin (undetectable), and a blood smear showed 7–9 schistocytes per field. Creatinine increased to 93 μmol/L. Electrolytes, acid–base balance, and plasma proteins were in normal range. Urine protein to creatinine ratio (UPr/UCr) was 1,921 μg/μmol (<20 μg/μmol). Basic coagulation parameters were normal. Blood pressure remained spontaneously in normal range and diuresis preserved, without involvement of other organs or systems. Patient was admitted to the pediatric ward.

Maximum plasma creatinine was attained on the second day of admission (106 μmol/L). Hemolysis markers started to descend from the third day. He was discharged on the sixth day with hemoglobin of 10.8 g/dl, platelets of 201,000/μl, LDH of 639 U/L, creatinine of 65 μmol/L, and UPr/UCr of 34 μg/μmol (**Figure 1**).

Additional studies performed during admission revealed the following: plasma homocysteine was normal at 11.4 μmol/L (<15 μmol/L), autoantibodies [antinuclear antibody (ANA), antineutrophil cytoplasmic antibody (ANCA), and antiextractable nuclear antigen (anti-ENA)] were negative, C3 was 51 mg/dl (75–135 mg/dl) and C4 was 21 mg/dl (14–60 mg/dl), and plasma ADAMTS13 activity was 81% (>5%). A stool sample was only obtained after 4 days of admission. Because of its completely normal appearance and the satisfactory evolution of HUS at that moment, it was only tested for Shigatoxin. Blood and urine culture were sterile. The patient was under careful observation during admission without needing renal replacement therapy or any drug. The spontaneous and very favorable evolution, the previous history of diarrhea, and the justification of a negative Shigatoxin assay due to a late stool collection suggested STEC-HUS as the most likely etiology.

Successive controls showed a complete recovery of renal function and absence of hemolytic activity, anemia, and thrombopenia. No treatment was needed during follow-up. However, decreased C3 levels (46–62 mg/dl) (**Figure 1**) persisted, and subsequent analysis of factor B plasma levels revealed that they were in the lower part of the normal range (85–170 μg/ml) (**Figure 2**). Hypocomplementemia is not unusual during a STEC-SHU episode, but the complement normalizes afterwards in these patients (16). The persistent hypocomplementemia in our patients did not correlate with his favorable evolution, raising the suspicion of an underlying constitutive complement abnormality that prompted us to the realization of a complete complement molecular and genetic analysis.

To search for mutations in complement genes, we used an in-house next generation sequencing (NGS) panel including all the complement genes relevant to aHUS (17). A complementary analysis of copy number variations was performed by multiplex ligation-dependent probe amplification (MLPA) with the P236 A1 ARMD mix 1 (MRC-Holland, Amsterdam, Netherlands). These analyses identified a C3 mutation in heterozygosis (c535T>C; p.S179P) that was confirmed by Sanger sequencing. This genetic variant has been found previously associated with aHUS (18). No other genetic alterations were found in this patient. Interestingly, none of his parents present this C3 variation (**Figure 2A**). Paternity was supported by the analysis of *CFH* and *MCP* polymorphisms. The patient carries the *CFH-H3* aHUS risk polymorphism in heterozygosis, inherited from his father (**Figure 2A**). He does not carry the *MCPggaac* aHUS risk polymorphism.

Annotation of $C3_{S179P}$ variant with six pathogenicity prediction algorithms (SIFT, POLYPHEN, Mutation Taster, MutAss, FATHMM and CADD) included in the ANNOVAR server (http://annovar.openbioinformatics.org/) indicated that it is most likely a benign C3 variant. However, because the C3 mutations associated with aHUS are gain-of-function mutations that normally are not predicted pathogenic, we purified the C3 protein from the patient's plasma and performed a complete functional characterization following standard procedures in our laboratory (15). These analyses demonstrated that the mutant $C3_{S179P}$ is present in the patient's plasma and shows an altered function with the characteristic of the C3 gain-of-function mutations that associate with aHUS (19–21). Briefly, when purified C3 from the patient was incubated with FB and FD, it completely activated to C3b, suggesting that $C3_{S179P}$ is normally activated by the AP C3 convertase (**Figure 2B**). When the patient C3b was tested for inactivation by FI in the presence of FH or MCP, we found that it was resistant to inactivation by FI in the

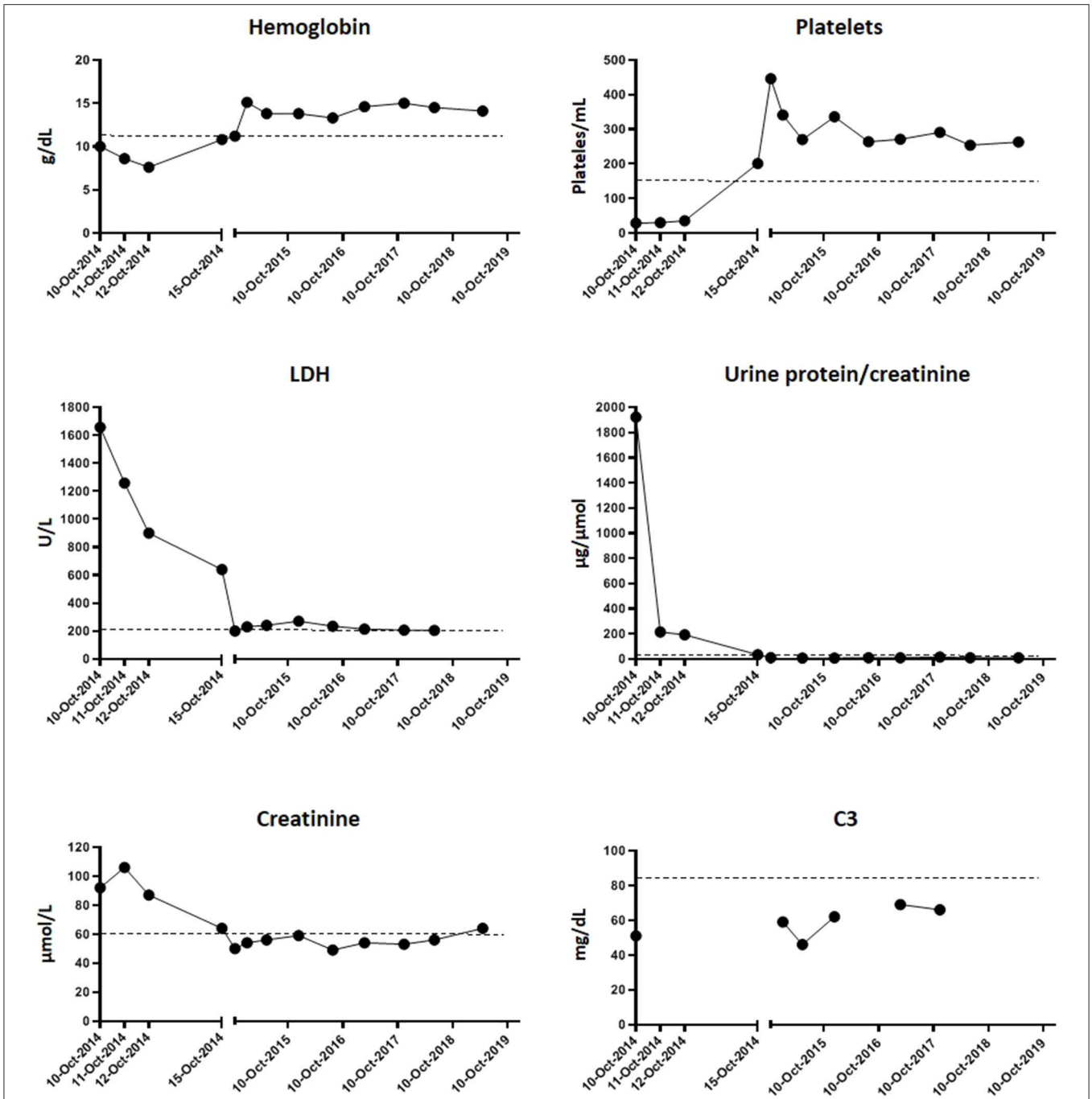

FIGURE 1 | Evolution of hematological parameters and renal activity. Graphics show the blood test determinations since the day of admission (10-Oct-2014) to the day of discharge (15-Oct-2014) and then of the successive routine controls in the following years. Dotted lines represent the upper or minimum value of each parameter from which it is considered pathogenic (hemoglobin > 11.5 g/dl; platelets < 150/ml; LDH > 220 U/L; urine protein/creatinine > 20 µg/µmol; creatinine > 61 µmol/l; C3 < 85 mg/dl).

presence of both cofactors, but much more resistant when MCP was the cofactor (**Figure 2C**).

The patient has remained completely asymptomatic without clinical or analytical data of disease activity or renal sequelae for 5 years, with an expectant attitude.

DISCUSSION

aHUS is a rare, life-threatening renal pathology associated with complement dysregulation. Mutations in genes encoding the regulatory proteins factor H (*CFH*), factor H-related protein

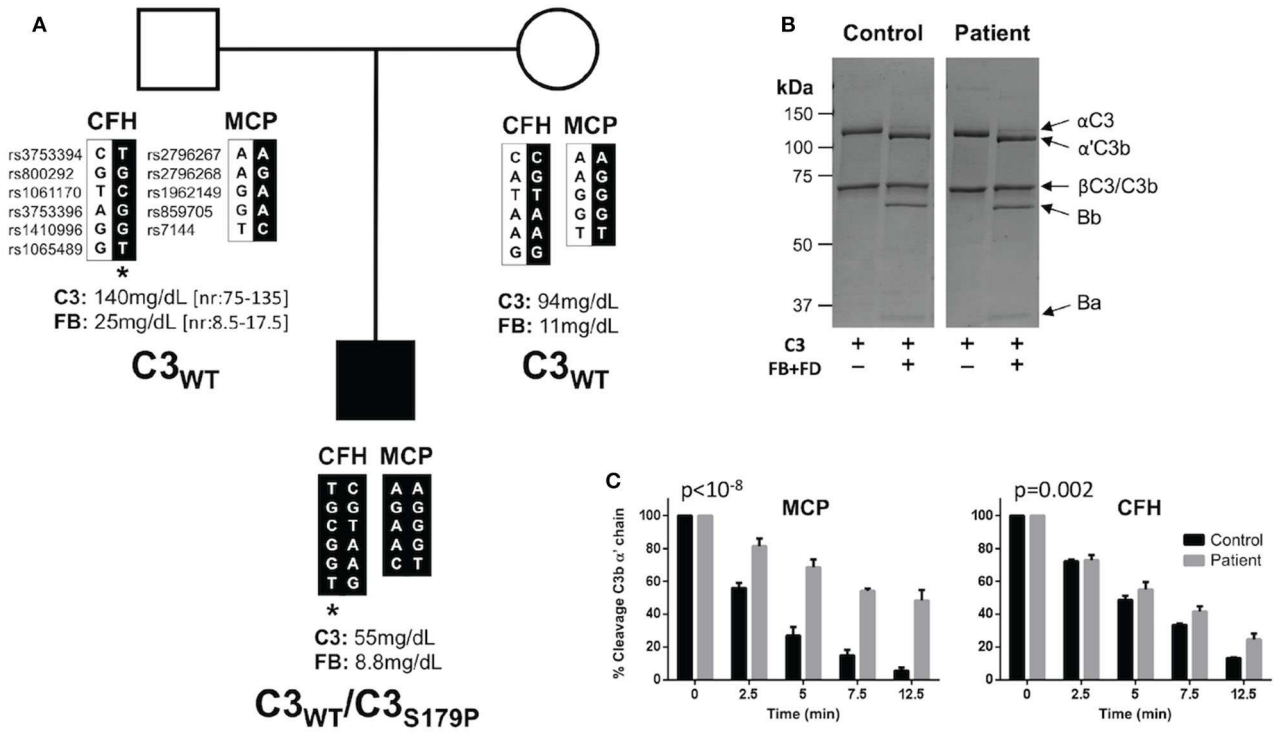

FIGURE 2 | $C3_{S179P}$ is a novel *de novo* gain-of-function mutations that impairs regulation by MCP. **(A)** Pedigree depicting the segregation of *CFH* and *MCP* polymorphisms organized in haplotype blocks. Single nucleotide polymorphisms are identified by their "rs" numbers. In black are the haplotypes inherited by the patient, identified by a solid square. Asterisk identifies the *CFH-H3* aHUS risk haplotype. Plasma levels of C3 and factor B (FB) are indicated for each individual. The patient is the only member of the pedigree carrying the $C3_{S179P}$ mutation. **(B)** C3 purified from the plasma-ethylenediaminetetraacetic acid (EDTA) of the patient activates normally to C3b by factor B (FB) and factor D (FD). Briefly, C3 was purified using a combination of sodium sulfate precipitation, lysine-sepharose chromatography, DEAE-Sepharose anion exchange chromatography, and Mono S HR 5/5 cation exchange chromatography as previously described (15). **(C)** C3b generated from the patient's C3 shows a marked resistant to inactivation by factor I in the presence of MCP. Differences between slopes were tested with a general linear model (GLM), with "time" as an integer variable and "strain" as a nominal one. The time × strain interaction was considered as the estimator of the differences between slopes. MCP ($p < 10^{-8}$). FH ($p = 0.002$).

1 (*CFHR1*), MCP (*MCP*), and factor I (*CFI*), as well as mutations in the complement components factor B (*CFB*) and C3 have been found in 50–70% of aHUS patients (13, 22). Importantly, while mutations in the complement regulators are loss-of-function, mutations in complement components like factor B and C3 are gain-of-function (13, 14). For C3, these aHUS-associated gain-of-function mutations result in C3b activated molecules being resistant to regulation by MCP, but not by factor H (19–21). The genetic and functional analyses performed in our patient concluded that he carries a C3 gain-of-function mutation that is prototypical of aHUS. This explains why our patient presents a constitutive complement alternative pathway activation with persistent consumption of C3. He has no familial history of aHUS because $C3_{S179P}$ is a *de novo* mutation, and he is the first in his pedigree carrying this genetic predisposition to aHUS. More interesting is the favorable disease outcome in our patient. Previous studies have shown that C3 mutations, like R161W, tend to be associated with severe aHUS presentations leading to end-stage renal disease. Others, like I1157T, associate with aHUS presentations characterized by multiple recurrences and prolonged favorable outcomes. Interestingly, the presence of the *MCPggaac* aHUS risk polymorphism influences the aHUS presentation in all carriers of C3 mutations (10, 19–21, 23), which may be justified because this polymorphism determines reduced expression of MCP on the cellular surface (8).

Our aHUS registry includes a total of 13 additional patients having a complete clinical record who carry a clearly pathogenic C3 mutation (**Table 1**). In total, this series comprises five different C3 mutations. Ten of these aHUS patients also carry the *MCPggaac* aHUS risk polymorphism (five in heterozygosis and five in homozygosis) (**Table 1**). This results in an allele frequency for the MCPggaac polymorphism in this group of patients ($n = 14$) of 0.54, which is significantly different ($p < 0.0037$) from that in the control Spanish population (AF = 0.28; $n = 107$). Notably, the only patient in this series who have had a relative favorable outcome is the only one who does not carry the *MCPggaac* risk polymorphism. Eculizumab treatment was initiated early after aHUS onset or to treat a bad evolution in three patients, and therefore, no conclusions can be reached in them regarding natural progression of aHUS. Notably, nine of the remaining 11 patients reached end-stage renal disease (ESRD) or

TABLE 1 | Atypical hemolytic uremic syndrome (aHUS) patients carrying C3 mutations in our aHUS registry.

	Patient	C3 mutation	*MCPggaac* risk polymorphism	Additional changes	ESRD	Eculizumab
1	HUS107	Arg161Trp	HET	No	Yes	No
2	HUS316	Lys65Gln	HOM	No	Yes	No
3	HUS416	Lys65Gln	HOM	No	Yes	No
4	HUS500	Lys65Gln	HET	*MCP:* Gly243Val	Yes	No
5	HUS835	Lys65Gln	HET	No	Yes	Yes
6	HUS787	Gln1161Lys	HET	No	No	Yes[a]
7	HUS594	Arg161Trp	HET	No	No	Yes[a]
8	HUS019	Ile1157Thr	HOM	No	No	No
9	HUS612	Lys65Gln	NO	*CFI:* Gly162Asp	Yes	Yes
10	HUS446	Lys65Gln	NO	*CFH:* Arg885Serfs*13	Yes	Yes
11	HUS843	Lys65Gln	NO	No	No[b]	No
12	HUS933	Lys65Gln	HOM	No	Yes	No
13	HUS962	Lys65Gln	HOM	*THBD*: (Ala43Thr)	No	Yes[c]
14	HUS657	Ser179Pro	No	No	No[d]	No

[a] *Treatment was initiated early after onset; no conclusions can be made regarding the natural progression of aHUS.*
[b] *Onset at 63 years old without recurrences until she was 78 years old. Treated with five doses of eculizumab she recovered enough renal function to leave hemodialysis. Currently, at 80 years old, she remains with chronic renal insufficiency but does not requires renal replacement therapy.*
[c] *Very bad evolution of the disease until the administration of eculizumab.*
[d] *This report.*

had multiple recurrences (**Table 1**). Eight of these patients carry, in addition to the C3 gain-of-function mutation, the *MCPggaac* risk polymorphism or additional pathogenic mutations in the *CFH*, *CFI*, *MCP*, and *THBD* genes. The only patient who, like our current patient, does not carry the *MCPggaac* risk polymorphisms or additional pathogenic mutations had a very late onset (63 years old) without recurrences until she was 76 years old. Currently (80 years old), the patient presents chronic kidney disease but does not require hemodialysis. These registry data suggest that the likely explanation for the favorable disease outcome in our patient is that he does not carry additional genetic risk factors, in particular the *MCPggaac* risk polymorphism. A relevant question is why our patient had an aHUS episode. It is known that several viral pathogens interact with MCP and that viral infections may lead to a reduction in the pathogen's receptor. Therefore, one possibility could be that our patient underwent a transient decrease in the cell surface levels of MCP as a consequence of the infection that triggered the aHUS episode. However, this is just a speculation because, when MCP levels were tested, months after the aHUS episode, they were found normal.

Although our patient is currently asymptomatic and presents normal renal function, our functional characterization of the $C3_{S179P}$ variant indicates that it is an important aHUS genetic risk factor. This has important implications. In fact, we cannot exclude that under exposure to a strong environmental trigger (e.g., an infection), our patient will experience a more severe aHUS recurrence. While we strongly recommend normal life to avoid unnecessary anxiety in the patient and its family, we also suggest active surveillance of the patient with specific recommendations. Regular determination of blood pressure, blood count, and measurement of biochemical markers for hemolysis (bilirubin, LDH, haptoglobin), as well as plasma creatinine, proteinuria, and albuminuria are performed. The patient and his parents are instructed to go the ER in case of presenting symptoms suggesting activity of his disease, such as hematuria, oliguria, edema, and significant general malaise in the context of some intercurrent process that can act as a trigger. Ultimately, it is reassuring to know that we have the "magic bullet" of eculizumab, if this patient should need it (24). In conclusion, complete understanding of the etiological factor in the TMA patient is critical to strengthen diagnosis and assist patient management.

DATA AVAILABILITY STATEMENT

All datasets presented in this study are included in the article/supplementary files.

ETHICS STATEMENT

Written informed consent was obtained from the participant's legal guardian/next of kin for the publication of any potentially identifiable images or data included in this article.

AUTHOR CONTRIBUTIONS

JL, MS, and SR designed the study. JL, MS, EA, and SR performed the experiments, collected, and analyzed the data. JL and SR drafted the manuscript, which was revised and approved by all

coauthors. All authors contributed to the article and approved the submitted version.

FUNDING

SR was supported by the Spanish Ministerio de Economía y Competitividad-FEDER (SAF2015-66287R) and the Autonomous Region of Madrid (S2017/BMD-3673).

ACKNOWLEDGMENTS

All the members of the Multidisciplinary Working Group on Thrombotic Microangiopathies from the Hospital Universitari Son Espases, in Palma de Mallorca, Spain are gratefully acknowledged. We are in debt to all patients and relatives participating in this study. This work was developed under the supervision of the Spanish Registry of atypical Hemolytic Uremic Syndrome and C3-Glomerulopathy (aHUS/C3G).

REFERENCES

1. Moake JL. Thrombotic microangiopathies. *N Engl J Med.* (2002) 347:589–600. doi: 10.1056/NEJMra020528
2. Ricklin D, Hajishengallis G, Yang K, Lambris JD. Complement: a key system for immune surveillance and homeostasis. *Nat Immunol.* (2010) 11:785–97. doi: 10.1038/ni.1923
3. de Cordoba SR, Tortajada A, Harris CL, Morgan BP. Complement dysregulation and disease: from genes and proteins to diagnostics and drugs. *Immunobiology*. (2012) 217:1034–46. doi: 10.1016/j.imbio.2012.07.021
4. Noris M, Brioschi S, Caprioli J, Todeschini M, Bresin E, Porrati F, et al. Familial haemolytic uraemic syndrome and an MCP mutation. *Lancet.* (2003) 362:1542–7. doi: 10.1016/S0140-6736(03)14742-3
5. Perez-Caballero D, Gonzalez-Rubio C, Gallardo ME, Vera M, Lopez-Trascasa M, Rodriguez de Cordoba S, et al. Clustering of missense mutations in the C-terminal region of factor H in atypical hemolytic uremic syndrome. *Am J Hum Genet.* (2001) 68:478–84. doi: 10.1086/318201
6. Richards A, Kemp EJ, Liszewski MK, Goodship JA, Lampe AK, Decorte R, et al. Mutations in human complement regulator, membrane cofactor protein (CD46), predispose to development of familial hemolytic uremic syndrome. *Proc Natl Acad Sci USA*. (2003) 100:12966–71. doi: 10.1073/pnas.2135497100
7. Warwicker P, Goodship TH, Donne RL, Pirson Y, Nicholls A, Ward RM, et al. Genetic studies into inherited and sporadic hemolytic uremic syndrome. *Kidney Int.* (1998) 53:836–44. doi: 10.1111/j.1523-1755.1998.00824.x
8. Esparza-Gordillo J, Goicoechea de Jorge E, Buil A, Carreras Berges L, Lopez-Trascasa M, Sanchez-Corral P, et al. Predisposition to atypical hemolytic uremic syndrome involves the concurrence of different susceptibility alleles in the regulators of complement activation gene cluster in 1q32. *Hum Mol Genet.* (2005) 14:703–12. doi: 10.1093/hmg/ddi066
9. Fremeaux-Bacchi V, Dragon-Durey MA, Blouin J, Vigneau C, Kuypers D, Boudailliez B, et al. Complement factor I: a susceptibility gene for atypical haemolytic uraemic syndrome. *J Med Genet.* (2004) 41:e84. doi: 10.1136/jmg.2004.019083
10. Fremeaux-Bacchi V, Miller EC, Liszewski MK, Strain L, Blouin J, Brown AL, et al. Mutations in complement C3 predispose to development of atypical hemolytic uremic syndrome. *Blood.* (2008) 112:4948–52. doi: 10.1182/blood-2008-01-133702
11. Goicoechea de Jorge E, Harris CL, Esparza-Gordillo J, Carreras L, Arranz EA, Garrido CA, et al. Gain-of-function mutations in complement factor B are associated with atypical hemolytic uremic syndrome. *Proc Natl Acad Sci USA*. (2007) 104:240–5. doi: 10.1016/j.molimm.2006.07.076
12. Goodship TH, Cook HT, Fakhouri F, Fervenza FC, Fremeaux-Bacchi V, Kavanagh D, et al. Atypical hemolytic uremic syndrome and C3 glomerulopathy: conclusions from a "kidney disease: improving global outcomes" (KDIGO) controversies conference. *Kidney Int.* (2017) 91:539–51. doi: 10.1016/j.kint.2016.10.005
13. de Cordoba SR. Complement genetics and susceptibility to inflammatory disease. Lessons from genotype-phenotype correlations. *Immunobiology*. (2016) 221:709–14. doi: 10.1016/j.imbio.2015.05.015
14. Nester CM, Barbour T, de Cordoba SR, Dragon-Durey MA, Fremeaux-Bacchi V, Goodship TH, et al. Atypical aHUS: state of the art. *Mol Immunol.* (2015) 67:31–42. doi: 10.1016/j.molimm.2015.03.246
15. Martinez-Barricarte R, Heurich M, Valdes-Canedo F, Vazquez-Martul E, Torreira E, Montes T, et al. Human C3 mutation reveals a mechanism of dense deposit disease pathogenesis and provides insights into complement activation and regulation. *J Clin Invest.* (2010) 120:3702–12. doi: 10.1172/JCI43343
16. Exeni RA, Fernandez-Brando RJ, Santiago AP, Fiorentino GA, Exeni AM, Ramos MV, et al. Pathogenic role of inflammatory response during Shiga toxin-associated hemolytic uremic syndrome (HUS). *Pediatr Nephrol.* (2018) 33:2057–71. doi: 10.1007/s00467-017-3876-0
17. Cavero T, Arjona E, Soto K, Caravaca-Fontan F, Rabasco C, Bravo L, et al. Severe and malignant hypertension are common in primary atypical hemolytic uremic syndrome. *Kidney Int.* (2019) 96:995–1004. doi: 10.1016/j.kint.2019.05.014
18. Osborne AJ, Breno M, Borsa NG, Bu F, Fremeaux-Bacchi V, Gale DP, et al. Statistical validation of rare complement variants provides insights into the molecular basis of atypical hemolytic uremic syndrome and C3 glomerulopathy. *J Immunol.* (2018) 200:2464–78. doi: 10.4049/jimmunol.1701695
19. Martinez-Barricarte R, Heurich M, Lopez-Perrote A, Tortajada A, Pinto S, Lopez-Trascasa M, et al. The molecular and structural bases for the association of complement C3 mutations with atypical hemolytic uremic syndrome. *Mol Immunol.* (2015) 66:263–73. doi: 10.1016/j.molimm.2015.03.248
20. Roumenina LT, Frimat M, Miller EC, Provot F, Dragon-Durey MA, Bordereau P, et al. A prevalent C3 mutation in aHUS patients causes a direct C3 convertase gain of function. *Blood.* (2012) 119:4182–91. doi: 10.1182/blood-2011-10-383281
21. Schramm EC, Roumenina LT, Rybkine T, Chauvet S, Vieira-Martins P, Hue C, et al. Mapping interactions between complement C3 and regulators using mutations in atypical hemolytic uremic syndrome. *Blood.* (2015) 125:2359–69. doi: 10.1182/blood-2014-10-609073
22. Vieira-Martins P, El Sissy C, Bordereau P, Gruber A, Rosain J, Fremeaux-Bacchi V. Defining the genetics of thrombotic microangiopathies. *Transfus Apher Sci.* (2016) 54:212–9. doi: 10.1016/j.transci.2016.04.011
23. Siomou E, Gkoutsias A, Serbis A, Kollios K, Chaliasos N, Fremeaux-Bacchi V. aHUS associated with C3 gene mutation: a case with numerous relapses and favorable 20-year outcome. *Pediatr Nephrol.* (2016) 31:513–7. doi: 10.1007/s00467-015-3267-3
24. Ferreira E, Oliveira N, Marques M, Francisco L, Santos A, Carreira A, et al. Eculizumab for the treatment of an atypical hemolytic uremic syndrome with mutations in complement factor I and C3. *Nefrologia.* (2016) 36:72–5. doi: 10.1016/j.nefro.2015.07.007

Conflict of Interest: SR has received honoraria from Alexion Pharmaceuticals for giving lectures and participating in advisory boards. JL has received honoraria from Alexion Pharmaceuticals for giving lectures. None of these activities has had any influence on the results or interpretation in this article.

The remaining authors declare that the research was conducted in the absence of any commercial or financial relationships that could be construed as a potential conflict of interest.

frontiers in Immunology

ORIGINAL RESEARCH
published: 07 August 2020
doi: 10.3389/fimmu.2020.01772

Circulating FH Protects Kidneys From Tubular Injury During Systemic Hemolysis

Nicolas S. Merle[1†], Juliette Leon[1†], Victoria Poillerat[1], Anne Grunenwald[1], Idris Boudhabhay[1], Samantha Knockaert[1], Tania Robe-Rybkine[1], Carine Torset[1], Matthew C. Pickering[2], Sophie Chauvet[1,3], Veronique Fremeaux-Bacchi[1,4] and Lubka T. Roumenina[1]*

[1] Centre de Recherche des Cordeliers, INSERM, Sorbonne Université, Université de Paris, Paris, France, [2] Centre for Complement and Inflammation Research, Imperial College London, London, United Kingdom, [3] Assistance Publique – Hôpitaux de Paris, Service de Nephrologie, Hôpital Européen Georges Pompidou, Paris, France, [4] Assistance Publique – Hôpitaux de Paris, Service d'Immunologie Biologique, Hôpital Européen Georges Pompidou, Paris, France

OPEN ACCESS

Edited by:
Marcin Okrój, Intercollegiate Faculty of Biotechnology of University of Gdańsk and Medical University of Gdańsk, Poland

Reviewed by:
Margarita López-Trascasa, Autonomous University of Madrid, Spain
Elena Goicoechea De Jorge, Universidad Complutense de Madrid, Spain

***Correspondence:**
Lubka T. Roumenina
lubka.roumenina@sorbonne-universite.fr

[†]These authors have contributed equally to this work

Specialty section:
This article was submitted to Molecular Innate Immunity, a section of the journal Frontiers in Immunology

Received: 30 April 2020
Accepted: 02 July 2020
Published: 07 August 2020

Citation:
Merle NS, Leon J, Poillerat V, Grunenwald A, Boudhabhay I, Knockaert S, Robe-Rybkine T, Torset C, Pickering MC, Chauvet S, Fremeaux-Bacchi V and Roumenina LT (2020) Circulating FH Protects Kidneys From Tubular Injury During Systemic Hemolysis. Front. Immunol. 11:1772. doi: 10.3389/fimmu.2020.01772

Intravascular hemolysis of any cause can induce acute kidney injury (AKI). Hemolysis-derived product heme activates the innate immune complement system and contributes to renal damage. Therefore, we explored the role of the master complement regulator Factor H (FH) in the kidney's resistance to hemolysis-mediated AKI. Acute systemic hemolysis was induced in mice lacking liver expression of FH (hepatoFH$^{-/-}$, ∼20% residual FH) and in WT controls, by phenylhydrazine injection. The impaired complement regulation in hepatoFH$^{-/-}$ mice resulted in a delayed but aggravated phenotype of hemolysis-related kidney injuries. Plasma urea as well as markers for tubular (NGAL, Kim-1) and vascular aggression peaked at day 1 in WT mice and normalized at day 2, while they increased more in hepatoFH$^{-/-}$ compared to the WT and still persisted at day 4. These were accompanied by exacerbated tubular dilatation and the appearance of tubular casts in the kidneys of hemolytic hepatoFH$^{-/-}$ mice. Complement activation in hemolytic mice occurred in the circulation and C3b/iC3b was deposited in glomeruli in both strains. Both genotypes presented with positive staining of FH in the glomeruli, but hepatoFH$^{-/-}$ mice had reduced staining in the tubular compartment. Despite the clear phenotype of tubular injury, no complement activation was detected in the tubulointerstitium of the phenylhydrazin-injected mice irrespective of the genotype. Nevertheless, phenylhydrazin triggered overexpression of C5aR1 in tubules, predominantly in hepatoFH$^{-/-}$ mice. Moreover, C5b-9 was deposited only in the glomeruli of the hemolytic hepatoFH$^{-/-}$ mice. Therefore, we hypothesize that C5a, generated in the glomeruli, could be filtered into the tubulointerstitium to activate C5aR1 expressed by tubular cells injured by hemolysis-derived products and will aggravate the tissue injury. Plasma-derived FH is critical for the tubular protection, since pre-treatment of the hemolytic hepatoFH$^{-/-}$ mice with purified FH attenuated the tubular injury.

Worsening of acute tubular necrosis in the hepatoFH$^{-/-}$ mice was trigger-dependent, as it was also observed in LPS-induced septic AKI model but not in chemotherapy-induced AKI upon cisplatin injection. In conclusion, plasma FH plays a key role in protecting the kidneys, especially the tubules, against hemolysis-mediated injury. Thus, FH-based molecules might be explored as promising therapeutic agents in a context of AKI.

Keywords: complement – immunological term, complement factor H, hemolysis, kidney, acute tubular damage

INTRODUCTION

Intravascular hemolysis is responsible for acute kidney injury (AKI), partly due to cellular damage induced by hemoglobin and its breakdown product heme (1). There are multiple nephrotoxic mechanisms of hemoglobin and heme, including direct toxicity, oxidative stress, vasoconstriction, NO scavenging and sterile inflammation.

Renal injury related to hemolysis has been described in genetic hemoglobinopathies (like sickle cell disease, SCD), in malaria or in transfusion of stored red blood cells, where hemolysis-derived products injure renal structures, particularly the proximal tubules (2, 3). Interestingly, these products and especially heme, have also been shown to activate the complement system (4).

Complement is a powerful plasmatic innate immune defense mechanism, which is tightly regulated to prevent tissue injury (5, 6). Recent studies have identified a key role of complement overactivation in tissue damage occurring in hemolytic diseases, including SCD (7–12). Notably, complement activation drives acute tubular injury, which was prevented in C3$^{-/-}$ mice (5, 6, 8). One explanation for this phenomenon is that heme directly triggers the alternative complement pathway (AP) in the circulation. Moreover, heme also renders the endothelial cells (EC) susceptible to complement attack (7, 9, 13).

Despite these studies, the mechanisms of complement regulation in the context of hemolysis remain poorly understood. Factor H (FH) is a major plasma regulator of the complement system acting at level of C3 (5). By interacting with C3b, FH controls the complement cascade activation both in the bloodstream and on cell surfaces, preventing the terminal C5b-9 complex formation (14–18). Impaired FH binding to tubular cells in a mouse model of renal ischemia/reperfusion resulted in aggravation of the phenotype, emphasizing the protective effect of the circulating FH against acute tubular necrosis (19, 20). However, the role of FH in the context of hemolysis-related AKI remains unknown.

Moreover, systemic FH is mainly (up to 80%) produced by the liver (21). The kidney is considered as a major extrahepatic producer of complement proteins, but the capacity of its cells to produce and bind FH at resting state is debated.

Here we showed that systemic FH protected the kidneys from hemolysis-induced renal injury. We used a mouse model hepatoFH$^{-/-}$ unable to produce hepatic FH to differentiate its role from local FH. These data identify the complement system as a key driver of tubular damage in hemolytic diseases and show the potential for administration of purified FH as a promising therapeutic strategy.

METHODS

Reagents

Stock solution of 25 mg/ml Phenylhydrazin (PHZ) (Sigma-Aldrich) and of 250 μg/ml LPS (LPS-EB from *E. coli* O111:B4, InVivogen) were prepared in sterile PBS (Gibco) immediately before use.

Animal Experimentation

Experimental protocols were approved by Charles Darwin ethical committee (Paris, France) and by the French Ministry of Agriculture (Paris, France) number APAFIS# 3764-201601121739330v3. All the experiments were conducted in accordance with their recommendations for care and use of laboratory animals. Two different strains, housed in specific germs-free conditions, were used: wild type C57BL/6 mice (WT) purchased from Charles River Laboratories (L'Arbresle, France) and hepatocyte-Cfh$^{-/-}$ C57BL/6 mice (hepatoFH$^{-/-}$) (21). HepatoFH$^{-/-}$ mice have been generated by crossing alb-Cre (Jackson Laboratories, 003574) with FH–loxP mice (Cfh$^{loxP/loxP}$).

Mouse Treatment

Mice were injected with intraperitoneal (IP) injection of 100 μL PBS or PHZ (900 μmol/kg, corresponding to 0.125 mg/g body weight) and the mice were sacrificed at day 1, 2, or 4 (**Figure S1A**). Blood and urines were collected 3 days before the first injection (baseline). Blood, urines and organs, including kidneys, heart and liver, were recovered at sacrifice. Eight to 16-week-old mice were sex- and age-matched for each experiment. Mouse blood samples were collected into heparin–containing Eppendorf tubes. Organs were frozen in nitrogen liquid and stored at −80°C or fixed in 4% paraformaldehyde during 24 h for paraffin inclusion with HistoCore® (Leica Biosystem). Alternatively, PBS, Cisplatin (Tocris Bioscience 15 mg/kg) or LPS (InvivoGen, 2 mg/kg) were injected IP and mice were sacrificed at day 2. To test the efficacy of FH, mice were pretreated with 2 intravenous injections of 250 μL human FH 1 mg/mL (corresponding to 0.025 mg/g body weight), at 3 h and 1 h before IP injection of PBS or PHZ. Concentrations and route of administration were chosen as described previously (8, 22).

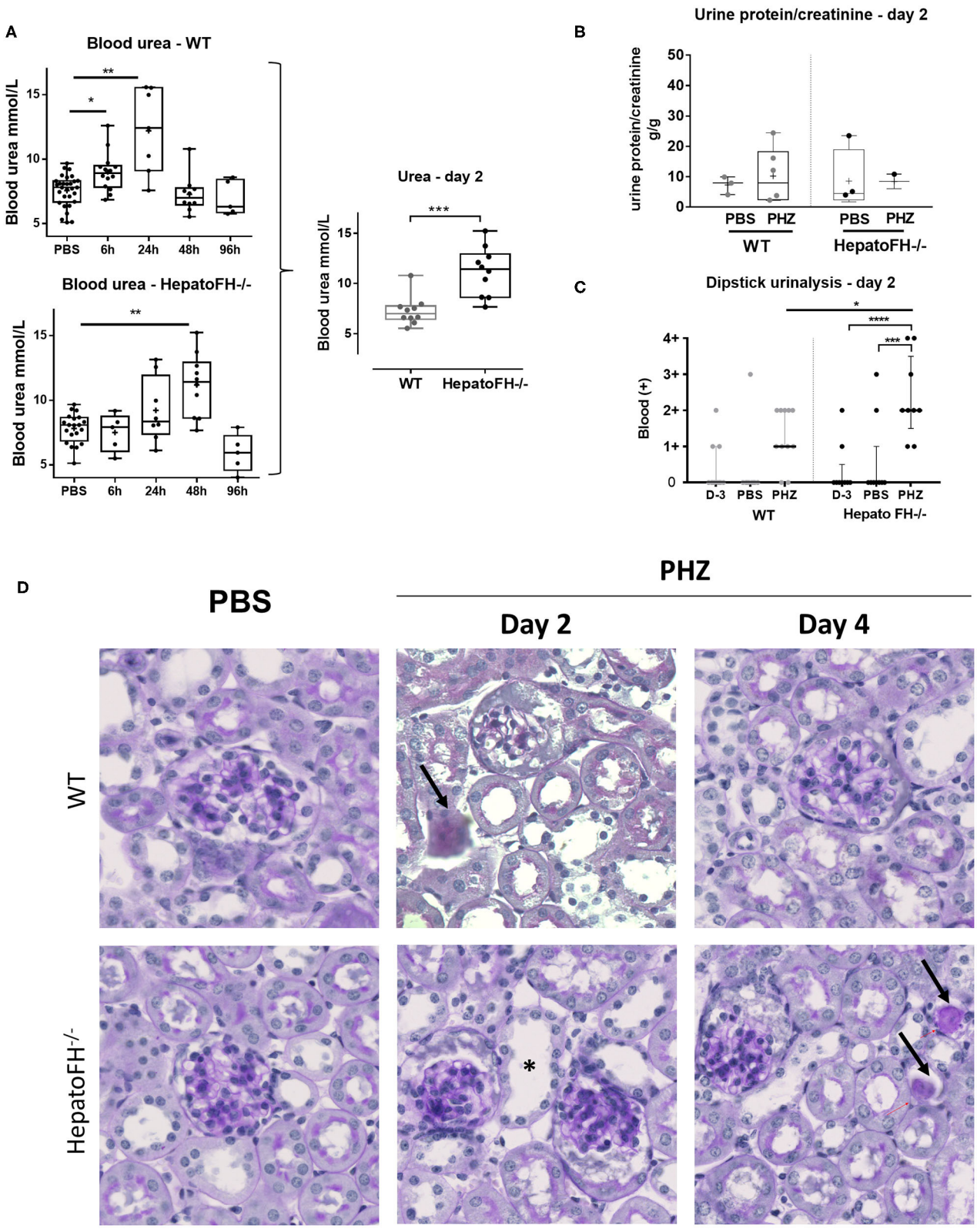

FIGURE 1 | Hemolysis induces clinicopathologic changes in HepatoFH$^{-/-}$ kidneys **(A–C)**. Evaluation of renal function by measurement of plasmatic urea level **(A)**, urine protein-creatinine ratio **(B)** and presence of blood in urine by urinary dipstick **(C)** in WT and hepatoFH$^{-/-}$ mice, at 6, 24, 48, and 96 h after PBS or PHZ

(Continued)

FIGURE 1 | injection. The dipstick scale is in **Figure S2**. **(D)** PAS coloration of paraffin-embedded renal section (x40) after PBS or PHZ injection in WT (upper panel) hepatoFH$^{-/-}$ (bottom panel) mice. Black arrows are showing the presence of casts inside the tubules. Asterix shows tubular injury with tubule dilation and loss of brush border. No significant changes are seen inside the glomeruli. *P*-values are derived from Two way ANOVA test with Sidak test correction: $^{*}p < 0.05$, $^{**}p < 0.005$, $^{***}p < 0.001$, $^{****}p < 0.0001$. The quantification values are box plots and dots with median and Min/Max points. Data from four independent experiments, each experimental group containing between 5 and 10 mice were pooled. PBS groups are composed of PBS-treated mice from each time points assessed with PHZ treatment. PBS-treated mouse were statistically equivalent from one another when analyzed over time. D, day.

Measurement of Renal and Hematologic Function

Plasma urea was measured using an enzymatic method by the analyzer KONELAB (ThermoFisher Scientific). Microscopic hematuria was detected with Multistix® 8SG Urin Strips (Siemens) using the following scale: negative, trace, 1+, 2+, 3+, and 4+. Urine protein and urine creatinine were measured by KONELAB on urine samples, in order to calculate the urine protein to creatinine ratio (UP/CR), used as a glomerular dysfunction marker. Hematocrit is the ratio between plasma volume after centrifugation and fresh blood volume collected from the mice.

Immunohistochemistry and PAS Coloration of Mouse Tissues

Four-µm-thick paraffin-embedded sections were cut with a microtome (RM2235, Leica Biosystem). Antigen retrieval was performed in a low pH buffer using the PT-Link™ Dako (Agilent Technologies). VCAM-1 (Abcam, ab134047) was stained and revealed with a one-step polymer goat anti-rabbit IgG coupled with horseradish peroxidase (HRP) (Dako Envision™, Agilent Technologies, #K4003). Staining was visualized using diaminobenzidine (DAB). Slides were scanned by Nanozoomer® (Hamamatsu) and analyzed with NDPview2® (Hamamatsu). Periodic acid–Schiff coloration was performed by routine procedures using sections of paraffin-embedded kidneys. Coloration of slides was scanned by Slide Scanner Axio Scan (Zeiss).

Immunofluorescence of Mouse Tissue

Five-µm-thick frozen sections of kidneys were cut with Cryostat (Leica AS-LMD, Leica Biosystem,) and fixed in acetone on ice for 10 min. C3 (Hycult Biotech, HM1065), C5b-9 (Abcam, ab55811), polyclonal anti-serum to human FH (Quidel, A312), goat IgG (Jackson Immunoresearch, 005-000-003), C5aR1 (Hycult Biotech, mAb 20/70), CD31 (Abcam, ab124432), and NGAL polyclonal IgG (R&D system, AF1857) were stained for 2 h at RT and revealed by secondary Donkey anti-Goat AF647 (ThermoScientific, A-21447) or goat anti-rat AF647 (ThermoScientific, A-21434). Nucleus were stained with DAPI. Stained tissues were scanned by Slide Scanner Axio Scan™ (Zeiss) and analyzed with Zen lite™ software (Zeiss).

Elisa for Detection of Human FH in Mouse Plasma

We used polyclonal antibody against FH (IgG purified in house from the goat anti-FH antiserum, Quidel A312), which was left native or was biotinylated. The native anti-FH antibodies was coated on a 96-well plate overnight at 4°C. After washing with PBS Tween 0.1% and blocking with PBS BSA 1% for 1 h at RT, the mouse plasma was added to the plate and incubated for 1 h at RT. After washing, plate was incubated with the biotinylated anti-FH antibody for 1 h at RT. After additional washings, streptavidin-HRP (Dako, P039701-2) was added for 1 h at RT. FH concentration was revealed by SureBlue TMB microwell peroxidase substrate (KPL) and the reaction was stopped by sulfuric acid 2 mol/L. Multiskan Ex (Thermofisher Scientific) was used to read the optical density at 450 nm. Results are expressed in µg/mL according to the standard curve, made using commercial purified FH (Comptech).

Measurement and Detection of Mouse FH and C3

Plasma FH and C3 levels were evaluated by WB using the Invitrogen™Novex™ (ThermoFisher Scientific) separated on Bis-tris gels and transferred onto nitrocellulose membranes, using diluted plasma at 1/50. Next, the membranes were blocked and incubated at 4°C overnight with an anti–human FH antiserum (Quidel, A312), an anti–serum against mouse C3 (MP Biomedicals, 0855463). Staining was revealed with HRP-linked secondary rabbit anti-goat antibody (Thermofisher, #31402) and detected by chemiluminescence with myECLimager® (Thermoscientific).

mRNA Level Analyses

Frozen kidney sections were recovered in RLT buffer (Macherey-nagel) + 1% β-mercaptoethanol (Gibco, Thermoscientific) and used for mRNA extraction using RNAse-free NucleoSpin® RNA (Macherey-nagel). The quality and quantity of mRNA were evaluated with the Agilent 2100 bioanalyzer using the Agilent TNA 6000 NanoKit (Agilent Technologies), followed by retrotranscription to cDNA (Qiagen).

Gene markers of acute tubular injury (NGAL and Kim-1), of endothelial activation (ICAM-1, VCAM-1, P-selectin, E-selectin), of inflammation (IL-6, Ki67, cNOS, Endothelin), of coagulation system (PAI-1), HO-1, and FH were analyzed by RT-qPCR (primers from ThermoFisher) using the Taqman 7900 (Life Technologies). Gene markers expression was analyzed with SDS 2.1® software (ThermoFisher), after normalization on actin housekeeping gene expression and comparison with gene expression from the pool of PBS-treated mice of each strain.

Statistical Analyses

Results were analyzed using statistical software GraphPad Prism 5 using Mann–Whitney test, Two-way ANOVA or Kruskall Wallis tests as indicated in the figures legends. Statistical significance was defined as $p < 0.05$.

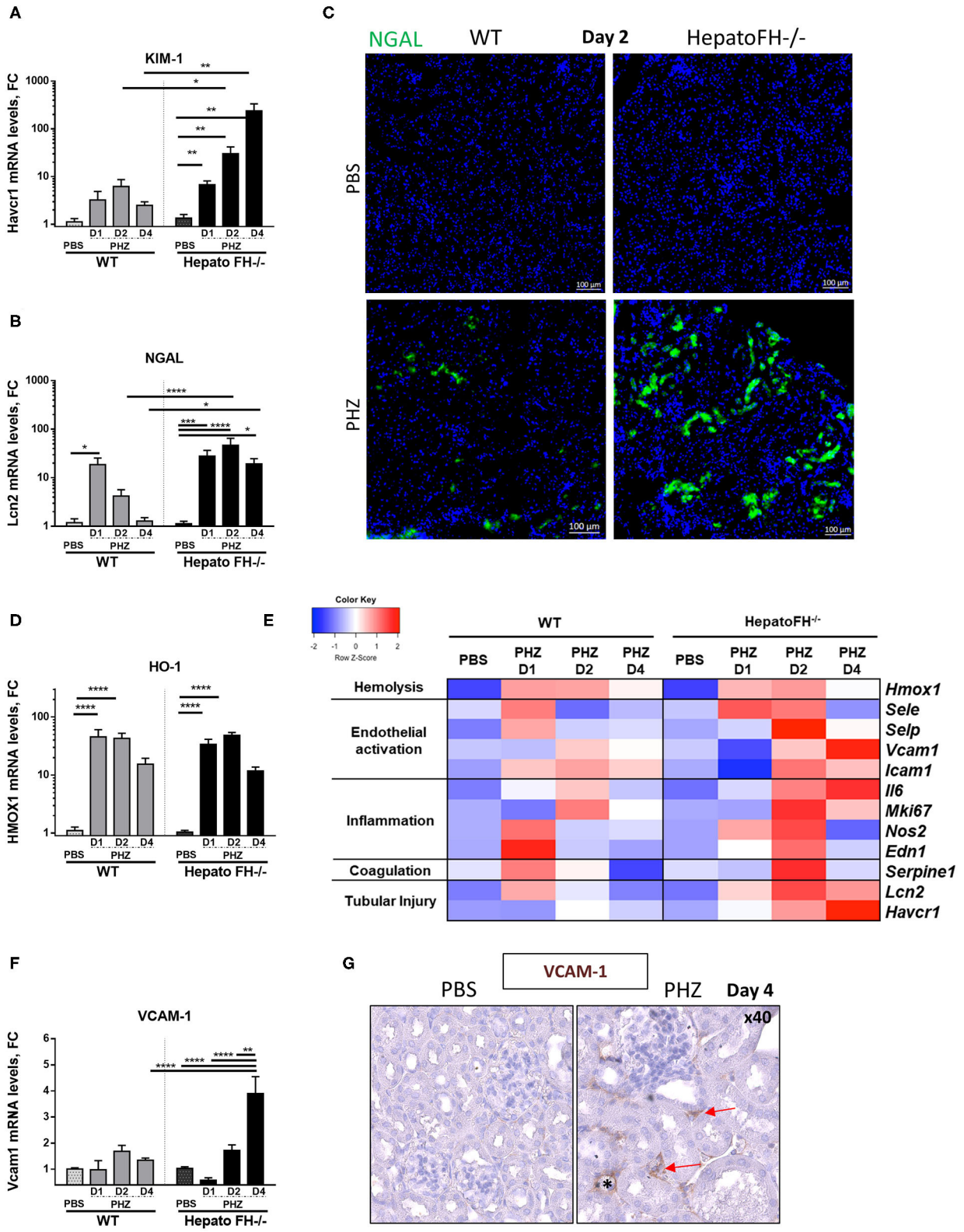

FIGURE 2 | Factor H deficiency increases tubular injury after hemolysis. **(A,B)** Assessment of acute tubular injury by mRNA renal expression of Kim1 (*Havcr1*) **(A)** and NGAL (*Lcn2*) **(B)**, after PBS or PHZ injection (day 1, 2, and 4) in WT and hepatoFH$^{-/-}$ mice. **(C)** Examples of NGAL staining (false green color) in tubular cells, by IF on frozen kidneys after PBS or PHZ injection in WT and HepatoFH$^{-/-}$ mice (5x). **(D)** Renal expression of Heme oxygenase 1 (HO-1, *Hmox1*) mRNA after PBS or PHZ injection (day 1, 2, and 4) in WT and hepatoFH$^{-/-}$ mice. **(E)** Heatmap summarizing the impact of hemolysis in renal mRNA expression: assessment of

(Continued)

FIGURE 2 | hemolysis, endothelial activation, inflammation, coagulation system, and acute tubular injury by mRNA renal gene expression at day 1, 2, and 4 after PBS or PHZ in WT and hepatoFH$^{-/-}$ mice: Endothelial activation reflected by renal mRNA expression of E-selectin (*Esel*), P-selectin (*Psel*), ICAM-1 (*Icam1*); Inflammatory status and coagulation system reflected by renal mRNA expression of Endothelin (*Edn1*), cNOS (*Nos2*), Ki67 (*Mki67*), IL6 (*Il6*), and PAI-1 (*Serpine1*). Each case represents the mean of mRNA values from mice with the same genotype and the same treatment. In red, the conditions were genes displaying the highest expression, and in blue the lowest expression. The heatmap incorporates for comparison the data from panels **(A,B,D,F)**. **(F)** Renal expression of VCAM-1 (*Vcam1*) mRNA after PBS orPHZ injection (day 1, 2, and 4) in WT and hepatoFH$^{-/-}$ mice. **(G)** Validation by VCAM-1 immunohistochemistry staining in embedded paraffin (false brown color), seen in peritubular capillaries (red arrow) and arteriols (*) in hepatoFH$^{-/-}$ at day 4 post PHZ vs. PBS injection (40x). *P*-values are derived from Two way ANOVA test with Sidak correction for multiple comparisons: $^{*}p < 0.05$; $^{**}p < 0.005$; $^{***}p < 0.001$; $^{****}p < 0.0001$. mRNA values are represented in fold change (FC), relatively to the mean expression of PBS treated mice for each strain. Values are represented as mean +/− SEM. Data from two independent experiments, experimental groups containing between 4 and 11 mice.

RESULTS

Hemolysis Triggers Stronger Kidney Injury but With Delayed Onset in HepatoFH$^{-/-}$ Mice

Well-characterized model of PHZ-induced intravascular hemolysis (8, 23) was induced in mice with a hepatic deficiency of FH (hepatoFH$^{-/-}$ mice) and in WT mice, described by Vernon et al. (21). Comparison between WT and hepatoFH$^{-/-}$ mouse strains revealed similar levels of hematocrit at day 2 (**Figure S1B**), showing that lack of FH does not impact on hemolysis induction. Blood urea increased in WT mice at 6 h and day 1 post treatment and returned to normal at day 2 and 4. HepatoFH$^{-/-}$ mice experienced delayed onset after PHZ treatment, with normal urea at 6 h, a trend toward increase at day 1, a peak at day 2, and normalization at day 4 (**Figure 1A**). Blood urea was higher at day 2 in hepatoFH$^{-/-}$ compare to WT mice. Concomitantly, urine protein/creatinine ratio was not altered by PHZ treatment in both strains (**Figure 1B**). Dipstick urinalysis revealed no difference in WT mice between untreated, PBS- and PHZ-treated mice (**Figures 1C**, **S2**). However, a positive dipstick for blood was found in hepatoFH$^{-/-}$ after PHZ treatment at day 2 compare to PBS and untreated hepatoFH$^{-/-}$ mice, $^{-}$but also compared to WT mice after PHZ treatment (**Figure 1C**). There was no evidence of glomerular lesions, such as hypercellularity, double contours or mesangiolysis. However, there was a clear damage in the tubulointerstitial area in hepatoFH$^{-/-}$ upon PHZ treatment, with a dilatation of tubular lumens and loss of brush border in proximal tubules at day 2 and tubular casts formation at day 4 (**Figure 1D**).

Hemolysis Promotes Gene Expression of Acute Tubular Injury Markers in HepatoFH$^{-/-}$

Hemolysis induces upregulation of acute tubular injury markers (8, 23, 24). Here, mRNA study revealed increased expression of proximal tubules injury marker KIM-1 at day 1, which was maintained at day 2 and declined at day 4 in WT mice after PHZ treatment (**Figure 2A**). Interestingly, KIM-1 expression constantly increased from day 1 to day 4 in hepatoFH$^{-/-}$ and was higher compared to its control PBS and to WT mice.

Further, tubular injury marker NGAL expression in WT mice acutely expressed (peak at day 1 and return to normal at day 4) as in (23) (**Figure 2B**). In hepatoFH$^{-/-}$, NGAL expression was increased at day 1, and reached a plateau at day 2. Moreover, NGAL expression was stronger in kidneys from hepatoFH$^{-/-}$ mice compared to the baseline and to WT mice, even at day 4. This different level of expression was confirmed by IF staining of NGAL, where NGAL in tubules from hepatoFH$^{-/-}$ was stronger compared to WT mice after PHZ treatment (**Figure 2C**). As a control, the heme detoxifying enzyme heme oxygenase 1 (HO-1) was equally upregulated in WT and in hepatoFH$^{-/-}$ mice (**Figure 2D**).

Hemolysis Induces Gene Expression of EC Stress Markers in HepatoFH$^{-/-}$

Endothelial cells get activated during hemolysis (8, 23). Here, we compared mRNA expression of endothelial stress markers in kidneys of WT and hepatoFH$^{-/-}$ mice (**Figure 2E**). P-selectin, E-selectin and cNOS increased at day 1 in WT mice after PHZ injection, and returned to baseline at day 2. At day 2, each of these markers increased in hepatoFH$^{-/-}$ after PHZ treatment compared to their PBS control and compared to WT mice treated with PHZ. Interestingly, expression of VCAM-1 showed a different kinetic Whereas VCAM-1 mRNA expression was found stable in WT mice under hemolysis after 4 days, its expression significantly increased in hepatoFH$^{-/-}$ mice at the latest time point (day 4) compared to PBS control and to WT mice treated with PHZ (**Figure 2F**). Interestingly, VCAM-1 was mostly found in peritubular capillaries and arterioles within kidneys, with no evidence of VCAM-1 staining within glomeruli (**Figure 2G**).

The Contribution of Hepatic FH Deficiency to Acute Tubular Necrosis Is Trigger-Dependent

Multiple agents induce AKI. To evaluate the impact of hepatic FH deficiency in other models of renal insult, we used models of LPS and cisplatin induced-nephrotoxicity (**Figure 3**). Both LPS (**Figures 3A–C**) and cisplatin (**Figures 3D–F**) triggered overexpression of NGAL, KIM-1 in WT mice at day 2. The expression was further enhanced in hepatoFH$^{-/-}$ mice in the LPS model, while remained unaltered in the cisplatin one. HO-1 was upregulated by LPS in hepatoFH$^{-/-}$ mice (**Figure 3C**) and in both strains by cisplatin (**Figure 3F**).

Complement Activation Is Increased in Plasma and Within Glomeruli of HepatoFH$^{-/-}$ Mice Upon Hemolytic Event

In agreement with Vernon et al. (21), the amount of plasma C3 in hepatoFH$^{-/-}$ was strongly reduced compare to WT,

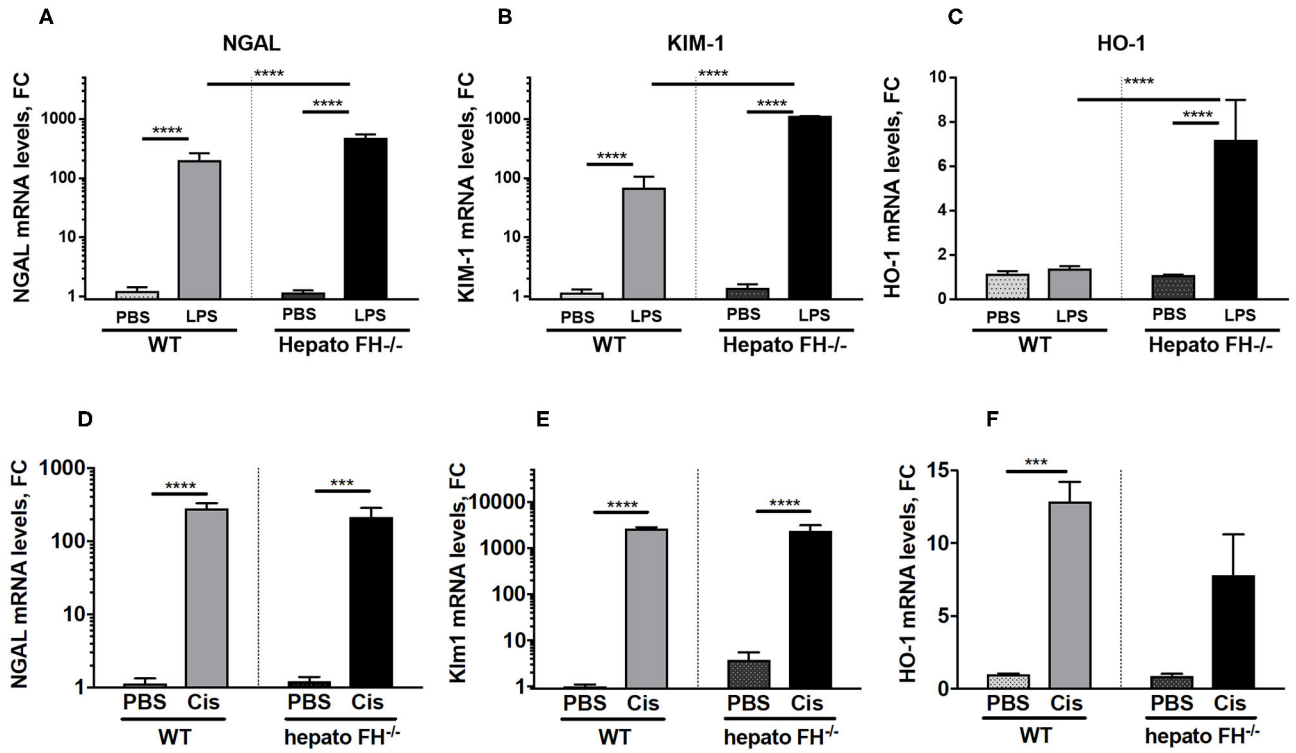

FIGURE 3 | LPS-induced but not Cisplatin-induced tubular injury is exacerbated by FH deficiency. WT and hepatoFH$^{-/-}$ received intraperitoneal injection of PBS, cisplatin (15 mg/kg) or LPS (LPS-EB from *E. coli* O111:B4) (2 mg/kg) at Day 0 and were sacrificed at Day 2. Renal mRNA expression in LPS treated mice of NGAL **(A)**, Kim-1 **(B),** and HO-1 **(C)** or Cisplatin treated mice of NGAL (*Lcn2*) **(D)**, Kim-1 (*Havcr1*) **(E)** and HO-1 (*Hmox1*) **(F)** were measured by RTqPCR. *P*-values are derived from two way ANOVA with Sidak correction: ***$P < 0.0005$; ****$P < 0.0001$. Values are mean +/- SEM. Cis, cisplatin. Data from two independent experiments, experimental group containing between 2 and 5 mice.

as shown by WB (**Figures 4A,B**). Triggering hemolysis with PHZ resulted in plasma C3 consumption, as evident by the appearance of the α' and increase in the α43 band in the WT and in hepatoFH$^{-/-}$ (day 2 data shown, **Figures 4A,B**). Further, we investigated the complement deposits in the kidneys (**Figures 4C–F**). Immunofluorescence staining of C3 revealed usual physiological traces of C3 fragment deposits surrounding the tubular cells in the WT mice, which disappeared in the hepatoFH$^{-/-}$ mice due to the complement consumption (8, 21). No enhancement of the C3 fragments deposits were detected in the tubulointerstitium upon PHZ injection neither in the WT mice [in agreement with our previous studies (8, 25)] nor in the hepatoFH$^{-/-}$ mice (data on day 2, **Figure 4C**). In contrast, the C3 fragments deposits were seen in glomeruli, which increased in both strains after PHZ treatment in a similar manner (**Figures 4C,E**). However, if C5b-9 was absent in kidneys in PBS-treated mice in WT and hepatoFH$^{-/-}$ mice, and WT mice injected with PHZ, it was found elevated exclusively in glomeruli of hepatoFH$^{-/-}$ after hemolysis at day 2 (**Figures 4D,F**). Even though we were not able to detect complement activation in tubular area with the detection limits of our methods, we found positive staining for C5aR1 on the WT mice, which was exacerbated in the tubules of the hepatoFH$^{-/-}$ mice, injected with PHZ (**Figure 4G**). The PBS-injected WT mice showed limited/no staining and only in glomeruli. It increased after treatment with PHZ. The hepatoFH$^{-/-}$ showed basal level of C5aR1 staining in the glomeruli and traces in the tubulointerstitium. The clear tubular staining appeared in these mice only after PHZ injection, making the tubular cells particularly responsive to C5a in this context.

FH Is Present in the Mouse Kidney

The circulating FH was lower in hepatoFH$^{-/-}$ compare to WT at resting state. In both mouse backgrounds, an increase was observed after PHZ treatment (**Figures 5A**, **S3A**). Exploring the mRNA expression for *Cfh* in the kidney showed that the expression was identical in the WT and hepatoFH$^{-/-}$ mice and was not affected by PHZ injection (**Figure 5B**). Exploring of FH staining in mouse kidney has been tricky and previous studies failed to detect it despite the clear evidence for mRNA production by various renal cell populations (26–31). The reason for this lack of staining in previous studies vs. the positive staining detected here is unclear and is likely related to the experimental conditions. Therefore, these staining results should be taken with caution, before being validated by an independent laboratory/method. Our conclusion that what we detect in the kidney is likely FH comes from the following arguments: Among the tested antibodies, we selected the anti-human factor H goat antiserum of Quidel, because it showed cross-reactivity with mouse FH by western blot (**Figures 5A**, **S3A**) with low

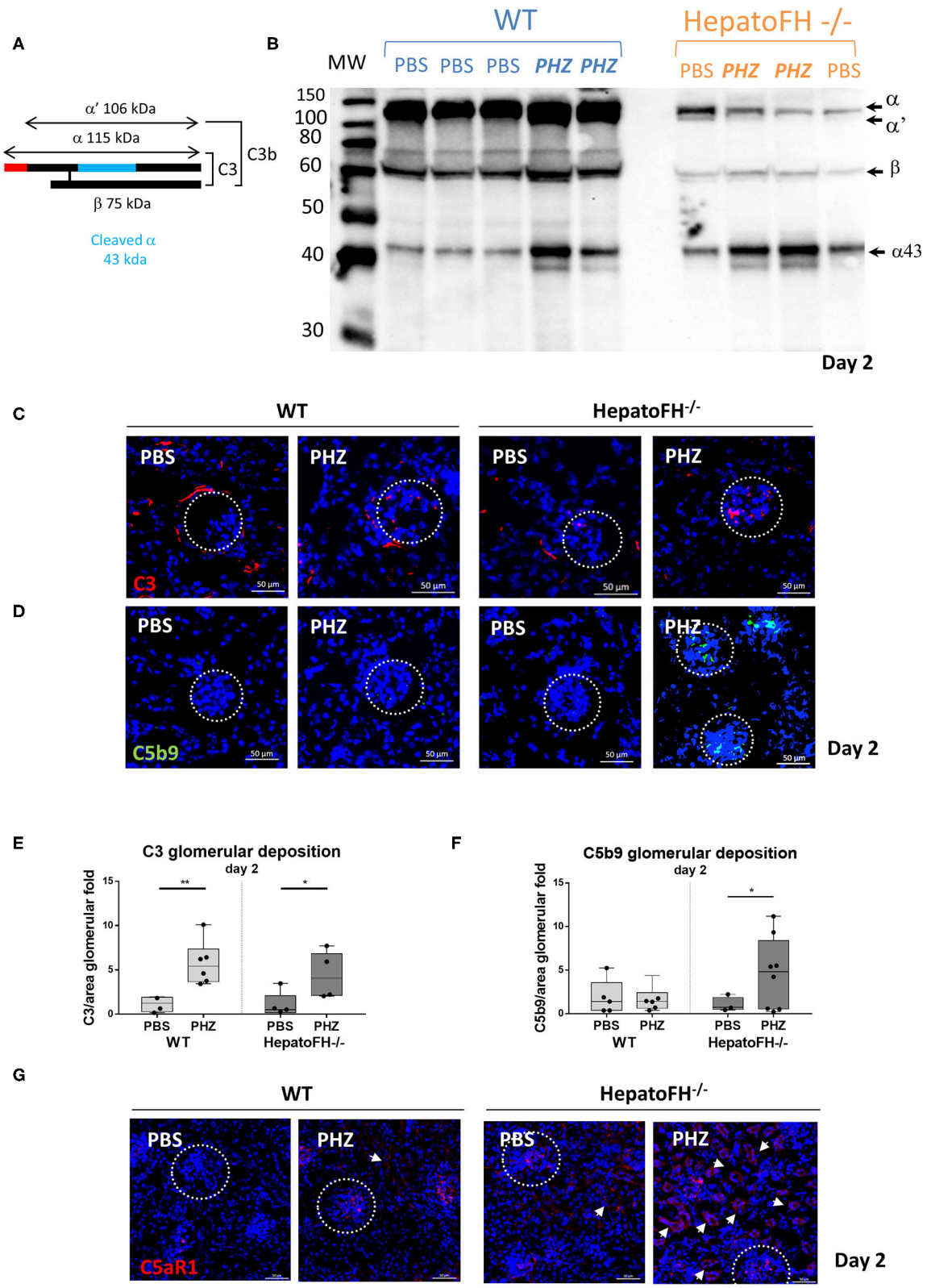

FIGURE 4 | Lack of circulating FH leads to formation of the membrane attack complex in glomeruli and C5aR1 upregulation in tubules. **(A)** Schematic represetation of complement C3, indicating the different chains and cleavage fragments to be detected by WB. **(B)** Evaluation of C3 cleavage by WB after PBS or PHZ injection (Day 2) in WT and hepatoFH$^{-/-}$ mice. Each lane correspond to 1 individual mouse. A mixture of purified C3 and C3b was used as a positive control to distinguish the

(Continued)

FIGURE 4 | presence of α and α' bands, characteristic for these two forms of C3, respectively. **(C,D)** Staining for C3 (false color red) **(C)**, and C5b-9 (false color green) **(D)** at day 2 after PBS or PHZ treatment in WT and hepatoFH$^{-/-}$ mice. The glomeruli are indicated by a dotted white circle (x40). **(E,F)** Immunofluorescence quantification of glomerular C3 **(E)** and C5b-9 **(F)**. **(G)** Staining of C5aR1 (false color red) at day 2 after PBS or PHZ treatment in WT and hepatoFH$^{-/-}$ mice. The arrowheads indicate the positive C5aR1 staining in the tubulointerstitium. In this figure, represetnative glomeruli are marked by a dotted circle. *P*-values are derived from Two way ANOVA test with Fisher test correction: $^{*}p < 0.05$, $^{**}p < 0.005$. The quantification values are represented in fold change (FC), relatively to the mean expression of PBS-treated mice for each strain. Values are box plots and dots with median and Min/Max points. D, day. Data from two independent experiments (except C5aR1, data from one experiment), experimental groups containing between 3 and 8 mice.

non-specific binding to other proteins in plasma (**Figure S3A**). We tested its specificity for mouse FH in tissues, taking the advantage of the hepatoFH$^{-/-}$ mice, which is invalidated for FH specifically in the hepatocytes (21). Upon optimization, the dilution 1/500 was selected, because it gave positive staining in the WT mice in hepatocytes and endothelial cells and positive staining in the EC of the hepatoFH$^{-/-}$ mouse but not in its hepatocytes (**Figure S3B**). With more diluted antibody this signal was lost. Nevertheless, we cannot fully exclude that part of the staining could be attributed to mouse factor H related proteins, which are produced by the liver but not by the kidney, and could come from the circulation. The presumed FH staining of frozen kidney sections from WT mice revealed strong staining within the glomeruli and positive staining in the tubules, which was unaffected by the PHZ treatment (data from day 2, **Figure S3C**). The glomerular staining partly co-localized with EC marker CD31 (**Figure S3D**). The hepatoFH$^{-/-}$ mice presented with a stronger staining in the glomeruli, likely due to binding of FH to the C3 fragments deposits present there at basal level, irrespective of the PHZ treatment. In contrast to the WT mice, the tubular staining in the hepatoFH$^{-/-}$ mice was very weak, suggesting that at least in part, the FH on the tubular cells comes from the circulation (**Figure S3C**).

Administration of Purified FH Prevents From Hemolysis-Driven AKI

To validate the importance of FH in the resistance to renal injury, we pre-treated hepatoFH$^{-/-}$ mice with purified human FH, known to regulate mouse complement (22). We established that human FH was detectable in comparable plasma concentrations in WT and hepatoFH$^{-/-}$ mice after a single intraperitoneal injection (**Figure 5C**). Furthermore, injected human FH was able to prevent from complement activation, as shown by WB on mouse plasma samples (**Figure 5D**) and bands quantification (**Figure 5E**). As a marker of AKI, we measured blood urea concentration 2 days after PHZ administration of WT and hepatoFH$^{-/-}$ mice pre-injected with human FH or PBS as a control. Blood urea did not increase in WT mice after PHZ treatment at day 2 and was comparable to the PBS-treated mice (**Figure 5F**). Therefore, pre-treatment of those mice with human FH did not affect blood urea concentration. However, PHZ treatment induced an increase of blood urea in hepatoFH$^{-/-}$ mice at day 2, which was prevented by pre-injection of human FH, normalizing to a similar level to PBS-treated mice (**Figure 5G**). Moreover, pre-injection of human FH partially prevented the increase of NGAL and KIM-1 expression in hepatoFH$^{-/-}$ mice observed at day 2 after PHZ treatment. No effect was detected in WT mice, since these markers had already returned to near normal spontaneously (**Figures 5H,I**). Of note, pre-injection of FH did not affect significantly the increase of HO-1 expression in both WT and hepatoFH$^{-/-}$ mice, suggesting that this marker is dependent on hemolytic status rather than complement-mediated tubular injury (**Figure 5J**).

DISCUSSION

Here we report the key role of systemic FH in protecting the kidneys against hemolysis-induced injury. Proximal tubules were particularly impacted by the reduced circulating FH and administration of purified FH partially prevented hemolysis-induced renal damage.

Despite the clear impact of intravascular hemolysis on the kidneys, hemolytic WT mice did not develop severe kidney failure (8, 23), suggesting an efficient underlying control mechanism. Since we have found that complement plays a major role in the hemolysis-induced kidney injury, we hypothesized that the tight regulation imposed by FH would contribute to renal protection. Interestingly, the disease course followed a different kinetic in the WT and hepatoFH$^{-/-}$ mice, with hepatoFH$^{-/-}$ mice having later onset but showing a more severe and persistent phenotype. The later onset could be explained by the partial C3 consumption, which was initially protective, since there was not enough C3 to be cleaved and deposited in order to promote the terminal pathway. Indeed, we found that C3$^{-/-}$ mice had attenuated expression of genes, triggered by intravascular hemolysis (8) and FH deficient mice were partially protected from ischemia/reperfusion injury due to the secondary consumption and therefore deficiency of C3 (19).

Hemolysis leads to pronounced tubular injury (2, 32–35). Complement AP activation is an important pathogenic mechanism in the development of AKI, especially in the tubulointerstitium, where it has been shown to drive severe injury (19, 20, 36). Moreover, we have recently demonstrated that in hemolytic conditions tubular injury markers were downregulated in C3$^{-/-}$ mice, confirming the harmful effect of complement activation on tubular cells (8). In line with these findings, we here detected further increases of NGAL and KIM-1 in hepatoFH$^{-/-}$, which were maintained at high levels at day 4 compared to WT mice. Furthermore, VCAM-1 was upregulated in peritubular capillaries in hepatoFH$^{-/-}$ mice at day 4.

The role of complement for the tubular injury during intravascular hemolysis may seem counterintuitive, since the deposition of complement activation fragments C3b/iC3b, as well as C5b-9 in the hepatoFH$^{-/-}$ mice, occurs in the glomeruli

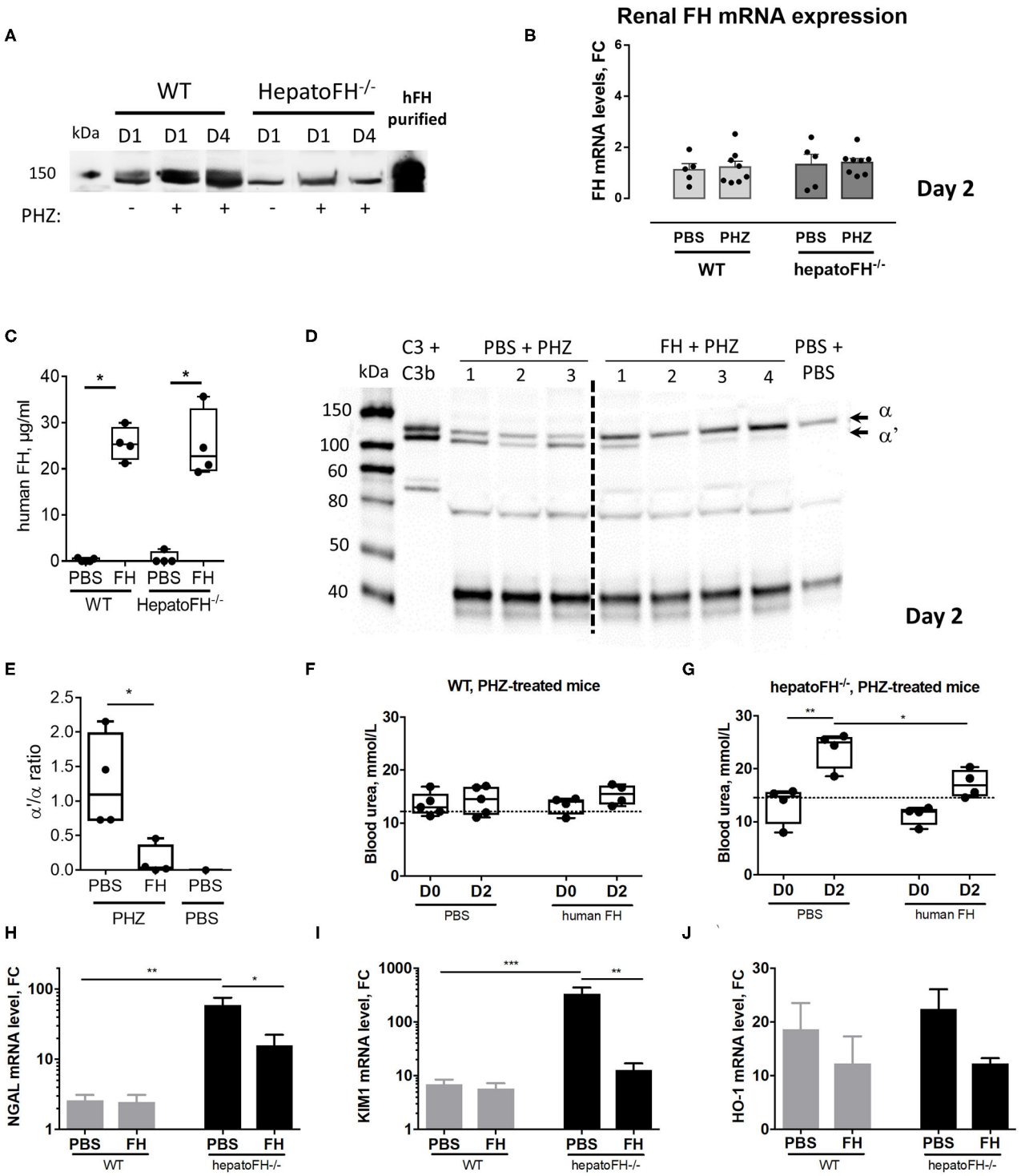

FIGURE 5 | Purified FH controls kidney injury in hemolytic conditions. **(A)** Measurement of plasma FH by WB after PBS or PHZ injection (Day 1 or 4 post-injection) in WT and hepatoFH$^{-/-}$ mice. Each lane correspond to 1 individual mouse. **(B)** Assessment of mRNA renal expression of FH in total kidney tissue. **(C)** Plasma human FH was assessed by ELISA at day 2 in WT and hepatoFH-/- mice, injected with human FH or PBS. **(D)** Plasma of hepatoFH$^{-/-}$ mice was resolved by electrophoresis and probed for C3 cleavage to C3b in hepatoFH$^{-/-}$ mice, treated or not with purified human FH. Each lane correspond to one individual mouse. **(E)** Quantification of the α'/α bands ratio, showing the absence of C3 activation in case of FH administration. **(F,G)** Blood urea was measured in plasma samples collected from PHZ-injected WT **(F)** or hepatoFH$^{-/-}$ **(G)** mice, pre-treated with human FH or PBS, at day 0 (D0) and day 2 (D2). **(H–J)** Assessment of mRNA renal expression for NGAL (*Lcn2*) **(H)**, Kim-1 (*Havcr1*) **(I)** and HO-1 (*Hmox1*) **(J)** at day 2 in PHZ-treated WT and hepatoFH$^{-/-}$ mice pre-treated with human FH or PBS. *P*-values are

(Continued)

FIGURE 5 | derived from Two way ANOVA test with Sidak correction for multiple comparisons: $*p < 0.05$; $**p < 0.005$; $***p < 0.001$. Plasma parameters are box plots and dots with median and Min/Max points. mRNA values are represented in fold change (FC), relatively to the mean expression of PBS-treated mice for each strain. Values are represented as mean +/- SEM for the gene expression and SD for the remaining panels. Data obtained from one experiment, experimental groups containing 4 mice.

and not on the tubules. Plasma FH protects the glomerular endothelium in the WT mice, since the cascade does not proceed to the terminal pathway during a hemolytic event, contrary to the hepatoFH$^{-/-}$ mice. However, processing of C3 and assembly of C5b-9 within glomeruli strongly suggest local endothelium damage and release of the anaphylatoxins C3a and C5a with a respective molecular weight of 10 and 11kDa. Proteins of this molecular weight are physiologically freely filtered by glomeruli to urine chamber and reabsorbed by proximal tubules. Expression of C5aR1 on damaged tubular epithelium, as depicted here under hemolytic conditions, could be locally activated by the excessive amount of C5a, filtered through glomeruli, contributing to nephrotoxicity (37, 38). Systemic FH could thus reduce the formation of systemic C3a and C5a in the circulation, without reaching the interstitium. Another possibility is that FH is coming from the peritubular capillaries, reaching and protecting the tubules locally. This is supported by the decreased tubular staining for FH of the hepatoFH$^{-/-}$ mice despite the identical intrarenal gene expression of *Cfh*. The intact endothelial barrier of peritubular capillaries, though, is likely to be an important limiting factor for access of complement proteins, including FH, to the tubular epithelium. The activation of plasma-derived complement at the basolateral border of tubules of mice in a model of ischemia/reperfusion injury, though, supports the idea of a diffusion of complement proteins from blood to the interstitium (39). Binding of the plasma-derived FH to the tubular cells could protect them from the hemolysis-mediated oxidative stress, by a mechanism, similar to the one described for the retinal pigment epithelial cells (40). This possibility requires further instigation. Nevertheless, our data shows that circulating FH is necessary to protect from acute tubular injury. This conclusion is supported also by the protective effect of the systemic injection of FH in the hepatoFH$^{-/-}$ mice against overexpression of tubular injury markers as well as complement activation in the circulation.

Besides tubular injuries, the glomerular function was particularly difficult to analyze in our model since hemoglobinuria might be a confounding factor for both, proteinuria and hematuria. We found a slight increase of blood in urines of hepatoFH$^{-/-}$ mice treated by PHZ in comparison to PHZ-treated WT mice, but without changes in light microscopy aspect. Thus, our histological results argue that tubular area is more susceptible to hemolysis related-damage than glomeruli, in agreement with previous studies (20, 41, 42). The glomerular cells, including the endothelial ones, produce FH, which likely contributes to the protection and prevents from exacerbated complement activation, even in case of reduced FH levels in plasma.

To find out if the observed protective effect of FH is restricted to the systemic hemolysis-associated AKI found here, and to the ischemia/reperfusion AKI (19, 20), we induced AKI in hepatoFH$^{-/-}$ mice by LPS-mediated sepsis and by cisplatin. LPS activates the AP (43) and triggers TLR-4 in a way similar to heme (9, 44). Therefore, mice injected with LPS showed the same sensitivity in regard to dysregulation of the complement system with aggravated tubular injury in hepatoFH$^{-/-}$. By contrast, while cisplatin-induced tubular injury occurs in a TLR-4-dependent manner (45), it does not activate complement (46) and the AKI here was thus FH-independent. These results account for a context-dependent protection provided by FH. FH is not implicated in all forms of acute tubular necrosis but likely restricted to complement triggering event, such as the ischemic tissue, LPS and heme.

Overall, these results demonstrate the importance of systemic FH for renal protection and raise the possibility of using purified FH or FH-derived molecules as therapeutic agents (22, 47–51) in hemolytic conditions. Indeed, pre-treatment of the hepatoFH$^{-/-}$ mice with FH prevented over-activation of hemolysis-mediated complement and the upregulation of the tubular injury markers.

In summary, this study highlights the specific role of FH to protect against AKI in case of systemic intravascular hemolysis. Liver-produced FH seems to be a key protective factor for tubular cells. Based on our data, we propose the following model. During intravascular hemolysis the activation of the complement cascade occurs systemically and on glomerular endothelium. Liver-derived FH binds to the glomerular EC, injured by heme and other hemolysis-derived products, and prevents formation of the membrane attack complex C5b-9. C3a and C5a are, though, generated locally and filter through the glomerular filtration barrier to reach tubulointerstitium. Hemoglobin dimers and heme also reach tubulointerstitium, activating the tubular cells. The tubular cells overexpress C5aR1 and become responsive to the filtered C5a, aggravating thus the tissue injury. Improvement of our understanding on the kidney protection mediated by FH opens a door for the development of future potential complement therapy for tubular injury in kidney diseases either related to complement dysregulation or intravascular hemolysis.

DATA AVAILABILITY STATEMENT

The original contributions presented in the study are included in the article/**Supplementary Material**, further inquiries can be directed to the corresponding author/s.

ETHICS STATEMENT

Experimental protocols were approved by Charles Darwin ethical committee (Paris, France) and by the French Ministry

of Agriculture (Paris, France) number APAFIS# 3764-201601121739330v3. All the experiments were conducted in accordance with their recommendations for care and use of laboratory animals. Written informed consent was obtained from the owners for the participation of their animals in this study.

AUTHOR CONTRIBUTIONS

LR and NM designed the research. NM, JL, VP, AG, IB, SK, TR-R, and CT performed the research. MP provided HepatoFH$^{-/-}$ mice. LR, NM, JL, AG, VP, and IB analyzed the data. LR, NM, JL, AG, VP, VF-B, SC, and MP discussed the data. LR, NM, JL, and AG wrote the manuscript. All authors contributed to the article and approved the submitted version.

FUNDING

This work was supported by a grant from Agence Nationale de la Recherche (ANR JCJC-INFLACOMP 2015–2018 ANR-15-CE15-0001 to LR and by INSERM. IB received a fellowship from the Société Francophone de Néphrologie Dialyse et Transplantation (SFNDT).

ACKNOWLEDGMENTS

We are grateful for excellent technical assistance from the Centre d'Expérimentations Fonctionnelles team of the Centre de Recherche des Cordeliers and for their support with animal experimentation. We also thank Dr. Gaëlle Brideau and the members of the Plateforme d'Exploration Fonctionnelle Rénale des Cordeliers for the help with the evaluation of the renal function parameters in blood and urine of the mice.

SUPPLEMENTARY MATERIAL

The Supplementary Material for this article can be found online at: https://www.frontiersin.org/articles/10.3389/fimmu.2020.01772/full#supplementary-material

REFERENCES

1. Tracz MJ, Alam J, Nath KA. Physiology and pathophysiology of heme: implications for kidney disease. *J Am Soc Nephrol.* (2007) 18:414–20. doi: 10.1681/ASN.2006080894
2. Van Avondt K, Nur E, Zeerleder S. Mechanisms of haemolysis-induced kidney injury. *Nat Rev Nephrol.* (2019) 15:671–92. doi: 10.1038/s41581-019-0181-0
3. Deuel JW, Schaer CA, Boretti FS, Opitz L, Garcia-Rubio I, Baek JH, et al. Hemoglobinuria-related acute kidney injury is driven by intrarenal oxidative reactions triggering a heme toxicity response. *Cell Death Dis.* (2016) 7:e2064. doi: 10.1038/cddis.2015.392
4. Roumenina LT, Rayes J, Lacroix-Desmazes S, Dimitrov JD. Heme: modulator of plasma systems in hemolytic diseases. *Trends Mol Med.* (2016) 22:200–13. doi: 10.1016/j.molmed.2016.01.004
5. Merle NS, Church SE, Fremeaux-Bacchi V, Roumenina LT. Complement system part i – molecular mechanisms of activation and regulation. *Front Immunol.* (2015) 6:262. doi: 10.3389/fimmu.2015.00262
6. Merle NS, Noe R, Halbwachs-Mecarelli L, Fremeaux-Bacchi V, Roumenina LT. Complement system part II: role in immunity. *Front Immunol.* (2015) 6:257. doi: 10.3389/fimmu.2015.00257
7. Frimat M, Tabarin F, Dimitrov JD, Poitou C, Halbwachs-Mecarelli L, Fremeaux-Bacchi V, et al. Complement activation by heme as a secondary hit for atypical hemolytic uremic syndrome. *Blood.* (2013) 122:282–92. doi: 10.1182/blood-2013-03-489245
8. Merle NS, Grunenwald A, Rajaratnam H, Gnemmi V, Frimat M, Figueres ML, et al. Intravascular hemolysis activates complement via cell-free heme and heme-loaded microvesicles. *JCI Insight.* (2018) 3:e96910. doi: 10.1172/jci.insight.96910
9. Merle NS, Paule R, Leon J, Daugan M, Robe-Rybkine T, Poillerat V, et al. P-selectin drives complement attack on endothelium during intravascular hemolysis in TLR-4/heme-dependent manner. *Proc Natl Acad Sci USA.* (2019) 116:6280–5. doi: 10.1073/pnas.1814797116
10. Vercellotti GM, Dalmasso AP, Schaid TR Jr., Nguyen J, Chen C, Ericson ME, et al. Critical role of C5a in sickle cell disease. *Am J Hematol.* (2019) 94:327–37. doi: 10.1002/ajh.25384
11. Lombardi E, Matte A, Risitano AM, Ricklin D, Lambris JD, De Zanet D, et al. Factor H interferes with the adhesion of sickle red cells to vascular endothelium: a novel disease-modulating molecule. *Haematologica.* (2019) 104:919–28. doi: 10.3324/haematol.2018.198622
12. Frimat M, Boudhabhay I, Roumenina LT. Hemolysis derived products toxicity and endothelium: model of the second hit. *Toxins.* (2019) 11:660. doi: 10.3390/toxins11110660
13. Pawluczkowycz AW, Lindorfer MA, Waitumbi JN, Taylor RP. Hematin promotes complement alternative pathway-mediated deposition of C3 activation fragments on human erythrocytes: potential implications for the pathogenesis of anemia in malaria. *J Immunol.* (2007) 179:5543–52. doi: 10.4049/jimmunol.179.8.5543
14. Bexborn F, Andersson PO, Chen H, Nilsson B, Ekdahl KN. The tick-over theory revisited: formation and regulation of the soluble alternative complement C3 convertase (C3(H2O)Bb). *Mol Immunol.* (2008) 45:2370–9. doi: 10.1016/j.molimm.2007.11.003
15. Elvington M, Liszewski MK, Bertram P, Kulkarni HS, Atkinson JP. A C3(H20) recycling pathway is a component of the intracellular complement system. *J Clin Investig.* (2017) 127:970–81. doi: 10.1172/JCI89412
16. Wu J, Wu Y-Q, Ricklin D, Janssen BJC, Lambris JD, Gros P. Structure of C3b-factor H and implications for host protection by complement regulators. *Nat immunol.* (2009) 10:728–33. doi: 10.1038/ni.1755
17. Perkins SJ, Nan R, Li K, Khan S, Miller A. Complement factor H-ligand interactions: self-association, multivalency and dissociation constants. *Immunobiology.* (2012) 217:281–97. doi: 10.1016/j.imbio.2011.10.003
18. Jokiranta TS, Hellwage J, Koistinen V, Zipfel PF, Meri S. Each of the three binding sites on complement factor H interacts with a distinct site on C3b. *J Biol Chem.* (2000) 275:27657–62. doi: 10.1074/jbc.M002903200
19. Renner B, Ferreira VP, Cortes C, Goldberg R, Ljubanovic D, Pangburn MK, et al. Binding of factor H to tubular epithelial cells limits interstitial complement activation in ischemic injury. *Kidney Int.* (2011) 80:165–73. doi: 10.1038/ki.2011.115
20. Goetz L, Laskowski J, Renner B, Pickering MC, Kulik L, Klawitter J, et al. Complement factor H protects mice from ischemic acute kidney injury but is not critical for controlling complement activation by glomerular IgM. *Eur J Immunol.* (2018) 48:791–802. doi: 10.1002/eji.201747240
21. Vernon KA, Ruseva MM, Cook HT, Botto M, Malik TH, Pickering MC. Partial complement factor H deficiency associates with C3 glomerulopathy and thrombotic microangiopathy. *J Am Soc Nephrol.* (2016) 27:1334–42. doi: 10.1681/ASN.2015030295
22. Fakhouri F, de Jorge EG, Brune F, Azam P, Cook HT, Pickering MC. Treatment with human complement factor H rapidly reverses renal complement deposition in factor H-deficient mice. *Kidney Int.* (2010) 78:279–86. doi: 10.1038/ki.2010.132
23. Merle NS, Grunenwald A, Figueres M-L, Chauvet S, Daugan M, Knockaert S, et al. Characterization of renal injury and inflammation in an experimental model of intravascular hemolysis. *Front Immunol.* (2018) 9:179. doi: 10.3389/fimmu.2018.00179

24. Graw JA, Yu B, Rezoagli E, Warren HS, Buys ES, Bloch DB, et al. Endothelial dysfunction inhibits the ability of haptoglobin to prevent hemoglobin-induced hypertension. *Am J Physiol Heart Circulat Physiol.* (2017) 312:H1120–7. doi: 10.1152/ajpheart.00851.2016
25. Poillerat VG, Thomas, Leon JW, Andreas, Edler M, Torset C, et al. Hemopexin as an inhibitor of hemolysis-induced complement activation. *Front. Immunol.* (2020). doi: 10.3389/fimmu.2020.01684
26. Zaferani A, Vivès RR, van der Pol P, Navis GJ, Daha MR, van Kooten C, et al. Factor h and properdin recognize different epitopes on renal tubular epithelial heparan sulfate. *J Biol Chem.* (2012) 287:31471–81. doi: 10.1074/jbc.M112.380386
27. Sartain SE, Turner NA, Moake JL. Brain microvascular endothelial cells exhibit lower activation of the alternative complement pathway than glomerular microvascular endothelial cells. *J Biol Chem.* (2018) 293:7195–208. doi: 10.1074/jbc.RA118.002639
28. Vastag M, Skopal J, Kramer J, Kolev K, Voko Z, Csonka E, et al. Endothelial cells cultured from human brain microvessels produce complement proteins factor H, factor B, C1 inhibitor, and C4. *Immunobiology.* (1998) 199:5–13. doi: 10.1016/S0171-2985(98)80059-4
29. Chen X, Li L, Liu F, Hoh J, Kapron CM, Liu J. Cadmium induces glomerular endothelial cell-specific expression of complement factor H via the−1635 AP-1 binding site. *J Immunol.* (2019) 202:1210–8. doi: 10.4049/jimmunol.1800081
30. Zoshima T, Hara S, Yamagishi M, Pastan I, Matsusaka T, Kawano M, et al. Possible role of complement factor H in podocytes in clearing glomerular subendothelial immune complex deposits. *Sci Rep.* (2019) 9:7857. doi: 10.1038/s41598-019-44380-3
31. Zhou W, Marsh JE, Sacks SH. Intrarenal synthesis of complement. *Kidney Int.* (2001) 59:1227–35. doi: 10.1046/j.1523-1755.2001.0590041227.x
32. Merle NS, Boudhabhay I, Leon J, Fremeaux-Bacchi V, Roumenina LT. Complement activation during intravascular hemolysis: Implication for sickle cell disease and hemolytic transfusion reactions. *Transfus Clin Biol.* (2019) 26:116–24. doi: 10.1016/j.tracli.2019.02.008
33. Chonat S, Quarmyne MO, Bennett CM, Dean CL, Joiner CH, Fasano RM, et al. Contribution of alternative complement pathway to delayed hemolytic transfusion reaction in sickle cell disease. *Haematologica.* (2018) 103:e483–5. doi: 10.3324/haematol.2018.194670
34. Dumas G, Habibi A, Onimus T, Merle J-C, Razazi K, Mekontso Dessap A, et al. Eculizumab salvage therapy for delayed hemolysis transfusion reaction in sickle cell disease patients. *Blood.* (2016) 127:1062–4. doi: 10.1182/blood-2015-09-669770
35. Dvanajscak Z, Walker PD, Cossey LN, Messias NC, Boils CL, Kuperman MB, et al. Hemolysis-associated hemoglobin cast nephropathy results from a range of clinicopathologic disorders. *Kidney Int.* (2019) 96:1400–7. doi: 10.1016/j.kint.2019.08.026
36. Gaarkeuken H, Siezenga MA, Zuidwijk K, van Kooten C, Rabelink TJ, Daha MR, et al. Complement activation by tubular cells is mediated by properdin binding. *Am J Physiol Renal Physiol.* (2008) 295:F1397–403. doi: 10.1152/ajprenal.90313.2008
37. Yiu WH, Li RX, Wong DWL, Wu HJ, Chan KW, Chan LYY, et al. Complement C5a inhibition moderates lipid metabolism and reduces tubulointerstitial fibrosis in diabetic nephropathy. *Nephrol Dial Transplant.* (2018) 33:1323–32. doi: 10.1093/ndt/gfx336
38. Noris M, Remuzzi G. Terminal complement effectors in atypical hemolytic uremic syndrome: C5a, C5b-9, or a bit of both? *Kidney Int.* (2019) 96:13–5. doi: 10.1016/j.kint.2019.02.038
39. Miao J, Lesher AM, Miwa T, Sato S, Gullipalli D, Song WC. Tissue-specific deletion of Crry from mouse proximal tubular epithelial cells increases susceptibility to renal ischemia-reperfusion injury. *Kidney Int.* (2014) 86:726–37. doi: 10.1038/ki.2014.103
40. Borras C, Canonica J, Jorieux S, Abache T, El Sanharawi M, Klein C, et al. CFH exerts anti-oxidant effects on retinal pigment epithelial cells independently from protecting against membrane attack complex. *Sci Rep.* (2019) 9:13873. doi: 10.1038/s41598-019-50420-9
41. Dennhardt S, Pirschel W, Wissuwa B, Daniel C, Gunzer F, Lindig S, et al. Modeling hemolytic-uremic syndrome: in-depth characterization of distinct murine models reflecting different features of human disease. *Front Immunol.* (2018) 9:1459. doi: 10.3389/fimmu.2018.01459
42. Paixao-Cavalcante D, Hanson S, Botto M, Cook HT, Pickering MC. Factor H facilitates the clearance of GBM bound iC3b by controlling C3 activation in fluid phase. *Mol Immunol.* (2009) 46:1942–50. doi: 10.1016/j.molimm.2009.03.030
43. Stover CM, Luckett JC, Echtenacher B, Dupont A, Figgitt SE, Brown J, et al. Properdin plays a protective role in polymicrobial septic peritonitis. *J Immunol.* (2008) 180:3313–8. doi: 10.4049/jimmunol.180.5.3313
44. Figueiredo RT, Fernandez PL, Mourao-Sa DS, Porto BN, Dutra FF, Alves LS, et al. Characterization of heme as activator of toll-like receptor 4. *J Biol Chem.* (2007) 282:20221–9. doi: 10.1074/jbc.M610737200
45. Zhang B, Ramesh G, Uematsu S, Akira S, Reeves WB. TLR4 signaling mediates inflammation and tissue injury in nephrotoxicity. *J Am Soc Nephrol.* (2008) 19:923–32. doi: 10.1681/ASN.2007090982
46. Zhang L, Fedorov Y, Adams D, Lin F. Identification of complement inhibitory activities of two chemotherapeutic agents using a high-throughput cell imaging-based screening assay. *Mol Immunol.* (2018) 101:86–91. doi: 10.1016/j.molimm.2018.06.009
47. Ricklin D, Mastellos DC, Reis ES, Lambris JD. The renaissance of complement therapeutics. *Nat Rev Nephrol.* (2018) 14:26–47. doi: 10.1038/nrneph.2017.156
48. Nichols EM, Barbour TD, Pappworth IY, Wong EK, Palmer JM, Sheerin NS, et al. An extended mini-complement factor H molecule ameliorates experimental C3 glomerulopathy. *Kidney Int.* (2015) 88:1314–22. doi: 10.1038/ki.2015.233
49. Yang Y, Denton H, Davies OR, Smith-Jackson K, Kerr H, Herbert AP, et al. An engineered complement factor H construct for treatment of C3 glomerulopathy. *J Am Soc Nephrol.* (2018) 29:1649–61. doi: 10.1681/ASN.2017091006
50. Hebecker M, Alba-Dominguez M, Roumenina LT, Reuter S, Hyvarinen S, Dragon-Durey MA, et al. An engineered construct combining complement regulatory and surface-recognition domains represents a minimal-size functional factor H. *J Immunol.* (2013) 191:912–21. doi: 10.4049/jimmunol.1300269
51. Schmidt CQ, Bai H, Lin Z, Risitano AM, Barlow PN, Ricklin D, et al. Rational engineering of a minimized immune inhibitor with unique triple-targeting properties. *J Immunol.* (2013) 190:5712–21. doi: 10.4049/jimmunol.1203548

Conflict of Interest: The authors declare that the research was conducted in the absence of any commercial or financial relationships that could be construed as a potential conflict of interest.

frontiers in Immunology

ORIGINAL RESEARCH
published: 07 August 2020
doi: 10.3389/fimmu.2020.01643

Properdin Pattern Recognition on Proximal Tubular Cells Is Heparan Sulfate/Syndecan-1 but Not C3b Dependent and Can Be Blocked by Tick Protein Salp20

Rosa G. M. Lammerts, Ditmer T. Talsma, Wendy A. Dam, Mohamed R. Daha, Marc A. J. Seelen, Stefan P. Berger and Jacob van den Born on behalf of the COMBAT Consortium*

Department of Internal Medicine, Division of Nephrology, University Medical Center Groningen, University of Groningen, Groningen, Netherlands

OPEN ACCESS

Edited by:
Marcin Okrój, Intercollegiate Faculty of Biotechnology of University of Gdańsk and Medical University of Gdańsk, Poland

Reviewed by:
Lubka T. Roumenina, INSERM U1138 Centre de Recherche des Cordeliers (CRC), France
Viviana P. Ferreira, University of Toledo, United States

***Correspondence:**
Rosa G. M. Lammerts
r.g.m.lammerts@umcg.nl

Specialty section:
This article was submitted to Molecular Innate Immunity, a section of the journal Frontiers in Immunology

Received: *17 April 2020*
Accepted: *19 June 2020*
Published: *07 August 2020*

Citation:
Lammerts RGM, Talsma DT, Dam WA, Daha MR, Seelen MAJ, Berger SP and van den Born J (2020) Properdin Pattern Recognition on Proximal Tubular Cells Is Heparan Sulfate/Syndecan-1 but Not C3b Dependent and Can Be Blocked by Tick Protein Salp20. Front. Immunol. 11:1643. doi: 10.3389/fimmu.2020.01643

Introduction: Proteinuria contributes to progression of renal damage, partly by complement activation on proximal tubular epithelial cells. By pattern recognition, properdin has shown to bind to heparan sulfate proteoglycans on tubular epithelium and can initiate the alternative complement pathway (AP). Properdin however, also binds to C3b(Bb) and properdin binding to tubular cells might be influenced by the presence of C3b(Bb) on tubular cells and/or by variability in properdin proteins *in vitro*. In this study we carefully evaluated the specificity of the properdin – heparan sulfate interaction and whether this interaction could be exploited in order to block alternative complement activation.

Methods: Binding of various properdin preparations to proximal tubular epithelial cells (PTEC) and subsequent AP activation was determined in the presence or absence of C3 inhibitor Compstatin and properdin inhibitor Salp20. Heparan sulfate proteoglycan dependency of the pattern recognition of properdin was evaluated on PTEC knocked down for syndecan-1 by shRNA technology. Solid phase binding assays were used to evaluate the effectivity of heparin(oids) and recombinant Salp20 to block the pattern recognition of properdin.

Results: Binding of serum-derived and recombinant properdin preparations to PTECs could be dose-dependently inhibited ($P < 0.01$) and competed off ($P < 0.01$) by recombinant Salp20 (IC50: ∼125 ng/ml) but not by Compstatin. Subsequent properdin-mediated AP activation on PTECs could be inhibited by Compstatin ($P < 0.01$) and blocked by recombinant Salp20 ($P < 0.05$). Syndecan-1 deficiency in PTECs resulted in a ∼75% reduction of properdin binding ($P = 0.057$). In solid-phase binding assays, properdin binding to C3b could be dose-dependently inhibited by recombinant Salp20> heparin(oid) > C3b.

Discussion: In this study we showed that all properdin preparations recognize heparan sulfate/syndecan-1 on PTECs with and without Compstatin C3 blocking

conditions. In contrast to Compstatin, recombinant Salp20 prevents heparan sulfate pattern recognition by properdin on PTECs. Both complement inhibitors prevented properdin-mediated C3 activation. Binding of properdin to C3b could also be blocked by heparin(oids) and recombinant Salp20. This work indicates that properdin serves as a docking station for AP activation on PTECs and a Salp20 analog or heparinoids may be viable inhibitors in properdin mediated AP activation.

Keywords: complement, properdin, C3, Salp20, syndecan-1

INTRODUCTION

Proteinuria is caused by the passage of proteins through the damaged glomerular filtration barrier and is an independent prognostic factor for the progression of chronic renal failure to end stage renal disease (1). Several mechanisms have been postulated on how proteinuria causes renal damage, one of them being via tubular complement activation. Evidence for involvement of the complement system in renal damage was already shown in 1985 by the finding of C3 deposits on the proximal tubular epithelial cells (PTECs) of nephrotic patients (2). Ultrafiltration of complement factors under proteinuric conditions may lead to alternative pathway activation within the renal tubules. This may be explained by the absence of a number of complement regulatory proteins on the apical membrane including decay accelerating factor (DAF), complement receptor 1 (CR1), and membrane cofactor protein (MCP) (3, 4) Complement regulatory protein CD59 is present on the brush border of proximal tubules, albeit weakly expressed (4). As a result, failure to downregulate the complement cascade might lead to tubular epithelial damage under proteinuric conditions.

The complement system consists of three pathways; the lectin pathway (LP), classical pathway (CP) and alternative pathway (AP). The LP and CP are initiated by pattern recognition molecules (e.g., MBL and C1q), whereas the current conception of the AP is thought to be a purely auto-activating route, via the spontaneous or induced formation of fluid-phase AP C3 convertase (5, 6). The three pathways merge at the formation of a C3 convertase, the major enzymes of the cascade (7, 8). For the CP and LP this is the C4bC2a complex, whilst in the AP the C3bBb complex is formed. The C3bBb complex is relatively unstable in plasma and requires stabilization by properdin, the only known positive regulator of the complement system (9). Properdin consists of seven thrombospondin repeat domains TSR0-TSR6 beginning at the N-terminus (10). However, understanding the complex biology of properdin has proven to be difficult due to the different sources of properdin used in biochemical studies and also its intricate self-associations. Through head-to-tail interactions of monomeric subunits, properdin can form cyclic dimers, trimers and tetramers under physiological conditions (11, 12). Additionally, non-physiological high molecular weight polymers can also form during long term storage and freeze/thaw cycles (12, 13). Moreover, stored properdin in the granules of neutrophils, which is released upon cell stimulation, may be structurally different than serum properdin either in its multimeric structure or in its posttranslational modifications (14, 15).

In the AP auto-activating theory it was thought that stabilizing the C3bBb complex was the only function of properdin. However, in the past decade data has accumulated stating that properdin can act as a pattern recognition molecule on PTECs, apoptotic, necrotic and bacterial cells (9). As ligands for properdin DNA and glycosaminoglycans have been proposed (16, 17). However, this theory was questioned by Harboe et al. since they showed that properdin binding to granulocyte MPO, endothelial cells and *Neisseria Meningitidis* is completely dependent on initial C3b binding, raising doubt on the conclusions of formerly published work (18). Their conclusion was based on properdin binding experiments in the presence or absence of Compstatin (18), a circular peptide inhibiting the cleavage of C3 into C3a and C3b. On the other hand, studies by the group of Van Kooten et al. in mice demonstrated that properdin can be found in glomeruli of C3 knockout mice during anti glomerular basement membrane disease indicating that C3 is not essential for properdin binding to tissues (19).

In proteinuric patients, AP activation has been linked to the presence of properdin on the PTEC brush border and *in vitro* binding of properdin and subsequent complement activation on HK-2 cells has also been shown. However, this is not the case for endothelial cells (20). In addition, urinary properdin excretion is associated with renal complement activation and worsening renal function (21, 22). More recently, our group showed that the binding of properdin to HK-2 cells is dependent on heparan sulfates (HS), since pretreatment of the cells with heparitinase abolished the binding of properdin (23). Moreover, competition experiments with heparin and non-anticoagulant heparinoids could reduce the binding of properdin to HK-2 cells, showing the treatment potential of heparinoids in AP mediated proteinuric damage (24). Co-localization of properdin with syndecan-1 on PTECs in an adriamycin induced nephropathy model suggested a role for the heparan sulfated proteoglycan (HSPG) syndecan-1 in the tubular binding of properdin (23). Syndecan-1 is a major membrane spanning HSPG in epithelial cells and has been shown to be upregulated on tubular epithelium in renal disease (25). Our group has previously shown that syndecan-1 expression on tubular epithelium correlates with activation of renal repair mechanisms (26), and that syndecan-1 deficiency in human tubular epithelial cells leads to reduced proliferation (25). However, a direct role for syndecan-1 in complement activation has never been described.

Although the AP has been shown to play a role in numerous diseases, no specific inhibitor for the AP is yet available. Salp20 is a protein derived from the deer tick Ixodes scapulari and has been shown to inhibit the AP via the displacement of properdin from the alternative pathway C3 convertase. This causes an accelerated decay of the C3bBb complex and subsequent inhibition of the AP by up to 70% (27, 28). *In vivo*, treatment with Salp20 in mice showed a reduction of AP mediated damage in ovalbumine-induced asthma, elastase-induced abdominal aortic aneurysm and after intraperitoneal injections with LPS (29). However, to the best of our knowledge, no experiments have been performed which assess the inhibition of the pattern recognition of properdin using Salp20. Therefore, in this study we investigated the interactions of properdin with PTECs, followed by AP activation and the inhibitory effects of Compstatin, Salp20 and heparinoids. To investigate the binding capacity of properdin from different sources and subsequent AP activation, experiments were performed with either normal human serum as a source of properdin, biochemically purified properdin and recombinant full length properdin.

METHODS

HK-2 Cells

The immortalized human kidney proximal tubular epithelial cell line HK-2 was obtained from ATCC (Manassas VA, USA). Cells were cultured in DMEM/F12 medium 1:1 (Invitrogen, Carlsbad, CA, USA), supplemented with 5 μg/ml insulin, 5 μg/ml transferrin, 5 μg/ml selenium, 36 ng/ml hydrocortisone, 10 ng/ml epidermal growth factor (All purchased from Sigma, Zwijndrecht, The Netherlands), and 50 U/ml penicillin, 50 μg/ml streptomycin and 25 mM Hepes (All purchased from Invitrogen, Carlsbad, CA, USA).

Syndecan-1 Knockout Cell Line

Production of the syndecan-1 knockout HK-2 cell line by shRNA technology has been described before (25, 30, 31). To confirm syndecan-1 knockdown and to evaluate the binding of properdin to wild type HK-2 cells or syndecan-1 knockout HK-2 cells, syndecan-1 expression and properdin binding on wild-type and syndecan-1 deficient HK-2 was determined by flow cytometry. Cells were plated in 6-wells cell culture plates at 37°C and were detached using cell dissociation solution (C5789, Sigma®, Zwijndrecht, The Netherlands), 900 μL/well at 37°C until cells were detached. Cells were collected in 4.5 mL tubes containing 2 mL cell medium, centrifuged at 300 × g for 5 min at 4°C and washed with ice-cold phosphate-buffered saline (PBS)/1% bovine serum albumin (BSA) (FACS buffer) (Sigma®, Zwijndrecht, The Netherlands). Cells were subsequently incubated with Alexa Fluor®647 mouse anti-human anti-syndecan-1 (CD138; Bio-Rad/AbD Serotec, California, USA) antibody in FACS buffer on ice, or purified properdin (human factor P, Millipore, Cat 341283-250 1.1mg/mL) followed by rabbit anti-human properdin, prepared as described before (20), and goat anti-rabbit FITC (Southern Biotech, Birmingham, USA) in FACS buffer on ice in the dark. After washing, cells were resuspended in 300 μL of FACS buffer and analyzed in a FACSCalibur™ (FACSCalibur, Becton Dickinson, New Jersey, USA). The purified properdin used was stored at −80°C and thawed only once for the experiments. Non-relevant mouse IgG served as an isotype control. Experiments were independently repeated 4 times. The percentage reduction was calculated as reduction in % = 100–[(MFI KO × 100)/MFI wild type].

Binding of Properdin to HK-2, Alternative Pathway Complement Activation and Inhibition by Compstatin

Properdin binding to the immortalized human kidney proximal epithelial cell line HK-2 was tested using properdin from various sources. Normal human serum (NHS) from a healthy volunteer with normal classical, alternative and lectin pathway activity, as detected by functional ELISA and determined before, was used as a serum properdin source (32). Concentrations of 5, 20, and 50% NHS diluted in DMEM/F12 culture medium were tested. Also purified properdin (human factor P, Millipore, Cat 341283-250 1.1 mg/mL) and recombinant full length properdin, produced in HEK E+ cells resulting in the same N-linked glycanation as plasma properdin, were used. Recombinant properdin had the physiological 1:2:1 ratio and did not contain non-physiological aggregates after purification. The recombinant properdin was aliquoted and stored at −80°C and thawed only once for the experiments (33).

Confluent HK-2 were cultured on a 6-well tissue culture plate and incubated for 36–48 h with 10 μg/ml Compstatin that was not exposed to freeze-thaw cycles before (a kind gift from professor J. D. Lambris, University of Pensylvania, Philadelphia, PA, United States) to prevent eventual C3b deposition. Cells were detached using cell dissociation solution (C5789, Sigma®, Zwijndrecht, The Netherlands), 900 μl/1mL at 37°C, collected in 4.5 mL tubes containing 2 mL cell medium and centrifuged twice at 250 g for 6 min at 20°C. For Compstatin mediated inhibition assays, cells were incubated with heat inactivated NHS in a serial dilution of 5, 20, or 50% NHS, purified properdin or recombinant properdin in the presence or absence of 10 μg/ml Compstatin for 30 min at 37°C. Hereafter, cells were centrifuged for 6 min at 250 g at 20°C. To detect bound properdin, cells were incubated with rabbit anti-human properdin (20), followed by goat anti-rabbit FITC (Southern Biotech, Birmingham, USA) in FACS buffer on ice in the dark.

To explore alternative pathway complement activation the same procedure as described above was followed. Subsequent to the incubation of properdin from NHS, purified properdin or recombinant properdin, cells were washed twice at 250 g without a break for 6 min at 20°C and were incubated in the presence or absence of 5% serum as a complement source for 45 min at 37°C. After incubation, cells were washed once with 2 mL 20°C FACS buffer at 250 g for 6 min at 4°C and once with 2 mL 4°C FACS buffer at 250 g without a break for 6 min at 4°C.

To detect activated C3, cells were incubated with mouse anti-human activated C3 recognizing C3b, iC3b, and C3c fragments (Clone bH6, HM2168S, Hycult biotech, Uden, The Netherlands) for 30 min on ice. Cells were washed twice with ice cold FACS buffer, centrifuged at 250 g for 6 min at 4°C, and incubated

goat anti-mouse FITC (Purchased from Southern Biotech, Birmingham, USA) for 30 min on ice in the dark. Propidium iodide 1 μg/ml (Molecular Probes, Leiden, The Netherlands) was added just before measuring to be able to exclude apoptotic and necrotic cells. Properdin binding and activated C3 deposition on viable non-apoptotic cells were analyzed in a FACSCalibur™ (FACSCalibur, Becton Dickinson, New Jersey, USA). Results are from six independent experiments.

Inhibition of Binding of Properdin to C3b

Competition ELISA was used to evaluate whether heparin-albumin (200 kDa), unfractionated heparin (15–18 kDa), low molecular weight (LMW)-heparin (4.5 kDa), C3b (185 kDa), and recombinant Salp20 (48 kDa) inhibit the binding of properdin to immobilized C3b. Heparin-albumin was from Sigma-Aldrich (Saint Louis, MO, USA). According to the data sheet, this artificial proteoglycan contained 4.8 moles heparin per mole albumin, with a protein content of 55%. Maxisorp 96-well flat bottom microtiter plates (U96 from Nunc International, Amsterdam, The Netherlands) were coated overnight with 1 μg/ml C3b in PBS at 4°C. C3b was purified as described before (34). After washing in PBS, wells were blocked with 1% BSA in PBS for 1 h at 37°C. A concentration range of heparin-albumin, unfractionated heparin, LMW-heparin, C3b or recombinant Salp20 was pre-incubated with 62.5 ng/ml properdin (Millipore, Billerica, Massachusetts, USA) in PBS, 0.05% Tween and 1% BSA for 15 min at room temperature. Thereafter the co-incubated heparin-albumin, unfractionated heparin, LMW-heparin, C3b and recombinant Salp20, together with properdin, was incubated on the C3b coated plate for 1 h at 37°C. Binding of properdin was detected with biotinylated rabbit anti-human properdin 1:3,000 diluted in PBS, 0.05% Tween and 1% BSA. After washing, streptavidin HRP (DAKO, Glostrup, Denmark) 1:5,000 was added to the plate and incubated for 1 h. Substrate reaction was performed with 3.3',5.5'-tetramethylbenzidine substrate (Sigma, Zwijndrecht, The Netherlands) for 15 min in the dark, and the reaction was stopped by adding 1.5 N H_2SO_4. Absorbance was measured at 450 nm in a microplate reader. All incubations were carried out in a volume of 100 μl/well. The experiment was independently repeated 3 times.

Dose Dependent Block and Dose Dependent Competition of Properdin Binding to HK-2 by Recombinant Salp20

To evaluate whether recombinant Salp20 can inhibit the binding of properdin to the immortalized human kidney proximal epithelial cell line HK-2, cells were cultured in 6-well tissue culture plates. Cells were detached with cell dissociation solution as described previously, transferred into a 5 mL FACS tube with medium and centrifuged at 200 g for 7 min at 20°C. After washing, cells were incubated with a serial dilution of recombinant Salp20 of 0, 125, 250, 500, 1,000, or 8,000 ng/mL recombinant Salp20 together with 10 μg/mL purified properdin for 30 min at 37°C.

To evaluate whether recombinant Salp20 can dose-dependently compete off bound properdin and the activation of C3 and C5b-9 on HK-2, cells were also cultured in a 6-well tissue culture plates. Cells were detached with cell dissociation solution as described before, transferred into a 5 mL FACS tube with medium and centrifuged at 200 g for 7 min at 20°C. Cells were incubated with or without 10 μg/mL purified properdin (human factor P, Millipore, Cat 341283-250 1,1 mg/mL) for 30 min at 37°C. Cells were washed twice at 200 g for 7 min at 20°C and incubated with a serial dilution of pre-incubated recombinant Salp20 of 0, 32, 125, and 500 ng/mL together with 5% NHS for 1 h at 37°C.

To detect bound properdin, activated C3 or neoantigen C9 (as a measure of C5b-9 formation), cells were incubated with either rabbit anti-human properdin, mouse anti-human activated C3 (Clone bH6, HM2168S, Hycult biotech, Uden, The Netherlands), or with mouse anti-human neoantigen C9 (Clone WU13-15, HM2264, Hycult biotech, Uden, The Netherlands), for 30 min on ice. Cells were washed with ice cold FACS buffer, centrifuged at 250 g for 6 min at 4°C, and incubated with goat anti-rabbit FITC or goat anti-mouse FITC (both purchased from Southern Biotech, Birmingham, USA) for 30 min on ice in the dark. Propidium iodide 1 μg/ml (Molecular Probes, Leiden, The Netherlands) was added just prior to measurement in order to exclude apoptotic cells. Properdin binding and activated C3 deposition on non-apoptotic cells were analyzed in a FACSCalibur™ (FACSCalibur, Becton Dickinson, New Jersey, USA). Experiments were repeated independently two times. The percentage effect was calculated based on the control data (0 ng/mL Salp20 + 10 μg/mL purified properdin) in median fluorescence intensity (MFI), % inhibition = 100–(MFI test result/MFI control) × 100.

Statistics

GraphPad Prism version 7.02 was used for statistical analyses. Data was examined by one-way ANOVA and the Mann-Whitney-U test and the Wilcoxon rank sum test were used as appropriate for the different experiments. A P-value <0.05 was considered statistically significant.

RESULTS

Properdin From Various Sources Binds With PTECs *in vitro* and Functions as a Docking Station for Alternative Pathway Complement Activation

Properdin binding to PTECs using properdin present in normal human serum, purified properdin and recombinant properdin was tested to investigate differences in properdin binding and complement activation between different preparations. Incubation for 30 min with 50% normal human serum (NHS), purified properdin and recombinant properdin, resulted in substantial binding of properdin detected by flow cytometry. Untreated samples served as a control. Means in median fluorescence intensity (MFI) were 35, 158, 68, and 7, respectively. Binding of all preparations was statistically different ($P = 0.02$, $P = 0.005$, $P = 0.049$, respectively) when compared as fold change (fold change = MFI treated cells/MFI untreated cells)

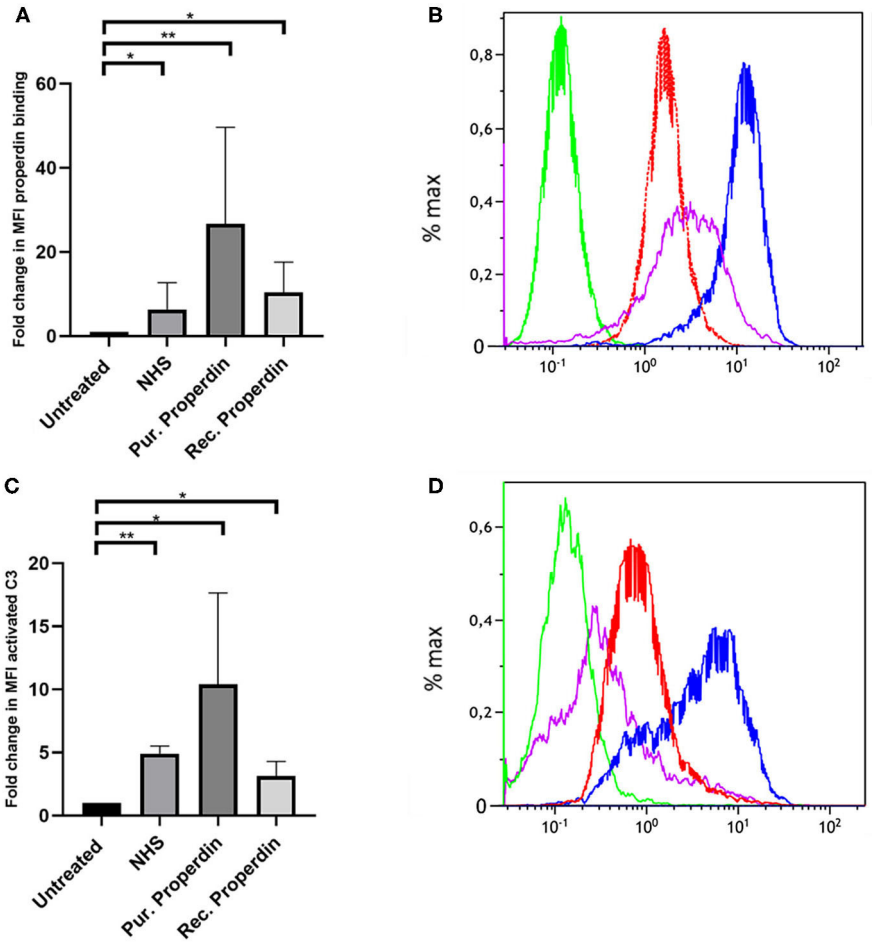

FIGURE 1 | Properdin from various sources bind with PTEC *in vitro* and functions as docking station for alternative pathway complement activation. **(A)** Properdin present in 50% normal human serum (NHS), purified properdin and recombinant properdin show binding with PTEC in comparison to the negative control. Data presented as fold change compared to the untreated control and analyzed by the Wilcoxon trank sum test (*$P < 0.05$, **$P < 0.01$). Asterisks above the capped lines denote significant differences between the untreated samples and the properdin binding from different sources ($n = 10$). **(B)** Representative flow cytometry experiment for properdin binding from 50% NHS (red line), purified properdin (blue line) and recombinant properdin (purple line) in comparison the untreated sample (green line). Data represented as % max (data normalized for the peak at 100%). **(C)** Complement C3 activation via properdin from NHS, purified properdin and recombinant properdin shows complement activation via the alternative pathway. Data presented as fold change compared to the untreated control and analyzed as described in **(A)** ($n = 6$). **(D)** Representative flow cytometry experiment for complement C3 activation via NHS (red line), purified properdin (blue line), recombinant properdin (purple line) and the untreated sample (green line).

to the untreated control. No statistically significant differences were found between recombinant properdin vs. either purified properdin or NHS ($P = 0.24$ and $P = 0.11$). A significant difference was found between 50% NHS vs. purified properdin ($P = 0.049$) (**Figures 1A,B**). In the presence of NHS as a complement source, deposition of activated C3 followed the same pattern (**Figures 1C,D**). Means in MFI were 31, 72, 16, and 6 for NHS, purified properdin, recombinant properdin and the untreated sample, respectively. Activated C3 deposition were statistically different ($P = 0.005$, $P = 0.01$, $P = 0.01$, respectively) when compared as fold change (fold change = MFI treated cells/MFI untreated cells) to the untreated control for all preparations. No statistically significant differences were found for activated C3 deposition between purified properdin vs. recombinant properdin ($P = 0.07$), NHS vs. recombinant properdin ($P = 0.06$) or NHS vs. purified properdin ($P = 0.17$). As properdin may serve as the docking station for AP complement activation and to unravel the role of properdin in C3 activation on PTEC, we decided to further investigate complement activation on PTEC with and without C3 inhibitor Compstatin.

AP Activation but Not Properdin Binding to PTECs Can Be Inhibited by Compstatin

HK-2 cells were incubated with Normal Human Serum (NHS) as a source of properdin in increasing concentrations of 5, 20, and 50%. Binding of properdin from serum to HK-2 was not affected by pre-incubation and co-incubation with the C3 inhibitor Compstatin, demonstrating that properdin binding with HK-2 cells is independent of the presence of C3b (5% NHS; $P =$

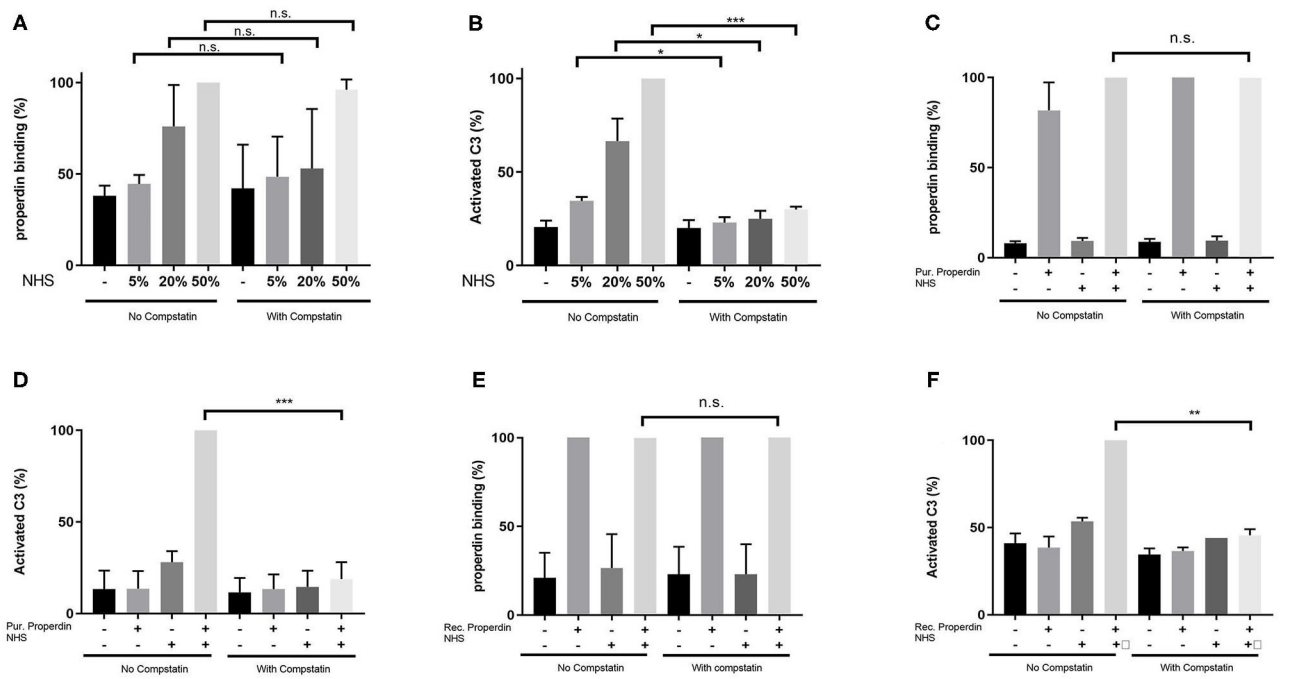

FIGURE 2 | Properdin binding with PTECs *in vitro* is not mediated via C3b. **(A)** Properdin binding from serum is not influenced by co-incubation with compstatin. Bars represent a serial dilution of 5, 20, and 50% NHS. **(B)** C3 complement activation mediated by properdin from serum is completely inhibited by compstatin. **(C)** Properdin binding purified from plasma is not influenced by compstatin. **(D)** C3 complement activation by purified properdin is completely inhibited by compstatin. **(E)** Recombinant properdin binding is not influenced by compstatin. **(F)** C3 complement activation by recombinant properdin is inhibited by compstatin. All graphs are normalized by the sample without compstatin but with NHS **(A,B)** or purified properdin with NHS **(C,D)** or recombinant properdin with NHS **(E,F)**. Data were analyzed by the Mann-Whitney U test with an option of multiple comparison (*$P < 0.05$, **$P < 0.01$, ***$P < 0.001$). Asterisks above the capped lines denote significant differences between the sample without Compstatin but with NHS **(A,B)** or purified properdin with NHS **(C,D)** or recombinant properdin with NHS **(E,F)** and the same sample with Compstatin. $N = 6$ for all experiments.

0.82, 20% NHS; $P = 0.49$ and 50% NHS; $P = 0.42$) (**Figure 2A**). Measurement of activated C3 deposition on HK-2 cells after incubation with NHS confirmed the functionality of Compstatin, since no increase in activated C3 deposition was seen during co-incubation with Compstatin (5% NHS; $P = 0.04$, 20% NHS; $P = 0.04$ and 50% NHS; $P = 0.0002$) (**Figure 2B**). This implies that properdin might act as a pattern recognition molecule on PTECs.

Similarly, when purified properdin or recombinant properdin was used as a source of properdin, pre-incubation and co-incubation of properdin with Compstatin did not affect the binding of properdin on HK-2 cells, further strengthening the finding that properdin binding to PTECs is independent of prior C3b deposition ($P = 0.23$ and $P = 0.50$, respectively) (**Figures 2C,E**). Co-incubation of serum with Compstatin after incubation of HK-2 cells with purified properdin or recombinant properdin resulted in the inhibition of activated C3 deposition, verifying the C3 inhibitory potential of Compstatin ($P < 0.0001$ and $P = 0.002$ respectively) (**Figures 2D,F**). In order to confirm the absence of C3 components (including C3b) on the PTEC cell surface to which properdin in NHS can bind, PTEC were stained for activated C3 (recognizing the cleavage fragments of C3b, iC3b, and C3c) before and after NHS treatment with and without pre-incubation with Compstatin (**Supplementary Figure 1**). C3 components were not detectable on untreated PTEC when compared to the background staining ($P = 0.48$). In conclusion, flow cytometry showed that properdin binds to HK-2 cells independent of C3b and regardless of properdin source.

Binding of Properdin to Proximal Tubular Epithelial Cells Is Partly Mediated by Syndecan-1

In former studies it was shown that heparitinase I treatment of HK-2 cells obliterated properdin binding, while immunofluorescent staining showed co-localization of properdin with syndecan-1 *in vivo* on tubular epithelium under nephrotic conditions (23). To identify the binding site of properdin on tubular cells, we tested properdin binding capacities of syndecan-1 silenced cells by short hairpin RNA technology. Stably transfected HK-2 *Synd1*$^{-/-}$ cells showed ∼80% reduction in syndecan-1 expression (**Figure 3A**). The HK-2 *Synd-1*$^{-/-}$ cells show a ∼70% reduced properdin binding potential compared to HK-2 WT cells($P = 0.057$) (**Figures 3B,C**).

AP Activation and Properdin Binding to PTECs Can Be Inhibited by Recombinant Salp20

It has been described that Salp20 (a deer tick protein) functions as a properdin-blocking agent, displacing properdin from the C3-convertase (27). To evaluate whether Salp20 inhibits the

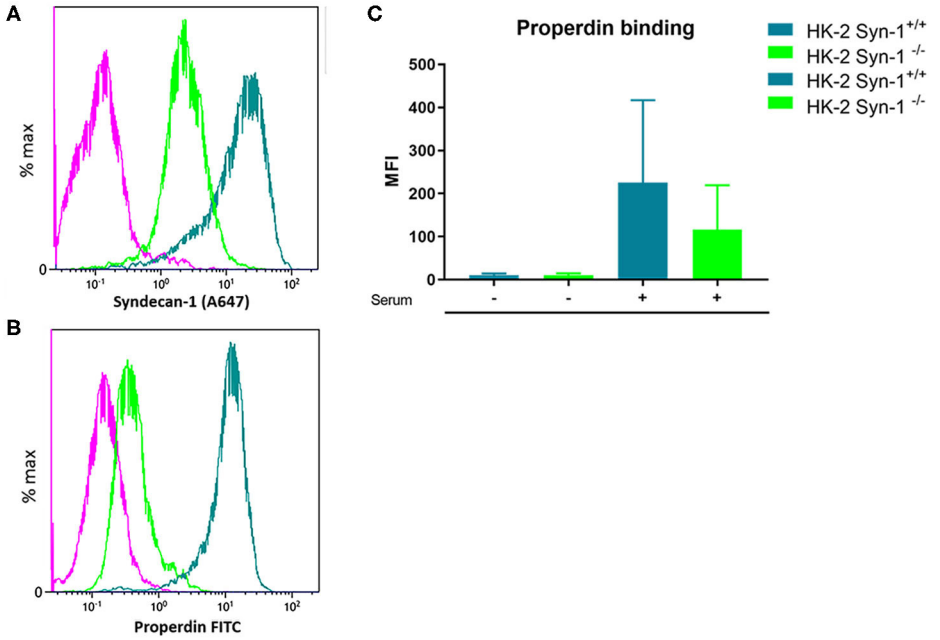

FIGURE 3 | Properdin binding with PTEC *in vitro* is largely via syndecan-1 associated heparan sulfate. **(A)** A representative experiment showing high expression of syndecan-1 in PTEC wild type (turquoise) and >80% less expression of syndecan-1 in syndecan-1 KO PTEC (Green). **(B)** A representative experiment showing strong properdin binding to PTEC wilde type (turquoise) and ∼75% less properdin binding to syndecan-1 KO PTEC (Green). The purple color represents the antibody binding of the isotype control. X-axis is a logarithmic scale, MFI noted in the figure. Data represented as % max (data normalized for the peak at 100%). **(C)** Syndecan-1 deficient cells show a reduction in properdin binding compared to HK-2 WT cells the difference was borderline significant ($n = 4$, $P = 0.057$). Data is expressed as mean ± SEM.

binding of properdin to HSPGs, resulting in inhibition of properdin's pattern recognition capacity of HSPGs, we co-incubated recombinant Salp20 with properdin in absence of activated C3 and measured the binding of properdin to heparin-albumin. Increasing concentrations of recombinant Salp20 showed dose dependent inhibition of properdin to heparin-albumin with an IC50 of 18 ng/ml (**Figure 4A**). Thus, showing that Salp20 indeed inhibited the binding of properdin to an HSPG analog, abolishing pattern recognition of HSPGs by properdin.

Recombinant Salp20 was also tested for properdin binding and AP inhibitory potential on HK-2 cells by flow cytometry. Incubation of 10 μg/mL purified properdin, in the absence of activated C3 conditions, led to properdin deposition on the HK-2 cells, while recombinant Salp20 led to a dose dependent reduction in binding of purified properdin to the cells (**Figures 4B,C**). An inhibitory effect of 70% was achieved when incubating the cells with 500 ng/ml recombinant Salp20 ($P = 0.01$) and an inhibitory effect of 98% ($P = 0.0003$) when incubating the cells with >1,000 ng/ml recombinant Salp20 (**Figure 4C**).

The dose dependent capacity of recombinant Salp20 to displace cell-bound properdin was also tested by flow cytometry. After pre-incubation with purified properdin, HK-2 cells were incubated with an increasing concentration of up to 500 ng/ml of Salp20 and NHS. Recombinant Salp20 dose-dependently displaced bound properdin with an inhibitory effect of 90% with 500 ng/ml Salp20 ($P = 0.003$) (**Figure 5A**). Recombinant Salp20 was also effective in the inhibition of AP activation, shown by dose-dependent reduction of activated C3 and C5b-9 deposition. Concentration dependent reduction of activated C3 and C5b-9 deposition by recombinant Salp20, showed a similar pattern compared to properdin binding (**Figures 5B,C**). The maximum concentration of recombinant Salp20, 500 ng/ml, resulted in an inhibition of 80% in activated C3 deposition ($P = 0.02$) and 90% in C5b-9 deposition ($P = 0.006$) compared to the non-inhibited control.

Inhibition of Properdin to C3b by Heparins, C3b and Recombinant Salp20

In the experiments described up to now we evaluated the properdin – syndecan-1/HS interaction as a focus point for intervention. In a last series of experiments, we evaluated the properdin-C3b interaction as a target point. Thus, we set out a series of competition experiments using the potential dose-dependent inhibitory activity of heparins, C3b or recombinant Salp20 on properdin binding to immobilized C3b. The results of the binding assay showed that heparin-albumin, unfractionated heparin, C3b and recombinant Salp20 inhibit properdin binding to C3b in a dose-dependent manner. (IC50 8.6 ng/mL for heparin-albumin, 63.4 ng/mL for unfractionated heparin, >1,000 ng/mL for LMW-heparin, 6,484 ng/mL for C3b and 33.5 ng/mL for recombinant Salp20). Also, the inhibitory capacity depends on the size of the heparin products (IC50

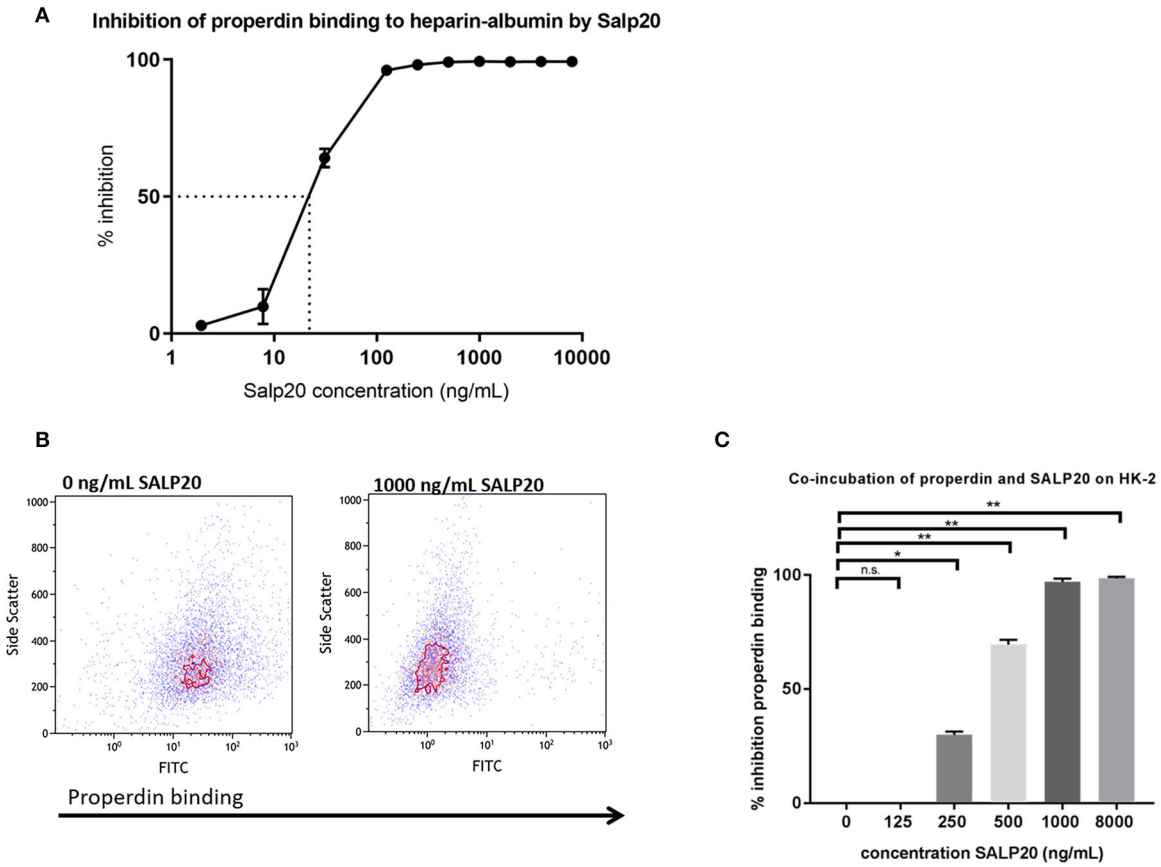

FIGURE 4 | Properdin binding to heparin-albumin in ELISA and to HK-2 cells can be dose-dependently blocked by recombinant Salp20. **(A)** Pre-incubation of properdin with Salp20 dose-dependently reduced properdin binding to immobilized heparin-albumin. Dotted line in figure *A* represents the IC50. Experiments were independently repeated in duplicate. **(B)** A representative flow cytometry experiment shows that properdin co-incubation with 1,000 ng Salp20 reduces properdin binding to HK-2 in comparison to properdin incubation with HK-2 without SALP20. **(C)** Quantitative analysis of multiple experiments ($n = 3$) shows that recombinant Salp20 significantly blocks the binding of properdin to HK-2 per dose. Data were analyzed by Mann-Whitney U test with an option of multiple comparison (*$P < 0.05$, **$P < 0.01$). Asterisks above the capped lines denote significant differences between the untreated samples and the recombinant Salp20 inhibition with different concentrations.

0.000043 nmol/mL for heparin-albumin, 0.004 nmol/mL for unfractionated heparin, >22.2 nmol/mL for LMW-heparin). Heparin has a lower IC50 compared to C3b (IC50 0.004 nmol/mL vs. IC50 0.035 nmol/mL). Recombinant Salp20 has a lower IC50 compared to heparin (IC50 0.0007 nmol/mL vs. IC50 0.004 nmol/mL, respectively) (**Table 1**). These data show that unfractionated heparin and recombinant Salp20 not only compete for properdin binding with heparan sulfates, but also for properdin binding with C3b.

DISCUSSION

In this study we provide evidence that properdin functions as a pattern recognition protein on PTECs where the binding is largely mediated via syndecan-1 associated heparan sulfate and is C3b-independent. Furthermore, we show that the tick protein Salp20 effectively blocks the heparan sulfate mediated pattern recognition by properdin, pointing toward the potential for therapeutic interventions at the tubular level in proteinuric conditions.

It has long been assumed that properdin, next to its stabilizing role of the alternative C3 convertase, could act as a pattern recognition molecule. We have shown previously that during proteinuria, properdin recognizes and binds to heparan sulfate proteoglycans (HSPG) on tubular epithelial cells (23). Our results in this study using the C3 inhibitor Compstatin, show that Compstatin can inhibit complement activation and therefore C3b deposition, but cannot preclude the deposition of properdin on PTECs. We display that this finding does not materially differ between properdin sources, including recombinant properdin. The latter confirms that our finding is robust, since different properdin isolates might differ in purity, conformation, multimerization, post-translational modifications, and the eventual presence of other co-purified or properdin-bound proteins. However, properdin in purified preparations is prone to aggregation which can be avoided to a certain extend by storage at 4°C for up to 2

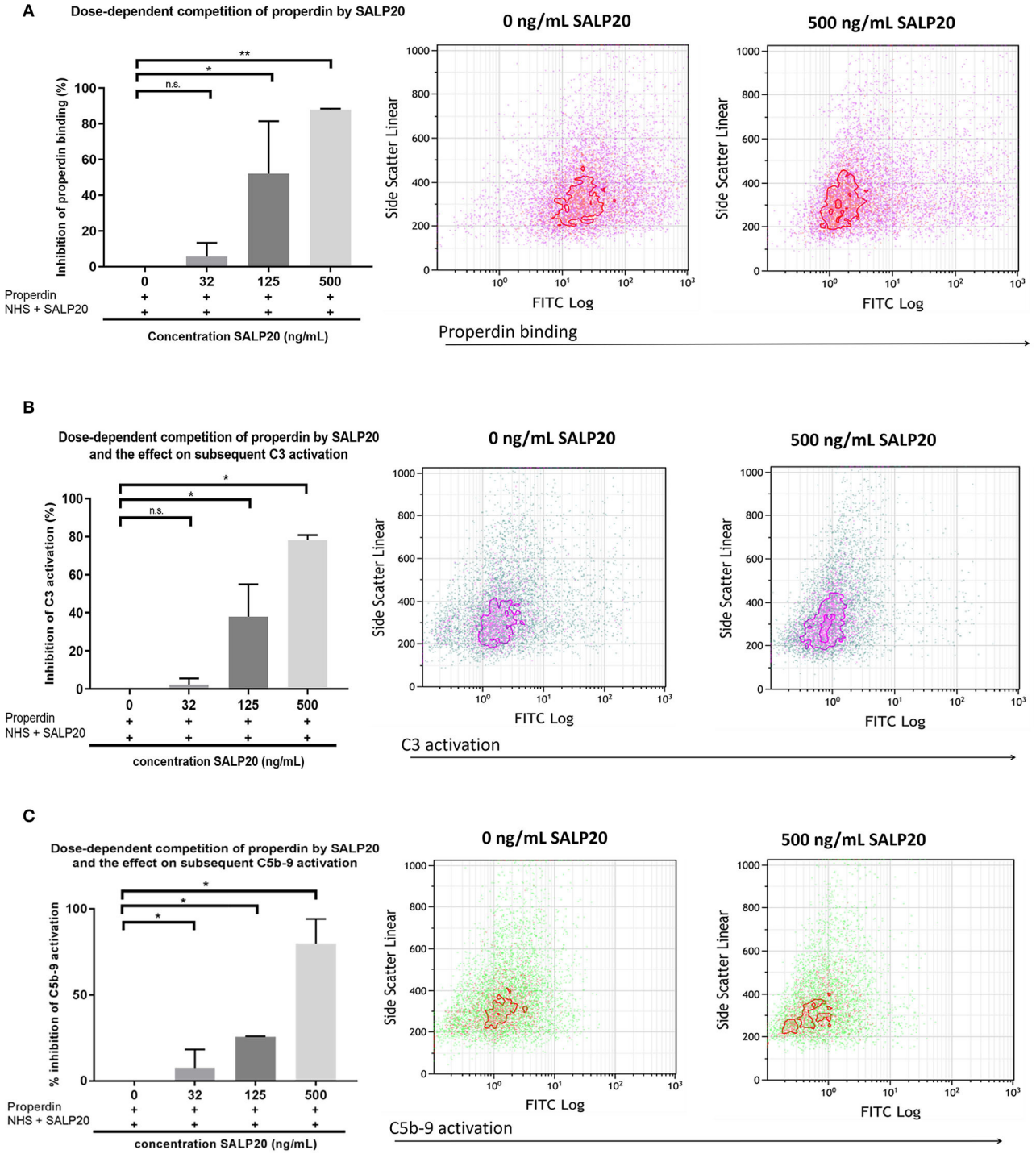

FIGURE 5 | Recombinant Salp20 dose-dependently competes with HK-2 bound properdin, thereby preventing AP complement activation. **(A)** PTECs were incubated with purified properdin followed by incubation with NHS and increasing concentrations of Salp20. Bars show quantitative analysis of multiple experiments ($n = 2$). Density plots of a representative experiment show the shift in PTEC-bound properdin in the presence of 500 ng/ml Salp20. **(B)** C3 activation can be dose dependently inhibited by recSALP20. The same experimental set up as in **(A)**, but now C3 activation was detected. **(C)** C5b-9 activation can be dose dependently inhibited by Salp20. The same experimental set up as in **(A,B)**, but now C5b-9 activation was detected. Data were analyzed by Mann-Whitney U test with an option of multiple comparison (*$P < 0.05$, **$P < 0.01$). Asterisks above the capped lines denote significant differences between the untreated samples and the recombinant Salp20 inhibition with different concentrations.

TABLE 1 | Inhibition of properdin binding to C3b; IC_{50}, Concentration causing 50% properdin binding inhibition expressed in ng/mL and nmol/mL.

Coating	Inhibitor	IC50 ng/mL	IC50 nmol/mL
C3b	Heparin-albumin	8.6 ng/mL	0.000043 nmol/mL
	Unfractionated heparin	63.4 ng/mL	0.004 nmol/mL
	LMW-heparin	>1,000 ng/mL	>22.2 nmol/mL
	C3b	6,484 ng/mL	0.035 nmol/mL
	Salp20	33.5 ng/mL	0.0007 nmol/mL

IC_{50} was calculated by non-linear regression with curve fitting in GraphPad Prism.

weeks without any additional freeze/thaw cycles (12, 35). Our properdin preparations were exposed to one freeze/thaw cycle and our preparations could therefore contain non-physiological aggregates. However, since unpurified properdin present in serum essentially showed the same binding to PTECs as purified and recombinant properdin, it is unlikely that properdin aggregates importantly contributed to our findings. Therefore, irrespective of the source, all experiments indicate a real C3b-independent binding of properdin to heparan sulfates (HS), most likely present on the PTEC cell membrane as the polysaccharide side chains of syndecan-1. These findings are in agreement with experimental studies in C3 knockout mice demonstrating C3 deposition in glomeruli of mice with anti- GBM disease, although the authors did not address the glomerular cell type to which properdin binds (19).

Conversely, Harboe et al. recently showed that properdin binding on endothelial cells and *Neisseria meningitidis* is dependent on initial C3 deposition (18). Consequently, our findings reopen the discussion whether properdin is a true pattern recognition molecule of the alternative pathway (AP). Pattern recognition of properdin has been indicated in other properdin interactions as well. Properdin binding to DNA and glycosaminoglycans on late apoptotic cells and necrotic cells has been suggested to be independent of initial C3 deposition (16, 17). Glycosaminoglycans and DNA share a strong negative charge, while properdin is strongly positively charged. Therefore, the interaction of properdin with glycosaminoglycans (and DNA), is based on charge - charge interactions, as we previously analyzed in detail (23).

Syndecan-1 and properdin co-localize on PTECs under proteinuric conditions (23). We present that syndecan-1 may be a ligand of properdin, using a syndecan-1 deficient HK-2 strain. Syndecan-1 is a major membrane spanning HSPG in epithelial cells and the interaction of properdin with sulfated glycosaminoglycans has been long known. In this study we found a reduced binding of properdin in syndecan-1 deficient HK-2 cells when compared to HK-2 wild type cells. It is likely that properdin not only binds to syndecan-1 but also to other epithelial HSPGs of which syndecan-1 is the most important properdin binding HSPG. Properdin consists of seven non-identical trombospondin-1 repeats (TSR), and literature has shown that a fragment consisting of TSR 4 & 5 forms the binding site for glycosaminoglycans, but also for C3b (30). Earlier work already showed that trypsin treatment of properdin, cleaving the TSR5 in half, results in an inability to bind C3b while the glycosaminoglycan binding remains intact. This suggests that TSR5 is the principal C3b binding site for properdin that receives a co-operative contribution from TSR4 (30, 36). Recent structural studies revealed TSR5 to be the dominant C3b binding domain with some contribution of TSR6 (33). Taken together, these studies showed that the binding site for C3b and glycosaminoglycans on properdin could be different, but are more likely very close. We show that inhibition of properdin to C3b by different heparinoid products is size dependent; the bigger the better, suggesting that larger heparins sterically hinder the C3b binding site on properdin as well. We also show that the deer tick protein Salp20 can inhibit both the binding of heparin-albumin and C3b to properdin. Salp20 has previously been shown to displace properdin from the alternative C3 convertase, resulting in accelerated decay of the convertase (27). Our results confirm that recombinant Salp20 can inhibit the binding of properdin to C3b and thereby reduce the AP activation on PTECs. However, we also show that recombinant Salp20 can inhibit the binding of properdin to heparin-albumin and to HS on PTECs, indicating a double inhibitory role for Salp20 in properdin mediated AP activation, namely inhibition of the active C3 convertase and inhibition of the initial pattern recognition function of properdin. The results further strengthen the data shown by others that C3b and glycosaminoglycans have a closely related binding epitope on properdin (27). Nevertheless, further molecular docking studies are needed to unravel the exact glycosaminoglycan-binding domain of properdin.

It has been demonstrated before that Salp20 can inhibit the AP of complement in multiple disease models (29, 37). This could be of major importance in the development of therapeutic modalities for tubular damage in proteinuric renal diseases. Our results demonstrate that in this setting, recombinant Salp20 may not only block the binding of properdin to proximal tubular epithelial cells, but also compete off properdin that was already bound to the cells and avoid AP activation, even when the initial pattern recognition step had already formed. Since properdin-deficient humans do not show a severely compromised immune function, apart from an increased risk for meningitis for which vaccination is possible, blocking properdin seems a relatively safe approach (38, 39). There are some *in vitro* and *ex vivo* studies describing properdin competing composites and properdin blocking antibodies in humans, however unexpected results in animal models teach us that not all lessons have yet been learned (30, 40–45). Bansal-Gupta et al. described a properdin targeting monoclonal antibody, showing exclusive AP blocking activity by influencing the interaction of C3 with properdin in an *in vitro* model (40). In addition, Pauly et al. reported the development of an anti-properdin monoclonal antibody that showed up to fifteen times more efficiency in blocking the complement cascade when compared to anti-Ba or anti-C5 antibodies in human blood samples (41). Currently one anti-properdin antibody is at the stage of a phase 2 clinical trial (42). However, properdin doesn't spill the beans that easily. In contrast to the studies described above, a protective role for properdin was described in two separate C3 glomerulopathy (C3G) mouse models. This is remarkable, as C3G occurs as a result of overactivity of the AP, leading to glomerular injury. Nonetheless, mice knocked

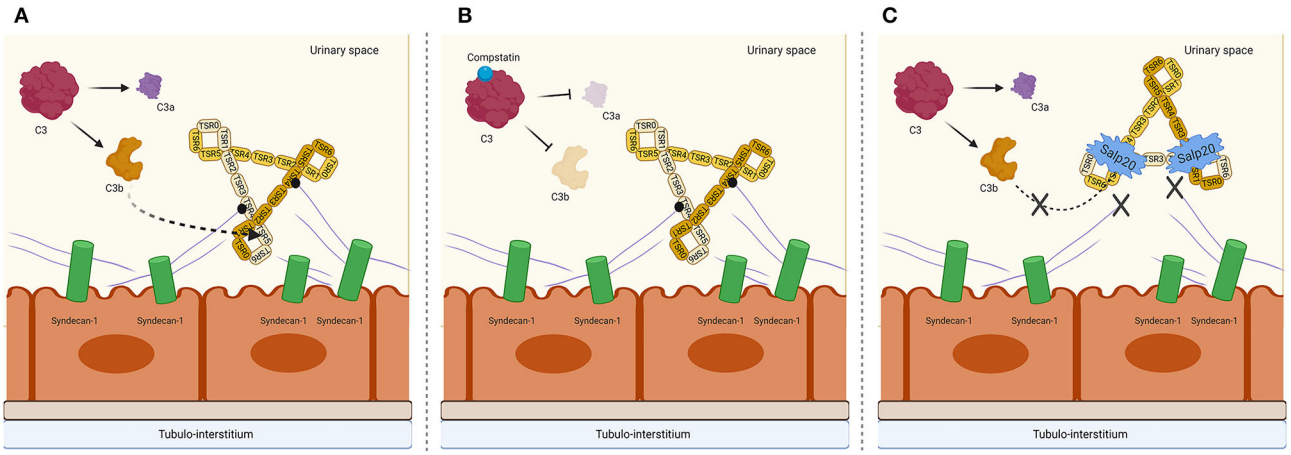

FIGURE 6 | Proposed mechanism on a tubular epithelial level of properdin binding to syndecan-1/heparan sulfate and interruption of AP complement activation by C3 cleavage inhibiting peptide Compstatin and properdin inhibitor Salp20. **(A)** Properdin is depicted in its trimeric form since this is the most abundant form of properdin. The binding of syndecan-1 is most likely to the trombospondin-1 repeat (TSR) 4 domain of properdin, receiving a cooperative contribution of TSR5. C3b most likely binds to TSR5, with a cooperative function of TSR4 and TSR6. **(B)** In the presence of Compstatin, C3 cleavage is inhibited. However, properdin is able to bind to heparan sulfate proteoglycan syndecan-1. **(C)** In the presence of Salp20, C3b cannot bind to the TSR5 domain of properdin, nor can properdin bind to syndecan-1. Figure created with BioRender.com.

out for properdin (and small amounts of truncated factor H) showed an injury exacerbation with increased accumulation of C3 along the glomerular basal membrane (44, 45). In conclusion, discovering the role of properdin remains challenging and not fully elucidated.

Salp20 is a new kid on the block in the field of properdin inhibition and since Salp20 is a tick protein, it would be expected to be strongly immunogenic. Therefore, prior to testing in animal models, small non-immunogenic molecule analogs of the Salp20 binding region should be produced and tested *in vitro* and *in vivo* for their AP inhibiting potential. Next to the inhibitory effect of Salp20, we have also shown in previous work that heparinoids compete for properdin binding with heparan sulfates on PTECs (24), and in that study we showed that non-anti-coagulant heparins also compete for properdin binding with C3b. This is promising for AP-driven diseases such as tubular activation secondary to proteinuria. Finally, we also show that Compstatin does not inhibit the binding of properdin to PTEC, but does prevent subsequent AP complement activation. Therefore, Compstatin holds promise in blocking undesired complement activation in numerous pathogenic conditions. A possible mechanism of AP complement inhibition on a tubular level by Compstatin and Salp20 is depicted in **Figure 6**. Overall, our study demonstrates the inhibitory effects of Compstatin, non-coagulant heparins and recombinant Salp20 at the level of proximal tubular epithelial cells. These results might be of great importance for reducing proteinuria induced AP activation and tubular injury.

DATA AVAILABILITY STATEMENT

The raw data supporting the conclusions of this article will be made available by the authors, without undue reservation.

AUTHOR CONTRIBUTIONS

RL was involved in study design, carrying out assays, interpreting data, statistical analysis, creating tables and figures, and writing of the manuscript. DT was involved in study design, interpreting data, and writing of the manuscript. WD was involved in carrying out assays and manuscript editing. MD and MS were involved in interpreting data and manuscript editing. SB and JB were involved in study design, interpreting data, statistical analysis, and manuscript editing. All authors contributed to the article and approved the submitted version.

FUNDING

This study was supported by the Dutch Kidney foundation (grant number: 13O CA27).

ACKNOWLEDGMENTS

We thank H. M. van der Lugt for her support for the preparation of this manuscript and Dr. J. D. Lambris for his generous gift of Compstatin. We also thank R. van den Bos and Dr. P. Gros (Bijvoet Center for Biomolecular Research, Utrecht University, Utrecht, The Netherlands) for their helpful gift of recombinant properdin and recombinant Salp20 and their support during the preparation of this manuscript.

SUPPLEMENTARY MATERIAL

The Supplementary Material for this article can be found online at: https://www.frontiersin.org/articles/10.3389/fimmu.2020.01643/full#supplementary-material

REFERENCES

1. Flanc RS, Roberts MA, Strippoli GF., Chadban SJ, Kerr PG, Atkins RC. Treatment of diffuse proliferative lupus nephritis: a meta-analysis of randomized controlled trials. *Am J Kidney Dis.* (2004) 43:197–208. doi: 10.1053/j.ajkd.2003.10.012
2. Camussi G, Stratta P, Mazzucco G, Gaido M, Tetta C, Castello R, et al. *In vivo* localization of C3 on the brush border of proximal tubules of kidneys from nephrotic patients. *Clin Nephrol.* (1985) 23:134–41.
3. Zhou W, Marsh JE, Sacks SH. Intrarenal synthesis of complement. *Kidney Int.* (2001) 59:1227–35. doi: 10.1046/j.1523-1755.2001.0590041227.x
4. Ichida S, Yuzawa Y, Okada H, Yoshioka K, Matsuo S. Localization of the complement regulatory proteins in the normal human kidney. *Kidney Int.* (1994) 46:89–96. doi: 10.1038/ki.1994.247
5. Lachmann PJ, Halbwachs L. The influence of C3b inactivator (KAF) concentration on the ability of serum to support complement activation. *Clin Exp Immunol.* (1975) 21:109–14.
6. Fredrik Bexborn, Per Ola Andersson, Hui Chen BN KNE. The Tick-over theory revisited: formation and regulation of the soluble alternative complement C3 convertase (C3(H20)Bb). *Mol Immunol.* (2008) 45:2370–9. doi: 10.1016/j.molimm.2007.11.003
7. Walport MJ. Complement. *N Engl J Med.* (2001) 344:1058–66. doi: 10.1056/NEJM200104053441406
8. Walport MJ. second of two parts. *N Engl J Med.* (2001) 344:1140–4. doi: 10.1056/NEJM200104123441506
9. Kemper C, Atkinson JP, Hourcade DE. Properdin: emerging roles of a pattern-recognition molecule. *Annu Rev Immunol.* (2010) 28:131–55. doi: 10.1146/annurev-immunol-030409-101250
10. Alcorlo M, Tortajada A, Rodriguez de Cordoba S, Llorca O. Structural basis for the stabilization of the complement alternative pathway C3 convertase by properdin. *Proc Natl Acad Sci USA.* (2013) 110:13504–9. doi: 10.1073/pnas.1309618110
11. Cortes C, Ohtola JA, Saggu G, Ferreira VP. Local release of properdin in the cellular microenvironment: role in pattern recognition and amplification of the alternative pathway of complement. *Front Immunol.* (2012) 3:1–7. doi: 10.3389/fimmu.2012.00412
12. Pangburn MK. Analysis of the natural polymeric forms of human properdin and their functions in complement activation. *J Immunol.* (1989) 142:202–7.
13. Farries TC, Finch JT, Lachmann PJ, Harrison RA. Resolution and analysis of 'native' and 'activated' properdin. *Biochem J.* (1987) 243:507–17. doi: 10.1042/bj2430507
14. Schwaeble W, Dippold WG, Schafer MKH, Pohla H, Jonas D, Luttig B, et al. Properdin, a positive regulator of complement activation, is expressed in human T cell lines and peripheral blood T cells. *J Immunol.* (1993) 151:2521–8.
15. Saggu G, Cortes C, Emch HN, Ramirez G, Worth RG, Ferreira VP. Identification of a novel mode of complement activation on stimulated platelets mediated by properdin and C3(H 2 O). *J Immunol.* (2013) 190:6457–67. doi: 10.4049/jimmunol.1300610
16. Xu W, Berger SP, Trouw LA, De HC, Schlagwein N, Mutsaers C, et al. Properdin binds to late apoptotic and necrotic cells independently of C3b and regulates alternative pathway complement activation. *J Immunol.* (2019) 180:7613–21. doi: 10.4049/jimmunol.180.11.7613
17. Kemper C, Mitchell LM, Zhang L, Hourcade DE. The complement protein properdin binds apoptotic T cells and promotes complement activation and phagocytosis. *Proc Natl Acad Sci USA.* (2008) 105:9023–8. doi: 10.1073/pnas.0801015105
18. Harboe M, Johnson C, Nymo S, Ekholt K, Schjalm C, Lindstad JK, et al. Properdin binding to complement activating surfaces depends on initial C3b deposition. *Proc Natl Acad Sci USA.* (2017) 114:E534–9. doi: 10.1073/pnas.1612385114
19. O'Flynn J, Kotimaa J, Faber-Krol R, Koekkoek K, Klar-Mohamad N, Koudijs A, et al. Properdin binds independent of complement activation in an *in vivo* model of anti–glomerular basement membrane disease. *Kidney Int.* (2018) 94:1141–50. doi: 10.1016/j.kint.2018.06.030
20. Gaarkeuken H, Siezenga MA, Zuidwijk K, Kooten C Van, Rabelink TJ, Daha MR, et al. Complement activation by tubular cells is mediated by properdin binding. *Am J Physiol Renal Physiol.* (2019) 295:1397–403. doi: 10.1152/ajprenal.90313.2008
21. Siezenga MA, Van Der Geest RN, Mallat MJK, Rabelink TJ, Daha MR, Berger SP. Urinary properdin excretion is associated with intrarenal complement activation and poor renal function. *Nephrol Dial Transplant.* (2010) 25:1157–61. doi: 10.1093/ndt/gfp630
22. Lammerts RGM, Eisenga MF, Alyami M, Daha MR, Seelen MA, Pol RA, et al. Urinary properdin and sc5b-9 are independently associated with increased risk for graft failure in renal transplant recipients. *Front Immunol.* (2019) 10:1–10. doi: 10.3389/fimmu.2019.02511
23. Zaferani A, Vivès RR, Van Der Pol P, Hakvoort JJ, Navis GJ, Van Goor H, et al. Identification of tubular heparan sulfate as a docking platform for the alternative complement component properdin in proteinuric renal disease. *J Biol Chem.* (2011) 286:5359–67. doi: 10.1074/jbc.M110.167825
24. Zaferani A, Vivès RR, Van Der Pol P, Navis GJ, Daha MR, Van Kooten C, et al. Factor H and properdin recognize different epitopes on renal tubular epithelial heparan sulfate*. *J Biol Chem.* (2012) 287:31471–81. doi: 10.1074/jbc.M112.380386
25. Celie JWAM, Katta KK, Adepu S, Melenhorst WBWH, Reijmers RM, Slot EM, et al. Tubular epithelial syndecan-1 maintains renal function in murine ischemia/reperfusion and human transplantation. *Kidney Int.* (2012) 81:651–61. doi: 10.1038/ki.2011.425
26. Adepu S, Rosman CWK, Dam W, van Dijk MCRF, Navis G, van Goor H, et al. Incipient renal transplant dysfunction associates with tubular syndecan-1 expression and shedding. *Am J Physiol Ren Physiol.* (2015) 309:F137–45. doi: 10.1152/ajprenal.00127.2015
27. Tyson KR, Elkins C, de Silva AM. A novel mechanism of complement inhibition unmasked by a tick salivary protein that binds to properdin. *J Immunol.* (2008) 180:3964–8. doi: 10.4049/jimmunol.180.6.3964
28. Tyson K, Elkins C, Patterson H, Fikrig E, De Silva A. Biochemical and functional characterization of Salp20, an Ixodes scapularis tick salivary protein that inhibits the complement pathway. *Insect Mol Biol.* (2007) 16:469–79. doi: 10.1111/j.1365-2583.2007.00742.x
29. Hourcade DE, Akk AM, Mitchell LM, Zhou H fang, Hauhart R, Pham CTN. Anti-complement activity of the Ixodes scapularis salivary protein Salp20. *Mol Immunol.* (2016) 69:62–9. doi: 10.1016/j.molimm.2015.11.008
30. Kouser L, Abdul-aziz M, Tsolaki AG, Singhal D, Schwaeble WJ, Urban BC, et al. A recombinant two-module form of human properdin is an inhibitor of the complement alternative pathway. *Mol Immunol.* (2016) 73:76–87. doi: 10.1016/j.molimm.2016.03.005
31. Campeiro JD, Dam W, Monte GG, Porta LC, Oliveira LCG de, Nering MB, et al. Long term safety of targeted internalization of cell penetrating peptide crotamine into renal proximal tubular epithelial cells *in vivo*. *Sci Rep.* (2019) 9:1–13. doi: 10.1038/s41598-019-39842-7
32. Roos A, Bouwman LH, Munoz J, Zuiverloon T, Faber-Krol MC, Fallaux-van den Houten FC, et al. Functional characterization of the lectin pathway of complement in human serum. *Mol Immunol.* (2003) 39:655–68. doi: 10.1016/S0161-5890(02)00254-7
33. van den Bos RM, Pearce NM, Granneman J, Brondijk THC, Gros P. Insights into enhanced complement activation by structures of properdin and its complex with the C-terminal domain of C3b. *Front Immunol.* (2019) 10:1–19. doi: 10.3389/fimmu.2019.02097
34. Lambris JD, Ross GD. Assay of membrane complement receptors (CR1 and CR2) with C3b- and C3d-coated fluorescent microspheres. *J Immunol.* (1982) 128:186–9. Available online at: http://www.ncbi.nlm.nih.gov/pubmed/7033372.
35. Ferreira VP, Cortes C, Pangburn MK. Native polymeric forms of properdin selectively bind to targets and promote activation of the alternative pathway of complement. *Immunobiology.* (2010) 215:932–40. doi: 10.1016/j.imbio.2010.02.002
36. Higgins JM, Wiedemann H, Timpl R, Reid KB. Characterization of mutant forms of recombinant human properdin lacking single thrombospondin type I repeats. Identification of modules important for function. *J Immunol.* (1995) 155:5777–85.
37. Michels MAHM, van de Kar NCAJ, van den Bos RM, van der Velden TJAM, van Kraaij SAW, Sarlea SA, et al. Novel assays to distinguish between properdin-dependent and properdin-independent C3 nephritic factors provide insight into properdin-inhibiting therapy. *Front Immunol.* (2019) 10:1–16. doi: 10.3389/fimmu.2019.01350

38. Fijen CA, van den Bogaard R, Schipper M, Mannens M, Schlesinger M, Nordin FG, et al. Properdin deficiency: molecular basis and disease association. *Mol Immunol.* (1999) 36:863–7. doi: 10.1016/S0161-5890(99)00107-8
39. Linton SM, Morgan BP. Properdin deficiency and meningococcal disease - Identifying those most at risk. *Clin Exp Immunol.* (1999) 118:189–91. doi: 10.1046/j.1365-2249.1999.01057.x
40. Gupta-Bansal R, Parent JB, Brunden KR. Inhibition of complement alternative pathway function with antiproperdin monoclonal antibodies. *Mol Immunol.* (2000) 37:191–201. doi: 10.1016/S0161-5890(00)00047-X
41. Pauly D, Nagel BM, Reinders J, Killian T, Wulf M, Ackermann S, et al. A novel antibody against human properdin inhibits the alternative complement system and specifically detects properdin from blood samples. *PLoS ONE.* (2014) 9:e96371. doi: 10.1371/journal.pone.0096371
42. Ricklin D, Mastellos DC, Reis ES, Lambris JD. The renaissance of complement therapeutics. *Nat Rev Nephrol.* (2018) 14:26–47. doi: 10.1038/nrneph.2017.156
43. Gullipalli D, Zhang F, Sato S, Ueda Y, Kimura Y, Golla M, et al. Antibody inhibition of properdin prevents complement-mediated intravascular and extravascular hemolysis. *J Immunol.* (2018) 201:1021–9. doi: 10.4049/jimmunol.1800384
44. Ruseva MM, Vernon KA, Lesher AM, Schwaeble WJ, Ali YM, Botto M, et al. Loss of properdin exacerbates C3 glomerulopathy resulting from factor H deficiency. *J Am Soc Nephrol.* (2013) 24:43–52. doi: 10.1681/ASN.2012060571
45. Lesher AM, Zhou L, Kimura Y, Sato S, Gullipalli D, Herbert AP, et al. Combination of factor H mutation and properdin deficiency causes severe C3 glomerulonephritis. *J Am Soc Nephrol.* (2013) 24:53–65. doi: 10.1681/ASN.2012060570

Conflict of Interest: The authors declare that the research was conducted in the absence of any commercial or financial relationships that could be construed as a potential conflict of interest.

frontiers in Immunology

ORIGINAL RESEARCH
published: 14 August 2020
doi: 10.3389/fimmu.2020.02072

Treatment of COVID-19 With Conestat Alfa, a Regulator of the Complement, Contact Activation and Kallikrein-Kinin System

Pascal Urwyler[1†], Stephan Moser[1†], Panteleimon Charitos[1], Ingmar A. F. M. Heijnen[2], Melanie Rudin[2], Gregor Sommer[3], Bruno M. Giannetti[4], Stefano Bassetti[1,5], Parham Sendi[6], Marten Trendelenburg[1,5] and Michael Osthoff[1,5‡]*

[1] Division of Internal Medicine, University Hospital Basel, Basel, Switzerland, [2] Laboratory Medicine, Division of Medical Immunology, University Hospital Basel, Basel, Switzerland, [3] Clinic of Radiology and Nuclear Medicine, University Hospital Basel, Basel, Switzerland, [4] Pharming Group, Leiden, Netherlands, [5] Department of Clinical Research and Department of Biomedicine, University Hospital Basel, Basel, Switzerland, [6] Department of Infectious Diseases and Hospital Epidemiology, University Hospital Basel, Basel, Switzerland

OPEN ACCESS

Edited by:
Marcin Okrój, Intercollegiate Faculty of Biotechnology of University of Gdańsk and Medical University of Gdańsk, Poland

Reviewed by:
Timothy M. Thomson, Consejo Superior de Investigaciones Científicas (CSIC), Spain
Zoltan Prohaszka, Semmelweis University, Hungary

***Correspondence:**
Michael Osthoff
michael.osthoff@usb.ch

[†] These authors have contributed equally to this work

[‡]ORCID:
Michael Osthoff
orcid.org/0000-0001-5439-957X

Specialty section:
This article was submitted to Molecular Innate Immunity, a section of the journal Frontiers in Immunology

Received: 17 June 2020
Accepted: 30 July 2020
Published: 14 August 2020

Citation:
Urwyler P, Moser S, Charitos P, Heijnen IAFM, Rudin M, Sommer G, Giannetti BM, Bassetti S, Sendi P, Trendelenburg M and Osthoff M (2020) Treatment of COVID-19 With Conestat Alfa, a Regulator of the Complement, Contact Activation and Kallikrein-Kinin System. Front. Immunol. 11:2072. doi: 10.3389/fimmu.2020.02072

A dysregulated immune response with hyperinflammation is observed in patients with severe coronavirus disease 2019 (COVID-19). The aim of the present study was to assess the safety and potential benefits of human recombinant C1 esterase inhibitor (conestat alfa), a complement, contact activation and kallikrein-kinin system regulator, in severe COVID-19. Patients with evidence of progressive disease after 24 h including an oxygen saturation <93% at rest in ambient air were included at the University Hospital Basel, Switzerland in April 2020. Conestat alfa was administered by intravenous injections of 8400 IU followed by 3 additional doses of 4200 IU in 12-h intervals. Five patients (age range, 53–85 years; one woman) with severe COVID-19 pneumonia (11–39% lung involvement on computed tomography scan of the chest) were treated a median of 1 day (range 1–7 days) after admission. Treatment was well-tolerated. Immediate defervescence occurred, and inflammatory markers and oxygen supplementation decreased or stabilized in 4 patients (e.g., median C-reactive protein 203 (range 31–235) mg/L before vs. 32 (12–72) mg/L on day 5). Only one patient required mechanical ventilation. All patients recovered. C1INH concentrations were elevated before conestat alfa treatment. Levels of complement activation products declined after treatment. Viral loads in nasopharyngeal swabs declined in 4 patients. In this uncontrolled case series, targeting multiple inflammatory cascades by conestat alfa was safe and associated with clinical improvements in the majority of severe COVID-19 patients. Controlled clinical trials are needed to assess its safety and efficacy in preventing disease progression.

Keywords: COVID-19, C1 esterase inhibitor, SARS-CoV-2, inflammation, complement system, kallikrein-kinin system, contact activation system

INTRODUCTION

The current pandemia of coronavirus disease 2019 (COVID-19) caused by severe acute respiratory syndrome coronavirus 2 (SARS-CoV-2) remains a major global health challenge. The clinical spectrum of COVID-19 ranges from asymptomatic carriers to respiratory failure. A dysregulated immune response with evidence of hyperinflammation is observed in patients with severe

COVID-19 (1). Siddiqi et al. suggested a disease stage model, where early disease is charaterized by infection and replication of the virus. Subsequently, pulmonary involvement and marked hyperinflammation occur during the next stage (2). The exact factors promoting disease progression are not yet known. However, sustained activation of the complement system (CS) induced by coronaviruses (CoV) seems to play a crucial role in this context.

The complement system (CS) is an integral part of the innate immune system and consists of a number of distinct plasma proteins that act as a first line of defense inducing an inflammatory response after opsonisation of pathogens and dying cells (3, 4). Inflammatory responses include the activation of macrophages, neutrophils, platelets and endothelial cells, and interactions with other plasmatic cascades. While the CS does not seem to be critical for controlling CoV replication, unregulated complement activation - induced by viruses including influenza and CoV - plays a crucial role in the pathogenesis of acute lung injury (ALI). Indeed, an animal model suggests that the CS mediates SARS-CoV-induced lung disease and regulates the proinflammatory response. Complement deficient mice infected with SARS-CoV were affected less severely and showed a reduced lung involvement and lower local and systemic cytokine levels compared to control mice (5). In line, inhibition of complement C5a signaling alleviated lung damage in animal infection models using MERS-CoV (6) and influenza H7N9 (7). Similar results were reported with inhibition of complement cascade C3a in an animal infection model using avian influenza (8). Gao et al. investigated the interaction of MERS-CoV, SARS-CoV, and SARS-CoV-2 with the lectin pathway of complement in more detail (9). They demonstrate an interaction of these highly pathogenic CoV with mannose-binding lectin associated serine protease-2 (MASP-2), the key activator of the lectin pathway of complement (10), leading to uncontrolled activation of the complement cascade. In line, MASP-2 knock-out mice and mice treated with MASP-2 inhibitors showed significantly milder symptoms in a virus protein mouse pneumonia model. Mannose-binding lectin, the pattern recognition molecule of the lectin pathway, that activates MASP-2 upon binding to pathogens, was found to bind to SARS-CoV spike glycoprotein (11). In COVID-19 patients, increased plasma levels of complement activation products C5a and soluble C5b-9 have been observed (12). Furthermore, autopsy findings from 5 patients with severe COVID-19 revealed excessive complement activation in lung tissue associated with complement-mediated microthrombotic disease (13).

TABLE 1 | Clinical characteristics of SARS-CoV-2 infected patients treated with conestat alfa.

Characteristics[a]	Patient 1	Patient 2	Patient 3	Patient 4	Patient 5
BMI	27.7	28.4	22.4	31.2	22.6
Smoking (ongoing or recent)	No	Yes	Yes	No	Yes
Comorbidity	CKD, hypertension, hypercholesterolemia, gout	CKD, CVD, diabetes, hypertension, PAD	CVD, hypertension	Asthma, hypertension, hypothyroidism	None
Days from symptom onset to admission	15	4	4	6	7
Days from admission to conestat alfa	1	1	7	1	2
Symptoms	Fever, diarrhea, fatigue, cough, chest pain	Cough, sore throat	Fatigue, diarrhea, muscle ache	Cough, diarrhea, fatigue, muscle ache, dyspnea	Fever, cough, fatigue, dyspnea
Lung involvement, %[b]	14	18	39	24	11
SOFA score day 0	1	2	2	1	2
NEWS2 score day 0	5	5	9	8	7
SARS-CoV-2 viral load day 0, copies/mL	23,500	36,046,600	1,000	611,900	33,400
Respiratory rate day 0, per minute	21	25	22	22	24
CRP day 0, mg/L	203	235	223	106	31
Ferritin day 0, μg/L	1,280	567	3,736	560	1,805
LDH day 0, U/L	379	466	483	366	584
D-dimer day 0, μg/ml	1.2	4.2	1.0	0.6	1.7
IL-6 day 0, ng/L	60	187	141	55	32
C1INH d0, g/l	0.71	0.45	0.57	0.52	0.64
C1INH d1, g/l	0.71	0.48	0.58	0.53	0.63

CKD, chronic kidney disease; CVD, cardiovascular disease; PAD, peripheral artery disease; BMI, body mass index; SOFA, sepsis-related organ failure assessment score; NEWS2, National Early Warning Score 2; CRP, C-reactive protein; LDH, lactate dehydrogenase; IL-6, interleukin-6.

[a] *Day 0 denotes the day of first administration.*

[b] *Lung involvement was determined from computed tomography scans of the chest.*

Beside CS activation, involvement of the contact activation (CAS) and kallikrein-kinin system (KKS) in thromboinflammation, capillary leakage and subsequent pulmonary angioedema has been suspected. Angiotensin-converting enzyme 2 (ACE2), a cell membrane bound protein used by SARS-CoV-2 to enter cells, also inactivates bradykinin degradation products, and expression of ACE2 as well as its enzymatic activity is decreased by SARS-CoV (14). Hence, the interaction of SARS-CoV-2 with ACE2 may impair its function, leading to a relative abundance of bradykinin degradation products and local pulmonary edema.

The role of the CAS has not been elucidated in COVID-19. However, dysregulated coagulation is commonly observed in critically-ill patients with COVID-19 and thromboembolism has been reported more frequently compared to other diseases causing severe sepsis (15, 16). This may be a consequence of over-activation of CAS since sepsis and ARDS are prototypic states that strongly activate the CAS (17, 18). Consistent with thromboinflammation, microthrombi have been observed in autopsy series in COVID-19 (19).

C1 esterase inhibitor (C1INH) is a strong inhibitor of the CS, CAS, and KKS and interacts with stressed endothelial cells. C1INH treatment was associated with reduced capillary leakage after stem cell transplantation and organ damage in human sepsis (20–22). Recently, C1INH was identified among other inflammatory proteins to be upregulated in severe vs. non-severe COVID-19 in a proteomic and metabolomic characterization (23). In a mouse model of highly pathogenic CoV, C1INH treatment was able to block MASP-2 mediated overactivation of the complement system and subsequent lung injury and death (9). Lastly, when examining published interactomes of SARS-CoV-1 and−2, a significant interaction of C1INH with CoV-1 proteins was documented including proteins that are highly similar to their orthologous CoV-2 proteins (24).

Investigating a regulator of the CS, CAS, and KKS for the first time in severe COVID-19, we report the experience of early administration of conestat alfa, a recombinant human C1INH, in non-critically ill patients to prevent deterioration.

MATERIALS AND METHODS

The treatments occurred at the University Hospital Basel from April 2, 2020, to April 28, 2020 and were approved by the Ethics Committee of Northwest and Central Switzerland (EKNZ 2020-1013). All participants consented to the compassionate use of conestat alfa and the acquisition of health-related personal data and biological material.

Study Drug

Conestat alfa is a recombinant human C1INH that shares an identical protein structure with plasma-derived C1INH but has a different glycosylation pattern. Comparable inhibition of most target proteases has been demonstrated (25). Despite the broad interference with several cascades and targets, major adverse events or unique toxicities have not been demonstrated in previous studies with the exception of a potential risk of allergic reactions in patients with rabbit dander allergy.

Patients and Intervention

Patients with polymerase chain reaction-confirmed and severe COVID-19 (26) were included if they were at least 18 years old, showed evidence of progressive disease after 24 h, and had a C-reactive protein level of at least 30 mg/L and oxygen saturation of <93% at rest in ambient air. Exclusion criteria included admission to ICU, immunosuppression, and known allergy to rabbit dander. Conestat alfa was administered by 4 intravenous injections in 12-h intervals over 48 h. The dosage was identical for all patients irrespective of body weight (8400 IU as initial dosage followed by 4200 IU).

Data Collection

Clinical information was collected from the electronic hospital information system. Affected lung tissue on a computed tomography (CT) scan was quantified semi-automatically using software for lung density analysis in Chest CT available at our radiology department [CT Pulmo 3D included in Syngo.Via VB30A, Siemens Healthineers, Forchheim, Germany; method similar as described recently (27)]. The processing included semi-automatic segmentation of the lungs followed by a threshold-analysis of Hounsfield units (HU), where pulmonary involvement was defined as the percentage of lung parenchyma with a CT-density between −600 and 0 HU. Concentration of complement proteins and C1INH antigen were analyzed in serum or plasma by standardized nephelometric assays (C3, C4, C1INH) or ELISA assays in duplicate according to the instructions of the manufacturer (C4d, C5a; Quidel, San Diego, U.S.A.). A control group was established from the database of all COVID-19 patients admitted during the same period (March and April 2020) at the University Hospital Basel ($n = 165$). Propensity score-matching (1:3 matching of cases and controls) was performed to adjust for relevant confounders (nearest-neighborhood method; caliper width of 0.25 times the standard deviation of the logit of propensity scores). The following variables were included in the matching model: gender (exact), age, lung involvement on CT scan of the chest and Charlson Comorbidity index. The maximum standardized difference of the mean was 0.05 and the area under the curve was 0.85. Characteristics of the group were compared with the use of the Fisher's exact test for categorical variables and the Mann-Whitney U-test for continuous variables.

RESULTS

Five patients (4 males, median age 60 years, range 53–85 years) were treated with conestat alfa. Four had preexisting medical conditions (**Table 1**). A CT scan of the chest demonstrated moderate to severe pneumonia with involvement of lung parenchyma ranging from 11 to 39% (**Figure 1A**). All patients received hydroxychloroquine and lopinavir/ritonavir (LPV/r) as per local treatment guideline at the time. Conestat alfa was administered a median of 1 day (range 1–7 days) after admission for 48 h and was well-tolerated. No treatment associated serious adverse events were recorded.

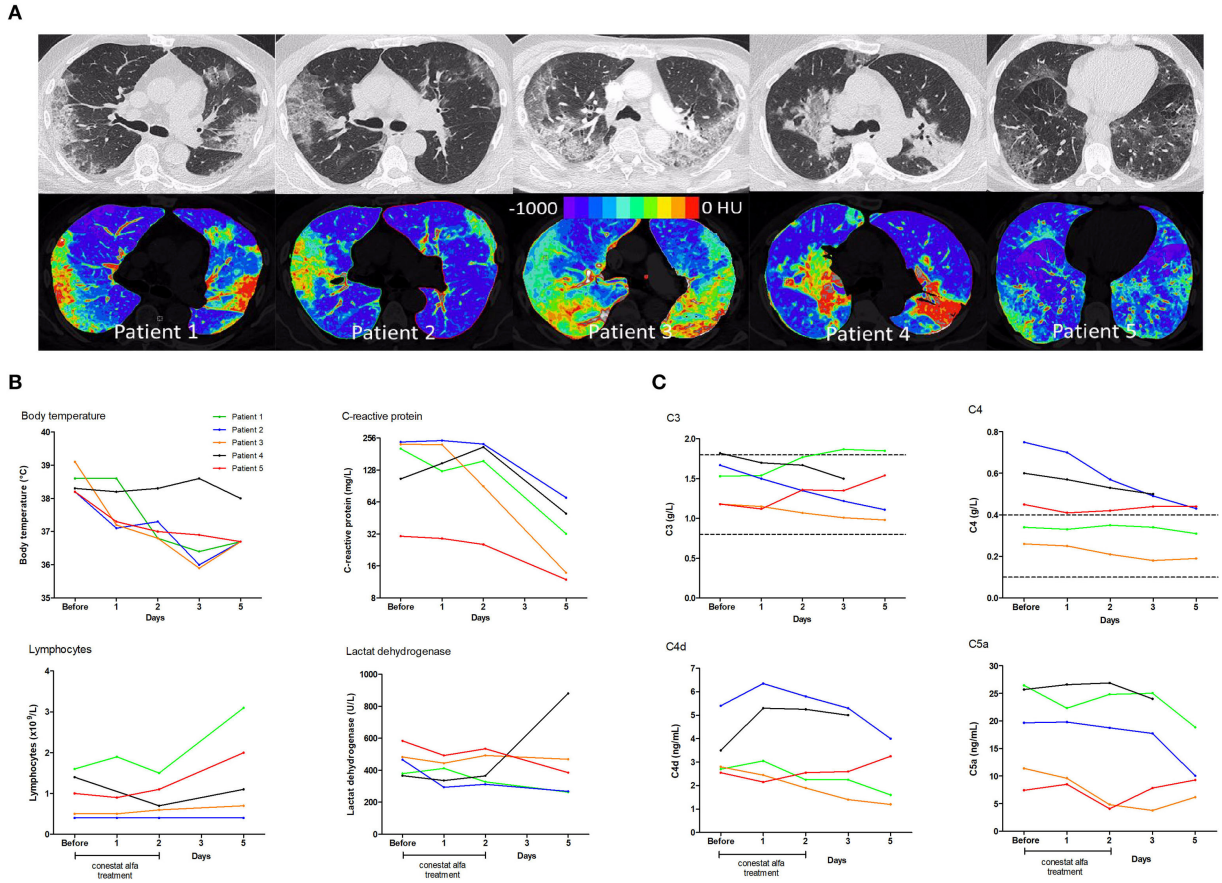

FIGURE 1 | Chest computed tomography scans and temporal changes of laboratory parameters in five patients treated with conestat alfa. **(A)** Upper row: Original images in lung kernel reconstruction showing ground-glass opacities and consolidations involving multiple segments of both lungs with subpleural predominance. Lower row: color-coded maps from lung density analysis used to quantify the percentage of affected lung volume. **(B)** Temporal changes of body temperature, plasma C-reactive protein levels, lymphocyte counts and lactate dehydrogenase levels. **(C)** Temporal changes in concentration of serum complement component C3 and C4, and plasma activation products complement component C4d and C5a. Reference ranges are depicted by dashed lines.

Outcome

Immediate defervescence occurred in all but one patient (patient 4) within 48 h (**Figure 1B**). Three patients were weaned off oxygen supplementation and discharged early. In patient 3, conestat alfa was administered late during admission (day 7) after rapid progression (pulmonary involvement increased from 7 to 39%). Hence, only 12 h after the start of conestat alfa tocilizumab was also administered. Only 1 patient deteriorated after 48 h of treatment and required mechanical ventilation. Tocilizumab and amoxicillin/clavulanic acid were administered. The patient was extubated after 10 days. All patients were discharged within 3 weeks (range 6–20 days).

Outcome was compared to a matched control population of 15 patients. Baseline characteristics, admission laboratory parameters and treatments administered were similar in both groups (**Table 2**), except for present smoking [3/5 (60%) of the conestat alfa group and 0/15 (0%) for the matched control population]. However, 8/15 (53%) patients in the control population required mechanical ventilation or died, compared to only 1 (20%) in the conestat alfa group.

Course of Laboratory Parameters

Inflammatory markers decreased or stabilized in 4/5 patients (**Figure 1B**). The individual course of inflammatory markers, which were measured inconsistently in the control population is depicted in **Figure S1**. C1INH concentrations were elevated in all patients before conestat alfa treatment (range, 0.45–0.71 g/L, normal range 0.21–0.39, for individual values see **Table 1**). Concentration of plasma complement activation products C4d and C5a decreased within 5 days in most patients (**Figure 1C**). SARS-CoV-2 viral loads in nasopharyngeal swabs declined in 4/5 patients.

Safety Events After Administration of Conestat Alfa

Patient 2 developed acute on chronic renal failure on day 2 attributed to severe diarrhea secondary to COVID-19 infection and LPV/r treatment. After hydration with Ringer's lactate and sodium bicarbonate solution and cessation of LPV/r, renal function returned to almost baseline before discharge. Grade 2 liver injury (alanine transaminase elevation >2.5–5.0x upper

TABLE 2 | Comparison of demographics, clinical features and outcome of 5 SARS-CoV-2 infected patients treated with conestat alfa and a matched control group.

Variable	Control group *N* = 15	Conestat alfa group *N* = 5	*P*-value*
Demographics			
Age in years	59 (51–71)	60 (54–81)	0.5
Male sex, *N* (%)	12 (80)	4 (80)	1.0
Obesity, *N* (%)	7 (47)	2 (40)	1.0
Arterial hypertension, *N* (%)	7 (57)	4 (80)	0.3
Diabetes mellitus, *N* (%)	2 (13)	1 (20)	1.0
Chronic lung disease, *N* (%)	3 (20)	1 (20)	1.0
Congestive heart failure, *N* (%)	2 (13)	1 (20)	1.0
Chronic renal failure, *N* (%)	3 (20)	2 (40)	0.6
Cardiovascular disease, *N* (%)	4 (27)	2 (40)	0.6
Charlson Comorbidity index	2 (1–5)	4 (1–4)	0.7
Findings on presentation			
Symptom duration in days	7 (1–9)	7 (5–8)	0.7
Fever, *N* (%)	13 (87)	2 (40)	0.07
Cough, *N* (%)	11 (73)	4 (80)	1.0
Diarrhea	4 (27)	3 (60)	0.3
Dyspnea	5 (33)	2 (40)	1.0
NEWS2 score	5 (3–8)	7 (5–8)	0.5
Lung involvement in %[a]	28 (18–36)	24 (14–36)	0.7
Lymphocytes, $\times 10^9$/l	0.7 (0.3–1.04)	1.1 (0.5–1.3)	0.3
CRP, mg/l	85 (69–166)	72 (28–230)	0.7
LDH, U/l	425 (319–506)	354 (238–433)	0.5
D-dimer, μg/ml[b]	1.1 (0.5–2.3)	1.2 (0.7–4.2)	0.4
Ferritin day, μg/L[b]	1817 (1,165–2,677)	906 (501–1,280)	0.1
Creatinine, μmol/L	91 (70–131)	106 (72–215)	0.7
Treatment			
Lopinavir/ritonavir, *N* (%)	13 (87)	5 (100)	1.0
Hydroxychloroquine, *N* (%)	14 (93)	5 (100)	1.0
Tocilizumab, *N* (%)	6 (40)	2 (40)	1.0
Antibiotic treatment, *N* (%)	9 (60)	4 (80)	0.6
Outcome			
Length of stay in days[c]	10 (8–13)	10 (7–22)	0.9
Intubation, *N* (%)	6 (40)	1 (20)	0.6
Death, *N* (%)	4 (27)	0 (0)	0.5
Intubation or death, *N* (%)	8 (53)	1 (20)	0.3

CRP, C-reactive protein; LDH, lactate dehydrogenase.

Numerical Data are Presented as Median and Interquartile Range, Categorical Data as Frequency and Percentage.

[a] *Lung involvement was determined from computed tomography scans of the chest. Reference values of laboratory parameters: CRP (normal range < 10 mg/L), LDH (normal range 135–225 U/L for males and 135–214 U/L for females), D-dimer (normal range 0.19–0.5 μg/ml), lymphocytes (normal range 0.9–3.3 x 10^9/l), ferritin (normal range 30–300 μg/l for males and 10–200 μg/l for females), creatinine (normal range 49–97 μmol/L for males and 42–80 μmol/L for females).*

[b] *For controls, measurements up to day 3 were considered; still, D-dimer and ferritin concentrations were not available in 4 and 5 control patients, respectively.*

[c] *only survivors were counted.*

**The Fisher's exact test was used for comparisons of categorical variables and the Mann-Whitney U-test to compare continuous variables in the control group of patients vs. the group of patients treated with conestat alfa. All testing was two-tailed.*

limit of normal) was documented in 3 patients, which was attributed to treatment with LPV/r, amoxicillin/clavulanic acid, tocilizumab or paracetamol. Incident asymptomatic deep venous thrombosis was diagnosed on routine ultrasound in one patient (patient 4) after admission to the ICU, and the patient was anticoagulated. Clot resolution was documented on a subsequent ultrasound before ICU discharge.

DISCUSSION

A range of strategies have been proposed and are being evaluated to dampen hyper-inflammation in COVID-19 such as corticosteroid therapies, antibodies against IL-1 or IL-6, treatments interfering with the interferon pathway and anti-tumor necrosis factor therapies (28). In particular, the CS has gained attention as a potential therapeutic target in COVID-19 patients (29, 30), and first experiences targeting C3 and C5 of the complement system have been published (31, 32). However, in this case series, we investigated – to the best of our knowledge – for the first time a strategy of interfering with 3 plasmatic cascades including the CS (i.e., CS, CAS, and KKS) in 5 non-critically ill patients with severe COVID-19. Treatment with conestat alfa over 48 h was well-tolerated. No signal of impaired viral clearance emerged from our case series.

The clinical condition improved in all but 1 patient, reflected by immediate defervescence, improvement in oxygen requirements, and a decline in systemic inflammation and markers of complement activation. Notably, 4/5 patients treated early did not require mechanical ventilation despite the presence of risk factors such as markedly elevated inflammatory proteins. In the majority of patients (4/5) IL-6 levels were markedly elevated (>80 ng/ml) during the disease course, a finding shown to predict respiratory failure and mechanical ventilation, previously (33).

Similar to previous studies in sepsis (20), C1INH protein levels were elevated in COVID-19 patients consistent with an acute phase response. However, elevated C1INH levels may not be sufficient to block ongoing extensive CS, CAS, and KKS activation in COVID-19. An increased amount of modified (cleaved) inactive C1INH in patients with severe sepsis was documented previously, which may indicate a relative C1INH-deficient state (34). Of note, concentration of complement activation products C4d and C5a decreased following conestat alfa administration. Early supplementation of C1INH with conestat alfa is thus a plausible treatment option in selected patients with COVID-19, thereby inhibiting upstream complement proteases and its associated over-activation of the CS in COVID-19 (13, 29).

Limitations

The present study has a number of limitations. First, this was a small case series with a heterogeneous patient population and no controls. Patients may have improved without conestat alfa treatment, although the immediate defervesence and decrease in inflammatory markers is reassuring. Second, sustained complement inhibition may not have been achieved with this

current regimen, given the short half-life of conestat alfa and limited treatment duration. Third, all patients were treated with multiple other agents used off-label for the treatment of COVID-19 including LPV/r and hydroxychloroquine.

CONCLUSION

In this uncontrolled case series of 5 non-critically ill patients with severe COVID-19 pneumonia, administration of conestat alfa over 48 h to inhibit the CS, CAS and KKS was well-tolerated and associated with improvement in the clinical condition of 4 patients. Consequently, we have initiated a randomized controlled trial to investigate this promising approach (ClinicalTrials.gov, number NCT04414631).

DATA AVAILABILITY STATEMENT

The raw data supporting the conclusions of this article will be made available by the authors, without undue reservation.

ETHICS STATEMENT

The studies involving human participants were reviewed and approved by Ethics Committee of Northwest and Central Switzerland (EKNZ 2020-1013). The patients/participants provided their written informed consent to participate in this study.

AUTHOR CONTRIBUTIONS

SM, BG, MT, and MO designed the study. MO, PU, SM, PC, IH, MR, PS, GS, MT, and SB performed the study, collected, analyzed, and interpreted the data. PU and MO drafted the manuscript. All authors critically revised the manuscript.

FUNDING

Funded by personal and departmental funds of the project leader (MO); Conestat alfa (Ruconest®, Pharming Biotechnologies B.V., Leiden, The Netherlands) was provided free of charge by the manufacturer.

ACKNOWLEDGMENTS

We are devoted to the nurses and physicians who cared for the COVID-19 patients during these stressful times.

SUPPLEMENTARY MATERIAL

The Supplementary Material for this article can be found online at: https://www.frontiersin.org/articles/10.3389/fimmu.2020.02072/full#supplementary-material

Figure S1 | Temporal changes of body temperature, plasma C-reactive protein levels, lymphocyte counts and lactate dehydrogenase levels in 15 control patients. For patient 9, no C-reactive protein and lactate dehydrogenase levels are available during the admission period. Day 0 denotes the day of admission.

REFERENCES

1. Giamarellos-Bourboulis EJ, Netea MG, Rovina N, Akinosoglou K, Antoniadou A, Antonakos N, et al. Complex immune dysregulation in COVID-19 patients with severe respiratory failure. *Cell Host Microbe.* (2020) 27:992–1000.e3. doi: 10.1016/j.chom.2020.04.009
2. Siddiqi HK, Mehra MR. COVID-19 illness in native and immunosuppressed states: a clinical-therapeutic staging proposal. *J Heart Lung Transplant.* (2020) 39:405–7. doi: 10.1016/j.healun.2020.03.012
3. Walport MJ. Complement. Second of two parts. *N Engl J Med.* (2001) 344:1140–4. doi: 10.1056/NEJM200104123441506
4. Walport MJ. Complement. First of two parts. *N Engl J Med.* (2001) 344:1058–66. doi: 10.1056/NEJM200104053441406
5. Gralinski LE, Sheahan TP, Morrison TE, Menachery VD, Jensen K, Leist SR, et al. Complement activation contributes to severe acute respiratory syndrome coronavirus pathogenesis. *mBio.* (2018) 9:e01753-18. doi: 10.1128/mBio.01753-18
6. Jiang Y, Zhao G, Song N, Li P, Chen Y, Guo Y, et al. Blockade of the C5a-C5aR axis alleviates lung damage in hDPP4-transgenic mice infected with MERS-CoV. *Emerg Microbes Infect.* (2018) 7:77. doi: 10.1038/s41426-018-0063-8
7. Sun S, Zhao G, Liu C, Fan W, Zhou X, Zeng L, et al. Treatment with anti-C5a antibody improves the outcome of H7N9 virus infection in African green monkeys. *Clin Infect Dis.* (2015) 60:586–95. doi: 10.1093/cid/ciu887
8. Sun S, Zhao G, Liu C, Wu X, Guo Y, Yu H, et al. Inhibition of complement activation alleviates acute lung injury induced by highly pathogenic avian influenza H5N1 virus infection. *Am J Respir Cell Mol Biol.* (2013) 49:221–30. doi: 10.1165/rcmb.2012-0428OC
9. Gao T, Hu M, Zhang X. Highly pathogenic coronavirus N protein aggravates lung injury by MASP-2-mediated complement over-activation. *medRxi [Preprint].* (2020). doi: 10.1101/2020.03.29.20041962
10. Heja D, Kocsis A, Dobo J, Szilagyi K, Szasz R, Zavodszky P, et al. Revised mechanism of complement lectin-pathway activation revealing the role of serine protease MASP-1 as the exclusive activator of MASP-2. *Proc Natl Acad Sci USA.* (2012) 109:10498–503. doi: 10.1073/pnas.1202588109
11. Zhou Y, Lu K, Pfefferle S, Bertram S, Glowacka I, Drosten C, et al. A single asparagine-linked glycosylation site of the severe acute respiratory syndrome coronavirus spike glycoprotein facilitates inhibition by mannose-binding lectin through multiple mechanisms. *J Virol.* (2010) 84:8753–64. doi: 10.1128/JVI.00554-10
12. Cugno M, Meroni PL, Gualtierotti R, Griffini S, Grovetti E, Torri A, et al. Complement activation in patients with Covid-19: A novel therapeutic target. *J Allergy Clin Immunol.* (2020)146:215–7. doi: 10.1016/j.jaci.2020.05.006
13. Magro C, Mulvey JJ, Berlin D, Nuovo G, Salvatore S, Harp J, et al. Complement associated microvascular injury and thrombosis in the pathogenesis of severe COVID-19 infection: a report of five cases. *Transl Res.* (2020) 220:1–13. doi: 10.1016/j.trsl.2020.04.007
14. Sodhi CP, Wohlford-Lenane C, Yamaguchi Y, Prindle T, Fulton WB, Wang S, et al. Attenuation of pulmonary ACE2 activity impairs inactivation of des-Arg(9) bradykinin/BKB1R axis and facilitates LPS-induced neutrophil infiltration. *Am J Physiol Lung Cell Mol Physiol.* (2018) 314:L17–31. doi: 10.1152/ajplung.00498.2016
15. Helms J, Tacquard C, Severac F, Leonard-Lorant I, Ohana M, Delabranche X, et al. High risk of thrombosis in patients with severe SARS-CoV-2 infection: a multicenter prospective cohort study. *Inten Care Med.* (2020) 4:1–10. doi: 10.1007/s00134-020-06062-x
16. Poissy J, Goutay J, Caplan M, Parmentier E, Duburcq T, Lassalle F, et al. Pulmonary embolism in COVID-19 patients: awareness of an increased prevalence. *Circulation.* (2020) 142:184–6. doi: 10.1161/CIRCULATIONAHA.120.047430
17. Carvalho AC, DeMarinis S, Scott CF, Silver LD, Schmaier AH, Colman RW. Activation of the contact system of plasma proteolysis in the adult respiratory distress syndrome. *J Lab Clin Med.* (1988) 112:270–7.
18. Schmaier AH. The contact activation and kallikrein/kinin systems: pathophysiologic and physiologic activities. *J*

Thromb Haemost. (2016) 14:28–39. doi: 10.1111/jth.13194
19. Menter T, Haslbauer JD, Nienhold R, Savic S, Hopfer H, Deigendesch N, et al. Post-mortem examination of COVID19 patients reveals diffuse alveolar damage with severe capillary congestion and variegated findings of lungs and other organs suggesting vascular dysfunction. *Histopathology.* (2020). doi: 10.1111/his.14134. [Epub ahead of print].
20. Igonin AA, Protsenko DN, Galstyan GM, Vlasenko AV, Khachatryan NN, Nekhaev IV, et al. C1-esterase inhibitor infusion increases survival rates for patients with sepsis*. *Crit Care Med.* (2012) 40:770–7. doi: 10.1097/CCM.0b013e318236edb8
21. Hack CE, Ogilvie AC, Eisele B, Eerenberg AJ, Wagstaff J, Thijs LG. C1-inhibitor substitution therapy in septic shock and in the vascular leak syndrome induced by high doses of interleukin-2. *Inten Care Med.* (1993) 19(Suppl. 1):S19–28. doi: 10.1007/BF01738946
22. Caliezi C, Zeerleder S, Redondo M, Regli B, Rothen HU, Zurcher-Zenklusen R, et al. C1-inhibitor in patients with severe sepsis and septic shock: beneficial effect on renal dysfunction. *Criti Care Med.* (2002) 30:1722–8. doi: 10.1097/00003246-200208000-00008
23. Shen B, Yi X, Sun Y, Bi X, Du J, Zhang C, et al. Proteomic and metabolomic characterization of COVID-19 patient sera. *Cell.* (2020) 182:59–72.e15. doi: 10.1016/j.cell.2020.05.032
24. Thomson TM, Toscano E, Casis E, Paciucci R. C1-INH and the contact system in COVID-19. *Br J Haematol.* (2020). doi: 10.20944/preprints202005.0262.v1. [Epub ahead of print].
25. van Veen HA, Koiter J, Vogelezang CJ, van Wessel N, van Dam T, Velterop I, et al. Characterization of recombinant human C1 inhibitor secreted in milk of transgenic rabbits. *J Biotechnol.* (2012) 162:319–26. doi: 10.1016/j.jbiotec.2012.09.005
26. Wu Z, McGoogan JM. Characteristics of and important lessons from the coronavirus disease 2019 (COVID-19) outbreak in China: summary of a report of 72314 cases from the Chinese center for disease control and prevention. *JAMA*. (2020). doi: 10.1001/jama.2020.2648. [Epub ahead of print].
27. Colombi D, Bodini FC, Petrini M, Maffi G, Morelli N, Milanese G, et al. Well-aerated lung on admitting chest CT to predict adverse outcome in COVID-19 pneumonia. *Radiology*. (2020) 2020:201433. doi: 10.1148/radiol.2020201433
28. Ye Q, Wang B, Mao J. The pathogenesis and treatment of the 'cytokine Storm' in COVID-19. *J Infect.* (2020) 80:607–13. doi: 10.1016/j.jinf.2020.03.037
29. Risitano AM, Mastellos DC, Huber-Lang M, Yancopoulou D, Garlanda C, Ciceri F, et al. Complement as a target in COVID-19? *Nat Rev Immunol.* (2020) 20:343–4. doi: 10.1038/s41577-020-0320-7
30. Campbell CM, Kahwash R. Will complement inhibition be the new target in treating COVID-19 related systemic thrombosis? *Circulation.* (2020) 141:1739–41. doi: 10.1161/CIRCULATIONAHA.120.047419
31. Mastaglio S, Ruggeri A, Risitano AM, Angelillo P, Yancopoulou D, Mastellos DC, et al. The first case of COVID-19 treated with the complement C3 inhibitor AMY-101. *Clin Immunol.* (2020) 215:108450. doi: 10.1016/j.clim.2020.108450
32. Diurno F, Numis FG, Porta G, Cirillo F, Maddaluno S, Ragozzino A, et al. Eculizumab treatment in patients with COVID-19: preliminary results from real life ASL Napoli 2 Nord experience. *Eur Rev Med Pharmacol Sci.* (2020) 24:4040–7. doi: 10.26355/eurrev_202004_20875
33. Herold T, Jurinovic V, Arnreich C, Lipworth BJ, Hellmuth JC, Bergwelt-Baildon MV, et al. Elevated levels of IL-6 and CRP predict the need for mechanical ventilation in COVID-19. *J Allergy Clin Immunol.* (2020) 146:128–36.e4. doi: 10.1016/j.jaci.2020.05.008
34. Nuijens JH, Eerenberg-Belmer AJ, Huijbregts CC, Schreuder WO, Felt-Bersma RJ, Abbink JJ, et al. Proteolytic inactivation of plasma C1- inhibitor in sepsis. *J Clin Investig.* (1989) 84:443–50. doi: 10.1172/JCI114185

Conflict of Interest: BG reports being employed by Pharming Group NV. MT reports receiving grants from the Swiss National Science Foundation, Roche, Novartis, and Idorsia outside of the submitted work. MO reports receiving consulting fees from Pharming Biotechnologies B.V. during the conduct of the study and grants from Pharming Biotechnologies B.V. outside the submitted work.

The remaining authors declare that the research was conducted in the absence of any commercial or financial relationships that could be construed as a potential conflict of interest.

frontiers in Immunology

REVIEW
published: 07 October 2020
doi: 10.3389/fimmu.2020.583853

SLE: Novel Postulates for Therapeutic Options

Kinga K. Hosszu[1†], Alisa Valentino[2†], Ellinor I. Peerschke[2] and Berhane Ghebrehiwet[3]*

[1] Department of Pediatrics, Memorial Sloan Kettering Cancer Center, New York, NY, United States, [2] Department of Lab Medicine, Memorial Sloan Kettering Cancer Center, New York, NY, United States, [3] The Department of Medicine, Stony Brook University, Stony Brook, NY, United States

Genetic deficiency in C1q is a strong susceptibility factor for systemic lupus erythematosus (SLE). There are two major hypotheses that potentially explain the role of C1q in SLE. The first postulates that C1q deficiency abrogates apoptotic cell clearance, leading to persistently high loads of potentially immunogenic self-antigens that trigger autoimmune responses. While C1q undoubtedly plays an important role in apoptotic clearance, an essential biological process such as removal of self- waste is so critical for host survival that multiple ligand-receptor combinations do fortunately exist to ensure that proper disposal of apoptotic debris is accomplished even in the absence of C1q. The second hypothesis is based on the observation that locally synthesized C1q plays a critical role in regulating the earliest stages of monocyte to dendritic cell (DC) differentiation and function. Indeed, circulating C1q has been shown to keep monocytes in a pre-dendritic state by silencing key molecular players and ensuring that unwarranted DC-driven immune responses do not occur. Monocytes are also able to display macromolecular C1 on their surface, representing a novel mechanism for the recognition of circulating "danger." Translation of this danger signal in turn, provides the requisite "license" to trigger a differentiation pathway that leads to adaptive immune response. Based on this evidence, the second hypothesis proposes that deficiency in C1q dysregulates monocyte-to-DC differentiation and causes inefficient or defective maintenance of self-tolerance. The fact that C1q receptors (cC1qR and gC1qR) are also expressed on the surface of both monocytes and DCs, suggests that C1q/C1qR may regulate DC differentiation and function through specific cell-signaling pathways. While their primary ligand is C1q, C1qRs can also independently recognize a vast array of plasma proteins as well as pathogen-associated molecular ligands, indicating that these molecules may collaborate in antigen recognition and processing, and thus regulate DC-differentiation. This review will therefore focus on the role of C1q and C1qRs in SLE and explore the gC1qR/C1q axis as a potential target for therapy.

Keywords: c1q, gC1qR, cC1qR, complement, SLE, novel hypothesis

OPEN ACCESS

Edited by:
Elena Volokhina, Radboud University Nijmegen Medical Centre, Netherlands

Reviewed by:
Mihaela Gadjeva, Harvard Medical School, United States
Kenneth Reid, University of Oxford, United Kingdom

***Correspondence:**
Berhane Ghebrehiwet
Berhane.Ghebrehiwet@stonybrook.edu;
Berhane.Ghebrehiwet@stonybrookmedicine.edu

† These authors have contributed equally to this work

Specialty section:
This article was submitted to Molecular Innate Immunity, a section of the journal Frontiers in Immunology

Received: *15 July 2020*
Accepted: *10 September 2020*
Published: *07 October 2020*

Citation:
Hosszu KK, Valentino A, Peerschke EI and Ghebrehiwet B (2020) SLE: Novel Postulates for Therapeutic Options. Front. Immunol. 11:583853. doi: 10.3389/fimmu.2020.583853

Abbreviations: gC1q, the globular heads of C1q; cC1q, the collagen domain of C1q; gC1qR, receptor for gC1q; cC1qR, receptor for cC1q; CR calreticulin, (another name for cC1qR); ghA, ghB, and ghC, globular heads (gh) of the A, B, and C chains of C1q.

C1q: A BRIEF OVERVIEW

The first component of complement, C1, is a multimeric protein comprised of C1q and the Ca^{2+} – dependent tetramer $C1r_2$–$C1s_2$ (1–6). C1q itself is a 460 kDa collagen-like glycoprotein that is comprised of six globular "heads" (gC1q) linked to six collagen-like "stalks" (cC1q), and serves as the recognition signal triggering the classical pathway of complement (7–9). Each subunit of C1q is made up of three different, but highly conserved polypeptide chains – A, B, and C (10, 11). C1q belongs to the collectin (collagen containing lectin) family of molecules that contain collagen-like sequences contiguous with non-collagen-like stretches. Although it lacks a consensus carbohydrate recognition domain (which allows other collectins to recognize glycoconjugates containing mannose and fucose on microorganisms but not on self-proteins), C1q contains collagen sequences which allow it to bind to protein motifs in immunoglobulin (Ig)G or IgM. These motifs allow C1q to bind to immune complexes and engage in complement-mediated microbial killing and phagocytosis (12–14). While the majority of C1q circulates in plasma, it is also synthesized by many cell types including macrophages and dendritic cells (DCs), and secreted locally at sites of inflammation (15–24). Approximately 80% of circulating C1q is associated with the C1 complex, while the remaining portion is in its monomeric, "free" form (25).

In recent decades multiple groups have shown evidence that C1q plays a role in recognizing and clearing altered self and apoptotic cells by binding to the apoptotic cell surface and initiating phagocytic uptake by macrophages and DCs through interaction with C1q receptors expressed both on the phagocytic cell, (e.g., cC1qR/CD91) and the apoptotic cell (gC1qR and phosphatidylserine) (26–29). This clearance of immune complexes and apoptotic debris is crucial for maintaining homeostasis to avoid immune recognition of hidden epitopes – a critical immunopathogenic event leading to autoimmune disease.

C1q RECEPTORS

C1q receptors mediate many immunologic functions involved in innate and adaptive immunity. There are at least two types of distinct, ubiquitously expressed cell surface molecules which bind human C1q: gC1qR, the receptor for the globular heads, and cC1qR, the receptor for the collagen tail (28, 30–35).

Predominantly found in the storage compartments of the endoplasmic reticulum, cC1qR (60 kDa), a homolog of calreticulin (CR) (sometimes also referred to as cC1qR/CR or the "collagen receptor") fulfills a multiplicity of functions. It is a molecular chaperone, an extracellular compartment protein, an intracellular mediator of integrin function, an inhibitor of steroid hormone-regulated gene expression, and a receptor for C1q (36–43). However, studies have shown that C1q can only bind stably to cC1qR after it has been immobilized, heat-treated, or bound to IgG, suggesting that cC1qR is a receptor for an altered conformation of C1q (44, 45).

cC1qR does not contain a transmembrane domain or a GPI-anchor attachment site, and instead needs other adaptor molecules for signal transduction. One such molecule is CD91 (46), which binds to cC1qR and C1q on the surface of monocytes to initiate uptake of apoptotic cells (26). However, the uptake process cannot be completely inhibited by antibody blockade or genetic deficiency of CD91, indicating that it is not actually required for the C1q-mediated enhancement of phagocytosis (26, 47). Additional co-receptors of cC1qR are scavenger receptor A on antigen presenting cells (48), CD59 on neutrophils (49), α2β1 integrin and glycoprotein VI on resting platelets (50), MHC class I on T cells (51), and CD69 on human peripheral blood mononuclear cells (PBMCs) (52).

GC1qR (p32/p33/HABP1) is another well-described C1q receptor. It is a highly acidic homotrimer, comprised of three 33-kDa chains with a ubiquitous and multi-compartmental distribution including on the cell surface. As a result, gC1qR has a highly asymmetric surface charge with a negatively charged "solution face" exposed to plasma and a neutral or basic "membrane face" on the reverse side, suggesting that the two sides have different functions (53–56). It is present on the surface of human monocytes, DCs, macrophages, and many other cells (19, 33, 34, 57, 58). Additionally, gC1qR's capacity to elicit biological responses and transduce intracellular signals affects a variety of cell types (32, 57, 59–64). Similar to cC1qR, it lacks a transmembrane segment, and requires a docking/signaling partner, some of which are β1-integrins on endothelial cells (32), vasopressin V2 receptor on the HEK 293 cell line, alpha(1B)-adrenergic receptor on the COS 7 cell line (65), DC-SIGN on DCs (66, 67) and LAIR-1 on DCs and T cells (68–71).

Due to gC1qR's ability to recognize and bind to a plethora of ligands, many pathogens employ immune escape mechanisms to exploit the normal regulatory functions of C1q/gC1qR. Among the growing list of pathogenic microorganisms are HIV (67, 72–74), adenovirus (75, 76), Epstein-Barr virus (77), Herpesvirus Saimiri (78), rubella virus (79–81), hepatitis B virus (82), hepatitis C virus (HCV) (59, 63, 74), *L. monocytogenes* (83), *S. aureus* (84), and *B. cereus* (85). These microorganisms have a strong affinity for gC1qR, which further indicates that gC1qR plays an important role in immune regulation. For example, *in vitro* studies have shown that HCV, which binds gC1qR at the C1q binding site, employs gC1qR on monocyte-DC precursors to prevent DC immunogenic activity (57, 58).

C1q AND SLE

The connection between C1q and autoimmune diseases such as rheumatoid arthritis (RA) and systemic lupus erythematosus (SLE) is well established. In RA, antibodies to C1q may cross-react with collagen type II and contribute to the disease process that leads to tissue destruction and inflammation (86, 87). In animal models of RA, C1q function is impaired by autoantibodies, indicating a regulatory role for C1q in suppressing immune activity (87, 88). Moreover, a synthetic decapeptide corresponding to the A-chain of C1q injected into

DBA/1 mice delays disease onset and reduces the severity of collagen-induced arthritis (86, 89).

Hereditary homozygous C1q deficiency, while rare, is the strongest known susceptibility factor for SLE (90–93). The vast majority of patients (≥95%) develop clinical symptoms closely related to SLE, with rashes, glomerulonephritis, and central nervous system disease (91, 94). Additionally, about a third of SLE patients have high affinity autoantibodies to C1q directed to a neo-epitope in the A-chain (91, 94). In a subset of patients who are C1q sufficient, the SLE disease process itself causes consumption of C1q, therefore mimicking the genetic deficiency of C1q. This acquired partial deficiency of C1q, either due to complement activation or to the presence of anti-C1q autoantibodies, is even more commonly observed in lupus patients than genetic C1q deficiency (92, 95, 96). Multiple studies have shown associations between the presence of anti-C1q antibodies and active nephritis in SLE (97–100). There is, however, evidence that the presence of anti-C1q antibodies is not associated with active lupus nephritis, but rather with SLE global activity, indicating that although C1q's main function is the clearance of immune complexes during apoptosis, it has other biologic functions with inhibitory/protective factors (30).

C1q plays a critical role in recognizing harmful molecules, ranging from pathogen-associated molecular ligands (non-self) to damage-associated molecular targets (altered self) (29). Therefore, in this manner, C1q acts as a molecular bridge between the phagocytic cell and the apoptotic debris to be cleared. While many studies suggest that failure to properly clear apoptotic cells in the absence of C1q could result in an immunogenic state (91, 94, 101), many observations have challenged this idea. Disruption of other apoptotic uptake processes, such as those mediated by CD14 (102), β3 or β5 integrin (103), mannose-binding lectin (104), all result in the accumulation of apoptotic bodies without triggering autoimmunity. In fact, apoptotic cells can actively inhibit the inflammatory program. For example, preincubating macrophages with apoptotic cells can significantly reduce the inflammatory response induced by lipopolysaccharide (LPS) (105–107). During this process, anti-inflammatory cytokines, such as transforming growth factor (TGF)-β and interleukin (IL)-10, are released and act via paracrine or autocrine mechanisms to sustain an anti-inflammatory state (107). Administration or accumulation of apoptotic cells have been shown to ameliorate multiple inflammatory disorders, such as diabetes (108, 109), Experimental Autoimmune Encephalomyelitis (110, 111), arthritis (112), colitis (113), pulmonary fibrosis (114–116), fulminant hepatitis (117), contact hypersensitivity (118, 119), acute and chronic graft rejection (120–123), and hematopoietic cell engraftment (124–127). Data from these studies indicate that apoptotic cells modulate immune responses and can prevent the onset and/or establishment of inflammatory disease. Based on these observations, it is likely that processes other than the accumulation of apoptotic debris play a decisive role in SLE development.

In recent years, increasing evidence has emerged that aside from the recognition and triggering of the classical complement pathway, C1q also modulates the acquired immune response. In this context, C1q provides active protection from autoimmunity by silencing key molecular markers or regulating autoreactive immune cells.

Multiple studies have shown that C1q regulates cytokine secretion and polarizes antigen presenting cells (APCs) toward a tolerogenic phenotype (17, 128–135). Specifically, macrophages and DCs that have been exposed to C1q exhibit enhanced production of anti−inflammatory and reduced pro-inflammatory cytokines (129, 134, 135). Immature DCs (iDC) in the presence of immobilized C1q have reduced capacity to induce allogeneic Th1 and Th17 cells, and demonstrate a trend toward increased Treg proliferation (130, 136). Furthermore, C1q-primed macrophages have elevated PD-L1 and PD-L2 and suppressed surface CD40, and C1q-polarized DCs have higher surface PD-L2 and reduced CD86 (130). Plasmacytoid DCs (pDCs), a major interferon-α (IFN-α)-producing cell type, also play a pivotal role in SLE pathogenesis (137–139). In the presence of immune complexes, C1q interacts with pDCs and strongly inhibits IFN-α production (140–142), while in the absence of C1q, immune complexes can preferentially engage pDCs and increase IFN-α production (143). These data suggest that C1q provides a protective, anti-inflammatory function by regulating IFN-α production in pDCs.

Our lab was the first to show that monocytes are able to display macromolecular C1 on their surface with the globular heads of C1q displayed outwardly, toward the extracellular milieu (144). Thus, membrane associated C1q can potentially recognize and capture circulating immune complexes or pathogen-associated molecular patterns and signal monocytes to migrate into tissues, differentiate into macrophages or DCs, and initiate the process of antigen elimination. Unoccupied C1q, on the other hand, may silence key molecular players, ensuring that unwarranted DC-driven immune responses do not occur.

Using a C1q-deficient mouse model of SLE, Ling et al. showed that C1q ameliorates the response to self-antigens by modulating the mitochondrial metabolism of CD8+ T cells (145). Conversely, C1q deficiency can trigger an effector CD8+ T cell response to chronic viral infection leading to lethal immunopathology.

Taken together, these data suggest that upon interacting with APCs, C1q regulates the subsequent activation of T effector functions to modulate the adaptive immune response and prevent the initiation/propagation of autoimmunity.

C1q RECEPTORS AS AN IMMUNE CHECKPOINT

While the wide array of immunological processes exhibited by C1q appear to be the principal component of its immune-modulatory function, its underlying mechanisms remain poorly described. The unique structure of C1q, which allows it to interact with its primary receptors, gC1qR and cC1qR, via either its globular head or collagen tail domains, may shed light to this dilemma. The observation that C1q functions as a molecular switch during the narrow window of monocyte to DC transition (128, 133) is also reflected by the differential expression of gC1qR and cC1qR during this process (**Figure 1**) (128). While gC1qR is steadily expressed, the expression of cC1qR is low on monocytes

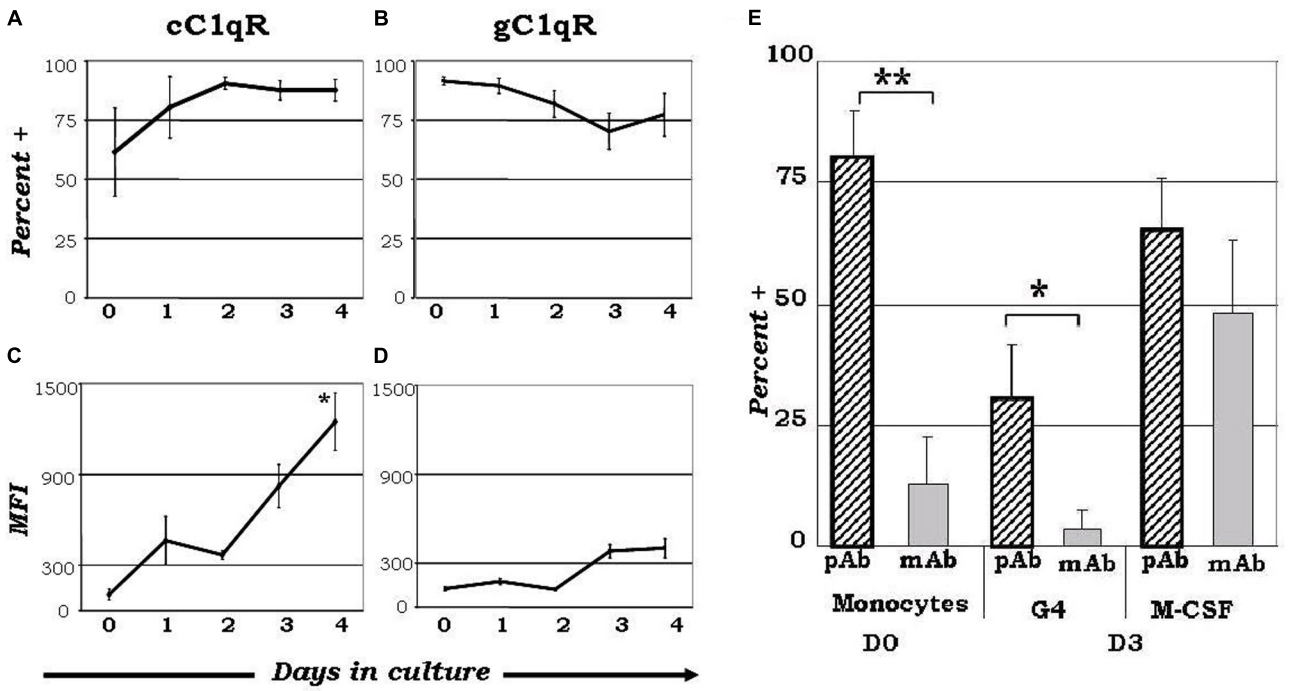

FIGURE 1 | Varied expression of C1q receptors and specific binding orientation of surface bound C1q on monocyte-DC precursors may regulate DC differentiation events. Mononuclear cells cultured in the presence of GM-CSF+ IL-4 were analyzed for the expression of cC1qR **(A,C)** and gC1qR **(B,D)** expression, and C1q binding orientation **(E)**. **(A)** The percentage of cC1qR expression was variable on monocytes, but by day 2 nearly all monocyte-DCs had the receptor on their surface (n = 4). (B) On day 0, gC1qR was present on almost all the cells, and its expression was only slightly reduced by day 4 (n = 4). **(C)** Mean fluorescence analysis revealed that cC1qR expression was dramatically amplified by days 3 and 4 (n = 4). **(D)** Mean fluorescence intensity of gC1qR remained at relatively steady levels throughout the days (n = 4). **(E)** C1q is bound to the monocyte and DC surface via its globular head regions, while on M-CSF treated monocyte-macrophages its orientation is reversed. Binding orientation of C1q was determined using monoclonal antibodies specific to the globular head regions of C1q as well as polyclonal antibodies to the whole protein, and assessed by flow cytometry (n = 3). Experiments were gated on HLA-DR$^+$ cells. *P < 0.05, **P < 0.01. [Adapted from ref (128)]

and increases as the cells commit to the dendritic cell lineage. At the time corresponding to firm commitment to the DC lineage, there is an inverse correlation between gC1qR and cC1qR expression on the cell surface, which, in turn, may influence the nature and specificity of the cells' response to C1q (128).

Upon binding to C1qR, specific pathways get activated to trigger downstream signaling. Incubating C1q or a monoclonal antibody which recognizes the C1q binding site on gC1qR, with T cells, inhibits T cell proliferation, possibly through the activation of PI3K, NADPH oxidase and p190 RhoGAP (53, 146). Additionally, it causes the inactivation of TC10, and the translocation of NKp44L from the cytoplasm to the plasma membrane (147). Ligand engagement of gC1qR at the C1q binding site (by HCV core protein and mAb) in LPS-stimulated monocytes increases PI3K activation and Akt phosphorylation, and in macrophages it induces A20 expression via P38, JNK and NF-κB signaling pathways, in an ERK independent manner (57, 58, 148). Similarly, engagement of gC1qR by C1q activates the MAPK and PI3K/AKT signaling pathways in macrophages (148). Furthermore, binding of HCV core protein to gC1qR down-regulates many inflammatory cytokines in macrophages, including IL-6 and IL-1β, indicating that gC1qR relays an anti-inflammatory signal (148). Conversely, ligation of cC1qR by a mAb increases TNFα and IL6 secretion, as well as the expression and phosphorylation of STAT6 in macrophages, indicating that cC1qR is a pro-inflammatory receptor (149).

C1q also engages in molecular complexing at the cell surface. In monocyte-derived iDCs, C1q, DC-SIGN and gC1qR form a trimolecular complex on the plasma membrane, which is presumed to modulate DC differentiation and function through DC-SIGN-mediated signaling pathways [26]. Signaling through DC-SIGN has been shown to increase phosphorylation of Raf-1 on Ser338 and Tyr340/341 (150). Furthermore, stimulation of DC-SIGN with a mannose receptor-1 Ab activates the MEK/ERK kinase cascade (151). However, whether direct stimulation of C1q participates in these signaling pathways still remains to be investigated.

The leukocyte-associated immunoglobulin-like receptor 1 (LAIR-1) is another C1q-binding transmembrane receptor that can serve as a potential co-receptor to gC1qR. On T cells, LAIR-1 engagement by C1q inhibits TCR signaling by decreasing the phosphorylation of LCK, LYN, ZAP-70, extracellular signal-regulated kinase, c-Jun N-terminal kinase 1/2, and p38, indicating that LAIR-1 activation may be a strategy for controlling inflammation (70). Studies by Son et al. showed that C1q and HMGB1 can cooperate to terminate inflammation, and induce the differentiation of monocytes to anti-inflammatory M2-like macrophages through a complex with RAGE and

LAIR-1 (71). In myelomonocytes, the globular head of C1q binds to CD33 and LAIR-1 and activates CD33/LAIR-1 inhibitory motifs (68). Binding of C1q to LAIR-1 on monocytes significantly up-regulates the expression of IL-8, IL-10, LAIR-1, and the phosphorylation of JNK, p38-MAPK, AKT, and NF-κ B (152).

Taken together, these data suggest that the regulatory effects of C1q may depend on specific C1q/C1qR interactions; and these interactions may in turn control the transition from the tolerogenic state toward a pro-inflammatory state. Fundamental to this mechanism is the differential expression of the C1q/C1qR system, which, through the engagement of distinct receptors (gC1qR versus cC1qR), and the resulting binding orientation of C1q – heads versus tails – actively avoids self-directed adaptive immune responses to modified-self as well as non-self antigens.

As illustrated by **Figure 2**, this functional duality of the C1q/gC1qR axis is very similar to the role of the PD1/PDL1 checkpoint in cancer, which helps maintain the balance between immune surveillance and cancer cell proliferation (153). In this setting, the C1q/C1qR axis would serve as an immune checkpoint supporting a tolerogenic/anti-inflammatory signal by the interaction between membrane-associated C1q on the signaling cell or soluble C1q in the extracellular milieu, and the membrane associated C1q receptors on the target cell. Conversely, when this interaction is blocked by antigen binding to the soluble or membrane-associated C1q, a pro-inflammatory signal is relayed through cC1qR. These specific interactions ensure that the immune system is activated only at the appropriate time in order to minimize the possibility of chronic autoimmune inflammation.

THE C1q/C1qR AXIS: A FUNCTIONAL EXAMPLE

The role of C1q in the regulation of DC differentiation and function has been greatly studied in recent years. A significant portion of the work has centered, around the potential regulatory role of C1q during DC maturation, once the cells have fully committed to the DC lineage. These data show that C1q treatment of LPS-primed human iDCs decreases the cell surface expression of CD80, CD83 and CD86, the secretion of IL-6, TNF-α, and IL-10, as well as the ability of the cells to stimulate T helper (T_H) 1 cell proliferation in a mixed leukocyte reaction (154). These results suggest that C1q treated iDCs may be resistant to LPS-induced maturation. Yamada and colleagues showed that C1q treatment after LPS-stimulation

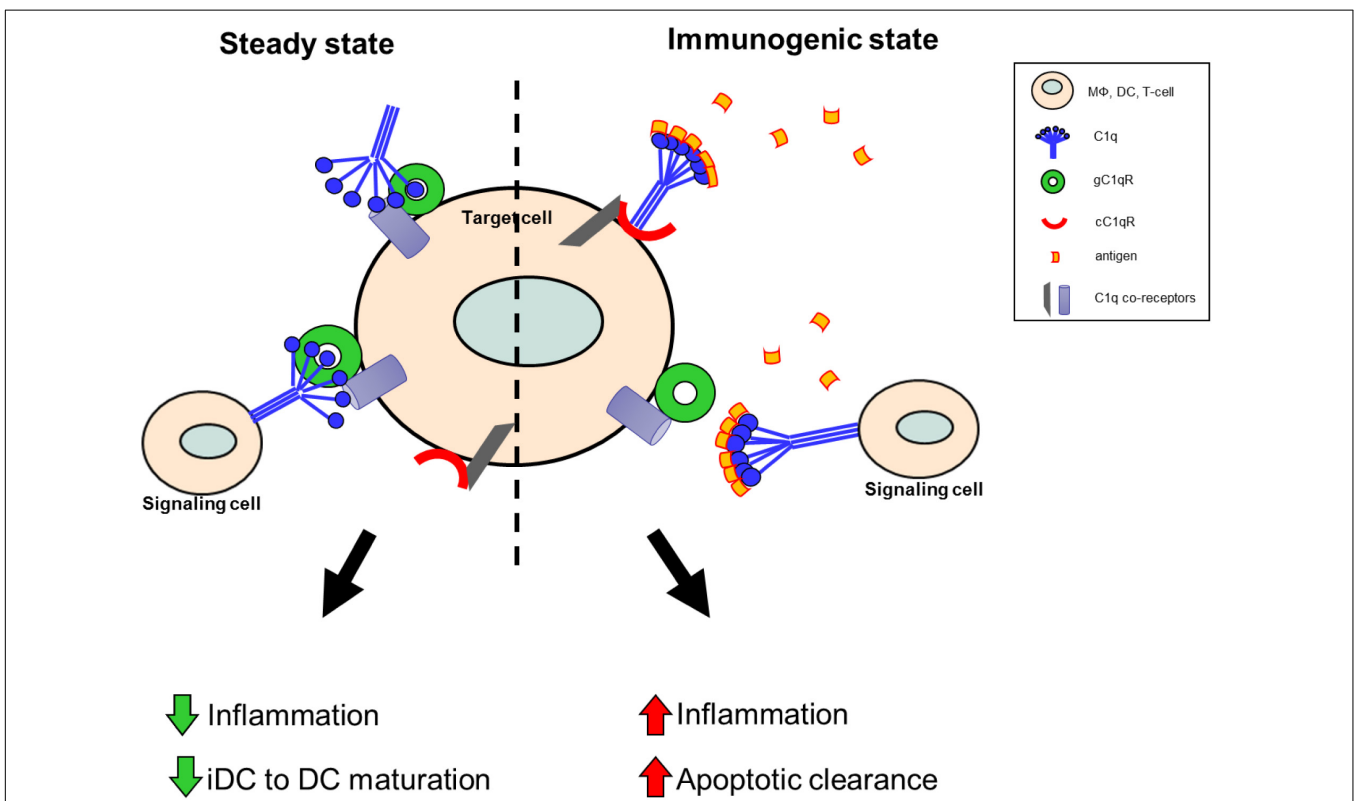

FIGURE 2 | Theoretical model of the C1q/gC1qR immune checkpoint in inflammation and autoimmunity. Under steady state conditions, in the absence of danger signals (PAMPs, DAMPs, etc.), membrane-associated C1q on the signaling cell, or soluble C1q in the extracellular milieu, is available to bind to gC1qR on the target cell to support a tolerogenic state. During these conditions anti-inflammatory processes are dominant and DC maturation is decreased to keep cells in a tolerogenic/immature state. When C1q recognizes and captures circulating immune complexes or pathogen-associated molecular patterns, it undergoes a conformational change and only the collagen tail is available to bind. Thus, the resulting C1q/cC1qR interactions drive increased pro-inflammatory signals and signal monocytes to migrate into tissues, differentiate into macrophages or DCs, and initiate the process of antigen elimination.

or CpG oligodeoxynucleotide induction suppresses IL-12p40 production in bone marrow-derived DCs, reduces NF-κB activity and delays the phosphorylation of p38, c-Jun N-terminal kinase, and extracellular signal-regulated kinase (155). These data further indicate that C1q may function by suppressing pro-inflammatory responses after DC activation. As ligation of gC1qR results in decreased secretion of pro-inflammatory cytokines like IL-6 and TNFα, soluble C1q in these experiments putatively acts through a gC1qR-mediated pathway.

However, in order to imitate the role of C1q as an opsonin *in vitro*, some studies employed immobilized C1q. Nauta and colleagues found that the uptake of C1q-opsonized apoptotic cells by iDCs stimulated the production of IL-6, IL-10, and TNF-α, without an effect on IL-12p70 (156). Additionally, iDCs placed on immobilized C1q, gC1q or cC1q, showed enhanced maturation, translocation of NF-κB to the nucleus and enhanced secretion of IL-12 and TNF-α, in addition to elevated T_H1-stimulating capacity (157). The increased secretion of pro-inflammatory cytokines in these studies suggest that fixation of C1q supports DC maturation and acts in a cC1qR-mediated pathway.

So far, very little data is available on how soluble C1q that is present in the plasma and interstitial tissues under steady state conditions might regulate DC differentiation during the earliest stages of mono-DC growth. These yet unexplored functions would provide important details of how C1q regulates adaptive immune functions via iDCs in the absence of infection or inflammation. Studies from our lab (158) and others (159) have shown that C1q acts as a chemoattractant to iDCs, but not mature DCs. C1q-induced migration is mediated through ligation of both gC1qR and cC1qR and activation of Akt and MAPK pathways. C1q treatment during DC differentiation was also shown to give rise to $CD1a^+$DC-$SIGN^+$ iDCs with high phagocytic capacity, and low expression of CD80, CD83, and CD86 (154). Because this narrow window of differentiation represents the important interface between innate and adaptive immunity, more work is needed to explore this crucial stage.

IMPLICATIONS FOR THERAPY AND CONCLUDING REMARKS

Since C1q and C1qRs are involved in a multitude of inflammatory processes that accompany various disease conditions, including infection, cancer, and autoimmune diseases, understanding the underlying mechanism is important to identify new targets for the design of therapeutic strategies. While the role of C1q in apoptotic clearance has been well described and is supported by a plethora of evidence, it is still not clear how deficiency of C1q contributes to the loss of tolerance. This review is aimed to provide new insights and stimulate discussion around the topic. Understanding how the interactions between C1q and C1qRs control the transition from steady state to a pro-inflammatory response, will not only give us insight into how the C1q/C1qR system regulates the immune response, but may also provide us with alternative approaches for designing better therapeutic options. Molecules or peptides that inhibit the interaction between antigen-bound C1q and cC1qR, or those that can mimic the interaction between C1q and gC1qR, can potentially be used as templates for the development of therapeutic interventions to reduce C1q-mediated pro-inflammatory responses. One potential target for an inhibitory-drug design is the N-terminal region (residues 160–283) on the collagen tail of C1q, which binds to cC1qR, and contains several short (7–10 amino acids) CH2-like motifs (ExKxKx) similar to the C1q binding motif found in the CH2 domain of IgG (160). For gC1qR, some therapeutic molecules already exist. One example is the use of mAb 74.5.2, which inhibits the binding of kininogen to gC1qR, thus blocking the generation of bradykinin and other vasoactive molecules that have been shown to contribute to inflammation (161). Another example of a therapeutic molecule is mAb 60.11, which is specific to the C1q binding site on gC1qR (aa 76–93). This antibody has been shown to reduce cell proliferation, decrease tumor growth, increase apoptosis, and impair angiogenesis (162). In summary, the data reviewed in this article supports the idea that the C1q/C1qR system is an ideal molecular target for the design of antibody- or peptide-based therapy to attenuate acute and chronic inflammation associated with autoimmune diseases, SLE in particular.

AUTHOR CONTRIBUTIONS

BG supervised the work. All authors contributed to the article and approved the submitted version.

FUNDING

The work included in this article was supported in part by grants from the National Institutes of Allergy and Infectious Diseases R01 AI 060866, R01 AI-084178, and R56-AI 1223476 (to BG) and the NIH/NCI cancer support grant P30 CA008748 (to MSKCC).

REFERENCES

1. Perkins SJ. Molecular modelling of human complement subcomponent C1q and its complex with C1r2C1s2 derived from neutron-scattering curves and hydrodynamic properties. *Biochem J*. (1985) 228:13–26. doi: 10.1042/bj2280013
2. Siegel RC, Schumaker VN. Measurement of the association constants of the complexes formed between intact C1q or pepsin-treated C1q stalks and the unactivated or activated C1r2C1s2 tetramers. *Mol Immunol*. (1983) 20:53–66. doi: 10.1016/0161-5890(83)90105-0
3. Weiss V, Fauser C, Engel J. Functional model of subcomponent C1 of human complement. *J Mol Biol*. (1986) 189:573–81. doi: 10.1016/0022-2836(86)90325-6
4. Calcott MA, Müller-Eberhard HJ. C1q protein of human complement. *Biochemistry*. (1972) 11:3443–50. doi: 10.1021/bi00768a018
5. Lepow IH, Naff GB, Todd EW, Pensky J, Hinz CF. Chromatographic resolution of the first component of human complement into three activities. *J Exp Med*. (1963) 117:983–1008. doi: 10.1084/jem.117.6.983
6. Muller-Eberhard HJ, Kunkel HG. Isolation of a thermolabile serum protein which precipitates gamma-globulin aggregates and participates in immune

hemolysis. *Proc Soc Exp Biol Med*. (1961) 106:291–5. doi: 10.3181/00379727-106-26313
7. Brodsky-Doyle B, Leonard KR, Reid KB. Circular-dichroism and electron-microscopy studies of human subcomponent C1q before and after limited proteolysis by pepsin. *Biochem J*. (1976) 159:279–86. doi: 10.1042/bj1590279
8. Reid KB, Porter RR. Subunit composition and structure of subcomponent C1q of the first component of human complement. *Biochem J*. (1976) 155:19–23. doi: 10.1042/bj1550019
9. Reid KB. Chemistry and molecular genetics of C1q. *Behring Inst Mitt*. (1989) 84:8–19.
10. Sasaki T, Yonemasu K. Chemical studies on the isolated collagen-like and globular fragment of complement component C1q. Comparative studies on bovine and human C1q. *Biochim Biophys Acta*. (1983) 742:122–8. doi: 10.1016/0167-4838(83)90367-9
11. Kishore U, Leigh LE, Eggleton P, Strong P, Perdikoulis MV, Willis AC, et al. Functional characterization of a recombinant form of the C-terminal, globular head region of the B-chain of human serum complement protein C1q. *Biochem J*. (1998) 333(Pt 1):27–32. doi: 10.1042/bj3330027
12. Lu J, Wiedemann H, Timpl R, Reid KB. Similarity in structure between C1q and the collectins as judged by electron microscopy. *Behring Inst Mitt*. (1993) 93:6–16.
13. Bobak DA, Gaither TA, Frank MM, Tenner AJ. Modulation of FcR function by complement: subcomponent C1q enhances the phagocytosis of IgG-opsonized targets by human monocytes and culture-derived macrophages. *J Immunol*. (1987) 138:1150–6.
14. Leist-Welsh P, Bjornson AB. Immunoglobulin-independent utilization of the classical complement pathway in opsonophagocytosis of *Escherichia coli* by human peripheral leukocytes. *J Immunol*. (1982) 128:2643–51. doi: 10.1016/0161-5890(82)90091-8
15. Schwaeble W, Schäfer MK, Petry F, Fink T, Knebel D, Weihe E, et al. Follicular dendritic cells, interdigitating cells, and cells of the monocyte-macrophage lineage are the C1q-producing sources in the spleen. Identification of specific cell types by in situ hybridization and immunohistochemical analysis. *J Immunol*. (1995) 155:4971–8.
16. Bensa JC, Reboul A, Colomb MG. Biosynthesis in vitro of complement subcomponents C1q, C1s and C1 inhibitor by resting and stimulated human monocytes. *Biochem J*. (1983) 216:385–92. doi: 10.1042/bj2160385
17. Castellano G, Woltman AM, Nauta AJ, Roos A, Trouw LA, Seelen MA, et al. Maturation of dendritic cells abrogates C1q production in vivo and in vitro. *Blood*. (2004) 103:3813–20. doi: 10.1182/blood-2003-09-3046
18. Kaul M, Loos M. Expression of membrane C1q in human monocyte-derived macrophages is developmentally regulated and enhanced by interferon-gamma. *FEBS Lett*. (2001) 500:91–8. doi: 10.1016/s0014-5793(01)02592-3
19. Vegh Z, Goyarts EC, Rozengarten K, Mazumder A, Ghebrehiwet B. Maturation-dependent expression of C1q-binding proteins on the cell surface of human monocyte-derived dendritic cells. *Int Immunopharmacol*. (2003) 3:345–57. doi: 10.1016/S1567-5769(02)00234-5
20. Dillon SP, D'Souza A, Kurien BT, Scofield RH. Systemic lupus erythematosus and C1q: a quantitative ELISA for determining C1q levels in serum. *Biotechnol J*. (2009) 4:1210–4. doi: 10.1002/biot.200800273
21. Hughes-Jones NC. Functional affinity constants of the reaction between 125I-labelled C1q and C1q binders and their use in the measurement of plasma C1q concentrations. *Immunology*. (1977) 32:191–8.
22. Schuller E, Helary M. Determination in the nanogram range of C1q in serum and unconcentrated CSF by electro-immunodiffusion. *J Immunol Methods*. (1983) 56:159–65. doi: 10.1016/0022-1759(83)90407-6
23. Breitner S, Störkel S, Reichel W, Loos M. Complement components C1q, C1r/C1s, and C1INH in rheumatoid arthritis. Correlation of in situ hybridization and northern blot results with function and protein concentration in synovium and primary cell cultures. *Arthritis Rheum*. (1995) 38:492–8. doi: 10.1002/art.1780380406
24. Soda K, Ando M, Sakata T, Sugimoto M, Nakashima H, Araki S. C1q and C3 in bronchoalveolar lavage fluid from patients with summer-type hypersensitivity pneumonitis. *Chest*. (1988) 93:76–80. doi: 10.1378/chest.93.1.76
25. Sjöholm AG, Mårtensson U, Laurell AB. C1 dissociation in serum: estimation of free C1q by electroimmunoassay. *Acta Pathol Microbiol Immunol Scand C*. (1985) 93:161–8. doi: 10.1111/j.1699-0463.1985.tb02939.x
26. Vandivier RW, Ogden CA, Fadok VA, Hoffmann PR, Brown KK, Botto M, et al. Role of surfactant proteins A, D, and C1q in the clearance of apoptotic cells in vivo and in vitro: calreticulin and CD91 as a common collectin receptor complex. *J Immunol*. (2002) 169:3978–86. doi: 10.4049/jimmunol.169.7.3978
27. Korb LC, Ahearn JM. C1q binds directly and specifically to surface blebs of apoptotic human keratinocytes: complement deficiency and systemic lupus erythematosus revisited. *J Immunol*. (1997) 158:4525–8.
28. Ogden CA, deCathelineau A, Hoffmann PR, Bratton D, Ghebrehiwet B, Fadok VA, et al. C1q and mannose binding lectin engagement of cell surface calreticulin and CD91 initiates macropinocytosis and uptake of apoptotic cells. *J Exp Med*. (2001) 194:781–95. doi: 10.1084/jem.194.6.781
29. Païdassi H, Tacnet-Delorme P, Garlatti V, Darnault C, Ghebrehiwet B, Gaboriaud C, et al. C1q binds phosphatidylserine and likely acts as a multiligand-bridging molecule in apoptotic cell recognition. *J Immunol*. (2008) 180:2329–38. doi: 10.4049/jimmunol.180.4.2329
30. Ghebrehiwet B, Lim BL, Peerschke EI, Willis AC, Reid KB. Isolation, cDNA cloning, and overexpression of a 33-kD cell surface glycoprotein that binds to the globular "heads" of C1q. *J Exp Med*. (1994) 179:1809–21. doi: 10.1084/jem.179.6.1809
31. Peterson KL, Zhang W, Lu PD, Keilbaugh SA, Peerschke EI, Ghebrehiwet B. The C1q-binding cell membrane proteins cC1q-R and gC1q-R are released from activated cells: subcellular distribution and immunochemical characterization. *Clin Immunol Immunopathol*. (1997) 84:17–26. doi: 10.1006/clin.1997.4374
32. Feng X, Tonnesen MG, Peerschke EIB, Ghebrehiwet B. Cooperation of C1q receptors and integrins in C1q-mediated endothelial cell adhesion and spreading. *J Immunol*. (2002) 168:2441–8. doi: 10.4049/jimmunol.168.5.2441
33. Herwald H, Dedio J, Kellner R, Loos M, Müller-Esterl W. Isolation and characterization of the kininogen-binding protein p33 from endothelial cells. Identity with the gC1q receptor. *J Biol Chem*. (1996) 271:13040–7. doi: 10.1074/jbc.271.22.13040
34. Peerschke EI, Reid KB, Ghebrehiwet B. Identification of a novel 33-kDa C1q-binding site on human blood platelets. *J Immunol*. (1994) 152:5896–901.
35. Sim RB, Moestrup SK, Stuart GR, Lynch NJ, Lu J, Schwaeble WJ, et al. Interaction of C1q and the collectins with the potential receptors calreticulin (cC1qR/collectin receptor) and megalin. *Immunobiology*. (1998) 199:208–24. doi: 10.1016/s0171-2985(98)80028-4
36. Malhotra R. Collectin receptor (C1q receptor): structure and function. *Behring Inst Mitt*. (1993) 93:254–61.
37. Malhotra R, Sim RB, Reid KB. Interaction of C1q, and other proteins containing collagen-like domains, with the C1q receptor. *Biochem Soc Trans*. (1990) 18:1145–8. doi: 10.1042/bst0181145
38. Nauseef WM, McCormick SJ, Clark RA. Calreticulin functions as a molecular chaperone in the biosynthesis of myeloperoxidase. *J Biol Chem*. (1995) 270:4741–7. doi: 10.1074/jbc.270.9.4741
39. Wada I, Imai S, Kai M, Sakane F, Kanoh H. Chaperone function of calreticulin when expressed in the endoplasmic reticulum as the membrane-anchored and soluble forms. *J Biol Chem*. (1995) 270:20298–304. doi: 10.1074/jbc.270.35.20298
40. Somogyi E, Petersson U, Hultenby K, Wendel M. Calreticulin–an endoplasmic reticulum protein with calcium-binding activity is also found in the extracellular matrix. *Matrix Biol*. (2003) 22:179–91. doi: 10.1016/S0945-053X(02)00117-8
41. Dedhar S. Novel functions for calreticulin: interaction with integrins and modulation of gene expression? *Trends Biochem Sci*. (1994) 19:269–71. doi: 10.1016/0968-0004(94)90001-9
42. Burns K, Duggan B, Atkinson EA, Famulski KS, Nemer M, Bleackley RC, et al. Modulation of gene expression by calreticulin binding to the glucocorticoid receptor. *Nature*. (1994) 367:476–80. doi: 10.1038/367476a0
43. Platet N, Cunat S, Chalbos D, Rochefort H, Garcia M. Unliganded and liganded estrogen receptors protect against cancer invasion via different mechanisms. *Mol Endocrinol*. (2000) 14:999–1009. doi: 10.1210/mend.14.7.0492
44. Vandenberg RJ, Easterbrook-Smith SB. Conformational changes in C1q upon binding to IgG oligomers. *FEBS Lett*. (1986) 207:276–9. doi: 10.1016/0014-5793(86)81504-6

45. Steinø A, Jørgensen CS, Laursen I, Houen G. Interaction of C1q with the receptor calreticulin requires a conformational change in C1q. *Scand J Immunol*. (2004) 59:485–95. doi: 10.1111/j.0300-9475.2004.01425.x
46. Basu S, Binder RJ, Ramalingam T, Srivastava PK. CD91 is a common receptor for heat shock proteins gp96, hsp90, hsp70, and calreticulin. *Immunity*. (2001) 14:303–13. doi: 10.1016/s1074-7613(01)00111-x
47. Lillis AP, Greenlee MC, Mikhailenko I, Pizzo SV, Tenner AJ, Strickland DK, et al. Murine low-density lipoprotein receptor-related protein 1 (LRP) is required for phagocytosis of targets bearing LRP ligands but is not required for C1q-triggered enhancement of phagocytosis. *J Immunol*. (2008) 181:364–73. doi: 10.4049/jimmunol.181.1.364
48. Berwin B, Hart JP, Rice S, Gass C, Pizzo SV, Post SR, et al. Scavenger receptor-A mediates gp96/GRP94 and calreticulin internalization by antigen-presenting cells. *EMBO J*. (2003) 22:6127–36. doi: 10.1093/emboj/cdg572
49. Ghiran I, Klickstein LB, Nicholson-Weller A. Calreticulin is at the surface of circulating neutrophils and uses CD59 as an adaptor molecule. *J Biol Chem*. (2003) 278:21024–31. doi: 10.1074/jbc.M302306200
50. Elton CM, Smethurst PA, Eggleton P, Farndale RW. Physical and functional interaction between cell-surface calreticulin and the collagen receptors integrin alpha2beta1 and glycoprotein VI in human platelets. *Thromb Haemost*. (2002) 88:648–54. doi: 10.1267/th02100648
51. Santos SG, Powis SJ, Arosa FA. Misfolding of major histocompatibility complex class I molecules in activated T cells allows cis-interactions with receptors and signaling molecules and is associated with tyrosine phosphorylation. *J Biol Chem*. (2004) 279:53062–70. doi: 10.1074/jbc.M408794200
52. Vance BA, Harley PH, Backlund PS, Ward Y, Phelps TL, Gress RE. Human CD69 associates with an N-terminal fragment of calreticulin at the cell surface. *Arch Biochem Biophys*. (2005) 438:11–20. doi: 10.1016/j.abb.2005.04.009
53. Ghebrehiwet B, Lu PD, Zhang W, Lim BL, Eggleton P, Leigh LE, et al. Identification of functional domains on gC1Q-R, a cell surface protein that binds to the globular "heads" of C1Q, using monoclonal antibodies and synthetic peptides. *Hybridoma*. (1996) 15:333–42. doi: 10.1089/hyb.1996.15.333
54. Ghebrehiwet B, Tantral L, Titmus MA, Panessa-Warren BJ, Tortora GT, Wong SS, et al. The exosporium of B. cereus contains a binding site for gC1qR/p33: implication in spore attachment and/or entry. *Adv Exp Med Biol*. (2007) 598:181–97. doi: 10.1007/978-0-387-71767-8_13
55. Jiang J, Zhang Y, Krainer AR, Xu RM. Crystal structure of human p32, a doughnut-shaped acidic mitochondrial matrix protein. *Proc Natl Acad Sci USA*. (1999) 96:3572–7. doi: 10.1073/pnas.96.7.3572
56. Ghebrehiwet B, Peerschke EIB. cC1q-R (calreticulin) and gC1q-R/p33: ubiquitously expressed multi-ligand binding cellular proteins involved in inflammation and infection. *Mol Immunol*. (2004) 41:173–83. doi: 10.1016/j.molimm.2004.03.014
57. Waggoner SN, Cruise MW, Kassel R, Hahn YS. gC1q receptor ligation selectively down-regulates human IL-12 production through activation of the phosphoinositide 3-kinase pathway. *J Immunol*. (2005) 175:4706–14. doi: 10.4049/jimmunol.175.7.4706
58. Waggoner SN, Hall CHT, Hahn YS. HCV core protein interaction with gC1q receptor inhibits Th1 differentiation of CD4+ T cells via suppression of dendritic cell IL-12 production. *J Leukoc Biol*. (2007) 82:1407–19. doi: 10.1189/jlb.0507268
59. Kittlesen DJ, Chianese-Bullock KA, Yao ZQ, Braciale TJ, Hahn YS. Interaction between complement receptor gC1qR and hepatitis C virus core protein inhibits T-lymphocyte proliferation. *J Clin Invest*. (2000) 106:1239–49. doi: 10.1172/JCI10323
60. Meenakshi J, Anupama, Goswami SK, Datta K. Constitutive expression of hyaluronan binding protein 1 (HABP1/p32/gC1qR) in normal fibroblast cells perturbs its growth characteristics and induces apoptosis. *Biochem Biophys Res Commun*. (2003) 300:686–93. doi: 10.1016/S0006-291X(02)02788-2
61. Moorman JP, Fitzgerald SM, Prayther DC, Lee SA, Chi DS, Krishnaswamy G. Induction of p38- and gC1qR-dependent IL-8 expression in pulmonary fibroblasts by soluble hepatitis C core protein. *Respir Res*. (2005) 6:105. doi: 10.1186/1465-9921-6-105
62. Yao ZQ, Nguyen DT, Hiotellis AI, Hahn YS. Hepatitis C virus core protein inhibits human T lymphocyte responses by a complement-dependent regulatory pathway. *J Immunol*. (2001) 167:5264–72. doi: 10.4049/jimmunol.167.9.5264
63. Yao ZQ, Eisen-Vandervelde A, Ray S, Hahn YS. HCV core/gC1qR interaction arrests T cell cycle progression through stabilization of the cell cycle inhibitor p27Kip1. *Virology*. (2003) 314:271–82. doi: 10.1016/S0042-6822(03)00419-7
64. Yao ZQ, Waggoner SN, Cruise MW, Hall C, Xie X, Oldach DW, et al. SOCS1 and SOCS3 are targeted by hepatitis C virus core/gC1qR ligation to inhibit T-cell function. *J Virol*. (2005) 79:15417–29. doi: 10.1128/JVI.79.24.15417-15429.2005
65. Xu Z, Hirasawa A, Shinoura H, Tsujimoto G. Interaction of the alpha(1B)-adrenergic receptor with gC1q-R, a multifunctional protein. *J Biol Chem*. (1999) 274:21149–54. doi: 10.1074/jbc.274.30.21149
66. Hosszu KK, Valentino A, Vinayagasundaram U, Vinayagasundaram R, Joyce MG, Ji Y, et al. C1q, and gC1qR form a trimolecular receptor complex on the surface of monocyte-derived immature dendritic cells. *Blood*. (2012) 120:1228–36. doi: 10.1182/blood-2011-07-369728
67. Pednekar L, Pandit H, Paudyal B, Kaur A, Al-Mozaini MA, Kouser L, et al. Complement protein C1q interacts with DC-SIGN via its globular domain and thus may interfere with HIV-1 transmission. *Front Immunol*. (2016) 7:600. doi: 10.3389/fimmu.2016.00600
68. Son M, Diamond B, Volpe BT, Aranow CB, Mackay MC, Santiago-Schwarz F. Evidence for C1q-mediated crosslinking of CD33/LAIR-1 inhibitory immunoreceptors and biological control of CD33/LAIR-1 expression. *Sci Rep*. (2017) 7:270. doi: 10.1038/s41598-017-00290-w
69. Son M, Diamond B. C1q-mediated repression of human monocytes is regulated by leukocyte-associated Ig-like receptor 1 (LAIR-1). *Mol Med*. (2015) 20:559–68. doi: 10.2119/molmed.2014.00185
70. Park J-E, Brand DD, Rosloniec EF, Yi A-K, Stuart JM, Kang AH, et al. Leukocyte-associated immunoglobulin-like receptor 1 inhibits T-cell signaling by decreasing protein phosphorylation in the T-cell signaling pathway. *J Biol Chem*. (2020) 295:2239–47. doi: 10.1074/jbc.RA119.011150
71. Son M, Porat A, He M, Suurmond J, Santiago-Schwarz F, Andersson U, et al. C1q and HMGB1 reciprocally regulate human macrophage polarization. *Blood*. (2016) 128:2218–28. doi: 10.1182/blood-2016-05-719757
72. Berro R, Kehn K, de la Fuente C, Pumfery A, Adair R, Wade J, et al. Acetylated Tat regulates human immunodeficiency virus type 1 splicing through its interaction with the splicing regulator p32. *J Virol*. (2006) 80:3189–204. doi: 10.1128/JVI.80.7.3189-3204.2006
73. Pednekar L, Valentino A, Ji Y, Tumma N, Valentino C, Kadoor A, et al. Identification of the gC1qR sites for the HIV-1 viral envelope protein gp41 and the HCV core protein: implications in viral-specific pathogenesis and therapy. *Mol Immunol*. (2016) 74:18–26. doi: 10.1016/j.molimm.2016.03.016
74. Ghebrehiwet B, Jesty J, Vinayagasundaram R, Vinayagasundaram U, Ji Y, Valentino A, et al. Targeting gC1qR domains for therapy against infection and inflammation. *Adv Exp Med Biol*. (2013) 735:97–110. doi: 10.1007/978-1-4614-4118-2_6
75. Matthews DA, Russell WC. Adenovirus core protein V interacts with p32–a protein which is associated with both the mitochondria and the nucleus. *J Gen Virol*. (1998) 79(Pt 7):1677–85. doi: 10.1099/0022-1317-79-7-1677
76. Ohrmalm C, Akusjärvi G. Cellular splicing and transcription regulatory protein p32 represses adenovirus major late transcription and causes hyperphosphorylation of RNA polymerase II. *J Virol*. (2006) 80:5010–20. doi: 10.1128/JVI.80.10.5010-5020.2006
77. Wang Y, Finan JE, Middeldorp JM, Hayward SD. P32/TAP, a cellular protein that interacts with EBNA-1 of Epstein-Barr virus. *Virology*. (1997) 236:18–29. doi: 10.1006/viro.1997.8739
78. Hall KT, Giles MS, Calderwood MA, Goodwin DJ, Matthews DA, Whitehouse A. The *Herpesvirus saimiri* open reading frame 73 gene product interacts with the cellular protein p32. *J Virol*. (2002) 76:11612–22. doi: 10.1128/JVI.76.22.11612-11622.2002
79. Beatch MD, Everitt JC, Law LJ, Hobman TC. Interactions between rubella virus capsid and host protein p32 are important for virus replication. *J Virol*. (2005) 79:10807–20. doi: 10.1128/JVI.79.16.10807-10820.2005
80. Beatch MD, Hobman TC. Rubella virus capsid associates with host cell protein p32 and localizes to mitochondria. *J Virol*. (2000) 74:5569–76. doi: 10.1128/JVI.74.12.5569-5576.2000
81. Mohan KVK, Ghebrehiwet B, Atreya CD. The N-terminal conserved domain of rubella virus capsid interacts with the C-terminal region of cellular p32

and overexpression of p32 enhances the viral infectivity. *Virus Res*. (2002) 85:151–61. doi: 10.1016/S0168-1702(02)00030-8
82. Lainé S, Thouard A, Derancourt J, Kress M, Sitterlin D, Rossignol JM. In vitro and in vivo interactions between the hepatitis B virus protein P22 and the cellular protein gC1qR. *J Virol*. (2003) 77:12875–80. doi: 10.1128/jvi.77.23.12875-12880.2003
83. Braun L, Ghebrehiwet B, Cossart P. gC1q-R/p32, a C1q-binding protein, is a receptor for the InlB invasion protein of *Listeria monocytogenes*. *EMBO J*. (2000) 19:1458–66. doi: 10.1093/emboj/19.7.1458
84. Peerschke EIB, Bayer AS, Ghebrehiwet B, Xiong YQ. gC1qR/p33 blockade reduces *Staphylococcus aureus* colonization of target tissues in an animal model of infective endocarditis. *Infect Immun*. (2006) 74:4418–23. doi: 10.1128/IAI.01794-05
85. Peerschke EIB, Ghebrehiwet B. The contribution of gC1qR/p33 in infection and inflammation. *Immunobiology*. (2007) 212:333–42. doi: 10.1016/j.imbio.2006.11.011
86. Maeurer MJ, Trinder PK, Störkel S, Loos M. C1q in autoimmune diseases: rheumatoid arthritis. *Behring Inst Mitt*. (1993) 93:262–78.
87. Trinder PK, Maeurer MJ, Stoerkel SS, Loos M. Altered (oxidized) C1q induces a rheumatoid arthritis-like destructive and chronic inflammation in joint structures in arthritis-susceptible rats. *Clin Immunol Immunopathol*. (1997) 82:149–56. doi: 10.1006/clin.1996.4293
88. Trinder PK, Maeurer MJ, Brackertz D, Loos M. The collagen-like component of the complement system, C1q, is recognized by 7 S autoantibodies and is functionally impaired in synovial fluids of patients with rheumatoid arthritis. *Immunology*. (1996) 87:355–61. doi: 10.1046/j.1365-2567.1996.495559.x
89. Maeurer MJ, Trinder PK, Störkel S, Loos M. Modulation of type II collagen-induced arthritis in DBA/1 mice by intravenous application of a peptide from the C1q-A chain. *Immunobiology*. (1992) 185:103–20. doi: 10.1016/S0171-2985(11)80321-9
90. Ghebrehiwet B, Peerschke EI. Role of C1q and C1q receptors in the pathogenesis of systemic lupus erythematosus. *Curr Dir Autoimmun*. (2004) 7:87–97. doi: 10.1159/000075688
91. Walport MJ, Davies KA, Botto M. C1q and systemic lupus erythematosus. *Immunobiology*. (1998) 199:265–85. doi: 10.1016/S0171-2985(98)80032-6
92. Frémeaux-Bacchi V, Weiss L, Demouchy C, Blouin J, Kazatchkine MD. Autoantibodies to the collagen-like region of C1q are strongly associated with classical pathway-mediated hypocomplementemia in systemic lupus erythematosus. *Lupus*. (1996) 5:216–20. doi: 10.1177/096120339600500309
93. Goulielmos GN, Zervou MI, Vazgiourakis VM, Ghodke-Puranik Y, Garyfallos A, Niewold TB. The genetics and molecular pathogenesis of systemic lupus erythematosus (SLE) in populations of different ancestry. *Gene*. (2018) 668:59–72. doi: 10.1016/j.gene.2018.05.041
94. Walport MJ. Complement and systemic lupus erythematosus. *Arthritis Res*. (2002) 4(Suppl. 3):S279–93. doi: 10.1186/ar586
95. Sharma M, Vignesh P, Tiewsoh K, Rawat A. Revisiting the complement system in systemic lupus erythematosus. *Expert Rev Clin Immunol*. (2020) 16:397–408. doi: 10.1080/1744666X.2020.1745063
96. Schur PH, Sandson J. Immunologic factors and clinical activity in systemic lupus erythematosus. *N Engl J Med*. (1968) 278:533–8. doi: 10.1056/NEJM196803072781004
97. Siegert C, Daha M, Westedt ML, van der Voort E, Breedveld F. IgG autoantibodies against C1q are correlated with nephritis, hypocomplementemia, and dsDNA antibodies in systemic lupus erythematosus. *J Rheumatol*. (1991) 18:230–4.
98. Trendelenburg M, Lopez-Trascasa M, Potlukova E, Moll S, Regenass S, Frémeaux-Bacchi V, et al. High prevalence of anti-C1q antibodies in biopsy-proven active lupus nephritis. *Nephrol Dial Transplant*. (2006) 21:3115–21. doi: 10.1093/ndt/gfl436
99. Gargiulo MDLÁ, Gómez G, Khoury M, Collado MV, Suárez L, Álvarez C, et al. Association between the presence of anti-C1q antibodies and active nephritis in patients with systemic lupus erythematosus. *Medicina*. (2015) 75:23–8.
100. Marto N, Bertolaccini ML, Calabuig E, Hughes GRV, Khamashta MA. Anti-C1q antibodies in nephritis: correlation between titres and renal disease activity and positive predictive value in systemic lupus erythematosus. *Ann Rheum Dis*. (2005) 64:444–8. doi: 10.1136/ard.2004.024943
101. Hurst NP, Nuki G, Wallington T. Evidence for intrinsic cellular defects of "complement" receptor-mediated phagocytosis in patients with systemic lupus erythematosus (SLE). *Clin Exp Immunol*. (1984) 55:303–12.
102. Devitt A, Parker KG, Ogden CA, Oldreive C, Clay MF, Melville LA, et al. Persistence of apoptotic cells without autoimmune disease or inflammation in CD14-/- mice. *J Cell Biol*. (2004) 167:1161–70. doi: 10.1083/jcb.200410057
103. Lucas M, Stuart LM, Zhang A, Hodivala-Dilke K, Febbraio M, Silverstein R, et al. Requirements for apoptotic cell contact in regulation of macrophage responses. *J Immunol*. (2006) 177:4047–54. doi: 10.4049/jimmunol.177.6.4047
104. Stuart LM, Ezekowitz RA. Phagocytosis: elegant complexity. *Immunity*. (2005) 22:539–50. doi: 10.1016/j.immuni.2005.05.002
105. Voll RE, Herrmann M, Roth EA, Stach C, Kalden JR, Girkontaite I. Immunosuppressive effects of apoptotic cells. *Nature*. (1997) 390:350–1. doi: 10.1038/37022
106. Fadok VA, Bratton DL, Konowal A, Freed PW, Westcott JY, Henson PM. Macrophages that have ingested apoptotic cells in vitro inhibit proinflammatory cytokine production through autocrine/paracrine mechanisms involving TGF-beta, PGE2, and PAF. *J Clin Invest*. (1998) 101:890–8. doi: 10.1172/JCI1112
107. Cvetanovic M, Ucker DS. Innate immune discrimination of apoptotic cells: repression of proinflammatory macrophage transcription is coupled directly to specific recognition. *J Immunol*. (2004) 172:880–9. doi: 10.4049/jimmunol.172.2.880
108. Xia C-Q, Peng R, Qiu Y, Annamalai M, Gordon D, Clare-Salzler MJ. Transfusion of apoptotic beta-cells induces immune tolerance to beta-cell antigens and prevents type 1 diabetes in NOD mice. *Diabetes*. (2007) 56:2116–23. doi: 10.2337/db06-0825
109. Xia C-Q, Qiu Y, Peng R-H, Lo-Dauer J, Clare-Salzler MJ. Infusion of UVB-treated splenic stromal cells induces suppression of beta cell antigen-specific T cell responses in NOD mice. *J Autoimmun*. (2008) 30:283–92. doi: 10.1016/j.jaut.2007.11.017
110. Qiu C-H, Miyake Y, Kaise H, Kitamura H, Ohara O, Tanaka M. Novel subset of CD8{alpha}+ dendritic cells localized in the marginal zone is responsible for tolerance to cell-associated antigens. *J Immunol*. (2009) 182:4127–36. doi: 10.4049/jimmunol.0803364
111. Miyake Y, Asano K, Kaise H, Uemura M, Nakayama M, Tanaka M. Critical role of macrophages in the marginal zone in the suppression of immune responses to apoptotic cell-associated antigens. *J Clin Invest*. (2007) 117:2268–78. doi: 10.1172/JCI31990
112. Gray M, Miles K, Salter D, Gray D, Savill J. Apoptotic cells protect mice from autoimmune inflammation by the induction of regulatory B cells. *Proc Natl Acad Sci USA*. (2007) 104:14080–5. doi: 10.1073/pnas.0700326104
113. Grau A, Tabib A, Grau I, Reiner I, Mevorach D. Apoptotic cells induce NF-κB and inflammasome negative signaling. *PLoS One*. (2015) 10:e0122440. doi: 10.1371/journal.pone.0122440
114. Yoon Y-S, Lee Y-J, Choi J-Y, Cho M-S, Kang JL. Coordinated induction of cyclooxygenase-2/prostaglandin E2 and hepatocyte growth factor by apoptotic cells prevents lung fibrosis. *J Leukoc Biol*. (2013) 94:1037–49. doi: 10.1189/jlb.0513255
115. Lee Y-J, Moon C, Lee SH, Park H-J, Seoh J-Y, Cho M-S, et al. Apoptotic cell instillation after bleomycin attenuates lung injury through hepatocyte growth factor induction. *Eur Respir J*. (2012) 40:424–35. doi: 10.1183/09031936.00096711
116. Yoon YS, Kim SY, Kim MJ, Lim JH, Cho MS, Kang JL. PPARγ activation following apoptotic cell instillation promotes resolution of lung inflammation and fibrosis via regulation of efferocytosis and proresolving cytokines. *Mucosal Immunol*. (2015) 8:1031–46. doi: 10.1038/mi.2014.130
117. Zhang M, Xu S, Han Y, Cao X. Apoptotic cells attenuate fulminant hepatitis by priming Kupffer cells to produce interleukin-10 through membrane-bound TGF-β. *Hepatology*. (2011) 53:306–16. doi: 10.1002/hep.24029
118. Ferguson TA, Herndon J, Elzey B, Griffith TS, Schoenberger S, Green DR. Uptake of apoptotic antigen-coupled cells by lymphoid dendritic cells and cross-priming of CD8(+) T cells produce active immune unresponsiveness. *J Immunol*. (2002) 168:5589–95. doi: 10.4049/jimmunol.168.11.5589
119. Griffith TS, Kazama H, VanOosten RL, Earle JK, Herndon JM, Green DR, et al. Apoptotic cells induce tolerance by generating helpless CD8+ T

cells that produce TRAIL. *J Immunol*. (2007) 178:2679–87. doi: 10.4049/jimmunol.178.5.2679

120. Wu C, Zhang Y, Jiang Y, Wang Q, Long Y, Wang C, et al. Apoptotic cell administration enhances pancreatic islet engraftment by induction of regulatory T cells and tolerogenic dendritic cells. *Cell Mol Immunol*. (2013) 10:393–402. doi: 10.1038/cmi.2013.16
121. Mougel F, Bonnefoy F, Kury-Paulin S, Borot S, Perruche S, Kantelip B, et al. Intravenous infusion of donor apoptotic leukocytes before transplantation delays allogeneic islet graft rejection through regulatory T cells. *Diabetes Metab*. (2012) 38:531–7. doi: 10.1016/j.diabet.2012.08.008
122. Wang Z, Shufesky WJ, Montecalvo A, Divito SJ, Larregina AT, Morelli AE. In situ-targeting of dendritic cells with donor-derived apoptotic cells restrains indirect allorecognition and ameliorates allograft vasculopathy. *PLoS One*. (2009) 4:e4940. doi: 10.1371/journal.pone.0004940
123. Sun E, Gao Y, Chen J, Roberts AI, Wang X, Chen Z, et al. Allograft tolerance induced by donor apoptotic lymphocytes requires phagocytosis in the recipient. *Cell Death Differ*. (2004) 11:1258–64. doi: 10.1038/sj.cdd.4401500
124. Bonnefoy F, Perruche S, Couturier M, Sedrati A, Sun Y, Tiberghien P, et al. Plasmacytoid dendritic cells play a major role in apoptotic leukocyte-induced immune modulation. *J Immunol*. (2011) 186:5696–705. doi: 10.4049/jimmunol.1001523
125. Bonnefoy F, Masson E, Perruche S, Marandin A, Borg C, Radlovic A, et al. Sirolimus enhances the effect of apoptotic cell infusion on hematopoietic engraftment and tolerance induction. *Leukemia*. (2008) 22:1430–4. doi: 10.1038/sj.leu.2405061
126. Kleinclauss F, Perruche S, Masson E, de Carvalho Bittencourt M, Biichle S, Remy-Martin JP, et al. Intravenous apoptotic spleen cell infusion induces a TGF-beta-dependent regulatory T-cell expansion. *Cell Death Differ*. (2006) 13:41–52. doi: 10.1038/sj.cdd.4401699
127. Perruche S, Kleinclauss F, de Bittencourt M, Paris D, Tiberghien P, Saas P. Intravenous infusion of apoptotic cells simultaneously with allogeneic hematopoietic grafts alters anti-donor humoral immune responses. *Am J Transplant*. (2004) 4:1361–5. doi: 10.1111/j.1600-6143.2004.00509.x
128. Hosszu KK, Santiago-Schwarz F, Peerschke EIB, Ghebrehiwet B. Evidence that a C1q/C1qR system regulates monocyte-derived dendritic cell differentiation at the interface of innate and acquired immunity. *Innate Immun*. (2010) 16:115–27. doi: 10.1177/1753425909339815
129. Fraser DA, Laust AK, Nelson EL, Tenner AJ. C1q differentially modulates phagocytosis and cytokine responses during ingestion of apoptotic cells by human monocytes, macrophages, and dendritic cells. *J Immunol*. (2009) 183:6175–85. doi: 10.4049/jimmunol.0902232
130. Clarke EV, Weist BM, Walsh CM, Tenner AJ. Complement protein C1q bound to apoptotic cells suppresses human macrophage and dendritic cell-mediated Th17 and Th1 T cell subset proliferation. *J Leukoc Biol*. (2015) 97:147–60. doi: 10.1189/jlb.3A0614-278R
131. Spivia W, Magno PS, Le P, Fraser DA. Complement protein C1q promotes macrophage anti-inflammatory M2-like polarization during the clearance of atherogenic lipoproteins. *Inflamm Res*. (2014) 63:885–93. doi: 10.1007/s00011-014-0762-0
132. Hosszu KK, Santiago-Schwarz F, Peerschke EI, Ghebrehiwet B. C1q is a molecular switch dictating the monocyte to dendritic cell (DC) transition and arrests DCs in an immature phenotype. *FASEB J*. (2008) 22:6731.
133. Hosszu KK, Santiago-Schwarz F, Peerschke EI, Ghebrehiwet B. C1q is a molecular switch that regulates dendritic cell maturation at the monocyte-to-dendritic cell transition. *FASEB J*. (2008) 45:4142–3. doi: 10.1016/j.molimm.2008.08.143
134. Lu J, Wu X, Teh BK. The regulatory roles of C1q. *Immunobiology*. (2007) 212:245–52. doi: 10.1016/j.imbio.2006.11.008
135. Espericueta V, Manughian-Peter AO, Bally I, Thielens NM, Fraser DA. Recombinant C1q variants modulate macrophage responses but do not activate the classical complement pathway. *Mol Immunol*. (2020) 117:65–72. doi: 10.1016/j.molimm.2019.10.008
136. Castellano G, Woltman AM, Schena FP, Roos A, Daha MR, van Kooten C. Dendritic cells and complement: at the cross road of innate and adaptive immunity. *Mol Immunol*. (2004) 41:133–40. doi: 10.1016/j.molimm.2004.03.018
137. Di Domizio J, Cao W. Fueling autoimmunity: type I interferon in autoimmune diseases. *Expert Rev Clin Immunol*. (2013) 9:201–10. doi: 10.1586/eci.12.106
138. Rönnblom L, Alm GV. A pivotal role for the natural interferon alpha-producing cells (plasmacytoid dendritic cells) in the pathogenesis of lupus. *J Exp Med*. (2001) 194:F59–63. doi: 10.1084/jem.194.12.f59
139. Cao W. Pivotal functions of plasmacytoid dendritic cells in systemic autoimmune pathogenesis. *J Clin Cell Immunol*. (2014) 5:212. doi: 10.4172/2155-9899.1000212
140. Lood C, Gullstrand B, Truedsson L, Olin AI, Alm GV, Rönnblom L, et al. C1q inhibits immune complex-induced interferon-alpha production in plasmacytoid dendritic cells: a novel link between C1q deficiency and systemic lupus erythematosus pathogenesis. *Arthritis Rheum*. (2009) 60:3081–90. doi: 10.1002/art.24852
141. Santer DM, Hall BE, George TC, Tangsombatvisit S, Liu CL, Arkwright PD, et al. C1q deficiency leads to the defective suppression of IFN-alpha in response to nucleoprotein containing immune complexes. *J Immunol*. (2010) 185:4738–49. doi: 10.4049/jimmunol.1001731
142. Mascarell L, Airouche S, Berjont N, Gary C, Gueguen C, Fourcade G, et al. The regulatory dendritic cell marker C1q is a potent inhibitor of allergic inflammation. *Mucosal Immunol*. (2017) 10:695–704. doi: 10.1038/mi.2016.87
143. Santer DM, Wiedeman AE, Teal TH, Ghosh P, Elkon KB. Plasmacytoid dendritic cells and C1q differentially regulate inflammatory gene induction by lupus immune complexes. *J Immunol*. (2012) 188:902–15. doi: 10.4049/jimmunol.1102797
144. Hosszu KK, Valentino A, Ji Y, Matkovic M, Pednekar L, Rehage N, et al. Cell surface expression and function of the macromolecular c1 complex on the surface of human monocytes. *Front Immunol*. (2012) 3:38. doi: 10.3389/fimmu.2012.00038
145. Ling GS, Crawford G, Buang N, Bartok I, Tian K, Thielens NM, et al. C1q restrains autoimmunity and viral infection by regulating CD8+ T cell metabolism. *Science*. (2018) 360:558–63. doi: 10.1126/science.aao4555
146. Chen A, Gaddipati S, Hong Y, Volkman DJ, Peerschke EI, Ghebrehiwet B. Human T cells express specific binding sites for C1q. Role in T cell activation and proliferation. *J Immunol*. (1994) 153:1430–40.
147. Fausther-Bovendo H, Vieillard V, Sagan S, Bismuth G, Debré P. HIV gp41 engages gC1qR on CD4+ T cells to induce the expression of an NK ligand through the PIP3/H2O2 pathway. *PLoS Pathog*. (2010) 6:e1000975. doi: 10.1371/journal.ppat.1000975
148. Song X, Yao Z, Yang J, Zhang Z, Deng Y, Li M, et al. HCV core protein binds to gC1qR to induce A20 expression and inhibit cytokine production through MAPKs and NF-κB signaling pathways. *Oncotarget*. (2016) 7:33796–808. doi: 10.18632/oncotarget.9304
149. Jiang Z, Chen Z, Hu L, Qiu L, Zhu L. Calreticulin blockade attenuates murine acute lung injury by inducing polarization of M2 subtype macrophages. *Front Immunol*. (2020) 11:11. doi: 10.3389/fimmu.2020.00011
150. Gringhuis SI, den Dunnen J, Litjens M, van Het Hof B, van Kooyk Y, Geijtenbeek TBH. C-type lectin DC-SIGN modulates Toll-like receptor signaling via Raf-1 kinase-dependent acetylation of transcription factor NF-kappaB. *Immunity*. (2007) 26:605–16. doi: 10.1016/j.immuni.2007.03.012
151. Caparrós E, Munoz P, Sierra-Filardi E, Serrano-Gómez D, Puig-Kröger A, Rodríguez-Fernández JL, et al. DC-SIGN ligation on dendritic cells results in ERK and PI3K activation and modulates cytokine production. *Blood*. (2006) 107:3950–8. doi: 10.1182/blood-2005-03-1252
152. Zhang Y, Li J, Rong Q, Xu Z, Ding Y, Cao Q, et al. The regulatory role of C1q on *Helicobacter* pylori-induced inflammatory cytokines secretion in THP-1 cells. *Microb Pathog*. (2019) 131:234–8. doi: 10.1016/j.micpath.2019.04.017
153. Pardoll DM. The blockade of immune checkpoints in cancer immunotherapy. *Nat Rev Cancer*. (2012) 12:252–64. doi: 10.1038/nrc3239
154. Castellano G, Woltman AM, Schlagwein N, Xu W, Schena FP, Daha MR, et al. Immune modulation of human dendritic cells by complement. *Eur J Immunol*. (2007) 37:2803–11. doi: 10.1002/eji.200636845
155. Yamada M, Oritani K, Kaisho T, Ishikawa J, Yoshida H, Takahashi I, et al. Complement C1q regulates LPS-induced cytokine production in bone marrow-derived dendritic cells. *Eur J Immunol*. (2004) 34:221–30. doi: 10.1002/eji.200324026

156. Nauta AJ, Castellano G, Xu W, Woltman AM, Borrias MC, Daha MR, et al. Opsonization with C1q and mannose-binding lectin targets apoptotic cells to dendritic cells. *J Immunol*. (2004) 173:3044–50.
157. Csomor E, Bajtay Z, Sándor N, Kristóf K, Arlaud GJ, Thiel S, et al. Complement protein C1q induces maturation of human dendritic cells. *Mol Immunol*. (2007) 44:3389–97. doi: 10.1016/j.molimm.2007.02.014
158. Vegh Z, Kew RR, Gruber BL, Ghebrehiwet B. Chemotaxis of human monocyte-derived dendritic cells to complement component C1q is mediated by the receptors gC1qR and cC1qR. *Mol Immunol*. (2006) 43:1402–7. doi: 10.1016/j.molimm.2005.07.030
159. Liu S, Wu J, Zhang T, Qian B, Wu P, Li L, et al. Complement C1q chemoattracts human dendritic cells and enhances migration of mature dendritic cells to CCL19 via activation of AKT and MAPK pathways. *Mol Immunol*. (2008) 46:242–9. doi: 10.1016/j.molimm.2008.08.279
160. Kovacs H, Campbell ID, Strong P, Johnson S, Ward FJ, Reid KB, et al. Evidence that C1q binds specifically to CH2-like immunoglobulin gamma motifs present in the autoantigen calreticulin and interferes with complement activation. *Biochemistry*. (1998) 37:17865–74. doi: 10.1021/bi973197p
161. Ghebrehiwet B, Jesty J, Xu S, Vinayagasundaram R, Vinayagasundaram U, Ji Y, et al. Structure-function studies using deletion mutants identify domains of gC1qR/p33 as potential therapeutic targets for vascular permeability and inflammation. *Front Immunol*. (2011) 2:58. doi: 10.3389/fimmu.2011.00058
162. Peerschke E, Stier K, Li X, Kandov E, de Stanchina E, Chang Q, et al. gC1qR/HABP1/p32 is a potential new therapeutic target against mesothelioma. *Front Oncol*. (2020) 10:1413. doi: 10.3389/fonc.2020.01413

Conflict of Interest: The authors declare that the research was conducted in the absence of any commercial or financial relationships that could be construed as a potential conflict of interest.

frontiers in Immunology

ORIGINAL RESEARCH
published: 16 October 2020
doi: 10.3389/fimmu.2020.575154

C2 IgM Natural Antibody Enhances Inflammation and Its Use in the Recombinant Single Chain Antibody-Fused Complement Inhibitor C2-Crry to Target Therapeutics to Joints Attenuates Arthritis in Mice

Nirmal K. Banda[1], Stephen Tomlinson[2], Robert I. Scheinman[3], Nhu Ho[1,3], Joseline Ramos Ramirez[1], Gaurav Mehta[1], Guankui Wang[3], Vivian Pham Vu[3], Dmitri Simberg[3], Liudmila Kulik[1] and V. Michael Holers[1]*

[1] Division of Rheumatology, Department of Medicine, University of Colorado Anschutz Medical Campus, Aurora, CO, United States, [2] Department of Microbiology and Immunology, Medical University of South Carolina, Charleston, SC, United States, [3] Skaggs School of Pharmacy and Pharmaceutical Sciences, University of Colorado Anschutz Medical Campus, Aurora, CO, United States

OPEN ACCESS

Edited by:
Elena Volokhina,
Radboud University Nijmegen Medical Centre, Netherlands

Reviewed by:
Roberta Bulla,
University of Trieste, Italy
Viviana P. Ferreira,
University of Toledo, United States

***Correspondence:**
Nirmal K. Banda
Nirmal.Banda@cuanschutz.edu;
Nirmal.Banda@UCDenver.edu

Specialty section:
This article was submitted to Molecular Innate Immunity, a section of the journal Frontiers in Immunology

Received: 22 June 2020
Accepted: 08 September 2020
Published: 16 October 2020

Citation:
Banda NK, Tomlinson S, Scheinman RI, Ho N, Ramirez JR, Mehta G, Wang G, Vu VP, Simberg D, Kulik L and Holers VM (2020) C2 IgM Natural Antibody Enhances Inflammation and Its Use in the Recombinant Single Chain Antibody-Fused Complement Inhibitor C2-Crry to Target Therapeutics to Joints Attenuates Arthritis in Mice. Front. Immunol. 11:575154. doi: 10.3389/fimmu.2020.575154

Natural IgM antibodies (NAbs) have been shown to recognize injury-associated neoepitopes and to initiate pathogenic complement activation. The NAb termed C2 binds to a subset of phospholipids displayed on injured cells, and its role(s) in arthritis, as well as the potential therapeutic benefit of a C2 NAb-derived ScFv-containing protein fused to a complement inhibitor, complement receptor-related y (Crry), on joint inflammation are unknown. Our first objective was to functionally test mAb C2 binding to apoptotic cells from the joint and also evaluate its inflammation enhancing capacity in collagen antibody-induced arthritis (CAIA). The second objective was to generate and test the complement inhibitory capacity of C2-Crry fusion protein in the collagen-induced arthritis (CIA) model. The third objective was to demonstrate *in vivo* targeting of C2-Crry to damaged joints in mice with arthritis. The effect of C2-NAb on CAIA in C57BL/6 mice was examined by inducing a suboptimal disease. The inhibitory effect of C2-Crry in DBA/1J mice with CIA was determined by injecting 2x per week with a single dose of 0.250 mg/mouse. Clinical disease activity (CDA) was examined, and knee joints were fixed for analysis of histopathology, C3 deposition, and macrophage infiltration. In mice with suboptimal CAIA, at day 10 there was a significant ($p < 0.017$) 74% increase in the CDA in mice treated with C2 NAb, compared to mice treated with F632 control NAb. In mice with CIA, at day 35 there was a significant 39% ($p < 0.042$) decrease in the CDA in mice treated with C2-Crry. Total scores for histopathology were also 50% decreased ($p < 0.0005$) in CIA mice treated with C2-Crry. C3 deposition was significantly decreased in the synovium (44%; $p < 0.026$) and on the surface of cartilage

(42%; $p < 0.008$) in mice treated with C2-Crry compared with PBS treated CIA mice. Furthermore, C2-Crry specifically bound to apoptotic fibroblast-like synoviocytes *in vitro*, and also localized in the knee joints of arthritic mice as analyzed by *in vivo* imaging. In summary, NAb C2 enhanced arthritis-related injury, and targeted delivery of C2-Crry to inflamed joints demonstrated disease modifying activity in a mouse model of human inflammatory arthritis.

Keywords: natural antibodies, single chain, C2-Crry, complement, complement inhibitor, arthritis

INTRODUCTION

Rheumatoid arthritis (RA) is the leading cause of autoimmune arthritis, and as the population ages RA-related disabilities in patients in the US have been projected to increase over the next 25 years by 40% (1), suggesting that this disease will continue to impact the public health care system dramatically (2). While the pathogenesis of RA is complex and no single mechanism or biomarker can explain its initiation and perpetuation, many potential risk factors for the development of RA have been identified (3). The complement system (CS), a component of innate immunity, plays an important role in the pathogenesis of RA (4). Complement activation is essential for disease progression in active and passive transfer mouse models of RA, and activated complement fragments have been found in the synovium of RA patients (5–7). Specifically, the alternative pathway (AP) and C5aR of complement is required for the perpetuation and severity of disease, as mice lacking complement MASP-1/3, factor D, factor B, C5, and C5aR are substantially resistant to arthritis while mice lacking C1q, C4, mannose-binding lectin, FCN A, Collectin 11, and FCN A are susceptible to arthritis (5, 8–12). In addition, mice lacking C3, C3aR, FCN B, and MASP-2 are partially resistant to arthritis (8, 13). Complement activation products have been shown to be generated locally during the pre-clinical initiation of RA (14). Furthermore, CS-based therapeutics have shown excellent therapeutic efficacy in mouse models of RA (15, 16), but have failed in RA clinical trials due to the complex nature of the late stage disease and potentially a failure to reach the injured joints in a sufficiently high concentration. For this and other reasons, there is an unmet need for the development of new therapeutics based on advancing understanding of the CS and its ability to damage local tissues in sites such as the joint through interactions with injured and apoptotic cells.

The CS gets activated by three different pathways: the classical pathway (CP), the lectin pathway (LP), and the AP (4). All of these pathways generate two potent pro-inflammatory molecules; C3a and C5a, via C3 and C5 convertases, respectively, as well as the C5b-9 membrane attack complex and C3 fragment ligands for other complement receptors. Normally, host cells are protected from an inadvertent self-attack of the CS through immediate intervention by deactivation of the early C3/C5 convertases steps or during the late assembly of the membrane attack complex (17). The deactivation of complement C3/C5 convertases is mediated by several soluble and membrane bound regulatory proteins (17) whose role is to protect tissue and organs from inappropriate CS-mediated damage. Both soluble and membrane bound regulatory proteins are essential to prevent immunopathology resulting from over activation of the CS in various autoimmune diseases such as RA. Specifically in mouse, one such membrane bound regulatory protein known as CR1-related gene/protein Y (Crry), a product of the *Crry* gene, is present. Crry is equivalent in several ways to human membrane cofactor protein (MCP; CD46) and also complement receptor 1 (CR1; CD35). CD46, CR1 and Crry are cofactors for the factor I (FI)-mediated cleavage of C3b and C4b, which are active products of C3 and C4 complement proteins (18). In contrast to MCP, though, Crry also possesses decay-accelerating activity for the CP but weak decay-accelerating activity for the AP C3 convertase (19–21). Crry has been shown to maintain homeostasis in mice, and mice lacking Crry demonstrate an embryonically lethal phenotype (21, 22). Crry has been shown play an important role in autoimmune disease such as lupus (MRL/lpr mice) (23, 24) and Alzheimer's disease (25, 26). However, Crry-Ig alone was not effective compared with anti-C5 mAb in protecting mice from collagen-induced arthritis (CIA) (27), suggesting its non-availability in the damaged joints or cartilage surface. Nonetheless, inhibition of complement by a fusion protein, CR2-Crry has been shown to reduce development of atherosclerosis (28) and collagen antibody-induced arthritis (CAIA) (29, 30). In an experimental autoimmune encephalomyelitis (EAE)-induced demyelination model in mice it has been shown that using adeno-associated viral (AAV)-mediated, *in vivo*, targeted gene delivery of Crry, there was a selective inhibition of activated C3 at presynaptic boutons protected structural synapses and visual function. The authors have achieved the inhibitory effect on C3 by overexpressing Crry fused to a domain of CR2 that only binds activated C3 in retinal ganglion cells, resulting in abundance of Crry protein in retinogeniculate presynaptic terminals following EAE (31).

Despite the presence of membrane bound regulatory proteins, abnormal complement activation occurs in many clinical conditions such as tissue inflammation, myocardial or intestinal ischemia, blunt trauma, hemorrhagic shock, glomerulonephritis, autoimmune diseases, and after exposure to bacterial toxins (32). In systemic autoimmune diseases such as arthritis and lupus, complement activation might be initiated by circulating

Abbreviations: AJM, all joint mean; AP, alternative pathway; CAIA, collagen antibody-induced arthritis; CDA, clinical disease activity; CIA, Collagen-induced arthritis; CII, Bovine type II collagen; CP, classical pathway; Crry, Mouse complement receptor-related y; CS, complement system; C2-scFv, C2scFv-Crry, C2-single-chain variable fragment; FLS, fibroblast-like synoviocyte; IgM, Immunoglobulin M; LP, lectin pathway; LPS, lipopolysacharide; mAb, monoclonal antibody; Nabs, natural antibodies; WT, wild type.

immune-complexes (ICs), which are characteristic features of these autoimmune diseases (4, 33).

To protect from viral and bacterial infections, healthy individuals express natural antibodies (NAbs), which are normally produced antibodies, subsets of which can recognize self, and/or foreign antigens. NAbs can cause direct neutralization of bacteria or viruses present in the circulation. NAbs/natural autoimmunity forms a network that serves to protect the organisms from exterior and interior danger, but may also contribute to autoimmune diseases (34). While NAbs are generally of the IgM or IgG3 isotype, nonetheless some IgA and IgG NAbs have also been identified (32). NAbs are typically encoded by germline variable (V) genes without extensive mutations (35). The major source of natural IgM are long lived peritoneal CD5 + B1 cells (36–38). It is not clear whether B1a (CD5C) or B1b (CD5K) B cells produce these NAbs (32, 39, 40). B1 cells are long lived which are positively selected for self-reactivity (34). Nonetheless some NAbs are synthesized by splenic $CD5^{-}$B2 cells (39).

In addition to direct or indirect lysis of pathogens by complement, NAbs have been shown to be involved in the clearance of senescent erythrocytes (41), intracellular debris and infectious agents from the circulation (42). Natural IgM has been shown bind to C1q and activate the complement cascade (43, 44). Furthermore, natural IgM also binds mannose-binding lectin (MBL), which is bound to apoptotic cells (45, 46) and clears ICs. These studies show that NAbs and the CS can act in some situations in concert to maintain homeostasis in an apoptotic microenvironment such as injury or inflammation.

In the recent past, we have cloned and purified one IgM NAb, designated C2, a mAb that recognizes an epitope expressed on a subset of phospholipids (PL), and shown that C2 mAb specifically bind to the intestine (47), brain (48), and heart following ischemia-reperfusion injury (49). Furthermore C2 binding to PL is not fatty acid dependent, as it binds to PL with different fatty acids, either saturated or unsaturated, and the epitope is not oxidized on double bound fatty acid (Kulik, L et al. unpublished data). We have also previously shown that certain IgM NAbs function as innate immune sensors of injury via recognition of neoepitopes expressed on damaged cells or within the spinal cord after injury (50). Other studies have shown that only cells undergoing apoptosis, but not normal viable cells, generate oxidation-specific neoepitopes, including biologically active oxidized low density lipoproteins, which in turn serve as dominant autoantigens as well as provide "pro-inflammatory" signals, mediating autoimmune and inflammatory responses (51).

In addition to tissue injury, many chemotherapeutics or biologics ultimately induce apoptosis as their mode of action (52, 53). Therefore, from a drug development prospective C2 as a mAb directed against specific apoptosis-induced PL biomarkers can be utilized for the targeted delivery of a complement inhibitory protein, for example, Crry, to create the tissue-targeted fusions protein C2-Crry. We hypothesized that a C3 complement inhibitor protein such as Crry can be directly and specifically delivered via C2 NAb targeting to the injured site, i.e., in the joints of arthritic mice, through binding of inflammation-associated PL generated during injury or inflammation. To this end, based on C2 neoepitope identification during injury, we constructed an anti-C2 single chain antibody (scFv), and then C2 scFv was linked to Crry to create a new fusion protein, C2-Crry with 6Histag. ScFv comprise the variable regions of the heavy (V_H) and light chains (V_L) of immunoglobulins, connected with a short linker peptide of ten to about 25 amino acids. We also hypothesized that these C2-specific neoepitopes are generated in the synovium or on the cartilage surface during inflammation in human RA and, therefore, Crry can be delivered clinically as the C2-Crry fusion protein to the site of inflammation, i.e., in the joints in early or late RA. Herein, to provide the proof-of-concept, we have used two mouse models of human RA, anti-collagen antibody induced arthritis (CAIA) and CIA. First to show that C2 mAb by itself, in mice, can enhance injury, i.e., arthritis, we used the mouse model of CAIA, which is dependent on the CS for it is involved in the effector phase of the arthritis. Mice deficient in C3 developed less severe arthritis while mice deficient in C5 are resistance of arthritis (54, 55). Second, to determine if C2-Crry as a fusion protein inhibitor can attenuate injury via suppression of the CS in the joints of mice, we used CIA, which is dependent on T and B cells, although complement is involved in the effector phase in this model. In CIA, active immunization with bovine type II collagen leads to the development of arthritis in which T and B cells are present, but not when preformed antibodies or T cells are used for disease induction (56). We also provided evidence using imaging analysis that Infrared Dye 800 (IRDye 800) labeled C2-Crry localized specifically within the damaged joints of arthritic mice.

MATERIALS AND METHODS

Cloning of C2-IgM NAb Sequences

The variable portion amino acid sequences from the heavy and light chains of C2-IgM with a spacer sequences $(4GS)_2$-4G and Crry protein on the C-terminus were cloned into pEE12.4 vector according to published methods (49). The construct was made both with and without 6xHis tag. The protein was produced in stably transfected Chinese Hamster Ovary (CHO) cells.

Generation and Purification of Natural Antibodies C2 and F632 IgM mAbs

The NAbs C2 and F632 were generated as mAbs and purified according to our previous published study (47). Briefly, C2 and F632 were developed by the fusion of spleen cells from wild type (WT) C57BL/6 mice with the Sp2/0-Ag14 myeloma cell line by the standard protocol to establish hybridomas. To purify C2 and F632 IgM NAbs, exhausted supernatants of cultured C2 and F632 hybridomas, were affinity purified on a column of agarose beads with goat anti-mouse IgM (Sigma-Aldrich, MO, United States). Bound Abs were eluted with a buffer containing 0.1 M glycine (pH 2.3) and collected into a buffer containing 1.5 M Tris (pH 8.8). Eluted mAb were dialyzed against 1 × PBS (pH 7.4) for 48 h and concentrated using centrifugal filtration on Centricon Plus-20 (Millipore, MA, United States). C2 mAb sequences were used to generate the fusion protein, C2-Crry, which recognizes

a subset of PL (47), and F632 IgM mAb used as a control recognizing 4-hydroxy-3-nitrophenylacetyl (49). Purified C2 and F632 IgM NAb concentrations for follow up *in vivo* studies were determined by measuring the $A_{280\ nm}$ of the sample, and purity was confirmed by analysis on a 10% SDS-PAGE gel (47).

Binding of C2 IgM NAb to Apoptotic Thymocytes

Thymocytes were isolated from 6-week old male C57BL6 mice. 6×10^6/ml cells were cultured in DMEM media for 16 h with 1 μM dexamethasone. Each sample of 1×10^6 thymocytes were re-suspended in staining buffer (Ca2+, Mg+ Dulbecco's Phosphate-Buffered Saline supplemented with 2% Fetal Bovine serum and 0.09% Na_3N) containing monoclonal antibody for 30 min on ice. Bound C2 antibody was detected with FITC labeled goat anti-IgM FITC. After washing cells were re-suspended in the Flow cytometry (FACS) staining buffer and analyzed. Before running samples through flow cytometer, 1 mg/ml propidium iodide (PI) was added to determine the level of apoptosis in thymocytes. Anti-D5 IgM Nab, which does not bind to PL and has no effect on injury (50), was used as a negative control.

C2 NAb-Mediated Injury in Collagen Antibody-Induced Arthritis

To examine the effect of purified C2 IgM NAb on arthritis, CAIA, was used as a mouse model of human RA. Wild type (WT) mice on C57BL6 (H-2^b haplotype) background were used for CAIA (5, 27). A suboptimal level of arthritis was induced in mice by an intraperitoneal (i.p.) injection at day 0 of a single dose (0.5 mg/mouse) of anti-collagen antibody a.k.a. Arthrogen-CIA 5-clone mixture (Chondrex, Inc., Redmond, WA, United States). At day 3, all mice were injected IP with a single dose (50 μg/mouse) of lipopolysaccharide (LPS; Escherichia coli strain; Chondrex, Inc., Redmond, WA, United States). All mice start showing signs of clinical disease, at day 4 when injected with Arthrogen alone but an injection of LPS is required as part of the standard protocol to inducing a sever disease to examine the exact efficacy of test fusion proteins *in vivo*. It has been shown that LPS exacerbate arthritis by inducing the secretion of IL-1β and TNF-α, which are not only involved in immune responses but also in inflammation itself (57). At day 4, i.e., after 24 h of LPS injection mice show the signs of disease and later on start developing severe disease. To determine the effect of anti-C2 NAb, mice were injected three times [0.1 mg/mouse intravenously (i.v.)] with C2 IgM or F632 ($n = 5$) or 1 × PBS ($n = 5$) at day 0, day 3, and at day 5. NAb F632 was used as an internal control to identify the specific pathogenic effects of C2 IgM on arthritis and serves as a Nab control. All mice were sacrificed at day 10. Clinical disease activity (CDA) starting at day 4 was scored each day blindly by two trained laboratory personals according to our published methods (5, 27).

Cloning, Expression and Purification of the C2-Crry Fusion Protein

The pEE12.4/C2scFv-Crry plasmid was transfected into Expi293 cells, which were grown for 7 days, following which the supernatants were collected and loaded on the His60 Ni Superflow column to purify the proteins. The pEE12.4/C2scFv-Crry plasmid encodes the six His tag at the C terminus of the peptide so protein was bound and then purified from Nickle column (His60 Ni Superflow Resion; Clontech company). The plasmids were transient transfected into Expi293 cells (Expi293^{TM} Expression System Kit, https://www.thermofisher.com/order/catalog/product/A14635) for 7 days, and the supernatant were collected and loaded on the His60 Ni Superflow column for C2-Crry purification (50).

Flow Cytometry Analysis for Binding of C2-Crry to Apoptotic Human Umbilical Vein Endothelial Cells

To determine whether the purified C2-Crry fusion protein binds to apoptotic human umbilical vein endothelial cells (HUVECs), flow cytometry was used. HUVEC cells were incubated over night with 10 mM Antimycin A (AMA) to induce apoptosis. Cell were de-attached from plates using Accutase (Sigma). Cells were incubated on ice for 30 min with C2-Crry protein at 10 μg/ml. The bound protein was detected with rabbit anti-6xHis-FITC. Flow cytometry analyses was performed on cells gated for live (G1 gate) and apoptotic (G2 gate) cells.

Binding of C2-Crry to the Phospholipid, Cardiolipin

Enzyme-linked immunosorbent assay (ELISA) was used to determine whether the purified C2-Crry fusion protein binds to specific PL. The ELISA plates were pre-coated over night with 10 μg/ml of cardiolipin (CL; phospholipid) re-suspended in Methanol and stored at 4°C with ELISA wells left uncovered for Methanol to evaporate overnight. PC-BSA (Phosphorylcholine hapten conjugated to bovine serum albumin by use of p-diazonium phenylphosphorylcholine) was added to plates in amount 5 μg/ml in PBS. After blocking the ELISA plates with BSA, different concentrations of C2-Crry were applied to wells. Bound C2-Crry was detected with anti-6xHis antibody.

Effect of C2-Crry on Collagen-Induced Arthritis

To examine the direct effect of C2-Crry fusion protein on disease, CIA, another mouse model human RA, was evaluated. Wild type DBA 1/J (H-2^q haplotype) mice were used due to the high susceptibility of this strain to CIA. CIA in mice was induced at day 0 by injecting an emulsion intra-dermally at the base of the tail containing a mixture of bovine type II collagen (BCII; 200 μg/mouse; Sigma) plus *Mybacterium tuberculosis* (MT; 200 μg/mouse; Complete Freund's Adjuvant; CFA; H37Ra; Difco Laboratories, Detroit, MI, United States). A booster injection was given at day 21 using identical doses of BCII and MT (58). To determine the inhibitory effect of C2-Crry, mice with CIA ($n = 14$), were injected with a dose of 0.250 mg/mouse/i.p. or 1 × PBS control 2x per week after the booster injection of CII/CFA at day 21. All mice were sacrificed at day 35. CDA was examined according to our published methods (58). At day 35, all four limbs (two forepaws, two hind paws with knee joint and

ankle) were surgically removed and fixed in 10% neutral buffered formalin (NBF) for histopathological analysis (58).

Histopathology and Immunohistochemical Staining for C3 Deposition and Macrophage Determination

All four joints (both fore limbs and the right hind limb, with knee joint, ankle and paw) from DBA 1/J mice with CIA treated with C2-Crry or controls and sacrificed at day 35 were fixed in 10% NBF to examine for overall histopathological changes and C3 deposition in the synovium and on the surface of cartilage. From CAIA mice, no limbs were processed for histopathology and C3 deposition. Histopathology with scores for inflammation, pannus, cartilage damage and bone damage was assessed by using Toluidine-blue (T-blue) according to our published criteria (5, 10, 15, 27, 58). C3 deposition was assessed by using a primary polyclonal goat anti-mouse C3 Ab (dilution 1:10,000; ICN Pharmaceuticals, Costa Mesa, CA, United States) and detected by goat anti-HRP polymer kit per manufacturer's instructions (Biocare Medical, Concord, CA, United States). immunohistochemical (IHC) visualization of C3 protein was carried out using 3′, 3′ diaminobenzidine solution substrate (DakoCytomation, Carpinteria, CA, United States) that reacts with HRP and generate a brown color stain on the sections. The presence of macrophages in the knee joints was also quantitated by IHC using F4/80 according to our published methods (13).

Measurements of Anti-collagen Antibodies

Serum was collected from each mouse with CIA treated with C2-Crry or controls by retro-orbital bleeding under anesthesia on day 0 (right eye), on day 21 (left eye), and on day 35 (right eye). Samples were used in triplicate to measure IgG1 and IgG2a anti-mouse CII antibodies by ELISA at a dilution of 1:2000 in 1 × PBS as previously describe (27, 58). A standard pool of anti-CII antibodies was made by mixing sera from several mice with severe arthritis and used to create a standard curve. Absorbance was read at 405 nm with a 492 nm correction filter.

Fibroblast-Like Synoviocyte Culture

Primary fibroblast-like synoviocytes (FLS) derived from mice with CIA (originally obtained from Dr. Gary Firestein (University of California–San Diego) were cultured in T25 tissue culture flasks in DMEM high-glucose medium (Sigma) containing 10% FBS, 1% penicillin-streptomycin, 1% L-glutamine, and 0.5% gentamicin (59). The FLS became confluent at 7–14 days. Cultured FLS were used up to 10 passages when a new aliquot of cells was thawed. FLS were used for evaluation of binding of IRDye 800 labeled C2-Crry to the apoptotic FLS.

Induction of Apoptosis in FLS

Apoptosis in FLS 1×10^5 in 0.5 ml media in a 24-well plate were induced by using serum starvation for hours 72 h to assess the binding of C2-Crry to apoptotic FLS. Serum was withdrawn from the FLS culture for 72 h to trigger apoptosis. Apoptosis in FLS was also confirmed using 1.2% agarose gel electrophoresis and identification of a cleaved DNA ladder.

Labeling of C2-Crry With IRDye 800CW

To show the binding of C2-Crry *in vitro* to apoptotic FLS, we labeled the protein with IRDye800-NHS ester (Li-COR Biosciences) as we have shown previously (60, 61). C2-Crry fusion protein was incubated with a 10-fold molar excess of dye for 5 h at 4°C in PBS. Unbound dye was removed with a 7 kDa Zeba desalting column (Thermo Fisher). After labeling C2-Crry with IRDye800 and addition to a Zeba column, the protein was eluted from the column with PBS and stored at 4°C before use according to our previously published study (60, 61). Similarly, Arthrogen (anti-CII) mAbs were labeled with IRDye 800 (60, 61).

Near-Infrared Microscopy for *ex vivo* IRDye 800 Labeled C2-Crry Binding With Apoptotic FLS

IRDye 800CW labeled C2-Crry (10 μg/ml) was added to the serum starved apoptotic FLS in a 24-well plate and incubated for 2 h at room temperature. Serum starved FLS for 6 h were used as negative and positive controls to show specific FLS apoptosis followed staining with Caspase 3/7 (2 mM) green detection reagent using a glass slide according to manufacturer's standard protocol (ThermoFisher Scientific). The cells were fixed in 4% formalin and imaged with Zeiss Axio Observer 5 epifluorescent microscope equipped with X-Cite 200DC light source and Axiocam 506 monochromatic camera. Near infrared fluorescence was detected using a Cy7 filter set, catalog number 49007, Chroma Corporation (McHenry, IL, United States). The plate fluorescence was read with a Li-COR Odyssey scanner at 800 nm, and the integrated density of gray 8-bit images (TIFF) of the wells was determined with ImageJ software.

In vivo Joint-Specific Detection of IRDye 800 Labeled Anti-CII Abs and C2-Crry

To examine joint-specific distribution of IRDye 800 labeled C2-Crry in WT C57B6 mice with CAIA, two experiments were done. First, to show that IRDye 800 labeled anti-CII Abs alone binds to the cartilage in the joints, and dye itself have no effect on antibody binding capacity, C57B6 WT mice were injected with a single low dose of IRDye 800 labeled anti-CII Abs (Arthrogen; 50 μg/mouse/i.v.) or murine IgG (50 μg/mouse/i.v.) or non-injected. After two weeks of antibody wash out period (15 days) mice were sacrificed to detect IRDye 800 labeled anti-CII Abs in the joints. IRDye 800 labeled anti-CII Abs clears very slowly from the circulation but firmly binds to the cartilage in joints even after a long wash period according to our published methods (60, 61). This binding of IRDye 800 anti-CII Abs also induced a low level of disease and it can compete with the unlabeled arthrogen (60). Our previous study show that IRDye 800 labeled anti-CII also does not bind non-specifically to spleen, kidney, lung, heart, liver and intestine but only to the arthritic joints (61). At day 15, bones of forelimbs and hind limbs were cleaned of muscle, sandwiched between two glass slides and scanned with a Li-COR Odyssey at 700 nm channel for autofluorescence and 800 nm channel for

IRDye 800. Mean fluorescence was determined from 8-bit images using ImageJ. No gross morphology and bright field images were taken due to clarity issues.

Second to show the specific binding of the IRDye 800 labeled fusion protein C2-Crry to the damaged cartilage or to the joints, a single dose of C2-Crry (50 μg/mouse/i.v.) was injected at day 15 in mice with suboptimal disease, i.e., CAIA. A suboptimal or a low level of disease was induced by using 50 μg/mouse of unlabeled Arthrogen i.v. followed by LPS (50 μg/mouse/i.p.) which is sufficient to bind and cause mild injury in the joints as mentioned above. At day 18, IRDye 800 labeled C2-Crry injected (i.v.) mice were sacrificed and scanned using Li-COR Odyssey as mentioned above. For control, mice were injected with unlabeled C2-Crry or not injected with anything. In order to determine the circulation half-life of IRDye 800 labeled C2-Crry, plasma collected at different time points during the 3 day (day 15 to day 18) period was applied in 2 μl triplicates on a 0.22 μm nitrocellulose membrane and scanned at 800 nm using Li-COR Odyssey (60). For this study, no gross morphology and bright field images were taken.

Statistics

p-values were calculated using Student's *t* test with the GraphPad Prism® 4 statistical program. ANOVA was used for CDA, histopathology, C3 deposition and macrophage data. The data in graphs, histograms and tables are shown as the mean ±SEM, with $p < 0.05$ considered significant.

RESULTS

Flow Cytometry Analysis Showing Binding of C2 IgM NAb to Apoptotic Thymocytes

Flow cytometry data show a significantly higher levels of anti-C2-IgM NAb binding to late apoptotic mouse thymocytes compared to control anti-D5-IgM NAb binding (**Figure 1**). At 16 h, 35% of dexamethasone treated thymocytes were positive for anti-C2-IgM antibody compared with only 3% for control anti-D5-IgM antibody (**Figures 1A,B**). Thus NAb C2-IgM specifically binds to apoptotic cells, rationalizing its study for enhancement of arthritis or its incorporation as a component of an scFv-linked complement inhibitor to deliver complement inhibition activity to injured cells or tissues.

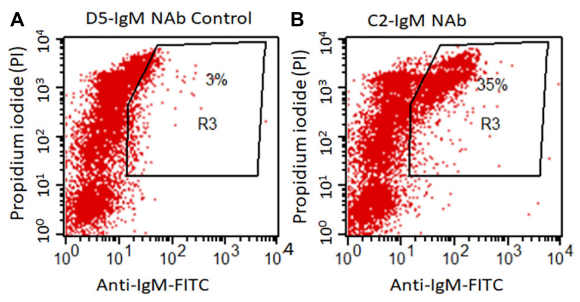

FIGURE 1 | C2-IgM antibody recognizes a subpopulation of late apoptotic thymocytes. Mouse thymocytes were cultured for 16 h in the presence of 1 mM Dexamethasone; apoptotic thymocytes were then analyzed by FACS analysis for the binding of C2-IgM antibody. **(A)** FACS analysis showing minimal (background level) binding of a non-specific NAb, anti-D5 IgM (anti-cytokeratin 19 antibody) to apoptotic cells. **(B)** Anti-C2-IgM NAb specific binding was detected on a subset of late apoptotic cells (PI^{high}).

Enhancement of Arthritis by C2-IgM NAb

The CAIA mouse model, wherein damage is dependent on an intact CS, was used to examine the potential inflammation or injury enhancing effect of C2-IgM NAb in suboptimally induced arthritis.

All WT mice were injected i.v., three times, before, during and after induction of disease, either with 1 × PBS or F632 IgM or C2 IgM (**Figure 2**). At day 10, the CDA was 2.6 ± 0.509, 2.4 ± 0.400 and 9.2 ± 0.374 in mice treated with 1 × PBS, F-632

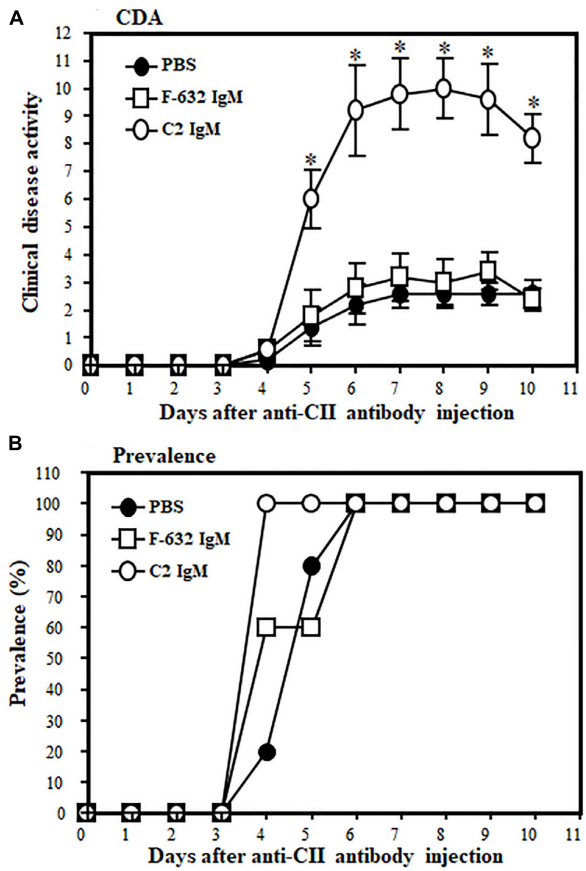

FIGURE 2 | Showing the disease modifying effect of C2-IgM or F632-IgM NAbs on suboptimal CAIA. A suboptimal level of arthritis in mice was induced by injecting Arthrogen 4 clone (anti-CII abs; 0.5 mg/mice) and LPS as mentioned in the Materials and Methods. Mice were injected (i.v.) with a single dose (0.1 mg/mouse) of C2-IgM ($n = 5$) or F632-IgM ($n = 5$) or 1 × PBS buffer control ($n = 5$) at day 0 (prior to arthritis induction with anti-CII abs), day 3 (prior to LPS injection), and at day 5 (after the induction of arthritis). Mice injected with F632-IgM or 1 × PBS served as controls. **(A)** An increase in the CDA in mice injected with C2-IgM compared with F632-IgM. **(B)** Prevalence (%) of disease. Data shown as Mean ± SEM. *$p < 0.05$ considered significant.

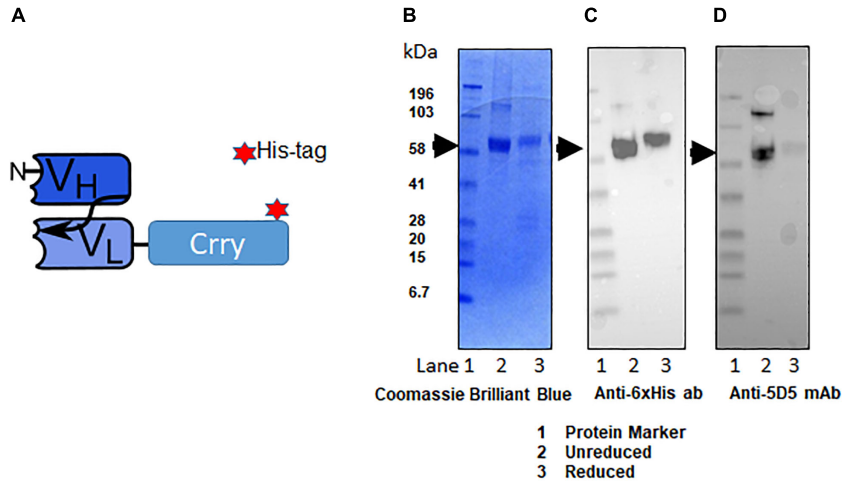

FIGURE 3 | Schematic representation of scFv-Crry construct and purification of C2-Crry fusion protein. **(A)** The variable portion amino acid sequences from heavy chain of C2-IgM and light chain C2-IgM with a spacer sequences $(4GS)_2$-4G and Crry protein on the C-terminus were cloned into pEE12.4 vector. The construct was made either with 6xHis tag or without 6xHis tag. The His tagged and non-His tag C2-Crry were purified from CHO cell supernatant by affinity chromatography on bound to sepharose anti-Crry mAb 5D5. Purified C2-Crry protein either was loaded into the gel in the loading sample buffer (1-unreduced) or boiled in a loading sample buffer containing 2-mercaptpethanol as a reducing agent (2-reduced). **(B)** The identity of purified C2-Crry band was confirmed separating reduced or unreduced samples using 10% Tris–glycine SDS gel followed by staining with Coomassie Brilliant Blue. **(C)** Western blot analysis confirming C2-Crry protein band (65.5 kDa) using HRP-conjugated anti 6xHis tag mAb. **(D)** Western blots using anti-Crry antibody, 5D5 confirmed the presence of Crry along with C2 in the C2-Crry fusion protein.

Nab, and C2-IgM Nab, respectively (**Figure 2A**). Overall, there was a 74% ($p < 0.017$) and 72% significant ($p < 0.006$) increase in the CDA in mice treated with C2-IgM compared with mice treated with control F632 NAb or 1 × PBS, respectively. At day 10, the prevalence of disease was 100% in all groups (**Figure 2B**). There was no toxic effect on mice for all experimental mice survived and also there was no significant loss of weight. These CDA data show that anti-C2-IgM NAb enhanced suboptimal inflammation to generate severe near maximal inflammation in CAIA mice. Representative pictures of forelimbs of mice with visible enhancement of inflammation or injury by C2-IgM NAb are shown in **Supplementary Figure 1**.

Purification and Assessment of the Quality of C2-Crry Fusion Protein

The fusion protein C2-Crry was originally generated tagged with a hexa-histidine tag (6xHis-tag; **Figure 3A**). C2-Crry was purified and its size of 65.5 kDa was confirmed by SDS-PAGE (**Figure 3B** lanes 1, 2). Commercially available anti-His-tag antibody was used to check the quality of C2-Crry fusion protein (**Figure 3C** lanes 1, 2). In parallel, additional Western blot confirmed that anti-Crry mAb 5D5 binds to a Crry conformational epitope, as reduced C2-Crry does not reveal any 5D5 epitope (**Figure 3D**, lanes 1, 2). Since 5D5 binds to Crry only, Western blot confirmed the presence of Crry in the C2-Crry fusion protein (**Figure 3D**, lanes 1, 2).

Binding of C2-Crry Fusion Protein to Apoptotic HUVECs

To determine if the C2-Crry fusion protein binds specifically to apoptotic HUVEC cells, apoptosis was induced using AMA as described in Materials and Methods. FACS analysis confirmed that C2-Crry preferentially binds to apoptotic cells present in the G2 gate as compared to the G1 gate. Bound C2-Crry protein was detected with rabbit anti-6xHis –FITC (**Figures 4A–C**).

Enzyme-Linked Immunosorbent Assay Showing Binding of C2-Crry to Phospholipids

Enzyme-linked immunosorbent assay was used to demonstrate retention of the specificity of C2-Crry binding to PL of the class present on the surface of apoptotic cells. ELISA results show that C2-Crry has similar PL characteristics as reported for C2 IgM (**Figure 5**). C2-Crry fusion protein specifically bound to CL and Phosphorylcholine-Bovine Serum Albumin (PC-BSA) in a dose dependent manner, but did not bind BSA alone (**Figure 5**). CL is a unique PL which is located in the inner mitochondrial cell membrane, and was specifically recognized by C2-Crry.

Phosphorylcholine-Bovine Serum Albumin was also used (**Figure 5**). In PC-BSA, Phosphorylcholine hapten is conjugated to BSA protein by use of p-diazonium phenylphosphorylcholine. Our ELISA data (**Figure 5**) and above FACS data (**Figure 4**) confirm that C2-Crry can specifically recognize PL found on the surface cells undergoing apoptosis.

Amelioration of Arthritis by Treatment With the C2-Crry Fusion Protein

To examine the direct effect of C2-Crry fusion protein on arthritis, we used the CIA model. Mice were injected four times (2 times per week) after the booster injection with a dose of 250 μg/mouse and sacrificed at day 35 (**Figure 6**). At day 35, the CDA in mice treated with 1 × PBS or C2-Crry was 11.14 ± 0.459

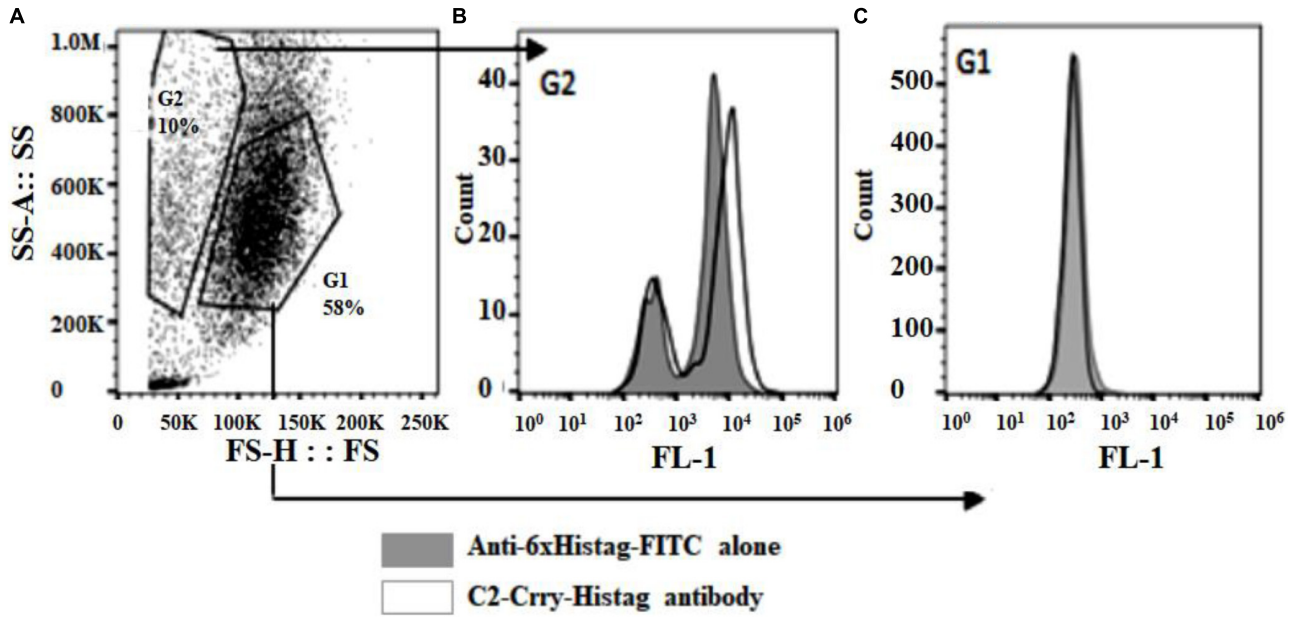

FIGURE 4 | Purified C2-Crry protein was analyzed by flow cytometry and demonstrated to bind apoptotic HUVEC cells. The HUVEC cells were incubated over night with 10 μM Antimycin A to induce apoptosis. After harvesting, cells were incubated on ice for 30 min with C2-Crry protein (10 μg/ml). The bound C2-Crry protein was detected with rabbit anti-6xHis-FITC conjugated antibody. **(A)** Flow cytometry analyses was performed on cells, **(B)** on apoptotic cells (boxed in G2 gate), or **(C)** on healthy cells (boxed in G1 gate).

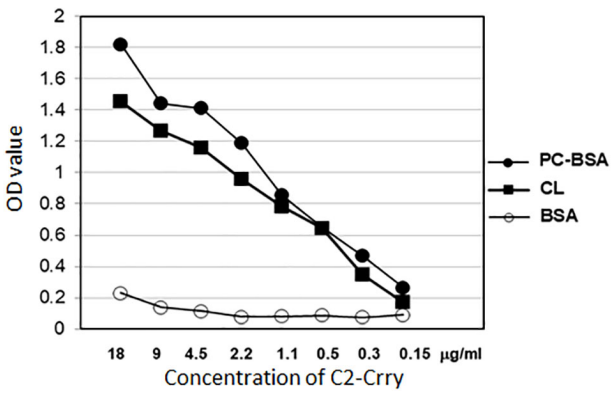

FIGURE 5 | Purified C2-Crry protein was analyzed in ELISA for binding the phospholipids cardiolipin (CL) and phosphatidylcholine-*b*ovine serum albumin (PC-BSA). The ELISA plates were covered over night with 10 μg/ml of cardiolipin dissolved in methanol and stored at 4°C with ELISA wells uncovered for methanol to dry out through the night. PC-BSA was added to plates in amount 5 μg/ml in PBS. After blocking the plates with BSA, different concentrations of C2-Crry (*X*-axis) were applied to wells. BSA was used as a control. Bound C2-Crry was detected with anti-6xHis antibody. Data shown as raw mean OD values (*Y*-axis). All samples were run in duplicate.

and 6.85 ± 1.89, respectively (**Figure 6A**). There was a significant 38.5% ($p < 0.042$) decrease in CDA in mice treated with the C2-Crry fusion protein (**Figure 6A**). The prevalence in mice treated with 1 × PBS or C2-Crry was 100% and 71%, respectively (**Figure 6B**). There was no significant change in weight in mice treated with C2-Crry compared with 1 × PBS treated mice (**Figure 6C**). None of the mice showed any type of toxicity, and all mice survived. These CDA and prevalence data in mice with CIA show that C2-Crry specifically decreased arthritis in mice with no toxicity or change in weight of treated mice.

Decreased IgG2a Anti-CII Levels in CIA Mice Treated With C2-Crry

IgG1 and Ig2a anti-CII Ab levels in sera from CIA mice treated with 1 × PBS or C2-Crry were examined by ELISA. There was no effect on IgG1 levels (**Figure 7A**). There was, however, a modest but significant ($p < 0.048$) decrease in the IgG2a anti-CII Ab levels at day 35 compared with PBS treated mice (**Figure 7B**). These data show that C2-Crry affects pathogenic IgG2a autoantibody levels, which is consist with the decrease in the CDA (**Figure 6A**).

Decreased Immunopathology, C3 Deposition but Not in Macrophage Scores in CIA Mice Treated With C2-Crry

There was a significant ($p < 0.0005$) decrease in immunopathology scores in mice treated with C2-Crry. Immunopathology scores decreased to 44, 46, 51, and 58% for inflammation, pannus formation, cartilage and bone damage, respectively (**Figure 8A**). C3 deposition was also significantly ($p < 0.026$) 42% decreased both on the cartilage and in the synovium (**Figure 8B**). No significant decrease in macrophage infiltration was seen in CIA mice treated with C2-Crry compared with the PBS treated mice (**Figure 8C**). Overall, these immunopathologic and C3 deposition IHC data

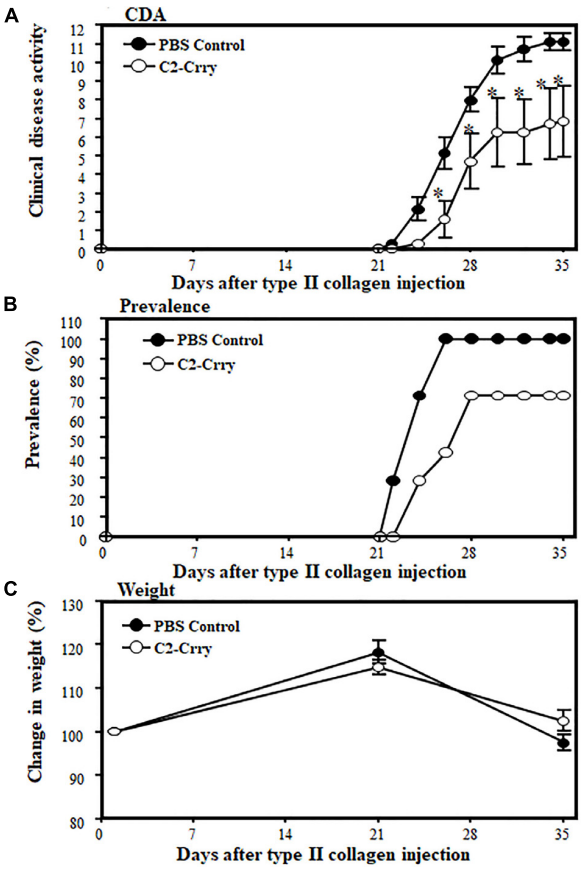

FIGURE 6 | Inhibitory effect of C2-Crry on the development of CIA. Mice were injected 4 times with a dose of 250 μg/mouse/i.p. of C2-Crry (n = 7) or 1 × PBS (n = 7) control 2x per week after the booster injection of type II collagen/CFA at day 21, at day 25, at day 29, and at day 32 as described in the Materials and Methods. All mice were sacrificed at day 35. **(A)** Mice injected with C2-Crry were protected (39%) significantly compared with mice treated with 1 × PBS. **(B)** Prevalence (%) was 66% and 100% in mice treated with C2-Crry and PBS, respectively. **(C)** Change in weight (%). Data shown as Mean ± SEM. *$p < 0.05$ considered significant.

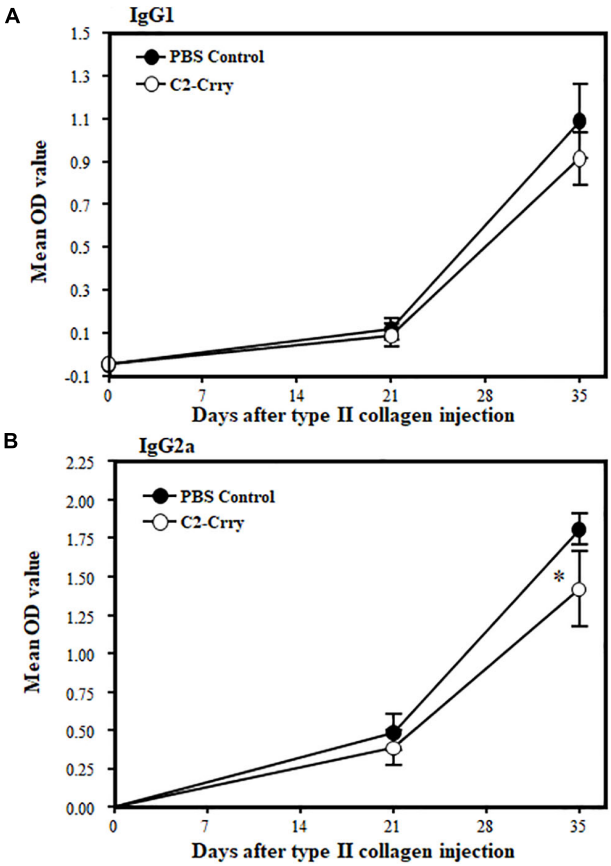

FIGURE 7 | Levels of IgG1 and IgG2a anti-CII antibodies in the sera from mice with CIA after treatment with C2-Crry and PBS. IgG1 and IgG2a antibodies were measured in the serum at day 0 (before induction of disease), day 22 (after booster injection and after one treatment), and at day 35 (after development of disease and after two treatments). **(A)** No decrease in IgG1 in mice treated with C2-Crry (n = 7) compared to 1 × PBS (n = 7) at day 22 or at day 35. **(B)** Significant decrease in IgG2a in serum in mice treated with C2-Crry (n = 7) compared with 1 × PBS control at day 35 only. Data shown as Mean ± SEM. *$p < 0.05$ considered significant.

were consistent with the decrease in CDA seen in mice with CIA (**Figure 6A**). Representative pictures of T-blue, C3 deposition and macrophage IHC are shown in **Supplementary Figure 2**.

Ex vivo Targeting of Apoptotic FLS With IRDye 800 Labeled C2-Crry

To determine that C2-Crry fusion protein target injured synovium in the joints of mice, we used FLS cells derived from the synovium of arthritic mouse (**Figure 9**). Serum starvation method was used to induce injury in the form of apoptosis in FLS. Therefore, FLS were serum starved for 72 h followed by the addition of IRDye 800 labeled C2-Crry as mentioned in the Methods so that it can be detected on apoptotic FLS. Binding of IRDye 800 labeled C2-Crry to apoptotic FLS was observed using a Zeiss Axio Observer 5 epifluorescent microscope (**Figure 9B**). Apoptotic cells with bound C2-Crry appeared green (**Figure 9B**) compared with non-apoptotic control FLS (**Figure 9A**). Apoptosis in FLS was separately confirmed using an agarose gel by visualizing a DNA ladder of 1 Kb, characteristic of apoptotic cells as shown in **Supplementary Figure 3**. Serum starved FLS for 6 h were used, as a negative and positive controls, and stained with Caspase 3/7 to show specific apoptosis of FLS induced by serum starvation under UV light (**Figures 9C,D**). These serum starved FLS data show that C2-Crry specifically targeted apoptotic, but not healthy FLS.

In vivo Targeting and Detection of IRDye 800 Labeled Anti-CII Antibodies and C2-Crry in the Joints of Arthritis Mice

To examine whether IRDye 800 labeled C2-Crry specifically targeted joints in mice with arthritis, two experiments were performed. In the first experiment, we injected WT C57BL/6 mice with IRDye 800 labeled (green color) anti-CII Abs, or with control IRDye 800 labeled mouse IgG in mice (**Figure 10**). At day

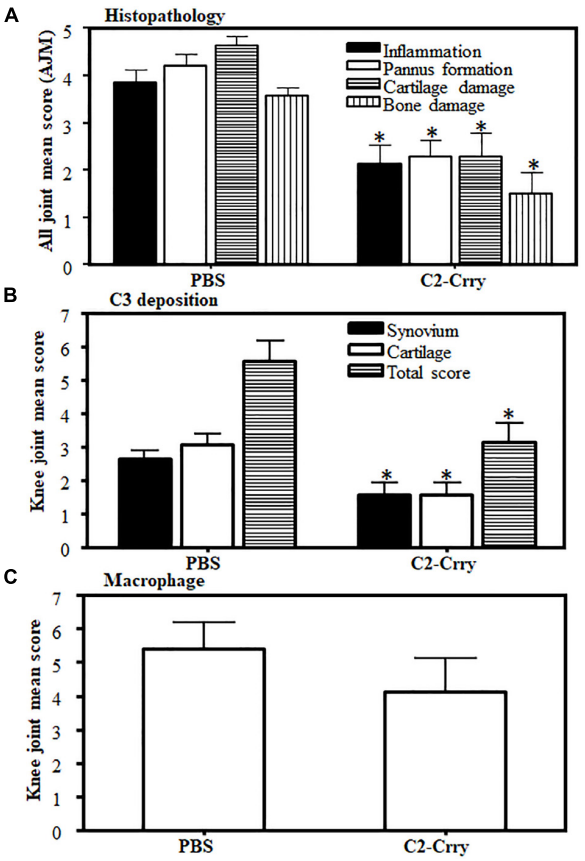

FIGURE 8 | Histopathology scores in CIA mice treated with C2-Crry substantially decreased compared with mice treated with PBS. All joints from mice sacrificed at day 35 were fixed in 10% neutral buffered formalin and processed for histopathology using T-blue and evaluated to determine all joints mean score (AJM). All sections from the joints were cut at a thickness of 5 μm and stained with T-blue. **(A)** Joint sections were scored for inflammation, pannus, cartilage damage and bone damage using a scale of 0–5 for each parameter. Data from all mice were included. **(B)** C3 deposition in the joints of mice treated with C2-Crry compared with 1 × PBS. Mean C3 deposition scores from both the knee joints only in the synovium, on the surface of cartilage and total scores (synovium plus cartilage). **(C)** Macrophage infiltration from the knee joints of mice treated with C2-Crry compared with 1 × PBS. Both the knee joints from each mouse were used to detect the presence of macrophages. All data represent the Mean ± SEM comparing C2-Crry ($n = 7$) or with PBS ($n = 7$). p-values were calculated using t-test. *$p < 0.05$ in comparison to the mice injected with PBS.

15, all mice were sacrificed after a long wash period of 3 days. Only labeled anti-CII Abs, but not murine labeled IgG, localized in the joints (**Figures 10A,B**). As expected no green color was detected in the joints of non-injected mice (**Figure 10C**). In separate studies, mice injected with 1 × PBS, appears identical to the non-injected mice (data not shown) and we have published it (61). No non-specific binding of IRD800 labeled anti-CII Ab was seen in other organs such as kidney, liver and lung which is consistent with our previous publication therefore no images were taken (61). These data show that IRDye 800 labeled antibodies or proteins can be detected in injured joints.

In the second experiment, a suboptimal disease was induced in WT C57BL6 mice by injecting unlabeled Arthrogen (**Figure 11**). At day 15, these mice were injected with IRDye 800 labeled C2-Crry or unlabeled C2-Crry and sacrificed after a wash period of 3 days, i.e., at day 18. Only IRDye 800 labeled C2-Crry bound to the knee joints, (**Figure 11A**). Although the binding of IRDye 800 labeled C2-Crry was not as robust when compared with IRDye 800 labeled anti-CII Abs, which might be due to the short half-life of C2-Crry, no distinct green color is visible in the joint of mice injected with non-labeled C2-Crry (**Figure 11B**). Similarly as expected no green color was detected in the joints of non-injected mice (**Figure 11C**). Of-note, some labeled C2-Crry was excreted rapidly in the urine of mice, which resulted in a non-specific binding on the paws (green color) of all mice even in non-injected mice for all these mice were kept in one cage due to blinding (**Figures 11A–C**). No non-specific binding of IRD800 labeled C2-Crry was seen in any other organs such as kidney, liver and lungs therefore no images were taken. These *in vivo* IRDye 800 C2-Crry labeling images show that C2-Crry can specifically target injured joints in mice.

DISCUSSION

In this study, we first showed that anti-C2 IgM NAb specifically recognized surface epitope(s) on apoptotic thymocytes. Second, C2-IgM NAb was shown to enhance suboptimal injury in CAIA, a complement-dependent mouse model of inflammatory arthritis. Third, we recombinantly linked C2scFv with the complement inhibitory protein Crry and then generated and purified a fusion protein, C2-Crry, in which the C2 sequences retained binding capacity to PL on apoptotic or injured cells. C2-Crry was also shown to attenuate arthritis in CIA, a separate complement dependent mouse model of arthritis. Finally, IRDye 800 labeled C2-Crry specifically bound *in vitro* to injured sFLS derived from an arthritic mouse, and *in vivo* imaging data showed that C2-Crry bound to the injured arthritic knee joints in mice. Overall, these data suggest that C2-Crry can be clinically useful for the treatment of arthritis or other autoimmune diseases involving apoptosis.

Notably, over one million cells die every second in the human body (62), and cell death can also occur due to infections such as viruses and bacteria as a primitive way of limiting their replication and systemic spread (63). Apoptosis pathways have also been linked to tolerance and immunity (64). The main purpose of apoptosis is to dispose of unwanted cells in a physiological controlled manner (65, 66) and in doing so cells expose eat me signals, e.g., phosphatidylserine, on their surface. We have shown previously that but C2-IgM binds to phosphatidylserine (48), although the actual epitope (s) to which C2 binds on apoptotic cells still unknown; however, it was speculated that C2 might bind to glycerol/fatty acid interface (48). The membrane contents of the cells undergoing apoptosis are well preserved and can still interact with the surrounding microenvironment, including NAbs already present in the blood.

Natural antibodies, in contrast to adaptive immune response generated antibodies, are present in mammals without previous

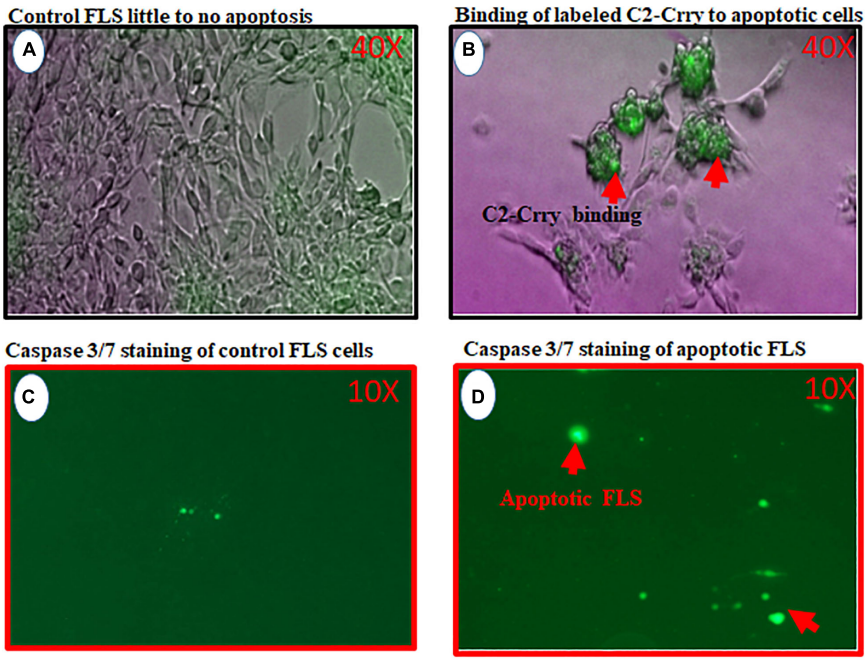

FIGURE 9 | *In vitro* study showing binding of IRDye 800 labeled C2-Crry (Green color) to serum starved FLS undergoing apoptosis. FLS were serum starved in 24-well tissue culture plates for 72 h followed by the addition of IRDye 800 labeled C2-Crry. **(A)** FLS control bright field showing little to no apoptosis. **(B)** Apoptotic FLS bound to labeled C2-Crry (Green color; red arrow) in 24-well plate. **(C)** Caspase 3/7 staining (2 mM) staining used for negative control FLS on the glass slide showing minimum background green color staining. **(D)** Caspase 3/7 staining used to show serum starved apoptotic FLS for 6 h on a glass slide with cover slip. Apoptotic cells and apoptotic bodies appeared green under UV light as shown by red arrows. Scanning/and or imaging using with Zeiss Axio Observer 5 epifluorescent microscope equipped with X-Cite 200 DC light source and Axiocam 506 monochromatic camera. Near infrared Fluorescence was imaged using Cy7 filter set (Chroma Corporation, McHenry, IL, United States). One representative experiment of C2-Crry binding to apoptotic FLS images is shown. No scale was added when the images were taken. But 40x magnification objective was used to take these pictures for images **(A,C)** and 10x objective was used for images **(C,D)**.

externally generated antigen exposure, vaccination or infection. In contrast to antigen-induced antibodies, which are mainly IgG and mono-reactive, many NAbs are IgM and polyreactive. NAbs are self-reactive IgM Abs and mainly secreted by CD5 + B1 cells even in germ free environments and constitute up to 80% of the systemic IgM levels (49, 67, 68). Because of the NAb ability to bind self-antigens, they may serve as templates for some of the high-affinity autoantibodies that emerge in patients with autoimmune disease, particularly those associated with a significant expansion of CD5 + B cells (69–71). Thus, chromic activation of the immune system can lead to expansion of naturally present auto poly-reactive clones of NAbs. Furthermore, in genetically predisposed individuals, this can lead to the development of autoimmune diseases such as arthritis and lupus.

Apoptotic and necrotic cell death, dependent on the CS, also occurs due to tissue reperfusion after ischemia (72). C2 NAb neoepitopes have also been shown to be exposed in post-ischemic mouse models of intestine and brain injury (47, 48). Previous studies have shown that other self-reactive IgM NAbs recognize non-muscle myosin and catalyze intestinal (73), myocardial (74), and skeletal muscle (75) ischemia reperfusion injury in Rag1 deficient mice; an identical antibody specificity is found in human serum (76). In another model of recognition of annexin-IV by a pathogenic Nab, by transplanting hearts from WT donor mice into antibody deficient mice reconstituted with specific self-reactive IgM mAbs neoepitope, Annexin-IV expressed on post-transplant heart was shown to be the key mechanisms for IgM recognition of neoepitopes in graft injury (49). Similarly, anti-Annexin scFV linked to Crry (a.k.a. B4-Crry) not only blocked graft IgM binding and complement activation but also reduced graft inflammation and injury (49). In that study, whether B4-Crry actually bound to the apoptotic cells or not was not clear. Our data clearly show that IRDye 800 labeled C2-Crry bound to the FLS, *in vitro*, undergoing apoptosis due to serums starvation (**Figure 9B**) and also, *in vivo*, bound to the knee joints of arthritic mice (**Figure 11A**). Apoptosis in serum starved FLS was also separately confirmed using annexin V plus propidium iodide by flow cytometry analysis (data not shown). All of above mentioned studies provided the fundamental concept that IgM NAbs can cause injury and targeted delivery of scFv-linked complement inhibitory proteins can reduce injury in ischemia reperfusion related injury mouse models. These results are consistent with our current study in which C2 IgM mAb induced inflammation but scFV-linked Crry with C2 reduced inflammation, i.e., arthritis probably by targeting to apoptotic sFLS in the knee joints.

In this study, we have targeted pathologically important epitopes in the form of PL generated during injury or inflammation in the synovium. FLS are the predominant cell

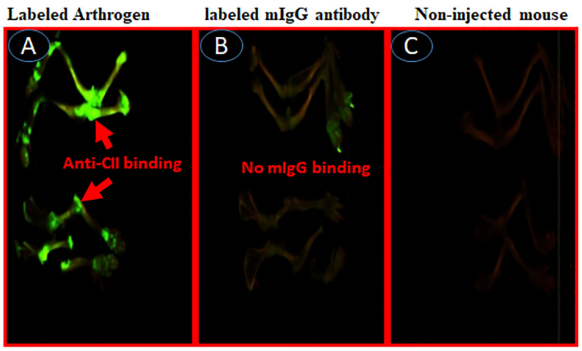

FIGURE 10 | *In vivo* imaging of binding of IRDye 800 labeled Arthrogen to the cartilage or joints in mice. Showing specific localization of IRDye 800 labeled-Arthrogen (green color), at day 15, to the cartilage in the joints of mice. All mice were injected i.v. with IRDye 800 labeled Arthrogen and sacrificed after a long wash period of 15 days **(A)** Labeled Arthrogen (green color) localized and specifically bound to the joints. **(B)** Labeled murine IgG control (no green color) s.c. injected mice showing no specific binding or localization to the joints. **(C)** Non-injected mice as control (no green color) in the joints. Scanning/and or imaging using Li-COR Odyssey. No scale was added when the images were taken and images of the entire limb(s) has been shown. These experiments were performed three times using three mice in with each treatment with excellent reproducibility.

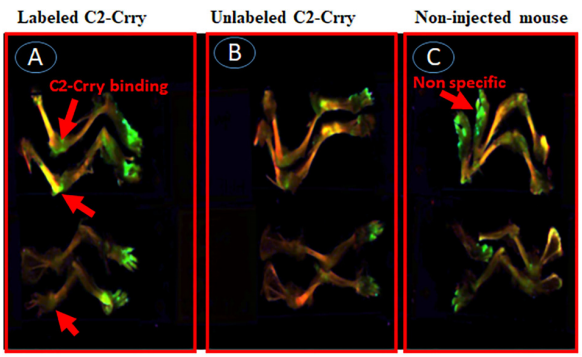

FIGURE 11 | *In vivo* scanning using Li-COR Odyssey of binding of IRDye 800 labeled C2-Crry binding to the cartilage in mice with CAIA. IRDye 800 labeled (Green color) C2-Crry localized and bound to the joints in arthritic mice with arthritis at day 15. Suboptimal disease (injury) was induced in mice joints by injecting Arthrogen and LPS as mentioned in Methods. All mice were sacrificed 3 days after injection (i.v.), due to short half-life, with labeled or unlabeled C2-Crry followed by imaging. **(A)** Labeled C2-Crry (green color shown by red arrow) bound to the joints of arthritic mice with CDA score 6. **(B)** Unlabeled C2-Crry not detected in the joints of arthritic mice with CDA 7. **(C)** Non-injected control mice show no binding as expected in the joints of normal mice with CDA 0. Non-specific fluorescence (shown by red arrow) has been seen on paws of all mice due to excretion of the dye in urine of labeled C2-Crry mice for all mice were kept in the same cage for the purpose of blinding. No scale was added when the images were taken and images of the entire limb(s) has been shown. These experiments were done two times using three mice each time.

type present in the pannus (multilayered synovium) of inflamed joints in RA. In addition, other cell types such as T cells, B cells, adipocytes, monocyte, neutrophil and macrophage are also present. Furthermore, the cartilage surface gets damaged during inflammation due to the direct binding of anti-CII antibodies (5, 77). Using a conjugate of C2-Crry, we systemically delivered Crry to targeting the site of injury due to the specific neoepitopes for C2 IgM NAb expressed on the surface of synoviocytes in the synovium or on chondrocytes on the surface of cartilage. This is based on the imaging data that IRDye 800 labeled C2-Crry localized in the knee joints of arthritic mice (**Figure 11A**) compared with non-labeled C2-Crry (**Figure 11B**) indicating that C2-Crry bound to the injured synoviocytes or damaged cartilage surface. In addition, C2 IgM NAb alone enhances injury (**Figure 2A**) which normally leads to more C3 deposition as it is evident from mice with CIA, i.e., only PBS treatment have more C3 deposition compared with C2-Crry treated CIA mice (**Supplementary Figure 2**). One of the important questions is that whether C2-Crry will be effective when CS is compromised, e.g., in C3 deficient mice? We speculate that it will equally be effective because C2 might be binding to PL on apoptotic or injured cells independently from C3. Furthermore Crry possesses decay-accelerating activity for the CP but weak decay-accelerating activity for the AP C3 convertase so it might be equally effective in the complete absence of C3 because it can still inhibit CP C5 convertase although it has not been tested. We then asked the question what is the relevance of C2-Crry for its clinical use as a medicine in RA patients because Crry is not present in humans? In this study we have provided the proof-of-concept, *in vitro* and *in vivo*, that complement inhibitory protein such as Crry can be specifically delivered to the injured cells or injured joints using C2 scFv. In humans, CR1 is the functional orthologue of Crry, as it expresses cofactor and decay-accelerating function for both the CP and AP. Thus, the approach of delivering complement inhibitory protein, Crry or potentially using CR1, through C2 scFV as an apoptotic cell guide has also advantage over currently available therapeutic approaches which delivers complement inhibitory proteins systematically instead of direct targeted delivery to the injured tissue.

There are several limitations in our current study. One of the limitations is that we have not used C2 scFv alone to determine its cause and effect on the CAIA model. However, C2 scFv alone should not demonstrate a substantial effect on arthritis because it lacks the Fc domain and, therefore, will not activate complement. However, it may block certain neoepitopes and diminish joint damage in CIA. That remains to be evaluated. Furthermore C2-Crry has no known complement-dependent cytotoxicity. It does not contain any part of Fc which can bind to C1q. It is a single chain mAb and only contains variable regions. The second limitation is that we were unable to show through *in vivo* imaging a comparable amount of IRDye 800 labeled C2-Crry deposited in the joints of arthritic mice compared with labeled control anti-CII antibody (**Figure 10A**). There can be many reasons for this low deposition of C2-Crry in the joints. First, it might be related to the half-life of C2-Crry fusion protein, which was less than 48 h but more than 24 h. Second, IRDye 800 labeled C2-Crry clearance through urine, perhaps because of its small size allowing passage through the glomerular basement membrane, suggest it has less availability to apoptotic cells in the joints. Third, there might be less apoptotic cells in the joints due to the use of a suboptimal level of injury to dissect the protective effect of C2-Crry. Finally, based on our experience, apoptotic cells might be cleared rapidly

from the synovium. In contrast, the reason, we do see more IRDye 800 labeled anti-CII deposited in the joints because it specifically binds to the collagen/chondrocytes on the surface of cartilage and causes injury. Some of the non-specific binding of IRDye labeled C2-Crry on the hair of paws of mice was noticed due to its excretion in the urine for all mice were kept in the same cage for the investigators were blinded to the treatment. Finally using and corroborating IRD800 labeled C2-Crry histology along with anti-C2-Crry immunohistochemistry might have yielded more valuable joint-specific binding information.

We also asked how the presence of NAbs and also the binding of C2 and C2-Crry have any clinical relevance to the treatment of RA. In early stages of apoptosis, nuclear chromatin condenses and DNA is digested into nucleosome-sized 180 base pair fragments (**Supplementary Figure 3**). Although there are not many reports related to the presence of apoptosis in RA synovium, it has been shown in 12 RA synovium and 4 OA synovium biopsies that apoptosis occurs and the primary site for apoptosis was the synovial sub lining (78). That study also showed that apoptosis can be induced in cultured sFLS with cytokines present in the inflamed joints of RA patients. It is consistent with our *in vitro* FLS data, in which apoptosis, was induced using serum starvation and then IRDye 800 labeled C2-Crry bound to these apoptotic FLS (**Figure 9B**). Interestingly, in the above mentioned study, synovial sub lining cells with fragmented DNA, i.e., apoptotic cells included macrophages and fibroblasts, but T cells in lymphoid aggregates, which expressed large amounts of bcl2, were spared (78). This study highlighted the fact that apoptosis specifically occur in the RA and OA synovium, but to what extend is not known. Furthermore, most of the rheumatology-related literature points out that apoptosis is a common feature of the RA synovium either because it occur naturally or it is induced by drugs which are currently being used for the treatment of RA. For example, Rituximab, anti-CD20 chimeric mouse/human mAb or CD40 fully humanized anti-CD20 mAb being used for the treatment of RA deplete B cells via apoptosis (79–81). In RA patients Fas and Fas-L have been detected in synovial cells and, also in activated mature T cells obtained at the time of arthroplasty (82) and these are highly susceptible to Fas-mediated apoptosis induced by anti-Fas mAb. Nonetheless, apoptosis pathways are defective in RA synovium and treatment with DMARD reduces Fas expression on the synovial tissue (82). In contrast, other studies have shown DMARD itself can initiate apoptosis both *in vitro* (83, 84) and *in vivo* (85). Another study support the concept that both Etanercept and Infliximab did induce apoptotic pathways in RA synovial tissue (86).

The exact relationship between pannus formation (synovial hyperplasia) and apoptosis in rheumatoid synovium is unknown. There might be an imbalance between cell proliferation and apoptosis in RA synovium that leads to pannus formation (87). Nonetheless apoptotic cells in the synovial lining can be a potential therapeutic target for fusion proteins like C2-Crry which specifically binds to PL. Even if apoptosis is not present then transient induction of apoptosis by drugs in the synovium or in the pannus could be a way to locally deliver C2-Crry in the RA synovium at very early or at very late stage of the disease.

We have previously shown that the LP of the CS plays an important role not only activating the AP but also directly playing an important role in inducing arthritis in mice (8, 88). But we do not know the precise interactions between NAbs, apoptosis and various LP components such as MBL or ficolins or collectins at very early stage in arthritis. We also do not know the extent of apoptosis in the peripheral blood or synovium or the presence of CD5 + B1 IgM NAbs producing cells in the synovium at very early stage disease in RA patients. Furthermore, whether rheumatoid factor (RF) IgM, which exists in RA, can act as a NAb is also not fully understood. RF are present in more than 70% of RA patients, and high titers are associated with severe disease (89). RF are also abundant in the RA synovium. Two types of RF exists, i.e., low affinity and high affinity RF. Low affinity RF are IgM NAbs, polyreactive, T cell independent and also produced by CD5 + B1 cells in normal subjects (89).

In sum, our study offers the potential for the development of new targeted drugs to inhibit complement activation in the joints at very early stage of RA that would be triggered by IgM Nabs as well as disease specific IgG antibodies. Other fusion proteins such as C2-MAp44 or C2-sMAP can be designed to directly deliver a LP inhibitors MAp44 or sMAP to the joints, or C2-Factor H to deliver an AP, could also be created and tested in studies going forward.

DATA AVAILABILITY STATEMENT

All datasets presented in this study are included in the article/**Supplementary Material**.

ETHICS STATEMENT

The studies involving human participants were reviewed and approved by IRB University of Colorado. The patients/participants provided their written informed consent to participate in this study. The animal study was reviewed and approved by IACUC University of Colorado.

AUTHOR CONTRIBUTIONS

VH conceived the idea for making fusion protein, C2-Crry, supervised the project and reviewed this manuscript in-depth. NB proposed the idea of testing of C2-Crry *in vivo*, planned and executed all *in vivo* CIA and CAIA experiments, designed labeling of Arthrogen and C2-Crry with IRDy800, analyzed all data and wrote the first and revised drafts of the manuscript. ST originally designed, constructed and purified fusion protein, C2-Crry-6Histag. LK cloned NAb C2, and purified already clones fusion protein, C2-Crry and checked the quality of all NAbs used and also C2-Crry, respectively. LK also done the functional assays such as ELISA and FACS to show the specificity of C2 mAb binding to phospholipids. NH, JR, and GM assisted in all *in vivo* CAIA and CIA as well as IHC studies. RS, VV, GW, and DS assisted in planning labeling of Arthrogen IRDy800 and standardization of *in vivo* injection planning, and strategy for

determining the *in vivo* half-life of C2-Crry and imaging joint of mice. All authors contributed to the article and approved the submitted version.

FUNDING

Supported by National Institutes of Health grant 2R56R01AR51749-15 to VH (PI) and NB (Co-I), R01 AI154959-05 to DS and U01AI132894 to ST, and by Department of Veteran's Affairs grant RX001141 to ST.

ACKNOWLEDGMENTS

All authors are grateful to Mr. Xiaofeng Yang, Department of Microbiology and Immunology, Medical University of South Carolina, Charleston, SC for helping in designing, constructing and purification of fusion protein, and C2-Crry 6Histag.

SUPPLEMENTARY MATERIAL

The Supplementary Material for this article can be found online at: https://www.frontiersin.org/articles/10.3389/fimmu.2020.575154/full#supplementary-material

Supplementary Figure 1 | Photographs of C2-IgM NAb enhanced inflammation in CAIA mice at day 3 and at day 10. **(A)** No visible inflammation (shown in circle by red arrow) on the forepaws of mice treated with control F-632 IgM NAb. **(B)** Visible inflammation (shown in circle by red arrow) on forepaws of mice treated with anti-C2-IgM. **(C)** Inflammation (shown in circle by red arrow) on forepaws of mice treated with 1 × PBS (control). **(D)** Inflammation (shown in circle by red arrow) on forepaws of mice treated with control F-632 IgM. **(E)** Substantial inflammation (shown in circle by red arrow) on forepaws of mice treated with anti-C2-IgM. All photographs were taken by simple polaroid camera under normal light.

Supplementary Figure 2 | Representative histopathologic images of inflammation, C3 deposition and macrophage staining from the knee joints of CIA mice injected i.p. four times with PBS or C2-Crry fusion protein. At day 35, all joints were fixed with 10% neutral buffered formalin, decalcified, paraffin embedded, and then sectioned at a thickness of 5 μm. The left hand side two panels top and bottom **(A,B)** show inflammation, i.e., staining with toluidine-blue (blue color) from the knee joints of CIA mice treated with PBS (left top panel) or with C2-Crry (right bottom panel). The middle set of two panels top and bottom **(C,D)** show C3 deposition (brown color) staining from the knee joints of CIA mice treated with PBS (Center top panel) or with C2-Crry (Center bottom panel). The right hand side two panels top and bottom **(E,F)** show macrophage F4/80 (red color) staining of knee joint of CIA mice treated with PBS (right top panel) or with C2-Crry (right bottom panel). Areas of synovium (S-black arrow), cartilage (C-black arrow), bone (B-black arrow), and meniscus (M-black arrow) are identified. The sections for inflammation (blue color) were photographed under the 20x objective while sections of C3 deposition and macrophage IHC staining were photographed under the 10x objective. Scale bars have shown in the red at the right bottom knee joint equal 0.05 mm (50 μm) for 20x and 0.01 mm (100 μm) for 10x objectives, respectively.

Supplementary Figure 3 | Detection of DNA apoptotic ladder in serum starved FLS. FLS with no serum starvation (lane 1; no DNA ladder) or FLS with serum starved for 3 days to induce apoptosis (lane 2; DNA ladder present) or DNA ladder marker of 1 Kb (lane 3). Genomic DNA from FLS grown in the presence or absence of serum was isolates using QIAGEN DNA kit. 4 μg of DNA from each sample was electrophoresed in 1 × TAE buffer, 90 volts for 1 h using 1.2% agarose gel containing Ethidium bromide followed by visualization under UV light.

REFERENCES

1. Hootman JM, Helmick CG. Projections of US prevalence of arthritis and associated activity limitations. *Arthritis Rheum.* (2006) 54:226–9.
2. Helmick CG, Felson DT, Lawrence RC, Gabriel S, Hirsch R, Kwoh CK, et al. Estimates of the prevalence of arthritis and other rheumatic conditions in the United States Part I. *Arthritis Rheum.* (2008) 58:15–25. doi: 10.1002/art.23177
3. Arend WP, Firestein GS. Pre-rheumatoid arthritis: predisposition and transition to clinical synovitis. *Nat Rev Rheumatol.* (2012) 8:573–86. doi: 10.1038/nrrheum.2012.134
4. Holers VM, Banda NK. Complement in the initiation and evolution of rheumatoid arthritis. *Front Immunol.* (2018) 9:1057. doi: 10.3389/fimmu.2018.01057
5. Banda NK, Thurman JM, Kraus D, Wood A, Carroll MC, Arend WP, et al. Alternative complement pathway activation is essential for inflammation and joint destruction in the passive transfer model of collagen-induced arthritis. *J Immunol.* (2006) 177:1904–12. doi: 10.4049/jimmunol.177.3.1904
6. Brodeur JP, Ruddy S, Schwartz LB, Moxley G. Synovial fluid levels of complement SC5b-9 and fragment Bb are elevated in patients with rheumatoid arthritis. *Arthritis Rheum.* (1991) 34:1531–7. doi: 10.1002/art.1780341209
7. Ammitzboll CG, Thiel S, Ellingsen T, Deleuran B, Jorgensen A, Jensenius JC, et al. Levels of lectin pathway proteins in plasma and synovial fluid of rheumatoid arthritis and osteoarthritis. *Rheumatol Int.* (2012) 32:1457–63. doi: 10.1007/s00296-011-1879-x
8. Banda NK, Acharya S, Scheinman RI, Mehta G, Takahashi M, Endo Y, et al. Deconstructing the lectin pathway in the pathogenesis of experimental inflammatory arthritis: essential role of the lectin ficolin B and mannose-binding protein-associated serine protease 2. *J Immunol.* (2017) 199:1835–45. doi: 10.4049/jimmunol.1700119
9. Banda NK, Takahashi K, Wood AK, Holers VM, Arend WP. Pathogenic complement activation in collagen antibody-induced arthritis in mice requires amplification by the alternative pathway. *J Immunol.* (2007) 179:4101–9. doi: 10.4049/jimmunol.179.6.4101
10. Banda NK, Takahashi M, Levitt B, Glogowska M, Nicholas J, Takahashi K, et al. Essential role of complement mannose-binding lectin-associated serine proteases-1/3 in the murine collagen antibody-induced model of inflammatory arthritis. *J Immunol.* (2010) 185:5598–606. doi: 10.4049/jimmunol.1001564
11. Wang Y, Kristan J, Hao L, Lenkoski CS, Shen Y, Matis LA. A role for complement in antibody-mediated inflammation: C5-deficient DBA/1 mice are resistant to collagen-induced arthritis. *J Immunol.* (2000) 164:4340–7. doi: 10.4049/jimmunol.164.8.4340
12. Wang Y, Rollins SA, Madri JA, Matis LA. Anti-C5 monoclonal antibody therapy prevents collagen-induced arthritis and ameliorates established disease. *Proc Natl Acad Sci USA.* (1995) 92:8955–9. doi: 10.1073/pnas.92.19.8955
13. Banda NK, Hyatt S, Antonioli AH, White JT, Glogowska M, Takahashi K, et al. Role of C3a receptors, C5a receptors, and complement protein C6 deficiency in collagen antibody-induced arthritis in mice. *J Immunol.* (2012) 188:1469–78. doi: 10.4049/jimmunol.1102310
14. Bemis EA, Norris JM, Seifert J, Frazer-Abel A, Okamoto Y, Feser ML, et al. Complement and its environmental determinants in the progression of human rheumatoid arthritis. *Mol Immunol.* (2019) 112:256–65. doi: 10.1016/j.molimm.2019.05.012
15. Banda NK, Mehta G, Kjaer TR, Takahashi M, Schaack J, Morrison TE, et al. Essential role for the lectin pathway in collagen antibody-induced arthritis revealed through use of adenovirus programming complement inhibitor MAp44 expression. *J Immunol.* (2014) 193:2455–68. doi: 10.4049/jimmunol.1400752
16. Mehta G, Scheinman RI, Holers VM, Banda NK. A new approach for the treatment of arthritis in mice with a novel conjugate of an anti-C5aR1 antibody

and C5 small interfering RNA. *J Immunol*. (2015) 194:5446–54. doi: 10.4049/jimmunol.1403012
17. Morgan BP, Meri S. Membrane proteins that protect against complement lysis. *Springer Semin Immunopathol*. (1994) 15:369–96. doi: 10.1007/bf01837366
18. Barilla-LaBarca ML, Liszewski MK, Lambris JD, Hourcade D, Atkinson JP. Role of membrane cofactor protein (CD46) in regulation of C4b and C3b deposited on cells. *J Immunol*. (2002) 168:6298–304. doi: 10.4049/jimmunol.168.12.6298
19. Foley S, Li B, Dehoff M, Molina H, Holers VM. Mouse Crry/p65 is a regulator of the alternative pathway of complement activation. *Eur J Immunol*. (1993) 23:1381–4. doi: 10.1002/eji.1830230630
20. Kim YU, Kinoshita T, Molina H, Hourcade D, Seya T, Wagner LM, et al. Mouse complement regulatory protein Crry/p65 uses the specific mechanisms of both human decay-accelerating factor and membrane cofactor protein. *J Exp Med*. (1995) 181:151–9. doi: 10.1084/jem.181.1.151
21. Wu X, Spitzer D, Mao D, Peng SL, Molina H, Atkinson JP. Membrane protein Crry maintains homeostasis of the complement system. *J Immunol*. (2008) 181:2732–40. doi: 10.4049/jimmunol.181.4.2732
22. Xu C, Mao D, Holers VM, Palanca B, Cheng AM, Molina H. A critical role for murine complement regulator crry in fetomaternal tolerance. *Science*. (2000) 287:498–501. doi: 10.1126/science.287.5452.498
23. Alexander JJ, Jacob A, Bao L, Macdonald RL, Quigg RJ. Complement-dependent apoptosis and inflammatory gene changes in murine lupus cerebritis. *J Immunol*. (2005) 175:8312–9. doi: 10.4049/jimmunol.175.12.8312
24. Alexander JJ, Jacob A, Vezina P, Sekine H, Gilkeson GS, Quigg RJ. Absence of functional alternative complement pathway alleviates lupus cerebritis. *Eur J Immunol*. (2007) 37:1691–701. doi: 10.1002/eji.200636638
25. Wyss-Coray T, Mucke L. Inflammation in neurodegenerative disease–a double-edged sword. *Neuron*. (2002) 35:419–32. doi: 10.1016/s0896-6273(02)00794-8
26. Wyss-Coray T, Yan F, Lin AH, Lambris JD, Alexander JJ, Quigg RJ, et al. Prominent neurodegeneration and increased plaque formation in complement-inhibited Alzheimer's mice. *Proc Natl Acad Sci USA*. (2002) 99:10837–42. doi: 10.1073/pnas.162350199
27. Banda NK, Kraus D, Vondracek A, Huynh LH, Bendele A, Holers VM, et al. Mechanisms of effects of complement inhibition in murine collagen-induced arthritis. *Arthritis Rheum*. (2002) 46:3065–75. doi: 10.1002/art.10591
28. Liu F, Wu L, Wu G, Wang C, Zhang L, Tomlinson S, et al. Targeted mouse complement inhibitor CR2-Crry protects against the development of atherosclerosis in mice. *Atherosclerosis*. (2014) 234:237–43. doi: 10.1016/j.atherosclerosis.2014.03.004
29. Song H, Qiao F, Atkinson C, Holers VM, Tomlinson S. A complement C3 inhibitor specifically targeted to sites of complement activation effectively ameliorates collagen-induced arthritis in DBA/1J mice. *J Immunol*. (2007) 179:7860–7. doi: 10.4049/jimmunol.179.11.7860
30. Banda NK, Levitt B, Glogowska MJ, Thurman JM, Takahashi K, Stahl GL, et al. Targeted inhibition of the complement alternative pathway with complement receptor 2 and factor H attenuates collagen antibody-induced arthritis in mice. *J Immunol*. (2009) 183:5928–37. doi: 10.4049/jimmunol.0901826
31. Werneburg S, Jung J, Kunjamma RB, Ha SK, Luciano NJ, Willis CM, et al. Targeted complement inhibition at synapses prevents microglial synaptic engulfment and synapse loss in demyelinating disease. *Immunity*. (2020) 52:167–82.e167.
32. Fleming SD. Natural antibodies, autoantibodies and complement activation in tissue injury. *Autoimmunity*. (2006) 39:379–86. doi: 10.1080/08916930600739381
33. Wener M. Immune complexes and autoantibodies to C1q. In: Kammer GM, Tsokos GC editors. *Lupus: Molecular and Cellular Pathogenesis*. Totowa, NJ: Humana Press. (1999). p. 574–98. doi: 10.1007/978-1-59259-703-1_35
34. Avrameas S, Alexopoulos H, Moutsopoulos HM. Natural autoantibodies: an undersugn hero of the immune system and autoimmune disorders-a point of view. *Front Immunol*. (2018) 9:1320. doi: 10.3389/fimmu.2018.01320
35. Ochsenbein AF, Zinkernagel RM. Natural antibodies and complement link innate and acquired immunity. *Immunol Today*. (2000) 21:624–30. doi: 10.1016/s0167-5699(00)01754-0
36. Baumgarth N, Herman OC, Jager GC, Brown LE, Herzenberg LA, Chen J. B-1 and B-2 cell-derived immunoglobulin M antibodies are nonredundant components of the protective response to influenza virus infection. *J Exp Med*. (2000) 192:271–80. doi: 10.1084/jem.192.2.271
37. Casali P, Notkins AL. CD5+ B lymphocytes, polyreactive antibodies and the human B-cell repertoire. *Immunol Today*. (1989) 10:364–8. doi: 10.1016/0167-5699(89)90268-5
38. Herzenberg LA, Kantor AB. B-cell lineages exist in the mouse. *Immunol Today*. (1993) 14:79–83; discussion 88–90.
39. Avrameas S. Natural autoantibodies: from 'horror autotoxicus' to 'gnothi seauton'. *Immunol Today*. (1991) 12:154–9. doi: 10.1016/0167-5699(91)90080-d
40. Avrameas S, Ternynck T. Natural autoantibodies: the other side of the immune system. *Res Immunol*. (1995) 146:235–48. doi: 10.1016/0923-2494(96)80259-8
41. Lutz HU, Bussolino F, Flepp R, Fasler S, Stammler P, Kazatchkine MD, et al. Naturally occurring anti-band-3 antibodies and complement together mediate phagocytosis of oxidatively stressed human erythrocytes. *Proc Natl Acad Sci USA*. (1987) 84:7368–72. doi: 10.1073/pnas.84.21.7368
42. Ochsenbein AF, Fehr T, Lutz C, Suter M, Brombacher F, Hengartner H, et al. Control of early viral and bacterial distribution and disease by natural antibodies. *Science*. (1999) 286:2156–9. doi: 10.1126/science.286.5447.2156
43. Ogden CA, Kowalewski R, Peng Y, Montenegro V, Elkon KB. IGM is required for efficient complement mediated phagocytosis of apoptotic cells in vivo. *Autoimmunity*. (2005) 38:259–64. doi: 10.1080/08916930500124452
44. Quartier P, Potter PK, Ehrenstein MR, Walport MJ, Botto M. Predominant role of IgM-dependent activation of the classical pathway in the clearance of dying cells by murine bone marrow-derived macrophages in vitro. *Eur J Immunol*. (2005) 35:252–60. doi: 10.1002/eji.200425497
45. Arnold JN, Wormald MR, Suter DM, Radcliffe CM, Harvey DJ, Dwek RA, et al. Human serum IgM glycosylation: identification of glycoforms that can bind to mannan-binding lectin. *J Biol Chem*. (2005) 280:29080–7. doi: 10.1074/jbc.m504528200
46. Nauta AJ, Raaschou-Jensen N, Roos A, Daha MR, Madsen HO, Borrias-Essers MC, et al. Mannose-binding lectin engagement with late apoptotic and necrotic cells. *Eur J Immunol*. (2003) 33:2853–63. doi: 10.1002/eji.200323888
47. Kulik L, Fleming SD, Moratz C, Reuter JW, Novikov A, Chen K, et al. Pathogenic natural antibodies recognizing annexin IV are required to develop intestinal ischemia-reperfusion injury. *J Immunol*. (2009) 182:5363–73. doi: 10.4049/jimmunol.0803980
48. Elvington A, Atkinson C, Kulik L, Zhu H, Yu J, Kindy MS, et al. Pathogenic natural antibodies propagate cerebral injury following ischemic stroke in mice. *J Immunol*. (2012) 188:1460–8. doi: 10.4049/jimmunol.1102132
49. Atkinson C, Qiao F, Yang X, Zhu P, Reaves N, Kulik L, et al. Targeting pathogenic postischemic self-recognition by natural IgM to protect against posttransplantation cardiac reperfusion injury. *Circulation*. (2015) 131:1171–80. doi: 10.1161/circulationaha.114.010482
50. Narang A, Qiao F, Atkinson C, Zhu H, Yang X, Kulik L, et al. Natural IgM antibodies that bind neoepitopes exposed as a result of spinal cord injury, drive secondary injury by activating complement. *J Neuroinflammation*. (2017) 14:120.
51. Chang MK, Binder CJ, Miller YI, Subbanagounder G, Silverman GJ, Berliner JA, et al. Apoptotic cells with oxidation-specific epitopes are immunogenic and proinflammatory. *J Exp Med*. (2004) 200:1359–70. doi: 10.1084/jem.20031763
52. Fulda S. Exploiting apoptosis pathways for the treatment of pediatric cancers. *Pediatr Blood Cancer*. (2009) 53:533–6. doi: 10.1002/pbc.21922
53. Fulda S, Debatin KM. Extrinsic versus intrinsic apoptosis pathways in anticancer chemotherapy. *Oncogene*. (2006) 25:4798–811. doi: 10.1038/sj.onc.1209608
54. Hietala MA, Nandakumar KS, Persson L, Fahlen S, Holmdahl R, Pekna M. Complement activation by both classical and alternative pathways is critical for the effector phase of arthritis. *Eur J Immunol*. (2004) 34:1208–16. doi: 10.1002/eji.200424895
55. Watson WC, Brown PS, Pitcock JA, Townes AS. Passive transfer studies with type II collagen antibody in B10.D2/old and new line and C57Bl/6 normal and beige (Chediak-Higashi) strains: evidence of important roles for C5 and multiple inflammatory cell types in the development of erosive arthritis. *Arthritis Rheum*. (1987) 30:460–5. doi: 10.1002/art.1780300418

56. Nandakumar KS, Holmdahl R. Antibody-induced arthritis: disease mechanisms and genes involved at the effector phase of arthritis. *Arthritis Res Ther*. (2006) 8:223.
57. Arend WP, Dayer JM. Inhibition of the production and effects of interleukin-1 and tumor necrosis factor alpha in rheumatoid arthritis. *Arthritis Rheum*. (1995) 38:151–60. doi: 10.1002/art.1780380202
58. Fridkis-Hareli M, Storek M, Or E, Altman R, Katti S, Sun F, et al. The human complement receptor type 2 (CR2)/CR1 fusion protein TT32, a novel targeted inhibitor of the classical and alternative pathway C3 convertases, prevents arthritis in active immunization and passive transfer mouse models. *Mol Immunol*. (2019) 105:150–64. doi: 10.1016/j.molimm.2018.09.013
59. Arend WP, Mehta G, Antonioli AH, Takahashi M, Takahashi K, Stahl GL, et al. Roles of adipocytes and fibroblasts in activation of the alternative pathway of complement in inflammatory arthritis in mice. *J Immunol*. (2013) 190:6423–33. doi: 10.4049/jimmunol.1300580
60. Gifford G, Vu VP, Banda NK, Holers VM, Wang G, Groman EV, et al. Complement therapeutics meets nanomedicine: overcoming human complement activation and leukocyte uptake of nanomedicines with soluble domains of CD55. *J Control Release*. (2019) 302:181–9. doi: 10.1016/j.jconrel.2019.04.009
61. Lofchy LA, Vu VP, Banda NK, Ramirez JR, Smith WJ, Gifford G, et al. Evaluation of targeting efficiency of joints with anticollagen II antibodies. *Mol Pharm*. (2019) 16:2445–51. doi: 10.1021/acs.molpharmaceut.9b00059
62. Nagata S, Hanayama R, Kawane K. Autoimmunity and the clearance of dead cells. *Cell*. (2010) 140:619–30. doi: 10.1016/j.cell.2010.02.014
63. Green DR, Ferguson T, Zitvogel L, Kroemer G. Immunogenic and tolerogenic cell death. *Nat Rev Immunol*. (2009) 9:353–63.
64. Galluzzi L, Vitale I, Abrams JM, Alnemri ES, Baehrecke EH, Blagosklonny MV, et al. Molecular definitions of cell death subroutines: recommendations of the nomenclature committee on cell death 2012. *Cell Death Differ*. (2012) 19:107–20. doi: 10.1038/cdd.2011.96
65. Campisi L, Cummings RJ, Blander JM. Death-defining immune responses after apoptosis. *Am J Transplant*. (2014) 14:1488–98. doi: 10.1111/ajt.12736
66. Kerr JF, Wyllie AH, Currie AR. Apoptosis: a basic biological phenomenon with wide-ranging implications in tissue kinetics. *Br J Cancer*. (1972) 26:239–57. doi: 10.1038/bjc.1972.33
67. Durandy A, Thuillier L, Forveille M, Fischer A. Phenotypic and functional characteristics of human newborns' B lymphocytes. *J Immunol*. (1990) 144:60–5.
68. Gadol N, Ault KA. Phenotypic and functional characterization of human Leu1 (CD5) B cells. *Immunol Rev*. (1986) 93:23–34. doi: 10.1111/j.1600-065x.1986.tb01500.x
69. Burastero SE, Casali P. Characterization of human CD5 (Leu-1, OKT1)+ B lymphocytes and the antibodies they produce. *Contrib Microbiol Immunol*. (1989) 11:231–62.
70. Burastero SE, Casali P, Wilder RL, Notkins AL. Monoreactive high affinity and polyreactive low affinity rheumatoid factors are produced by CD5+ B cells from patients with rheumatoid arthritis. *J Exp Med*. (1988) 168:1979–92. doi: 10.1084/jem.168.6.1979
71. Casali P, Notkins AL. Probing the human B-cell repertoire with EBV: polyreactive antibodies and CD5+ B lymphocytes. *Annu Rev Immunol*. (1989) 7:513–35. doi: 10.1146/annurev.iy.07.040189.002501
72. Weiser MR, Williams JP, Moore FD Jr., Kobzik L, Ma M, Hechtman HB, et al. Reperfusion injury of ischemic skeletal muscle is mediated by natural antibody and complement. *J Exp Med*. (1996) 183:2343–8. doi: 10.1084/jem.183.5.2343
73. Zhang M, Austen WG Jr., Chiu I, Alicot EM, Hung R, Ma M, et al. Identification of a specific self-reactive IgM antibody that initiates intestinal ischemia/reperfusion injury. *Proc Natl Acad Sci USA*. (2004) 101:3886–91. doi: 10.1073/pnas.0400347101
74. Zhang M, Michael LH, Grosjean SA, Kelly RA, Carroll MC, Entman ML. The role of natural IgM in myocardial ischemia-reperfusion injury. *J Mol Cell Cardiol*. (2006) 41:62–7.
75. Zhang M, Alicot EM, Chiu I, Li J, Verna N, Vorup-Jensen T, et al. Identification of the target self-antigens in reperfusion injury. *J Exp Med*. (2006) 203:141–52. doi: 10.1084/jem.20050390
76. Haas MS, Alicot EM, Schuerpf F, Chiu I, Li J, Moore FD, et al. Blockade of self-reactive IgM significantly reduces injury in a murine model of acute myocardial infarction. *Cardiovasc Res*. (2010) 87:618–27. doi: 10.1093/cvr/cvq141
77. Banda NK, Kraus DM, Muggli M, Bendele A, Holers VM, Arend WP. Prevention of collagen-induced arthritis in mice transgenic for the complement inhibitor complement receptor 1-related gene/protein y. *J Immunol*. (2003) 171:2109–15. doi: 10.4049/jimmunol.171.4.2109
78. Firestein GS, Yeo M, Zvaifler NJ. Apoptosis in rheumatoid arthritis synovium. *J Clin Invest*. (1995) 96:1631–8. doi: 10.1172/jci118202
79. Al-Zoobi L, Salti S, Colavecchio A, Jundi M, Nadiri A, Hassan GS, et al. Enhancement of rituximab-induced cell death by the physical association of CD20 with CD40 molecules on the cell surface. *Int Immunol*. (2014) 26:451–65. doi: 10.1093/intimm/dxu046
80. Bryant A, Moore J. Rituximab and its potential for the treatment of rheumatoid arthritis. *Ther Clin Risk Manag*. (2006) 2:207–12. doi: 10.2147/tcrm.2006.2.2.207
81. Edwards JC, Cambridge G. B-cell targeting in rheumatoid arthritis and other autoimmune diseases. *Nat Rev Immunol*. (2006) 6:394–403. doi: 10.1038/nri1838
82. Smith MD, Weedon H, Papangelis V, Walker J, Roberts-Thomson PJ, Ahern MJ. Apoptosis in the rheumatoid arthritis synovial membrane: modulation by disease-modifying anti-rheumatic drug treatment. *Rheumatology*. (2010) 49:862–75. doi: 10.1093/rheumatology/kep467
83. Doering J, Begue B, Lentze MJ, Rieux-Laucat F, Goulet O, Schmitz J, et al. Induction of T lymphocyte apoptosis by sulphasalazine in patients with Crohn's disease. *Gut*. (2004) 53:1632–8. doi: 10.1136/gut.2003.037911
84. Swierkot J, Miedzybrodzki R, Szymaniec S, Szechinski J. Activation dependent apoptosis of peripheral blood mononuclear cells from patients with rheumatoid arthritis treated with methotrexate. *Ann Rheum Dis*. (2004) 63:599–600. doi: 10.1136/ard.2003.015370
85. Nakazawa F, Matsuno H, Yudoh K, Katayama R, Sawai T, Uzuki M, et al. Methotrexate inhibits rheumatoid synovitis by inducing apoptosis. *J Rheumatol*. (2001) 28:1800–8.
86. Catrina AI, Trollmo C, af Klint E, Engstrom M, Lampa J, Hermansson Y, et al. Evidence that anti-tumor necrosis factor therapy with both etanercept and infliximab induces apoptosis in macrophages, but not lymphocytes, in rheumatoid arthritis joints: extended report. *Arthritis Rheum*. (2005) 52:61–72. doi: 10.1002/art.20764
87. Mountz JD, Wu J, Cheng J, Zhou T. Autoimmune disease. A problem of defective apoptosis. *Arthritis Rheum*. (1994) 37:1415–20. doi: 10.1002/art.1780371002
88. Banda NK, Desai D, Scheinman RI, Pihl R, Sekine H, Fujita T, et al. Targeting of liver mannan-binding lectin-associated serine protease-3 with RNA interference ameliorates disease in a mouse model of rheumatoid arthritis. *Immunohorizons*. (2018) 2:274–95. doi: 10.4049/immunohorizons.1800053
89. Posnett DN, Edinger J. When do microbes stimulate rheumatoid factor? *J Exp Med*. (1997) 185:1721–3. doi: 10.1084/jem.185.10.1721

Conflict of Interest: NB: C2-MAp44 fusion protein licensed to AdMIRx. ST, LK, and VH: AdMIRx.

The remaining authors declare that the research was conducted in the absence of any commercial or financial relationships that could be construed as a potential conflict of interest.

frontiers in Immunology

ORIGINAL RESEARCH
published: 26 October 2020
doi: 10.3389/fimmu.2020.583305

Development of Complement Factor H–Based Immunotherapeutic Molecules in Tobacco Plants Against Multidrug-Resistant *Neisseria gonorrhoeae*

Jutamas Shaughnessy[1], *Y Tran*[2], *Bo Zheng*[1], *Rosane B. DeOliveira*[1], *Sunita Gulati*[1], *Wen-Chao Song*[3], *James M. Maclean*[2], *Keith L. Wycoff*[2] *and Sanjay Ram*[1]*

[1] Division of Infectious Diseases and Immunology, University of Massachusetts Medical School, Worcester, MA, United States, [2] Planet Biotechnology, Inc., Hayward, CA, United States, [3] Department of Systems Pharmacology and Translational Therapeutics, Perelman School of Medicine, University of Pennsylvania School of Medicine, Philadelphia, PA, United States

OPEN ACCESS

Edited by:
Marcin Okrój,
University of Gdańsk and Medical University of Gdańsk, Poland

Reviewed by:
Kevin James Marchbank,
Newcastle University, United Kingdom
Peter F. Zipfel,
Leibniz Institute for Natural Product Research and Infection Biology, Germany

***Correspondence:**
Sanjay Ram
Sanjay.ram@umassmed.edu

Specialty section:
This article was submitted to Vaccines and Molecular Therapeutics, a section of the journal Frontiers in Immunology

Received: 14 July 2020
Accepted: 24 September 2020
Published: 26 October 2020

Citation:
Shaughnessy J, Tran Y, Zheng B, DeOliveira RB, Gulati S, Song W-C, Maclean JM, Wycoff KL and Ram S (2020) Development of Complement Factor H–Based Immunotherapeutic Molecules in Tobacco Plants Against Multidrug-Resistant Neisseria gonorrhoeae. Front. Immunol. 11:583305. doi: 10.3389/fimmu.2020.583305

Novel therapeutics against the global threat of multidrug-resistant *Neisseria gonorrhoeae* are urgently needed. Gonococci possess several mechanisms to evade killing by human complement, including binding of factor H (FH), a key inhibitor of the alternative pathway. FH comprises 20 short consensus repeat (SCR) domains organized in a head-to-tail manner as a single chain. *N. gonorrhoeae* binds two regions in FH; domains 6 and 7 and domains 18 through 20. We designed a novel anti-infective immunotherapeutic molecule that fuses domains 18–20 of FH containing a D-to-G mutation in domain 19 at position 1119 (called FH*) with human IgG1 Fc. FH*/Fc retained binding to gonococci but did not lyse human erythrocytes. Expression of FH*/Fc in tobacco plants was undertaken as an alternative, economical production platform. FH*/Fc was expressed in high yields in tobacco plants (300–600 mg/kg biomass). The activities of plant- and CHO-cell produced FH*/Fc against gonococci were similar *in vitro* and in the mouse vaginal colonization model of gonorrhea. The addition of flexible linkers [e.g., $(GGGGS)_2$ or $(GGGGS)_3$] between FH* and Fc improved the bactericidal efficacy of FH*/Fc 2.7-fold. The linkers also improved PMN-mediated opsonophagocytosis about 11-fold. FH*/Fc with linker also effectively reduced the duration and burden of colonization of two gonococcal strains tested in mice. FH*/Fc lost efficacy: i) in $C6^{-/-}$ mice (no terminal complement) and ii) when Fc was mutated to abrogate complement activation, suggesting that an intact complement was necessary for FH*/Fc function *in vivo*. In summary, plant-produced FH*/Fc represent

promising prophylactic or adjunctive immunotherapeutics against multidrug-resistant gonococci.

Keywords: *Neisseria gonorrhoeae*, gonorrhea, factor H, immunotherapeutic, Fc fusion protein, *Nicotiana benthamiana*, complement, factor H (FH)

INTRODUCTION

Gonorrhea is caused by the Gram-negative bacterium *Neisseria gonorrhoeae*. Each year about 87 million new cases of gonorrhea occur worldwide (1). Gonorrhea commonly manifests as cervicitis, urethritis, proctitis, and conjunctivitis and can result in serious sequelae in woman including infertility, ectopic pregnancy, and chronic pelvic pain. Concomitant infection with HIV and gonorrhea enhances the rate of HIV transmission (2–4). Over the years *N. gonorrhoeae* has become resistant to almost every antibiotic that has been used for treatment (5, 6). The recent emergence of azithromycin-resistant isolates in several countries (7–10) could render the first-line therapy, ceftriaxone plus azithromycin, recommended by the Centers for Disease Control and Prevention (https://www.cdc.gov/std/tg2015/default.htm), ineffective in the near future.

In light of rapidly emerging multidrug-resistant *N. gonorrhoeae* worldwide, development of safe and effective vaccines and novel therapeutics against gonorrhea is a high priority (11). An approach for developing new and effective therapeutics against gonorrhea is to target key bacterial virulence mechanisms. One of these is the ability of *N. gonorrhoeae* to bind factor H (FH), a key inhibitor of the alternative pathway of complement (12). FH comprises 20 short consensus repeat (SCR) domains that are organized as a single chain (13). *N. gonorrhoeae* binds FH through domains 6 and 7 (14, 15) and the C-terminal domains 18 through 20 (12, 16). We previously designed a novel anti-infective immunotherapeutic molecule combining the *N. gonorrhoeae*-binding C-terminal domains 18–20 of FH, with a D to G mutation at position 1119 in FH (termed FH*) to minimize binding to human tissue while retaining binding to *N. gonorrhoeae*, with human IgG1 Fc (the antibody-like effector region of the modified molecule [termed FH*/Fc]) (17). We showed that FH*/Fc possessed complement-dependent bactericidal activity against gonococci *in vitro* and shortened the duration and diminished bacterial loads in the mouse model of vaginal colonization (17).

One of the important variables that we considered when we designed FH*/Fc is the choice of linker length and sequence (18–20). Linkers may offer some advantages for the production of fusion protein, such as improving biological activity and increasing expression yield (19). One of the most commonly used flexible linkers has the sequence of (Gly-Gly-Gly-Gly-Ser)n, where "n" can be optimized to achieve appropriate separation of the functional domains (18). We previously used a simple AAAGG-containing linker between FH* and Fc domain (17). In this work, we explored the role of different linker lengths in the efficacy of protein by generating FH*/Fc with no linker, AAAGG, $(GGGGS)_2$, and $(GGGGS)_3$. In addition, we expressed these molecules in tobacco plants because of the ability for large scale production, low cost and the absence of animal products (21–24). We also compared the functions of these molecules to CHO-cell-produced FH*/Fc.

MATERIALS AND METHODS

Bacterial Strains

Strains F62 (25), Ctx-r(Spain) (similar to strain F89) (26), H041 (also known as World Health Organization reference strain X) (27, 28), MS11 (29), UMNJ60_06UM (NJ-60) (30), and FA1090 (31) have all been described previously. Strains Ctx-r(Spain), H041, and NJ-60 are resistant to ceftriaxone. Opacity protein (Opa)–negative mutants of FA1090 (32) (all *opa* genes deleted) have been described previously.

Expression and Purification of FH/Fc Fusion Proteins in Tobacco Plants

A nucleotide sequence encoding human FH SCR18-20 (GenBank accession no. NP_000177) [aa 1048-1231, incorporating the D1119G mutation (33)], designed to employ optimal codon usage for expression in *Nicotiana benthamiana*, was synthesized by GENEWIZ (South Plainfield, NJ). This sequence (and the encoded protein fragment) was designated FH*.

The synthetic FH* sequence was cloned into the plant binary expression vector pTRAkc (34) upstream and in-frame with codon-optimized hinge, C_H2 and C_H3 domains from human IgG1 (hFc) and downstream of the signal peptide of the murine mAb24 heavy-chain (lph) (35). Additional clones encoding N-terminal amino acid extensions to the FH* sequence or linkers between FH* and Fc were made using overlap extension PCR. The molecular constructs that were assembled are listed in **Table 1**. Throughout the text these are referred to by *Agrobacterium tumefaciens* strain number.

Transient expression of recombinant proteins was accomplished by whole-plant vacuum infiltration (36) of *N. benthamiana* ΔXT/FT (37) using *A. tumefaciens* GV3101 (pMP90RK) (38) containing one of the binary expression vectors, co-infiltrated with *A. tumefaciens* GV3101 (pMP90RK)

TABLE 1 | Description of plant-produced FH*/Fc molecules.

Strain	Modifications	Binary expression vector name
S2366	AAAGG linker	pTRAk-c-lph-FH*-(AAAGG)-hFc
S2368	$(GGGGS)_2$ [$(G_4S)_2$] linker	pTRAk-c-lph-FH*-(GGGGS)2-hFc
S2370	$(GGGGS)_3$ [$(G_4S)_3$] linker	pTRAk-c-lph-FH*-(GGGGS)3-hFc
S2381	no linker	pTRAk-c-lph-FH*-hFc
S2477	N-terminal TS	pTRAk-c-lph-(TS)FH*-$(G_4S)_2$-hFc
S2493	N-terminal TS "complement-inactive"	pTRAk-c-lph-(TS)FH*-$(G_4S)_2$-hFc (D270A/K322A)

containing the binary vector pTRAkc-P19, encoding the post-transcriptional silencing suppressor P19 (39). Glycoproteins produced in *N. benthamiana* ΔXT/FT contain almost homogeneous N-glycan species without plant-specific β1,2-xylose and α1,3-fucose residues (37). After infiltration, the plants were maintained in a grow room under continuous light at 25°C for 5–7 days prior to harvest and protein purification.

Leaves were collected 5–7 days after vacuum infiltration and frozen at −80°C until use. Purification of FH*/Fc fusion proteins was accomplished using a protocol previously used with another plant-produced Fc fusion (40), which incorporates affinity chromatography with Protein A-MabSelect SuRe (GE HealthCare). Purified proteins were concentrated to ≥2 mg/ml using 10 kDa cut-off centrifugal concentrators, buffer exchanged into PBS, and rendered sterile by filtration through 0.22-μm PES membrane filters. Protein concentrations were quantified using absorption at 280 nm and extinction coefficients predicted from the amino acid sequences.

Purified protein samples were analyzed using standard methods. Samples were subjected to SDS-polyacrylamide gel electrophoresis (under reducing and non-reducing conditions) on 4%–20% Mini-PROTEAN® TGX Stain-Free™ Protein Gels (Bio-Rad, Hercules, CA). Gel images were obtained using a Bio-Rad Gel Doc EZ imaging system.

Expression and Purification of FH/Fc Fusion Proteins in CHO Cells

Cloning, expression in CHO cells and purification from cell culture supernatants of a chimeric protein comprising human FH (HuFH) domains 18–20 (D1119G) fused to the hinge, C_H2 and C_H3 domains of human IgG1 (hFc) has been described previously (17). Protein concentrations were determined using absorption at 280 nm and the BCA protein Assay kit (Pierce); mass was determined by Coomassie Blue staining of proteins separated by SDS-PAGE.

Human Complement

IgG- and IgM-depleted normal human serum (human complement) was purchased from Pel-Freez.

Antibodies

Anti-human IgG–FITC was from Sigma-Aldrich and was used at a dilution of 1:100 in HBSS containing 0.15 mM $CaCl_2$ and 1 mM $MgCl_2$ ($HBSS^{++}$) and 1% BSA ($HBSS^{++}$/BSA) in flow cytometry assays. Goat anti-human FH, alkaline phosphatase conjugated anti-human IgG (Southern Biotechnology), and donkey anti-goat IgG were used in Western blots a dilution of 1:1,000 in PBS with 5% non-fat dry milk.

Flow Cytometry

Binding of FH*/Fc to bacteria was measured by flow cytometry as described previously (17). Data were acquired on a BD LSR II flow cytometer, and data were analyzed using FlowJo software.

Serum Bactericidal Assay

Serum bactericidal assays using bacteria grown in gonococcal liquid media supplemented with CMP-Neu5Ac (2 μg/ml) were performed as described previously (17, 41). Approximately, 2,000 colony forming units (CFUs) of *N. gonorrhoeae* were incubated with 20% human complement [IgG and IgM depleted normal human serum (Pel-Freez)] in the presence or the absence of the FH*/Fc fusion protein (concentration indicated for each experiment). The final volume of the bactericidal reaction mixture was 150 μl. Aliquots of 25μl reaction mixtures were plated onto chocolate agar in duplicate at the beginning of the assay (t_0) and again after incubation at 37°C for 30 min (t_{30}). Survival was calculated as the number of viable colonies at t_{30} relative to t_0.

Opsonophagocytosis Assay

Opsonophagocytic killing of gonococci with freshly isolated human polymorphonuclear leukocytes (PMNs) was performed as described previously (15, 17). Briefly, heparinized venous blood was obtained from a healthy adult volunteer in accordance with a protocol approved by the Institutional Review Board. PMNs were isolated using Mono-Poly Resolving Medium (MP Biomedicals) according to the manufacturer's instructions. Isolated PMNs were washed and suspended in HBSS without added divalent cations, counted, and diluted to 1×10^7/ml in HEPES-buffered RPMI 1640 medium supplemented with L-glutamine and 1% heat-inactivated FBS. To measure survival of gonococci in the presence of PMNs, Opa-negative mutant of *N. gonorrhoeae* strain FA1090 was added to 1×10^6 PMNs at a multiplicity of infection of 1 (two bacteria to one PMN). Opa-negative (Opa^-) *N. gonorrhoeae* was used because select Opa proteins serve as ligands for human carcinoembryonic Ag–related cell adhesion molecule 3 (CEACAM3) that is expressed by PMNs and results in phagocytosis (42). FH*/Fc was added at different concentrations, followed by 10% human complement (Pel-Freez). The reaction mixtures were incubated for 60 min at 37°C in a shaking water bath. Bacteria were serially diluted and plated at 0 and 60 min on chocolate agar plates. Percentage survival of gonococci in each reaction was calculated as a ratio of CFU at 60 min to CFU at the start of the assay (0 min).

Mouse Strains

Human FH and C4b-binding protein (C4BP) (FH/C4BP) transgenic mice) in a BALB/c background have been described previously (43). FH/C4BP Tg mice express levels of FH and C4BP that are comparable to those found in human serum and show similar responses to a variety of stimuli as wild-type (wt) BALB/c mice (43). Wild-type C57BL/6 mice were purchased from Jackson laboratories. Construction and characterization of $C6^{-/-}$ mice (C57BL/6 background) have been described previously (44).

Mouse Vaginal Colonization Model of Gonorrhea

Use of animals in this study was performed in strict accordance with the recommendations in the *Guide for the Care and Use of Laboratory Animals* by the National Institutes of Health. The protocol was approved by the Institutional Animal Care and Use Committee at the University of Massachusetts Medical

School. Female mice 6–8 weeks of age in the diestrus phase of the estrous cycle were started on treatment with 0.1-mg Premarin (Pfizer; conjugated estrogens) in 200 µl of water given s.c. on each of 3 days: −2, 0, and +2 (2 days before, the day of, and 2 days after inoculation) to prolong the estrus phase of the reproductive cycle and promote susceptibility to *N. gonorrhoeae* infection. Antibiotics (vancomycin and streptomycin) ineffective against *N. gonorrhoeae* were also used to reduce competitive microflora (45). Mice were infected on day 0 with either strain H041 or FA1090 (inoculum specified for each experiment). Mice were treated daily with 1 or 10 µg FH*/Fc intravaginally from day 0 until the conclusion of the experiment or were given a corresponding volume of PBS (vehicle controls).

Statistical Analysis

Concentration-dependent complement-mediated killing by FH/Fc across strains was compared using two-way ANOVA. Experiments that compared clearance of *N. gonorrhoeae* in independent groups of mice estimated and tested three characteristics of the data (15, 17, 46): time to clearance, longitudinal trends in mean $\log_{10}$ CFU, and the cumulative CFU as area under the curve (AUC). Statistical analyses were performed using mice that initially yielded bacterial colonies on days 1 and/or 2. Median time to clearance was estimated using Kaplan-Meier survival curves; times to clearance were compared between groups using the Mantel-Cox log-rank test. Mean $\log_{10}$ CFU trends over time were compared between groups using two-way ANOVA and Dunnett's multiple comparison test. The mean AUC ($\log_{10}$ CFU versus time) was computed for each mouse to estimate the bacterial burden over time (cumulative infection). The means under the curves of two groups were compared using the nonparametric Mann-Whitney test because distributions were skewed or kurtotic. The Kruskal-Wallis equality-of-populations rank test was also applied to compare more than two groups in an experiment.

RESULTS

Production of FH*/Fc Molecules in *Nicotiana benthamiana*

We cloned a plant codon-optimized FH* DNA sequence upstream and in-frame with sequences encoding the hinge, CH_2 and CH_3 domains (Fc) of human IgG1 in a plant expression vector, then produced the FH*/Fc using a rapid *N. benthamiana* expression system. One variant (S2366) included an AAAGG linker between FH* and Fc, resulting in the same protein that had previously been expressed in CHO cells (17). We also produced three new FH*/hFc variants containing either no linker (S2381) or two or three copies of a GGGGS (G_4S) linker (S2368 and S2370, respectively). Yield of these proteins following Protein A affinity chromatography ranged from 300 to 600 mg per kg plant fresh weight (**Figure 1A**). Characterization of the plant produced proteins by protein staining of SDS-PAGE gels and western blotting with anti-human FH is shown in **Supplemental Figure S1**.

Effect of Linkers on Efficacy of FH*/Fc

We initially characterized four FH*/Fc molecules made in tobacco plants: FH*/Fc without a linker, or with AAAGG, two G_4S or three G_4S linkers (called $(G_4S)_2$ and $(G_4S)_3$, respectively). FH*/Fc with AAAGG linker made in CHO cells was used as a control. As we expected, since all proteins possessed the same FH* sequence they showed similar binding to *N. gonorrhoeae* strain H041 when tested at dilutions ranging from 1.1 to 30 µg/ml (**Figure 1B**). In human complement-dependent bactericidal assays using *N. gonorrhoeae* strain H041, S2368 and S2370 (FH*/Fc with $(G_4S)_2$ and $(G_4S)_3$, respectively) showed improved bactericidal activities compared to S2366 (FH*/Fc with AAAGG) or S2381 (FH*/Fc without a linker) (**Figure 1C**). The concentrations required for 50% bactericidal activity (BC_{50}) were lower for S2368 and S2370 than for S2366 and S2381 (BC_{50} of 2.1 µg/ml with S2368 and S2370 vs. 5.9 and 7.2 µg/ml with S2366 and S2381, respectively). FH*/Fc with AAAGG generated in CHO cells or tobacco plants (S2366) showed similar bactericidal activity (BC_{50} of 6.3 and 5.9 µg/ml, respectively). S2381 (no linker) showed the least killing.

We next evaluated the effect of linkers on opsonophagocytic activity. We have shown previously that FH*/Fc made in CHO cells enhanced complement-dependent killing by PMN (17). In this experiment, we used an Opacity protein negative (Opa-) mutant derivative of *N. gonorrhoeae* strain FA1090, where all 11 *opa* genes have been inactivated, to eliminate Opa-CAECAM3 induced uptake of gonococci by PMNs (42). As shown in **Figure 1D**, S2368 and S2370 enhanced PMN-mediated killing significantly more than S2366 or S2381 (BC_{50} of 2.3 and 2.6 µg/ml with S2368 and S2370 vs. 27.4 and 19.1 µg/ml with S2366 and S2381, respectively).

Collectively, the data above showed that S2368 and S2370 [$(G_4S)_2$ and $(G_4S)_3$ linkers, respectively] improved bactericidal and PMN-mediated opsonophagocytic killing about 2.7- and 11- fold, respectively, compared to S2366. We chose S2370 for further bactericidal testing using five additional gonococcal strains (**Figure 1E**) and observed killing of four of the six strains tested [H041, NJ60, F62, and MS11, but not FA1090 or CTX-r(Sp)]. These six strains showed the same pattern of susceptibility to FH*/Fc with the AAAGG linker produced in CHO cells (17).

Efficacy of S2370 Against *N. gonorrhoeae* in the Mouse Vaginal Colonization Model

We next evaluated the efficacy of S2370 against *N. gonorrhoeae* in the mouse vaginal colonization model of gonorrhea using FH/C4BP transgenic mice. We used two strains that differed in their susceptibility to killing in the human complement-dependent bactericidal assay; sensitive strain H041 and resistant strain FA1090 (**Figure 1E**).

As shown in **Figure 2**, S2370 given daily intravaginally at doses of either 1 or 10 µg/d significantly attenuated both the duration and the burden of gonococcal vaginal colonization compared to vehicle control treated groups, when challenged with either 10^6 (**Figure 2A**) or 10^7 CFU (**Figure 2B**) of strain H041. Overall, there were no significant differences in clearance between the 1 or 10 µg doses. S2370 was also efficacious against

A

	Protein			
	S2366	S2368	S2370	S2381
Linker	AAAGG	$(GGGGS)_2$	$(GGGGS)_3$	none
Yield (mg/kg)	615-815	400	330	450
% intact band	72%	83%	81%	92%

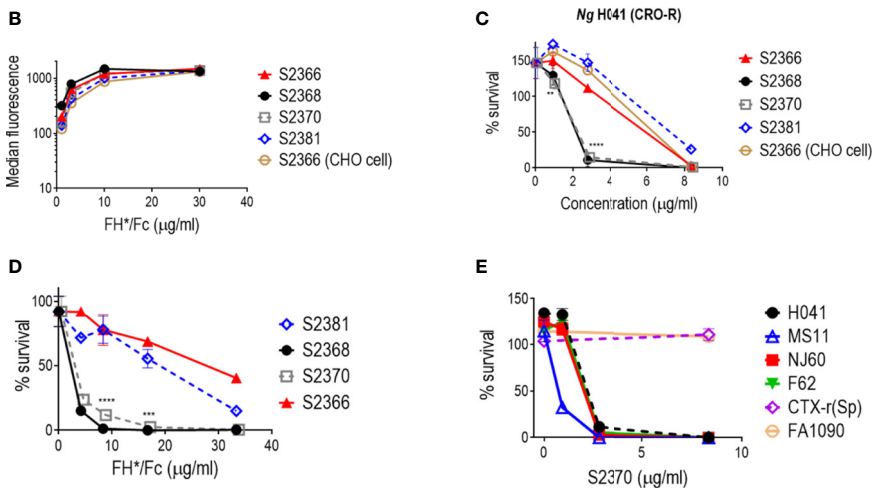

FIGURE 1 | Effect of linkers in efficacy of FH/Fc produced in *N. benthamiana* against *N. gonorrhoeae in vitro*. **(A)** Yields and stability of the four human IgG1 Fc variants produced in tobacco plants. **(B)** Binding of FH*/Fc fusion proteins to sialylated *N. gonorrhoeae* H041. CHO cell-produced FH*/Fc that was used in previous studies was used as a comparator. **(C)** Bactericidal activity of the FH*/Fc fusion proteins against *N. gonorrhoeae* H041. S2368 [$(G_4S)_2$ linker] and S2370 [$(G_4S)_3$ linker] show improved activity. **(D)** Comparison of the opsonophagocytic activity of S2368, S2370 and S2381 (no linker) against *N. gonorrhoeae* FA1090. Presence of the G_4S linker improves function. **(E)** Activity of S2370 against six sialylated strains of *N. gonorrhoeae*.

strain FA1090 in FH/C4BP transgenic mice when administered intravaginally at a dose of 10 μg/d (**Figure 3**).

Capping the N-terminal Cys in FH*/Fc Improves Protein Yields and Retains Function

We observed that concentration and sterile filtration of all variants of FH*/Fc resulted in dramatic losses of protein; close to 50% versus the ~20% loss seen with other plant-produced Fc fusions (40, 47). A distinctive feature of FH*/Fc is the presence of an N-terminal cysteine. Proteins with N-terminal cysteines are able to undergo a reaction called native chemical ligation, whereby the cysteine reacts with free thioester groups (48, 49). We suspected this might be responsible for the protein loss during concentration. We therefore designed, expressed, and purified a new FH*/Fc (S2477) with two additional amino acids (TS) that are normally N-terminal to the cysteine in the native FH sequence, which overcame the previously noted loss during purification. As shown in **Figure 4A**, S2477 showed fewer degradation products after purification compared to S2370.

A comparison of the bactericidal activity of S2370 and S2477 against six strains of *N. gonorrhoeae* [H041, NJ-60, F62, MS11, FA1090, and Ctx-r(Sp)] grown in media containing CMP-Neu5Ac to sialylate LOS showed that S2477 has slightly better activity than S2370 (**Figure 4B**). The efficacy of S2477 against another ceftriaxone-resistant isolate, NJ60, was also confirmed (BC_{50} of 1.5 μg/ml) (**Figure 4C**). By comparison, S2493 [a derivative of S2477 that contained D270A and K322A in Fc, abrogating C1q binding (50)] was included as a negative control and showed no killing (**Figure 4C**).

S2477 Requires an Intact Terminal Complement Pathway for Efficacy

C1q engagement by Fc is critical for the activity of CHO cell-produced FH*/Fc (15), suggesting that the classical complement pathway is required for efficacy of FH*/Fc. To determine whether complement alone acting through killing by membrane attack complex (MAC) insertion was necessary and sufficient for efficacy of FH*/Fc, we used $C6^{-/-}$ mice (44). C6 is the second step in the formation of the C5b-9 MAC pore. While $C6^{-/-}$ mice lack the capacity to form MAC pores, they can generate C5a, which is important for chemotaxis of PMNs and opsonophagocytic killing of Neisseriae (51, 52). Wild-type C57BL/6 control mice or $C6^{-/-}$ mice (n = 6/group) were infected with H041 and treated with either S2477 or S2493 (each given at 5μg intravaginally daily, starting on day 0, through day 7) or PBS vehicle control (**Figure 5**). Although S2477 was efficacious in WT C57BL/6 mice, all efficacy was lost

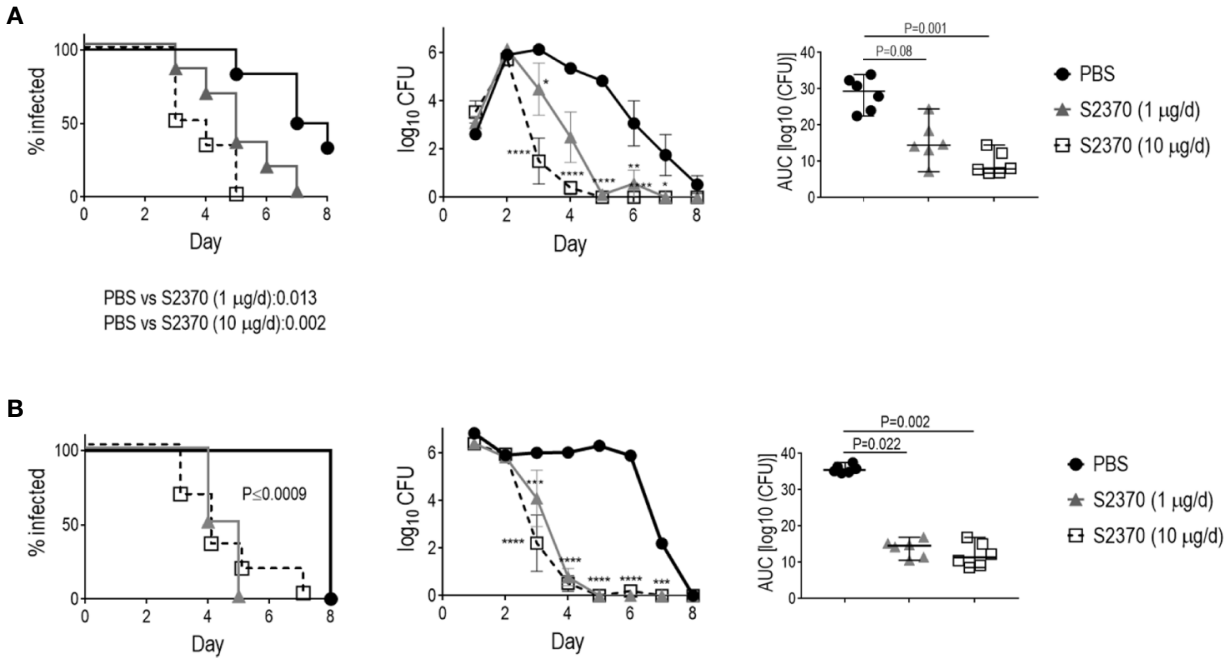

FIGURE 2 | Efficacy of S2370 against *N. gonorrhoeae* H041 in human FH/C4BP transgenic mice. Premarin®-treated 6- to 8-week-old human FH/C4BP transgenic mice (n = 6/group) were infected with either 10^6 CFU **(A)** or 10^7 CFU **(B)** *N. gonorrhoeae* strain H041. Mice were treated daily (starting 2 h before infection) intravaginally either with PBS (vehicle control) or with 1 μg or 10 μg of FH*/Fc molecule S2370. *Left graphs*: Kaplan Meier curves showing time to clearance, analyzed by the Mantel-Cox (log-rank) test. Significance was set at 0.017 (Bonferroni's correction for comparisons across three groups). *Middle graphs*: $\log_{10}$ CFU versus time. X-axis, day; Y-axis, $\log_{10}$ CFU. Comparisons of the CFU over time between each treatment group and the respective saline control was made by two-way ANOVA and Dunnett's multiple comparison test. *P < 0.05; **P < 0.01; ***P < 0.001; ****P < 0.0001. *Right graphs*: bacterial burdens consolidated over time (area under the curve [$\log_{10}$ CFU] analysis). The three groups were compared by one-way ANOVA using the non-parametric Kruskal-Wallis equality of populations rank test. The χ^2 with ties were 12.12 (P = 0.0002) and 11.94 (P = 0.0002) for the graphs in panels **(A, B)**, respectively. Pairwise AUC comparisons across groups was made with Dunn's multiple comparison test.

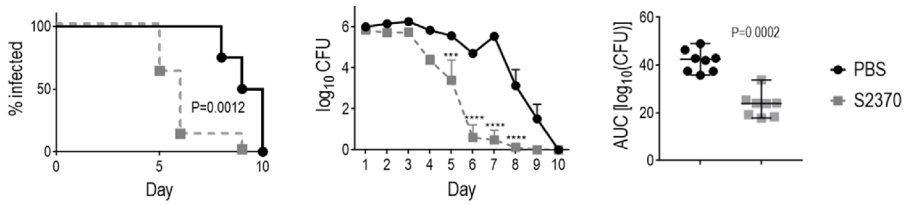

FIGURE 3 | Efficacy of S2370 (FH/Fc with $(GGGGS)_3$ linker) against *N. gonorrhoeae* FA1090 in human FH/C4BP transgenic mice. Premarin®-treated 6 week-old human FH/C4BP transgenic mice (n = 8/group) were infected with 4×10^7 CFU *N. gonorrhoeae* strain FA1090. Mice were treated daily (starting 2 h before infection) intravaginally either with PBS (vehicle control) or with 10 μg of FH*/Fc molecule S2370. Left graph: Kaplan Meier curves showing time to clearance, analyzed by the Mantel-Cox (log-rank) test. Middle graph: $\log_{10}$ CFU versus time. X-axis, day; Y-axis, $\log_{10}$ CFU. Comparisons of the CFU over time between each treatment group and the respective saline control was made by two-way ANOVA and Dunnett's multiple comparison test. ***P < 0.001; ****P < 0.0001. Right graphs: bacterial burdens consolidated over time (area under the curve [$\log_{10}$ CFU] analysis). Comparisons were made by Mann-Whitney's non-parametric test.

in $C6^{-/-}$ mice. FH*/Fc that lacked the ability to activate complement (S2493) was inactive in both $C6^{-/-}$ and wt mice. Taken together, these data show that complement alone is necessary and sufficient for efficacy of FH*/Fc in the mouse vaginal colonization model of gonorrhea.

DISCUSSION

N. gonorrhoeae has developed resistance to almost every antibiotic used for treatment and poses an urgent threat to human health worldwide. The "Global action plan to control the spread and

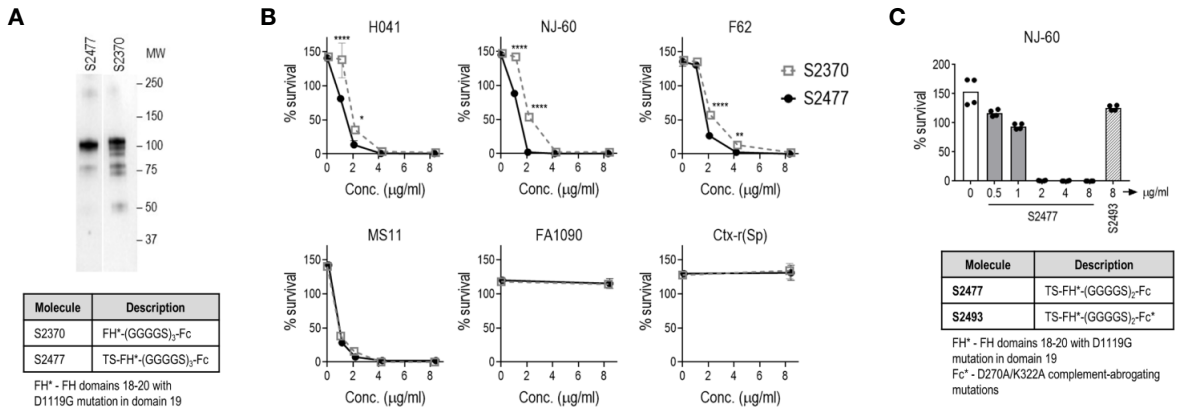

FIGURE 4 | Improved stability and efficacy of FH*/Fc bearing two amino acids (TS) at the N-terminus (S2477) *in vitro*. **(A)** S2477 shows fewer degradation products compared to S2370. Western blot of purified S2477 (lane 1) and S2370 (lane 2) using anti-human IgG alkaline phosphatase as the detection reagent. Note that irrelevant lanes between lanes 1 and 2 have been excluded. MW, molecular weight (kDa). **(B)** S2477 (TS-FH*-$(G_4S)_2$/Fc) and S2370 (FH*-$(G_4S)_3$/Fc) (concentrations indicated on the X-axis) were incubated with sialylated strains H041, NJ-60, F62, MS11, FA1090, and Ctx-r(Sp) and complement and survival at 30 min (relative to 0 min) was measured in a bactericidal assay. Comparisons were made by two-way ANOVA. *P < 0.05; **P < 0.01; ****P < 0.0001. **(C)** Complement-dependent bactericidal efficacy of S2477 against *N. gonorrhoeae* strain NJ-60. Negative controls included bacteria incubated with complement alone (open bar on left) and bacteria incubated with 8 μg/ml S2493 (TS-FH*-$(G_4S)_2$/Fc-D270A/K322A (complement-inactive Fc mutations); hatched bar on right).

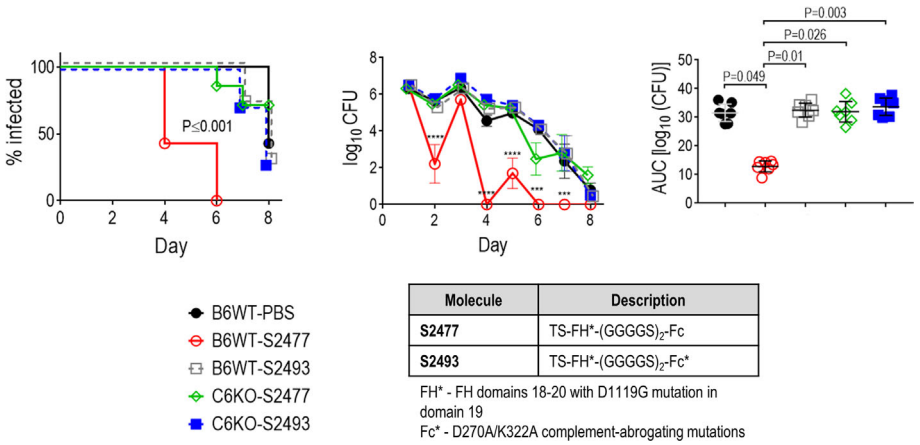

FIGURE 5 | Terminal complement is required for efficacy of FH/Fc against *N. gonorrhoeae* H041 *in vivo*. The activities of S2477 (TS-FH*/Fc with $(G_4S)_2$ linker) and S2493 (the corresponding FH/Fc molecule with D270A/K322A mutations in Fc that abrogates complement activation) were tested in *C6*$^{-/-}$ mice or wt C57BL/6 control mice. Mice (n = 7/group) were infected with 4.2×10^6 CFU *N. gonorrhoeae* H041 and treated daily (starting 2 h before infection) with 5 μg of the indicated FH/Fc protein intravaginally; control animals received PBS. *Left graph*: Kaplan Meier curves showing time to clearance, analyzed by the Mantel-Cox (log-rank) test. Significance was set at 0.005 (Bonferroni's correction for comparisons across five groups). *Middle graph*: $\log_{10}$ CFU versus time. X-axis, day; Y-axis, $\log_{10}$ CFU. Comparisons of the CFU over time between each treatment group and the respective PBS control was made by two-way ANOVA and Dunnett's multiple comparison test. ***P < 0.001; ****P < 0.0001. *Right graph*: bacterial burdens consolidated over time (area under the curve [$\log_{10}$ CFU] analysis). The five groups were compared by one-way ANOVA using the non-parametric Kruskal-Wallis equality of populations rank test. The χ^2 with ties was 17.15 (P = 0.0018). Pairwise AUC comparisons across groups was made with Dunn's multiple comparison test.

impact of antimicrobial resistance in *N. gonorrhoeae*" emphasizes the need for novel approaches to prevent and treat gonorrhea (53). The complement system is a critical component of innate immune defense that is central to controlling bacterial infections. *N. gonorrhoeae* have evolved several strategies to escape complement, including binding of FH, a key inhibitor of the alternative pathway of complement (12, 54). Sialylation of gonococcal LOS occurs in humans (55) and also during experimental infection of mice (56). Loss of the ability to sialylate its LOS is associated with a significant decrease in the ability of gonococci to colonize mice (56, 57). Targeting a gonococcal virulence factor has a distinct advantage over conventional antibiotics because resistance, if it were to develop, would result in a less fit organism due to loss of the virulence factor.

Gonococcal surface antigens show extensive antigenic and phase variability (58, 59). Thus, the identification of protective epitopes that are shared by a wide array of strains has been challenging. To overcome this obstacle, we designed an immunotherapeutic molecule combining the gonococcal-binding C-terminal domains 18, 19, and 20 of FH with human IgG1 Fc. This molecule has the advantage of targeting a broad array of gonococcal isolates. Introducing a D-to-G mutation at position 1119 in FH domain 19 (FH*) abrogated lysis of human RBCs that was seen when unmodified FH domains 18–20 were fused to Fc, while retaining binding to and activity against gonococci *in vitro* and *in vivo* (17).

In this study, we examined the efficacy of tobacco plant-produced FH*/Fc. Tobacco plants have been used for over three decades to produce antibodies and proteins (60). The tobacco plant expression system has advantages over mammalian cells because of the scalability of production, the potentially low costs and the absence of animal viruses or prions (22). FH*/Fc molecules were expressed in high yields in tobacco plants (>300 mg/kg biomass). Plant-produced FH*/Fc showed activity against *N. gonorrhoeae* that was comparable with CHO cell-produced FH*/Fc.

Linkers between the binding domain and Fc can positively impact production and/or function of fusion proteins (19, 20, 61). Accordingly, insertion of $(G_4S)_2$ and $(G_4S)_3$ flexible linkers between FH* and Fc improved the functional efficacy of FH*/Fc, evidenced by approximately 3- and 11-fold increases in bactericidal activity and PMN-mediated killing, respectively, compared to FH*/Fc with an AAAGG linker. The $(G_4S)_3$ linker-containing FH*/Fc was efficacious in mice against ceftriaxone-resistant isolate H041 when given topically at a dose as low as 1 μg/d.

Complement is a central arm of innate immune defenses against Neisserial infections. Defects of terminal complement components (C5 through C9) are associated with increased risk from invasive Neisserial infections, including disseminated gonococcal infection (62–68). We used mice deficient in complement C6 ($C6^{-/-}$ mice) to assess the role of terminal pathway in enabling FH*/Fc to clear *N. gonorrhoeae*. The opsonophagocytic activity in $C6^{-/-}$ mice is intact because they can generate C5a, a chemotaxin shown to be important for killing of *N. meningitidis* in blood where C7 function was blocked (52). FH*/Fc lost activity in $C6^{-/-}$ mice, suggesting terminal complement was required for FH*/Fc activity. The lack of FH*/Fc activity in $C6^{-/-}$ mice was not because of species incongruity between (human) Fc and (mouse) FcR; human IgG1 binds to all mouse FcγRs and can mediate Ab-mediated cellular cytotoxicity (ADCC) and Ab-dependent cellular phagocytosis (ADCP) with mouse effector cells in a manner similar to human cells (69). FH*/Fc with the complement-inactivating D270A/K322A Fc mutations was also ineffective in mice. Taken together with our prior observation of loss of FH*/Fc activity in $C1q^{-/-}$ mice (15), these data reiterate the role of classical pathway activation for FH*/Fc activity *in vivo*. A different $C6^{-/-}$ mouse constructed by back-crossing the naturally C6-deficient Peru-Coppock strain into the C3H/He background (70) and subsequently backcrossing the C3H/He $C6^{-/-}$ mice into the C57BL/6 background (71) showed impaired PMN function including defective phagocytosis and generation of reactive oxygen species (72). Whether the function of phagocytes in our $C6^{-/-}$ mice that were created by targeted deletion of *C6* directly in the C57BL/6 background is compromised remains to be determined. Nevertheless, collectively our data suggest that the classical and terminal pathways of complement were necessary for FH*/Fc function.

In summary, we have designed novel FH/Fc fusion proteins, expressed in tobacco plants, that show promising activity both *in vivo* and *in vitro* against *N. gonorrhoeae*. The modification of flexible linkers between FH* and Fc improves the potency of FH*/Fc. Intact classical and terminal complement pathways are required for FH*/Fc activity.

DATA AVAILABILITY STATEMENT

The raw data supporting the conclusions of this article will be made available by the authors, without undue reservation.

ETHICS STATEMENT

The animal study was reviewed and approved by Institutional Animal Care and Use Committee at the University of Massachusetts Medical School.

AUTHOR CONTRIBUTIONS

JS, YT, KW, and SR designed the experiments, analyzed data and wrote the manuscript. JS, YT, BZ, SG, JM, and RBD performed the experiments and W-CS provided critical reagents. All authors contributed to the article and approved the submitted version.

FUNDING

This work was supported by National Institutes of Health/National Institutes for Allergy and Infectious Disease grants R01 AI132296 and R44 AI147930 (both to SR and KW).

ACKNOWLEDGMENTS

We thank Nancy Nowak (University of Massachusetts) for excellent technical assistance. The authors at the University of Massachusetts and Planet Biotechnology have contributed equally to this work.

SUPPLEMENTARY MATERIAL

The Supplementary Material for this article can be found online at: https://www.frontiersin.org/articles/10.3389/fimmu.2020.583305/full#supplementary-material

REFERENCES

1. Rowley J, Vander Hoorn S, Korenromp E, Low N, Unemo M, Abu-Raddad LJ, et al. Chlamydia, gonorrhoea, trichomoniasis and syphilis: global prevalence and incidence estimates, 2016. *Bull World Health Organ* (2019) 97(8):548–62P. doi: 10.2471/BLT.18.228486
2. Laga M, Manoka A, Kivuvu M, Malele B, Tuliza M, Nzila N, et al. Non-ulcerative sexually transmitted diseases as risk factors for HIV- 1 transmission in women: results from a cohort study [see comments]. *Aids* (1993) 7(1):95–102. doi: 10.1097/00002030-199301000-00015
3. Cohen MS. Sexually transmitted diseases enhance HIV transmission: no longer a hypothesis. *Lancet* (1998) 351 (Suppl 3):5–7. doi: 10.1016/s0140-6736(98)90002-2
4. Cohen MS, Hoffman IF, Royce RA, Kazembe P, Dyer JR, Daly CC, et al. Reduction of concentration of HIV-1 in semen after treatment of urethritis: implications for prevention of sexual transmission of HIV-1. *AIDSCAP Malawi Res Group Lancet* (1997) 349(9069):1868–73. doi: 10.1016/s0140-6736(97)02190-9
5. Unemo M, Seifert HS, Hook EW3rd, Hawkes S, Ndowa F, Dillon JR. Gonorrhoea. *Nat Rev Dis Primers* (2019) 5(1):79. doi: 10.1038/s41572-019-0128-6
6. Unemo M, Shafer WM. Antimicrobial resistance in *Neisseria gonorrhoeae* in the 21st century: past, evolution, and future. *Clin Microbiol Rev* (2014) 27 (3):587–613. doi: 10.1128/CMR.00010-14
7. Brunner A, Nemes-Nikodem E, Jeney C, Szabo D, Marschalko M, Karpati S, et al. Emerging azithromycin-resistance among the *Neisseria gonorrhoeae* strains isolated in Hungary. *Ann Clin Microbiol Antimicrob* (2016) 15(1):53. doi: 10.1186/s12941-016-0166-9
8. Liang JY, Cao WL, Li XD, Bi C, Yang RD, Liang YH, et al. Azithromycin-resistant *Neisseria gonorrhoeae* isolates in Guangzhou, China (2009-2013): coevolution with decreased susceptibilities to ceftriaxone and genetic characteristics. *BMC Infect Dis* (2016) 16:152. doi: 10.1186/s12879-016-1469-3
9. Xue J, Ni C, Zhou H, Zhang C, van der Veen S. Occurrence of high-level azithromycin-resistant *Neisseria gonorrhoeae* isolates in China. *J Antimicrob Chemother* (2015) 70(12):3404–5. doi: 10.1093/jac/dkv266
10. Katz AR, Komeya AY, Kirkcaldy RD, Whelen AC, Soge OO, Papp JR, et al. Cluster of *Neisseria gonorrhoeae* Isolates With High-level Azithromycin Resistance and Decreased Ceftriaxone Susceptibility, Hawaii, 2016. *Clin Infect Dis* (2017) 65(6):918–23. doi: 10.1093/cid/cix485
11. Alirol E, Wi TE, Bala M, Bazzo ML, Chen XS, Deal C, et al. Multidrug-resistant gonorrhea: A research and development roadmap to discover new medicines. *PLoS Med* (2017) 14(7):e1002366. doi: 10.1371/journal.pmed.1002366
12. Ram S, Sharma AK, Simpson SD, Gulati S, McQuillen DP, Pangburn MK, et al. A novel sialic acid binding site on factor H mediates serum resistance of sialylated *Neisseria gonorrhoeae*. *J Exp Med* (1998) 187(5):743–52. doi: 10.1084/jem.187.5.743
13. Ripoche J, Day AJ, Harris TJ, Sim RB. The complete amino acid sequence of human complement factor H. *Biochem J* (1988) 249(2):593–602. doi: 10.1042/bj2490593
14. Lewis LA, Rice PA, Ram S. Role of Gonococcal Neisserial Surface Protein A (NspA) in Serum Resistance and Comparison of Its Factor H Binding Properties with Those of Its Meningococcal Counterpart. *Infect Immun* (2019) 87(2):e00658–18. doi: 10.1128/IAI.00658-18
15. Shaughnessy J, Lewis LA, Zheng B, Carr C, Bass I, Gulati S, et al. Human Factor H Domains 6 and 7 Fused to IgG1 Fc Are Immunotherapeutic against *Neisseria gonorrhoeae*. *J Immunol* (2018) 201(9):2700–9. doi: 10.4049/jimmunol.1701666
16. Shaughnessy J, Ram S, Bhattacharjee A, Pedrosa J, Tran C, Horvath G, et al. Molecular characterization of the interaction between sialylated *Neisseria gonorrhoeae* and factor H. *J Biol Chem* (2011) 286(25):22235–42. doi: 10.1074/jbc.M111.225516
17. Shaughnessy J, Gulati S, Agarwal S, Unemo M, Ohnishi M, Su XH, et al. A Novel Factor H-Fc Chimeric Immunotherapeutic Molecule against Neisseria gonorrhoeae. *J Immunol* (2016) 196(4):1732–40. doi: 10.4049/jimmunol.1500292
18. Silacci M, Baenziger-Tobler N, Lembke W, Zha W, Batey S, Bertschinger J, et al. Linker length matters, fynomer-Fc fusion with an optimized linker displaying picomolar IL-17A inhibition potency. *J Biol Chem* (2014) 289 (20):14392–8. doi: 10.1074/jbc.M113.534578
19. Chen X, Zaro JL, Shen WC. Fusion protein linkers: property, design and functionality. *Adv Drug Deliv Rev* (2013) 65(10):1357–69. doi: 10.1016/j.addr.2012.09.039
20. Klement M, Liu C, Loo BL, Choo AB, Ow DS, Lee DY. Effect of linker flexibility and length on the functionality of a cytotoxic engineered antibody fragment. *J Biotechnol* (2015) 199:90–7. doi: 10.1016/j.jbiotec.2015.02.008
21. Buyel JF, Fischer R. Predictive models for transient protein expression in tobacco (*Nicotiana tabacum* L.) can optimize process time, yield, and downstream costs. *Biotechnol Bioeng* (2012) 109(10):2575–88. doi: 10.1002/bit.24523
22. Nandi S, Kwong AT, Holtz BR, Erwin RL, Marcel S, McDonald KA. Techno-economic analysis of a transient plant-based platform for monoclonal antibody production. *MAbs* (2016) 8(8):1456–66. doi: 10.1080/19420862.2016.1227901
23. Kaufman J, Kalaitzandonakes N. The economic potential of plant-made pharmaceuticals in the manufacture of biologic pharmaceuticals. *J Commercial Biotechnol* (2011) 17):173–82. doi: 10.1057/jcb.2010.37
24. Tuse D, Tu T, McDonald KA. Manufacturing economics of plant-made biologics: case studies in therapeutic and industrial enzymes. *BioMed Res Int* (2014) 2014:256135. doi: 10.1155/2014/256135
25. Shafer WM, Joiner K, Guymon LF, Cohen MS, Sparling PF. Serum sensitivity of *Neisseria gonorrhoeae*: the role of lipopolysaccharide. *J Infect Dis* (1984) 149 (2):175–83. doi: 10.1093/infdis/149.2.175
26. Camara J, Serra J, Ayats J, Bastida T, Carnicer-Pont D, Andreu A, et al. Molecular characterization of two high-level ceftriaxone-resistant *Neisseria gonorrhoeae* isolates detected in Catalonia, Spain. *J Antimicrob Chemother* (2012) 67(8):1858–60. doi: 10.1093/jac/dks162
27. Ohnishi M, Golparian D, Shimuta K, Saika T, Hoshina S, Iwasaku K, et al. Is *Neisseria gonorrhoeae* initiating a future era of untreatable gonorrhea?: detailed characterization of the first strain with high-level resistance to ceftriaxone. *Antimicrob Agents Chemother* (2011) 55(7):3538–45. doi: 10.1128/AAC.00325-11
28. Unemo M, Golparian D, Sanchez-Buso L, Grad Y, Jacobsson S, Ohnishi M, et al. The novel 2016 WHO *Neisseria gonorrhoeae* reference strains for global quality assurance of laboratory investigations: phenotypic, genetic and reference genome characterization. *J Antimicrob Chemother* (2016) 71 (11):3096–108. doi: 10.1093/jac/dkw288
29. Schneider H, Griffiss JM, Boslego JW, Hitchcock PJ, Zahos KM, Apicella MA. Expression of paragloboside-like lipooligosaccharides may be a necessary component of gonococcal pathogenesis in men. *J Exp Med* (1991) 174:1601–5. doi: 10.1084/jem.174.6.1601
30. Chakraborti S, Lewis LA, Cox AD, St Michael F, Li J, Rice PA, et al. Phase-Variable Heptose I Glycan Extensions Modulate Efficacy of 2C7 Vaccine Antibody Directed against *Neisseria gonorrhoeae* Lipooligosaccharide. *J Immunol* (2016) 196(11):4576–86. doi: 10.4049/jimmunol.1600374
31. Hitchcock PJ, Hayes SF, Mayer LW, Shafer WM, Tessier SL. Analyses of gonococcal H8 antigen. Surface location, inter- and intrastrain electrophoretic heterogeneity, and unusual two-dimensional electrophoretic characteristics. *J Exp Med* (1985) 162(6):2017–34. doi: 10.1084/jem.162.6.2017
32. Lewis LA, Ram S, Prasad A, Gulati S, Getzlaff S, Blom AM, et al. Defining targets for complement components C4b and C3b on the pathogenic neisseriae. *Infect Immun* (2008) 76(1):339–50. doi: 10.1128/IAI.00613-07
33. Jokiranta TS, Jaakola VP, Lehtinen MJ, Parepalo M, Meri S, Goldman A. Structure of complement factor H carboxyl-terminus reveals molecular basis of atypical haemolytic uremic syndrome. *EMBO J* (2006) 25(8):1784–94. doi: 10.1038/sj.emboj.7601052
34. Maclean J, Koekemoer M, Olivier AJ, Stewart D, Hitzeroth II, Rademacher T, et al. Optimization of human papillomavirus type 16 (HPV-16) L1 expression in plants: comparison of the suitability of different HPV-16 L1 gene variants and different cell-compartment localization. *J Gen Virol* (2007) 88(Pt 5):1460–9. doi: 10.1099/vir.0.82718-0
35. Voss A, Niersbach M, Hain R, Hirsch HJ, Liao YC, Kreuzaler F, et al. *Reduced virus infectivity in N. tabacum secreting a TMV-specific full-size antibody, Molecular breeding : new strategies in plant improvement*. Dordrecht; Boston: Kluwer Academic Publishers (1995). p. 39–50.
36. Fischer R, Liao YC, Drossard J. Affinity-purification of a TMV-specific recombinant full-size antibody from a transgenic tobacco suspension culture. *J Immunol Methods* (1999) 226(1-2):1–10. doi: 10.1016/s0022-1759(99)00058-7
37. Strasser R, Stadlmann J, Schahs M, Stiegler G, Quendler H, Mach L, et al. Generation of glyco-engineered *Nicotiana benthamiana* for the production of monoclonal antibodies with a homogeneous human-like N-glycan structure. *Plant Biotechnol J* (2008) 6(4):392–402. doi: 10.1111/j.1467-7652.2008.00330.x

38. Koncz C, Schell J. The promoter of TL-DNA gene 5 controls the tissue-specific expression of chimaeric genes carried by a novel type of Agrobacterium binary vector. *Mol Gen Genet* (1986) 204:383–96. doi: 10.1007/BF00331014
39. Garabagi F, Gilbert E, Loos A, McLean MD, Hall JC. Utility of the P19 suppressor of gene-silencing protein for production of therapeutic antibodies in Nicotiana expression hosts. *Plant Biotechnol J* (2012) 10(9):1118–28. doi: 10.1111/j.1467-7652.2012.00742.x
40. Wycoff KL, Belle A, Deppe D, Schaefer L, Maclean JM, Haase S, et al. Recombinant anthrax toxin receptor-Fc fusion proteins produced in plants protect rabbits against inhalational anthrax. *Antimicrob Agents Chemother* (2011) 55(1):132–9. doi: 10.1128/AAC.00592-10
41. Gulati S, Rice PA, Ram S. Complement-Dependent Serum Bactericidal Assays for *Neisseria gonorrhoeae*. *Methods Mol Biol* (2019) 1997:267–80. doi: 10.1007/978-1-4939-9496-0_16
42. Sarantis H, Gray-Owen SD. The specific innate immune receptor CEACAM3 triggers neutrophil bactericidal activities via a Syk kinase-dependent pathway. *Cell Microbiol* (2007) 9(9):2167–80. doi: 10.1111/j.1462-5822.2007.00947.x
43. Ermert D, Shaughnessy J, Joeris T, Kaplan J, Pang CJ, Kurt-Jones EA, et al. Virulence of Group A Streptococci Is Enhanced by Human Complement Inhibitors. *PLoS Pathog* (2015) 11(7):e1005043. doi: 10.1371/journal.ppat.1005043
44. Ueda Y, Miwa T, Ito D, Kim H, Sato S, Gullipalli D, et al. Differential contribution of C5aR and C5b-9 pathways to renal thrombic microangiopathy and macrovascular thrombosis in mice carrying an atypical hemolytic syndrome-related factor H mutation. *Kidney Int* (2019) 96(1):67–79. doi: 10.1016/j.kint.2019.01.009
45. Jerse AE, Wu H, Packiam M, Vonck RA, Begum AA, Garvin LE. Estradiol-Treated Female Mice as Surrogate Hosts for *Neisseria gonorrhoeae* Genital Tract Infections. *Front Microbiol* (2011) 2:107. doi: 10.3389/fmicb.2011.00107
46. Gulati S, Beurskens FJ, de Kreuk BJ, Roza M, Zheng B, DeOliveira RB, et al. Complement alone drives efficacy of a chimeric antigonococcal monoclonal antibody. *PLoS Biol* (2019) 17(6):e3000323. doi: 10.1371/journal.pbio.3000323
47. Wycoff K, Maclean J, Belle A, Yu L, Tran Y, Roy C, et al. Anti-infective immunoadhesins from plants. *Plant Biotechnol J* (2015) 13(8):1078–93. doi: 10.1111/pbi.12441
48. Dawson PE, Muir TW, Clark-Lewis I, Kent SB. Synthesis of proteins by native chemical ligation. *Science* (1994) 266(5186):776–9. doi: 10.1126/science.7973629
49. Gentle IE, De Souza DP, Baca M. Direct production of proteins with N-terminal cysteine for site-specific conjugation. *Bioconjug Chem* (2004) 15 (3):658–63. doi: 10.1021/bc049965o
50. Hezareh M, Hessell AJ, Jensen RC, van de Winkel JG, Parren PW. Effector function activities of a panel of mutants of a broadly neutralizing antibody against human immunodeficiency virus type 1. *J Virol* (2001) 75(24):12161–8. doi: 10.1128/JVI.75.24.12161-12168.2001
51. Densen P, MacKeen LA, Clark RA. Dissemination of gonococcal infection is associated with delayed stimulation of complement-dependent neutrophil chemotaxis in vitro. *Infect Immun* (1982) 38:563–72. doi: 10.1128/IAI.38.2.563-572.1982
52. Konar M, Granoff DM. Eculizumab treatment and impaired opsonophagocytic killing of meningococci by whole blood from immunized adults. *Blood* (2017) 130(7):891–9. doi: 10.1182/blood-2017-05-781450
53. WHO. *Global action plan to control the spread and impact of antimicrobial resistance in Neisseria gonorrhoeae*. World Health Organization (WHO), Geneva, Switzerland: Department of Reproductive Health and Research (2012). p. 1–36.
54. Ram S, McQuillen DP, Gulati S, Elkins C, Pangburn MK, Rice PA. Binding of complement factor H to loop 5 of porin protein 1A: a molecular mechanism of serum resistance of nonsialylated *Neisseria gonorrhoeae*. *J Exp Med* (1998) 188 (4):671–80. doi: 10.1084/jem.188.4.671
55. Apicella MA, Mandrell RE, Shero M, Wilson ME, Griffiss JM, Brooks GF, et al. Modification by sialic acid of *Neisseria gonorrhoeae* lipooligosaccharide epitope expression in human urethral exudates: an immunoelectron microscopic analysis. *J Infect Dis* (1990) 162(2):506–12. doi: 10.1093/infdis/162.2.506
56. Wu H, Jerse AE. Alpha-2,3-sialyltransferase enhances *Neisseria gonorrhoeae* survival during experimental murine genital tract infection. *Infect Immun* (2006) 74(7):4094–103. doi: 10.1128/IAI.00433-06
57. Lewis LA, Gulati S, Burrowes E, Zheng B, Ram S, Rice PA. alpha-2,3-Sialyltransferase Expression Level Impacts the Kinetics of Lipooligosaccharide Sialylation, Complement Resistance, and the Ability of Neisseria gonorrhoeae to Colonize the Murine Genital Tract. *MBio* (2015) 6(1):e02465–14. doi: 10.1128/mBio.02465-14
58. Srikhanta YN, Dowideit SJ, Edwards JL, Falsetta ML, Wu HJ, Harrison OB, et al. Phasevarions mediate random switching of gene expression in pathogenic Neisseria. *PLoS Pathog* (2009) 5(4):e1000400. doi: 10.1371/journal.ppat.1000400
59. Tan A, Atack JM, Jennings MP, Seib KL. The Capricious Nature of Bacterial Pathogens: Phasevarions and Vaccine Development. *Front Immunol* (2016) 7:586. doi: 10.3389/fimmu.2016.00586
60. Hiatt A, Cafferkey R, Bowdish K. Production of antibodies in transgenic plants. *Nature* (1989) 342(6245):76–8. doi: 10.1038/342076a0
61. Klein JS, Jiang S, Galimidi RP, Keeffe JR, Bjorkman PJ. Design and characterization of structured protein linkers with differing flexibilities. *Protein Eng Des Sel* (2014) 27(10):325–30. doi: 10.1093/protein/gzu043
62. Crew PE, Abara WE, McCulley L, Waldron PE, Kirkcaldy RD, Weston EJ, et al. Disseminated Gonococcal Infections in Patients Receiving Eculizumab: A Case Series. *Clin Infect Dis* (2019) 69(4):596–600. doi: 10.1093/cid/ciy958
63. Ellison RT,3, Curd JG, Kohler PF, Reller LB, Judson FN. Underlying complement deficiency in patients with disseminated gonococcal infection. *Sex Transm Dis* (1987) 14(4):201–4. doi: 10.1097/00007435-198710000-00004
64. McWhinney PH, Langhorne P, Love WC, Whaley K. Disseminated gonococcal infection associated with deficiency of the second component of complement. *Postgrad Med J* (1991) 67(785):297–8. doi: 10.1136/pgmj.67.785.297
65. Keiser HD. Recurrent disseminated gonococcal infection in a patient with hypocomplementemia and membranoproliferative glomerulonephritis. *J Clin Rheumatol* (1997) 3(5):286–9. doi: 10.1097/00124743-199710000-00009
66. Figueroa JE, Densen P. Infectious diseases associated with complement deficiencies. *Clin Microbiol Rev* (1991) 4(3):359–95. doi: 10.1128/cmr.4.3.359
67. Ram S, Lewis LA, Rice PA. Infections of people with complement deficiencies and patients who have undergone splenectomy. *Clin Microbiol Rev* (2010) 23 (4):740–80. doi: 10.1128/CMR.00048-09
68. Snyderman R, Durack DT, McCarty GA, Ward FE, Meadows L. Deficiency of the fifth component of complement in human subjects. Clinical, genetic and immunologic studies in a large kindred. *Am J Med* (1979) 67(4):638–45. doi: 10.1016/0002-9343(79)90247-x
69. Overdijk MB, Verploegen S, Ortiz Buijsse A, Vink T, Leusen JH, Bleeker WK, et al. Crosstalk between human IgG isotypes and murine effector cells. *J Immunol* (2012) 189(7):3430–8. doi: 10.4049/jimmunol.1200356
70. Orren A, Wallance ME, Horbart MJ, Lachmann PJ. C6 polymorphism and C6 deficiency in site strains of the mutation-prone Peru-Coppock mice. *Complement Inflamm* (1989) 6:295–6. doi: 10.1159/000463108
71. Banda NK, Hyatt S, Antonioli AH, White JT, Glogowska M, Takahashi K, et al. Role of C3a receptors, C5a receptors, and complement protein C6 deficiency in collagen antibody-induced arthritis in mice. *J Immunol* (2012) 188(3):1469–78. doi: 10.4049/jimmunol.1102310
72. Fattahi F, Grailer JJ, Parlett M, Lu H, Malan EA, Abe E, et al. Requirement of Complement C6 for Intact Innate Immune Responses in Mice. *J Immunol* (2020) 205(1):251–60. doi: 10.4049/jimmunol.1900801

Conflict of Interest: YT, KW, and JM are employed by the company Planet Biotechnology, Inc.

The remaining authors declare that the research was conducted in the absence of any commercial or financial relationships that could be construed as a potential conflict of interest.

frontiers in Immunology

ORIGINAL RESEARCH
published: 19 November 2020
doi: 10.3389/fimmu.2020.584509

Monitoring of the Complement System Status in Patients With B-Cell Malignancies Treated With Rituximab

*Anna Felberg[1], Michał Taszner[2], Aleksandra Urban[1], Alan Majeranowski[2], Kinga Jaskuła[1], Aleksandra Jurkiewicz[1], Grzegorz Stasiłojć[1], Anna M. Blom[3], Jan M. Zaucha[2] and Marcin Okrój[1]**

[1] Department of Cell Biology and Immunology, Intercollegiate Faculty of Biotechnology, University of Gdańsk and Medical University of Gdańsk, Gdańsk, Poland, [2] Department of Hematology and Transplantology, Medical University of Gdańsk, Gdańsk, Poland, [3] Department of Translational Medicine, Lund University, Malmö, Sweden

OPEN ACCESS

Edited by:
Zvi Fishelson, Tel Aviv University, Israel

Reviewed by:
Mark S. Cragg, University of Southampton, United Kingdom
Christian Drouet, INSERM U1016 Institut Cochin, France

***Correspondence:**
Marcin Okrój
marcin.okroj@gumed.edu.pl

Specialty section:
This article was submitted to Molecular Innate Immunity, a section of the journal Frontiers in Immunology

Received: *17 July 2020*
Accepted: *19 October 2020*
Published: *19 November 2020*

Citation:
Felberg A, Taszner M, Urban A, Majeranowski A, Jaskuła K, Jurkiewicz A, Stasiłojć G, Blom AM, Zaucha JM and Okrój M (2020) Monitoring of the Complement System Status in Patients With B-Cell Malignancies Treated With Rituximab. Front. Immunol. 11:584509. doi: 10.3389/fimmu.2020.584509

Rituximab is a pioneering anti-CD20 monoclonal antibody that became the first-line drug used in immunotherapy of B-cell malignancies over the last twenty years. Rituximab activates the complement system *in vitro*, but there is an ongoing debate on the exact role of this effector mechanism in therapeutic effect. Results of both *in vitro* and *in vivo* studies are model-dependent and preclude clear clinical conclusions. Additional confounding factors like complement inhibition by tumor cells, loss of target antigen and complement depletion due to excessively applied immunotherapeutics, intrapersonal variability in the concentration of main complement components and differences in tumor burden all suggest that a personalized approach is the best strategy for optimization of rituximab dosage and therapeutic schedule. Herein we critically review the existing knowledge in support of such concept and present original data on markers of complement activation, complement consumption, and rituximab accumulation in plasma of patients with chronic lymphocytic leukemia (CLL) and non-Hodgkin's lymphomas (NHL). The increase of markers such as C4d and terminal complement complex (TCC) suggest the strongest complement activation after the first administration of rituximab, but not indicative of clinical outcome in patients receiving rituximab in combination with chemotherapy. Both ELISA and complement-dependent cytotoxicity (CDC) functional assay showed that a substantial number of patients accumulate rituximab to the extent that consecutive infusions do not improve the cytotoxic capacity of their sera. Our data suggest that individual assessment of CDC activity and rituximab concentration in plasma may support clinicians' decisions on further drug infusions, or instead prescribing a therapy with anti-CD20 antibodies like obinutuzumab that more efficiently activate effector mechanisms other than complement.

Keywords: obinutuzumab (GA101), non-Hodgkin's lymphoma, complement system, chronic lymphocytic leukemia, rituximab

INTRODUCTION

CD20, a surface molecule present on most developmental stages of B lymphocytes, fulfills many conditions attributable to being a promising target for immunotherapy (1–5). The first anti-CD20 immunotherapeutic rituximab was clinically approved in 1997 (6). It became the first-line drug (usually in combination with chemotherapy), which significantly improved the survival of patients suffering from B cell leukemias and lymphomas (7, 8). Rituximab contains a human IgG1 Fc portion capable of activating immune effector mechanisms in man and rodents, including activation of the complement system and complement-dependent cytotoxicity (CDC) next to antibody-dependent cellular cytotoxicity (ADCC) and phagocytosis mediated by either Fc—or complement receptors (2, 9). On the other hand, immune escape and modulation of immune response by tumor cells and supracellular factors like the number of tumor cells and bioavailability of the drug influence the effectiveness of cancer eradication. Accordingly, indications that many patients are refractory to rituximab (10) reasoned the studies on the pivotal effector and resistance mechanisms, which often brought contradictory results. Our goal was to form coherent conclusions in the light of published data, with an emphasis on the role of the complement system. We also supplement these conclusions with original data showing the status of the complement system and the retention of the drug in patients with B cell malignancies receiving rituximab. In our opinion, monitoring of such parameters contributes to a personalized therapeutic approach highly appreciated in patients undergoing treatment with anti-CD20 antibodies.

An Interplay Between Effector Mechanisms of Rituximab

Based on predominant effector mechanisms, anti-CD20 mAbs are classified into type I and type II antibodies (1, 3). Type I specimens are potent complement activators in contrast to type II, which directly exert cell death upon binding to the target cell. There are reports on limited rituximab-induced cell death in certain tumor B cell lines (11), nonetheless, rituximab is more efficient in the complement-mediated killing and categorized as a representative of type I. Notably, both type I and type II anti-CD20 mAbs can support ADCC induced by the binding of the Fc portion of antibody to Fc receptors localized on effector cells (predominantly NK cells). ADCC and CDC mechanisms may compete with each other as complement activation on the platform of cell-bound rituximab imposes the occupation of its Fc portion and results in a steric hindrance for the interaction with FcγRIII. This phenomenon was proven for the first time *in vitro* by Wang et al., who noticed that normal human serum or C5-depleted serum but not heat-inactivated serum, C1- and C3-depleted serum blocks NK cell activation (12). Further experiments in a syngeneic murine lymphoma model showed that complement depletion by application of cobra venom factor (CVF) before mAb administration resulted in longer survival than the application of mAb alone, thus suggesting that the ADCC mechanism is pivotal and complement activation is detrimental for the therapeutic effect of type I mAbs (13). However, one limitation of this and many other syngeneic mouse models is the usage of anti-CD20 other than rituximab whereas even subtle differences in target epitope or Ig structure outside of CDR regions may be critical for type I/II characteristics (14). A few studies analyzed effector mechanisms of type I anti-CD20 antibodies in transgenic mice expressing human CD20 (15–17). Beers et al. reported a dispensable role of the complement system in the elimination of CD20-positive cells by rituximab converted to mouse IgG2a isotype (equally efficient in CDC as the original rituximab) (16). Results of Tipton and colleagues suggest that antibody-mediated phagocytosis is the crucial effector mechanism (17) whereas Gong et al. showed that effective depletion of B cells may need different effectors depending on their location. Complement was found crucial for the elimination of B cells from the marginal zone in the spleen but not important in other sites (15). The other limitation in the context of the translational potential of *in vivo* studies in mouse models is the fact that mouse complement is very weak compared to other mammals (18, 19), and therefore experiments performed in the mouse model introduce the risk of under-appreciation of CDC as an effector mechanism. Nonetheless, there is a number of the mouse *in vivo* studies that either support (20–22) or question (16, 17, 23, 24) the critical role of complement in the therapeutic effect of rituximab. There is a lack of conclusive *in vivo* studies performed in animal models with complement activity comparable to humans (e.g., rat, guinea pig, and dog). A single study in nude rats with intracerebral lymphoma xenograft successively treated with rituximab suggests complement involvement (25). However, a separate and more detailed investigation must ensure the extrapolation of this conclusion.

Observations from clinics and *ex vivo* experiments in man also bring ambiguous conclusions. ADCC reactions may play a role in the therapeutic effect of rituximab as a low number of NK cells correlated with poor clinical outcome (26). A higher response rate to rituximab and higher progression-free survival of patients with follicular lymphoma was shown in individuals with a polymorphism in FcγRIIIa (CD16), which renders a high affinity to IgG1 (27, 28) but these findings were not confirmed in a larger clinical study (29). Additionally, clinical response and duration of response to rituximab were correlated with polymorphism of the C1qA gene that associates with low levels of C1q—the first component of the classical complement pathway (30). Contrarily, addition of fresh frozen plasma to CLL patients markedly improved their clinical outcome, even when previous administrations of rituximab were ineffective (31, 32). These data suggest that the CDC/ADCC interplay depends either on model or supracellular factors like the number of tumor cells and the expression of the target antigen. Since the threshold necessary for effective ADCC is lower than that for CDC (33), these two competitive effector mechanisms may act cooperatively, i.e. in case of a heterogeneous population of tumor cells, ADCC eliminates these of low CD20

Abbreviations: ADCC, antibody-dependent cellular cytotoxicity; CDC, complement-dependent cytotoxicity; CLL, chronic lymphocytic leukemia; CR3, complement receptor 3; CVF, cobra venom factor; MAC, membrane attack complex; NHL, non-Hodgkin's lymphoma; NHP, normal human plasma; NHS, normal human serum; TCC, terminal complement complex; Δ NHS, heat-inactivated normal human serum.

expression whereas complement eradicates cells with high CD20 content. The number of tumor cells is another parameter important in the context of rituximab's effector mechanisms. Boross et al. showed that injection of rituximab to FcRγ-deficient mice was ineffective at a high load of tumor cells and that, in contrast to a challenge with a low number of tumor cells, effective elimination demands the cooperation of complement and ADCC and the presence of functional complement receptor 3 (CR3) on blood phagocytes (34). The role of receptors for complement-derived opsonins is also underlined by Lee at al., who developed rituximab RA801 mutant non-bondable to human or mouse Fc receptors but retaining complement activation potential (35). While PBMC and PMN were not able to eliminate RA801-opsonized CD20-positive cells *ex vivo* without the addition of serum depleted of the C9 component, there was no difference in human CD20-positive Ramos cells' eradication in *in vivo* nude mouse model between original rituximab and RA801 mutant (35). Yet, eradication of mouse EL4 lymphoma cells expressing human CD20 by rituximab, but not RA801, was impaired in mice additionally lacking all Fc receptors. This can be explained by the higher CDC efficacy of RA801 (4.5-fold lower CH_{50} value) compared to rituximab. Nonetheless, such results underline two important issues: i) extrapolation of conclusions obtained from the studies on one mAb to the other, even closely related mAb, is not reliable, and ii) the relative importance of rituximab's effector mechanisms heavily depends on the target cells. Therefore the seemingly contradictory results showing successful depletion of B cells by rituximab-like antibodies in mice with functional macrophages and Fcγreceptor-dependent pathways but lacking functional complement or ADCC mechanism (16, 23, 36) should not be surprising.

Rituximab (Type I) or Type II Anti-CD20 Immunotherapeutics?

Since both type I and type II anti-CD20 antibodies are nowadays available in clinics, a relevant dilemma is which of these two types is superior for particular patients. Complicated interplay between effector mechanisms and heterogeneity of targets in B cell malignancies in conjunction with supracellular factors make a unanimous answer problematic. Due to the same reason, the role of the complement system in the therapeutic effect cannot be generally ruled out or confirmed. However, assuming that under certain circumstances patients may benefit from complement activation by rituximab, parallel monitoring of the complement system parameters enables selecting subjects with functional impairment, saturation, or unresponsiveness of this effector mechanism, who may benefit more from type II antibodies, e.g., obinutuzumab that more efficiently activates effectors other than complement (37). Another parameter deserving control in case of usage of type I anti-CD20 antibodies is their retention in blood. When excessively administered, they may lead to loss of target antigen *via* internalization (3) and trogocytic removal (38, 39). Conversely, administering type II antibodies results in higher stability of surface CD20 antigen (40). In experimental models, the saturation of the CDC takes place much faster than the saturation of C3b deposition on target cells, thus overdosing provokes exhaustion of the complement system (41, 42). Such exhaustion affects mostly the initial components of the classical pathway, namely, C1 and C2, which are present in serum at much lower molar concentrations than C3 and act as a bottleneck of the whole pathway. Since malignant B cells are typically equipped with a set of complement inhibitors that affect C3/C5 convertases (43, 44), their activity will also lead to the consumption of downstream components C1 and C2. Therefore, too high concentration of rituximab and potent intrinsic complement inhibition by tumor cells may not only dampen CDC at consecutive infusions of the drug but also lead to the selection of tumor cells with low expression of CD20 antigen. Transient loss of CD20 on tumor B cells following rituximab infusion was observed in CLL patients and considered as one of the causes of the limited efficacy of antitumor mAbs (42, 45).

Previously we proposed a calcein release assay on Raji cells as a method for monitoring CDC potential of serum collected from patients treated with type I anti-CD20 antibodies (46). There are several advantages of this method over the routinely used CH_{50} assay performed on sensitized sheep erythrocytes: i) usage of human tumor cells bearing both molecular target (CD20) for dedicated immunotherapeutics and human complement inhibitors (CD46, CD55, CD59) (43) fully compatible with human complement, ii) adequate sensitivity of target cells to complement-mediated lysis and iii) lower inter-assay variability compared to CH_{50} assay (46). Using this approach, we measured the CDC potential of serum samples collected before and after each infusion of rituximab in 17 patients with various B cell malignancies. In another version of these experiments, we supplemented the analyzed sera with saturating concentration of rituximab to evaluate whether putative post-infusion complement depression overlapped with consecutive infusions. In parallel, we measured rituximab concentrations in each sample. The combined results of these experiments reveal the net functional effect of rituximab retention and individual competence of the complement system, which altogether may support the clinician's decision on modification of the therapeutic schedule or switch into type II anti-CD20 antibodies.

METHODS

Patients and Treatment

All samples collected from patients and healthy volunteers were obtained after written informed consent, in accordance with the Declaration of Helsinki and with approval from The Local Bioethical Committee at Medical University of Gdańsk (approval number: NKBBN/500/2016). The cohort consisted of 17 patients admitted to Dept. of Hematology and Transplantology of Medical University of Gdańsk, 7 of which were diagnosed with CLL and 10 with different forms of NHL. All patients had no prior therapies. They were administered with 375 mg/m2 rituximab over the period from 2 to 5 h in four-week intervals for 4 to 8 cycles. All but two patients received concomitant chemotherapy. Detailed patients' characteristics are given in **Table 1**. Response to treatment was assessed according to iwCLL guidelines (47). Blood drawn immediately before and after rituximab infusions was used for

TABLE 1 | Patients' characteristics.

Patient #	Diagnosis	Combined chemotherapy	Clinical response (the way of assessment)	Lymphocyte count before infusions 1-4 (CLL patients only) [10^9/ml]			
				1st	2nd	3rd	4th
1	DLBCL	CHOP	mCR (PET)				
6	HGL	EPOCH	PROG (PET)				
8	PMBCL	EPOCH	mCR (PET)				
9	DLBCL	CHOP	PROG (CT)				
10	BL	codox/ivac	mCR (PET)				
11	FL	COP	PR (CT)				
12	MZL	none	mCR (PET)				
17	CLL	none	PR (clinical)	91.44	42.79	15.03	9.44
18	CLL	FC	CR (clinical)	46.16	3.42	1.73	0.75
19	HGL	CHOP	PROG (CT)				
20	MZL	COP/bendamustine	PR (CT)				
21	CLL	FC	CR (clinical)	64.76	0.83	0.23	0.34
23	CLL	FC	CR (clinical)	128.0	4.37	2.58	0.85
26	CLL	FC	CR (clinical)	81.63	0.48	0.56	0.32
27	CLL	FC	PR (clinical)	90.96	2.29	2.63	0.93
31	FL	COP	CR (CT)				
33	CLL	FC	CR (MRD -)	6.67	2.82	0.17	1.05

Diagnosis: DLBCL, diffused large B cell lymphoma; HGL, high grade lymphoma; PMBCL, primary mediastinal B cell lymphoma; FL, follicular lymphoma; BL, Burkitt lymphoma; MZL, marginal zone B cell lymphoma; CLL, chronic lymphocytic leukemia.

Chemotherapy: CHOP, cyclophosphamide + hydroxydaunorubicin + oncovin + prednisone; EPOCH, etoposide + prednisone + oncovin + cyclophosphamide + hydroxydaunorubicin; COP, cyclophosphamide + oncovin + prednisone; FC, fludarbine + cyclophosphamide.

Clinical response: CR, complete response; mCR, metabolic clinical response; PR, partial response, PROG, progression; PET, positron emission tomography; CT, computed tomography; MRD, minimal residual disease.

serum preparation, as described in (48) and for preparation of EDTA-plasma.

Sample Handling

After collection and preparation, which was accomplished in approximately 30 min after blood collection, serum and plasma samples were aliquoted and kept at −80°C until the time of the experiment. Repetitive freezing and thawing were avoided, and the same rule was applied to normal human serum (NHS) and normal human plasma (NHP), which were prepared from the blood of healthy volunteers and pooled. NHS was then used as a positive control in the CDC assay. NHP was used as a milieu for the preparation of the calibration curve in ELISA-based measurements of C4d and TCC. Heat-inactivated normal human serum (Δ NHS) was prepared from NHS heated to 56°C for 30 min and then cleared by centrifugation at 3000 x G for 5 min. Δ NHS was used as a negative control in CDC assays as heat-inactivation depletes complement activity. Working dilutions of serum and plasma were prepared only before experiments in chilled tubes or microplates kept on ice.

Cell Lines

Raji, Ramos, Namalwa, SU-DHL-4 cells were obtained from the American Type Culture Collection. Cells were aliquoted and cryopreserved after the first few passages. Cells used for experiments were grown from such stock aliquots in RPMI 1640 medium with l-glutamine (ATCC) supplemented with 10% fetal bovine serum (ATCC) at 37 °C and humidified 5% CO_2 atmosphere. Cells were routinely checked for Mycoplasma contamination by DAPI staining (49) when cultured and never kept in continuous culture for more than 10 passages. The primary culture of CLL cells was established from heparinized patients' blood. Lymphocyte fraction was isolated using Lymphoprep (Stemcell Technologies) according to the manufacturer's instruction and assessed as a homogenous population by flow cytometry (>98% of gated objects) showing CD20 expression. Then CLL cells were cultured in a 1:1 mixture of RPMI 1640: DMEM (HyCult) medium supplemented with 10% FBS.

Assessment of Rituximab Concentrations

Rituximab concentration in samples collected just before and just after each infusion was measured using an enzyme-linked immunosorbent assay. 96-well ELISA MaxiSorp plates (ThermoFisher Scientific) were coated with 1 μg/ml of anti-rituximab (anti-idiotype) antibody RB01 (R&D Systems) and blocked with washing buffer (50 mM Tris-HCl, 0.15 M NaCl, 0.1% Tween, pH 7.5) supplemented with 3% fish skin gelatin (Sigma-Aldrich). Patients' serum was diluted to the final concentration of 0,125% in PBS with 0.02% Tween-20 and 0.02M EDTA. Rituximab (Roche) serially diluted in NHS was used for the preparation of the calibration curve. The horseradish peroxidase-conjugated goat anti-mouse antibody (Dako, P0447) was used for detection. The assay was developed using 3,3′,5,5′-Tetramethylbenzidine (TMB) (Sigma-Aldrich), and absorbance readout at 450 nm was measured using a Synergy H1 microplate reader (Biotek).

CDC Assay

Complement-dependent cytotoxicity (CDC) functional assay was performed as described in (46). Briefly, cells previously loaded with calcein-AM (Sigma) were pelleted onto V-shape microplate wells and overlaid with 50 μl of the indicated serum with or without addition of rituximab. After 30 min of

incubation fluorescence of calcein released into the supernatant was measured at 490 nm/520 nm excitation/emission wavelength in Synergy H1 microplate reader (Biotek).

Measurement of Complement Activation Markers

Measurements of the early activation marker of the classical complement pathway, C4d, and the marker of terminal complement pathway activation TCC were performed as described in (50), with slight modifications regarding the TCC sandwich ELISA assay. Instead of zymosan-activated serum, serial dilutions of purified sC5b-9 complex (Complement Technology) in 5% NHP solution in PBS with 0.02% Tween-20 and 0.02M EDTA were used for calibration curve. Detection was achieved using polyclonal rabbit anti-human sC5b-9 neo antibody (Complement Technology) followed by horseradish peroxidase-conjugated goat anti-rabbit antibody (Dako).

Statistics

The grouped analyses of differences in CDC potential and concentration of complement activation markers between pre- and post-infusion serum samples collected at each infusion were performed by multiple Sidak's comparison tests. Calculations were supported by GraphPad 6 software (Prism).

RESULTS

We analyzed the CDC activity of patients' sera collected immediately before and after each infusion of rituximab in two different experimental settings: i) without the addition of a new dose of rituximab and ii) with saturating concentration of rituximab added to patients' serum. The first measurement aimed to assess the cytotoxic activity of serum during the treatment, which reflected the retention of rituximab and the competence of the complement system. The second measurement was performed upon conditions, which imposed complement activity but not rituximab concentration, as a CDC-limiting factor. Thus, the latter assessed the immediate post-infusion complement depletion and whether such putative depletion overlapped with the next infusion. The results obtained for CLL and NHL patients are shown in **Figures 1** and **2**, respectively.

Only one CLL patient (#18) showed spectacular, significantly lower CDC of rituximab-supplemented post-infusion serum sample compared to the analogical pre-infusion sample and such CDC depletion was only observed at the first infusion (**Figure 1** and **Supplementary Statistics File**). Out of seven CLL patients included in the study, four accumulated more than 100 mg/ml of rituximab before infusion 3 (patient #27), infusion 4 (patients #18 and #33), and infusion 6 (patient #26). Similarly, six out of ten patients with NHL accumulated rituximab at the level of 100 mg/ml before infusion 2 (patient #12), infusion 3 (#1, #8, and #11) infusion 5 (#9) and infusion 8 (#20), respectively (**Figure 2**). In both groups of patients, there was a significant correlation between rituximab concentration and CDC exerted on Raji cells, with the saturation level of CDC achieved at rituximab concentration around 50 mg/ml (inlets in **Figures 1** and **2**). We found one NHL patient (#19) who presented depressed CDC throughout all infusions, even when serum samples were supplemented with extra rituximab (**Figure 2**). Interestingly, this patient did not respond to the therapy. One NHL patient (#31) exhibited a low level of CDC in both pre- and post-infusion serum samples, but all his samples regained functionality when supplemented with extra rituximab. Nonetheless, patient #31 achieved a complete response to the treatment.

Previously we characterized Raji as a cell line moderately sensitive to CDC exerted by anti-CD20 mAbs. Incubation of Raji cells in 50% NHS supplemented with CDC-saturating concentration of rituximab (50 μg/ml) yielded in c.a. 50% of lysis (43). In the current experiments performed in 10% of patients' sera (**Figures 1** and **2**), we observed the highest impact of rituximab on the CDC in a concentration range from 10 to 100 μg/ml. Therefore we attempted to assess the effect of the same concentration range either at the different load of tumor cells or on other CD20-positive tumor cells of different sensitivity to CDC (**Figure 3**). Experiments performed in 50% NHS should demonstrate the highest CDC effect theoretically attainable in blood. Raji cells showed CDC increase from 35% to 53% at 100.000 cells and from 25 to 35% at 1M cells when rituximab concentration increased from 10 to 100 μg/ml. Ramos cells showed increased CDC from 44 to 61% of full lysis but there was no effect of increased cell number. Similarly, a 10-fold increase of cell number did not significantly affect the lysis of SU-DHL-4 cells, where the CDC oscillated from 65% at 10 μg/ml of rituximab to 77% at 100 μg/ml of rituximab. Rituximab was ineffective in the killing of Namalwa cells and fresh culture of CLL cells, irrespectively on concentration (**Figure 3**).

CLL patients possess tumor cells circulating in their bloodstream, which are much better accessible for effector mechanisms than tumor cells residing in bone marrow, lymph nodes or other extravascular locations. We analysed appearance of complement activation markers in plasma samples from the CLL patients during the first four infusions (when available). Significant increase of either C4d and TCC were observed (if any) mainly after the first infusions (**Figure 4**), corresponding with the high number of circulating tumor cells further eliminated during the treatment (see **Table 1**). However, patients #21 and #27 did not show signs of strong systemic complement activation, despite the ability of their sera to exert CDC *in vitro* (**Figure 1**). Importantly, levels of both C4d and TCC markers do not correlate with CDC exerted on different target cells (**Supplementary Figure 1**) and should be considered as qualitative rather than quantitative measures of CDC *in vivo*.

DISCUSSION

There is no unanimous opinion on the role of complement in the therapeutic effect of type I anti-CD20 antibodies. Results of *in vivo* animal studies seem to be model-dependent (reviewed in (4)), and the predictive value of *ex vivo* CDC assays in uncertain. Bordon et al. reported the vulnerability of isolated CD20-positive tumor cells to the CDC as a predictor of clinical response to rituximab (51), but

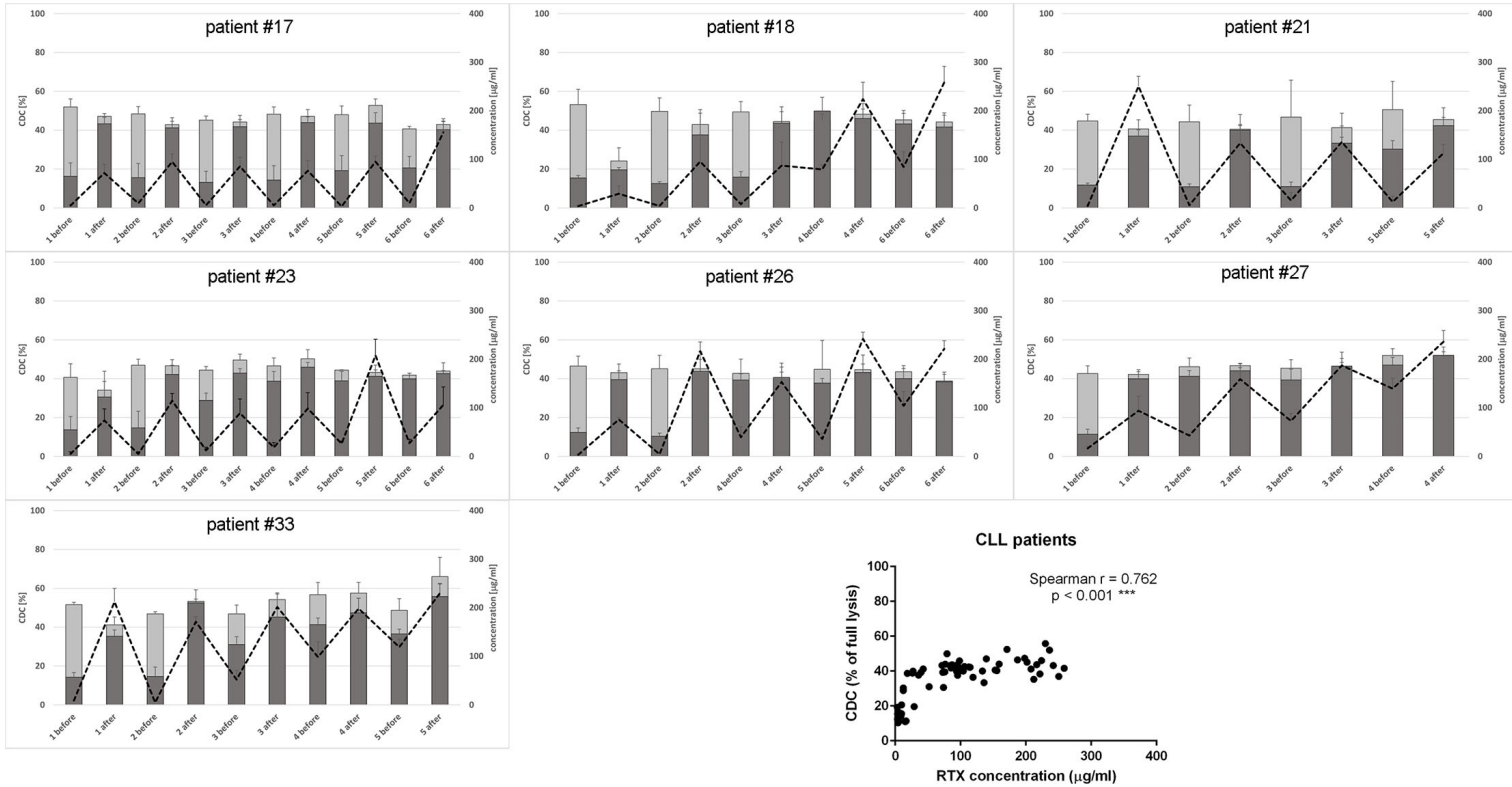

FIGURE 1 | CDC potential and rituximab concentration in serum samples collected from CLL patients. CDC potential was assessed in calcein release assay performed using Raji cells incubated with 10% patient's serum. Dark bars represent CDC levels of patients' sera non-supplemented with extra rituximab, grey bars represent CDC levels when sera were supplemented with 50 µg/ml of rituximab. Dotted line represents rituximab concentration (right Y axis). Each serum was tested in three independent experiments, error bars indicate standard deviation.

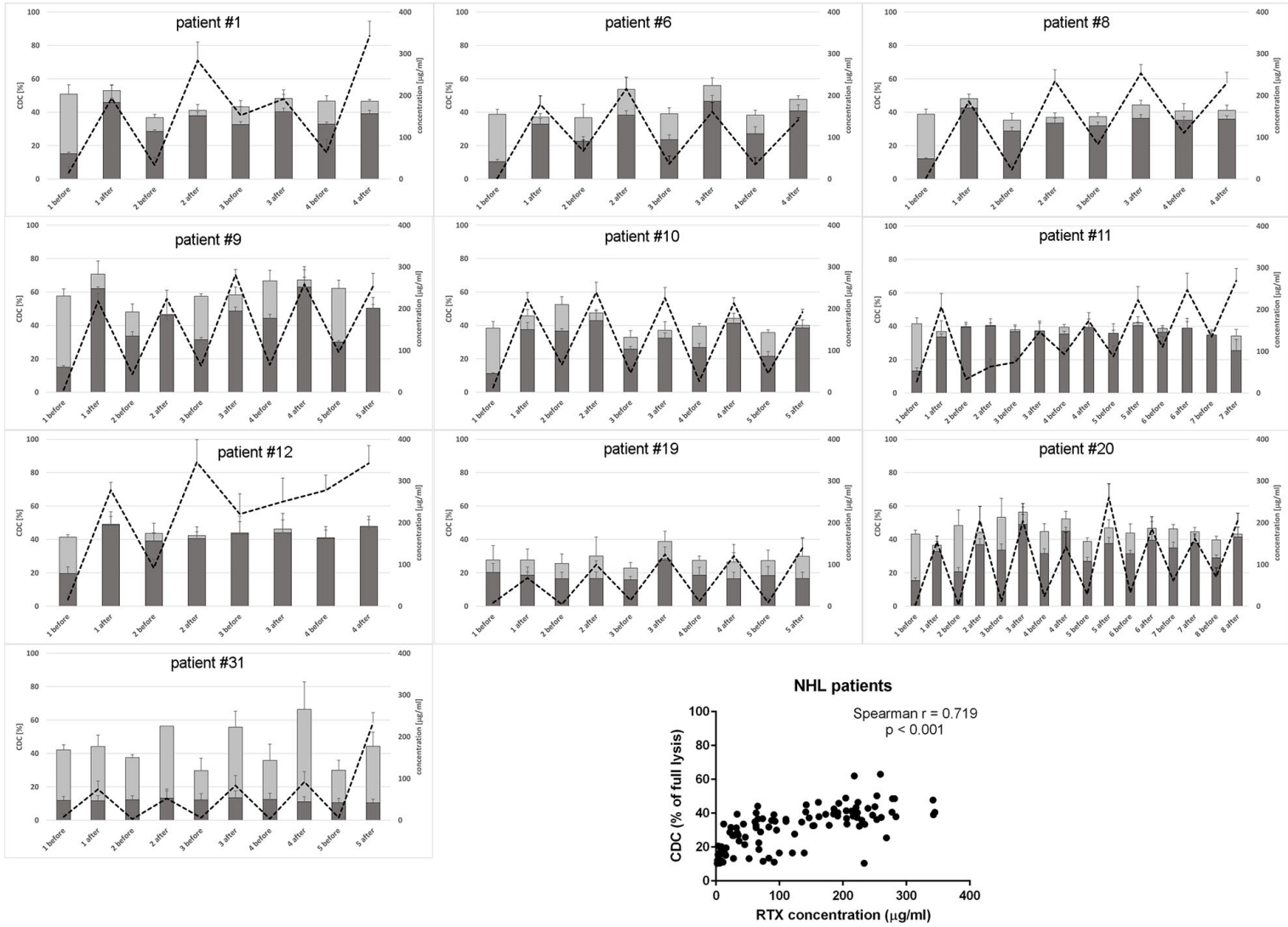

FIGURE 2 | CDC potential and rituximab concentration in serum samples collected from NHL patients. CDC potential was assessed in calcein release assay performed using Raji cells incubated with 10% patient's serum. Dark bars represent CDC level of patients' sera non-supplemented with extra rituximab, grey bars represent CDC level when sera were supplemented with 50 µg/ml of rituximab. Dotted line represents rituximab concentration (right Y axis). Each serum was tested in three independent experiments, error bars indicate standard deviation.

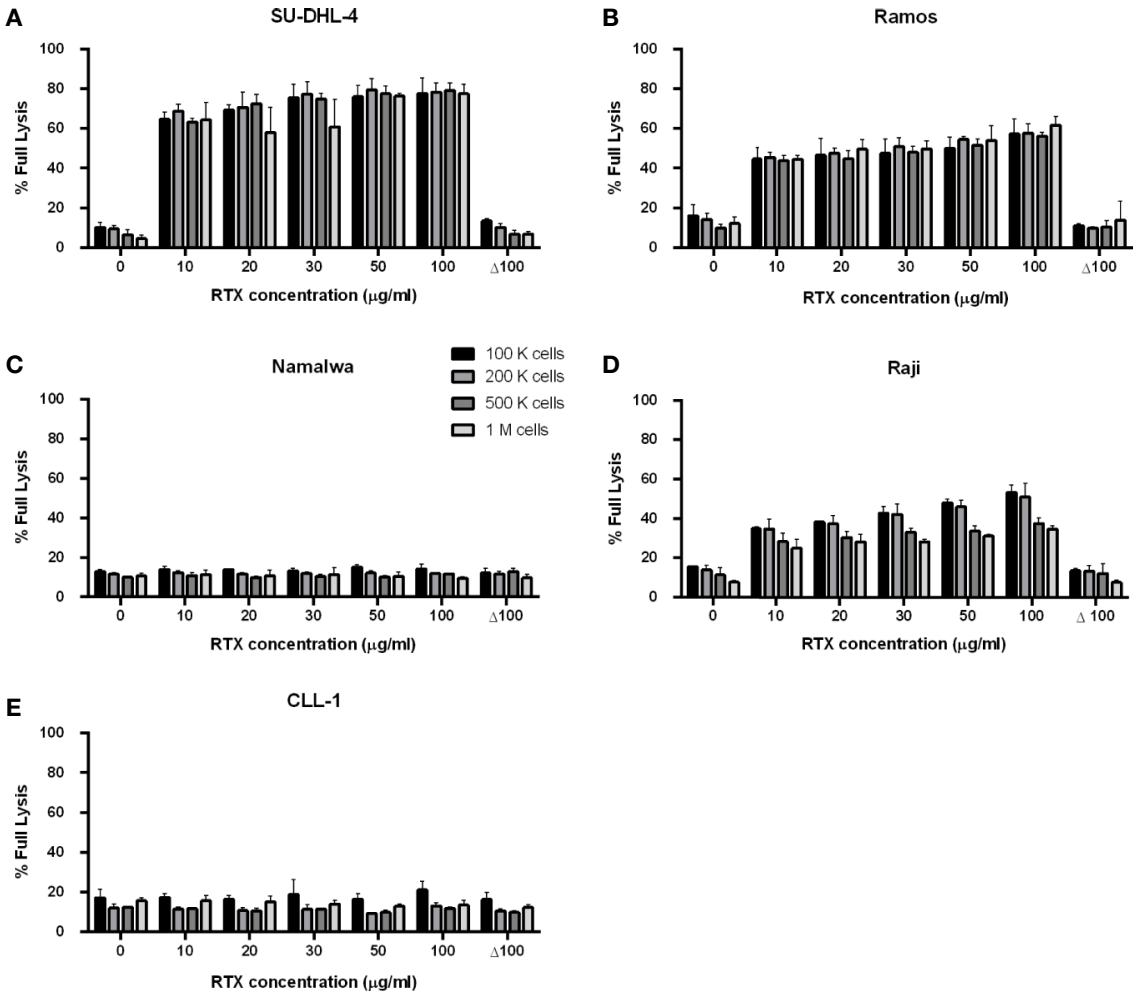

FIGURE 3 | CDC exerted in 50% normal human serum by rituximab at concentration range 10-100 μg/ml. CDC was examined on four CD20-positive cell lines: SU-DHL-4 **(A)**, Ramos **(B)**, Namalwa **(C)**, Raji **(D)** and fresh culture of CLL cells **(E)**. Supernatant collected from calcein-labelled cells lysed with 30% DMSO diluted in PBS served as the indicator of 100% (full) lysis. Readout obtained for heat-inactivated serum (Δ NHS) served as negative control, i.e. background lysis independent on complement activation. Cells were tested at quantities 1, 2, 5, and 10 × 10^5 cells/50 μl, Δ 100 group represents heat-inactivated normal human serum supplemented with 100 μg/ml of rituximab. Data were collected from three independent experiments, error bars indicate standard deviation.

two other studies presented contradictory results (52, 53). A strong argument for the complement role in CLL immunotherapy is the observation that clinical response to rituximab improved after supplementation with fresh-frozen plasma (31, 32). On the other hand, up to 40% of CLL patients may have deficiencies or low levels of circulating complement proteins (54). Therefore the first question we asked in the current study is whether the CDC activity of sera collected from the patients receiving rituximab is sufficient to lyse a model CD20-positive Raji cells. The functional assay we performed to answer this question is much more informative than measurements of the main complement components, whose physiological concentration range varies substantially (e.g., 0.6–1.4 g/L for C3 and 0.1–0.33 g/L for C4) (55). Notably, even C3 concentration as low as 0.18 g/L was reported sufficient to maintain a proper complement function (56).

Raji cell line is characterized as a moderately sensitive to rituximab compared to other B-cell lymphomas, thus enabling observation of either depressed or higher than average complement activity in CDC assays (43). Previously we demonstrated the utility of this model for the mirroring of the anti-CD20 antibody-driven complement consumption and found superior sensitivity of the assay when 10% instead of 50% serum was used (46). Importantly, 10% serum is a surrogate of the complement content in lymph or extravascular fluids, a natural microenvironment of lymphoma (13, 57, 58). However, an increase of NHS concentration from 10% to 50% did not result in a significant increase of CDC in Raji cells, as demonstrated in (43). In the current study, the readout of CDC assay at 10% patients' serum that contained saturating concentration of rituximab (**Figures 1** and **2**) in most of the cases

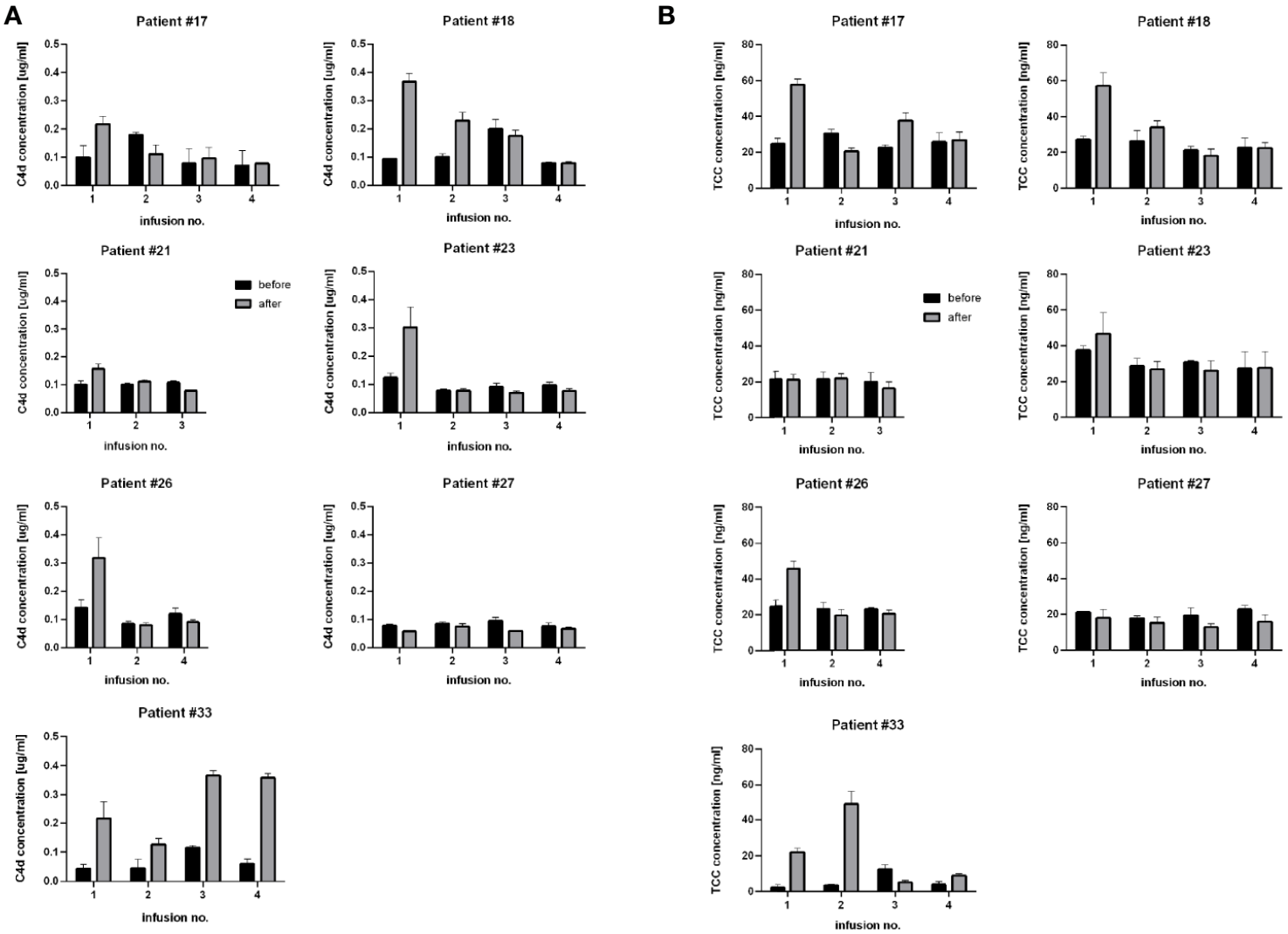

FIGURE 4 | Determination of levels of C4d and TCC, complement activation markers. Graphs show C4d concentration **(A)** and TCC concentration **(B)** in sera collected before (black bars) and after (grey bars) consecutive rituximab infusions in CLL patients. Data were collected from three independent measurements, error bars represent standard deviation.

was not significantly different from the readout obtained at 50% NHS (see **Figure 3D**, bar for the concentration of 50 μg/ml and 100 k cells). Nonetheless, there were few exceptions from this rule. All post-infusion samples of patients #19 and #31 had low CDC activity. Supplementation with additional 50 μg/ml of rituximab markedly improved the CDC readout in patient #31.

We did not study the complement activity of serum over several hours after infusion as others did (41, 59) but found only one patient (#18) who showed signs of complement exhaustion immediately after infusion. Importantly, such exhaustion did not overlap with the next infusion indicating that a four-week interval is enough for the restoration of the complement pool. These results are in agreement with another study, which analyzed the effect of ofatumumab, a stronger CDC-activating anti-CD20 antibody (60), applied in a 2-week interval (46).

CDC potential of pre-infusion serum samples (without addition of rituximab) correlated with the amount of accumulated rituximab in both CLL and NHL patients (inlets in **Figures 1** and **2**). The study by Berinstein et al. evaluated pharmacokinetics of rituximab in 137 non-Hodgkin's lymphoma patients, who received the 375 mg/m^2 dose once weekly for four injections (61). The median difference in rituximab concentration between post- and pre-infusion serum was approx. 250-270 μg/ml, whereas the median level of rituximab in pre-infusion samples was 63 μg/ml, 124 μg/ml, and 186 μg/ml at second, third, and fourth administration, respectively. Significantly higher accumulation of rituximab was noticed in responders to the therapy before the second and fourth infusion. Accumulation of the drug may be explained by a decreased number of accessible tumor cells in responders, but further studies also suggest the loss of target antigen due to internalization and trogocytic removal as a possible explanation (3, 62–64). In our cohort, the differences between post- and pre-infusion levels of serum rituximab were from 25 to 246 μg/ml in CLL patients and from 30 to 279 μg/ml in NHL patients. NHL patients who gradually accumulated rituximab throughout all infusions achieved complete response (#1, #8, and #12), partial response (#11, #20) or progression (#9). Part of the NHL patients with no gradual accumulation of rituximab had progressive disease (#6, #19), but the other part (#10 and #31) showed complete response, so there was no clear segregation into responders and non-responders in terms of rituximab accumulation. These results, opposite to the previous study, can be explained by a four-week instead of one-week interval in rituximab dosing. However, our results show that even at a four-week interval, there are patients (#1, #8, #11, and #12), which accumulate the amounts rituximab comparable to these delivered at the first infusion. Excessively administrated rituximab provides a risk for the selection of a CD20-low population of tumor cells (62). On the other hand, the bioavailability of rituximab in lymph nodes and other extravascular sites is lower than in serum (65). Such a high accumulation of rituximab and concomitant saturation of CDC potential in pre-infusion sera imposes a question if the additional dosing is necessary or counterproductive. Thus, a biopsy of lymphoma cells stained for either cell-bound rituximab or free antigenic CD20 sites will give a valuable hint on whether the therapeutic schedule should be modified or the therapy should be changed to type-II anti-CD20 antibodies such as obinutuzumab, which is superior for the killing of tumor cells *via* ADCC and direct mechanisms (37).

Circulating CD20-positive cells in CLL patients are much more accessible for complement than NHL cells in extravascular locations. Therefore, complement activation by rituximab on circulating CLL cells should be immediately mirrored by the appearance of complement activation markers such as C4d and TCC. C4d is a marker of early stages of the classical complement pathway activation, which leads to opsonization (and complement-dependent phagocytosis) and anaphylaxis. Soluble TCC is formed upon assembly of membrane attack complex (MAC) and indicates CDC. Previously we validated C4d and TCC assays on the cohort of 31 CLL patients and found that increase of TCC in the post-infusion samples took place when an increase of C4d was also observed (50). Nonetheless, the formation of C4d and TCC must depend on the expression level of either CD20 or complement inhibitors present on tumor cells and in patients' sera. We characterized numerous CD20-positive cell lines (including these presented in **Supplementary Figure 1**) and fresh CLL cultures for their expression of CD20 and endogenous complement inhibitors (43). As substantial differences were found in these cells, we assume similar variability in patients. Therefore, the concentration of detected markers cannot be directly associated with CDC intensity, as shown in **Supplementary Figure 1**, and directly compared between individuals. The appearance of C4d and TCC markers indicates whether the complement activation took place and whether it proceeded up to the terminal stages, respectively. The highest increase of complement activation markers should be expected after the first infusion when a high number of CD20-positive tumor cells is present. Indeed, most CLL patients had increased levels of C4d and TCC after the first infusion with a tendency to flatten the differences at consecutive infusions. Except for patient #17, who received rituximab as monotherapy and except for patient #33, the drop in absolute lymphocyte count after the first rituximab infusion in CLL patients was greater than 90% (**Table 1**). Patient #17 achieved a partial response and showed neither gradual accumulation of rituximab nor saturation of CDC serum activity in any of the pre-infusion samples (**Figure 2**). Two CLL patients showed a marginal (#21) or no increase (#27) in C4d. Accordingly, both patients showed no increase in TCC (**Figure 4**). Notably, patient #21 achieved a complete response, unlike patient #27, who responded partially and showed accumulated rituximab throughout all infusions and saturated serum CDC potential already before the second infusion (**Figure 1**).

Our analyses of the complement system competence accompanied by the measurements of rituximab concentration in serum during consecutive infusions performed in the group of 17 patients with heterologous B-cell malignancies are not sufficient to answer the question about the role of complement in the therapeutic effect of rituximab. However, there are two important observations from our study. Irrespectively of serum and drug concentration, rituximab could not exert CDC in freshly isolated CLL cultures (**Figure 3E**) and in Namalwa cells (**Figure 3C**), which express the relative levels of CD20 and complement inhibitors comparable to these observed in CLL cultures (33, 40, 43). These results are in line with our previous publication showing the inability of rituximab to

lyse CLL cells isolated from six patients (43). We conclude that CDC cannot be a sole killing mechanism of CLL cells *in vivo* when rituximab is applied as a monotherapy (as in patient #17), however, concomitant chemotherapy may additionally sensitize tumor cells for CDC, and complement receptor-driven phagocytosis cannot be ruled out. The second issue worth underlining is the fact that even in such a small group of heterologous patients treated with a standard rituximab dose, there were examples of individuals, who deserved a personalized approach. These examples were patient #27 who accumulated a high concentration of rituximab in serum and had fully functional complement but presented no increase of complement activation markers, patients #19 and #31 who had depressed or non-functional complement, and patients #1, #8, #11, and #12 who showed substantial accumulation of rituximab and additionally (#11 and #12) saturated CDC potential of their sera. Monitoring of the complement status and concentration of cell-free rituximab may suggest to clinicians that the ongoing therapy should be continued with type II anti-CD20 antibodies, impose the re-evaluation of a molecular target for the drug, or a delay of further infusions, respectively.

DATA AVAILABILITY STATEMENT

The original contributions presented in the study are included in the article/**Supplementary Material**. Further inquiries can be directed to the corresponding author.

ETHICS STATEMENT

The studies involving human participants were reviewed and approved by The Local Bioethical Committee at Medical University of Gdańsk. The patients/participants provided their written informed consent to participate in this study.

AUTHOR CONTRIBUTIONS

AF, AU, KJ, AJ, and GS performed the experiments and/or optimized assays used in the study. MT, AM, and JZ diagnosed the patients and collected clinical material. AB, MO, and JZ wrote the manuscript. MO conceived the idea of the study. All authors contributed to the article and approved the submitted version.

FUNDING

This work was supported by National Science Centre Poland grant no. 2014/14/E/NZ6/00182 and Cancerfonden.

SUPPLEMENTARY MATERIAL

The Supplementary Material for this article can be found online at: https://www.frontiersin.org/articles/10.3389/fimmu.2020.584509/full#supplementary-material

REFERENCES

1. Winiarska M, Glodkowska-Mrowka E, Bil J, Golab J. Molecular mechanisms of the antitumor effects of anti-CD20 antibodies. *Front Biosci* (2010) 16:277–306. doi: 10.2741/3688
2. Glennie MJ, French RR, Cragg MS, Taylor RP. Mechanisms of killing by anti-CD20 monoclonal antibodies. *Mol Immunol* (2007) 44:3823–37. doi: 10.1016/j.molimm.2007.06.151
3. Beers SA, French RR, Chan HT, Lim SH, Jarrett TC, Vidal RM, et al. Antigenic modulation limits the efficacy of anti-CD20 antibodies: implications for antibody selection. *Blood* (2010) 115:5191–201. doi: 10.1182/blood-2010-01-263533
4. Okroj M, Osterborg A, Blom AM. Effector mechanisms of anti-CD20 monoclonal antibodies in B cell malignancies. *Cancer Treat Rev* (2013) 39:632–9. doi: 10.1016/j.ctrv.2012.10.008
5. Marshall MJE, Stopforth RJ, Cragg MS. Therapeutic Antibodies: What Have We Learnt from Targeting CD20 and Where Are We Going? *Front Immunol* (2017) 8:1245. doi: 10.3389/fimmu.2017.01245
6. Maloney DG, Grillo-Lopez AJ, White CA, Bodkin D, Schilder RJ, Neidhart JA, et al. IDEC-C2B8 (Rituximab) anti-CD20 monoclonal antibody therapy in patients with relapsed low-grade non-Hodgkin's lymphoma. *Blood* (1997) 90:2188–95. doi: 10.1182/blood.V90.6.2188.2188_2188_2195
7. Murawski N, Pfreundschuh M. New drugs for aggressive B-cell and T-cell lymphomas. *Lancet Oncol* (2010) 11:1074–85. doi: 10.1016/S1470-2045(10)70210-2
8. Marcus R, Davies A, Ando K, Klapper W, Opat S, Owen C, et al. Obinutuzumab for the First-Line Treatment of Follicular Lymphoma. *N Engl J Med* (2017) 377:1331–44. doi: 10.1056/NEJMoa1614598
9. Harjunpaa A, Junnikkala S, Meri S. Rituximab (anti-CD20) therapy of B-cell lymphomas: direct complement killing is superior to cellular effector mechanisms. *Scand J Immunol* (2000) 51:634–41. doi: 10.1046/j.1365-3083.2000.00745.x
10. Solal-Celigny P, Leconte P, Bardet A, Hernandez J, Troussard X. A retrospective study on the management of patients with rituximab refractory follicular lymphoma. *Br J Haematol* (2018) 180:217–23. doi: 10.1111/bjh.15023
11. Awasthi A, Ayello J, Van de Ven C, Elmacken M, Sabulski A, Barth MJ, et al. Obinutuzumab (GA101) compared to rituximab significantly enhances cell death and antibody-dependent cytotoxicity and improves overall survival against CD20(+) rituximab-sensitive/-resistant Burkitt lymphoma (BL) and precursor B-acute lymphoblastic leukaemia (pre-B-ALL): potential targeted therapy in patients with poor risk CD20(+) BL and pre-B-ALL. *Br J Haematol* (2015) 171:763–75. doi: 10.1111/bjh.13764
12. Wang SY, Racila E, Taylor RP, Weiner GJ. NK-cell activation and antibody-dependent cellular cytotoxicity induced by rituximab-coated target cells is inhibited by the C3b component of complement. *Blood* (2008) 111:1456–63. doi: 10.1182/blood-2007-02-074716
13. Wang SY, Veeramani S, Racila E, Cagley J, Fritzinger DC, Vogel CW, et al. Depletion of the C3 component of complement enhances the ability of rituximab-coated target cells to activate human NK cells and improves the efficacy of monoclonal antibody therapy in an in vivo model. *Blood* (2009) 114:5322–30. doi: 10.1182/blood-2009-01-200469
14. Meyer S, Evers M, Jansen JHM, Buijs J, Broek B, Reitsma SE, et al. New insights in Type I and II CD20 antibody mechanisms-of-action with a panel of novel CD20 antibodies. *Br J Haematol* (2018) 180:808–20. doi: 10.1111/bjh.15132
15. Gong Q, Ou Q, Ye S, Lee WP, Cornelius J, Diehl L, et al. Importance of cellular microenvironment and circulatory dynamics in B cell immunotherapy. *J Immunol* (2005) 174:817–26. doi: 10.4049/jimmunol.174.2.817
16. Beers SA, Chan CH, James S, French RR, Attfield KE, Brennan CM, et al. Type II (tositumomab) anti-CD20 monoclonal antibody out performs type I (rituximab-like) reagents in B-cell depletion regardless of complement activation. *Blood* (2008) 112:4170–7. doi: 10.1182/blood-2008-04-149161
17. Tipton TR, Roghanian A, Oldham RJ, Carter MJ, Cox KL, Mockridge CI, et al. Antigenic modulation limits the effector cell mechanisms employed by type I

anti-CD20 monoclonal antibodies. *Blood* (2015) 125:1901–9. doi: 10.1182/blood-2014-07-588376
18. Ong GL, Mattes MJ. Mouse strains with typical mammalian levels of complement activity. *J Immunol Methods* (1989) 125:147–58. doi: 10.1016/0022-1759(89)90088-4
19. Bergman I, Basse PH, Barmada MA, Griffin JA, Cheung NK. Comparison of in vitro antibody-targeted cytotoxicity using mouse, rat and human effectors. *Cancer Immunol Immunother* (2000) 49:259–66. doi: 10.1007/s002620000120
20. Di Gaetano N, Cittera E, Nota R, Vecchi A, Grieco V, Scanziani E, et al. Complement activation determines the therapeutic activity of rituximab in vivo. *J Immunol* (2003) 171:1581–7. doi: 10.4049/jimmunol.171.3.1581
21. Cragg MS, Glennie MJ. Antibody specificity controls in vivo effector mechanisms of anti-CD20 reagents. *Blood* (2004) 103:2738–43. doi: 10.1182/blood-2003-06-2031
22. Golay J, Cittera E, Di Gaetano N, Manganini M, Mosca M, Nebuloni M, et al. The role of complement in the therapeutic activity of rituximab in a murine B lymphoma model homing in lymph nodes. *Haematologica* (2006) 91:176–83. doi: 10.3324/%25x
23. Uchida J, Hamaguchi Y, Oliver JA, Ravetch JV, Poe JC, Haas KM, et al. The innate mononuclear phagocyte network depletes B lymphocytes through Fc receptor-dependent mechanisms during anti-CD20 antibody immunotherapy. *J Exp Med* (2004) 199:1659–69. doi: 10.1084/jem.20040119
24. Minard-Colin V, Xiu Y, Poe JC, Horikawa M, Magro CM, Hamaguchi Y, et al. Lymphoma depletion during CD20 immunotherapy in mice is mediated by macrophage FcgammaRI, FcgammaRIII, and FcgammaRIV. *Blood* (2008) 112:1205–13. doi: 10.1182/blood-2008-01-135160
25. Miyake Y, Okoshi Y, Machino T, Chiba S. Treatment of central nervous system lymphoma in rats with intraventricular rituximab and serum. *Int J Hematol* (2010) 92:474–80. doi: 10.1007/s12185-010-0669-7
26. He L, Zhu HY, Qin SC, Li Y, Miao Y, Liang JH, et al. Low natural killer (NK) cell counts in peripheral blood adversely affect clinical outcome of patients with follicular lymphoma. *Blood Cancer J* (2016) 6:e457. doi: 10.1038/bcj.2016.67
27. Cartron G, Dacheux L, Salles G, Solal-Celigny P, Bardos P, Colombat P, et al. Therapeutic activity of humanized anti-CD20 monoclonal antibody and polymorphism in IgG Fc receptor FcgammaRIIIa gene. *Blood* (2002) 99:754–8. doi: 10.1182/blood.v99.3.754
28. Weng WK, Levy R. Two immunoglobulin G fragment C receptor polymorphisms independently predict response to rituximab in patients with follicular lymphoma. *J Clin Oncol* (2003) 21:3940–7. doi: 10.1200/JCO.2003.05.013
29. Ghesquieres H, Cartron G, Seymour JF, Delfau-Larue MH, Offner F, Soubeyran P, et al. Clinical outcome of patients with follicular lymphoma receiving chemoimmunotherapy in the PRIMA study is not affected by FCGR3A and FCGR2A polymorphisms. *Blood* (2012) 120:2650–7. doi: 10.1182/blood-2012-05-431825
30. Racila E, Link BK, Weng WK, Witzig TE, Ansell S, Maurer MJ, et al. A polymorphism in the complement component C1qA correlates with prolonged response following rituximab therapy of follicular lymphoma. *Clin Cancer Res* (2008) 14:6697–703. doi: 10.1158/1078-0432.CCR-08-0745
31. Xu W, Miao KR, Zhu DX, Fang C, Zhu HY, Dong HJ, et al. Enhancing the action of rituximab by adding fresh frozen plasma for the treatment of fludarabine refractory chronic lymphocytic leukemia. *Int J Cancer* (2011) 128:2192–201. doi: 10.1002/ijc.25560
32. Klepfish A, Gilles L, Ioannis K, Rachmilewitz EA, Schattner A. Enhancing the action of rituximab in chronic lymphocytic leukemia by adding fresh frozen plasma: complement/rituximab interactions & clinical results in refractory CLL. *Ann N Y Acad Sci* (2009) 1173:865–73. doi: 10.1111/j.1749-6632.2009.04803.x
33. van Meerten T, van Rijn RS, Hol S, Hagenbeek A, Ebeling SB. Complement-induced cell death by rituximab depends on CD20 expression level and acts complementary to antibody-dependent cellular cytotoxicity. *Clin Cancer Res* (2006) 12:4027–35. doi: 10.1158/1078-0432.CCR-06-0066
34. Boross P, Jansen JH, de Haij S, Beurskens FJ, van der Poel CE, Bevaartj L, et al. The in vivo mechanism of action of CD20 monoclonal antibodies depends on local tumor burden. *Haematologica* (2011) 96:1822–30. doi: 10.3324/haematol.2011.047159
35. Lee CH, Romain G, Yan W, Watanabe M, Charab W, Todorova B, et al. IgG Fc domains that bind C1q but not effector Fcgamma receptors delineate the importance of complement-mediated effector functions. *Nat Immunol* (2017) 18:889–98. doi: 10.1038/ni.3770
36. Montalvao F, Garcia Z, Celli S, Breart B, Deguine J, Van Rooijen N, et al. The mechanism of anti-CD20-mediated B cell depletion revealed by intravital imaging. *J Clin Invest* (2013) 123:5098–103. doi: 10.1172/JCI70972
37. Tobinai K, Klein C, Oya N, Fingerle-Rowson G. A Review of Obinutuzumab (GA101), a Novel Type II Anti-CD20 Monoclonal Antibody, for the Treatment of Patients with B-Cell Malignancies. *Adv Ther* (2017) 34:324–56. doi: 10.1007/s12325-016-0451-1
38. Li Y, Williams ME, Cousar JB, Pawluczkowycz AW, Lindorfer MA, Taylor RP. Rituximab-CD20 complexes are shaved from Z138 mantle cell lymphoma cells in intravenous and subcutaneous SCID mouse models. *J Immunol* (2007) 179:4263–71. doi: 10.4049/jimmunol.179.6.4263
39. Dahal LN, Huang CY, Stopforth RJ, Mead A, Chan K, Bowater JX, et al. Shaving Is an Epiphenomenon of Type I and II Anti-CD20-Mediated Phagocytosis, whereas Antigenic Modulation Limits Type I Monoclonal Antibody Efficacy. *J Immunol* (2018) 201:1211–21. doi: 10.4049/jimmunol.1701122
40. Herter S, Herting F, Mundigl O, Waldhauer I, Weinzierl T, Fauti T, et al. Preclinical activity of the type II CD20 antibody GA101 (obinutuzumab) compared with rituximab and ofatumumab in vitro and in xenograft models. *Mol Cancer Ther* (2013) 12:2031–42. doi: 10.1158/1535-7163.MCT-12-1182
41. Beurskens FJ, Lindorfer MA, Farooqui M, Beum PV, Engelberts P, Mackus WJ, et al. Exhaustion of cytotoxic effector systems may limit monoclonal antibody-based immunotherapy in cancer patients. *J Immunol* (2012) 188:3532–41. doi: 10.4049/jimmunol.1103693
42. Kennedy AD, Beum PV, Solga MD, DiLillo DJ, Lindorfer MA, Hess CE, et al. Rituximab infusion promotes rapid complement depletion and acute CD20 loss in chronic lymphocytic leukemia. *J Immunol* (2004) 172:3280–8. doi: 10.4049/jimmunol.172.5.3280
43. Okroj M, Eriksson I, Osterborg A, Blom AM. Killing of CLL and NHL cells by rituximab and ofatumumab under limited availability of complement. *Med Oncol* (2013) 30:759. doi: 10.1007/s12032-013-0759-5
44. Horl S, Banki Z, Huber G, Ejaz A, Windisch D, Muellauer B, et al. Reduction of complement factor H binding to CLL cells improves the induction of rituximab-mediated complement-dependent cytotoxicity. *Leukemia* (2013) 27:2200–8. doi: 10.1038/leu.2013.169
45. Jilani I, O'Brien S, Manshuri T, Jilani I, O'Brien S, Manshuri T, et al. Transient down-modulation of CD20 by rituximab in patients with chronic lymphocytic leukemia. *Blood* (2003) 102:3514–20. doi: 10.1182/blood-2003-01-0055
46. Stasilojc G, Felberg A, Urban A, Kowalska D, Ma S, Blom AM, et al. Calcein release assay as a method for monitoring serum complement activity during monoclonal antibody therapy in patients with B-cell malignancies. *J Immunol Methods* (2020) 476:112675. doi: 10.1016/j.jim.2019.112675
47. Hallek M, Cheson BD, Catovsky D, Caligaris-Cappio F, Dighiero G, Dohner H, et al. iwCLL guidelines for diagnosis, indications for treatment, response assessment, and supportive management of CLL. *Blood* (2018) 131:2745–60. doi: 10.1182/blood-2017-09-806398
48. Blom AM, Volokhina EB, Fransson V, Stromberg P, Berghard L, Viktorelius M, et al. A novel method for direct measurement of complement convertases activity in human serum. *Clin Exp Immunol* (2014) 178:142–53. doi: 10.1111/cei.12388
49. Uphoff CC, Brauer S, Grunicke D, Gignac SM, MacLeod RA, Quentmeier H, et al. Sensitivity and specificity of five different mycoplasma detection assays. *Leukemia* (1992) 6:335–41.
50. Blom AM, Osterborg A, Mollnes TE, Okroj M. Antibodies reactive to cleaved sites in complement proteins enable highly specific measurement of soluble markers of complement activation. *Mol Immunol* (2015) 66:164–70. doi: 10.1016/j.molimm.2015.02.029
51. Bordron A, Bagacean C, Mohr A, Tempescul A, Bendaoud B, Deshayes S, et al. Resistance to complement activation, cell membrane hypersialylation and relapses in chronic lymphocytic leukemia patients treated with rituximab and chemotherapy. *Oncotarget* (2018) 9:31590–605. doi: 10.18632/oncotarget.25657
52. Weng WK, Levy R. Expression of complement inhibitors CD46, CD55, and CD59 on tumor cells does not predict clinical outcome after rituximab treatment in follicular non-Hodgkin lymphoma. *Blood* (2001) 98:1352–7. doi: 10.1182/blood.v98.5.1352
53. Bannerji R, Kitada S, Flinn IW, Pearson M, Young D, Reed JC, et al. Apoptotic-regulatory and complement-protecting protein expression in

chronic lymphocytic leukemia: relationship to in vivo rituximab resistance. *J Clin Oncol* (2003) 21:1466–71. doi: 10.1200/JCO.2003.06.012
54. Middleton O, Cosimo E, Dobbin E, McCaig AM, Clarke C, Brant AM, et al. Complement deficiencies limit CD20 monoclonal antibody treatment efficacy in CLL. *Leukemia* (2014) 29:107–14. doi: 10.1038/leu.2014.146
55. Ferriani VP, Barbosa JE, de Carvalho IF. Complement haemolytic activity (classical and alternative pathways), C3, C4 and factor B titres in healthy children. *Acta Paediatr* (1999) 88:1062–6. doi: 10.1080/08035259950168081
56. da Silva KR, Fraga TR, Lucatelli JF, Grumach AS, Isaac L. Skipping of exon 27 in C3 gene compromises TED domain and results in complete human C3 deficiency. *Immunobiology* (2016) 221:641–9. doi: 10.1016/j.imbio.2016.01.005
57. Olszewski WL, Engeset A. Haemolytic complement in peripheral lymph of normal men. *Clin Exp Immunol* (1978) 32:392–8.
58. Kaartinen M, Kosunen TU, Makela O. Complement and immunoglobulin levels in the serum and thoracic duct lymph of the rat. *Eur J Immunol* (1973) 3:556–9. doi: 10.1002/eji.1830030906
59. Baig NA, Taylor RP, Lindorfer MA, Church AK, LaPlant BR, Pettinger AM, et al. Induced resistance to ofatumumab-mediated cell clearance mechanisms, including complement-dependent cytotoxicity, in chronic lymphocytic leukemia. *J Immunol* (2014) 192:1620–9. doi: 10.4049/jimmunol.1302954
60. Teeling JL, French RR, Cragg MS, van den Brakel J, Pluyter M, Huang H, et al. Characterization of new human CD20 monoclonal antibodies with potent cytolytic activity against non-Hodgkin lymphomas. *Blood* (2004) 104:1793–800. doi: 10.1182/blood-2004-01-0039
61. Berinstein NL, Grillo-Lopez AJ, White CA, Bence-Bruckler I, Maloney D, Czuczman M, et al. Association of serum Rituximab (IDEC-C2B8) concentration and anti-tumor response in the treatment of recurrent low-grade or follicular non-Hodgkin's lymphoma. *Ann Oncol* (1998) 9:995–1001. doi: 10.1023/A:1008416911099
62. Taylor RP, Lindorfer MA. Analyses of CD20 Monoclonal Antibody-Mediated Tumor Cell Killing Mechanisms: Rational Design of Dosing Strategies. *Mol Pharmacol* (2014) 86:485–91. doi: 10.1124/mol.114.092684
63. Taylor RP, Lindorfer MA. Fcgamma-receptor-mediated trogocytosis impacts mAb-based therapies: historical precedence and recent developments. *Blood* (2015) 125:762–6. doi: 10.1182/blood-2014-10-569244
64. Vaughan AT, Chan CH, Klein C, Glennie MJ, Beers SA, Cragg MS. Activatory and inhibitory Fcgamma receptors augment rituximab-mediated internalization of CD20 independent of signaling via the cytoplasmic domain. *J Biol Chem* (2015) 290:5424–37. doi: 10.1074/jbc.M114.593806
65. Hekman A, Honselaar A, Vuist WM, Sein JJ, Rodenhuis S, ten Bokkel Huinink WW, et al. Initial experience with treatment of human B cell lymphoma with anti-CD19 monoclonal antibody. *Cancer Immunol Immunother* (1991) 32:364–72. doi: 10.1007/BF01741331

Conflict of Interest: The authors declare that the research was conducted in the absence of any commercial or financial relationships that could be construed as a potential conflict of interest.

frontiers in Immunology

ORIGINAL RESEARCH
published: 10 December 2020
doi: 10.3389/fimmu.2020.612402

Monoclonal Antibodies Capable of Inhibiting Complement Downstream of C5 in Multiple Species

Wioleta M. Zelek * *and B. Paul Morgan* *

Systems Immunity Research Institute, Division of Infection and Immunity and Dementia Research Institute, School of Medicine, Cardiff University, Wales, United Kingdom

OPEN ACCESS

Edited by:
Marcin Okrój, University of Gdańsk and Medical University of Gdańsk, Poland

Reviewed by:
Christoph Q. Schmidt, University of Ulm, Germany
Lubka T. Roumenina, INSERM U1138 Centre de Recherche des Cordeliers (CRC), France

***Correspondence:**
B. Paul Morgan
morganbp@cardiff.ac.uk
Wioleta M. Zelek
zelekw@cardiff.ac.uk

Specialty section:
This article was submitted to Molecular Innate Immunity, a section of the journal Frontiers in Immunology

Received: *30 September 2020*
Accepted: *09 November 2020*
Published: *10 December 2020*

Citation:
Zelek WM and Morgan BP (2020) Monoclonal Antibodies Capable of Inhibiting Complement Downstream of C5 in Multiple Species. Front. Immunol. 11:612402. doi: 10.3389/fimmu.2020.612402

Better understanding of roles of complement in pathology has fuelled an explosion of interest in complement-targeted therapeutics. The C5-blocking monoclonal antibody (mAb) eculizumab, the first of the new wave of complement blocking drugs, was FDA approved for treatment of Paroxysmal Nocturnal Hemoglobinuria in 2007; its expansion into other diseases has been slow and remains restricted to rare and ultra-rare diseases such as atypical hemolytic uremic syndrome. The success of eculizumab has provoked other Pharma to follow this well-trodden track and made C5 blockade the busiest area of complement drug development. C5 blockade inhibits generation of C5a and C5b, the former an anaphylatoxin, the latter the nidus for formation of the pro-inflammatory membrane attack complex. In order to use anti-complement drugs in common complement-driven diseases, more affordable and equally effective therapeutics are needed. To address this, we explored complement inhibition downstream of C5. Novel blocking mAbs targeting C7 and/or the C5b-7 complex were generated, identified using high throughput functional assays and specificity confirmed by immunochemical assays and surface plasmon resonance (SPR). Selected mAbs were tested in rodents to characterize pharmacokinetics, and therapeutic capacity. Administration of a mouse C7-selective mAb to wildtype mice, or a human C7 specific mAb to C7-deficient mice reconstituted with human C7, completely inhibited serum lytic activity for >48 h. The C5b-7 complex selective mAb 2H2, most active in rat serum, efficiently inhibited serum lytic activity *in vivo* for over a week from a single low dose (10 mg/kg); this mAb effectively blocked disease and protected muscle endplates from destruction in a rat myasthenia model. Targeting C7 and C7-containing terminal pathway intermediates is an innovative therapeutic approach, allowing lower drug dose and lower product cost, that will facilitate the expansion of complement therapeutics to common diseases.

Keywords: complement, therapeutics, monoclonal antibody, C7, C5b-7, human, rat, mouse

INTRODUCTION

The complement system comprises over 50 proteins, regulators and receptors circulating in plasma or on cells. Activation of the system by three distinct pathways, classical, lectin, and alternative, the latter comprising a common amplification loop, leads to formation of C3 convertases, followed by C5 convertases which cleave C5 into the potent chemotactic anaphylatoxin C5a, and C5b, the nidus for formation of the cytotoxic proinflammatory membrane attack complex (MAC). C5b while associated with the convertase, sequentially binds the plasma proteins C6 and C7, generating the C5b-7 complex that undergoes conformational change, triggering release from the convertase and exposing a labile hydrophobic membrane binding surface. The C5b-7 complex through its hydrophobic surface tightly binds membrane and sequentially recruits C8 and C9 to create the MAC, a transmembrane pore comprising one molecule each of C5b, C6, C7, and C8 and up to 18 copies of C9 that are recruited sequentially. The MAC pore allows metabolites and small proteins to leak out of the cell and water to flood into the cell due to osmotic pressure leading to lytic cell death (1–3).

Complement is critical to immune defense, providing recognition, tagging and elimination of bacteria and other foreign intruders and immune complexes; however, inappropriate activation of the system can lead to self-tissue and self-cell damage, driving disease. Hence, there is a need for therapies that block complement. For more than a decade, there was only one anti-complement drug in the clinic, the anti-C5 monoclonal antibody (mAb) eculizumab; this drug was FDA approved in 2007 for the ultra-rare hemolytic disease paroxysmal nocturnal hemoglobinuria (PNH), in 2011 for the ultra-rare renal disease atypical hemolytic uremic syndrome (aHUS), and for myasthenia gravis (MG) therapy in 2017 and in 2019 for the treatment of anti-aquaporin-4 (AQP4) antibody positive neuromyelitis optica spectrum disorder (NMOSD) in adults (1). At a list price of approximately $500,000 per patient per year, eculizumab, remains one of the most expensive therapies in the world. The drug must be given bi-weekly by intravenous infusion, 0.9 to 1.2 g/dose (1–5). These factors restrict progress toward therapy of more common complement-driven diseases. A step change is now needed to enable the use of anti-complement drugs in these conditions where there is considerable unmet need and many patients do not respond adequately to currently available agents. Anti-complement drugs for common conditions must be safer, cheaper and easier to administer.

Although the complement cascade can be targeted at many stages, anti-complement drugs in development are focused on very few targets, with agents mimicking eculizumab and targeting C5 or its breakdown products predominating. This is at least in part because inhibition of C5 has proven to be relatively low risk; the increased risk of Neisserial infections is managed by vaccination before treatment and prophylactic use of antibiotics. There are numerous agents in development that target C5, for example, crovalimab (SKY59), a C5 blocking mAb utilizing a pH-dependent recycling technology to increase drug half-life, and reduce the dose required to block C5 (in phase III clinical trials; (1, 6) https://clinicaltrials.gov/ct2/show/NCT04432584), and ravulizumab, the "next generation" eculizumab that also incorporates recycling technology enabling an increase in dosing interval to eight weeks. Ravulizumab has been FDA approved for PNH (2018) and aHUS (2019) (7).

Currently, only one drug targeting MAC downstream of C5 has progressed to clinical trials; AAVCAGsCD59 is a gene therapy agent in development for age-related macular degeneration (AMD); the agent is injected into the eye to locally express a non-anchored form of the MAC inhibitor CD59 (8). An anti-C6 mAb (CP010), developed by Complement Pharma and now partnered with Alexion, is in pre-clinical testing. (https://globalgenes.org/2018/06/12/alexion-and-complement-pharma-form-partnership-to-co-develop-complement-inhibitor-for-neurodegenerative-disorders/). In the wider literature there are a few preclinical reports describing targeting MAC beyond C5. An anti-C8 mAb was tested in hyperacute rejection (HAR) and cardiopulmonary bypass (CPB) rodent models; (9, 10) in HAR, mAb treatment protected hearts perfused with human serum while in CPB the mAb reduced platelet activation. A polyclonal antibody against C6 inhibited clinical symptoms in an experimental MG (EAMG) model in rats (11). Neither of these agents was advanced further. A very recent report described a monoclonal anti-C6 that inhibited hemolysis in human and rhesus monkey serum (12). These reports not only highlight the therapeutic potential of developing anti-terminal pathway drugs beyond C5, but also demonstrate the crucial role of MAC as a pathology driver.

Here we describe a panel of terminal pathway blocking mAbs, generated in C7-knockout (KO) mice hyper-immunized with human or rat C5b-7 and/or C7. The selected anti-human mAbs were equivalent or better inhibitors of human complement when compared to eculizumab in standard activity assays. Some of the mAbs showed cross-species activity when tested against human and rodent sera and the relevant mAbs efficiently inhibited complement activity *in vivo* in rodents. For one mAb, reactive against rat C5b-7, a single low dose inhibited complement for over a week in rats and blocked disease in the rat EAMG model.

MATERIALS AND METHODS

Reagents and Sera

All chemicals, except where otherwise stated, were obtained from either Fisher Scientific UK (Loughborough, UK) or Sigma Aldrich (Gillingham, UK) and were of analytical grade. All tissue culture reagents and plastics were from Invitrogen Life Technologies (Paisley, UK). Sheep and guinea pig erythrocytes in Alsever's solution were from TCS Biosciences (Claydon, UK). Eculizumab was kindly donated by Prof. David Kanavagh (Newcastle University, UK), and crovalimab by Roche Diagnostics (Basel, Switzerland). Cynomolgus monkey serum was purchased from Serlab (#S-118-D-24526, London, UK). Human and animal sera were prepared in house from freshly collected blood. For human, rabbit and rat, blood was clotted at room temperature (RT) for 1 h, then placed on ice for 2 h for clot retraction before centrifugation and harvesting of serum. For mouse, blood was placed on ice immediately after harvest and clotted for 2 h on ice

before serum harvest. Sera were stored in aliquots at −80°C and not subjected to freeze–thaw cycles.

Generation of mAbs

Monoclonal antibodies against C7/C5b-7 protein were generated by first establishing a line of C7 deficient mice. CRISP-generated heterozygous C7 KO mice (C57BL/6NJ-C7$^{em1(IMPC)J}$/Mmjax) were purchased from Jackson Laboratories (Bar Harbour, Maine, USA) and back-crossed to obtain homozygous C7 deficient mice. The absence of C7 was confirmed by western blotting (WB) and hemolytic assays (data not shown). Wildtype (WT) and C7 KO mice were immunized with rat C7 and human C7/C5b-7 (both purified in-house) using standard schedules (13). The C7 KO mice were also used as a source of feeder macrophages during the cloning process. Immunized mice were screened using enzyme-linked immunosorbent assay (ELISA), mice with the highest titer response against the immunized proteins were selected and re-boosted before killing and harvesting of spleens. Plasma cells were harvested, fused with SP2 myeloma and aliquoted into 96-well plates. Hybridoma supernatants were screened using high-throughput hemolytic assay (described below) to identify blocking mAbs; supernatants with blocking activity were also screened for antibody responses by ELISA. Complement blocking mAb-secreting clones were sub-cloned by limiting dilution to monoclonality. Mouse mAbs were isotyped using IsoStrips (# 11493027001; Roche).

Hemolytic Assays

The capacity of the mAbs to inhibit complement in human and animal sera was investigated by classical pathway (CP; CH50) hemolysis assay using antibody-sensitized sheep erythrocytes (ShEA); sheep blood was from TCS Bioscience and anti-ShE antiserum (#ORLC25, Siemens Amboceptor) was from Cruinn Diagnostics (Dublin, UK). ShEA were suspended in HEPES-buffered saline (HBS) containing Ca^{2+} and Mg^{2+} at 2% (vol:vol) (14). For measurement of activity in male mouse serum, ShEA were additionally incubated with mouse anti-rabbit IgG at 25 μg/ml (#3123; Invitrogen) for 30 min at 37°C before washing in HBS. A serial dilution series of each test mAb (100–0 μg/ml; 50 μl/well) was prepared in HBS and aliquoted in triplicate into a 96-well round-bottomed plate at 50 μl/well, then serum and 2% ShEA (50 μl/well of each) added. Serum dilutions for each species were selected in preliminary experiments to give near complete hemolysis in the absence of test mAb: 2.5%: normal human serum (NHS); 10%: normal Cynomolgus monkey serum (Cyno); 2.5% normal rat serum (NRS); 25%: normal rabbit serum (NRbS); 25%: normal male mouse serum (NMS) (using the double-sensitized cells as described above). Plates were incubated at 37°C for 30 min, centrifuged and hemoglobin in the supernatant was measured by absorbance at 405 nm. Percentage lysis was calculated according to: % Lysis = Absorbance (Abs) sample − Abs background)/(Abs max − Abs background) × 100%. GraphPad Prism was used for data analysis. Hybridoma supernatants were screened for blocking mAbs using the same assay but with neat tissue culture supernatant in place of the purified mAb.

Reactive lysis assays were used to identify mechanism of mAb inhibition. Guinea pig blood was from TCS; erythrocytes (GPE) at 2% in HBS (50 μl/well) were incubated sequentially with C5b6, C7, C8 and C9 (in house, affinity purified (15)), each for 10 min at 37°C, at doses titrated to give ~75% to 90% hemolysis in the absence of inhibitor. The concentrations (per well) of the purified components used were as follow; C5b6; 45 ng/ml, C7; 184 ng/ml, C8; 168 ng/ml, C9; 383 ng/ml. Molarities in nM; C5b6, 0.16; C7, 1.99; C8, 1.11; C9, 5.39 (Ratios: 1: 13: 10: 34). Serial dilutions (in triplicate) of the mAb (1–0 μg/ml) were made into HBS and added to the wells at different stages of MAC formation to determine the inhibition. Test and control mAb were added either prior to addition of C7 (human or rat), or prior to addition of C8/C9 and incubated for 30 min at 37°C. In some assay rat-EDTA serum was used as source of rat C8 and C9 to develop lysis of C5b-7 (human or rat C7) coated cells. Plates were centrifuged at 2000 rpm for 3 min at 4°C, supernatants removed to a flat-welled microtiter plate, absorbances measured spectrophometrically (A_{405}nm) and % lysis calculated.

To reduce the need for large volumes of fresh mouse serum, add-back hemolytic assays were used for testing of lytic activity in mice treated with the mAb. NHS depleted of C7 (C7D) or C5 (C5D) was used as source of the rest of the complement proteins; mouse serum was added (1:2 v:v; mouse serum:C7D/C5D) to restore the relevant component. The serum mix was diluted to 10% in HBS then plated in a dilution series (50 μl/well; 10–0%) in HBS in a round bottom microwell plate; 50 μl 2% ShEA and 50 μl HBS were added (final concentrations of serum mix in wells: 3.3–0%), incubated for 30 min at 37°C. Plates were centrifuged, supernatants removed to a flat-welled microtiter plate and absorbance measured spectrophometrically (A_{405}nm). % lysis was calculated.

Characterization of Novel mAbs by ELISA and WB

Direct ELISA was used to test whether the new mAb bound C7 from different species. Sandwich ELISA were used to confirm C7 binders, to eliminate issues around denaturation by protein binding on plastic, and to test whether the mAbs competed for the same binding epitope. Standard curves were generated using in-house human or animal (rat, mouse, monkey) C7 proteins, immunoaffinity purified as previously described (15). In the direct ELISA, Maxisorp (Nunc, Loughborough, UK) 96-well plates were coated with C7 (0.5 μg/ml in bicarbonate buffer, pH 9.6) at 4°C overnight; wells were blocked (1 h) at 37°C with 2% bovine serum albumin (BSA) in phosphate-buffered saline (PBS), washed in PBS containing 0.05% Tween 20 (PBS-T). Dilutions of purified mAb, 1000–0 ng/ml (stock concentrations of all proteins used established using the BCA assay) in 0.2% BSA-PBS, were added in triplicate to wells coated with each of the antigens and incubated for 1 h at 37°C. Wells were washed with PBS-T then incubated (1 h, 37°C) with secondary antibody (donkey anti-mouse-horseradish peroxidase (HRP); Jackson ImmunoResearch, Ely, UK) for 1 h at 37°C. In the sandwich ELISA, Maxisorp plates were coated with mAb (2 μg/ml in bicarbonate buffer, pH 96) at 4°C overnight; wells were

blocked (1 h at 37°C with 2% BSA-PBS) and washed in PBS-T. Standard curves were generated using in-house purified C7 protein serially diluted in 0.2% BSA-PBS, added in triplicate and incubated for 1 h at 37°C. Wells were washed with PBS-T then incubated (1 h, 37°C) with the paired HRP-labeled mAb (1 in 1000 dilution in PBS-T; Pierce, #31489). After washing, plates were developed using O-phenylenediamine dihydrochloride (OPD, Sigma FAST™; Sigma-Aldrich) and absorbance (492 nm) was measured. GraphPad Prism was used for data analysis.

To confirm specificity for C7 and the species reactivity, C7 protein (in house; 0.5 μg) or human or animal (mouse, rat, monkey) sera diluted 1:100 in PBS were placed in separate wells and resolved on 4–20% sodium dodecyl sulphate–polyacrylamide gel (SDS-PAGE) electrophoresis gels (#4561093; Biorad, Hemel Hempstead, UK) under reducing (R) and non-reducing (NR) conditions, then electrophoretically transferred onto 0.45 μm nitrocellulose membrane (GE Healthcare, Amersham, UK). After transfer, non-specific sites on the membrane were blocked with 5% BSA in PBS-T. After washing in PBS-T, membrane strips were incubated overnight at 4°C with individual test mAb (each at 1 μg/ml in 5% BSA PBS-T) or polyclonal (goat) anti-human C7 (2 μg/ml, CompTech, Tyler, TX; A224). After washing, bound test mAb were detected by incubation with donkey anti-mouse IgG-HRP (#715-035-150, Jackson ImmunoResearch) and polyclonal anti-C7 with rabbit anti-goat IgG HRP conjugate (#305-035-045; Jackson ImmunoResearch) at 1: 10000 in 5% BSA PBS-T. Blots were washed, developed with enhanced chemiluminescence (GE Healthcare) and visualized by autoradiography.

To characterize mAb binding to soluble terminal complement complexes (TCC), biotinylated mAbs (Pierce, #21327) were individually added to human or rat serum (100 μg/ml in 3 ml serum) and the mix activated *via* both classical and alternative pathways by incubation with Zymosan A (7 mg/ml; #21327, Pierce) and aggregated human IgG (1 mg/ml; in house) for 32 h at 37°C in a shaking water bath. The reaction was stopped by centrifugation at 2500 rpm for 15 min at 4°C and the supernatant (activated serum) collected. For analysis by WB, supernatant was mixed with 0.25 ml Avidin-coated beads (prepared by coupling avidin to HiTrap N-hydroxysuccinimide-activated beads; #17-0716-01, GE Healthcare, Little Chalfont, UK). The mixture was incubated for 1 hat RT while mixing gently, the beads washed five times in PBS by centrifugation (1000 rpm for 1 min) and the bound mAb-complex eluted by incubation (10 min at 100°C) in reducing or non-reducing SDS-PAGE running buffer. Supernatants were subjected to SDS-PAGE and WB as above. Blots were blocked with 5% BSA, washed, cut into strips and individual strips incubated with goat anti-C5, -C6, -C7, -C8 or -C9 antibodies (at 2 μg/ml, Comptech, Tyler, TX; A220, 223, 224, 225, 226) for 1 h, washed then incubated with horseradish peroxidase HRP-conjugated anti-goat immunoglobulin (1: 10 000 dilutions, #305-035-045; Jackson ImmunoResearch) for 1 h at RT with constant mixing. After washing, blots were developed as described above. For analysis by ELISA, supernatant was added to 96-well plates coated with Avidin (10 μg/ml), incubated 1 h at 37°C and blocked with 2% BSA (1 h at 37°C); after washing, terminal pathway components in the pull-down samples were detected with Goat anti-C5, C6, C7, C8 or C9 antibodies as above at 2 μg/ml diluted in 0.2% BSA PBS-T then developed with rabbit anti-Goat-HRP, #305-035-045; Jackson ImmunoResearch). Controls for each antibody comprised biotinylated mAb alone or incubated with C7. The assay was developed as described above.

Binding of the mAbs to pre-formed TCC was tested in ELISA; serum activated as above in the absence of mAbs (1 in 50 dilution in 0.2% BSA-PBS-T) was transferred to plates coated with aE11 anti-C9 neo-specific antibody (5 μg/ml, Hycult Biotech, # HM2167), incubated 1 h at 37°C and blocked with 2% BSA (1 h at 37°C); after washing, the new biotinylated mAb or as positive control, an in house mAb known to bind aE11-captured TCC (E2 anti-C8; 1 in 1000 dilution in 0.2% BSA-PBS-T) were added and incubated for 1 h at 37°C, after washing, Streptavidin-HRP (1 in 5000 dilution in 0.2% BSA-PBS-T, Fisher Scientific, # 21130) was added, plates incubated 1 h at 37°C and the assay developed as described above.

SPR Analysis to Determine Test mAbs Binding Affinity to Human C7

The mAbs binding analyses were carried out on a Biacore T200 instrument (GE Healthcare); for mAb of isotype IgG, an antibody capture kit (GE Healthcare, # BR-1008-38) was used to immobilize the mAb on a CM5 sensor chip (GE Healthcare, #29-1496-03) as recommended by the manufacturer. mAb isotype IgM was immobilized on a Protein L Series S sensor chip (GE Healthcare #29-2051-38). mAb were flowed to saturate the surface, then C7, human, rat or mouse, diluted in EP-HBS (10 mM HEPES, pH 7.4, 150 mM NaCl, 0.005% surfactant P20) in the range 0 to 68 nM, flowed over the immobilized mAb. For kinetic analysis the flow rate was maintained at 30 μl/min, and data were collected at 25°C. Data from a reference cell were subtracted to control for bulk refractive index changes. The Rmax was kept low and the flow rate high to eliminate mass transfer. All reagents used were of high purity and polished by size exclusion chromatography immediately before use to ensure removal of any aggregates. Data were evaluated using Biacore Evaluation Software (GE Healthcare).

In Vivo Testing of mAbs

To test *in vivo* mAb that blocked mouse complement in hemolysis assays, wild type (WT) mice (C57BL/6J, bred in house) were administered mAb by IP injection (1 mg in PBS, 40 mg/kg dose); controls included the blocking anti-mouse C5 mAb BB5.1 at the same dose. Blood was collected before mAb administration and at intervals up to 48 h after for measurement of hemolytic activity.

To test mAb that blocked human complement in hemolysis assays, C7 deficient mice (homozygous C57BL/6NJ-C7$^{em1(IMPC)J}$/Mmjax, bred in house, n= 10) were injected intraperitoneally (IP) with human C7 (500 μg), then split into test and control groups (5 in each). One hour later, test group animals were injected subcutaneously (SC) with blocking mAb (1 mg in PBS, 40 mg/kg dose), while control group mice were injected with an

irrelevant mAb at the same dose; blood was collected from all the animals just before the experiment, 1 h after C7 administration (immediately before giving the mAb) and at intervals after mAb injection up to 48 h for measurement of hemolytic activity.

To test mAb that blocked rat complement in hemolysis assays, Lewis rats (100–150 g; Charles River Laboratories, Edinburgh, UK) were injected IP with 10, 20 or 40 mg/kg dose of mAb (2 per group); blood was collected from all the animals just before the experiment, and at intervals post-injection over a time course of 7 days for measurement of hemolytic activity.

Testing mAb in an Experimental Autoimmune Myasthenia Gravis (EAMG) Rat Model

A rat complement-blocking mAb was tested in the rat EAMG model. Lewis rats (100–150 g) were injected IP with anti-Acetylcholine receptor (AChR) mAb35 at 1 mg/kg in PBS as described previously (16–18). mAb35 binds the main immunogenic region of AChR, activating complement and damaging the neuromuscular junction endplates, causing severe damage to motor function. Animals were assessed hourly post-disease initiation as described previously. Clinical symptoms were assigned based on a standardized scale 0 to 5: 0, no disease; 1, reduced grip strength in front legs (can grip cage lid but cannot lift) and floppy tail; 2, loss of grip in front legs; 3, loss of grip and hind limb weakness and wasting; 4, loss of grip and hind limb paralysis; 5, moribund. mAb35-injected rats were split into two groups (n= 5 each), the test group received blocking mAb at 10 mg/kg SC (determined in the dosing experiment) at time zero, the control group received an irrelevant isotype control antibody (D1.3) at the same times, routes and doses. Blood was taken at intervals for hemolysis assays; all animals were sacrificed at 48 h post-induction.

Soleus muscles were harvested and frozen in OCT mounting medium for sectioning as described previously (16–18). Sections were fixed in ice-cold acetone for 15 min at −80°C and then blocked for 30 min in 10% horse serum/2% BSA. After washing in PBS, sections were stained overnight at 4°C with primary antibodies, C3/30 anti-C3b/iC3b mAb (in house) at 10 μg/ml, and rabbit anti-rat C9/MAC polyclonal IgG (in house) at 50 μg/ml, both in the block buffer. Anti-C3b/iC3b sections were washed and incubated for 15 min at RT with amplifier antibody goat anti-mouse (VectaFluor DyLight 488, # DK-2488; Vector Labs, Peterborough, UK). After washing, secondary antibody, horse anti-goat IgG–Alexa Fluor 488 (DyLight 488, # DK2488) for C3b/iC3b or goat anti-rabbit-FITC (#45002; Oxford Biomedical Research, Rochester Hills, MI, USA) for anti-C9/MAC were added as appropriate, together with α-bungarotoxin-TRITC (BtX) (labels AChR; Boitum, # 00012) at 0.5% and Hoechst stain 1: 10 000 dilution (# 62249; ThermoFisher), then incubated 40 min at RT in the dark. Sections were washed in PBS and mounted in VectorShield Vibrance (#H-1700-2; Vector Labs) before analysis using an Apotome fluorescence microscope (Zeiss Apotome Axio Observer microscope, Carl Zeiss Microscopy, Cambridge, UK). Ten fields were captured from comparable regions of muscle in each sample at the same exposure and magnification (×20) and the number of BuTx-reactive endplates in each section was measured using density slicing in an image analysis system (ImageJ, University of Wisconsin-Maddison, Maddison, WI, USA). For co-localization of complement activation products, sections were additionally imaged on a Zeiss confocal microscope (Zeiss LSM800 confocal laser scanning microscope).

Statistical Analysis

All statistical analyses were performed using GraphPad Prism software (v. 5.0, San Diego, California). Statistical significance between two groups was obtained using the unpaired t-test and for multiple groups using one-way ANOVA after testing for normality. For all analyses, $p<0.05$ was considered significant. Error bars in all figures represent mean ± standard error of triplicates (unless otherwise stated. The SPR analysis was performed in an automated manner using T200 Biacore Evaluation Software version 2 (GE Healthcare).

RESULTS

The Novel Blocking mAb Work Across Species and Block Hemolysis by Binding C7 and/or the C5b-7 Complex

In total, 15 fusions were performed; ~15,000 hybridoma clones were generated and screened, 7 confirmed to be inhibitory, and five of these, 2H2 (IgG2b, κ), 3B11 (IgM, κ), 17E7 (IgG2a, κ), 59E7 (IgG2b, κ), and 73D1 (IgG2a, κ), chosen for full characterization based upon the capacity of clone supernatants to cause inhibition of CP hemolysis of ShEA by NHS, NRS or NMS. All selected mAbs except mAb 17E7 were generated in C7 KO mice; 17E7 was produced in a WT mouse. All mAbs except 3B11 were purified using protein G chromatography, mAb 3B11, an IgM mAb, was purified using ammonium sulphate precipitation. The purified mAbs were tested in hemolysis assays with different species sera (**Figures 1A–D**). Anti-C5 blocking mAbs were used as positive controls; commercial mAbs eculizumab and crovalimab for NHS, BB5.1 for NMS and in house mAb 7D4 for NRS (18, 19). As expected from the selection process, each of the selected mAbs efficiently inhibited CP hemolysis in one or more species sera; In NHS, mAbs 17E7, 59E7, 3B11 and 73D1 all inhibited in that order of efficiency; 2H2 inhibited weakly (**Figure 1A**). In NMkS 59E7, 73D1, and 17E7 inhibited in that order of efficiency; no inhibition was observed with 2H2 (**Figure 1D**). In NRS, 2H2 was an exceptionally strong inhibitor, at least ten-fold better than other mAbs in the assay; 73D1 and 3B11 also inhibited NRS in that order of efficiency, but 17E7, 59E7, and the commercial anti-human C5 mAb had no inhibitory activity in NRS (**Figure 1B**). In NMS, mAbs 73D1, 2H2, and 3B11 inhibited in that order of efficiency, but 17E7, 59E7, and the C5-blocking controls 7D4 and eculizumab had no inhibitory activity in NMS (**Figure 1C**). The 73D1 inhibition profile closely matched that of BB5.1, the blocking anti-C5 mAb used as positive control in this assay; crovalimab also inhibited NMS as previously reported (**Figure 1C**) (19). None of the new

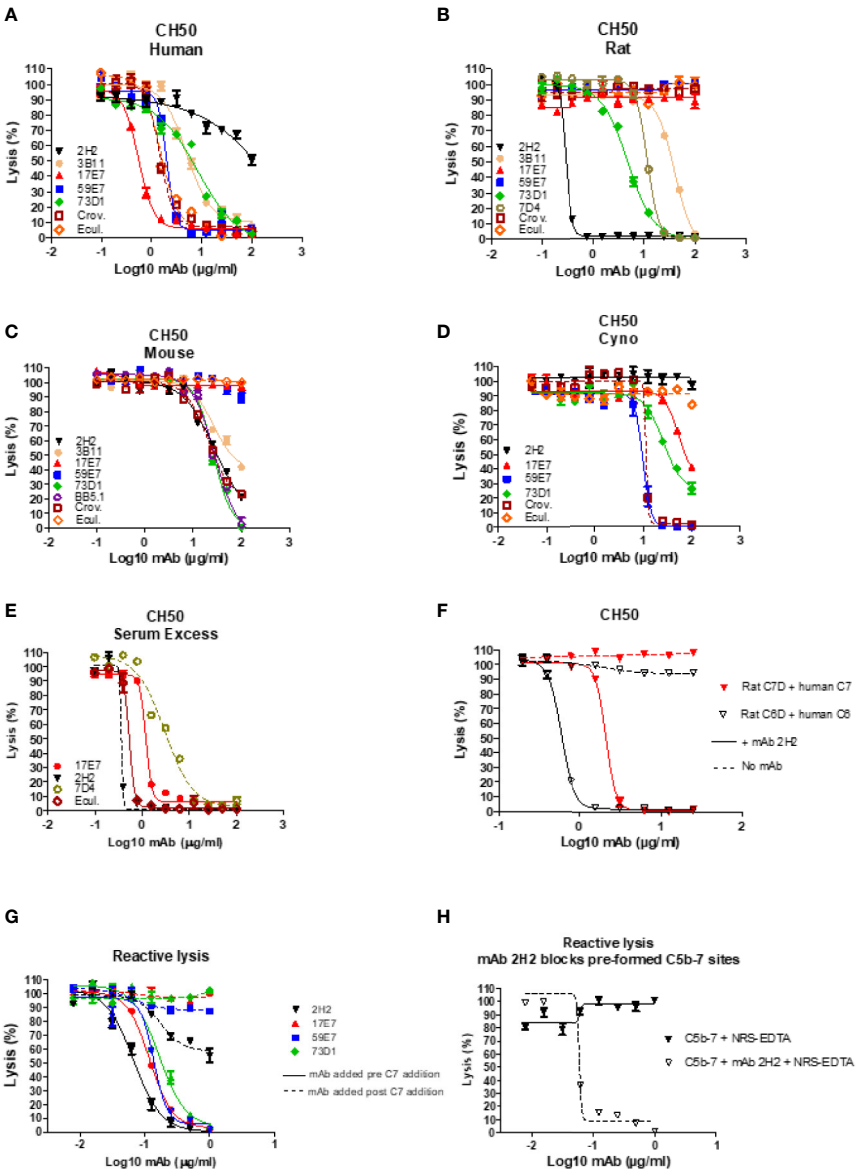

FIGURE 1 | Functional assays of C7-blocking mAbs. **(A–D)** Anti-C7 mAb were tested for blocking activity in classical pathway (CP) hemolysis (CH50) assays across species. Sera tested were human **(A)**, rat **(B)**, mouse **(C)** and cynomolgus monkey (Cyno) **(D)**. Anti-C5 mAb crovalimab (Crov), eculizumab (Ecul), BB5.1 and 7D4 were used as comparators. Test and control mAb were titrated in range 0–100 µg/ml. **(E)** Serum excess assay using NHS or NRS concentration 10-fold that used in the standard CP assay; solid lines are NHS, dashed lines are NRS. **(F)** human C6D and C7D were reconstituted with purified human C6 or C7 (dashed lines) respectively and the capacity of mAb 2H2 to inhibit hemolysis tested. **(G, H)** Reactive lysis assays using guinea pig erythrocytes (GpE) as target; for mAb 17E7, 59E7, and 73D1, purified human complement proteins (C5b6, C7, C8 and C9) were used; for mAb 2H2 and 73D1 human C5b6 and rat C7 were used with normal rat serum (NRS) as the source of rodent C8 and C9. The mAb were either added to GpE-C5b6 before or after C7 addition **(G)**; solid and dotted line respectively. mAb 2H2 was added to washed GPE- C5b-$7_{(rat)}$ prior to addition of NRS as source of C8 and C9 **(H)**. All experiments were repeated three times with the same results. The error bars are standard errors of triplicates.

mAb inhibited in NRbS (negative data not shown). The cross-species inhibitory activities of the mAbs are summarized in **Table 1;** the calculated 50% complement inhibitory doses and hemolytic units (HU) of all mAbs in the different sera are shown. Serum excess assays (25% serum;10-fold serum dose compared to titration assays above) were used to test mAb 17E7 and 2H2 in conditions that better reflect those prevailing in whole blood (**Figures 1E, F**), confirming that these mAbs are efficient complement inhibitors in human and rat serum respectively.

To identify the precise mechanism of complement inhibition by the novel mAbs, reactive lysis assays were used. GPE were first incubated with C5b6; blocking mAbs (17E7, 59E7, 73D1, 2H2) at

TABLE 1 | Summary of novel anti-C7 and control anti-C5 blocking mAb tested.

Antibody	Isotype	Species	Hemolytic Units (HU)	50% Inhibitory Dose (ng/ml)	Reactivity
mAb anti-C7					
17E7	IgG2a,κ	Human	55.1	181.6	Strong
		Monkey	1.9	530.3	Strong
59E7	IgG2b,κ	Human	47.7	209.7	Strong
		Monkey	10.1	98.7	Strong
3B11	IgM,κ	Human	19.9	501.9	Strong
		Rat	11.9	839.5	Moderate
2H2	IgG2b,κ	Human	1.0	9977.0	Weak
		Rat	264.8	33.9	Strong
		Mouse	2.7	3715.4	Weak
73D1	IgG2a,κ	Human	17.2	581.8	Strong
		Monkey	3.8	261.1	Strong
		Rat	19.8	505.5	Strong
		Mouse	13.9	720.3	Strong
mAb anti-C5 controls					
7D4	IgG2b,κ	Human	69.3	144.2	Strong
		Rat	9.5	1054.4	Moderate
BB5.1	IgG1,κ	Mouse	16.3	613.6	Strong
Crovalimab	IgG1,κ	Human	49.9	212.3	Strong
		Monkey	8.6	115.5	Strong
		Mouse	1.4	1862.1	Weak
Eculizumab	IgG2/4,κ	Human	47.1	181.6	Strong

Inhibitory dose: <750, strong; 750–1500, moderate; >1500, weak.

various doses (0–1 μg/ml) added either before or after C7 addition, followed by C8, C9. All mAb except 2H2 were tested with purified human proteins; for mAb 2H2, purified rat C7 and EDTA-NRS as a source of rat C8 and C9 were used with human C5b6. All the 22 tested mAbs showed strong inhibition when added to GPE-C5b6 before C7 was added. When added after C7, mAb 17E7, 59E7, and 73D1 all showed no inhibition of lysis (**Figure 1G**). To further test the mode of inhibition of mAb 17E7 the mAb was either pre-incubated with C7 prior to addition to GPE-C5b6 or added simultaneously with C7; inhibition of lysis was essentially the same with or without the pre-incubation step, suggesting that the mAb efficiently captures fluid-phase C7 to prevent formation of an active C5b-7 complex (data not shown).

In contrast to the other mAb, the rat-selective mAb 2H2 caused a dose-dependent inhibition of lysis even when added to pre-formed GPE-C5b-7, implying that this mAb had a distinct mechanism of inhibition compared to the other mAb, working at least in part by binding and blocking C5b-7 thus preventing C8 binding to the complex (**Figure 1H**). When tested in a reactive lysis system using human C5b6, rat C7 and either human C8/C9 or NRS as a source of C8/C9, mAb 22H2 effectively blocked lysis when incubated with pre-formed GPE-C5b-$7_{(rat)}$ and washed to remove free mAb prior to addition of either human C8/C9 or NRS, confirming the findings with human C7 above and demonstrating that the species source of C8/C9 (human or rat) did not impact the effect (**Figure 1H**). To further test species specificity of mAb 2H2, rat C6D was reconstituted with human C6 and rat C7D with human C7; in each case, 2H2 strongly inhibited lysis in a dose-dependent manner, implying that this mAb is selective for the C5b-7 complex (**Figure 1F**).

The Novel mAbs Bind Native C7 and C7 in the TCC Complex in Serum

The direct ELISA showed that all the selected new mAbs recognized human C7; mAb 2H2, 3B11, and 73D1 also bound rat C7, while mAb 73D1 bound mouse C7. mAb 17E7 and 73D1 were strongly cross-reactive with non-human primate (cynomolgus) C7 (**Figure 2A; Table 1**). In competitive sandwich ELISA, C7 was not detected with any mAb pair suggesting that they compete for similar epitopes on C7; all mAb worked in sandwich ELISA with goat anti-C7 as either capture or detect (**Figure 2B**). mAb 2H2 when used as capture and goat anti-C7 as detection also detected rat C7, demonstrating that the mAb recognizes C7 from both species.

WB was used to confirm binding of mAbs to C7. The human-specific mAb 59E7 and 17E7 detected C7 in human and cynomolgus monkey serum under NR conditions (**Figure 3A**); these mAb did not detect C7 in other species sera, confirming the ELISA results above. The species cross-reactive mAb 73D1 and 3B11 specifically detected C7 in human, rat, mouse and cynomolgus monkey sera under NR conditions (**Figures 3B, C**). None of the mAb detected C7 in sera under R conditions (negative data not shown). mAb 2H2 did not bind the human C7 standard, detected by all other mAbs; it did weakly detect C7 in all sera tested under NR conditions but also identified multiple high molecular weight bands in the MW range 160 to 260 kDa that may represent C7 aggregates or terminal pathway complexes in serum (**Figure 3D**). To further explore the nature of these, pull-down assay from rat or human serum activated with zymosan and aggregated IgG in the presence of biotinylated 2H2 was performed; remarkably, mAb 2H2 pulled down all the terminal pathway proteins from both rat and human serum, indicating that it bound the fluid phase TCC when present during activation (**Figures 3F, G**). Pull-downs from activated human serum performed as above but using biotinylated mAb 17E7, 59E7, and 73D1, showed that each of the antibodies also pulled down all the terminal pathway proteins C5b–C9, demonstrating capacity of each of these mAbs to bind C7 in the forming TCC (**Figures 3H–J**).

Binding of the novel mAbs to TCC when present during serum activation was confirmed in sandwich ELISA on pull-downs from rat or human serum using the mAbs as above. All terminal pathway proteins: C5b, C6, C7, C8, and C9 were detected in the pull-downs; the strongest signals were observed with C5b, C6, and C7 proteins (**Figure 2D**). All the new mAb also bound the pre-formed TCC (captured on aE11 anti-C9 neospecific antibody) in activated human serum, giving signals at similar levels to the positive control E2 anti-C8 antibody, confirming that they bind C7 in the pre-formed TCC (**Figure 2C**). The aE11 mAb also captured TCC from activated rat serum and this was detected using the rat C7-reactive mAb 2H2 (**Figure 2C**). Taken together, the data show that each of the mAb recognize C7 in the TCC both when present in the fluid phase during TCC generation, and when added post-activation to the preformed complex.

SPR analysis on immobilized antibody with human or rat C7 flowed over confirmed binding of the novel mAbs to human and/or rat C7. The measured kinetics/affinity are summarized in

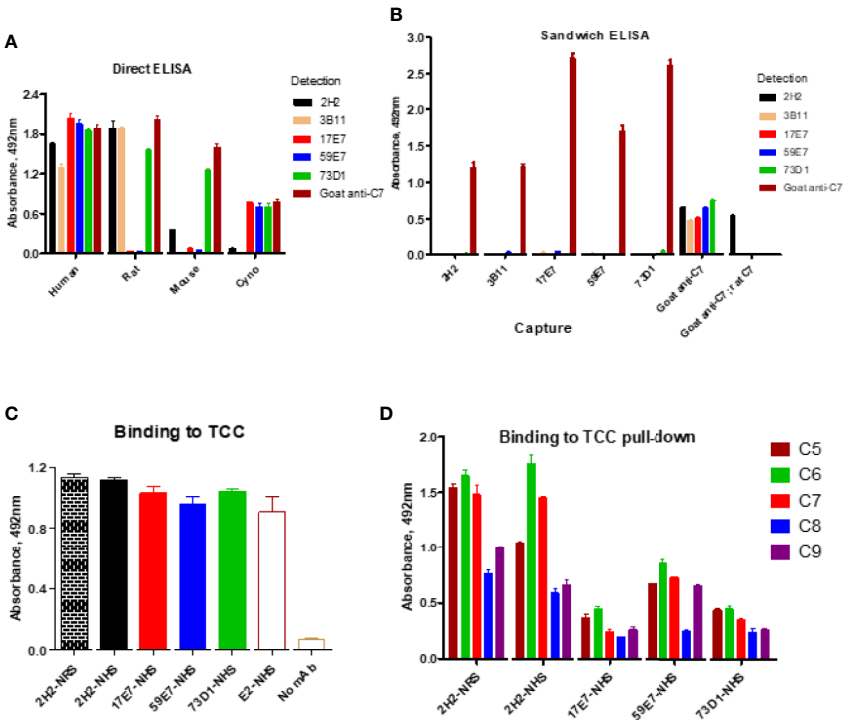

FIGURE 2 | Direct and sandwich ELISA to determine mAb binding to human, monkey, rat and mouse C7. **(A)** Direct ELISA: plates were coated with human, monkey (cyno), rat or mouse C7; mAbs were tested in a dilution series (0–10 μg/ml). The graph shows representative binding with the 10 μg/ml capture. **(B)** Sandwich ELISA: the new mAbs were paired as capture and detect with human C7 used in a dilution series (0–5 μg/ml). The graph shows representative binding with 5 μg/ml C7. As a positive control, polyclonal anti-C7 (goat anti-C7) was used as capture with each of the mAb as detect; rat C7 captured on goat anti-C7 (goat anti-C7; rat C7) was also tested with the mAb as detect. **(C)** Sandwich ELISA to detect pre-formed TCC in activated NHS; TCC in activated NHS (and NRS for 2H2) was captured on aE11 anti-C9 and the novel mAbs and the positive control E2 anti-C8 mAb used to detect the TCC complex captured. **(D)** TCC complexes generated in NHS (or NRS for 2H2) in the presence of each of the new mAb (biotinylated) were captured on avidin-coated plates, then polyclonal antibodies against each of the terminal complement proteins used to test the presence of the respective components in the complex. The error bars are standard errors of triplicates. All experiments were repeated three times with the same results.

Table 2. The mAb 17E7 and 59E7 showed very strong binding to human C7 in SPR analyses (KD = 1.02×10^{-9}, 9.31×10^{-10} respectively) (**Figure 3K**) with negligible off rates, suggesting that 17E7 and 59E7 are promising candidates for human therapeutics. Binding of mAb 3B11 and 73D1 to human or rat C7 was relatively weak (human KD = 2.30×10^{-7} and 5.55×10^{-8}; rat KD =1.93×10^{-7} and 8.17×10^{-8}) (**Supplementary Figure 1**); however, both these mAb showed a slow off rate for rat C7 offering promise for use *in vivo*. Additionally, mAb 73D1 showed strong binding to mouse C7 (KD = 2.31×10^{-9}) with a very slow off rate, promising for testing in mouse models. Analysis by SPR of immobilized 2H2 showed no measurable binding to native human, rat or mouse C7 in multiple analyses (negative data not shown).

The Novel mAbs Are Efficient Complement Inhibitors *In Vivo*

The capacity of mAbs to inhibit complement *in vivo* was tested in mice and rats. To test the capacity of the anti-mouse C7 mAb 73D1 to inhibit complement *in vivo*, WT mice were administered 73D1 (or BB5.1 anti-mouse C5 as positive control) IP and complement activity in serum was tested at intervals over a time course of 48 h. Complement was inhibited by both mAb over the full course of the experiment up to end-point at 48 h (**Figure 4A**). To test the capacity of the anti-human C7 mAb 17E7 to inhibit C7 *in vivo*, mAb was administered to C7-deficient mice reconstituted with human C7. Human C7 effectively restored hemolytic activity in the mice, and administration of mAb 17E7 efficiently inhibited hemolytic activity in the mice (>70% inhibited at 3 h post-administration) compared to irrelevant antibody, demonstrating that the mAb blocked human C7 *in vivo* (**Figure 4B**). The rat-selective mAb 2H2 was tested for complement inhibition in rats to determine dose requirement and antibody half-life. Rats were injected with mAb 2H2 at 10, 20, and 40 mg/kg and blood collected at intervals for testing hemolytic activity. Even at the lowest dose, the mAb was an effective inhibitor, blocking complement activity for >48 h, and at the highest dose blocked complement for at least a week (**Figure 4C**). The 10-mg/kg dose was used for the EAMG experiment described below.

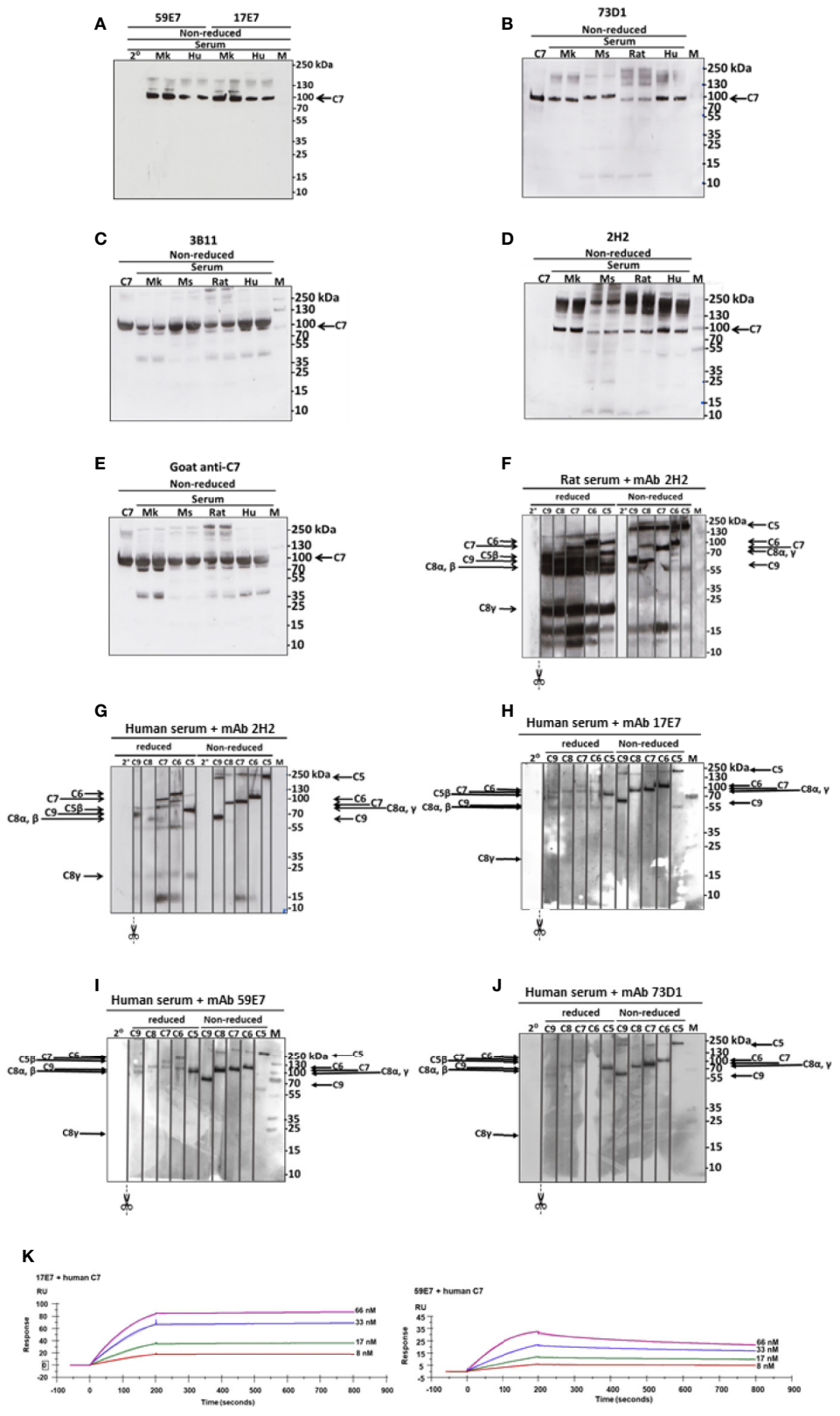

FIGURE 3 | Continued

FIGURE 3 | Western blotting to detect C7 binding in serum and in TCC. **(A)** The human-specific mAbs 59E7 and 17E7 were used to probe WB of NHS (Hu) and Cynomolgus monkey (Mk) serum under non-reducing (NR) conditions. Secondary only control was included (2°). **(B–E)** The cross-species reactive mAbs 73D1 **(B)**, 3B11 **(C)** and 2H2 **(D)** and as control the polyclonal goat anti-C7 **(E)** were used to probe WB of NHS (Hu), monkey (Mk), mouse (Mo) and rat sera; purified human C7 was used as standard. All sera were run in duplicate. Polyclon3B11 **(C)**, 2H2 **(D)**, and positive control goat anti-C7 **(E)**. Results are representative of three independent experiments. M; protein molecular weight marker. **(F–J)** The novel mAbs were used to pull down complexes from activated serum; these were then run on WB under non-reduced and reduced conditions and probed with polyclonal antibodies against each of the terminal complement proteins. mAb 2H2 was used in rat **(F)** and human **(G)** serum; the other mAbs in human serum only **(H–J)**. The blots were cut into strips prior to probing to detect the individual terminal pathway proteins. Molecular weights used were: NR: C5, 190 kDa; C6, 105 kDa; C7, 95 kDa, C8αγ; 70 kDa; C9, 65 kDa. R: C6, 110 kDa; C7, 95 kDa; C5β, 75 kDa; C9, 70 kDa; C8α/β, 65 kDa; C8γ, 22 kDa. Results are representative of at least three analyses. M; protein molecular weight marker, 2°; secondary antibody. **(K)** The novel mAbs 17E7, 59E7 and 73D1 were separately immobilized on mouse IgG capture sensor chips (GE Healthcare, # BR-1008-38) and mAb 3B11 (IgM) on protein L Series S sensor chip (GE Healthcare #29-2051-38) at approximately 60 RU. Human, rat or mouse C7 was flowed in HEPES-buffered saline (HBS) in a dilution range of 66 to 8 nM and interactions with the immobilized mAbs were analyzed. Sensorgrams were collected and KDs were calculated using the Langmuir 1: 1 binding model with RI values set to zero. Representative sensorgrams for 17E7 and 59E7 binding of human C7 are shown with raw data in colored lines and fitted data in dotted line (average of 3); all binding data and analyses are included in **Table 2**. The sensorgrams of clones 3B11 and 73D1 are included in Supplementary. The SPR analysis was performed in an automated manner using T200 Biacore Evaluation Software version 2 (GE Healthcare).

TABLE 2 | SPR analysis of the binding of C7 to the immobilized mAb.

Antibody	KD (M)	Ka (1/Ms)	Kd (1/s)
17E7	Human; 1.02×10^{-9}	6.83×10^{4}	6.94×10^{-5}
59E7	Human; 9.31×10^{-10}	1.45×10^{6}	1.4×10^{-3}
3B11 (protein L captured)	Human; 2.30×10^{-7}	5.05×10^{3}	1.20×10^{-3}
	Rat; 1.93×10^{-7}	2.91×10^{3}	5.61×10^{-4}
73D1	Human; 5.55×10^{-8}	2.63×10^{4}	1.5×10^{-3}
	Rat; 8.17×10^{-8}	6.98×10^{3}	5.70×10^{-4}
	Mouse; 2.31×10^{-9}	1.02×10^{5}	2.36×10^{-4}

The Rat-Selective mAb 2H2 Prevents Clinical Disease and Pathology in a Myasthenia Model

EAMG was passively induced in rats; at the time of disease induction, the rat-selective mAb 2H2 or isotype control (10 mg/kg; 5 per group) was administered SC. As expected, all isotype control treated rats began to lose weight and show symptoms, comprising limp tails, piloerection, hind limb weakness and reduced grip strength within 24 h; all had a clinical score of 4 by endpoint (**Figures 4D, E**). (15–17) In contrast, animals given mAb 2H2 subcutaneously at the time of disease induction continued to gain weight over the time course of the experiment and did not develop detectable weakness or other clinical manifestations for the duration of the experiment (**Figures 4D, E**). Animals were sacrificed by a Schedule 1 method when weight loss was equal to or exceeded 20% of original bodyweight, when clinical score reached 4, or at the 48 h endpoint. CP hemolytic activity in serum was absent in the 2H2-treated group throughout the experiment (**Figure 4F**). As expected, serum from the untreated control animals retained full hemolytic activity across the time course. Soleus muscles were harvested at sacrifice, stained with α-Bungarotoxin-TRITC and receptor numbers quantified. The number of endplates in isotype control treated animals was significantly lower than in mAb 2H2-treated animals (~three-fold less; $P < 0.0001$, **Figure 4G**); endplate numbers in the 2H2-treated rat were comparable to numbers in naïve animals (data not shown). Endplates in muscles from the EAMG group were frequently fragmented, whereas most endplates in the 2H2-treated group were intact and linear, as in naïve animals. There was no significant difference in C3 fragment staining between the 2H2-treated and isotype control-treated animals ($P = 0.9792$, **Figure 4H**); however, the intensity of C9/MAC staining was reduced more than threefold in the 2H2-treated group ($P = 0.0011$, **Figure 4I**). Confocal analysis demonstrated co-localization of C3b/iC3b and C9/MAC deposition at the endplate in isotype control animals at 48 h (**Figure 4J**); in 2H2-treated animals, C3b/iC3b was deposited to a similar degree at endplates but C9/MAC deposition was weak or absent (**Figure 4K**).

DISCUSSION

The pathological role of complement in diverse diseases has been apparent for more than 50 years (20–23). Despite this long history, to date the use of anti-complement drugs has been restricted to a handful of rare diseases, including hemolytic disorders such as PNH and renal diseases, notably aHUS, where they have had a transformational impact (1–3). Eculizumab was first approved for treatment of PNH thirteen years ago, but only very recently have new anti-complement drugs reached the market and disease targets remain restricted to rare conditions (1). Recent reports provide irrefutable evidence that complement drives pathology in more common diseases including multiple sclerosis, NMOSD and AMD (24–26); however, because of the cost and route of administration, use of eculizumab in these diseases is not feasible; more affordable and effective drugs are needed. Complement proteins are abundant in plasma (~5% of total plasma protein), and the majority are acute phase reactants, increasing synthesis and plasma concentration in response to infection. This is a particular issue for C5 blockade; breakthrough hemolysis is a recognized complication in patients on eculizumab, likely because even a tiny amount of free C5 (<0.1%) is sufficient to restore hemolytic activity (27–29). These issues led us to consider other targets in the terminal pathway; we focused on C7 for four reasons: i). Plasma concentrations of C7 are lower than those of C5 (~2-fold lower molar concentration); ii). Unlike the other terminal pathway components, C7 is not synthesized by hepatocytes and is not an acute phase reactant, hence levels of C7 are stable in acute phase conditions (30); iii). Blocking C7 is likely to be less of an infection hazard compared to C5 blockade because C5a-mediated neutrophil recruitment is unimpaired - indeed, the majority of patients with C7 deficiency are healthy, although at increased risk of Neisserial infections (31); iv).

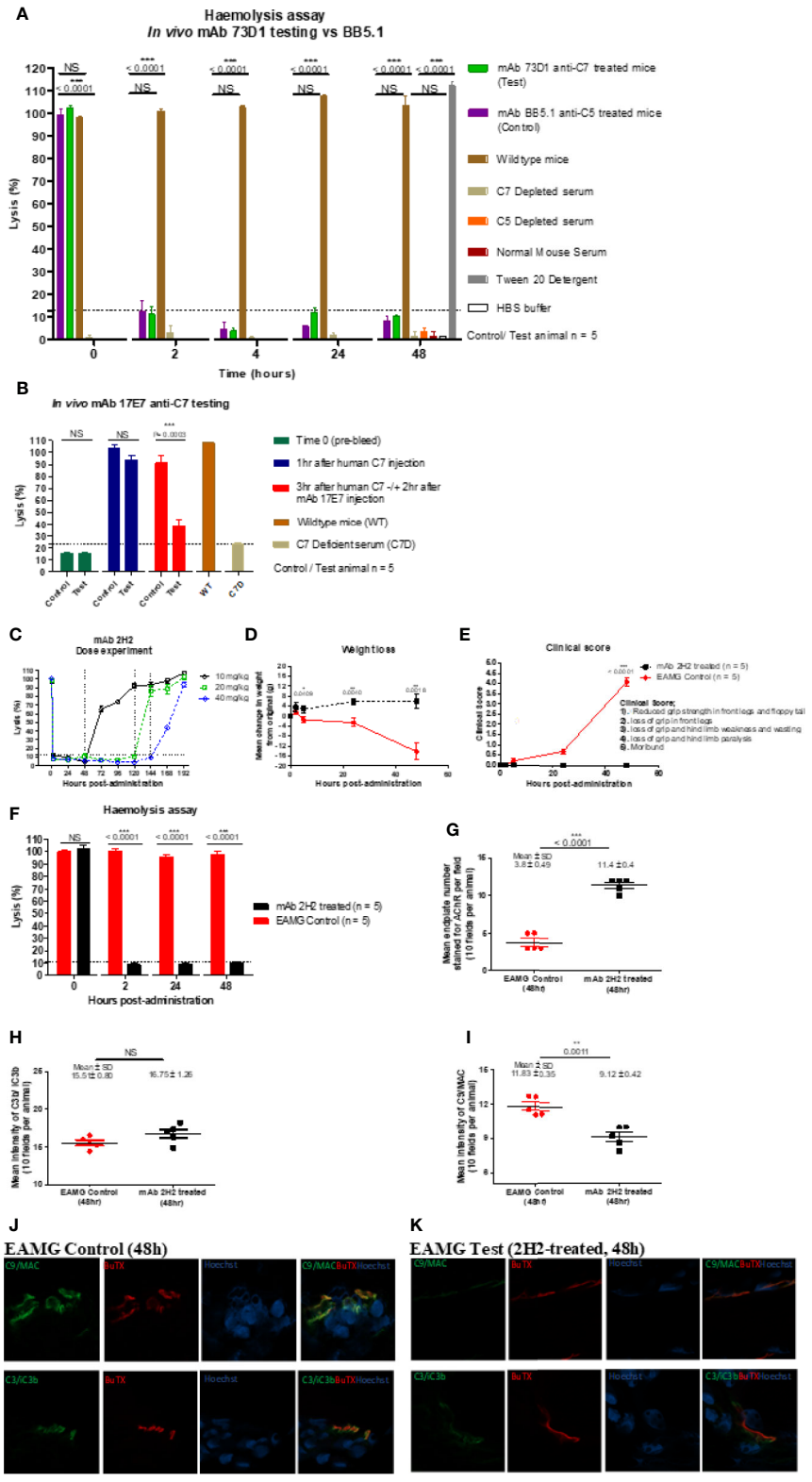

FIGURE 4 | Continued

FIGURE 4 | Testing anti-C7 mAbs *in vivo*. **(A)** mAb 73D1 or BB5.1 anti-mouse C5 as positive control was administered IP at a dose of 1 mg/kg to female wildtype mice (n=5 per group); blood was sampled at intervals serum obtained and added to human C7D or C5D serum respectively prior to measuring CP hemolytic activity measured. Controls included C7D and C5D human sera at the same dose, NMS to demonstrate the requirement for human depleted sera and 1% Tween-20 and HBS to set 100% and 0% lysis in the assay. Significance of differences between groups was determined by one-way ANOVA; significant differences and p values are shown in the figure. Error bars are standard errors of triplicates. **(B)** C7-deficient mice (10 females) were reconstituted with human C7 (500µg; IP), then split into test and control groups (5 in each). After 1 h, test and control animals were injected subcutaneously (SC) with 17E7 mAb or irrelevant isotype control mAb (1 mg) respectively. Blood was collected prior to administration of C7, immediately prior to administration of mAb and 3 h after mAb administration. Hemolytic activity was measured as above. Significance of differences between groups was determined using an unpaired t test; significant differences and p values are shown in the figure. Error bars are standard errors of triplicates. **(C)** Female Lewis rats were divided into three groups (n = 2 each) and injected intraperitoneally with mAb 2H2 at doses of 10, 20, and 40 mg/kg; blood was collected from all the animals just before mAb administration, 2 h after mAb 2H2 administration, and then every 12 h over 1 week. Sera prepared and hemolytic activity tested in standard CP assays. Significance of differences between groups was determined using an unpaired t test; significant differences and p values are shown in the figure. Error bars are standard errors of triplicates. **(D–F)** EAMG was induced in rats (5 per group) and either mAb 2H2 or isotype control mAb(10mg/kg) administered at induction. Weight loss **(D)** and clinical score **(E)** were measured at intervals; mice were bled at 0, 2, 24, and 48 h, serum harvested and hemolytic activity measured **(F)**. All animals were killed at 48 h. Results are means of five in each group and vertical bars represent SD. Significance of differences between groups was determined using an unpaired *t* test except panel E where paired t test was used; significant differences and p values are shown in the figures. **(G–K).** Soleus muscles were harvested at time of sacrifice (48 h) and snap frozen in OCT. Sections (10 µm) were stained for AChR with TRITC-conjugated a-BuTX; AChR-positive endplates were counted in 10 fields from each animal using ImageJ software. **(G)**. Sections were stained for C3b/iC3b **(H)** and C9/MAC **(I)** and staining quantified as above. Tissue sections from isotype control **(J)** or 2H2 **(K)** treated animals were double-stained for AChR together with anti-C3b/iC3b (top panel) or C9/MAC (bottom panel) and imaged on a Zeiss confocal microscope. The scale bar shown is 10 µm; all images were captured at identical magnification. Statistical significance was obtained by unpaired t-test and $P < 0.05$ was considered significant; significant differences and p values, mean and SD are shown in the figures.

C7 has been neglected as a therapeutic target, in contrast to C5 where numerous Pharma companies are developing blocking mAb or other drugs.

To identify clones secreting blocking anti-C7 mAbs early in clone screening we used a high-throughput hemolysis assay; notably, C7-blocking mAb were rare events, only 7 inhibitory clones identified from 15,000 screened clones over 15 separate fusions. Although we did not test for non-blocking anti-C7 mAbs in all fusions, this was done in early fusions and C7-binding activity was detected in ~5% of clones screened. This contrasts markedly with our experience with C5 where ~10% of the anti-C5 mAb generated were strong function blockers (17). The mAb described here bound C7 in ELISA (**Figure 2A**) and inhibited lysis of ShEA in CP assays (**Figure 1**) with mAb 17E7 and 59E7 being the most efficient for human serum; these mAb gave similar inhibition profiles to the currently available therapeutic anti-C5 mAb eculizumab and crovalimab. The mAb were generated in C7-deficient mice and several showed strong cross-species activity. The mAb 2H2 was most effective for rat serum and 73D1 for mouse serum; mAb 3B11 efficiently inhibited both human and rat serum (**Table 1**). Inhibition by 17E7 and 2H2 was confirmed in a modified CP assay using near-physiological serum concentrations. The *in vitro* inhibition data was confirmed *in vivo* for the mouse C7-blocking mAb 73D1, and for the human C7-specific mAb 17E7, the latter tested in C7-deficient mice administered human C7. Mouse serum inhibition by 73D1 was equivalent to the anti-C5 blocker BB5.1 (**Figure 4A**), widely used in animal models (19) and catalyzing the enthusiasm for anti-C5 therapeutics; the efficient inhibition of mouse complement by mAb 73D1 make it a valuable tool for animal studies targeting MAC specifically without interfering with C5a generation.

Both of the human C7-specific mAbs, 17E7 and 59E7, showed strong and stable binding to human C7 in SPR ($KD = 1.02 \times 10^{-9}$, 9.31×10^{-10}, respectively; **Table 2**). Strong binding of mAb 73D1 to mouse C7 was also confirmed by SPR analysis ($KD = 2.31 \times 10^{-9}$, **Table 2**). Epitope specificity was tested in ELISA; surprisingly, all of the antibodies reactive with a given species C7 gave no signal when used as a pair in sandwich ELISA, showing that they bound the same or overlapping epitopes on C7 (**Figure 2B**). All the mAb worked as detect or capture in sandwich ELISA in conjunction with a polyclonal anti-C7, demonstrating that all bound C7 in this context. These observations suggest that there is a dominant epitope or surface of the C7 molecule that is critical for function and the target for all selected mAb. We plan structural studies to identify this epitope as we recently described for the anti-C5 mAb BB5.1 (19).

The mAb 2H2 stood out from the other mAb generated; this rat-selective mAb was a highly efficient complement inhibitor *in vitro* inhibiting at a dose at least 10-fold lower than the other in-house blocking mAb; at this dose, C7 is in ~10-fold molar excess compared to the mAb. Although 2H2 recognized C7 protein immobilized on plastic in direct ELISA, when tested in SPR immobilized on the chip surface, this mAb did not capture either human or rat C7 flowed over the surface. *In vivo*, this mAb completely blocked serum lytic activity at a quarter of the dose routinely used in rodent models (10 mg/kg versus 40 mg/kg body weight) for other terminal pathway inhibitory mAb, including BB5.1, the in-house anti-rat C5 4G2, and the 73D1 anti-C7 mAb (18, 19). When administered at the standard dose, 2H2 effectively blocked complement for at least seven days in rats, compared to 48 h for the other mAb at the same dose. Rats treated with the lowest dose of mAb 2H2 showed complete loss of hemolytic activity and were protected from disease compared to controls in the EAMG model; treated rats did not lose weight or develop paralysis, endplates were protected from damage and MAC deposition at endplates was markedly reduced (**Figures 4D–K**).

Taken together, the above data demonstrating that mAb 2H2 binds denatured but not native C7 and blocks hemolytic activity *in vitro* and *in vivo* at much lower concentrations than other blocking mAb and when C7 is in molar excess, suggested that 2H2 has a different mechanism of action to the other blocking mAb. We reasoned that it might inhibit by binding the transient

C5b-7 complex. To test this, we used reactive lysis assays; all the blocking mAb, including 2H2, inhibited lysis when added to C5b6-bearing cells prior to addition of C7, indicating that they either prevented binding of C7 to C5b6 or its unfolding to reveal C8-binding sites. When the blocking mAb were added to preformed C5b-7 cells, only 2H2 inhibited suggesting that it additionally bound to C5b-7 and blocked C8 binding (**Figures 1G, H**). It was not possible to test directly the impact of 2H2 on the fluid-phase C5b-7 complex in these assays because of the transience of C5b-7 membrane-binding activity; instead, we explored binding of 2H2 and the other blocking mAb to forming and formed TCC in the fluid phase. Pull-downs from rat serum activated in the presence of mAb 2H2 included all terminal pathway proteins C5b–C9, demonstrating that the mAb captures intermediates in the fluid phase while permitting binding of later components to generate a mAb-TCC complex (**Figures 3F, G**). The anti-human C7 mAb 17E7, 59E7, and 73D1, when incubated in human serum during activation as above, each pulled down all the TCC components demonstrating that they too bound C7 in the complex and did not interfere with fluid-phase TCC generation (**Figures 3H–J**). Binding of the novel mAbs to pre-formed TCC was confirmed by sandwich ELISA capturing the complex on the aE11 anti-C9 neo-specific antibody (**Figures 2C, D**).

In some respects, the mechanism of action of mAb 2H2 resembles that of the naturally occurring MAC inhibitor clusterin; this fluid phase regulator binds C5b-7, preventing membrane attachment and insertion of the complex, but allows recruitment of C8 and C9 to form the TCC (32–34). Clusterin is a weak inhibitor of hemolysis that "buffers" bystander effects. The Streptococcal inhibitor of complement (SIC) protein similarly binds fluid-phase intermediates (predominantly C5b-7) and blocks the capacity of the complex to associate with membranes (35, 36). In contrast to 2H2, neither clusterin nor SIC caused inhibition in reactive lysis when C5b-7 was already on the target surface, confirming that they only interfere with membrane binding of nascent C5b-7. The capacity of 2H2 to bind and inhibit membrane-bound C5b-7 complexes suggests a dual impact on C5b-9 assembly; these properties make mAb 2H2 a powerful MAC inhibitor, a "super-clusterin" working with much greater efficiency to inhibit MAC assembly and resultant lysis.

In summary, we have demonstrated that, with regard to blocking hemolytic activity *in vivo* and *in vitro*, targeting MAC downstream of C5 is at least as effective as targeting C5. We describe anti-C7 mAbs that are powerful blockers of human, primate, rat and mouse C7, several working across species. We describe one mAb, 2H2, that shows selectivity for the C5b-7 complex and inhibits at greatly reduced dose compared to component-specific mAbs; although this mAb is predominantly active in rat, it is proof of principle that complex-specific mAb can be generated. These have potentially great advantages over current anti-complement drugs in terms of dose, frequency of administration and infection risk; they have the potential to open up new therapeutic fields for anti-complement drugs with significantly lower cost of treatment and more suited to treatment of common, chronic diseases. Current efforts are focused on the development of 2H2-like mAb that bind and block the human C5b-7 complex.

DATA AVAILABILITY STATEMENT

The raw data supporting the conclusions of this article will be made available by the authors, without undue reservation.

ETHICS STATEMENT

The animal study was reviewed and approved by UK Home Office; license numbers: PF4167C0A and P8159A562.

AUTHOR CONTRIBUTIONS

WZ performed all the laboratory analyses and wrote the first draft of the manuscript. BPM conceived and planned the study and oversaw the data handling and manuscript preparation. All authors contributed to the article and approved the submitted version.

FUNDING

WZ was supported by a PhD Studentship from the Life Sciences Research Network Wales (LSRN), LSRN Translational Support Fund, and by a Consolidator Award supported by Wellcome Trust ISSF funding to Cardiff University. BPM is supported by the UK Dementia Research Institute Cardiff.

ACKNOWLEDGMENTS

We thank Prof. David Kanavagh for providing eculizumab and Roche Diagnostics for donating crovalimab. We acknowledge Michelle Somerville for assistance with the Zeiss confocal microscope.

SUPPLEMENTARY MATERIAL

The Supplementary Material for this article can be found online at: https://www.frontiersin.org/articles/10.3389/fimmu.2020.612402/full#supplementary-material

SUPPLEMENTARY FIGURE 1 | Binding sensorgrams of the novel mAbs to C7 protein. mAb 3B11 (IgM) was immobilized on a protein L Series S sensor chip (GE Healthcare #29-2051-38) and mAb 73D1 (IgG2a, κ) immobilized on a mouse IgG capture sensor chip (GE Healthcare, # BR-1008-38) at approximately 60 RU. Human, rat or mouse C7 was flowed in HEPES-buffered saline (HBS) in a dilution range of 66 to 4 nM (3B11) or 66 to 8 nM (73D1) and interactions with the immobilized mAbs were analyzed. Sensorgrams were collected and KDs calculated using the Langmuir 1: 1 binding model with RI values set to zero. Sensorgrams are shown with raw data in colored lines and fitted data in dotted lines (average of 3); all binding data and analyses are included in **Table 2**. The SPR analysis was performed in an automated manner using T200 Biacore Evaluation Software version 2 (GE Healthcare).

REFERENCES

1. Zelek WM, Xie L, Morgan BP, Harris CL. Compendium of current complement therapeutics. *Mol Immunol* (2019) 114:341–52. doi: 10.1016/j.molimm.2019.07.030
2. Harris CL, Pouw RB, Kavanagh D, Sun R, Ricklin D. Developments in anti-complement therapy; from disease to clinical trial. *Mol Immunol* (2018) 102:89–119. doi: 10.1016/j.molimm.2018.06.008
3. Morgan BP, Harris CL. Complement, a target for therapy in inflammatory and degenerative diseases. *Nat Rev Drug Discov* (2015) 14:857–77. doi: 10.1038/nrd4657
4. Rother RP, Rollins SA, Mojcik CF, Brodsky RA, Bell L. Discovery and development of the complement inhibitor eculizumab for the treatment of paroxysmal nocturnal hemoglobinuria. *Nat Biotechnol* (2007) 25:1256–64. doi: 10.1038/nbt1344
5. Hillmen P, Young NS, Schubert J, Brodsky RA, Socié G, Muus P, et al. The complement inhibitor eculizumab in paroxysmal nocturnal hemoglobinuria. *N Engl J Med* (2006) 355:1233–43. doi: 10.1056/NEJMoa061648
6. Röth A, Nishimura JI, Nagy Z, Gaàl-Weisinger J, Panse J, Yoon SS, et al. The complement C5 inhibitor crovalimab in paroxysmal nocturnal hemoglobinuria. *Blood* (2020) 135:912–20. doi: 10.1182/blood.2019003399
7. McKeage K. Ravulizumab: First Global Approval. *Drugs* (2019) 79:347–52. doi: 10.1007/s40265-019-01068-2
8. Cashman SM, Ramo K, Kumar-Singh R. A non membrane-targeted human soluble CD59 attenuates choroidal neovascularization in a model of age related macular degeneration. *PloS One* (2011) 6:19078. doi: 10.1371/journal.pone.0019078
9. Rollins SA, Matis LA, Springhorn JP, Setter E, Wolff DW. Monoclonal antibodies directed against human C5 and C8 block complement-mediated damage of xenogeneic cells and organs. *Transplantation* (1995) 60:1284–92. doi: 10.1097/00007890-199512000-00017
10. Rinder CS, Rinder HM, Smith MJ, Tracey JB, Fitch J, Li L, et al. Selective blockade of membrane attack complex formation during simulated extracorporeal circulation inhibits platelet but not leukocyte activation. *J Thorac Cardiovasc Surg* (1999) 118:460–6. doi: 10.1016/S0022-5223(99)70183-2
11. Biesecker G, Gomez CM. Inhibition of acute passive transfer experimental autoimmune myasthenia gravis with Fab antibody to complement C6. *J Immunol* (1989) 142(8):2654–9.
12. Lin K, Zhang L, Kong M, Yang M, Chen Y, Poptic E, et al. Development of an anti-human complement C6 monoclonal antibody that inhibits the assembly of membrane attack complexes. *Blood Adv* (2020) 4:2049–57. doi: 10.1182/bloodadvances.2020001690
13. Köhler G, Milstein C. Continuous cultures of fused cells secreting antibody of predefined specificity. *Nature* (1975) 256:495–7. doi: 10.1038/256495a0
14. Zelek WM, Harris CL, Morgan BP. Extracting the barbs from complement assays: Identification and optim of a safe substitute for traditional buffers. *Immunobiology* (2018) 223:744–9. doi: 10.1016/j.imbio.2018.07.016
15. Morgan BP. *Complement Methods and Protocols*. Totowa, New Jersey: Humana Press (2000). doi: 10.1385/159259056x
16. Chamberlain-Banoub J, Neal JW, Mizuno M, Harris CL, Morgan BP. Complement membrane attack is required for endplate damage and clinical disease in passive experimental myasthenia gravis in Lewis rats. *Clin Exp Immunol* (2006) 146:278–86. doi: 10.1111/j.1365-2249.2006.03198.x
17. Morgan BP, Chamberlain-Banoub J, Neal JW, Song W, Mizuno M, Harris CL. The membrane attack pathway of complement drives pathology in passively induced experimental autoimmune myasthenia gravis in mice. *Clin Exp Immunol* (2006) 146:294–302. doi: 10.1111/j.1365-2249.2006.03205.x
18. Zelek WM, Taylor PR, Morgan BP. Development and characterization of novel anti-C5 monoclonal antibodies capable of inhibiting complement in multiple species. *Immunology* (2019) 157:283–95. doi: 10.1111/imm.13083
19. Zelek WM, Menzies GE, Brancale A, Stockinger B, Morgan BP. Characterizing the original anti-C5 function-blocking antibody, BB5.1, for species specificity, mode of action and interactions with C5. *Immunology* (2020) 161:103–13. doi: 10.1111/imm.13228
20. Pickering RJ. Significance of abnormalities of serum complement in human disease. *Postgrad Med* (1968) 43:39–43. doi: 10.1080/00325481.1968.11693275
21. Schur PH, Austen KF. Complement in human disease. *Annu Rev Med* (1968) 19:1–24. doi: 10.1146/annurev.me.19.020168.000245
22. Nesargikar P, Spiller B, Chavez R. The complement system: History, pathways, cascade and inhibitors. *Eur J Microbiol Immunol* (2012) 2:103–11. doi: 10.1556/eujmi.2.2012.2.2
23. Sim RB, Schwaeble W, Fujita T. Complement research in the 18th–21st centuries: Progress comes with new technology. *Immunobiology* (2016) 221:1037–45. doi: 10.1016/j.imbio.2016.06.011
24. Zelek WM, Fathalla D, Morgan A, Touchard S, Loveless S, Tallantyre E, et al. Cerebrospinal fluid complement system biomarkers in demyelinating disease. *Mult Scler J* (2019) 1352458519887905:1–9. doi: 10.1177/1352458519887905
25. Carpanini SM, Torvell M, Morgan BP. Therapeutic inhibition of the complement system in diseases of the central nervous system. *Front Immunol* (2019) 10:1–17. doi: 10.3389/fimmu.2019.00362
26. Clark SJ, Bishop PN. The eye as a complement dysregulation hotspot. *Semin Immunopathol* (2018) 40:65–74. doi: 10.1007/s00281-017-0649-6
27. Zelek WM, Stott M, Walters D, Harris CL, Morgan BP. Characterizing a pH-switch anti-C5 antibody as a tool for human and mouse complement C5 purification and cross-species inhibition of classical and reactive lysis. *Immunology* (2018) 155:396–403. doi: 10.1111/imm.12982
28. Harder MJ, Höchsmann B, Dopler A, Anliker M, Weinstock C, Skerra A, et al. Different levels of incomplete terminal pathway inhibition by eculizumab and the clinical response of PNH patients. *Front Immunol* (2019) 10:1–7. doi: 10.3389/fimmu.2019.01639
29. Hill A, Piatek CI, Peffault de Latour R, Wong LL, Wells RA, Brodsky RA, et al. Breakthrough Hemolysis in Adult Patients with Paroxysmal Nocturnal Hemoglobinuria Treated with Ravulizumab: Results of a 52-Week Extension from Two Phase 3 Studies. *Blood* (2019) 134:952–2. doi: 10.1182/blood-2019-128929
30. Würzner R, Joysey VC, Lachmann PJ. Complement component C7. Assessment of *in vivo* synthesis after liver transplantation reveals that hepatocytes do not synthesize the majority of human C7. *J Immunol* (1994) 152(9):4624–9.
31. Wurzner R, Platonov AE, Beloborodov VB, Pereverzev AI, Vershinina IV, Fernie BA, Orren A, et al. How partial C7 deficiency with chronic and recurrent bacterial infections can mimic total C7 deficiency: temporary restoration of host C7 levels following plasma transfusion. *Immunology* (1996) 88:407–11. doi: 10.1046/j.1365-2567.1996.d01-663.x
32. Nam-Ho C, Toshio M, Motowo T. A serum protein SP40,40 modulates the formation of membrane attack complex of complement on erythrocytes. *Mol Immunol* (1989) 26:835–40. doi: 10.1016/0161-5890(89)90139-9
33. Jenne DE, Tschopp J. Molecular structure and functional characterization of a human complement cytolysis inhibitor found in blood and seminal plasma: Identity to sulfated glycoprotein 2, a constituent of rat testis fluid. *Proc Natl Acad Sci U S A* (1989) 86:7123–7. doi: 10.1073/pnas.86.18.7123
34. Hallström T, Uhde M, Singh B, Skerka C, Riesbeck K, Zipfel PF. Pseudomonas aeruginosa uses Dihydrolipoamide dehydrogenase (Lpd) to bind to the human terminal pathway regulators vitronectin and clusterin to inhibit terminal pathway complement attack. *PloS One* (2015) 10:1–21. doi: 10.1371/journal.pone.0137630
35. Hadders MA, Bubeck D, Roversi P, Hakobyan S, Forneris F, Morgan BP, et al. Assembly and Regulation of the Membrane Attack Complex Based on Structures of C5b6 and sC5b9. *Cell Rep* (2012) 1:200–7. doi: 10.1016/j.celrep.2012.02.003
36. Fernie-King BA, Seilly DJ, Willers C, Würzner R, Davies A, Lachmann PJ. Streptococcal inhibitor of complement (SIC) inhibits the membrane attack complex by preventing uptake of C567 onto cell membranes. *Immunology* (2001) 103:390–8. doi: 10.1046/j.1365-2567.2001.01249.x

Conflict of Interest: BPM has provided advice on complement to Roche and is a consultant to RaPharma. The authors are named inventors on a patent (PCT/EP2020/073430) describing the anti-C7 mAbs.

frontiers in Immunology

REVIEW
published: 10 December 2020
doi: 10.3389/fimmu.2020.578069

Therapeutic Lessons to be Learned From the Role of Complement Regulators as Double-Edged Sword in Health and Disease

Esther C. W. de Boer[1,2], *Anouk G. van Mourik*[1] *and Ilse Jongerius*[1,2]*

[1] Sanquin Research, Department of Immunopathology, and Landsteiner Laboratory, Amsterdam University Medical Centre, Amsterdam Infection and Immunity Institute, Amsterdam, Netherlands, [2] Department of Pediatric Immunology, Rheumatology, and Infectious Diseases, Emma Children's Hospital, Amsterdam University Medical Centre, Amsterdam, Netherlands

The complement system is an important part of the innate immune system, providing a strong defense against pathogens and removing apoptotic cells and immune complexes. Due to its strength, it is important that healthy human cells are protected against damage induced by the complement system. To be protected from complement, each cell type relies on a specific combination of both soluble and membrane-bound regulators. Their importance is indicated by the amount of pathologies associated with abnormalities in these complement regulators. Here, we will discuss the current knowledge on complement regulatory protein polymorphisms and expression levels together with their link to disease. These diseases often result in red blood cell destruction or occur in the eye, kidney or brain, which are tissues known for aberrant complement activity or regulation. In addition, complement regulators have also been associated with different types of cancer, although their mechanisms here have not been elucidated yet. In most of these pathologies, treatments are limited and do not prevent the complement system from attacking host cells, but rather fight the consequences of the complement-mediated damage, using for example blood transfusions in anemic patients. Currently only few drugs targeting the complement system are used in the clinic. With further demand for therapeutics rising linked to the wide range of complement-mediated disease we should broaden our horizon towards treatments that can actually protect the host cells against complement. Here, we will discuss the latest insights on how complement regulators can benefit therapeutics. Such therapeutics are currently being developed extensively, and can be categorized into full-length complement regulators, engineered complement system regulators and antibodies targeting complement regulators. In conclusion, this review provides an overview of the complement regulatory proteins and their links to disease, together with their potential in the development of novel therapeutics.

Keywords: complement, complement regulators, complement therapeutics, complement antibodies, complement-mediated disease

OPEN ACCESS

Edited by:
Cees Van Kooten,
Leiden University, Netherlands

Reviewed by:
Simon John Clark,
University of Tübingen, Germany
Arvind Sahu,
National Centre for Cell Science, India

***Correspondence:**
Ilse Jongerius
i.jongerius@sanquin.nl

Specialty section:
This article was submitted to Molecular Innate Immunity, a section of the journal Frontiers in Immunology

Received: *30 June 2020*
Accepted: *12 October 2020*
Published: *10 December 2020*

Citation:
de Boer ECW, van Mourik AG and Jongerius I (2020) Therapeutic Lessons to be Learned From the Role of Complement Regulators as Double-Edged Sword in Health and Disease. Front. Immunol. 11:578069. doi: 10.3389/fimmu.2020.578069

INTRODUCTION

The Complement System

Upon its discovery at the end of the 19th century, the complement system was considered to consist of only one component. Nowadays it is known that the complement system is a complex part of the innate immune system, consisting of a large number of proteins and associated regulators (1, 2). In order to respond quickly to pathogens, the components of the complement system are present in plasma and thus are readily available throughout the body (3, 4). Three different pathways can initiate complement activity: the classical pathway (CP), the lectin pathway (LP) and the alternative pathway (AP). Activation of these pathways takes place *via* antibody-binding, recognition of specific sugar patterns or spontaneous C3 hydrolysis, all resulting in formation of a C3 convertase. C3 convertases cleave C3, resulting in opsonization of pathogens and formation of C5 convertases. With C5 convertases the terminal pathway is initiated which will result in chemotaxis and formation of the membrane attack complex (MAC) (3).

Although all three complement pathways result in the formation of a C3 convertase, their initiation and intermediate steps differ (**Figure 1**). The CP is mainly initiated by antibody binding to target cells. The C1 complex consists of C1q, C1r and C1s. C1q is the pattern recognition molecule, and upon surface binding of C1q, the protease C1r is activated, cleaving and activating C1s. C1s can then cleave C2 and C4, which leads to the formation of C3 convertase C4bC2a (3, 5, 6). The LP is activated in a similar way, with ficolin and mannose-binding lectin (MBL) acting as pattern recognition molecules. These molecules recognize microbial carbohydrate structures. Upon recognition, the MBL-associated serine proteases (MASPs), can cleave C2 and C4, to form the C4bC2a C3 convertase (5–7). Lastly, the AP is activated by C3b coming from the other two pathways. In addition, constant background spontaneous hydrolysis of C3 results in formation of C3(H_2O) which also serves as a platform for the AP. C3b or C3(H_2O) will bind Factor

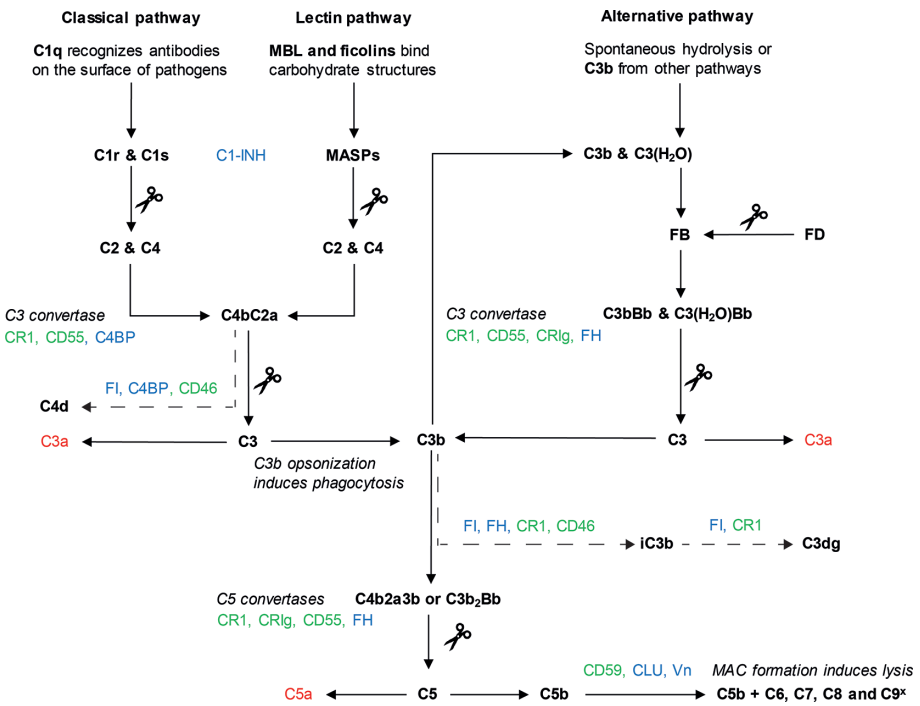

FIGURE 1 | The complement system. Three pathways can lead to complement activation: the classical pathway (CP), the lectin pathway (LP) and the alternative pathway (AP). Activation of the CP (left) starts with binding of C1q to target cells, often *via* antibodies. Binding of C1q leads to cleavage of C1r, which in turn cleaves C1s. The proteolytic activity of C1s results in the cleavage of C2 and C4. These components form the C3 convertase of the CP, C4bC2a. Activation of the LP (middle) starts with the binding of MBL or ficolins to carbohydrate structures on target cell surfaces. As a result, the proteases of the LP, MASPs, cleave C2 and C4, also leading to the formation of C4bC2a. The AP pathway (right) is activated by spontaneous hydrolysis of C3, which leads to the formation of C3(H_2O), or by C3b from the CP or LP. After assembly of C3b, FB binds to C3b or C3(H_2O) and is cleaved by protease FD. This results in the formation of the C3 convertases of the AP, C3bBb or C3(H_2O)Bb. C3 convertases of the CP/LP and the AP cleave C3 into C3b and C3a. Usage of C3b in the AP causes an amplification loop, which can amplify the CP and LP. In addition, C3b deposition leads to formation of two C5 convertases: C4b2aC3b (CP/LP) or $C3b_2Bb$ (AP). C5 convertases cleave C5 in C5a and C5b. C5b is used for the formation of the MAC which is formed after assembly of C6, C7, C8 and multiple C9 molecules ($C9^x$). The MAC is inserted into the membrane to induce lysis. C3a and C5a (depicted in red) are anaphylatoxins important for chemotaxis and the initiation of inflammation. Complement components are depicted in bold, scissors indicate cleavage. Complement regulators can be divided in two groups: soluble (depicted in blue) and membrane-bound (depicted in green). These regulators prevent complement activation by targeting the complement pathway in different places, as depicted here. The inactivating breakdown pathways of C3b and C4b respectively by complement regulators are indicated here with a dotted arrow, showing the different breakdown products.

B (FB), which is cleaved by the protease Factor D (FD), leading to the formation of C3bBb, another C3 convertase (5, 8). The AP mechanisms enable it to work as an amplification loop for the CP and LP (9, 10).

After the formation of a C3 convertase, the three pathways all continue with the terminal complement pathway. The C3 convertases cleave C3 into C3a and C3b, which leads to the formation of two different C5 convertases: C4b2a3b and $C3b_2Bb$. The C5 convertase cleaves C5, after which C5b associates with C6 and C7 and inserts itself into the cell membrane. Upon binding of C8 and several C9 units, a lytic pore is formed: the MAC (5). Whilst the main cleavage products of complement ensure the downstream continuation of the pathway, the smaller cleavage products C3a and C5a are anaphylatoxins (3). Anaphylatoxins act as chemoattractant for immune cells and are important mediators in inflammation (11).

Next to its well-known role, it has become evident that intracellular complement plays an important role in homeostasis [reviewed in (12, 13)]. It has been shown that complement proteins are expressed by a large variety of cells that secrete these proteins into the local environment when needed. Recent studies also indicate that T cells not only express C3 but actually need intracellular C3 activation fragments for their survival (12, 13). Next, complement receptor CD46, described in more detail below, has also been identified as an important player in T cell homeostasis (14). Taken together, the complement system is well-orchestrated and highly effective in clearing invading pathogens. In addition, this system also plays an important role in activation of the adaptive immune system (11) and important for T cell homeostasis.

Complement Regulators

The complement system is key in eradicating pathogens, but also plays an important role in clearance of for instance apoptotic or tumor cells. Due to the strength and omnipresence of the complement system regulation of this system is key to prevent damage to host cells (5, 15). However, complement dysregulation can be beneficial in certain circumstances. In retinitis pigmentosa complement overactivation on the levels of C3 results in enhanced phagocytic clearance of apoptotic photoreceptors by microglia resulting in limiting photoreceptor loss (16). In addition, the positive effect of complement activation on human cells was also shown for neuronal development (17). To ensure proper regulation of complement on host cells where needed, and to distinguish these from pathogens, complement regulators are in place. Most of these regulators of complement activity are encoded at the same locus on chromosome 1q32 and are formed by repeated complement control protein (CCP) domains (18). Up to date, a variety of soluble and membrane-bound complement regulators has been identified, which will be described here.

The soluble complement regulators can be found in plasma: Factor I (FI), Factor H (FH), C1-inhibitor (C1-INH), C4b binding protein (C4BP), clusterin (CLU) and vitronectin (Vn) (19, 20). FI is a protease specific for C3b and C4b, that can cleave these proteins in presence of a co-factor, forming their inactive counterparts iC3b and C4d. These co-factors are C4BP, FH and the membrane-bound complement receptor 1 (CR1) and CD46. By acting on C3b and C4b, FI can regulate all the complement pathways (21). Two soluble regulators act exclusively on the CP and LP: C4BP and C1-INH. C4BP prevents the formation of C3 convertase in the LP and CP, by binding to C4b. After C4BP binding of C4b, FI cleaves and inactivates C4b to C4d (19, 22). C1-INH has several roles in the suppression of inflammation and vascular permeability, but in the complement system it blocks the proteolytic activity of C1s, C1r and MASPs (23, 24). As a result, cleavage of C2 and C4 is inhibited resulting in less formation of the C3 convertase, C4bC2a.

FH is a regulator of the AP, next to its co-factor activity for FI. FH binds to sialic acid residues on host cells and to C3b, regulating the formation of C3bBb. FH can remove Bb from C3b, reversing convertase formation (25, 26). FH also has an alternative splice variant, Factor H-like 1 (FHL-1). FHL-1 consists of the first 7 CCP domains and is thereby able to fulfill the AP regulatory capacity similar to FH. However, as FHL-1 lacks the sialic acid residue binding domains of FH (CCP 19-20) its fails to distinguish effectively between host and foreign surfaces (27). FHL-1 CCP domain 7 is able to bind to sulphated glycosaminoglycans (GAGs) therefore, it is postulated that FHL-1 is mainly important in controlling the AP in local tissues such as the such as for example in the eye (28) Next to FH and FHL-1, humans also have five different Factor H-related proteins (FHR), which have arisen from duplication events of the *CFH* gene (29). These molecules share some domains with FH, but lack the complement inhibiting domains. Currently, there is no consensus on the precise function of these molecules *in vivo*, which is why they will not be discussed in detail here (30–32).

The last soluble complement regulators are CLU and Vn, both acting on the terminal complement pathway, inhibiting MAC formation. CLU binds to C7 to prevent membrane attachment, and can also bind C8 and C9 to prevent C9 assembly. Vn prevents the insertion of the MAC into the membrane by binding at the membrane-binding site of C5b-7 (19). Apart from their function as complement regulators, CLU and Vn have a range of cellular functions in lipid transport and cell adhesion respectively (22).

Next to the soluble complement regulators, five different membrane-bound regulators have been discovered that play an important role in regulation: CR1 (also known as CD35), membrane co-factor protein (CD46), decay accelerating factor (DAF, also known as CD55), CD59 and complement receptor immunoglobin (CRIg) (22). CR1 is a transmembrane protein that acts as a cofactor for FI and is a receptor for C3b, iC3b and C4b, inducing decay of C3 and C5 convertases (33). In this way, CR1 inhibits the CP, LP and AP. CR1 also plays a role in other immune functions, such as B and T cell regulation and phagocytosis and particle binding (34, 35). The other membrane-bound co-factor for FI is CD46, a transmembrane glycoprotein. Like CR1 it binds to the C3 and C4 fragments, but it does not have any decay activity, as opposed to CR1 (36, 37). CRIg is another transmembrane protein and an inhibitor of the AP. It is suggested to bind C3b, preventing C3bBb from

cleaving C5. Unlike the other membrane-bound regulators that are widely expressed, CRIg is only present on a subset of cells: specific macrophages and dendritic cells (38, 39). Lastly, two other membrane-bound complement regulators are glycosylphosphatidylinositol- (GPI) anchored proteins CD55 and CD59 (3). CD55 accelerates the decay of the C3 convertases (22, 40). CD59, on the other hand, prevents the formation of the MAC by binding to C9 and preventing MAC insertion into the membrane (22, 40).

As the complement system needs to be regulated so tightly by a large number of proteins, it is to be expected that abnormalities in the complement system or the complement regulators are associated with a range of diseases. For many of these diseases, no adequate therapeutics are currently available, which is unsurprising considering that only two complement therapeutics are currently approved: anti-C5 antibodies (eculizumab and ravulizumab) and C1-INH (41, 42). Here, we will first describe the pathologies that complement regulators are involved in. Then, we will explore how the complement regulators can be used as potential therapeutics for these and other pathologies, and discuss relevant therapeutics currently in development. Altogether, this will give an insight in the significance and broad therapeutic applications for complement regulatory proteins.

THE ROLE OF COMPLEMENT REGULATORS IN PATHOLOGIES

As described above, different cell types and tissues rely on different combinations of complement regulators and abnormalities in complement regulators are associated with a variety of pathologies (22). Amongst these are for example several red blood cell (RBC) mediated diseases, but also different cancerous malignancies and neurological diseases. The pathologies have been linked to both genetic and acquired abnormalities in complement regulators. Here, we will describe the different ways in which complement regulators have been linked to pathologies and focus on the diseases that are most well-studied. The most important polymorphisms and deficiencies are described in **Figure 2**. An overview of other diseases that have been linked to complement regulators, but are not discussed in detail here, are presented in **Table 1**.

The Role of Complement Regulators in Anemic Pathologies

Many of the diseases in which aberrant complement regulation plays a role affect RBCs, which leads to hemolysis and anemia. As RBCs are continuously exposed to the complement system in the blood it is to be expected that they are highly vulnerable to complement-mediated lysis when their complement regulatory proteins are affected (54). The most well-described example of this is paroxysmal nocturnal hemoglobinuria (PNH). PNH is characterized by intra- and extravascular hemolysis and venous thrombosis, caused by the complement system. The disease arises from acquired somatic mutations in *PIGA* in hematopoietic stem cells, which encodes for phosphatidylinositol N-acetylglucosaminyltransferase subunit A, an essential enzyme in the synthesis of GPI-anchored proteins. As a consequence, GPI-anchored proteins are not present on cells arising from these stem cells, such as RBCs, platelets and neutrophils. Amongst these proteins are complement regulators CD55 and CD59, which cause the increased sensitivity to complement-mediated hemolysis (55–57).

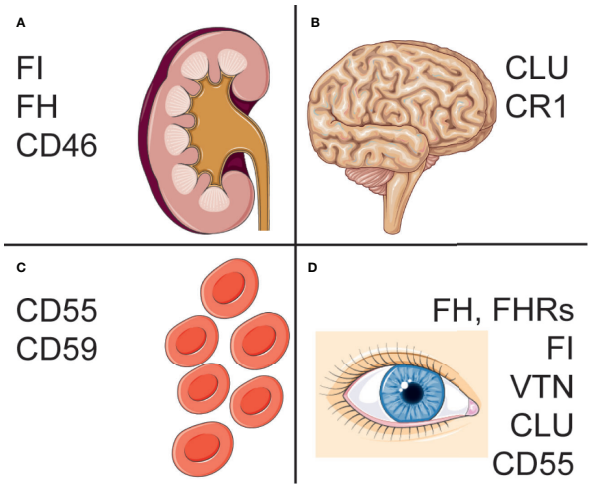

FIGURE 2 | Complement regulators associated with pathologies. Overview of the major pathologies associated with complement regulators and polymorphisms or deficiencies associated with disease. **(A)** In the kidney, mutations in *CFH*, *CFI* and *CD46* are associated with aHUS, C3 glomerulopathy and IgA nephropathy. **(B)** Polymorphisms in *CLU* and *CR1* have been found to increase risk of AD. One of these *CLU* polymorphisms is also a risk factor for PD. **(C)** On erythrocytes, deficiencies of CD55 and CD59 on blood cells contribute to PNH, with isolated CD59-deficiency also associating with chronic hemolysis. **(D)** *CFH, CFI* and *VTN*, as well as a *CFHR1-3* deletion have been associated with AMD. A *CLU* polymorphism was found in pseudoexfoliation syndrome and Fuchs' endothelial dystrophy. Lastly, a *CD55* polymorphism is a risk factor for pathological myopia. Figure designed using Servier Medical Art.

Currently, the only treatments approved for PNH are eculizumab and ravulizumab, both C5 monoclonal antibodies, inhibiting C5a generation and formation of the MAC. Eculizumab is able to reduce intravascular hemolysis, fatigue and transfusion requirements in PNH patients, although responses are variable between patients (58–60). The variability of responses can in some cases be explained by a C5 mutation that prevents eculizumab binding (61). However, the main variation arises from the fact that eculizumab does not prevent C3b deposition on RBCs. Opsonization by C3b induces removal of the RBCs by phagocytosis, which leads to an increase in extravascular hemolysis as shown in PNH patients receiving eculizumab treatment (62). Susceptibility to extravascular hemolysis upon eculizumab treatment has been linked to a CR1 polymorphism. Decreased CR1 on the RBC surface would lead to a decrease in C3b decay and thus for increased opsonization that can induce extravascular hemolysis. *CR1* has

TABLE 1 | Additional pathologies where complement regulators were identified to play a role, that were not described in the text.

Pathology	Regulator	Association	Observations	Ref.
Allergic respiratory disease	CD55	Polymorphism	A CD55 SNP linked to decreased transcriptional activity, was associated with susceptibility to pollen and mite-induced respiratory allergies and enhanced specific IgE responses.	(43)
Geographic atrophy	CD46	Protein levels	Retinal pigment epithelial CD46 expression is altered early on in geographic atrophy development.	(44)
Traumatic brain injury	CR1 and CD59	Protein levels	CR1 and CD59 were significantly reduced in the first week after acute brain injury.	(45)
Recurrent miscarriages	C4BP	Polymorphism	C4BP mutations, of which some affecting expression level and FI co-factor activity, were found in women with recurrent miscarriages.	(46)
Cardiovascular disease	CR1	Polymorphism	CR1 polymorphisms are associated with increased risk of coronary artery disease.	(47)
	FH	Polymorphism	The FH Y402H polymorphism in FH was suggested to determine myocardial infarction susceptibility.	(48)
Sudden sensorineural hearing loss	FH	Polymorphism	The FH Y402H polymorphism has been associated with risk of sudden sensorineural hearing loss.	(49)
Idiopathic pulmonary fibrosis	CR1	Polymorphism	A CR1 polymorphism was associated with development of idiopathic pulmonary fibrosis.	(50)
Preeclampsia	CD46 and FH	Polymorphism	Two fetal CD46 SNPs were associated with preeclampsia, where placentas have increased complement deposition. An interaction with maternal FH and a C3 SNP might play a role as well.	(51)
Rheumatic disease	CD55 and CD59	Deficiency	CD55 and/or CD59 erythrocytes are present in a majority of patients with rheumatic disease.	(52)
Schizofrenia	Clusterin	Polymorphism	A clusterin polymorphism was associated with schizophrenia in Chinese patients with family history of disease.	(53)

two co-dominant alleles that lead to either high (H) or low (L) expression of the regulator respectively. It has been shown that PNH patients with a H/L or L/L genotype have a lower expression of CR1 and require more transfusions (63). Although it has been shown that compstatin is a highly effective inhibitor of C3 that can prevent extravascular hemolysis (64, 65), it is not FDA approved yet (66).

Next to the combined CD55- and CD59 deficiency in PNH, a few isolated CD55- and CD59 deficiencies have been described. Isolated genetic CD59-deficiencies have been associated with chronic hemolysis like PNH, as well as with other symptoms such as neuronal damage and recurrent strokes (67, 68). Interestingly, RBCs specific isolated deficiencies of CD55 do not seem to induce hemolysis. A small group of patients has been found to have CD55-deficient RBCs, named the Inab phenotype. These individuals do not have any specific complaints and have a variety of CD55 silencing mutations (69, 70). Although *in vitro* research showed an increase in C3b deposition on the RBCs of this phenotype compared to healthy cells, an increase in hemolysis was not found (71). Not all of these patients are however fully deficient in CD55, which *in vivo* might prevent some complement-mediated activity on RBCs. Furthermore, a CD55 loss-of-function mutation causes an autosomal recessive disorder characterized by hyperactivation of complement, angiopathic thrombosis, and protein-losing enteropathy (CHAPLE) syndrome. Here, the lack of CD55 leads to overactivation of the complement system, which leads to gut inflammation induced by anaphylatoxins in these patients (72–74). Interestingly, again increased hemolysis was not reported in any of the CD55-deficient patients, which could be an indication that CD59 is more important in complement regulation on RBCs. The important role of CD59 is further illustrated by the fact that CD59-deficient RBCs are highly sensitive to complement-mediated lysis. However, RBCs of a PNH patient showed the highest sensitivity for complement mediated lysis compared to the RBCs with a single complement regulator deficiency (75).

Hereditary hemolytic anemias are a group of anemias that share the common feature of decreased RBC survival leading to anemia, which is caused by inherited disorders in certain membranes, enzymes or hemoglobin. Examples are hereditary spherocytis, caused by membrane protein deficiencies, congenital microcytosis, caused by defects in hemoglobin (76) and sickle cells disease, caused by a hemoglobin mutation inducing deformation of affected RBCs under stress conditions, that leads to anemia in homozygous patients (77). The expression of membrane-bound complement regulators CD55 and CD59 in patients with hereditary spherocytis and congenital microcytosis has been investigated. FACS analysis showed a decrease in CD55 expression on erythrocytes of both patient groups compared to controls. However, immunoblot showed a less clear difference. CD59 was unaffected in both patient groups indicating that the decrease in CD55 expression is not caused by a *PIGA* mutation, similar to PNH patients, as a GPI anchor defect would affect both CD55 and CD59. It remains debatable whether low CD55 expression contributes to the anemia in these patients as a correlation between the expression of CD55 and severity of the anemia was not found and the effect on complement-mediated RBCs destruction was not studied (78). Like in the before mentioned anemias, differential expression of CD55 and CD59 on erythrocytes was also found in sickle cell disease patients. Although these patients expressed decreased CD55 and CD59 expression on RBCs, this could not be linked to disease severity, suggesting that these regulators do not play a significant role in the pathophysiology of hemolysis in sickle cell disease (79). Recent research does however suggest a role for complement activation in sickle cell disease pathophysiology, where overactivation of complement has been found on sickle cell erythrocytes compared to healthy erythrocytes (80). Altogether, these studies indicate directions for future research into the mechanistic role of complement regulators and complement activity in hereditary hemolytic anemias to determine the exact role of complement regulators in these pathologies.

The Involvement of Complement Regulators in Renal Disease

Complement is differentially regulated in the kidney compared to other tissues. The glomerular basement membrane is very sensitive to complement damage and relies completely on soluble complement regulators, as it is directly exposed to blood and the complement system, unlike most other basement membranes (81, 82). It is therefore understandable that different kidney pathologies have been associated with anomalies in soluble complement regulators, which results in overactivation of the complement system (83).

Atypical hemolytic uremic syndrome (aHUS) is a kidney disease that can have serious complications, with a mortality rate of 25% without eculizumab treatment (84). Characterized by microangiopathic hemolysis, thrombocytopenia and renal failure, it is caused by disbalance between regulation and activation of the AP. This disbalance is caused by decreased activity of complement regulators, or increased activity of complement proteins. Many aHUS cases have an identified genetic basis. Mutations linked to aHUS have been identified in several complement-related proteins, of which mutations in FH, FI, CD46 and C3 are found in approximately half of the patients. These mutations often lead to altered function or expression (85–87). More rarely, mutations in C2 and FB are found in aHUS patients (83, 88). In around 10% of the patients, autoantibodies against FH have been found. Most of the FH mutations as well as the FH autoantibodies target FH CCP 20. As FH CCP 19-20 is most important for FH binding to GAGs predominantly expressed in the glomeruli basement membrane, it might not come as a surprise that exactly these mutations and antibodies are linked to aHUS (89–91). Current treatment of aHUS consists of either plasma infusion or exchange, or eculizumab. Plasma infusion and exchange can replenish complement regulators in the blood of the patient and is especially beneficial in patients with FH and FI mutations (92). Eculizumab is now the preferred treatment, as it prevents complement-mediated damage as described above for PNH and is more safe than plasma transfusions (84).

Next to aHUS patients, C3 glomerulopathy patients suffer from dysregulation of the AP as well. In contrast to aHUS patients, these patients are characterized by C3 deposits in glomeruli, which leads to disruption of kidney function, but the disease is not associated with thrombocytopenia, anemia, or other systemic involvement (93). The pathophysiology of disease is not always clear, but in some cases it is known to be caused by autoantibody formation against C3bBb, which stabilizes the convertase and thus increases its activity, or by mutations in C3 or the complement regulatory proteins FH or FI (94–96). Another kidney disease where an FH polymorphism increases susceptibility is IgA nephropathy, a form of glomerulonephritis where C3 depositions are found on affected kidney tissue, together with IgA. The FH polymorphism identified for IgA nephropathy has not been linked to aHUS. A meta-analysis showed significant association between this minor allele and IgA nephropathy risk (97). This strengthens the hypothesis that IgA nephropathy is caused by overactivation of complement, although no functional implications of this specific polymorphism have been described.

Lastly, chronic kidney disease (CKD) is a condition where decreased kidney condition takes place over a longer period of time, regardless of the underlying cause. Although the pathologies mentioned above can cause CKD, the majority of cases is caused by diabetes and hypertension (98). Anemia is found in almost half of the CKD patients, being more prevalent in end-stage disease (99). A study of anemic CKD patients investigated CD55 and CD59 expression and showed that patients had an altered expression of CD55 and CD59 on RBCs, with more CD55- and CD59-deficient RBCs in patients than in healthy controls. CD55- and CD59-deficiency would make RBCs more susceptible to complement-mediated hemolysis. Increased hemolysis was confirmed in patients with high levels of CD55- and CD59 deficient RBCs. The underlying cause of CKD in these patients was not reported, making it difficult to speculate on the mechanisms involved (100). Furthermore, *VTN* has been shown to be upregulated in chronic kidney disease. This is possibly related to the fact that it functions as a ligand for the urokinase-type plasminogen activator receptor. This receptor is not found on healthy kidney cells, only getting expressed in diseased kidney cells, where it is involved in cell recruitment and migration (101). Up to date, no studies have been conducted that assess the role of Vn on complement regulation in CKD.

Complement Regulators in Diseases Affecting the Eye

Complement activation in the eye is highly reliant on local production of complement proteins, due to its anatomical characteristics (102). The inner part of the eye is shielded off by a sheet of extracellular matrix called the Bruch's membrane. Like the glomerular basement membrane in the kidney, it is directly exposed to circulation and thus to complement activity, making it vulnerable to dysfunctional complement regulators (103). Bruch's membrane is impermeable to larger proteins, these thus need to be locally produced. This also holds for the larger proteins of the complement cascade, such as C3b, FH, FB, and FI. It has been shown that FHL-1, a truncated splice variant of FH, is small enough to diffuse over Bruch's membrane and could thus play an important role in the eye (28). The importance of complement in the eye has been illustrated in age-related macular degeneration (AMD). As one of the leading causes of blindness AMD is affecting more than 5% of the elderly above 75 years old, for which the role of complement in disease has been widely studied.

AMD is marked by progressive destruction of the macula, as the retinal pigment epithelial cells that normally maintain retinal homeostasis are unable to do so. Currently, AMD is considered to be caused by a combination of genetic and environmental risk factors. Different complement genes have been associated with AMD, which can altogether account for 40–60% of the heritability of the disease. Amongst these genes are *CFH*, *CFI* and *VTN* which indicates that a dysregulation of complement activation is at play here.

Several mutations were found for *CFH*, amongst which the common Y402H variant, and were all associated with decreased protein expression or functionality of FH and FHL-1 (104, 105). Similarly, the *CFI* mutations found were associated with decreased serum levels of FI, although the effect of these polymorphisms on FI production within the eye is not known (106). For the *VTN* polymorphism identified no functional consequences have been described yet (107). Lastly, serum levels of FHR-4 were increased in AMD patients compared to healthy controls, while complete *CFHR1* and *CFHR3* deletion has been described to be protective against AMD (32, 108). While FHR-3 is locally produced in the retina, FHR-4 expression has not been demonstrated here yet (109, 110). It has been suggested that FHR-4 might inhibit FHL-1 functioning in AMD, as competition assays showed that FHR-4 outcompetes FHL-1 in C3b binding (32).

Pseudoexfoliation syndrome is a pathology characterized by the deposition of abnormal fibrillar extracellular material in both non-ocular and ocular tissue, which can lead to glaucoma (111, 112). CLU is reduced at both mRNA and protein levels in several parts of the eyes of pseudoexfoliation syndrome patients compared to healthy controls (113). Under stress conditions CLU would be conventionally expected to be increased: amongst its biological functions are its role as an extracellular chaperone, which inhibits stress-induced precipitation and the aggregation of misfolded proteins (114). Thus, its downregulation here could be a contributing factor to the accumulation of fibrillar extracellular material (113). A polymorphism in *CLU* might contribute to genetic risk of pseudoexfoliation syndrome, but was not relevant when the age of controls was corrected for, and was not significant in logistic regression. Thus, common genetic variation in the CLU gene does not seem to play a major role (115). Next to the involvement of CLU in pseudoexfoliation syndrome, C3 was found to be significantly upregulated in aqueous humor in eyes of patients with pseudoexfoliation syndrome indicating an important role for complement activation during this disease (112). The mechanisms behind the role of complement in pseudoexfolation syndrome have not been elucidated yet, calling for more research to indicate whether other complement regulators might be implicated in its development.

Furthermore, a *CLU* polymorphism was associated with Fuchs' endothelial dystrophy, which is a degenerative disease of the corneal endothelium. This polymorphism results in overexpression of CLU in the corneal endothelial cells of these patients. It was hypothesized by the authors that this specific polymorphism in the *CLU* gene might affect its secretion by corneal endothelial cells, which would expose these cells to physiological stress (116). Lastly, a polymorphism in CD55 was repeatedly associated with the risk of development of myopia. Myopia, more commonly known as nearsightedness, is the leading cause of vision loss in young people, stemming from excessive axial elongation of the eye (117, 118). The effect of this polymorphism on CD55 function or expression has not been described yet. Complement activity as measured by C3, C4 and CH50 activity in serum is increased in pathological myopia patients, which could be an indication that dysregulation of complement is at play here (119). However, as measurements of complement activity in serum are not proper indications of complement activity in the eye, care should be taken in concluding complement plays a role in myopia patients, for which further research is needed.

Taken together, there are multiple strong links between mutations in complement regulatory proteins and pathology in eye diseases. Studying complement activation and regulation within the eye is difficult, limiting our current knowledge. Although some *in vitro* models have been developed, the current *in vivo* models are still insufficient to mimic complement activity in the human eye (102, 105, 120, 121). Knowledge considering the effect of the currently identified polymorphisms in the eye, could improve our understanding of the pathology and aid in the development of therapeutics.

Complement Regulators in Neurological Disease

The blood–brain barrier is largely impermeable for plasma proteins, like the complement proteins. As only a fraction of complement proteins passes the blood–brain barrier and there is minimal local production, the healthy brain expresses low levels of complement proteins. In diseased brain however, the blood–brain barrier can get disrupted and local production can be increased, contributing to a rise in complement activity. If complement is activated in the brain, the brain's glia cells and neurons have a low tolerance for it, due to low levels of complement regulators (122). The role of complement in diseases of the central nervous system has become more apparent in recent years. It has been shown to play a role in brain development, acute brain trauma and neurogenerative disease (123). Here, we discuss the links between complement regulators and Alzheimer's disease (AD) or Parkinson's disease (PD) as the role of regulators here has been most well-studied and the diseases largely impact global health.

AD is a common neurodegenerative disease, with almost 30 million cases worldwide in 2019, that leads to loss of cognitive function, caused by neuropathologic lesions in the brain (124). These lesions can be caused by amyloid plaques or neurofibrillary degeneration. Complement has been shown to contribute to the inflammation of the brain that occurs in AD, and to be activated in and around the amyloid plaques (122). The overactivation of complement contributes to disease progression, resulting in synapse loss and neurodegeneration (125). The evidence for the association of complement regulatory genes with AD has been given multiple times. Polymorphisms in both *CR1* and *CLU* have been repeatedly demonstrated to increase risk of AD (126–129). *CLU* has been shown to be upregulated in the AD brain, as well as to play a role in the clearance of β amyloid, which is the major component of the amyloid plaques (124). How this upregulation of *CLU* in the AD brain affects local complement activation has not been investigated. The functionality behind *CR1* polymorphisms in AD have not been fully elucidated either. One of the risk-increasing *CR1* polymorphisms results in a single amino acid change that has been associated with mildly increased sCR1 levels and binding affinity for C1q (130). The other is an intronic mutation associated with increased length of

the final protein by duplication, resulting in more C3b binding sites which could increase CR1 effectivity (122, 131). However, this variant is also associated with decreased expression levels. Overall, it seems that AD patients with the long CR1 isoform show an progressively decreased expression of CR1 on cells, thus reducing the total effectiveness of CR1 (132). Future research should indicate what the effects of the found *CR1* and *CLU* polymorphisms are on protein levels and functionality within the brain.

PD is another common neurodegenerative disease, which is also characterized by protein depositions in the brain. Research on the brains of PD patients has repeatedly shown complement activation in affected tissues (133, 134), and the dysregulated complement system has been suggested to play a role in pathology of PD (123). This was reason to investigate the abovementioned found polymorphisms for AD in PD. Only one of the *CLU* polymorphisms found for AD also showed to be a risk factor for the development of PD (135). However, levels of CLU in cerebrospinal fluid and plasma were not found to differ between patients and healthy controls. A correlation between CLU levels and amyloid- ß42, T-tau and P-tau levels was found, which are proteins that play a role in both AD and PD. Altogether these results suggest a direct interaction between amyloid- ß42, tau and CLU (136). It might not be surprising to see that CLU is associated with several neurological diseases, as it has been implicated in neuronal synapse function (53). Further research should indicate whether CLU also contributes *via* its role as complement regulatory protein in this system.

Complement Regulators in Oncology

The complement system has become strongly implicated in different types of cancer in recent years, but its role in oncology has not been well defined (137). In fact, the role of complement in carcinogenesis, has been described as a dual-edged sword (138). The dual mechanism of complement in carcinogenesis could be similar to that of inflammation, in which complement is a large contributing factor. Initially, acute inflammation can cause early detection and clearance of malignant cells, but chronic inflammation might also contribute to the spread of malignant cells (139). Specifically, the anaphylatoxins C3a and C5a have been described to contribute to an inflammatory tumor microenvironment. Their production upon local activity of the CP and AP on the tumor creates an environment that favors tumor growth and metastatic spread, contributing to tumor progression (137, 139–141). This role for C3a and C5a has been shown in different cancer types, in the form of promoting angiogenesis, inhibiting anti-tumor immune responses and by triggering tumorigenic, survival and anti-apoptotic pathways in tumor cells (141).

Although the importance of complement in cancer has been demonstrated, its function and overall effect have not been fully elucidated. The currently available literature on complement regulators in cancer specifically is limited and sometimes contradictory. This could in part be explained by the fact that only few human studies are available, with most of the data stemming from animal models or *in vitro* studies (137). In addition, complement regulators do not only have impact on the complement system, but also play an important role in the adaptive immune system by regulating and activating T-cells (142), making studies regarding their role extremely difficult. In general, it is believed that high expression of complement regulatory proteins is linked to worse clinical outcome (142). Here, we will give a brief overview of the currently available human studies of complement regulators in cancer.

Colon cancer is the second-most lethal cancer in the world (143). Although no complement regulator polymorphisms for risk of colon cancer have been identified, CD46, CD55, and CD59 were all upregulated in colon cancer compared to adjacent healthy tissue (144, 145), with CD55 and CD59 expression correlating with tumor stage and differentiation level (146). In addition, patients with an increased CD55 expression in their tumor tissue had a worse 7-year survival rate, with tumors with high levels of CD55 more aggressive than tumors with low CD55-levels (147). Patients with colorectal cancer also showed increased soluble CD55 in stool specimens compared to healthy controls and to patients with other gastrointestinal disease. Whether the soluble CD55 was secreted as such, or whether it arose from cleaved membrane-bound CD55, was unclear (148). These studies combined suggest that the increased expression of complement regulators protects malignant colorectal cells from being attacked by the human immune system, especially for CD55. A mouse xenograft study has shown that a blocking CD55-antibody inhibits tumor growth and increases survival of mice. *In vitro*, the combination of a blocking CD55-antibody with regular chemotherapy has a synergistic effect (149). This therapeutic effect suggests a clinical relevance for CD55 in colon cancer.

Another common and deadly cancer type is non-small cell lung cancer (NSCLC). NSCLC has been associated with the complement system in multiple ways, but the precise mechanisms in place have not been elucidated yet (150). On the genetic level, both a CD55 and a CR1 polymorphism have been associated with risk of NSCLC development (138, 151). The CD55 polymorphism found in NSCLC is associated with decreased transcriptional activity of CD55. This was a surprising finding, as complement regulation was initially expected to be increased on malignant cells, protecting them from detection by the complement system (151, 152). There might be a differential effect of CD55 between healthy and cancer cells at play here, as CD55 in NSCLC is not only down-regulated, but also sialylated. Possibly, sialylated CD55 can execute its function longer than regular CD55, as it has a high resistance against proteolysis and can thus be retained on the cell surface for a longer time (153). Another explanation could be that NSCLC tissue does not require complement regulation as much, as the bulky tissue formation ensures that not all cells are exposed to the alveolar cavity, and thus to complement activity (153). The CR1 polymorphism found in NSCLC was not further functionally described. Furthermore, at the protein level *in vivo* xenograft study in mice showed that FH expression is critical for NSCLC tumor growth. Whilst NSCLC cells *in vitro*

were shown to be insensitive to complement-mediated lysis, even largely when FH was blocked, blocking FH *in vivo* significantly decreased xenograft size (154).

Apart from the solid tumors described above, some research is available that links different types of leukemia and lymphoma to complement regulators. In a group of leukemia patients, comprised of patients with acute myeloid leukemia, acute lymphoblastic leukemia and chronic lymphocytic leukemia, soluble CR1 was found in high concentrations, regardless of specific leukemia type (155). The soluble CR1 originates from cleaved and shed membrane-bound CR1. This soluble CR1 maintains its complement regulatory activity, allowing for complement regulation in serum. Although it seems unlikely that this would lead to reduced overall complement activity in plasma *in vivo*, it could be that soluble CR1 shedding leads to local down-regulation of complement activity at sites of tumor infiltration, which could aid the malignant cells locally (155). This regulating characteristic of soluble CR1 has also been demonstrated in other studies, and soluble CR1 is now used to therapeutic advantage in complement-mediated diseases (156–158) as discussed below. The effects found for soluble complement regulators could be caused by their effects on the tumor microenvironment. The tumor microenvironment is the total of cancer cells, stromal cells and extracellular components around the tumor, where complement has been shown to play a regulatory role to which soluble regulators might contribute (159, 160).

The last type of tumor to be described here is non-Hodgkin's lymphoma. Non-Hodgkin's lymphoma is the most common type of lymphoma, with around half a million new cases a year and diffuse large B cell lymphoma and follicular lymphoma as its most common subtypes (161). In follicular lymphoma, a CD46 polymorphism is associated with decreased event-free survival, while the CD55 and FH polymorphisms are associated with increased event free survival. In diffuse large B cell lymphoma, a possible association with increased event-free survival was found for a *CLU* polymorphism (162). Unfortunately, there are no studies available linking any of these polymorphisms to expression levels or functionality of the protein, and there is no consensus on the role of complement in these diseases. A more recent study acknowledged that the role of complement in lymphoma is complex, but could indicate FHR-3 as a biomarker for the response to specific immunotherapies (163).

In conclusion, both solid malignancies and blood cancers have been associated with complement regulators. Here, we have described a selection of cancer types related to complement regulators, based on the extent to which they have been studied in humans. Based on this research, it is not possible to be conclusive on the role of complement regulators in cancer. The current indications of the many polymorphisms in complement regulators involved in cancer, can be used as directions for future research into the mechanisms and purposes of complement regulation in cancer.

Overall, we have demonstrated the broad range of diseases in which complement plays a role, giving examples from RBCs, the eyes, kidney, brain and oncology. In addition, **Table 1** shows other pathologies found linked to complement regulators in the current research. Altogether, the great amount of pathologies linking to dysfunction of complement regulators implies that future therapeutics based on complement regulators could potentially be applied widely. Next, we will explore the potential of such therapeutics currently available and under development.

FUTURE POTENTIAL OF UTILIZING COMPLEMENT REGULATORS IN THERAPEUTICS

As discussed above, a broad range of pathologies arises from dysfunction of complement regulation, leading to overactivation of the complement system on healthy cells, or insufficient complement activation on malignant cells (22, 137). Currently, only two therapeutics are approved to target the complement system, eculizumab/ravulizumab and C1-INH, which is insufficient to treat the wide range of complement-related pathologies. Other complement-targeting therapeutics are currently in development, such as compstatin, and FB and FD inhibitors (42, 164). The clinical success of these drugs has been limited to this date. The anti-C5 antibody eculizumab, as mentioned previously, is currently approved for diseases such as PNH and aHUS. When effective, eculizumab treatment increases patients' life expectancy to that of healthy person (165, 166). However, the drug is not effective in all patients (165, 166). Around 15% of aHUS patients do not respond to treatment, as well as 3% of PNH patients, with 30% of treated patients still requiring regular blood transfusions (61, 167, 168). In AMD, a phase III trial with eculizumab and a similar trial with an anti-FD antibody did not show a slowing effect on geographic atrophy development (169, 170). Together, this data indicates that although the fact that complement plays an important role in AMD, complement modulation seems a challenging and uncertain therapeutic option. Lastly, compstatin is a small cyclic peptide that binds C3 and inhibits convertase formation and C3 cleavage, of which two analogs have been clinically evaluated: AMY-101 and APL-2. To this date, AMY-101 has only been tested in a phase I trial, with phase II trials still expected to start (66). APL-2, a compstatin variant with an increased half-life due to adapted pegylation, has been successfully tested in PNH patients in phase I studies, with a phase III study on its way (66, 83).

Finding targets for complement therapeutics is not easy, as it is often unclear which of the many complement components is involved in the pathology of disease and the functions of the system are broad, meaning that side-effects of drugs interfering with the complement system are likely to occur. Furthermore, the plasma concentrations and turnover rate of the complement proteins are high and their production occurs at different sites in the body which can complicate drug delivery (4). The field of complement therapeutics has been evolving to solve these challenges, looking at complement regulators to prevent side-effects of targeting complement systemically. Here, we discuss

therapeutics based on complement regulators currently in the pipeline, and future possibilities to use the mechanisms of complement regulators in therapeutics (**Figure 3**).

Plasma-Derived and Recombinant Full-Length Complement Regulators

Full-length complement regulators can be therapeutically used to aid patients with deficiencies functional defects in their regulators. The best example of this approach is the use of C1-INH in hereditary angioedema. Hereditary angioedema is caused by a genetic C1-INH deficiency which can result in life-threatening edema from excessive bradykinin release (171, 172). The plasma-derived C1-INH can prevent angioedema attacks completely, providing a safe treatment option with no significant side effects (171, 173). Additionally, C1-INH has been recombinantly produced from the milk of transgenic New Zealand white rabbits (174). The recombinant and plasma-derived C1-INH did show comparable activity in hereditary angioedema, but the half-life of recombinant C1-INH was much shorter (171). This might pose a problem when using recombinant C1-INH for complement mediated diseases such as ischemia–reperfusion injury, acute myocardial infarction, autoimmune hemolytic anemia and renal transplantation (175–178).

Another complement regulator for which both a plasma-derived and a recombinant variant is in development is FH. As described, mutations of FH are clearly linked to development of complement-mediated renal diseases. As described above for aHUS, patients with functional FH mutations can be treated with plasma infusions. However, plasma infusions are not without risks, as they can lead to allergic reactions or fluid overload (179). Plasma-derived or recombinant FH could potentially be more purposeful in supplementing mutated non-functional FH. FH-deficient mice, mimicking C3 glomerulopathy, have been treated with human plasma-derived FH, resulting in a reduction in complement activity and C3 deposition on the glomerular basement membrane (180–182). Recombinant FH has been produced in insect cells, the yeast *Pichia pastoris*, mammalian HEK and COS7 cell lines (91, 183, 184). Although the produced proteins were biologically active, success was limited by low yield and aberrant glycosylation patterns. Currently, the most

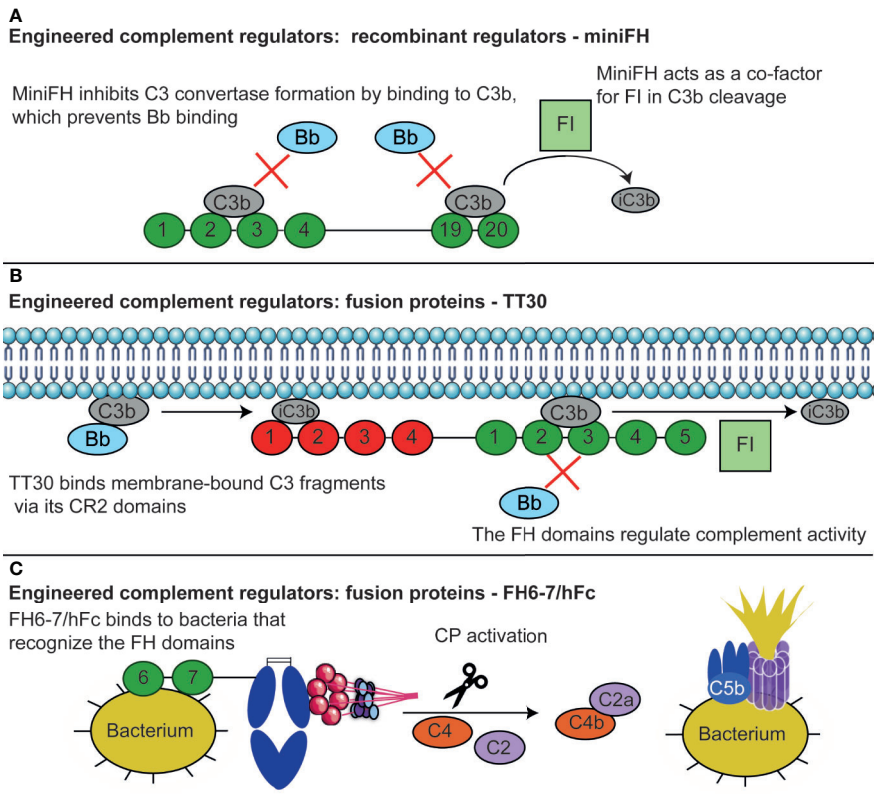

FIGURE 3 | Therapeutics based of complement regulators. **(A)** MiniFH has been designed from FH CCPs 1-4 and 19-20 to open up an extra C3b binding domain. This means it can bind two C3b molecules simultaneously, where regular FH can only bind one. MiniFH inhibits C3bBb formation and exert FI co-factor activity. **(B)** TT30 is a fusion protein of the first 4 domains of CR2 and the first 5 domains of FH. The CR2 domains recognize tissue-bound C3 fragments, while the FH domains regulate complement activity. Thus, the protein is targeted towards tissues where complement is already activated, where the FH domains can then exert complement regulatory activity. **(C)** FH6-7/hFc contains FH CCP 6 and 7, and the Fc part of an antibody. Certain bacteria bind FH *via* CCP FH6-7, normally to evade the complement system. These CCPs are utilized here to target these bacteria, upon which the hFc induces CP activation by C1q binding resulting in complement activation *via* the CP finally resulting in opsonization and lysis of bacteria. Figure designed using Servier Medical Art.

successful production of recombinant FH with full human glycosylation pattern has been achieved in the moss *Physcomitrella patens* (FHmoss) (185, 186). FHmoss has full biological activity and was shown to reduce complement activation and hemolysis in aHUS patient sera. Experiments in FH-deficient mice treated with FHmoss showed a reduction of glomerular C3 accumulation and AP activity. These experiments also showed that FHmoss is cleared from the circulation faster than plasma-derived FH and could not be detected anymore in plasma after 6 h, which is a potential obstacle for the clinical use of FHmoss (185). The success of the *P. patens* system has been further illustrated by the production of MFHR1, which is a recombinant regulator with domains from FH and FHR-1. This is a biologically stable protein that has an even stronger *in vitro* regulatory activity on the AP than FH (187).

Next to the fluid-phase regulators C1-INH and FH, recombinant soluble variants of membrane-bound regulators have been developed. While soluble CR1 (sCR1), CD46, CD55 and CD59 were all produced and tested successfully *in vitro* (188–190), only sCR1 has progressed to clinical trials (158). With regards to sCR1, two highly similar recombinant molecules have been designed (TP10 and TP20). Both are effective inhibitors of C3 and C5 convertases and were shown to prevent complement-mediated tissue damage in different animal models of vascular injury (158, 191). TP20 is a derivative of TP10 that contains Sialyl-Lewis X tetrasaccharide (sLe^x) groups to target it towards the endothelium *via* binding of E- and P-selectin receptors. This modification has made it more effective in *in vivo* models of cardiovascular and lung disease than TP10 (191, 192). Recently, TP10 has been clinically evaluated in several indications requiring cardiopulmonary bypass, as complement activity has been shown to play a role in the inflammatory response after acute myocardial infarction. Intravenous administration of TP10 reduced complications and mortality in male patients undergoing cardiopulmonary bypass, but not in female patients, although this gender difference was not caused by the complement suppressing effects of sCR1 (156). In lung transplantations, TP10 administration led to a shorter intubation time, although other clinical outcomes were not affected by TP10 (156). Taken together, use of full length complement regulators seems an efficient strategy. Use of plasma-derived proteins is limited due to the availability of plasma, while recombinant proteins struggle with a short half-life. In addition to the proteins described here, we could imagine the use of full length FI to be further explored, as it has been shown that plasma infusions are also successful in aHUS patients suffering from a mutation in FI (92, 193).

Engineered Complement Regulators

Apart from the variety of full-length complement regulators researched for therapeutic usage, engineered complement regulators are also under development. These proteins are recombinant complement regulators, but rather than being designed to mimic the human regulator as closely as possible, they are adapted to enhance their therapeutic effects (194). For FH, two engineered variants have been designed: miniFH and midiFH. MiniFH contains CCP 1-4 and 19-20 of FH, whilst midiFH is its duplicated variant, coupling two miniFH molecules with a short linker (**Figure 3A**). MiniFH was designed specifically to enhance C3b binding activity, as the CCPs masking the C-terminal C3b binding domain in full-length FH are deleted. Both proteins are more effective in decay accelerating activity than FH and FHL-1, but less effective in FI co-factor activity (195, 196). MidiFH outcompetes miniFH in the inhibition of AP activation, which can probably be explained by its extra C3b binding sites (195). Engineered variants of FH could be relevant in the treatment of PNH as *in vitro* studies already showed that both miniFH and midiFH are effective in protecting PNH erythrocytes from complement-mediated lysis (195, 197). The efficacy of miniFH could even be improved by introducing the dimerization domain of FHRs in the protein, which lead to the formation of homodimers and prolonged its half-life. These homomeric miniFHs have been tested *in vivo* in FH-deficient mice, where they showed a reduction in glomerular accumulation of C3 (198). Taken together, engineered complement regulators such a miniFH show promising results both *in vitro* as well as *in vivo*. To date, Amyndas has engineered a mini FH for which phase-1 clinical studies for treatment of AMD are planned (42).

A different approach to engineered complement regulators is the design of fusion proteins to optimally utilize their regulatory activity. Currently, fusion proteins have been described containing (parts of) CR1, CD55, CD46, and FH to target the AP, CP and/or the LP. Mirococept is a fusion molecule containing the first three CR1 SCRs, containing the complement regulatory activity, followed by an amphiphilic peptide that increases its affinity for cell surfaces. *In vitro*, Mirococept can inhibit C3 and C5 convertase activity similar to CR1 (199). Mirococept is also beneficial *in vivo*, which was demonstrated using rat models for intestinal ischaemia and reperfusion injury and for kidney transplantation (199, 200). Mirococept was shown to be safe in a phase I clinical trial, with a phase II clinical trial in kidney transplantations currently underway (201). To the best of our knowledge, the results of this trial have not been published yet (202).

TT30 is an FH and CR2 fusion protein that has been designed to selectively inhibit the AP locally at activation sites in order to minimize the risk of infection or autoimmune disease which could increase upon systemic complement inhibition (**Figure 3B**) (203). To this end CR2 domains were used, as CR2 only binds to the tissue-bound C3b breakdown products iC3b, C3dg, and C3d, thereby specifically acting at sites of complement activation on tissue. TT30 contains the first four CCPs of CR2, which bind to the C3b breakdown products, and the first five domains of FH, which regulate AP activity. *In vitro*, TT30 is effective in both inhibiting the C3 and C5 convertase. Next, subcutaneous administration of TT30 in cynomolgus monkeys showed almost complete inhibition of the AP, lasting up to 24 h, and partial inhibition of the CP (203).

The above-mentioned fusion proteins utilize CR1 and CR2, which mainly target the AP. Although the role of the AP has been well described in diseases as PNH and aHUS, it is not the only

complement pathway to think of when aiming to target the complement system with therapeutics. Recently, fusion proteins to target the LP were developed and suggested to have potential in the treatment of ischemia–reperfusion injury and delayed kidney graft function (204). These proteins consist of the first domains of CR1, CD55 or FH with MAP-1 or sMAP in order to inhibit LP activation at the C3 level and prevent MAC formation. MAP-1 and sMAP are alternative splice variants of MASP-1 and MASP-3 respectively, lacking the proteolytic site, thus binding to the pattern recognition molecules of the LP without inducing subsequent C2 and C4 cleavage (7, 205). MAP-1:CD55$^{1-4}$ and MAP-1:CD35$^{1-3}$ effectively inhibit the LP in *in vitro* assays that measured deposition of C3, C4, and MAC on mannan. The effects of MAP-1:CD55$^{1-4}$ were stronger, especially at the terminal pathway level. The root of this difference could not be pinpointed, although it was suggested to be caused by the absence of certain CD35 domains in MAP-1:CD35$^{1-3}$ that are normally involved in its co-factor activity (205). A different study fused full-length murine MAP-1, murine sMAP or human sMAP to the same FH domains. The murine MAP-1 FH fusion protein, MAp44-FH, showed only limited activity both *in vitro* and *in vivo*, while the murine sMAP-FH inhibited the activity of both the AP and LP. Human sMAP-FH showed an inhibitory effect on the AP and LP in human serum as well, which was stronger than the effect of the sMAP or FH domains separately (206). The stronger effect of sMAP-FH than of MAp44-FH could possibly be explained by their competition with MASPs to form complexes with the pattern recognition molecules. sMAP competes with MASP-2 for binding, while MAp44 competes with MASP-1 and -3. MASP-1 is 13.6 times more abundant in serum than MASP-2, which results in MASP-1 outcompeting MAp44-FH in serum at the studied concentrations, which were constant between MAp44-FH and sMAP-FH (206). To conclude, several LP inhibiting complement regulators have been engineered, of which the FH domain also targets the AP. The AP and LP both contribute to diseases as AMD and ischemia–reperfusion injuries, were MAP-1:CD55$^{1-4}$, MAP-1:CD35$^{1-3}$, and sMAP-FH could potentially aid in the treatment of such pathologies.

The last fusion protein composed of two different complement regulators to be described here is decay-cofactor protein (DCP), a fusion product of CD55 and CD46 (207) that was designed to target both the AP and CP. Different CCPs of CD55 and CD46 were combined into fusion proteins that would retain their inhibitory effect on CP and AP activation. A fusion protein of CD55 CCP2-3 and CD46 CCP3-4 showed the largest inhibitory activity *in vitro*, upon which DCP with maximal inhibitory effect was achieved by selecting the most effective mutant (207). Although successful inhibition of the AP and CP could be achieved *in vitro*, this protein has to this date not been tested *in vivo*.

Next to the fusions of complement proteins with the regulators, other fusion proteins contain (parts of) antibodies. Three different types of regulators fuse parts of antibodies with a complement regulator, which have been developed to target myasthenia gravis, the AP in several pathologies or bacterial infections respectively. Firstly, the fusion protein designed to treat myasthenia gravis contains CD55 and an antibody fragment. Myasthenia gravis is an autoantibody-mediated disease, where damage to neurons at the neuromuscular junction is enhanced by complement activity (208). The fusion protein to treat this disease consists of an scFv antibody fragment targeting the nicotine acetylcholine receptor, that did not affect ion channel function, and CD55, which would regulate complement activation on the neuron surface. This fusion protein induced a reduction in complement activation *in vitro* and reduced clinical severity *in vivo* (208, 209). Secondly, a fusion protein of CRIg and Fc of a murine IgG1 (CRIg-Fc) is a soluble version of CRIg and was designed to inhibit the AP selectively by binding to cells opsonized with antibodies and inhibiting C3 convertase (210, 211). Successful reduction of inflammation was shown *in vivo* in mouse models of experimental arthritis, ischemia/reperfusion injury and FH-deficient mice that mimick C3 glomerulopathy (210, 212, 213).

While most engineered proteins focus on inhibiting complement-mediated diseases, complement regulators can also be used in a different way. A fusion protein consisting of FH CCP 6 -7 and the Fc region of a human IgG is designed to treat bacterial infections by activating the complement system (**Figure 3C**). This protein makes clever use of the fact that pathogenic bacteria often bind to FH CCP 6-7 in order to evade the complement system (19). In addition, the Fc domain would then be able to initiate the CP by binding to C1q, which can in turn lead to C3b deposition and phagocytosis (214). This protein has been effective in enhancing complement-mediated killing *in vivo* for *Streptococcus pyogenes*, *Haemophilus influenzae* and *Neisseria meningitidis* (214–216). The increased killing of *S. pyogenes* upon FH6-7/hFC administration demonstrate that the protein can induce opsonophagocytosis, as this Gram-positive pathogen cannot be lysed by the MAC. Furthermore, FH6-7/hFc was also shown to outcompete FH for *S. pyogenes* binding, resulting in reduced complement evasion by the pathogen. This shows that the activating effect of FH6-7/hFC on the complement system is two-fold: it reduces complement evasion by outcompeting FH for binding, and it initiates more complement activation by binding to C1q (215).

Altogether, the engineered complement regulators are designed to enhance therapeutic efficacy of the regulators with two main aims. The engineered regulators are either designed to increase the regulatory power of the original protein, or they are designed to be targeted to a specific tissue and prevent systemic effects. These engineered regulators have shown promising results in a range of *in vivo* studies, although most have not been evaluated clinically to this date.

Potentiating and Inhibiting Complement Regulation Using Antibodies

Next to the use of plasma-derived and full-length regulators and the development of engineered therapeutics, we here discuss the therapeutic use of antibodies. While those antibodies are mainly used in development of cancer therapeutics, as will be described below, we have recently developed an antibody that could be

used to treat complement-mediated aHUS. The anti-FH antibodies anti-FH.07 and FH07.1 are designed to potentiate the regulatory function of FH. The antibodies bind to FH domain 18, and enhance its activity specifically on human cells. Hence, these antibodies have the potential as a therapeutic in aHUS, especially in patients that suffer from FH dysfunction. This could be an alternative to eculizumab, which has the disadvantage of inhibiting complement activity against pathogens as well. This antibody can restore FH activity in aHUS patient sera (217). In addition, we recently showed that this potentiating antibody not only potentiates wild type FH, but also four common aHUS mutated FHs *in vitro* (218).

Most antibodies that are currently developed to target complement regulators are used to target these in cancer. As discussed above, complement regulatory proteins are often highly expressed on tumor cells and have been described to compromise the efficiency of antibody-based immunotherapies. This has raised the interests in finding blocking antibodies for the complement regulators. The effects of these antibodies can be twofold: either, complement regulators can be targeted with immunotherapy, as they are specifically upregulated in certain tumor cells, or, they can be targeted to block their function and make the tumor cells more susceptible to complement-mediated killing (**Figure 4**) (149, 154, 219, 220). However, targeting complement regulators with antibodies is not without risk. As described in the previous section, different membrane-bound regulators seem to be differentially expressed on tumor cells, but where some studies show upregulation of complement regulators, others do not. This means that usage of these antibodies would require a personalized medicine approach, in which the tumor is first extensively characterized before a drug is selected for a specific patient. More importantly, the regulators are also expressed on many other cell types throughout the body. Several studies have shown successful usage of neutralizing CD55 or CD59 antibodies in colon cancer or NSCLC, but these were investigated in cell lines or in mouse xenograft models. Here, antibodies directed against the human regulators would give rise to only very limited off-target effects, as the antibodies will only minimally recognize the mouse homologs (149, 221, 222). In addition to complement regulatory inhibiting antibodies, oligonucleotides such as anti-sense phosphorothioate oligonucleotides (S-ODNs) and small interfering RNAs (siRNAs) have been designed to silence to complement regulators. Successful silencing has been shown *in vitro*, but further developments with regards to their stability and targeting *in vivo* are still required (219, 220)

The prevention of healthy host cell targeting by these complement regulator-targeted antibodies and oligonucleotides is one of the main challenges in developing such therapeutics, as inhibiting complement regulators on healthy cells is undesirable. By administering antibodies that solely target complement regulators, a dangerous situation could arise where healthy cells expressing complement regulators are also targeted by the antibody. This poses a serious challenge for this therapeutic approach, as all healthy cells express complement regulators and most complement regulators are expressed by a majority of cells. Several possibilities are under investigation to circumvent this problem, such as bispecific antibodies or a biotin–avidin system, or circumventing the usage of antibodies altogether (220). Firstly, the bispecific antibodies are composed of Fabs of two different monoclonal antibodies: one that recognizes a complement regulator, and another that targets a tumor-specific antigen. These showed to be promising in animal models, but have not been clinically tested yet (220, 223, 224). Another possible strategy is to use a biotin–avidin system, which combines biotin-labeled mini-antibodies against CD55 and CD59 with biotin-rituximab, which targets CD20, and avidin. The mini-antibodies do not work independently, but only when combined with biotin-rituximab *via* avidin. This was shown to be effective in an *in vivo* model of B-cell lymphoma (225).

Summarizing, one potentiating antibody for a complement regulator has been successfully produced, targeting FH. The development of complement regulator inhibiting antibodies to be used as a cancer therapeutic is however still in its infancy. Several practical challenges remain to be overcome in order to test these antibodies in the clinic.

DISCUSSION

In conclusion, this review described the wide range of human pathologies involving complement regulators. Most of the pathologies identified affect tissues where complement or complement regulation is organized in a different way than in the rest of the body, such as the kidney, eyes and brain (28, 81, 122). The role of complement regulators in cancer was also discussed, however, there is no consensus yet on the role of complement itself in cancer (137–139) and the current evidence does not allow us to make a general statement about the role of complement regulators in cancer, which seems to differ per cancer type.

All in all, a diverse group of complement regulatory therapeutics is currently in development (4, 42, 164). There are however still challenges to overcome before these therapeutics can be used in the clinic. Although the effects of plasma-derived and recombinant molecules are highly similar, with recombinant molecules easier to produce, a shortcoming of the recombinant regulators is that their half-life is often much shorter (171, 185), which might hinder their clinical applications. In addition, the targeting or inhibiting of complement regulatory proteins in cancer is still in its infancy. Although some promising results have been shown *in vitro* and *in vivo* (149, 154, 219–221), current knowledge on expression and role of the regulators in different tumor types is lacking, which should be further clarified to develop future therapeutics. However, other drugs have found clever ways to ensure specificity of the complement regulatory effect, as has been described for the fusion proteins. The therapeutics described here have not been clinically evaluated, with the exception of recombinant soluble CR1, which would be interesting possibilities for future research (156). Their clinical success remains to be seen, as for most pathologies described in this paper targeting the complement system has not yet been proven a successful strategy. An interesting point of contention is whether this lack of success can be contributed to the specific

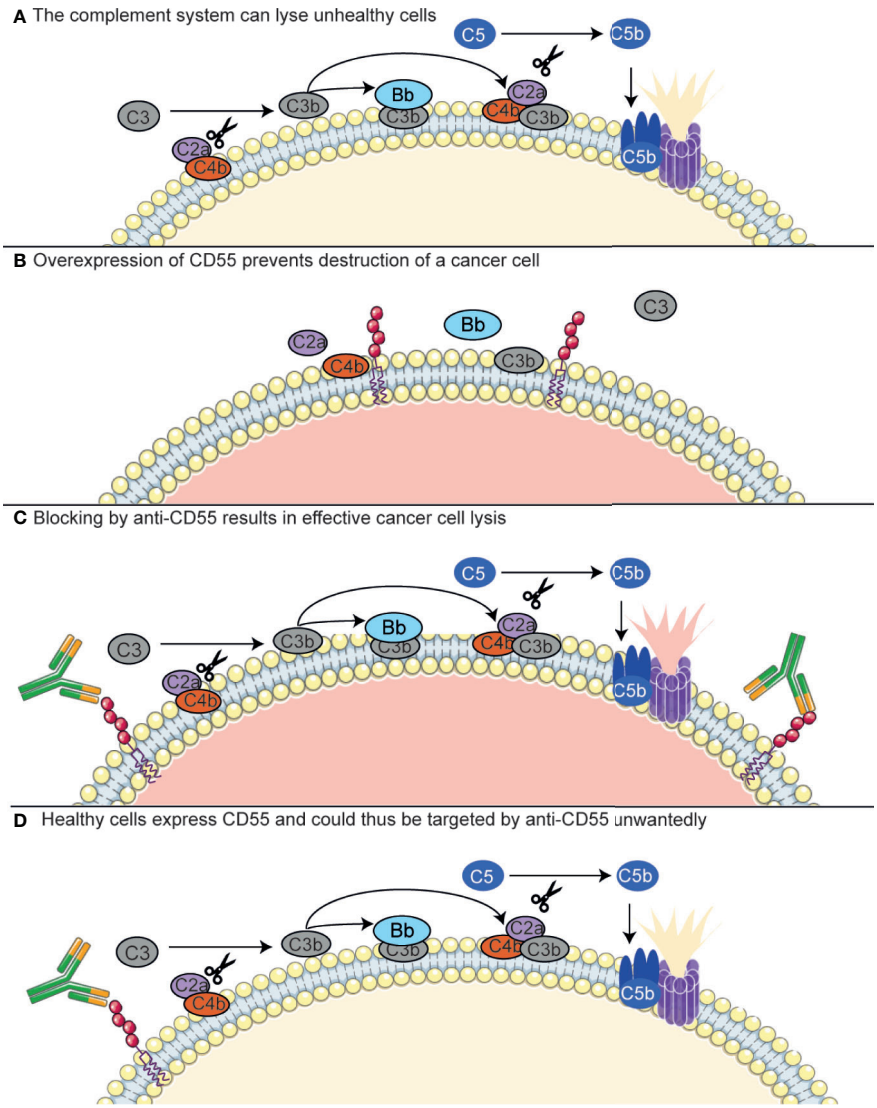

FIGURE 4 | Antibodies targeting complement regulators. Antibodies targeting complement regulators can be used as immunotherapy in cancer, as some cancer types upregulate these regulators. CD55 has been shown to be overexpressed in NSCLC and colon cancer. **(A)** The complement system contributes to killing of unhealthy cells, such as cancer cells, both *via* lysis by the MAC and opsonization inducing phagocytosis (not depicted here). For MAC-mediated lysis, the complement system depends on C5 convertase (CP convertase depicted here) formation. **(B)** Cancer cells overexpressing CD55 are protected from the complement system, as CD55 has a decay accelerating activity on the C3 convertases. **(C)** An anti-CD55 antibody targets the CD55-overexpressing cancer cells and inhibits the complement regulatory activity of CD55. Thus, the cancer cells are resensitized to the complement system. **(D)** Healthy cells, conventionally expressing CD55, can also be targeted by anti-CD55 and lysed unwantedly. Figure designed using Servier Medical Art.

complement modulators used in previous studies, for example in AMD, or whether a different treatment strategy should be pursued altogether.

The current research also indicates some starting points for the development of future therapeutics, if the abovementioned limitations with regards to specificity and half-time can be overcome. One clear shortcoming of the currently available therapeutics, is that there is no possibility to target the complement system at the C3 level specifically on the target tissue. As has been described above, there is a clear need for this in specific groups of PNH patients, that suffer from extravascular hemolysis under eculizumab treatment. Potentially, treatments based on complement regulatory proteins that target C3, could be a solution there, as for example FH-CR2, miniFH and anti-FH07 (197, 218). Next, the successful *in vivo* tests of FH-IgG chimeric proteins in bacterial infections, indicate that there might lie success in similar approaches using C4BP, C1-INH or Vn, which all are used by bacteria in complement evasion mechanisms (19). Lastly, future research could focus at the development of plasma-purified complement regulators other than C1-INH. Successful plasma-purification could especially be useful for FH and FI, of which mutations have been shown to

affect several eye and kidney diseases and of which recombinant variants have not yet been successfully tested in a clinical setting (106, 226).

To conclude, we have described the significant role of complement regulators in a broad range of diseases. Currently, there are many therapeutics under development that use complement regulators, ranging from full-length and engineered regulators to antibodies targeting complement regulators. Altogether, the current research shows several promising directions for future clinical studies and applications of complement therapeutics based on regulators.

AUTHOR CONTRIBUTIONS

All authors contributed to the article and approved the submitted version.

FUNDING

This work is part of the research programme Aspasia with project number 015.014.069, which is (partly) financed by the Netherlands Organisation for Scientific Research (NWO).

REFERENCES

1. Ehrnthaller C, Ignatius A, Gebhard F, Huber-Lang M. New insights of an old defense system: Structure, function, and clinical relevance of the complement system. *Mol Med* (2011) 17(3–4):317–29. doi: 10.2119/molmed.2010.00149
2. Nesargikar P, Spiller B, Chavez R. The complement system: History, pathways, cascade and inhibitors. *Eur J Microbiol Immunol* (2012) 2 (2):103–11. doi: 10.1556/EuJMI.2.2012.2.2
3. Merle NS, Church SE, Fremeaux-Bacchi V, Roumenina LT. Complement system part I - molecular mechanisms of activation and regulation. *Front Immunol* (2015) 6:1–30. doi: 10.3389/fimmu.2015.00262
4. Harris CL. Expanding horizons in complement drug discovery: challenges and emerging strategies. *Semin Immunopathol* (2017) 40(1):125–40. doi: 10.1007/s00281-017-0655-8
5. Ricklin D, Hajishengallis G, Yang K, Lambris JD. Complement: A key system for immune surveillance and homeostasis. *Nat Immunol* (2010) 11 (9):785–97. doi: 10.1038/ni.1923
6. Mathern DR, Heeger PS. Molecules great and small: The complement system. *Clin J Am Soc Nephrol* (2015) 10(9):1636–50. doi: 10.2215/CJN.06230614
7. Garred P, Genster N, Pilely K, Bayarri-Olmos R, Rosbjerg A, Ma YJ, et al. A journey through the lectin pathway of complement—MBL and beyond. *Immunol Rev* (2016) 274(1):74–97. doi: 10.1111/imr.12468
8. Bexborn F, Andersson PO, Chen H, Nilsson B, Ekdahl KN. The tick-over theory revisited: Formation and regulation of the soluble alternative complement C3 convertase (C3(H2O)Bb). *Mol Immunol* (2008) 45 (8):2370–9. doi: 10.1016/j.molimm.2007.11.003
9. Harboe M, Ulvund G, Vien L, Fung M, Mollnes TE. The quantitative role of alternative pathway amplification in classical pathway induced terminal complement activation. *Clin Exp Immunol* (2004) 138(3):439–46. doi: 10.1111/j.1365-2249.2004.02627.x
10. Harboe M, Garred P, Karlstrøm E, Lindstad JK, Stahl GL, Mollnes TE. The down-stream effects of mannan-induced lectin complement pathway activation depend quantitatively on alternative pathway amplification. *Mol Immunol* (2009) 47(2–3):373–80. doi: 10.1016/j.molimm.2009.09.005
11. Merle NS, Noe R, Halbwachs-Mecarelli L, Fremeaux-Bacchi V, Roumenina LT. Complement system part II: Role in immunity. *Front Immunol* (2015) 6 (MAY):1–26. doi: 10.3389/fimmu.2015.00257
12. West EE, Kunz N, Kemper C. Complement and human T cell metabolism: location, location, location. *Immunol Rev* (2020) 295(1):68–81. doi: 10.1111/imr.12852
13. West EE, Kemper C. Complement and T Cell Metabolism: Food for Thought. *Immunometabolism* (2019) 1(T Cell Metabolic Reprogramming): e190006. doi: 10.1111/imr.12852
14. Liszewski MK, Kolev M, Le Friec G, Leung M, Bertram PG, Fara AF, et al. Intracellular Complement Activation Sustains T Cell Homeostasis and Mediates Effector Differentiation. *Immunity* (2013) 39(6):1143–57. doi: 10.1016/j.immuni.2013.10.018
15. Trouw LA, Blom AM, Gasque P. Role of complement and complement regulators in the removal of apoptotic cells. *Mol Immunol* (2008) 45:1199–207. doi: 10.1016/j.molimm.2007.09.008
16. Silverman SM, Ma W, Wang X, Zhao L, Wong WT. C3- And CR3-dependent microglial clearance protects photoreceptors in retinitis pigmentosa. *J Exp Med* (2019) 216(8):1925–43. doi: 10.1084/jem.20190009
17. Veerhuis R, Nielsen HM, Tenner AJ. Complement in the brain. *Mol Immunol* (2011) 48(14):1592–603. doi: 10.1016/j.molimm.2011.04.003
18. Ojha H, Ghosh P, Singh Panwar H, Shende R, Gondane A, Mande SC, et al. Spatially conserved motifs in complement control protein domains determine functionality in regulators of complement activation-family proteins. *Commun Biol* (2019) 2(1):1–12. doi: 10.1038/s42003-019-0529-9
19. Hovingh ES, van den Broek B, Jongerius I. Hijacking complement regulatory proteins for bacterial immune evasion. *Front Microbiol* (2016) 7(DEC):1–20. doi: 10.3389/fmicb.2016.02004
20. Ermert D, Ram S, Laabei M. The hijackers guide to escaping complement: Lessons learned from pathogens. *Mol Immunol* (2019) 114:49–61. doi: 10.1016/j.molimm.2019.07.018
21. Nilsson SC, Sim RB, Lea SM, Fremeaux-Bacchi V, Blom AM. Complement factor I in health and disease. *Mol Immunol* (2011) 48:1611–20. doi: 10.1016/j.molimm.2011.04.004
22. Zipfel PF, Skerka C. Complement regulators and inhibitory proteins. *Nat Rev Immunol* (2009) 9(10):729–40. doi: 10.1038/nri2620
23. Davis AE, Mejia P, Lu F. Biological activities of C1 inhibitor. *Mol Immunol* (2008) 45:4057–63. doi: 10.1016/j.molimm.2008.06.028
24. Zeerleder S. C1-inhibitor: More than a serine protease inhibitor. *Semin Thromb Hemost* (2011) 37(4):362–74. doi: 10.1055/s-0031-1276585
25. Blaum BS, Hannan JP, Herbert AP, Kavanagh D, Uhrín D, Stehle T. Structural basis for sialic acid-mediated self-recognition by complement factor H. *Nat Chem Biol* (2015) 11(1):77–82. doi: 10.1038/nchembio.1696
26. Parente R, Clark SJ, Inforzato A, Day AJ. Complement factor H in host defense and immune evasion. *Cell Mol Life Sci* (2017) 74:1605–24. doi: 10.1007/s00018-016-2418-4
27. Dopler A, Guntau L, Harder MJ, Palmer A, Höchsmann B, Schrezenmeier H, et al. Self versus Nonself Discrimination by the Soluble Complement Regulators Factor H and FHL-1. *J Immunol* (2019) 202(7):2082–94. doi: 10.4049/jimmunol.1801545
28. Clark SJ, Schmidt CQ, White AM, Hakobyan S, Morgan BP, Bishop PN. Identification of Factor H–like Protein 1 as the Predominant Complement Regulator in Bruch's Membrane: Implications for Age-Related Macular Degeneration. *J Immunol* (2014) 193(10):4962–70. doi: 10.4049/jimmunol.1401613
29. Skerka C, Chen Q, Fremeaux-Bacchi V, Roumenina LT. Complement factor H related proteins (CFHRs). *Mol Immunol [Internet]* (2013) 56(3):170–80. doi: 10.1016/j.molimm.2013.06.001
30. Józsi M. Factor H family proteins in complement evasion of microorganisms. *Front Immunol* (2017) 8:1–8. doi: 10.3389/fimmu.2017.00571
31. Józsi M, Tortajada A, Uzonyi B, Goicoechea de Jorge E, Rodríguez de Córdoba S. Factor H-related proteins determine complement-activating surfaces. *Trends Immunol* (2015) 36:374–84. doi: 10.1016/j.it.2015.04.008
32. Cipriani V, Lorés-Motta L, He F, Fathalla D, Tilakaratna V, McHarg S, et al. Increased circulating levels of Factor H-Related Protein 4 are strongly associated with age-related macular degeneration. *Nat Commun* (2020) 11 (1):1–15. doi: 10.1038/s41467-020-14499-3

33. Java A, Liszewski MK, Hourcade DE, Zhang F, Atkinson JP. Role of complement receptor 1 (CR1; CD35) on epithelial cells: A model for understanding complement-mediated damage in the kidney. *Mol Immunol* (2015) 67(2):584–95. doi: 10.1016/j.molimm.2015.07.016
34. Khera R, Das N. Complement Receptor 1: Disease associations and therapeutic implications. *Mol Immunol* (2009) 46:761–72. doi: 10.1016/j.molimm.2008.09.026
35. Ernst JD. Macrophage Receptors for Mycobacterium tuberculosis. *Infect Immun* (1998) 66(4):1277–81. doi: 10.1128/IAI.66.4.1277-1281.1998
36. Liszewski MK, Kemper C. Complement in Motion: The Evolution of CD46 from a Complement Regulator to an Orchestrator of Normal Cell Physiology. *J Immunol* (2019) 203(1):3–5. doi: 10.4049/jimmunol.1900527
37. Ni Choileain S, Astier AL. CD46 processing: A means of expression. *Immunobiology* (2012) 217:169–75. doi: 10.1016/j.imbio.2011.06.003
38. Small AG, Al-Baghdadi M, Quach A, Hii C, Ferrante A. Complement receptor immunoglobulin: a control point in infection and immunity, inflammation and cancer. *Swiss Med Wkly* (2016) 146(April):w14301. doi: 10.4414/smw.2016.14301
39. He JQ, Wiesmann C, van Lookeren Campagne M. A role of macrophage complement receptor CRIg in immune clearance and inflammation. *Mol Immunol* (2008) 45(16):4041–7. doi: 10.1016/j.molimm.2008.07.011
40. Kim DD, Song WC. Membrane complement regulatory proteins. *Clin Immunol* (2006) 118(2–3):127–36. doi: 10.1016/j.clim.2005.10.014
41. Zelek WM, Xie L, Morgan BP, Harris CL. Compendium of current complement therapeutics. *Mol Immunol* (2019) 114(July):341–52. doi: 10.1016/j.molimm.2019.07.030
42. Harris CL, Pouw RB, Kavanagh D, Sun R, Ricklin D. Developments in anti-complement therapy; from disease to clinical trial. *Mol Immunol* (2018) 102 (May):89–119. doi: 10.1016/j.molimm.2018.06.008
43. Kawai T, Takeshita S, Imoto Y, Matsumoto Y, Sakashita M, Suzuki D, et al. Associations between decay-accelerating factor polymorphisms and allergic respiratory diseases. *Clin Exp Allergy* (2009) 39(10):1508–14. doi: 10.1111/j.1365-2222.2009.03316.x
44. Vogt SD, Curcio CA, Wang L, Li CM, McGwin G, Medeiros NE, et al. Retinal pigment epithelial expression of complement regulator CD46 is altered early in the course of geographic atrophy. *Exp Eye Res* (2011) 93 (4):413–23. doi: 10.1016/j.exer.2011.06.002
45. Goetzl EJ, Yaffe K, Peltz CB, Ledreux A, Gorgens K, Davidson B, et al. Traumatic brain injury increases plasma astrocyte-derived exosome levels of neurotoxic complement proteins. *FASEB J* (2020) 34(2):3359–66. doi: 10.1096/fj.201902842R
46. Mohlin FC, Mercier E, Fremeaux-Bacchi V, Liszewski MK, Atkinson JP, Gris JC, et al. Analysis of genes coding for CD46, CD55, and C4b-binding protein in patients with idiopathic, recurrent, spontaneous pregnancy loss. *Eur J Immunol* (2013) 43(6):1617–29. doi: 10.1002/eji.201243196
47. de Vries MA, Trompet S, Mooijaart SP, Smit RAJ, Böhringer S, Castro Cabezas M, et al. Complement receptor 1 gene polymorphisms are associated with cardiovascular risk. *Atherosclerosis* (2017) 257:16–21. doi: 10.1016/j.atherosclerosis.2016.12.017
48. Kardys I, Klaver CCW, Despriet DDG, Bergen AAB, Uitterlinden AG, Hofman A, et al. A Common Polymorphism in the Complement Factor H Gene Is Associated With Increased Risk of Myocardial Infarction. The Rotterdam Study. *J Am Coll Cardiol* (2006) 47(8):1568–75. doi: 10.1016/j.jacc.2005.11.076
49. Nishio N, Teranishi M, Uchida Y, Sugiura S, Ando F, Shimokata H, et al. Contribution of complement factor H Y402H polymorphism to sudden sensorineural hearing loss risk and possible interaction with diabetes. *Gene* (2012) 499(1):226–30. doi: 10.1016/j.gene.2012.02.027
50. Zorzetto M, Ferrarotti I, Trisolini R, Agli LL, Scabini R, Novo M, et al. Complement receptor 1 gene polymorphisms are associated with idiopathic pulmonary fibrosis. *Am J Respir Crit Care Med* (2003) 168(3):330–4. doi: 10.1164/rccm.200302-221OC
51. Banadakoppa M, Balakrishnan M, Yallampalli C. Common variants of fetal and maternal complement genes in preeclampsia: pregnancy specific complotype. *Sci Rep* (2020) 10(1):1–9. doi: 10.1038/s41598-020-60539-9
52. Asimakopoulos JV, Terpos E, Papageorgiou L, Kampouropoulou O, Christoulas D, Giakoumis A, et al. The presence of CD55- and/or CD59-deficient erythrocytic populations in patients with rheumatic diseases reflects an immunemediated bone-marrow derived phenomenon. *Med Sci Monit* (2014) 20:123–39. doi: 10.12659/MSM.889727
53. Zhou Y, Wang J, Wang K, Li S, Song X, Ye Y, et al. Association analysis between the rs11136000 single nucleotide polymorphism in clusterin gene, rs3851179 single nucleotide polymorphism in clathrin assembly lymphoid myeloid protein gene and the patients with schizophrenia in the Chinese population. *DNA Cell Biol* (2010) 29(12):745–51. doi: 10.1089/dna.2010.1075
54. Flegel WA. Pathogenesis and mechanisms of antibody-mediated hemolysis. *Transfusion* (2015) 55(July):S47–58. doi: 10.1111/trf.13147
55. Rosti V. The molecular basis of paroxysmal nocturnal hemoglobinuria. *Hametologica* (2000) 85:82–7. doi: 10.3324/%25x
56. Takeda J, Miyata T, Kawagoe K, Iida Y, Endo Y, Fujita T, et al. Deficiency of the GPI anchor caused by a somatic mutation of the PIG-A gene in paroxysmal nocturnal hemoglobinuria. *Cell* (1993) 73(4):703–11. doi: 10.1016/0092-8674(93)90250-T
57. Lee SCW, Abdel-Wahab O. The mutational landscape of paroxysmal nocturnal hemoglobinuria revealed: New insights into clonal dominance. *J Clin Invest* (2014) 124(10):4227–30. doi: 10.1172/JCI77984
58. Brodsky RA, Young NS, Antonioli E, Risitano AM, Schrezenmeier H, Gaya A, et al. Multicenter phase 3 study of eculizumab for the treatment of PNH. *Blood* (2008) 111(4):1840–7. doi: 10.1182/blood-2007-06-094136
59. Hillmen P, Young NS, Schubert J, Brodsky RA, Socié G, Muus P, et al. The complement inhibitor eculizumab in paroxysmal nocturnal hemoglobinuria. *N Engl J Med* (2006) 355(12):1233–43. doi: 10.1056/NEJMoa061648
60. Socié G, Caby-Tosi MP, Marantz JL, Cole A, Bedrosian CL, Gasteyger C, et al. Eculizumab in paroxysmal nocturnal haemoglobinuria and atypical haemolytic uraemic syndrome: 10-year pharmacovigilance analysis. *Br J Haematol* (2019) 185(2):297–310. doi: 10.1111/bjh.15790
61. Nishimura JI, Yamamoto M, Hayashi S, Ohyashiki K, Ando K, Brodsky AL, et al. Genetic variants in C5 and poor response to eculizumab. *N Engl J Med* (2014) 370(7):632–9. doi: 10.1056/NEJMoa1311084
62. Lin Z, Schmidt CQ, Koutsogiannaki S, Ricci P, Risitano AM, Lambris JD, et al. Complement C3dg-mediated erythrophagocytosis: Implications for paroxysmal nocturnal hemoglobinuria. *Blood* (2015) 126(7):891–4. doi: 10.1182/blood-2015-02-625871
63. Rondelli T, Risitano AM, de Latour RP, Sica M, Peruzzi B, Ricci P, et al. Polymorphism of the complement receptor 1 gene correlates with the hematologic response to eculizumab in patients with paroxysmal nocturnal hemoglobinuria. *Haematologica* (2014) 99(2):262–6. doi: 10.3324/haematol.2013.090001
64. Baas I, Delvasto-Nuñez L, Ligthart, Peter Brouwer C, Folman C, Reis ES, et al. Complement C3 inhibition by compstatin Cp40 prevents intra- and extravascular hemolysis of red blood cells. *Haemotologica* (2020) 105 (57):471–3. doi: 10.3324/haematol.2019.216028
65. Mastellos DC, Yancopoulou D, Kokkinos P, Huber-Lang M, Hajishengallis G, Biglarnia AR, et al. Compstatin: A C3-targeted complement inhibitor reaching its prime for bedside intervention. *Eur J Clin Invest* (2015) 45:423–40. doi: 10.1111/eci.12419
66. Risitano AM, Marotta S, Ricci P, Marano L, Frieri C, Cacace F, et al. Anti-complement Treatment for Paroxysmal Nocturnal Hemoglobinuria: Time for proximal complement inhibition? A position paper from the SAAWP of the EBMT. *Front Immunol* (2019) 10(4):43–52. doi: 10.3389/fimmu.2019.01157
67. Haliloglu G, Maluenda J, Sayinbatur B, Aumont C, Temucin C, Tavil B, et al. Early-onset chronic axonal neuropathy, strokes, and hemolysis. *Neurology* (2015) 84:1220–4. doi: 10.1212/WNL.0000000000001391
68. Karbian N, Eshed-Eisenbach Y, Tabib A, Hoizman H, Paul Morgan B, Schueler-Furman O, et al. Molecular pathogenesis of human CD59 deficiency. *Neurol Genet* (2018) 4(6):1–9. doi: 10.1212/NXG.0000000000000280
69. Lublin DM. Cromer and DAF: role in health and disease. *Immunohematology* (2005) 21(2):39–47.
70. Hue-Roye K, Powell VI, Patel G, Lane D, Maguire M, Chung A, et al. Novel molecular basis of an Inab phenotype. *Immunohematology* (2005) 21(2):53–5.
71. Holguin MH, Martin CB, Bernshaw NJ, Parker CJ. Analysis of the effects of activation of the alternative pathway of complement on erythrocytes with an isolated deficiency of decay accelerating factor. *J Immunol* (1992) 148 (2):498–502.

72. Kurolap ARN, Eshach-Adiv O, Hershkovitz T, Paperna T, Mory A, Oz-Levi D, et al. Loss of CD55 in Eculizumab-Responsive Protein-Losing Enteropathy. *N Engl J Med* (2017) 377:87–9. doi: 10.1056/NEJMc1707173
73. Ozen A, Comrie WA, Ardy RC, Conde CD, Dalgic B, Beser ÖF, et al. CD55 deficiency, early-onset protein-losing enteropathy, and thrombosis. *N Engl J Med* (2017) 377(1):52–61. doi: 10.1056/NEJMoa1615887
74. Ozen A. CHAPLE syndrome uncovers the primary role of complement in a familial form of Waldmann's disease. *Immunol Rev* (2019) 287(1):20–32. doi: 10.1111/imr.12715
75. Shichishima T, Saitoh Y, Terasawa T, Noji H, Kai T, Maruyama Y. Complement sensitivity of erythrocytes in a patient with inherited complete deficiency of CD59 or with the Inab phenotype. *Br J Haematol* (1999) 104(2):303–6. doi: 10.1046/j.1365-2141.1999.01188.x
76. Mohandas N. Inherited hemolytic anemia: A possessive beginner's guide. *Hematology* (2018) 2018(1):377–81. doi: 10.1182/asheducation-2018.1.377
77. Wastnedge E, Waters D, Patel S, Morrison K, Goh MY, Adeloye D, et al. The global burden of sickle cell disease in children under five years of age: A systematic review and meta-analysis. *J Glob Health* (2018) 8(2):1–9. doi: 10.7189/jogh.08.021103
78. Loniewska-Lwowska A, Koza K, Mendek-Czajkowska E, Wieszczy P, Adamowicz-Salach A, Branicka K, et al. Diminished presentation of complement regulatory protein CD55 on red blood cells from patients with hereditary haemolytic anaemias. *Int J Lab Hematol* (2018) 40(2):128–35. doi: 10.1111/ijlh.12752
79. Al-Faris L, Al-Rukhayes M, Al-Humood S. Expression pattern of CD55 and CD59 on red blood cells in sickle cell disease. *Hematology* (2017) 22(2):105–13. doi: 10.1080/10245332.2016.1231988
80. Roumenina LT, Chadebech P, Bodivit G, Vieira-Martins P, Grunenwald A, Boudhabhay I, et al. Complement activation in sickle cell disease: Dependence on cell density, hemolysis and modulation by hydroxyurea therapy. *Am J Hematol* (2020) 95(5):456–64. doi: 10.1002/ajh.25742
81. De Vriese AS, Sethi S, Van Praet J, Nath KA, Fervenza FC. Kidney disease caused by dysregulation of the complement alternative pathway: An etiologic approach. *J Am Soc Nephrol* (2015) 26(12):2917–29. doi: 10.1681/ASN.2015020184
82. Jayadev R, Sherwood DR. Basement membranes. *Curr Biol* (2017) 27(6):R207–11. doi: 10.1016/j.cub.2017.02.006
83. Wong EKS, Kavanagh D. Diseases of complement dysregulation—an overview. *Semin Immunopathol* (2018) 40(1):49–64. doi: 10.1007/s00281-017-0663-8
84. Raina R, Krishnappa V, Blaha T, Kann T, Hein W, Burke L, et al. Atypical Hemolytic-Uremic Syndrome: An Update on Pathophysiology, Diagnosis, and Treatment. *Ther Apher Dial* (2019) 23(1):4–21. doi: 10.1111/1744-9987.12763
85. De Córdoba SR. aHUS: A disorder with many risk factors. *Blood* (2010) 115(2):158–60. doi: 10.1182/blood-2009-11-252627
86. Nester CM, Barbour T, de Cordoba SR, Dragon-Durey MA, Fremeaux-Bacchi V, Goodship THJ, et al. Atypical aHUS: State of the art. *Mol Immunol [Internet]* (2015) 67(1):31–42. doi: 10.1016/j.molimm.2015.03.246
87. Arjona E, Huerta A, Goicoechea De Jorge E, Rodríguez de Córdoba S. The familial risk of developing atypical Hemolytic Uremic Syndrome. *Blood* (2020) 136(13):1558–61. doi: 10.1182/blood.2020006931
88. Urban A, Volokhina E, Felberg A, Stasiłojć G, Blom AM, Jongerius I, et al. Gain-of-function mutation in complement C2 protein identified in a patient with aHUS. *J Allergy Clin Immunol* (2020) 146(4):1–4 doi: 10.1016/j.jaci.2020.02.014
89. Moore I, Strain L, Pappworth I, Kavanagh D, Barlow PN, Herbert AP, et al. Association of factor H autoantibodies with deletions of CFHR1, CFHR3, CFHR4, and with mutations in CFH, CFI, CD46, and C3 in patients with atypical hemolytic uremic syndrome. *Blood* (2010) 115(2):379–87. doi: 10.1182/blood-2009-05-221549
90. Strobel S, Dahse H, Liu W, Hoyer PF, Oppermann M, Skerka C, et al. Brief report Anti – factor H autoantibodies block C-terminal recognition function of factor H in hemolytic uremic syndrome. *Blood* (2007) 110(5):1516–8. doi: 10.1182/blood-2007-02-071472
91. Sánchez-Corral P, Pérez-Caballero D, Huarte O, Simckes AM, Goicoechea E, López-Trascasa M, et al. Structural and functional characterization of factor H mutations associated with atypical hemolytic uremic syndrome. *Am J Hum Genet* (2002) 71(6):1285–95. doi: 10.1086/344515
92. Caprioli J, Noris M, Brioschi S, Pianetti G, Castelletti F, Bettinaglio P, et al. Genetics of HUS: The impact of MCP, CFH, and IF mutations on clinical presentation, response to treatment, and outcome. *Blood* (2006) 108(4):1267–79. doi: 10.1182/blood-2005-10-007252
93. Bajwa R, Depalma JA, Khan T, Cheema A, Kalathil SA, Hossain MA, et al. C3 Glomerulopathy and Atypical Hemolytic Uremic Syndrome: Two Important Manifestations of Complement System Dysfunction. *Case Rep Nephrol Dial* (2018) 8(1):25–34. doi: 10.1159/000486848
94. Servais A, Noël LH, Roumenina LT, Le Quintrec M, Ngo S, Dragon-Durey MA, et al. Acquired and genetic complement abnormalities play a critical role in dense deposit disease and other C3 glomerulopathies. *Kidney Int* (2012) 82(4):454–64. doi: 10.1038/ki.2012.63
95. Chauvet S, Roumenina LT, Bruneau S, Marinozzi MC, Rybkine T, Schramm EC, et al. A familial C3GN secondary to defective C3 regulation by complement receptor 1 and complement factor H. *J Am Soc Nephrol* (2016) 27(6):1665–77. doi: 10.1681/ASN.2015040348
96. Caravaca-Fontán F, Lucientes L, Cavero T, Praga M. Update on C3 Glomerulopathy: A Complement-Mediated Disease. *Nephron* (2020) 144(6):1–9. doi: 10.1159/000507254
97. Yeo SC, Liu X, Liew A. Complement factor H gene polymorphism rs6677604 and the risk, severity and progression of IgA nephropathy: A systematic review and meta-analysis. *Nephrology* (2018) 23(12):1096–106. doi: 10.1111/nep.13210
98. Webster AC, Nagler EV, Morton RL, Masson P. Chronic Kidney Disease. *Lancet* (2017) 389(10075):1238–52. doi: 10.1016/S0140-6736(16)32064-5
99. McClellan W, Aronoff SL, Bolton WK, Hood S, Lorber DL, Tang KL, et al. The prevalence of anemia in patients with chronic kidney disease. *Curr Med Res Opin* (2004) 20(9):1501–10. doi: 10.1185/030079904X2763
100. Al-Faris L, Al-Humood S, Behbehani F, Sallam H. Altered expression pattern of CD55 and CD59 on red blood cells in Anemia of Chronic Kidney Disease. *Med Princ Pract* (2018) 26(6):516–22. doi: 10.1159/000481823
101. Zhang G, Eddy AA. Urokinase and its receptors in chronic kidney disease. *Front Biosci* (2008) 13(14):5462–78. doi: 10.2741/3093
102. Clark SJ, McHarg S, Tilakaratna V, Brace N, Bishop PN. Bruch ' s Membrane compartmentalizes complement regulation in the eye with implications for Therapeutic Design in age-related Macular Degeneration. *Front Immunol* (2017) 8(December):1–10. doi: 10.3389/fimmu.2017.01778
103. Clark SJ, Bishop PN. The eye as a complement dysregulation hotspot. *Semin Immunopathol* (2018) 40(1):65–74. doi: 10.1007/s00281-017-0649-6
104. Geerlings MJ, de Jong EK, den Hollander AI. The complement system in age-related macular degeneration: A review of rare genetic variants and implications for personalized treatment. *Mol Immunol* (2017) 84:65–76. doi: 10.1016/j.molimm.2016.11.016
105. Toomey CB, Johnson LV, Bowes Rickman C. Complement factor H in AMD: Bridging genetic associations and pathobiology. *Prog Retin Eye Res* (2018) 62:38–57. doi: 10.1016/j.preteyeres.2017.09.001
106. Kavanagh D, Yu Y, Schramm EC, Triebwasser M, Wagner EK, Raychaudhuri S, et al. Rare genetic variants in the CFI gene are associated with advanced age-related macular degeneration and commonly result in reduced serum factor I levels. *Hum Mol Genet* (2015) 24(13):3861–70. doi: 10.1093/hmg/ddv091
107. Fritsche LG, Igl W, Bailey JNC, Grassmann F, Sengupta S, Bragg-Gresham JL, et al. A large genome-wide association study of age-related macular degeneration highlights contributions of rare and common variants. *Nat Genet* (2016) 48(2):134–43. doi: 10.1038/ng.3448
108. Hughes AE, Orr N, Esfandiary H, Diaz-Torres M, Goodship T, Chakravarthy U. A common CFH haplotype, with deletion of CFHR1 and CFHR3, is associated with lower risk of age-related macular degeneration. *Nat Genet* (2006) 38(10):1173–7. doi: 10.1038/ng1890
109. Sánchez-Corral P, Pouw RB, López-Trascasa M, Józsi M. Self-damage caused by dysregulation of the complement alternative pathway: Relevance of the factor H protein family. *Front Immunol* (2018) 9(JUL):1–19. doi: 10.3389/fimmu.2018.01607
110. Schäfer N, Grosche A, Reinders J, Hauck SM, Pouw RB, Kuijpers TW, et al. Complement regulator FHR-3 is elevated either locally or systemically in a

selection of autoimmune diseases. *Front Immunol* (2016) 7(NOV):1–16. doi: 10.3389/fimmu.2016.00542
111. Tekin K, Inanc M, Elgin U. Monitoring and management of the patient with pseudoexfoliation syndrome: Current perspectives. *Clin Ophthalmol* (2019) 13:453–64. doi: 10.2147/OPTH.S181444
112. Botling Taube A, Konzer A, Alm A, Bergquist J. Proteomic analysis of the aqueous humour in eyes with pseudoexfoliation syndrome. *Br J Ophthalmol* (2019) 103(8):1190–4. doi: 10.1136/bjophthalmol-2017-310416
113. Zenkel M, Kruse FE, Jünemann AG, Naumann GOH, Schlötzer-Schrehardt U. Clusterin Deficiency in Eyes with Pseudoexfoliation Syndrome May Be Implicated in the Aggregation and Deposition of Pseudoexfoliative Material. *Invest Ophthalmol Vis Sci* (2006) 47(5):1982–90. doi: 10.1167/iovs.05-1580
114. Wyatt AR, Yerbury JJ, Berghofer P, Greguric I, Katsifis A, Dobson CM, et al. Clusterin facilitates in vivo clearance of extracellular misfolded proteins. *Cell Mol Life Sci* (2011) 68(23):3919–31. doi: 10.1007/s00018-011-0684-8
115. Burdon KP, Sharma S, Hewitt AW, McMellon AE, Wang JJ, Mackey DA, et al. Genetic analysis of the clusterin gene in pseudoexfoliation syndrome. *Mol Vis* (2008) 14(August):1727–36.
116. Kuot A, Hewitt AW, Griggs K, Klebe S, Mills R, Jhanji V, et al. Association of TCF4 and CLU polymorphisms with Fuchs endothelial dystrophy and implication of CLU and TGFBI proteins in the disease process. *Eur J Hum Genet* (2012) 20(6):632–8. doi: 10.1038/ejhg.2011.248
117. Cheng CY, Schache M, Ikram MK, Young TL, Guggenheim JA, Vitart V, et al. Nine loci for ocular axial length identified through genome-wide association studies, including shared loci with refractive error. *Am J Hum Genet* (2013) 93(2):264–77. doi: 10.1016/j.ajhg.2013.06.016
118. Yoshikawa M, Yamashiro K, Miyake M, Oishi M, Akagi-Kurashige Y, Kumagai K, et al. Comprehensive replication of the relationship between myopia-related genes and refractive errors in a large Japanese cohort. *Invest Ophthalmol Vis Sci* (2014) 55(11):7343–54. doi: 10.1167/iovs.14-15105
119. Long Q, Ye J, Li Y, Wang S, Jiang Y. C-reactive protein and complement components in patients with pathological myopia. *Optom Vis Sci* (2013) 90 (5):501–6. doi: 10.1097/OPX.0b013e31828daa6e
120. Mohlin C, Sandholm K, Kvanta A, Ekdahl KN, Johansson K. A model to study complement involvement in experimental retinal degeneration. *Ups J Med Sci* (2018) 123(1):28–42. doi: 10.1080/03009734.2018.1431744
121. Lyzogubov VV, Bora PS, Wu X, Horn LE, de Roque R, Rudolf XR, et al. The Complement Regulatory Protein CD46 Deficient Mouse Spontaneously Develops Dry-Type Age-Related Macular Degeneration-Like Phenotype. *Am J Pathol* (2016) 186(8):2088–2104. doi: 10.1016/j.ajpath.2016.03.021
122. Morgan BP. Complement in the pathogenesis of Alzheimer's disease. *Semin Immunopathol* (2018) 40(1):113–24. doi: 10.1007/s00281-017-0662-9
123. Lee JD, Coulthard LG, Woodruff TM. Complement dysregulation in the central nervous system during development and disease. *Semin Immunol* (2019) 45(June):1–13. doi: 10.1016/j.smim.2019.101340
124. Foster EM, Dangla-Valls A, Lovestone S, Ribe EM, Buckley NJ. Clusterin in Alzheimer's disease: Mechanisms, genetics, and lessons from other pathologies. *Front Neurosci* (2019) 13(FEB):1–27. doi: 10.3389/fnins.2019.00164
125. Yang J, Wise L, Fukuchi KI. TLR4 Cross-Talk With NLRP3 Inflammasome and Complement Signaling Pathways in Alzheimer's Disease. *Front Immunol* (2020) 11(April):1–16. doi: 10.3389/fimmu.2020.00724
126. Misra A, Charkabati SS, Gambhir IS. New genetic players in late-onset Alzheimer's disease: Findings of genome-wide association studies. *Indian J Med Res* (2018) 148):135–44. doi: 10.4103/ijmr.IJMR_473_17
127. Lambert JC, Heath S, Even G, Campion D, Sleegers K, Hiltunen M, et al. Genome-wide association study identifies variants at CLU and CR1 associated with Alzheimer's disease. *Nat Genet* (2009) 41(10):1094–9. doi: 10.1038/ng.439
128. Figueiredo Almeida JF, Ramos dos Santos L, Trancozo M, de Paula F. Updated Meta-Analysis of BIN1, CR1, MS4A6A, CLU,and ABCA7 Variants in Alzheimer's Disease. *J Mol Neurosci* (2018) 64:471–7. doi: 10.1007/s12031-018-1045-y
129. Shen N, Chen B, Jiang Y, Feng R, Liao M, Zhang L, et al. An Updated Analysis with 85,939 Samples Confirms the Association Between CR1 rs6656401 Polymorphism and Alzheimer's Disease. *Mol Neurobiol* (2015) 51(3):1017–23. doi: 10.1007/s12035-014-8761-2
130. Fonseca MI, Chu S, Pierce AL, Brubaker WD, Hauhart RE, Mastroeni D, et al. Analysis of the putative role of CR1 in Alzheimer's disease: Genetic association, expression and function. *PloS One* (2016) 11(2):1–21. doi: 10.1371/journal.pone.0149792
131. Kucukkilic E, Brookes K, Barber I, Guetta-Baranes T, Morgan K, Hollox EJ. Complement receptor 1 gene (CR1) intragenic duplication and risk of Alzheimer's disease. *Hum Genet* (2018) 137(4):305–14. doi: 10.1007/s00439-018-1883-2
132. Mahmoudi R, Feldman S, Kisserli A, Duret V, Tabary T, Bertholon LA, et al. Inherited and acquired decrease in complement receptor 1 (CR1) density on red blood cells associated with high levels of soluble CR1 in Alzheimer's disease. *Int J Mol Sci* (2018) 19(8):1–18. doi: 10.3390/ijms19082175
133. Loeffler DA, Camp DM, Conant SB. Complement activation in the Parkinson's disease substantia nigra: An immunocytochemical study. *J Neuroinflammation* (2006) 3:1–8. doi: 10.1186/1742-2094-3-29
134. Yamada T, McGeer PL, McGeer EG. Lewy bodies in Parkinson's disease are recognized by antibodies to complement proteins. *Acta Neuropathol* (1992) 84(1):100–4. doi: 10.1007/BF00427222
135. Gao J, Huang X, Park YY, Hollenbeck A, Chen H. An exploratory study on CLU, CR1 and PICALM and Parkinson disease. *PloS One* (2011) 6(8):4–8. doi: 10.1371/journal.pone.0024211
136. Van Dijk KD, Jongbloed W, Heijst JA, Teunissen CE, Groenewegen HJ, Berendse HW, et al. Cerebrospinal fluid and plasma clusterin levels in Parkinson's disease. *Parkinsonism Relat Disord* (2013) 19(12):1079–83. doi: 10.1016/j.parkreldis.2013.07.016
137. Roumenina LT, Daugan MV, Petitprez F, Sautès-Fridman C, Fridman WH. Context-dependent roles of complement in cancer. *Nat Rev Cancer* (2019) 19:698–715. doi: 10.1038/s41568-019-0210-0
138. Yu X, Rao J, Lin J, Zhang Z, Cao L, Zhang X. Tag SNPs in complement receptor-1 contribute to the susceptibility to non-small cell lung cancer. *Mol Cancer* (2014) 13(1):1–7. doi: 10.1186/1476-4598-13-56
139. Rutkowski MJ, Sughrue ME, Kane AJ, Mills SA, Parsa AT. Cancer and the complement cascade. *Mol Cancer Res* (2010) 8(11):1453–65. doi: 10.1158/1541-7786.MCR-10-0225
140. Pio R, Ajona D, Ortiz-Espinosa S, Mantovani A, Lambris JD. Complementing the cancer-immunity cycle. *Front Immunol* (2019) 10(APR):1–12. doi: 10.3389/fimmu.2019.00774
141. Ajona D, Ortiz-Espinosa S, Pio R. Complement anaphylatoxins C3a and C5a: Emerging roles in cancer progression and treatment. *Semin Cell Dev Biol* (2019) 85:153–63. doi: 10.1016/j.semcdb.2017.11.023
142. Geller A, Yan J. The role of membrane bound complement regulatory proteins in tumor development and cancer immunotherapy. *Front Immunol* (2019) 10(MAY):1–13. doi: 10.3389/fimmu.2019.01074
143. Xie YH, Chen YX, Fang JY. Comprehensive review of targeted therapy for colorectal cancer. *Signal Transduct Target Ther* (2020) 5(1):1–30. doi: 10.1038/s41392-020-0116-z
144. Nakagawa M, Mizuno M, Kawada M, Uesu T, Nasu J, Takeuchi K, et al. Polymorphic expression of decay-accelerating factor in human colorectal cancer. *J Gastroenterol Hepatol* (2001) 16:184–9. doi: 10.1046/j.1440-1746.2001.02418.x
145. Inoue H, Mizuno M, Uesu T, Ueki T, Tsuji T. Distribution of complement regulatory proteins, decay-accelerating factor, CD59/homologous restriction factor 20 and membrane cofactor protein in human colorectal adenoma and cancer. *Acta Med Okayama* (1994) 48(5):271–7. doi: 10.18926/AMO/31112
146. Shang Y, Chai N, Gu Y, Ding L, Yang Y, Zhou J, et al. Systematic immunohistochemical analysis of the expression of CD46, CD55, and CD59 in colon cancer. *Arch Pathol Lab Med* (2014) 138(7):910–9. doi: 10.5858/arpa.2013-0064-OA
147. Durrant LG, Chapman MA, Buckley DJ, Spendlove I, Robins RA, Armitage NC. Enhanced expression of the complement regulatory protein CD55 predicts a poor prognosis in colorectal cancer patients. *Cancer Immunol Immunother* (2003) 52(10):638–42. doi: 10.1007/s00262-003-0402-y
148. Mizuno M, Nakagawa M, Uesu T, Inoue H, Inaba T, Ueki T, et al. Detection of decay-accelerating factor in stool specimens of patients with colorectal cancer. *Gastroenterology* (1995) 109(3):826–31. doi: 10.1016/0016-5085(95)90390-9
149. Dho SH, Cho EH, Lee JY, Lee SY, Jung SH, Kim LK, et al. A novel therapeutic anti–CD55 monoclonal antibody inhibits the proliferation and metastasis of colorectal cancer cells. *Oncol Rep* (2019) 42(6):2686–93. doi: 10.3892/or.2019.7337

150. Kleczko EK, Kwak JW, Schenk EL, Nemenoff RA. Targeting the complement pathway as a therapeutic strategy in lung cancer. *Front Immunol* (2019) 10:1–16. doi: 10.3389/fimmu.2019.00954
151. Zhang Y, Zhang Z, Cao L, Lin J, Yang Z, Zhang X. A common CD55 rs2564978 variant is associated with the susceptibility of non-small cell lung cancer. *Oncotarget* (2017) 8(4):6216–21. doi: 10.18632/oncotarget.14053
152. Zhou J, To KKW, Dong H, Cheng ZS, Lau CCY, Poon VKM, et al. A functional variation in CD55 increases the severity of 2009 pandemic H1N1 influenza a virus infection. *J Infect Dis* (2012) 206(4):495–503. doi: 10.1093/infdis/jis378
153. Higuchi M, Endo Y, Suzuki H, Osuka F, Shio Y, Fujiu K, et al. Identification of the decay-accelerating factor CD55 as a peanut agglutinin-binding protein and its alteration in non-small cell lung cancers. *Clin Cancer Res* (2006) 12 (21):6367–72. doi: 10.1158/1078-0432.CCR-06-0836
154. Ajona D, Hsu Y-F, Corrales L, Montuenga LM, Pio R. Down-Regulation of Human Complement Factor H Sensitizes Non-Small Cell Lung Cancer Cells to Complement Attack and Reduces In Vivo Tumor Growth. *J Immunol* (2007) 178(9):5991–8. doi: 10.4049/jimmunol.178.9.5991
155. Sadallah S, Lach E, Schwarz S, Gratwohl A, Spertini O, Schifferli JA. Soluble complement receptor 1 is increased in patients with leukemia and after administration of granulocyte colony-stimulating factor. *J Leukoc Biol* (1999) 65(1):94–101. doi: 10.1002/jlb.65.1.94
156. Li JS, Jaggers J, Anderson PAW. The use of TP10, soluble complement receptor 1, in cardiopulmonary bypass. *Expert Rev Cardiovasc Ther* (2006) 4 (5):649–54. doi: 10.1586/14779072.4.5.649
157. Tomlinson S, Thurman JM. Tissue-targeted complement therapeutics. *Mol Immunol* (2018) 102:120–8. doi: 10.1016/j.molimm.2018.06.005
158. Mulligan MS, Yeh CG, Rudolph AR, Ward PA. Protective effects of soluble CR1 in complement- and neutrophil-mediated tissue injury. *J Immunol* (1992) 148(5):1479–85.
159. Singel KL, Emmons TR, Khan ANH, Mayor PC, Shen S, Wong JT, et al. Mature neutrophils suppress T cell immunity in ovarian cancer microenvironment. *JCI Insight* (2019) 4(5):1–19. doi: 10.1172/jci.insight.122311
160. Zhang R, Liu Q, Li T, Liao Q, Zhao Y. Role of the complement system in the tumor microenvironment. *Cancer Cell Int [Internet]* (2019) 19(1):1–12. doi: 10.1186/s12935-019-1027-3
161. Miranda-Filho A, Piñeros M, Znaor A, Marcos-Gragera R, Steliarova-Foucher E, Bray F. Global patterns and trends in the incidence of non-Hodgkin lymphoma. *Cancer Causes Control* (2019) 30(5):489–99. doi: 10.1007/s10552-019-01155-5
162. Charbonneau B, Maurer MJ, Fredericksen ZS, Zent CS, Link BK, Novak AJ, et al. Germline variation in complement genes and event-free survival in follicular and diffuse large B-cell lymphoma. *Am J Hematol* (2012) 87 (9):880–5. doi: 10.1002/ajh.23273
163. Rogers LM, Mott SL, Smith BJ, Link BK, Sahin D, Weiner GJ. Complement-regulatory proteins CFHR1 and CFHR3 and patient response to anti-CD20 monoclonal antibody therapy. *Clin Cancer Res* (2017) 23(4):954–61. doi: 10.1158/1078-0432.CCR-16-1275
164. Mastellos DC, Ricklin D, Lambris JD. Clinical promise of next-generation complement therapeutics. *Nat Rev Drug Discovery* (2019) 18(9):707–29. doi: 10.1038/s41573-019-0031-6
165. De Andrade LGM, Contti MM, Nga HS, Bravin AM, Takase HM, Viero RM, et al. Long-term outcomes of the Atypical Hemolytic Uremic Syndrome after kidney transplantation treated with eculizumab as first choice. *PloS One* (2017) 12(11):1–14. doi: 10.1371/journal.pone.0188155
166. Schubert J, Röth A. Update on paroxysmal nocturnal haemoglobinuria: On the long way to understand the principles of the disease. *Eur J Haematol* (2015) 94(6):464–73. doi: 10.1111/ejh.12520
167. Cavero T, Rabasco C, López A, Román E, Ávila A, Sevillano Á, et al. Eculizumab in secondary atypical haemolytic uraemic syndrome. *Nephrol Dial Transplant* (2017) 32(3):466–74. doi: 10.1093/ndt/gfw453
168. Risitano AM. Anti-Complement Treatment in Paroxysmal Nocturnal Hemoglobinuria: Where we Stand and Where we are Going. *Transl Med UniSa* (2014) 8(6):43–52. doi: 10.1517/21678707.2015.1041376
169. Holz FG, Sadda SR, Busbee B, Chew EY, Mitchell P, Tufail A, et al. Efficacy and safety of lampalizumab for geographic atrophy due to age-related macular degeneration: Chroma and spectri phase 3 randomized clinical trials. *JAMA Ophthalmol* (2018) 136(6):666–77. doi: 10.1001/jamaophthalmol.2018.1544
170. Yehoshua Z, Alexandre De Amorim Garcia Filho C, Nunes RP, Gregori G, Penha FM, Moshfeghi AA, et al. Systemic complement inhibition with eculizumab for geographic atrophy in age-related macular degeneration: The COMPLETE study. *Ophthalmology* (2014) 121(3):693–701. doi: 10.1016/j.ophtha.2013.09.044
171. Perego F, Wu MA, Valerieva A, Caccia S, Suffritti C, Zanichelli A, et al. Current and emerging biologics for the treatment of hereditary angioedema. *Expert Opin Biol Ther* (2019) 19(6):517–26. doi: 10.1080/14712598.2019.1595581
172. Schröder-Braunstein J, Kirschfink M. Complement deficiencies and dysregulation: Pathophysiological consequences, modern analysis, and clinical management. *Mol Immunol* (2019) 114(August):299–311. doi: 10.1016/j.molimm.2019.08.002
173. Emmens RW, Wouters D, Zeerleder S, van Ham SM, Niessen HWM, Krijnen PAJ. On the value of therapeutic interventions targeting the complement system in acute myocardial infarction. *Transl Res* (2017) 182:103–22. doi: 10.1016/j.trsl.2016.10.005
174. Koles K, van Berkel PHC, Pieper FR, Nuijens JH, Mannesse MLM, Vliegenthart JFG, et al. N- and O-glycans of recombinant human C1 inhibitor expressed in the milk of transgenic rabbits. *Glycobiology* (2004) 14(1):51–64. doi: 10.1093/glycob/cwh010
175. Wouters D, Wagenaar-Bos I, Van Ham M, Zeerleder S. C1 inhibitor: Just a serine protease inhibitor? New and old considerations on therapeutic applications of C1 inhibitor. *Expert Opin Biol Ther* (2008) 8(8):1225–40. doi: 10.1517/14712598.8.8.1225
176. Caliezi C, Wuillemin WA, Zeerleder S, Redondo M, Eisele B, Hack CE. C1-esterase inhibitor: An anti-inflammatory agent and its potential use in the treatment of diseases other than hereditary angioedema. *Pharmacol Rev* (2000) 52(1):91–112.
177. Wouters D, Stephan F, Strengers P, de Haas M, Brouwer C, Hagenbeek A, et al. C1-esterase inhibitor concentrate rescues erythrocytes from complement-mediated destruction in autoimmune hemolytic anemia. *Blood* (2013) 121(7):1242–4. doi: 10.1182/blood-2012-11-467209
178. Jordan SC, Choi J, Aubert O, Haas M, Loupy A, Huang E, et al. A phase I/II, double-blind, placebo-controlled study assessing safety and efficacy of C1 esterase inhibitor for prevention of delayed graft function in deceased donor kidney transplant recipients. *Am J Transplant* (2018) 18(12):2955–64. doi: 10.1111/ajt.14767
179. Pandey S, Vyas GN. Adverse Effects of Plasma Transfusion. *Transfusion* (2012) 52:1–23. doi: 10.1111/j.1537-2995.2012.03663.x
180. Kasanmoentalib ES, Valls Serón M, Engelen-Lee JY, Tanck MW, Pouw RB, Van Mierlo G, et al. Complement factor H contributes to mortality in humans and mice with bacterial meningitis. *J Neuroinflammation* (2019) 16 (1):1–14. doi: 10.1186/s12974-019-1675-1
181. Fakhouri F, De Jorge EG, Brune F, Azam P, Cook HT, Pickering MC. Treatment with human complement factor H rapidly reverses renal complement deposition in factor H-deficient mice. *Kidney Int* (2010) 78 (3):279–86. doi: 10.1038/ki.2010.132
182. Pickering MC, Cook HT, Warren J, Bygrave AE, Moss J, Walport MJ, et al. Uncontrolled C3 activation causes membranoproliferative glomerulonephritis in mice deficient in complement factor h. *Nat Genet* (2002) 31(4):424–8. doi: 10.1038/ng912
183. Feng S, Liang X, Cruz MA, Vu H, Zhou Z, Pemmaraju N, et al. The Interaction between Factor H and Von Willebrand Factor. *PloS One* (2013) 8 (8):1–15. doi: 10.1371/journal.pone.0073715
184. Sharma AK, Pangburn MK. Biologically active recombinant human complement factor H: synthesis and secretion by the baculovirus system. *Gene* (1994) 143(2):301–2. doi: 10.1016/0378-1119(94)90116-3
185. Michelfelder S, Parsons J, Bohlender LL, Hoernstein SNW, Niederkrüger H, Busch A, et al. Moss-produced, glycosylation-optimized human Factor H for therapeutic application in complement disorders. *J Am Soc Nephrol* (2017) 28(5):1462–74. doi: 10.1681/ASN.2015070745
186. Büttner-Mainik A, Parsons J, Jérôme H, Hartmann A, Lamer S, Schaaf A, et al. Production of biologically active recombinant human factor H in Physcomitrella. *Plant Biotechnol J* (2011) 9(3):373–83. doi: 10.1111/j.1467-7652.2010.00552.x

187. Top O, Parsons J, Bohlender LL, Michelfelder S, Kopp P, Busch-Steenberg C, et al. Recombinant production of MFHR1, a novel synthetic multitarget complement inhibitor, in moss bioreactors. *Front Plant Sci* (2019) 10 (March):1–14. doi: 10.3389/fpls.2019.00260
188. Sugita Y, Ito K, Shiozuka K, Suzuki H, Gushima H, Tomita M, et al. Recombinant soluble CD59 inhibits reactive haemolysis with complement. *Immunology* (1994) 82(1):34–41.
189. Christiansen D, Milland J, Thorley BR, McKenzie IFC, Loveland BE. A functional analysis of recombinant soluble CD46 in vivo and a comparison with recombinant soluble forms of CD55 and CD35 in vitro. *Eur J Immunol* (1996) 26(3):578–85. doi: 10.1002/eji.1830260312
190. Moran P, Beasley H, Gorrell A, Martin E, Gribling P, Fuchs H, et al. Human recombinant soluble decay accelerating factor inhibits complement activation in vitro and in vivo. *J Immunol* (1992) 149(5):1736–43.
191. Smith GP, Smith RAG. Membrane-targeted complement inhibitors. *Mol Immunol* (2001) 38(2–3):249–55. doi: 10.1016/S0161-5890(01)00047-5
192. Schmid RA, Hillinger S, Hamacher J, Stammberger U. TP20 is superior to TP10 in reducing ischemia/reperfusion injury in rat lung grafts. *Transplant Proc* (2001) 33(1–2):948–9. doi: 10.1016/S0041-1345(00)02279-X
193. Sellier-Leclerc AL, Fremeaux-Bacchi V, Dragon-Durey MA, Macher MA, Niaudet P, Guest G, et al. Differential impact of complement mutations on clinical characteristics in atypical hemolytic uremic syndrome. *J Am Soc Nephrol* (2007) 18(8):2392–400. doi: 10.1681/ASN.2006080811
194. Ricklin D, Mastellos DC, Reis ES, Lambris JD. The renaissance of complement therapeutics. *Physiol Behav* (2018) 14(1):1–47. doi: 10.1038/nrneph.2017.156
195. Harder MJ, Anliker M, Höchsmann B, Simmet T, Huber-Lang M, Schrezenmeier H, et al. Comparative Analysis of Novel Complement-Targeted Inhibitors, MiniFH, and the Natural Regulators Factor H and Factor H–like Protein 1 Reveal Functional Determinants of Complement Regulation. *J Immunol* (2016) 196(2):866–76. doi: 10.4049/jimmunol.1501919
196. Schmidt CQ, Bai H, Lin Z, Risitano AM, Barlow PN, Ricklin D, et al. Rational Engineering of a Minimized Immune Inhibitor with Unique Triple-Targeting Properties. *J Immunol* (2013) 190(11):5712–21. doi: 10.4049/jimmunol.1203548
197. Schmidt CQ, Harder MJ, Nichols EM, Hebecker M, Anliker M, Höchsmann B, et al. Selectivity of C3-opsonin targeted complement inhibitors: A distinct advantage in the protection of erythrocytes from paroxysmal nocturnal hemoglobinuria patients. *Immunobiology* (2016) 221(4):503–11. doi: 10.1016/j.imbio.2015.12.009
198. Yang Y, Denton H, Davies OR, Smith-Jackson K, Kerr H, Herbert AP, et al. An engineered complement factor H construct for treatment of C3 glomerulopathy. *J Am Soc Nephrol* (2018) 29(6):1649–61. doi: 10.1681/ASN.2017091006
199. Souza DG, Esser D, Bradford R, Vieira AT, Teixeira MM. APT070 (Mirococept), a membrane-localised complement inhibitor, inhibits inflammatory responses that follow intestinal ischaemia and reperfusion injury. *Br J Pharmacol* (2005) 145(8):1027–34. doi: 10.1038/sj.bjp.0706286
200. Patel H, Smith RAG, Sacks SH, Zhou W. Therapeutic strategy with a membrane-localizing complement regulator to increase the number of usable donor organs after prolonged cold storage. *J Am Soc Nephrol* (2006) 17(4):1102–11. doi: 10.1681/ASN.2005101116
201. Kassimatis T, Qasem A, Douiri A, Ryan EG, Rebollo-Mesa I, Nichols LL, et al. A double-blind randomised controlled investigation into the efficacy of Mirococept (APT070) for preventing ischaemia reperfusion injury in the kidney allograft (EMPIRIKAL): Study protocol for a randomised controlled trial. *Trials* (2017) 18(1):1–11. doi: 10.1186/s13063-017-1972-x
202. Drage M. *An investigation into the treatment of the donor kidney to see if this improves the recovery of the kidney after transplantation*. ISCRTN Registry. doi: 10.1186/ISRCTN49958194
203. Fridkis-Hareli M, Storek M, Mazsaroff I, Risitano AM, Lundberg AS, Horvath CJ, et al. Design and development of TT30, a novel C3d-targeted C3/C5 convertase inhibitor for treatment of human complement alternative pathway-mediated diseases. *Blood* (2011) 118(17):4705–13. doi: 10.1182/blood-2011-06-359646
204. Dobó J, Kocsis A, Gál P. Be on target: Strategies of targeting alternative and lectin pathway components in complement-mediated diseases. *Front Immunol* (2018) 9(AUG):1–22. doi: 10.3389/fimmu.2018.01851
205. Pérez-Alós L, Bayarri-Olmos R, Skjoedt MO, Garred P. Combining MAP-1: CD35 or MAP-1:CD55 fusion proteins with pattern-recognition molecules as novel targeted modulators of the complement cascade. *FASEB J* (2019) 33 (11):12723–34. doi: 10.1096/fj.201901643R
206. Takasumi M, Omori T, Machida T, Ishida Y, Hayashi M, Suzuki T, et al. A novel complement inhibitor sMAP-FH targeting both the lectin and alternative complement pathways. *FASEB J* (2020) 34(5):1–15. doi: 10.1096/fj.201902475R
207. Panwar HS, Ojha H, Ghosh P, Barage SH, Raut S, Sahu A. Molecular engineering of an efficient four-domain DAF-MCP chimera reveals the presence of functional modularity in RCA proteins. *PNAS* (2019) 116 (20):9953–8. doi: 10.1073/pnas.1818573116
208. Song C, Xu Z, Miao J, Xu J, Wu X, Zhang F, et al. Protective effect of scFv-DAF fusion protein on the complement attack to acetylcholine receptor: A possible option for treatment of myasthenia gravis. *Muscle Nerve* (2012) 45 (5):668–75. doi: 10.1002/mus.23247
209. Kusner LL, Satija N, Cheng G, Kaminski HJ. Targeting therapy to the neuromuscular junction: Proof of concept. *Muscle Nerve* (2014) 49(5):749–56. doi: 10.1002/mus.24057
210. Katschke KJ, Helmy KY, Steffek M, Xi H, Yin JP, Lee WP, et al. A novel inhibitor of the alternative pathway of complement reverses inflammation and bone destruction in experimental arthritis. *J Exp Med* (2007) 204 (6):1319–25. doi: 10.1084/jem.20070432
211. Helmy KY, Katschke KJ, Gorgani NN, Kljavin NM, Elliott JM, Diehl L, et al. CRIg: A macrophage complement receptor required for phagocytosis of circulating pathogens. *Cell* (2006) 124(5):915–27. doi: 10.1016/j.cell.2005.12.039
212. Chen M, Muckersie E, Luo C, Forrester JV, Xu H. Inhibition of the alternative pathway of complement activation reduces inflammation in experimental autoimmune uveoretinitis. *Eur J Immunol* (2010) 40 (10):2870–81. doi: 10.1002/eji.201040323
213. Wang X, Van Lookeren Campagne M, Katschke KJ, Gullipalli D, Miwa T, Ueda Y, et al. Prevention of Fatal C3 Glomerulopathy by Recombinant Complement Receptor of the Ig Superfamily. *J Am Soc Nephrol* (2018) 29 (8):2053–9. doi: 10.1681/ASN.2018030270
214. Shaughnessy J, Vu DM, Punjabi R, Serra-Pladevall J, De Oliveira RB, Granoff DM, et al. Fusion protein comprising factor H domains 6 and 7 and human IgG1 Fc as an antibacterial immunotherapeutic. *Clin Vaccine Immunol* (2014) 21(10):1452–9. doi: 10.1128/CVI.00444-14
215. Blom AM, Magda M, Kohl L, Shaughnessy J, Lambris JD, Ram S, et al. Factor H–IgG Chimeric Proteins as a Therapeutic Approach against the Gram-Positive Bacterial Pathogen Streptococcus pyogenes. *J Immunol* (2017) 199 (11):3828–39. doi: 10.4049/jimmunol.1700426
216. Wong SM, Shaughnessy J, Ram S, Akerley BJ. Defining the binding region in factor H to develop a therapeutic factor H-Fc fusion protein against non-typeable Haemophilus influenzae. *Front Cell Infect Microbiol* (2016) 6 (APR):1–10. doi: 10.3389/fcimb.2016.00040
217. Pouw RB, Brouwer MC, de Gast M, van Beek AE, van den Heuvel LP, Schmidt CQ, et al. Potentiation of complement regulator factor H protects human endothelial cells from complement attack in aHUS sera. *Blood Adv* (2019) 3(4):621–32. doi: 10.1182/bloodadvances.2018025692
218. Dekkers G, Brouwer M, Jeremiasse J, Kamp A, Biggs RM, Van G. Unravelling the effect of a potentiating anti-Factor H antibody on atypical hemolytic uremic syndrome associated factor H variants. *J Immunol* (2020) 205(9):1–9. doi: 10.1101/2020.04.08.026906
219. Zell S, Geis N, Rutz R, Schultz S, Giese T, Kirschfink M. Down-regulation of CD55 and CD46 expression by anti-sense phosphorothioate oligonucleotides (S-ODNs) sensitizes tumour cells to complement attack. *Clin Exp Immunol* (2007) 150(3):576–84. doi: 10.1111/j.1365-2249.2007.03507.x
220. Kourtzelis I, Rafail S. The dual role of complement in cancer and its implication in anti-tumor therapy. *Ann Transl Med* (2016) 4(14):1–14. doi: 10.21037/atm.2016.06.26
221. Zhao W-P, Zhu B, Duan Y-Z, Chen Z-T. Neutralization of complement regulatory proteins CD55 and CD59 augments therapeutic effect of herceptin against lung carcinoma cells WEI-PENG. *Oncol Rep* (2009) 21:1405–11. doi: 10.3892/or_00000368
222. Dho SH, Kim SY, Chung C, Cho EH, Lee SY, Kim JY, et al. Development of a radionuclide-labeled monoclonal anti-CD55 antibody with theranostic

potential in pleural metastatic lung cancer. *Sci Rep* (2018) 8(1):1–12. doi: 10.1038/s41598-018-27355-8

223. Gelderman KA, Blok VT, Fleuren GJ, Gorter A. The inhibitory effect of CD46, CD55, and CD59 on complement activation after immunotherapeutic treatment of cervical carcinoma cells with monoclonal antibodies or bispecific monoclonal antibodies. *Lab Investig* (2002) 82(4):483–93. doi: 10.1038/labinvest.3780441
224. Gelderman KA, Kuppen PJK, Okada N, Fleuren GJ, Gorter A. Tumor-specific inhibition of membrane-bound complement regulatory protein Crry with bispecific monoclonal antibodies prevents tumor outgrowth in a rat colorectal cancer lung metastases model. *Cancer Res* (2004) 64(12):4366–72. doi: 10.1158/0008-5472.CAN-03-2131
225. Macor P, Tripodo C, Zorzet S, Piovan E, Bossi F, Marzari R, et al. In vivo targeting of human neutralizing antibodies against CD55 and CD59 to lymphoma cells increases the antitumor activity of rituximab. *Cancer Res* (2007) 67(21):10556–63. doi: 10.1158/0008-5472.CAN-07-1811
226. Bresin E, Rurali E, Caprioli J, Sanchez-Corral P, Fremeaux-Bacchi V, De Cordoba SR, et al. Combined complement gene mutations in atypical hemolytic uremic syndrome influence clinical phenotype. *J Am Soc Nephrol* (2013) 24(3):475–86. doi: 10.1681/ASN.2012090884

Conflict of Interest: The authors declare that the research was conducted in the absence of any commercial or financial relationships that could be construed as a potential conflict of interest.

frontiers in Immunology

REVIEW
published: 08 January 2021
doi: 10.3389/fimmu.2020.603039

Nanoparticle-Induced Complement Activation: Implications for Cancer Nanomedicine

Ninh M. La-Beck[1,2]*, *Md. Rakibul Islam*[1] *and Maciej M. Markiewski*[1]*

[1] Department of Immunotherapeutics and Biotechnology, Jerry H. Hodge School of Pharmacy, Texas Tech University Health Sciences Center, Abilene, TX, United States, [2] Department of Pharmacy Practice, Jerry H. Hodge School of Pharmacy, Texas Tech University Health Sciences Center, Abilene, TX, United States

Nanoparticle-based anticancer medications were first approved for cancer treatment almost 2 decades ago. Patients benefit from these approaches because of the targeted-drug delivery and reduced toxicity, however, like other therapies, adverse reactions often limit their use. These reactions are linked to the interactions of nanoparticles with the immune system, including the activation of complement. This activation can cause well-characterized acute inflammatory reactions mediated by complement effectors. However, the long-term implications of chronic complement activation on the efficacy of drugs carried by nanoparticles remain obscured. The recent discovery of protumor roles of complement raises the possibility that nanoparticle-induced complement activation may actually reduce antitumor efficacy of drugs carried by nanoparticles. We discuss here the initial evidence supporting this notion. Better understanding of the complex interactions between nanoparticles, complement, and the tumor microenvironment appears to be critical for development of nanoparticle-based anticancer therapies that are safer and more efficacious.

Keywords: nanomedicine, complement, activation, immunosuppression, tumor microenvironment, cancer, nanoparticle

OPEN ACCESS

Edited by:
Marcin Okrój, University of Gdańsk and Medical University of Gdańsk, Poland

Reviewed by:
Karin Fromell, Uppsala University, Sweden
Janos Szebeni, Semmelweis University, Hungary

***Correspondence:**
Maciej M. Markiewski
maciej.markiewski@ttuhsc.edu
Ninh M. La-Beck
irene.la-beck@ttuhsc.edu

Specialty section:
This article was submitted to Molecular Innate Immunity, a section of the journal Frontiers in Immunology

Received: *04 September 2020*
Accepted: *23 November 2020*
Published: *08 January 2021*

Citation:
La-Beck NM, Islam MR and Markiewski MM (2021) Nanoparticle-Induced Complement Activation: Implications for Cancer Nanomedicine. Front. Immunol. 11:603039. doi: 10.3389/fimmu.2020.603039

OVERVIEW OF CANCER NANOMEDICINE

Nanomedicine is a submicroscopic platform for effective and smart drug delivery, which enables direct drug interactions with cancer cells and their biological milieu. The main tool of this platform are nanoparticles, a heterogeneous group of engineered drug carriers, defined by a size within the nanometer scale, which includes: liposomes, polymer-conjugates, and micelles (1). The therapeutic potential of nanoparticles for cancer treatment lies in their ability to passively deliver drug to tumor tissue *via* the enhanced permeability and retention (EPR) effect (2). The EPR effect results from an increased vascular permeability of tumor blood vessels, which is linked to neoangiogenesis (3). Importantly, the size of nanoparticles enables their extravasation only in tumors but not in normal tissues. The nanoparticle formulation increases their half-life in circulation, leading to an increased number of passages of drug/carrier complex through the tumor vascular beds. The optimal size range to assure EPR effect appears to be between 20 and 200 nm (in approximate diameter). This ability of nanoparticles to specifically target tumors significantly attenuates drug toxicity.

Additionally, the encapsulation of nanoparticles protects the drug from degradation (4). Several nanoparticle-based therapies have been approved because of improved efficacy and tolerability. The most common nanoparticles among the approved agents are liposomes, however, there are other nanoparticle-delivery platforms, including albumin-conjugated micelles and polyethylene glycol (PEG) conjugates (5) (**Table 1**). Additionally, a large repertoire of nanoparticle systems is under preclinical and early phase clinical development including biopolymers (chitosan, alginate, cellulose, hyaluronic acid), dendrimers, inorganic nanoparticles (Au, Ag, iron oxide, silica, etc.), quantum dots, and the combinations thereof (12–14). These novel nanoparticle systems are likely to become more clinically relevant as there is an increasing interest and research efforts focused on the integration of diagnostics and therapeutics within the cancer nanomedicine field (15, 16).

The transformation of a "free" drug, usually less than 1–2 nm size, into a nanoparticle, with ~1 million-fold greater volume and loaded with thousands of drug molecules, is an extraordinary pharmaceutical challenge with significant pharmacological and biological consequences. For example, unlike traditional small molecule drugs, nanoparticles have a tendency to interact with the innate immune system (17). The cells that primarily interact with systemically administered nanoparticles are mononuclear phagocytes such as tissue-resident macrophages, including hepatic Kupffer cells, and circulating monocytes. These interactions result in the clearance of nanoparticle-delivered drugs from the circulation and their sequestration in organs enriched in macrophages such as liver and spleen (18, 19). The nanoparticles also interact with plasma proteins like immunoglobulins, IgG and IgM, and complement proteins (20). These proteins adsorb to the surface of nanoparticles forming a protein corona (21, 22), which contributes to nanoparticle opsonization, phagocytic clearance, the formation of immune complexes, generation of immunogenic epitopes from self-antigens, and activation or suppression of the immune responses (21–23). The composition of the protein corona is dynamic, highly variable, and depends on the physicochemical characteristics of the nanoparticle and fluctuations in the host circulating proteins. The interactions of nanoparticles with circulating complement proteins leads to the activation of complement cascade (17, 24–26) and the subsequent generation of opsonins (e.g., C3b), anaphylatoxins (e.g., C3a and C5a), and C5b-9 complex, known as terminal complement complex (TCC) or membrane attack complex (MAC). The anaphylatoxins, especially C5a, are associated with acute infusion reactions in patients, known as complement activation-related pseudoallergy (CARPA) (27).

MECHANISMS OF NANOPARTICLE-INDUCED COMPLEMENT ACTIVATION

Nanoparticle-mediated complement activation is a multifaceted process that depends on the physicochemical characteristics of the nanoparticle including: surface chemistry and topography, charge (zeta potential), size, and shape (28–38). Depending on the composition, nanoparticles may induce complement activation through the classical (IgG/IgM/C-reactive protein-mediated), mannose-binding lectin (MBL), or alternative (properdin-mediated) pathways, or any combination of these canonical pathways (39–44) (**Figure 1**).

Size and Shape

In general, as size increases, nanoparticles induce greater complement activation and are also more likely to be internalized by phagocytic cells, presumably due to enhanced opsonization by complement proteins (45, 46). Nanoparticles between 40 to 250 nm in size induce a potent activation of the complement system through the classical pathway similar to dextran coated nanoparticles with a size of ~250 nm (33). However, if the size of the particle is very large (~600 nm diameter), the activation of complement is reduced when adjusted for surface area (38, 46). Dextran-coated superparamagnetic iron oxide (SPIO) core-shell nanoworms of a size of ~200 nm are opsonized by C3b.This C3b engages with

TABLE 1 | Nanoparticle formulations used clinically for treatment of cancer.

Brand Name	Initial Approval	API	Platform	Indication
Oncaspar® (6)	1994	Asparaginase	Polymeric Protein Conjugate	Acute lymphoblastic leukemia
Doxil® (6) Lipodox® (7)	1995	Doxorubicin	Pegylated liposome	Ovarian cancer, breast cancer,Kaposi's sarcoma
DaunoXome® (6)	1996*	Daunorubicin	Non-pegylated liposome	HIV-associated Kaposi's sarcoma
Depocyt® (6)	1999*	Cytarabine	Non-pegylated liposome	Lymphomatous meningitis
Myocet® (8)	2000	Doxorubicin	Non-pegylated liposome	Metastatic breast cancer
Eligard® (6)	2002	Leuprolide Acetate	PLG Polymer	Prostate cancer
Mepact® (9)	2004	Mifamurtide	Non-pegylated liposome	Osteosarcoma
Abraxane® (6)	2005	Paclitaxel	Albumin-conjugated micelle	Breast cancer
NanoTherm® (10, 11)	2010	Iron Oxide	Iron oxide nanoparticle	Glioblastoma (thermo-ablative therapy)
Marqibo® (6)	2012	Vincristine Sulfate	Non-pegylated liposome	Philadelphia chromosome negative acute lymphoblastic leukemia
Onivyde® (6)	2015	Irinotecan	Pegylated (Stealth)	Pancreatic adenocarcinoma
Vyxeos® (6)	2017	Cytarabine and Daunorubicin	Non-Pegylated	Therapy-relatedacute myeloid leukemia

Discontinued and no longer in clinical use.

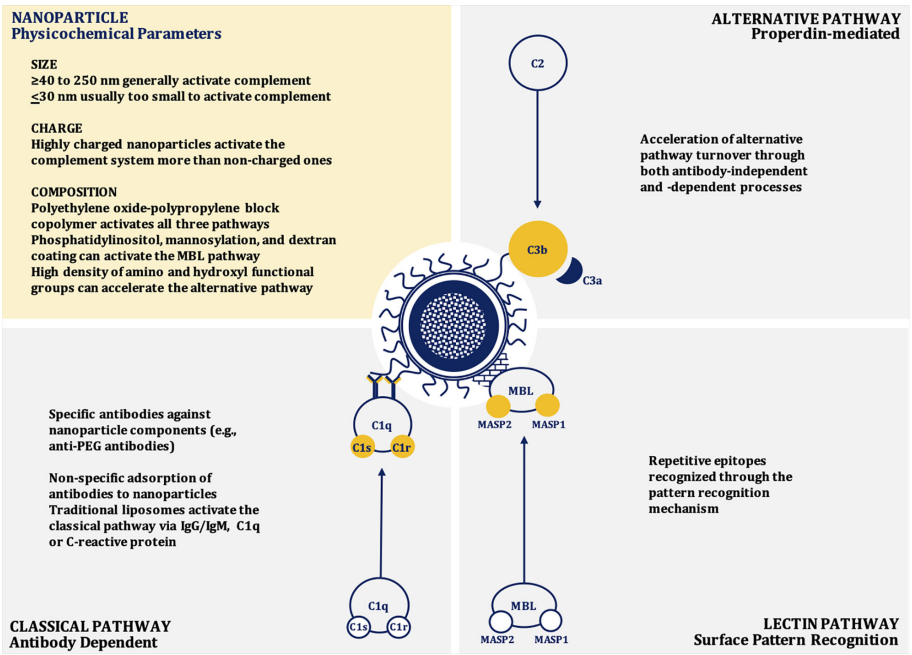

FIGURE 1 | Mechanisms of nanoparticle-induced complement activation.

properdin to recruit more C3b to form C3bBb, the C3 convertase of the alternative pathway (47, 48). When the size of the nanoparticle is at or below 30 nm diameter, they are usually too small to efficiently trigger the calcium-dependent complement activation pathways, such as the classical or lectin pathways, due to the relatively large size of C3b. The complement opsonin C3b occupies an area of about 40 nm^2, therefore, very small nanoparticles do not have enough surface area to adsorb C3b molecules. Consequently, most of the C3 cleavage fragments will be released rather than be deposited on to the surface of these nanoparticles (38, 46, 49).

In addition to size, the particle shape and curvature also play roles in complement activation. Studies with SiO_2 nanoparticles of different sizes (8, 32, and 68 nm) demonstrate that surfaces with the sharp curvature can reduce complement activation. Peptidoglycan particles with a diameter of 50–100 nm and curvature in the range of 0.02–0.04 nm^{-1} induce stronger complement activation when compared to particles with shallower or sharper curvatures. If the curvature is sharper or shallower than 0.02–0.04 nm^{-1}, the conformation requirement for complement activation through IgM and C1q is not optimal and leads to poor induction of the complement cascade (38, 50). Prolate ellipsoidal (rod) and oblate ellipsoidal (disk) shaped carboxylated polystyrene nanoparticles induce more profound and robust activation of the complement system than spherical nanoparticles when tested in porcine blood. However, when tested in human blood, the difference in complement activation between nanoparticles with different shapes were negligible (51). This phenomenon is also seen with spherical gold nanoparticles, gold nanorods, and gold nanostars (52). More research is needed to understand the mechanisms for this difference of complement activation between species.

Composition, Surface Charge, and Zeta Potential

While nanoparticles less than 30 nm are less likely to induce the activation of the complement system, their composition also affects this process because of the interaction of a particular material with the surrounding biological milieu. Polyethylene oxide-polypropylene block copolymer poloxamer 407 micelles of ~25 nm significantly activate the complement system *via* all three canonical pathways, while similar sized PEG-phospholipid micelles fail to activate the complement system (46, 53, 54). The closer inspection revealed that the poloxamer 407 component leads to the generation of larger particles with a range of 100 nm to nearly 1 μm in human plasma. Likely these particles interact with chylomicrons and other lipoprotein classes to form large aggregates that lead to the more potent activation of the complement system (54).

The surface charge of nanoparticles also impacts their interaction with complement. Nanoparticles with anionic surfaces (e.g., liposomes) attract Ca^{2+} ions that are vital for the activation of complement system through the classical pathway (28, 55, 56). These anionic charges derive from cardiolipin, phosphatidylserine, phosphatidic acid, and phosphatidylglycerol incorporated within the structure of liposomes. The complement protein C1q can also directly bind to these anions through hydrophobic interactions and/or hydrogen bonding (57, 58). Cationic or positively charged liposomes containing lipids, including stearylamine or 1,2-bis

(oleoyloxy)-3-(trirnethylammonio) propane, activate the complement system by interacting with proteins of the alternative pathway. Neutral liposomes poorly interact with the complement components and poorly activate the complement system (28, 56, 59). Consequently, nanoparticles containing polypropylene sulfide, lipid nanocapsules, polycations, polyplexes, and polystyrene that are highly charged are more potent activators of complement than particles with low or no charge (60–63). The important role of surface chemistry in complement activation is obvious when nanoparticles are coated with surface-charge-neutralizing polymers, such as polyethylene glycol (PEG). This coating leads to a reduction in nanoparticle-mediated complement activation (60). Suppression of complement activation by neutralizing polymers on the surface of anionic nanoparticles can occur even if the net charge remains slightly negative. For example reducing the net charge from −27.17 to −6.046 mV was sufficient to mitigate nanoparticle-induced complement activation (64).

Lipid bearing nanoparticles (e.g., liposomes) can activate the classical complement pathway *via* interactions between IgG and/or IgM and the phospholipid head-groups and cholesterol components (43, 57, 65, 66). Anti-phospholipid antibodies can also bind to other suitable epitopes found on the liposome surface, such as apolipoprotein H (66, 67). However, there is significant inter-individual variability in the specificity of these antibodies, which may contribute to heterogeneity in nanoparticle-induced complement activation in patients (65, 66). The classical pathway can also be activated by liposomes through the adsorption of C-Reactive Protein (CRP) to the liposomal surface. This CRP subsequently interacts with C1q (66, 68, 69). Liposomes containing phosphatidylinositol may also trigger the lectin pathway through binding to MBL. This initial event leads to MBL-Associated Serine Protease-2 (MASP-2) activation, triggering the complement cascade (40, 66). Similar mechanisms appear to be applicable to mannosylated liposomes. Liposomes can also contribute to the alternative pathway through antibody-independent direct C3 adsorption and C3 conformational changes that lead to the generation of structures resembling C3b and subsequent formation of the alternative pathway C3 (C3bBb) convertase. The alternative pathway is also triggered when the C3 binds to the Fab portion of liposome-bound antibodies (41, 42, 66, 70). In addition to charge neutralization, incorporating mPEG may reduce or delay complement activation through steric hinderance preventing interactions with blood proteins (39, 53). A high density of polymeric chains may lead to the compression of the chains on the surface of the nanoparticle. Whereas a low density may lead to interpenetration of protein molecules on the surface of the mPEG coated nanoparticles. Compression of the polymeric chains may cause steric hindrance that results in reduced protein interactions, consequently, the reduction in complement activation (71). When the surfaces of nanoparticles are modified, however, this can lead to different conformations of nanoparticle surface architectures that can have varying effect on the complement system. If the said surface is modified with mPEG, for example, different conformations can be generated, such as "mushroom," "mushroom-brush," or "brush." Changing the surface conformation from "mushroom"-like to the other conformations leads to a reduced complement activation and shifts the pathway from the classical to the lectin (35).

Topography and Surface Chemistry

Nanoparticle surfaces that have repetitive epitopes may trigger the activation of the complement system through the pattern recognition mechanisms, which are dependent on the surface topography. For example, the nanoparticles coated with star-shaped polyethylene oxide-polypropylene block copolymer (poloxamine 908) have the repetitive patterns of polarity and hydrophobicity. These patterns can be manipulated by altering the density of poloxamine on the nanoparticle surface, and, therefore, the docking sites for complement pattern recognition receptors can be altered (35, 46, 72).

A high density of amino and hydroxyl functional groups on the surfaces of nanoparticles can induce a nucleophilic attack by these chemical moieties on the internal thioester bond within the α-chain of nascent C3b, resulting in the acceleration of alternative complement activation pathway (46, 73, 74). Additionally, nanoparticles with surface polysaccharides that are cross-linked facilitate the activation of the complement system. This activation is partially inhibited if the hydroxyl groups are substituted with carboxymethyl groups (75, 76). The impact of the surface chemistry on the activation of the complement system becomes very complex when the interspecies variation is considered. For example, superparamagnetic iron oxide (SPIO) nanoparticles coated with dextran activate the classical complement pathway in mice, but when tested in human serum, the alternative pathway was found to be activated (76–80).

Drug Payload

The composition of the nanoparticle carrier clearly plays a role in complement activation, however, the influence of the payload (i.e. encapsulated or conjugated drug molecules) on the complement system has not been thoroughly studied. Doxil®, a PEGylated liposomal doxorubicin (PLD), activates the complement system more than liposomes of similar size and formulations that do not contain doxorubicin (46, 81). One of the characteristic features of PLD liposomes is their oblate/disc shape, whereas placebo liposomes are spherical. The oblate shape of PLD is due to deformation of the liposomes by crystalized doxorubicin that is loaded into these liposomes. PLD may trigger more complement activation *via* classical and/or alternative pathways, partly due to the altered phospholipid arrangement and partly due to the surface presence of doxorubicin crystals. It has also been observed that the administration of placebo PEGylated liposomes in rats induced an IgM-mediated complement activation, which increased the hepatic clearance of the second dose of the liposome. In the case of the doxorubicin encapsulated PEGylated liposomes, however, the second dose showed similar long-circulating half-life. This phenomenon is

believed to be related to the action of doxorubicin, which can kill B cells, responsible for producing IgM (26, 46, 82, 83).

CLINICAL IMPACT OF NANOPARTICLE-INDUCED COMPLEMENT ACTIVATION

Complement activation triggered by nanoparticles results in both the liberation of proinflammatory mediators such as anaphylatoxins and the opsonization of nanoparticles with C3b, which interacts with phagocytes (84). The anaphylatoxins (C3a, C4a, and C5a) stimulate the release of additional inflammatory mediators (e.g. histamine) by the immune cells. This sequence of inflammatory events was observed in connection with CARPA reactions in porcine and canine models (85). Several formulations of nanoparticles in clinical use (Doxil®/PLD, DaunoXome®, AmBisome®, Abelcet®, Amphocil®) have been shown to cause hypersensitivity reactions in patients that are consistent with CARPA (86). After intravenous administration, PLD activates complement in the blood of cancer patients, and the extent of complement activation (as measured by formation of s5b-9) correlated with the development of acute infusion reactions (27). Although complement activation induced by nanoparticles is well established (86), the clinical occurrence of CARPA does not appear to be as prevalent as would be expected from *in vitro* studies. For example, PLD induces significant complement activation *in vitro*, however, the occurrence of acute infusion reactions in patients is typically less than 10% and can be mitigated with premedications and by slowing the rate of infusion (27). Nonetheless, undesired interactions with circulating complement proteins can affect the pharmacokinetics and tolerability of nanoparticle-mediated drugs.

Coating nanoparticles with polyethylene glycol ("pegylation") has become widely used to reduce complement activation, improve stability in plasma, and prolong circulation time, which are all important for effective tumor targeting (87, 88). However, these approaches do not entirely abolish the immune reactions to nanoparticles (39). Several groups have demonstrated that the initial systemic administration of pegylated nanoparticles induces production of anti-PEG IgM antibodies that enhance immune recognition and clearance of the second dose of nanoparticles in preclinical models. Of note, this "accelerated blood clearance" (ABC) phenomenon has not been reported in patients, and its clinical relevance is currently unclear. In fact, the opposite has been observed in patients treated with PLD, where clearance rates decreased with repeat administration, up to 30% by the third cycle (89).

Nanoparticle-induced complement activation is generally perceived as undesirable when nanoparticles administered systemically lead to complement-mediated infusion reactions (27, 90). While uncontrolled complement activation can induce inflammatory and life-threatening consequences, controlled complement activation by nanoparticles may be beneficial for vaccination strategies (91–93). Opsonization of pathogens by complement proteins facilitates their uptake by antigen presenting cells *via* complement receptors CD21 and CD33 (94). In the case of nanoparticle-based vaccines, particle-induced complement activation products can act as endogenous vaccine adjuvants to enhance antigen uptake and recognition by antigen-presenting cells. Production of the complement cleavage products C5a and C3a locally at the APC and T cell interface is important for T cell costimulation and survival (95). Antigens that are opsonized by complement C3d engage both B cell receptors and the complement CD21 costimulatory receptor, activating antibody responses more efficiently (96, 97). These complement components can be leveraged by nanoparticle vaccines, where the localized activation of the complement system enhances the immune response against the nanoparticle-delivered antigens (98). Thus, the propensity of nanoparticles to induce complement activation can theoretically be leveraged to facilitate their efficacy as antigen carriers for vaccinations (98, 99).

Several studies of the last decade clearly demonstrated that complement proteins and complement activation accelerates tumor growth in mouse models and patients. Therefore, given the propensity of nanoparticles that are administrated often to cancer patients to activate complement, it is conceivable that this activation may have also reduced therapeutic efficacy of nanoparticles-based drugs. We will explore this possibility through the remaining sections of this review.

THE ROLE OF COMPLEMENT IN CANCER-ASSOCIATED IMMUNE DYSFUNCTION, ANGIOGENESIS, AND METASTASIS

The role of the complement system in cancer has been implicated for decades. The early studies demonstrated that several complement proteins are expressed or deposited in common human solid tumors (100). Given a well-established role of complement in innate immunity and in the initiation and propagation of the subsequent adaptive immune responses against microbial pathogens, these findings were thought to support the theory that complement also contributes to antitumor immune responses and tumor immune surveillance (100). This notion appears to be strengthened by a significant role of complement and complement-dependent cytotoxicity (CDC) in killing tumor cells by therapeutic monoclonal antibodies (101). However, the studies of the last decade clearly indicate that complement proteins and complement activation, in the absence of therapeutic antibodies, promote tumor growth in mouse models and cancer patients (102). The original discovery of tumor-promoting roles of complement linked these complement functions to the complement anaphylatoxin C5a receptor 1 (C5aR1)-dependent regulation of myeloid-derived suppressor cells (MDSC) and their C5aR1-dependent recruitment to tumors (103). MDSC have recently emerged as one of the most important cell subsets in the tumor microenvironment (TME), responsible for suppression of

antitumor T cell-responses, enhancement of tumor-angiogenesis, and resistance to therapy (104). In fact, C5aR1-dependent regulations of MDSC led to the suppression of antitumor $CD8^+$T cells because depletion of these cells by anti-CD8 neutralizing antibody erased beneficial effects of C5aR1 blockade on tumor growth in a mouse model of HPV-induced cancer (103). This study has linked the complement activation in tumors to the classically pathway, as C3 cleavage fragments colocalized with C1q in tumors. C1q initiates the classical pathway (105). In addition, mice deficient in complement fragments C4, which is required for the classical and lectin pathways to progress, had reduced tumor growth. Conversely, mice deficient in factor B, a key protein of the alternative pathway grew tumors in a similar rate as wild type littermate controls (103). Several follow-up studies have confirmed these initial findings in different mouse models (106) and discovered other complement-mediated mechanisms contributing to immune suppression in TME (102).

MDSC also play an important role in inducing another immunosuppressive subset-T regulatory cells (Tregs). Consistent with this MDSC function, the reduced number of Tregs were found in blood and the lungs of C5aR1-deficient mice in a model of metastatic breast cancer (107). The mechanisms of C5aR1-mediated induction of Tregs were connected to the regulation of TGF-β1 and IL-10 in cells of myeloid-origin in the lungs (107). TGF-β1 and IL-10 secreted from myeloid cells have been previously implicated in generation of Tregs in tumors (108). Upon C5aR1 inhibition, the reduced numbers of Tregs in the lungs correlated with the reduced lung metastatic burden (107). C5aR1 signaling is also implicated in generation of Tregs in tumors in a transgenic Her2/neu-driven model of breast cancer (109). The reduced generation of Tregs when C5aR1 signaling was blocked, with a specific C5aR1 inhibitor (PMX53) (110), was caused by the decreased production of TGF-β1 and increased expression of IL-6 in myeloid cells in tumor infiltrating lymph nodes (109), as the interplay between these two cytokines is pivotal for generating various subsets of T cell effectors (111).

In addition to regulating myeloid-origin cells such as MDSC and tumor-associated macrophages (TAM) (112), C5aR1 and the complement anaphylatoxin C3a receptor (C3aR) synergistically impair cytolytic activity of tumor infiltrating $CD8^+$T cells (TIL) by inhibiting expression of IL-10 in these cells (113). C3, required for complement activation and generation of the complement anaphylatoxins C3a and C5a, was shown to be produced by TIL. Through their reciprocal receptors expressed in TIL, C3a and C5a blocked IL-10 expression in these cells in autocrine manner (113). The expression of C3aR and C5aR1 in TIL indicates that TME favors expression of these receptors in T cells because non-activated T cells in the blood, spleen, or lymphoid organs were repeatedly shown to lack C3aR and C5aR1 protein (114).

Interestingly, complement appears to promote tumor angiogenesis, as indicated by reduced vascular density and impairment of endothelial cell function in C3aR-and C5aR1-deficient mice in a transgenic model of ovarian cancer (115). C1q, which initiates the classical complement pathway of activation, was found in stroma and vasculature of several human cancers, and C1q-deficient mice exhibited reduced vascular density in tumors in a B16 melanoma model (116). The most recent study, showing the striking impact of complement genes on outcomes in renal cell carcinoma (RCC), found that C3aR-deficiency or blockade and C5aR1 blockade were all associated with reduced vascular density of tumors in a mouse model of RCC (117). Similar to the first study reporting tumor promoting role of complement (103), this recent work linked the activation of complement in a mouse model to the classical pathway. Interestingly, the comprehensive analysis of TME transcriptome of tumors from RCC patients revealed a significant association of complement genes including C1q signature with highly aggressive inflammatory subtype of RCC (117). Consistent with these finding, another report on a role of complement in RCC found associations of genes encoding early complement fragments, involved in the classical pathway, with poor prognosis (118).

Finally, complement promotes tumor growth through autocrine signaling in tumor cells, and this effect was independent of TIL in a model of ovarian carcinoma. C5aR1 and C3aR signal through the PI3K/AKT pathway, and silencing the *PI3K* or *AKT* gene in tumor cells reduced impact of C5aR1 and C3aR stimulation on tumor growth. In patients with ovarian or lung cancer, higher C3 or C5aR mRNA levels in tumors were associated with decreased overall survival (119). These studies together support a key role of complement system in regulating TME, however, they mainly focused on growth of tumors in primary sites. Several recent comprehensive review articles cover this topic in detail (102, 120).

Recent work extends the findings on TME to the metastasis promoting functions of complement. The C5a/C5aR1 regulatory axis was demonstrated to recruit MDSC to the lung and liver premetastatic niches in a model of metastatic breast cancer (107). This recruitment and activation of MDSC resulted in the reduced infiltration of these organs by $CD8^+$T cells that appears to eliminate metastasizing tumor cells in these sites, as the depletion of $CD8^+$T cells eliminated the beneficial effect of C5aR1 blockade on lung metastatic burden. Furthermore, impact of C5aR1 on antitumor immunity in metastatic sites was linked to Th2-oriented responses that rendered $CD8^+$T cells dysfunctional (107). In addition to recruiting lung infiltrating MDSC, C5aR1 appears to be involved in regulating self-renewal of tissue-resident pulmonary alveolar macrophages (AM) in the lung premetastatic niche that, like MDSC, inhibit antitumor T cell responses by favoring generation of Th2 cells. In addition, AM reduced the number and maturation of lung dendritic cells by regulating TGF-β1 in the lung environment (121). Similar to findings from primary tumor sites (103, 117, 118), complement activation in the premetastatic niches seems to be associated with C1q-deposition and the classically pathway (122). C1q was demonstrated to bind to IgM-deposited in the premetastatic niche. These IgM likely belong to natural IgM that bind dying or damaged cells as demonstrated by colocalization of Annexin

V (binding to apoptotic cells) with IgM fluorescence in the lungs prior metastasis (122).

In summary complement activation and generation of complement effectors seem to be pivotal for protumor complement functions. Several studies linked mechanistically activation of the complement cascade in tumors to the classical pathway. However, the alternative pathway is known to contribute to 80% of C5a generation when the complement cascade is activated through the classical pathway (123). Therefore, the alternative pathway amplification loop is very likely to contribute to complement activation in cancer. Of course, which mechanism is pivotal for complement activation is expected to tumor type-dependent. Finally, some complement functions do not require the activation of complement cascade. For example a proangiogenic role of C1q is not associated with the classical pathway but seems to involve the direct interaction of a globular C1q head with C1q receptors expressed on endothelial cells (116).

IMPLICATIONS OF NANOPARTICLE DRUG DELIVERY-INDUCED INFLAMMATION FOR CANCER

Complement cleavage products and the uptake of nanoparticles by immune cells mediated by complement receptors may induce chronic inflammatory responses that could potentially negate the therapeutic effect of the payload. Indeed, there is an increasing evidence that nanoparticles could promote tumor growth in mice (124, 125). Polymer nanoparticles that are able to activate the complement system were found to increase tumor growth in a C5aR1-dependent manner, presumably through the liberation of C5a and the recruitment and activation of proinflammatory macrophages and Tregs (103, 126). We have also found that systemic administration of PLD to mice was associated with the increased infiltration of tumors by MDSC and the deposition of the complement cleavage products in tumors (**Figure 2**). Recently, we tested this pegylated liposomal carrier without any drug payload, and observed the significantly enhanced tumor growth in a syngeneic HPV-induced mouse tumor model (125). This enhanced tumor growth was associated with the suppression of antitumor immunity, indicated by blunting the production of cytokines in TAM and $CD8^+$ T cells and the suppression of tumor antigen-specific immune responses. Moreover, tumor vascular density was significantly increased in mice receiving pegylated liposomes, suggesting enhanced angiogenesis. Mechanistically, *in vivo* treatment with liposomes increased expression of arginase-1 (typical of M2 macrophages and MDSC) associated with the accumulation of TAMs with a mixed M1/M2 phenotype when compared to vehicle treated mice that had predominantly M1 macrophages in tumors (127). These findings suggest that nanoparticle-induced immune modulation may theoretically attenuate therapeutic efficacy of nano-encapsulated drugs (120, 128–130). This may be especially relevant for cancer patients as a result of profound and heterogenous immune dysfunction (131).

While complement activation associated with these "placebo" nanoparticles have the potential to promote tumor growth, this effect was not associated with drug-loaded nanoparticles. It is likely that the anticancer drug, loaded within the nanoparticle, mitigates the harmful carrier-related effects by inhibiting both tumor cells and TAMs that internalize the nanoparticles. Thus, for cytotoxic chemotherapies, the tumor-enhancing potential of nanoparticle-induced complement activation may not be fully appreciated. However, when nanoparticles are used for delivery of other drugs including immunotherapeutics, which do not act *via* direct tumor cell killing, nanoparticle-induced complement activation could conceivably diminish their efficacy. Another consideration is that complement activation in the blood, which occurs after intravenous infusion of nanoparticle drugs, is transient and likely do not persist long enough to impact tumor growth in the long term. Nonetheless, chronic inflammation and complement activation can promote tumor progression, although it has not been determined whether nanoparticles that accumulate in the tumor tissue induce chronic complement activation.

The major pitfall in the studies of the complex interactions between nanoparticles and the innate immunity is that *in vitro* studies and studies in "healthy" animals do not sufficiently mirror the biological interactions of nanomedicines with the immunity of cancer patients. The xenograft tumor models are the predominant *in vivo* models used to demonstrate anticancer efficacy of drugs including nanomedicines. However, they rely on immunodeficient mice. The genetically engineered and syngeneic tumor models that utilize immunocompetent mice would be better options for assessing the complex interplay between the tumor immunologic milieu and nanomedicine. The selection of animal species for use in preclinical tests of nanomedicines also has a major impact on the preclinical toxicology results. Some conventional preclinical models (rats and non-human primates) may be insensitive to complement activation and cytokine-storm induction by nanoparticles (132–137). In such cases, supplementing *in vivo* studies with *in vitro* assays utilizing human blood should be considered. Another consideration for selecting an animal model is related to the variable sensitivity of animal strains to a particular type of immunotoxicity. For example, rabbits are more sensitive to cytokine and complement-mediated toxicities than rodents. Among rodents, strains may differ in their selectivity to nanoparticle clearance. For example, Balb/c and C57BL/6 mice commonly used in preclinical studies demonstrate a different pattern of nanoparticle uptake due to their Th2 and Th1 bias, respectively (138).

CONCLUSIONS

Over two decades after the approval of the first nanoparticle-mediated anticancer drug, there has yet to be a major shift in cancer treatment paradigms linked to nanoparticles, contrary to what was expected based on preclinical studies of cancer nanomedicines (130). Only two anticancer nanoparticles are

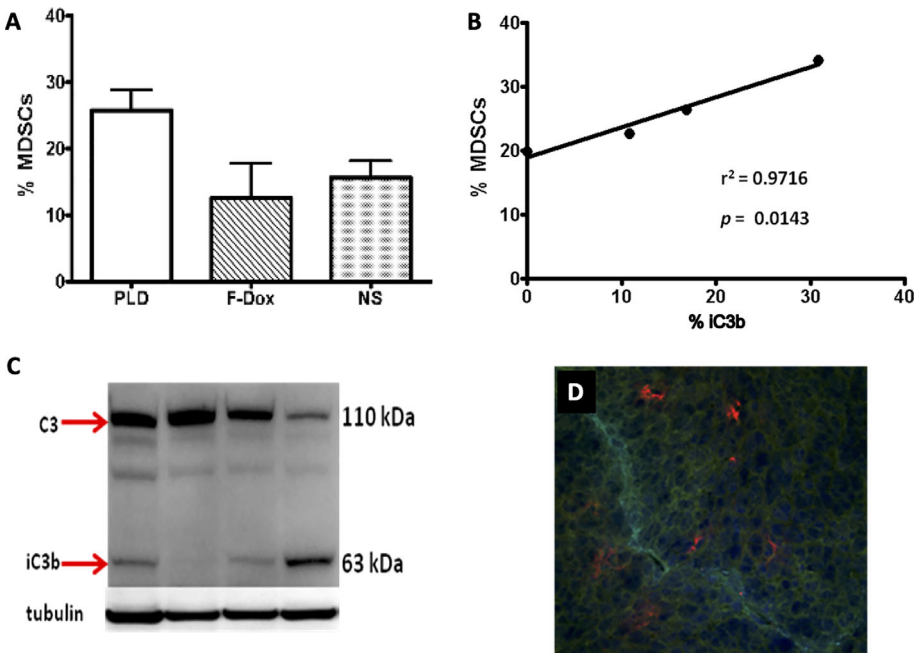

FIGURE 2 | Liposome-associated complement activation in tumor tissue correlates with myeloid-derived suppressor cell infiltration. **(A)** Pegylated liposomal doxorubicin (PLD) treatment increased MDSC in tumors ($p = 0.03$) whereas free doxorubicin (F-Dox) showed no change in %MDSC ($p > 0.05$). Treatments were intravenously administered in C57Bl6 mice bearing TC-1 tumors implanted on the hind flank: PLD (n = 4), F-Dox (n = 4), and saline (NS; n = 5). **(B)** Increasing levels of complement activation in tumor correlates with increased tumor MDSC in PLD treated mice. **(C)** Complement activation was quantified using immunoblot analysis of tumor lysate and verified by immunohistochemical analysis of frozen tumor sections. **(D)** A representative image is shown; red = iC3b, aqua = CD31 (vasculature), blue = DAPI (cell nuclei).

used as front-line therapies: nanoparticle albumin-bound paclitaxel (*nab*-paclitaxel; Abraxane®) for advanced non-small cell lung cancer and metastatic pancreatic adenocarcinoma, and liposomal daunorubicin cytarabine (CPX-351; Vyxeos®) for treatment-related acute myeloid leukemia and acute myeloid leukemia with myelodysplastic changes. Nonetheless, nanoparticle-mediated drug delivery is a proven strategy to mitigate toxicity of anticancer drugs in patients (139–141). The future of cancer nanomedicine is promising as recent new insights in understanding the role of the complement system in cancer will perhaps facilitate our understanding of how nanoparticle interactions with the innate immune system impacts drug pharmacology. If this knowledge gap can be addressed, it will lay the foundation for future work that will uncover the full clinical potential of cancer nanomedicines (18).

AUTHOR CONTRIBUTIONS

All authors listed have made a substantial, direct, and intellectual contribution to the work and approved it for publication.

FUNDING

This work was funded by the National Institute of Health (RO1CA190209 to MM).

ACKNOWLEDGMENTS

We thank Elizabeth Daugherity for the critical revision of this manuscript.

REFERENCES

1. Duncan R, Gaspar R. Nanomedicine(s) under the microscope. *Mol Pharmaceutics* (2011) 8:2101–41. doi: 10.1021/mp200394t
2. Maeda H, Fang J, Inutsuka T, Kitamoto Y. Vascular permeability enhancement in solid tumor: various factors, mechanisms involved and its implications. *Int Immunopharmacol* (2003) 3:319–28. doi: 10.1016/S1567-5769(02)00271-0
3. Maeda H, Nakamura H, Fang J. The EPR effect for macromolecular drug delivery to solid tumors: Improvement of tumor uptake, lowering of systemic toxicity, and distinct tumor imaging in vivo. *Adv Drug Delivery Rev* (2013) 65:71–9. doi: 10.1016/j.addr.2012.10.002
4. Allen TM, Cullis PR. Liposomal drug delivery systems: from concept to clinical applications. *Adv Drug Delivery Rev* (2013) 65:36–48. doi: 10.1016/j.addr.2012.09.037
5. Anchordoquy TJ, Barenholz Y, Boraschi D, Chorny M, Decuzzi P, Dobrovolskaia MA, et al. Mechanisms and Barriers in Cancer Nanomedicine: Addressing Challenges, Looking for Solutions. *ACS Nano* (2017) 11:12–8. doi: 10.1021/acsnano.6b08244
6. U.S. Food and Drug Administration. *Drugs@FDA: FDA-Approved Drugs*. (2020). https://www.accessdata.fda.gov/scripts/cder/daf/ [Accessed September 04, 2020].
7. Chou H, Lin H, Liu JM. A tale of the two PEGylated liposomal doxorubicins. *Onco Targets Ther* (2015) 8:1719–20. doi: 10.2147/OTT.S79089

8. European Medicines Agency. *Myocet liposomal (previously Myocet)*. (2020). https://www.ema.europa.eu/en/medicines/human/EPAR/myocet-liposomal-previously-myocet [Accessed September 04, 2020].
9. European Medicines Agency. *Assessment Report for Mepact*. (2009). https://www.ema.europa.eu/en/documents/assessment-report/mepact-epar-public-assessment-report_en.pdf [Accessed September 04, 2020].
10. Bobo D, Robinson KJ, Islam J, Thurecht KJ, Corrie SR. Nanoparticle-Based Medicines: A Review of FDA-Approved Materials and Clinical Trials to Date. *Pharm Res* (2016) 33:2373–87. doi: 10.1007/s11095-016-1958-5
11. Thiesen B, Jordan A. Clinical applications of magnetic nanoparticles for hyperthermia. *Int J Hyperthermia* (2008) 24:467–74. doi: 10.1080/02656730802104757
12. Salvioni L, Rizzuto MA, Bertolini JA, Pandolfi L, Colombo M, Prosperi D. Thirty Years of Cancer Nanomedicine: Success, Frustration, and Hope. *Cancers* (2019) 11:1855. doi: 10.3390/cancers11121855
13. Irvine DJ, Dane EL. Enhancing cancer immunotherapy with nanomedicine. *Nat Rev Immunol* (2020) 20:321–34. doi: 10.1038/s41577-019-0269-6
14. Norouzi M, Amerian M, Amerian M, Atyabi F. Clinical applications of nanomedicine in cancer therapy. *Drug Discovery Today* (2020) 25:107–25. doi: 10.1016/j.drudis.2019.09.017
15. Wu PH, Opadele AE, Onodera Y, Nam JM. Targeting Integrins in Cancer Nanomedicine: Applications in Cancer Diagnosis and Therapy. *Cancers (Basel)* (2019) 11:1783. doi: 10.3390/cancers11111783
16. Kang C, Kim D. Nanoconfinement-mediated cancer theranostics. *Arch Pharm Res* (2020) 43:110–7. doi: 10.1007/s12272-020-01217-2
17. Dobrovolskaia MA, Aggarwal P, Hall JB, McNeil SE. Preclinical studies to understand nanoparticle interaction with the immune system and its potential effects on nanoparticle biodistribution. *Mol Pharm* (2008) 5:487–95. doi: 10.1021/mp800032f
18. La-Beck NM, Gabizon AA. Nanoparticle Interactions with the Immune System: Clinical Implications for Liposome-Based Cancer Chemotherapy. *Front Immunol* (2017) 8:416. doi: 10.3389/fimmu.2017.00416
19. Caron WP, Lay JC, Fong AM, La-Beck NM, Kumar P, Newman SE, et al. Translational studies of phenotypic probes for the mononuclear phagocyte system and liposomal pharmacology. *J Pharmacol Exp Ther* (2013) 347:599–606. doi: 10.1124/jpet.113.208801
20. Bonte F, Juliano RL. Interactions of liposomes with serum proteins. *Chem Phys Lipids* (1986) 40:359–72. doi: 10.1016/0009-3084(86)90079-4
21. Caracciolo G. Liposome-protein corona in a physiological environment: challenges and opportunities for targeted delivery of nanomedicines. *Nanomed Nanotechnol Biol Med* (2015) 11:543–57. doi: 10.1016/j.nano.2014.11.003
22. Corbo C, Molinaro R, Parodi A, Toledano Furman NE, Salvatore F, Tasciotti E. The impact of nanoparticle protein corona on cytotoxicity, immunotoxicity and target drug delivery. *Nanomed (Lond)* (2016) 11:81–100. doi: 10.2217/nnm.15.188
23. Barbero F, Russo L, Vitali M, Piella J, Salvo I, Borrajo ML, et al. Formation of the Protein Corona: The Interface between Nanoparticles and the Immune System. *Semin Immunol* (2017) 34:52–60. doi: 10.1016/j.smim.2017.10.001
24. Alving CR. Immunologic aspects of liposomes: presentation and processing of liposomal protein and phospholipid antigens. *Biochim Biophys Acta* (1992) 1113:307–22. doi: 10.1016/0304-4157(92)90004-T
25. Verma JN, Rao M, Amselem S, Krzych U, Alving CR, Green SJ, et al. Adjuvant effects of liposomes containing lipid A: enhancement of liposomal antigen presentation and recruitment of macrophages. *Infect Immun* (1992) 60:2438–44. doi: 10.1128/IAI.60.6.2438-2444.1992
26. Szebeni J, Baranyi L, Savay S, Milosevits J, Bunger R, Laverman P, et al. Role of complement activation in hypersensitivity reactions to doxil and hynic PEG liposomes: experimental and clinical studies. *J Liposome Res* (2002) 12:165–72. doi: 10.1081/LPR-120004790
27. Chanan-Khan A, Szebeni J, Savay S, Liebes L, Rafique NM, Alving CR, et al. Complement activation following first exposure to pegylated liposomal doxorubicin (Doxil): possible role in hypersensitivity reactions. *Ann Oncol* (2003) 14:1430–7. doi: 10.1093/annonc/mdg374
28. Chonn A, Cullis PR, Devine DV. The role of surface charge in the activation of the classical and alternative pathways of complement by liposomes. *J Immunol* (1991) 146:4234–41.
29. Devine DV, Wong K, Serrano K, Chonn A, Cullis PR. Liposome-complement interactions in rat serum: implications for liposome survival studies. *Biochim Biophys Acta* (1994) 1191:43–51. doi: 10.1016/0005-2736(94)90231-3
30. Madani F, Bessodes M, Lakrouf A, Vauthier C, Scherman D, Chaumeil JC. PEGylation of microspheres for therapeutic embolization: preparation, characterization and biological performance evaluation. *Biomaterials* (2007) 28:1198–208. doi: 10.1016/j.biomaterials.2006.10.017
31. Salvador-Morales C, Flahaut E, Sim E, Sloan J, Green ML, Sim RB. Complement activation and protein adsorption by carbon nanotubes. *Mol Immunol* (2006) 43:193–201. doi: 10.1016/j.molimm.2005.02.006
32. Sevast'ianov VI, Tseytlina EA. The activation of the complement system by polymer materials and their blood compatibility. *J BioMed Mater Res* (1984) 18:969–78. doi: 10.1002/jbm.820180902
33. Salvador-Morales C, Basiuk EV, Basiuk VA, Green ML, Sim RB. Effects of covalent functionalization on the biocompatibility characteristics of multi-walled carbon nanotubes. *J Nanosci Nanotechnol* (2008) 8:2347–56. doi: 10.1166/jnn.2008.090
34. Hamad I, Christy Hunter A, Rutt KJ, Liu Z, Dai H, Moein Moghimi S. Complement activation by PEGylated single-walled carbon nanotubes is independent of C1q and alternative pathway turnover. *Mol Immunol* (2008) 45:3797–803. doi: 10.1016/j.molimm.2008.05.020
35. Hamad I, Al-Hanbali O, Hunter AC, Rutt KJ, Andresen TL, Moghimi SM. Distinct polymer architecture mediates switching of complement activation pathways at the nanosphere-serum interface: implications for stealth nanoparticle engineering. *ACS Nano* (2010) 4:6629–38. doi: 10.1021/nn101990a
36. Al-Hanbali O, Rutt KJ, Sarker DK, Hunter AC, Moghimi SM. Concentration dependent structural ordering of poloxamine 908 on polystyrene nanoparticles and their modulatory role on complement consumption. *J Nanosci Nanotechnol* (2006) 6:3126–33. doi: 10.1166/jnn.2006.406
37. Sou K, Tsuchida E. Electrostatic interactions and complement activation on the surface of phospholipid vesicle containing acidic lipids: effect of the structure of acidic groups. *Biochim Biophys Acta* (2008) 1778:1035–41. doi: 10.1016/j.bbamem.2008.01.006
38. Pedersen MB, Zhou X, Larsen EK, Sorensen US, Kjems J, Nygaard JV, et al. Curvature of synthetic and natural surfaces is an important target feature in classical pathway complement activation. *J Immunol* (2010) 184:1931–45. doi: 10.4049/jimmunol.0902214
39. Moghimi SM, Szebeni J. Stealth liposomes and long circulating nanoparticles: critical issues in pharmacokinetics, opsonization and protein-binding properties. *Prog Lipid Res* (2003) 42:463–78. doi: 10.1016/S0163-7827(03)00033-X
40. Kuroki Y, Honma T, Chiba H, Sano H, Saitoh M, Ogasawara Y, et al. A novel type of binding specificity to phospholipids for rat mannose-binding proteins isolated from serum and liver. *FEBS Lett* (1997) 414:387–92. doi: 10.1016/S0014-5793(97)01022-3
41. Szebeni J, Baranyi L, Savay S, Milosevits J, Bodo M, Bunger R, et al. The interaction of liposomes with the complement system: in vitro and in vivo assays. *Methods Enzymol* (2003) 373:136–54. doi: 10.1016/S0076-6879(03)73010-9
42. Szebeni J, Wassef NM, Hartman KR, Rudolph AS, Alving CR. Complement activation in vitro by the red cell substitute, liposome-encapsulated hemoglobin: mechanism of activation and inhibition by soluble complement receptor type 1. *Transfusion* (1997) 37:150–9. doi: 10.1046/j.1537-2995.1997.37297203517.x
43. Alving CR, Kinsky SC, Haxby JA, Kinsky CB. Antibody binding and complement fixation by a liposomal model membrane. *Biochemistry* (1969) 8:1582–7. doi: 10.1021/bi00832a038
44. Neun BW, Ilinskaya AN, Dobrovolskaia MA. Analysis of Complement Activation by Nanoparticles. *Methods Mol Biol* (2018) 1682:149–60. doi: 10.1007/978-1-4939-7352-1_13
45. Malachowski T, Hassel A. Engineering nanoparticles to overcome immunological barriers for enhanced drug delivery. *Engineered Regeneration* (2020) 1:35–50. doi: 10.1016/j.engreg.2020.06.001
46. Moghimi SM, Andersen AJ, Ahmadvand D, Wibroe PP, Andresen TL, Hunter AC. Material properties in complement activation. *Adv Drug Delivery Rev* (2011) 63:1000–7. doi: 10.1016/j.addr.2011.06.002

47. Chen F, Wang G, Griffin JI, Brenneman B, Banda NK, Holers VM, et al. Complement proteins bind to nanoparticle protein corona and undergo dynamic exchange in vivo. *Nat Nanotechnol* (2017) 12:387–93. doi: 10.1038/nnano.2016.269
48. Kouser L, Paudyal B, Kaur A, Stenbeck G, Jones LA, Abozaid SM, et al. Human Properdin Opsonizes Nanoparticles and Triggers a Potent Pro-inflammatory Response by Macrophages without Involving Complement Activation. *Front Immunol* (2018) 9:131. doi: 10.3389/fimmu.2018.00131
49. Janssen BJ, Christodoulidou A, McCarthy A, Lambris JD, Gros P. Structure of C3b reveals conformational changes that underlie complement activity. *Nature* (2006) 444:213–6. doi: 10.1038/nature05172
50. Westas Janco E, Hulander M, Andersson M. Curvature-dependent effects of nanotopography on classical immune complement activation. *Acta Biomater* (2018) 74:112–20. doi: 10.1016/j.actbio.2018.04.053
51. Wibroe PP, Anselmo AC, Nilsson PH, Sarode A, Gupta V, Urbanics R, et al. Bypassing adverse injection reactions to nanoparticles through shape modification and attachment to erythrocytes. *Nat Nanotechnol* (2017) 12:589–94. doi: 10.1038/nnano.2017.47
52. Quach QH, Kah JC. Non-specific adsorption of complement proteins affects complement activation pathways of gold nanomaterials. *Nanotoxicology* (2017) 11:382–94. doi: 10.1080/17435390.2017.1306131
53. Moghimi SM, Hamad I, Andresen TL, Jorgensen K, Szebeni J. Methylation of the phosphate oxygen moiety of phospholipid-methoxy(polyethylene glycol) conjugate prevents PEGylated liposome-mediated complement activation and anaphylatoxin production. *FASEB J* (2006) 20:2591–3. doi: 10.1096/fj.06-6186fje
54. Hamad I, Hunter AC, Moghimi SM. Complement monitoring of Pluronic 127 gel and micelles: suppression of copolymer-mediated complement activation by elevated serum levels of HDL, LDL, and apolipoproteins AI and B-100. *J Control Release* (2013) 170:167–74. doi: 10.1016/j.jconrel.2013.05.030
55. Szeto GL, Lavik EB. Materials design at the interface of nanoparticles and innate immunity. *J Mater Chem B* (2016) 4:1610–8. doi: 10.1039/C5TB01825K
56. Pham CT, Mitchell LM, Huang JL, Lubniewski CM, Schall OF, Killgore JK, et al. Variable antibody-dependent activation of complement by functionalized phospholipid nanoparticle surfaces. *J Biol Chem* (2011) 286:123–30. doi: 10.1074/jbc.M110.180760
57. Bradley AJ, Brooks DE, Norris-Jones R, Devine DV. C1q binding to liposomes is surface charge dependent and is inhibited by peptides consisting of residues 14-26 of the human C1qA chain in a sequence independent manner. *Biochim Biophys Acta* (1999) 1418:19–30. doi: 10.1016/S0005-2736(99)00013-9
58. Devine DV, Marjan JM. The role of immunoproteins in the survival of liposomes in the circulation. *Crit Rev Ther Drug Carrier Syst* (1997) 14:105–31. doi: 10.1615/CritRevTherDrugCarrierSyst.v14.i2.10
59. Klapper Y, Hamad OA, Teramura Y, Leneweit G, Nienhaus GU, Ricklin D, et al. Mediation of a non-proteolytic activation of complement component C3 by phospholipid vesicles. *Biomaterials* (2014) 35:3688–96. doi: 10.1016/j.biomaterials.2013.12.085
60. Vonarbourg A, Passirani C, Saulnier P, Simard P, Leroux JC, Benoit JP. Evaluation of pegylated lipid nanocapsules versus complement system activation and macrophage uptake. *J BioMed Mater Res A* (2006) 78:620–8. doi: 10.1002/jbm.a.30711
61. Thomas SN, van der Vlies AJ, O'Neil CP, Reddy ST, Yu SS, Giorgio TD, et al. Engineering complement activation on polypropylene sulfide vaccine nanoparticles. *Biomaterials* (2011) 32:2194–203. doi: 10.1016/j.biomaterials.2010.11.037
62. Meszaros T, Kozma GT, Shimizu T, Miyahara K, Turjeman K, Ishida T, et al. Involvement of complement activation in the pulmonary vasoactivity of polystyrene nanoparticles in pigs: unique surface properties underlying alternative pathway activation and instant opsonization. *Int J Nanomed* (2018) 13:6345–57. doi: 10.2147/IJN.S161369
63. Hall A, Lachelt U, Bartek J, Wagner E, Moghimi SM. Polyplex Evolution: Understanding Biology. *Optimizing Performance Mol Ther* (2017) 25:1476–90. doi: 10.1016/j.ymthe.2017.01.024
64. Shan X, Yuan Y, Liu C, Tao X, Sheng Y, Xu F. Influence of PEG chain on the complement activation suppression and longevity in vivo prolongation of the PCL biomedical nanoparticles. *BioMed Microdevices* (2009) 11:1187–94. doi: 10.1007/s10544-009-9336-2
65. Alving CR, Swartz GM Jr. Antibodies to cholesterol, cholesterol conjugates and liposomes: implications for atherosclerosis and autoimmunity. *Crit Rev Immunol* (1991) 10:441–53.
66. Moghimi SM, Hamad I. Liposome-mediated triggering of complement cascade. *J Liposome Res* (2008) 18:195–209. doi: 10.1080/08982100802309552
67. Horkko S, Miller E, Branch DW, Palinski W, Witztum JL. The epitopes for some antiphospholipid antibodies are adducts of oxidized phospholipid and beta2 glycoprotein 1 (and other proteins). *Proc Natl Acad Sci U.S.A.* (1997) 94:10356–61. doi: 10.1073/pnas.94.19.10356
68. Richards RL, Gewurz H, Osmand AP, Alving CR. Interactions of C-reactive protein and complement with liposomes. *Proc Natl Acad Sci U.S.A.* (1977) 74:5672–6. doi: 10.1073/pnas.74.12.5672
69. Volanakis JE, Wirtz KW. Interaction of C-reactive protein with artificial phosphatidylcholine bilayers. *Nature* (1979) 281:155–7. doi: 10.1038/281155a0
70. Moore FD Jr., Austen KF, Fearon DT. Antibody restores human alternative complement pathway activation by mouse erythrocytes rendered functionally deficient by pretreatment with pronase. *J Immunol* (1982) 128:1302–6.
71. Pannuzzo M, Esposito S, Wu LP, Key J, Aryal S, Celia C, et al. Overcoming Nanoparticle-Mediated Complement Activation by Surface PEG Pairing. *Nano Lett* (2020) 20:4312–21. doi: 10.1021/acs.nanolett.0c01011
72. Moghimi SM, Hunter AC, Murray JC. Long-circulating and target-specific nanoparticles: theory to practice. *Pharmacol Rev* (2001) 53:283–318.
73. Toda M, Kitazawa T, Hirata I, Hirano Y, Iwata H. Complement activation on surfaces carrying amino groups. *Biomaterials* (2008) 29:407–17. doi: 10.1016/j.biomaterials.2007.10.005
74. Salvador-Morales C, Zhang L, Langer R, Farokhzad OC. Immunocompatibility properties of lipid-polymer hybrid nanoparticles with heterogeneous surface functional groups. *Biomaterials* (2009) 30:2231–40. doi: 10.1016/j.biomaterials.2009.01.005
75. Carreno MP, Labarre D, Jozefowicz M, Kazatchkine MD. The ability of Sephadex to activate human complement is suppressed in specifically substituted functional Sephadex derivatives. *Mol Immunol* (1988) 25:165–71. doi: 10.1016/0161-5890(88)90064-8
76. Wang G, Chen F, Banda NK, Holers VM, Wu L, Moghimi SM, et al. Activation of Human Complement System by Dextran-Coated Iron Oxide Nanoparticles Is Not Affected by Dextran/Fe Ratio, Hydroxyl Modifications, and Crosslinking. *Front Immunol* (2016) 7:418. doi: 10.3389/fimmu.2016.00418
77. Karmali PP, Chao Y, Park JH, Sailor MJ, Ruoslahti E, Esener SC, et al. Different effect of hydrogelation on antifouling and circulation properties of dextran-iron oxide nanoparticles. *Mol Pharm* (2012) 9:539–45. doi: 10.1021/mp200375x
78. Park JH, von Maltzahn G, Zhang L, Derfus AM, Simberg D, Harris TJ, et al. Systematic surface engineering of magnetic nanoworms for in vivo tumor targeting. *Small* (2009) 5:694–700. doi: 10.1002/smll.200801789
79. Simberg D, Park JH, Karmali PP, Zhang WM, Merkulov S, McCrae K, et al. Differential proteomics analysis of the surface heterogeneity of dextran iron oxide nanoparticles and the implications for their in vivo clearance. *Biomaterials* (2009) 30:3926–33. doi: 10.1016/j.biomaterials.2009.03.056
80. Park JH, von Maltzahn G, Zhang L, Schwartz MP, Ruoslahti E, Bhatia SN, et al. Magnetic Iron Oxide Nanoworms for Tumor Targeting and Imaging. *Adv Mater* (2008) 20:1630–5. doi: 10.1002/adma.200800004
81. Szebeni J, Baranyi L, Savay S, Lutz HU, Jelezarova E, Bunger R, et al. The Role of Complement Activation in Hypersensitivity to Pegylated Liposomal Doxorubicin (Doxil®). *J Liposome Res* (2000) 10:467–81. doi: 10.3109/08982100009031112
82. Ishida T, Wang X, Shimizu T, Nawata K, Kiwada H. PEGylated liposomes elicit an anti-PEG IgM response in a T cell-independent manner. *J Control Release* (2007) 122:349–55. doi: 10.1016/j.jconrel.2007.05.015
83. Wang X, Ishida T, Kiwada H. Anti-PEG IgM elicited by injection of liposomes is involved in the enhanced blood clearance of a subsequent dose of PEGylated liposomes. *J Control Release* (2007) 119:236–44. doi: 10.1016/j.jconrel.2007.02.010

84. Moghimi SM, Simberg D, Skotland T, Yaghmur A, Hunter AC. The Interplay Between Blood Proteins, Complement, and Macrophages on Nanomedicine Performance and Responses. *J Pharmacol Exp Ther* (2019) 370:581–92. doi: 10.1124/jpet.119.258012
85. Szebeni J, Muggia F, Gabizon A, Barenholz Y. Activation of complement by therapeutic liposomes and other lipid excipient-based therapeutic products: prediction and prevention. *Adv Drug Deliver Rev* (2011) 63:1020–30. doi: 10.1016/j.addr.2011.06.017
86. Szebeni J. Complement activation-related pseudoallergy: a new class of drug-induced acute immune toxicity. *Toxicology* (2005) 216:106–21. doi: 10.1016/j.tox.2005.07.023
87. Yang A, Liu W, Li Z, Jiang L, Xu H, Yang X. Influence of polyethyleneglycol modification on phagocytic uptake of polymeric nanoparticles mediated by immunoglobulin G and complement activation. *J Nanosci Nanotechnol* (2010) 10:622–8. doi: 10.1166/jnn.2010.1738
88. Woodle MC, Lasic DD. Sterically stabilized liposomes. *Biochim Biophys Acta* (1992) 1113:171–99. doi: 10.1016/0304-4157(92)90038-C
89. Gabizon A, Isacson R, Rosengarten O, Tzemach D, Shmeeda H, Sapir R. An open-label study to evaluate dose and cycle dependence of the pharmacokinetics of pegylated liposomal doxorubicin. *Cancer Chemother Pharmacol* (2008) 61:695–702. doi: 10.1007/s00280-007-0525-5
90. Szebeni J. Complement activation-related pseudoallergy: a stress reaction in blood triggered by nanomedicines and biologicals. *Mol Immunol* (2014) 61:163–73. doi: 10.1016/j.molimm.2014.06.038
91. Salehen N, Stover C. The role of complement in the success of vaccination with conjugated vs. unconjugated polysaccharide antigen. *Vaccine* (2008) 26:451–9. doi: 10.1016/j.vaccine.2007.11.049
92. Kurtovic L, Boyle MJ, Opi DH, Kennedy AT, Tham WH, Reiling L, et al. Complement in malaria immunity and vaccines. *Immunol Rev* (2020) 293:38–56. doi: 10.1111/imr.12802
93. Kim YJ, Kim KH, Ko EJ, Kim MC, Lee YN, Jung YJ, et al. Complement C3 Plays a Key Role in Inducing Humoral and Cellular Immune Responses to Influenza Virus Strain-Specific Hemagglutinin-Based or Cross-Protective M2 Extracellular Domain-Based Vaccination. *J Virol* (2018) 92:e00969–18. doi: 10.1128/JVI.00969-18
94. Suzuki K, Grigorova I, Phan TG, Kelly LM, Cyster JG. Visualizing B cell capture of cognate antigen from follicular dendritic cells. *J Exp Med* (2009) 206:1485–93. doi: 10.1084/jem.20090209
95. Strainic MG, Liu J, Huang D, An F, Lalli PN, Muqim N, et al. Locally produced complement fragments C5a and C3a provide both costimulatory and survival signals to naive CD4+ T cells. *Immunity* (2008) 28:425–35. doi: 10.1016/j.immuni.2008.02.001
96. Carroll MC, Isenman DE. Regulation of humoral immunity by complement. *Immunity* (2012) 37:199–207. doi: 10.1016/j.immuni.2012.08.002
97. Dempsey PW, Allison ME, Akkaraju S, Goodnow CC, Fearon DT. C3d of complement as a molecular adjuvant: bridging innate and acquired immunity. *Science* (1996) 271:348–50. doi: 10.1126/science.271.5247.348
98. Reddy ST, van der Vlies AJ, Simeoni E, Angeli V, Randolph GJ, O'Neil CP, et al. Exploiting lymphatic transport and complement activation in nanoparticle vaccines. *Nat Biotechnol* (2007) 25:1159–64. doi: 10.1038/nbt1332
99. Fearon DT, Carroll MC. Regulation of B lymphocyte responses to foreign and self-antigens by the CD19/CD21 complex. *Annu Rev Immunol* (2000) 18:393–422. doi: 10.1146/annurev.immunol.18.1.393
100. Markiewski MM, Lambris JD. Is complement good or bad for cancer patients? *A New Perspect an old dilemma Trends Immunol* (2009) 30:286–92. doi: 10.1016/j.it.2009.04.002
101. Taylor RP, Lindorfer MA. Cytotoxic mechanisms of immunotherapy: Harnessing complement in the action of anti-tumor monoclonal antibodies, Semin. *Immunology* (2016) 28:309–16. doi: 10.1016/j.smim.2016.03.003
102. Reis ES, Mastellos DC, Ricklin D, Mantovani A, Lambris JD. Complement in cancer: untangling an intricate relationship. *Nat Rev Immunol* (2017) 18:5–18. doi: 10.1038/nri.2017.97
103. Markiewski MM, DeAngelis RA, Benencia F, Ricklin-Lichtsteiner SK, Koutoulaki A, Gerard C, et al. Modulation of the antitumor immune response by complement. *Nat Immunol* (2008) 9:1225–35. doi: 10.1038/ni.1655
104. Talmadge JE, Gabrilovich DI. History of myeloid-derived suppressor cells. *Nat Rev Cancer* (2013) 13:739–52. doi: 10.1038/nrc3581
105. Ricklin D, Lambris JD. Complement in immune and inflammatory disorders: pathophysiological mechanisms. *J Immunol* (2013) 190:3831–8. doi: 10.4049/jimmunol.1203487
106. Corrales L, Ajona D, Rafail S, Lasarte JJ, Riezu-Boj JI, Lambris JD, et al. Anaphylatoxin C5a creates a favorable microenvironment for lung cancer progression. *J Immunol* (2012) 189:4674–83. doi: 10.4049/jimmunol.1201654
107. Vadrevu SK, Chintala NK, Sharma SK, Sharma P, Cleveland C, Riediger L, et al. Complement c5a receptor facilitates cancer metastasis by altering T-cell responses in the metastatic niche. *Cancer Res* (2014) 74:3454–65. doi: 10.1158/0008-5472.CAN-14-0157
108. Ostrand-Rosenberg S, Sinha P, Beury DW, Clements VK. Cross-talk between myeloid-derived suppressor cells (MDSC), macrophages, and dendritic cells enhances tumor-induced immune suppression, Semin. *Cancer Biol* (2012) 22:275–81. doi: 10.1016/j.semcancer.2012.01.011
109. Markiewski MM, Vadrevu SK, Sharma SK, Chintala NK, Ghouse S, Cho JH, et al. The Ribosomal Protein S19 Suppresses Antitumor Immune Responses via the Complement C5a Receptor 1. *J Immunol* (2017) 198:2989–99. doi: 10.4049/jimmunol.1602057
110. Monk PN, Scola AM, Madala P, Fairlie DP. Function, structure and therapeutic potential of complement C5a receptors. *Br J Pharmacol* (2007) 152:429–48. doi: 10.1038/sj.bjp.0707332
111. Bettelli E, Carrier Y, Gao W, Korn T, Strom TB, Oukka M, et al. Reciprocal developmental pathways for the generation of pathogenic effector TH17 and regulatory T cells. *Nature* (2006) 441:235–8. doi: 10.1038/nature04753
112. Bonavita E, Gentile S, Rubino M, Maina V, Papait R, Kunderfranco P, et al. PTX3 is an extrinsic oncosuppressor regulating complement-dependent inflammation in cancer. *Cell* (2015) 160:700–14. doi: 10.1016/j.cell.2015.01.004
113. Wang Y, Sun SN, Liu Q, Yu YY, Guo J, Wang K, et al. Autocrine Complement Inhibits IL10-Dependent T-cell-Mediated Antitumor Immunity to Promote Tumor Progression. *Cancer Discovery* (2016) 6:1022–35. doi: 10.1158/2159-8290.CD-15-1412
114. Karsten CM, Laumonnier Y, Eurich B, Ender F, Broker K, Roy S, et al. Monitoring and cell-specific deletion of C5aR1 using a novel floxed GFP-C5aR1 reporter knock-in mouse. *J Immunol* (2015) 194:1841–55. doi: 10.4049/jimmunol.1401401
115. Nunez-Cruz S, Gimotty PA, Guerra MW, Connolly DC, Wu YQ, DeAngelis RA, et al. Genetic and pharmacologic inhibition of complement impairs endothelial cell function and ablates ovarian cancer neovascularization. *Neoplasia* (2012) 14:994–1004. doi: 10.1593/neo.121262
116. Bulla R, Tripodo C, Rami D, Ling GS, Agostinis C, Guarnotta C, et al. C1q acts in the tumour microenvironment as a cancer-promoting factor independently of complement activation. *Nat Commun* (2016) 7:10346. doi: 10.1038/ncomms10346
117. Reese B, Silwal A, Daugherity E, Daugherity M, Arabi M, Daly P, et al. Complement as Prognostic Biomarker and Potential Therapeutic Target in Renal Cell Carcinoma. *J Immunol* (2020) 205:3218–29. doi: 10.4049/jimmunol.2000511
118. Roumenina LT, Daugan MV, Noe R, Petitprez F, Vano YA, Sanchez-Salas R, et al. Tumor Cells Hijack Macrophage-Produced Complement C1q to Promote Tumor Growth. *Cancer Immunol Res* (2019) 7:1091–105. doi: 10.1158/2326-6066.CIR-18-0891
119. Cho MS, Vasquez HG, Rupaimoole R, Pradeep S, Wu S, Zand B, et al. Autocrine effects of tumor-derived complement. *Cell Rep* (2014) 6:1085–95. doi: 10.1016/j.celrep.2014.02.014
120. Kolev M, Markiewski MM. Targeting complement-mediated immunoregulation for cancer immunotherapy, Semin. *Immunology* (2018) 37:85–97. doi: 10.1016/j.smim.2018.02.003
121. Sharma SK, Chintala NK, Vadrevu SK, Patel J, Karbowniczek M, Markiewski MM. Pulmonary alveolar macrophages contribute to the premetastatic niche by suppressing antitumor T cell responses in the lungs. *J Immunol* (2015) 194:5529–38. doi: 10.4049/jimmunol.1403215
122. Ghouse SM, Vadrevu SK, Manne S, Reese B, Patel J, Patel B, et al. Therapeutic Targeting of Vasculature in the Premetastatic and Metastatic Niches Reduces Lung Metastasis. *J Immunol* (2020) 204:990–1000. doi: 10.4049/jimmunol.1901208

123. Harboe M, Mollnes TE. The alternative complement pathway revisited. *J Cell Mol Med* (2008) 12:1074–84. doi: 10.1111/j.1582-4934.2008.00350.x
124. Moghimi SM. Cancer nanomedicine and the complement system activation paradigm: Anaphylaxis and tumour growth. *J Controlled Release Off J Controlled Release Soc* (2014) 190:556–62. doi: 10.1016/j.jconrel.2014.03.051
125. Sabnani MK, Rajan R, Rowland B, Mavinkurve V, Wood LM, Alberto AG, et al. Liposome promotion of tumor growth is associated with angiogenesis and inhibition of antitumor immune responses. *Nanomed Nanotechnol Biol Med* (2014) 11:259–62. doi: 10.1016/j.nano.2014.08.010
126. Moghimi SM, Andresen TL. Complement-mediated tumour growth: implications for cancer nanotechnology and nanomedicines. *Mol Immunol* (2009) 46:1571–2. doi: 10.1016/j.molimm.2009.02.014
127. Rajan R, Sabnani MK, Mavinkurve V, Shmeeda H, Mansouri H, Bonkoungou S, et al. Liposome-induced immunosuppression and tumor growth is mediated by macrophages and mitigated by liposome-encapsulated alendronate. *J Controlled Release Off J Controlled Release Soc* (2018) 271:139–48. doi: 10.1016/j.jconrel.2017.12.023
128. Moghimi SM, Farhangrazi ZS. Just so stories: The random acts of anti-cancer nanomedicine performance. *Nanomed Nanotechnol Biol Med* (2014) 10:1661–6. doi: 10.1016/j.nano.2014.04.011
129. Lammers T, Kiessling F, Hennink WE, Storm G. Drug targeting to tumors: principles, pitfalls and (pre-) clinical progress. *J Controlled Release Off J Controlled Release Soc* (2012) 161:175–87. doi: 10.1016/j.jconrel.2011.09.063
130. Petersen GH, Alzghari SK, Chee W, Sankari SS, La-Beck NM. Meta-analysis of clinical and preclinical studies comparing the anticancer efficacy of liposomal versus conventional non-liposomal doxorubicin. *J Controlled Release Off J Controlled Release Soc* (2016) 232:255–64. doi: 10.1016/j.jconrel.2016.04.028
131. Rosenberg SA. Progress in human tumour immunology and immunotherapy. *Nature* (2001) 411:380–4. doi: 10.1038/35077246
132. Dyer O. Experimental drug that injured UK volunteers resumes in human trials. *BMJ* (2015) 350:h1831. doi: 10.1136/bmj.h1831
133. Eastwood D, Bird C, Dilger P, Hockley J, Findlay L, Poole S, et al. Severity of the TGN1412 trial disaster cytokine storm correlated with IL-2 release. *Br J Clin Pharmacol* (2013) 76:299–315. doi: 10.1111/bcp.12165
134. Finco D, Grimaldi C, Fort M, Walker M, Kiessling A, Wolf B, et al. Cytokine release assays: current practices and future directions. *Cytokine* (2014) 66:143–55. doi: 10.1016/j.cyto.2013.12.009
135. Kenter MJ, Cohen AF. The return of the prodigal son and the extraordinary development route of antibody TGN1412 - lessons for drug development and clinical pharmacology. *Br J Clin Pharmacol* (2015) 79:545–7. doi: 10.1111/bcp.12605
136. Tranter E, Peters G, Boyce M, Warrington S. Giving monoclonal antibodies to healthy volunteers in phase 1 trials: is it safe? *Br J Clin Pharmacol* (2013) 76:164–72. doi: 10.1111/bcp.12096
137. Vessillier S, Eastwood D, Fox B, Sathish J, Sethu S, Dougall T, et al. Cytokine release assays for the prediction of therapeutic mAb safety in first-in man trials - Whole blood cytokine release assays are poorly predictive for TGN1412 cytokine storm. *J Immunol Methods* (2015) 424:43–52. doi: 10.1016/j.jim.2015.04.020
138. Jones SW, Roberts RA, Robbins GR, Perry JL, Kai MP, Chen K, et al. Nanoparticle clearance is governed by Th1/Th2 immunity and strain background. *J Clin Invest* (2013) 123:3061–73. doi: 10.1172/JCI66895
139. Gibson JM, Alzghari S, Ahn C, Trantham H, La-Beck NM. The role of pegylated liposomal doxorubicin in ovarian cancer: a meta-analysis of randomized clinical trials. *Oncologist* (2013) 18:1022–31. doi: 10.1634/theoncologist.2013-0126
140. Gabizon AA, Patil Y, La-Beck NM. New insights and evolving role of pegylated liposomal doxorubicin in cancer therapy. *Drug Resist Update* (2016) 29:90–106. doi: 10.1016/j.drup.2016.10.003
141. Golan T, Grenader T, Ohana P, Amitay Y, Shmeeda H, La-Beck NM, et al. Pegylated liposomal mitomycin C prodrug enhances tolerance of mitomycin C: a phase 1 study in advanced solid tumor patients. *Cancer Med* (2015) 4:1472–83. doi: 10.1002/cam4.491

Conflict of Interest: The authors declare that the research was conducted in the absence of any commercial or financial relationships that could be construed as a potential conflict of interest.

frontiers in Immunology

REVIEW
published: 11 January 2021
doi: 10.3389/fimmu.2020.599117

Immunological Basis of the Endometriosis: The Complement System as a Potential Therapeutic Target

Chiara Agostinis[1†], *Andrea Balduit*[2†], *Alessandro Mangogna*[1*], *Gabriella Zito*[1], *Federico Romano*[1], *Giuseppe Ricci*[1,3], *Uday Kishore*[4*] and *Roberta Bulla*[2]

[1] Institute for Maternal and Child Health, IRCCS (Istituto di Ricovero e Cura a Carattere Scientifico) "Burlo Garofolo", Trieste, Italy, [2] Department of Life Sciences, University of Trieste, Trieste, Italy, [3] Department of Medical, Surgical and Health Science, University of Trieste, Trieste, Italy, [4] Biosciences, College of Health, Medicine and Life Sciences, Brunel University London, Uxbridge, United Kingdom

Endometriosis (EM) is a chronic disease characterized by the presence and proliferation of functional endometrial glands and stroma outside the uterine cavity. Ovaries and pelvic peritoneum are the most common locations for endometrial ectopic tissue, followed by deep infiltrating EM sites. The cyclic and recurrent bleeding, the progressive fibrosis and the peritoneal adhesions of ectopic endometrial glands, may cause different symptoms depending on the origin involved. EM is a frequent clinical condition affecting around 10% of women of mainly reproductive age, as well as in post-menopausal women and adolescents, especially with uterine anomalies. The risk of developing EM depends on a complex interaction between genetic, immunological, hormonal, and environmental factors. It is largely considered to arise due to a dysfunction of immunological surveillance. In fact, women with EM exhibit altered functions of peritoneal macrophages, lymphocytes and natural killer cells, as well as levels of inflammatory mediators and growth factors in the peritoneal fluid. In EM patients, peritoneal macrophages are preponderant and highly active compared to healthy women. Peritoneal macrophages are able to regulate the events that determine the production of cytokines, prostaglandins, growth factors and complement components. Several studies have shown alteration in the regulation of the complement activation, leading to chronic inflammation characteristic of EM. Aberrant regulation/activation of the complement system has been observed in the peritoneal cavity of women affected by EM. Thus, complement inhibition may represent a new approach for the treatment of EM, given that a number of complement inhibitors are under pre-clinical and clinical development. Such an intervention may provide a broader therapeutic control of complement-mediated inflammatory damage in EM patients. This review will focus on our current understanding of the role of complement activation in EM and possible modalities available for complement-based therapy.

Keywords: endometriosis, inflammation, innate immunity, complement system, immunotherapy

OPEN ACCESS

Edited by:
Marcin Okrój, Intercollegiate Faculty of Biotechnology of University of Gdańsk and Medical University of Gdańsk, Poland

Reviewed by:
Péter Gál, Hungarian Academy of Sciences (MTA), Hungary
Ilse Jongerius, Sanquin Research, Netherlands

***Correspondence:**
Alessandro Mangogna
alessandro.mangogna@burlo.trieste.it
Uday Kishore
uday.kishore@brunel.ac.uk; ukishore@hotmail.com

[†]These authors have contributed equally to this work

Specialty section:
This article was submitted to Molecular Innate Immunity, a section of the journal Frontiers in Immunology

Received: *26 August 2020*
Accepted: *27 November 2020*
Published: *11 January 2021*

Citation:
Agostinis C, Balduit A, Mangogna A, Zito G, Romano F, Ricci G, Kishore U and Bulla R (2021) Immunological Basis of the Endometriosis: The Complement System as a Potential Therapeutic Target. Front. Immunol. 11:599117. doi: 10.3389/fimmu.2020.599117

INTRODUCTION

Endometriosis (EM) is a common inflammatory disease caused by the dissemination or growth of endometrium-like tissue at abnormal locations, or through the onset of endometrial tissue *via* metaplasia outside the usual location (1, 2). The disease is considered a heterotopia; the endometrium-like heterotopic tissues are characterized by glands and stroma functionally responsive to local, endogenous and exogenous hormonal stimuli (3). In fact, the ectopic endometrium is affected, like the normal uterine mucosa, by the ovarian hormones, especially estrogens, and therefore, become proliferative and functional (characterized by flaking and bleeding during the menstrual period) similar to those that occur in the normal endometrium (3). It is, therefore, a disease invariably of fertile age when ovarian activity is present; it occurs exceptionally in puberty and rarely in adolescence. It tends to regress in post-menopause or after castration. It is more frequent in nulliparous women (4, 5).

The ectopic EM is usually found on the pelvic peritoneum and in the pelvic organs (ovaries, tubes, intestine, rectum-sigmoid, uterine ligaments, recto-vaginal septum, and bladder) (6). EM can also occur in organs and tissues outside or far from the pelvis (navel, vulva, scars of laparotomy operations, appendix, and lungs) (6, 7). The etiology of EM remains unclear (8). Even though the precise frequency of EM in the general population is unknown, it represents a recurrent pathology among women of reproductive age (2). The estimates of the incidence of the disease (which can vary enormously) are around 10% in reproductive-age women (4). Endometriotic lesions, in particular ovary endometrioma (**Figure 1**), present a 2–3-fold increased risk of transformation in clear-cell or endometrioid ovarian carcinomas. Recent findings have demonstrated that somatic mutations in cancer-associated genes, such as *KRAS, PIK3CA, ARID1A*, and *PPP2R1A*, are commonly found in different types of EM (9). EM is an estrogen-dependent disease since estrogen appears to play a primary role in the development and maintenance of endometriotic lesions (10). Several proposals have been put forward to explain the pathogenic mechanisms involved in EM (2) (**Figure 1**), which are as follows:

Tubal Reflux of Menstrual Blood and Implantation of Endometrial Frustules in Various Tissues

Frustules of uterine mucosa not only have the ability to implant, but can be stimulated to proliferate by the cyclic action of ovarian estrogens. Since retrograde menstruation is so frequent (almost considered a physiological phenomenon), the possibility of developing EM is likely to depend on the relationship between the quantity of endometrium refluxed into the peritoneal cavity, and the receptivity intrinsic to the implant of endometrial cells (11, 12).

Dissemination *via* Lymphatic or Blood

Viable endometrial cells could enter the blood vessels and lymphatics with consequent embolization and implantation at ectopic sites (13–15).

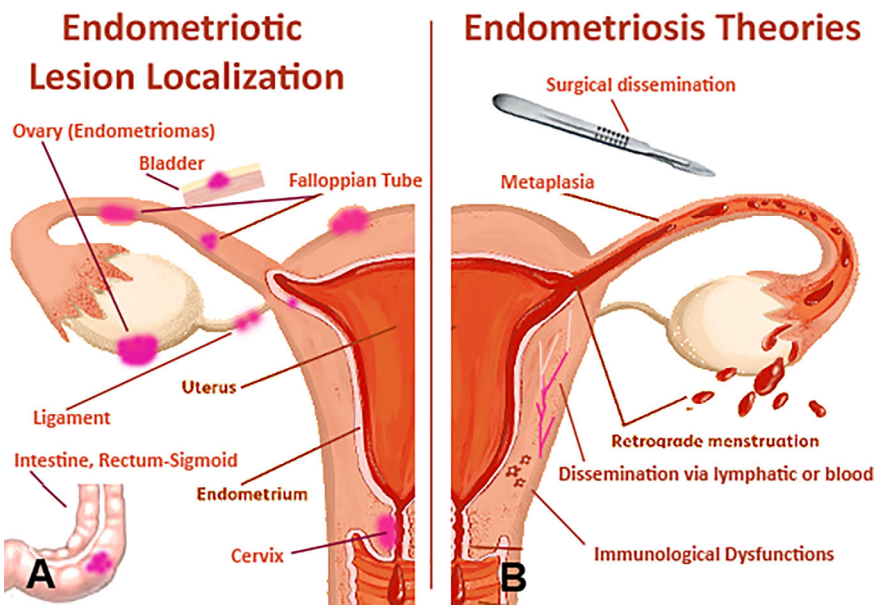

FIGURE 1 | Pathophysiological features of endometriosis (EM). **(A)** the female anatomy with areas that are commonly affected by EM. **(B)** likely pathogenic mechanisms involved in EM: potential origins of the endometriotic lesions include surgical dissemination, transplantation of endometrial tissue through retrograde menstruation, and *in situ* coelomic metaplasia of the peritoneal lining. Vascular or lymphatic metastasis occurs rarely, in cases of extrapelvic lesions. Superficial and deep endometriotic lesions are established and maintained through interacting molecular mechanisms that promote cellular adhesion and proliferation, systemic and localized steroidogenesis, localized inflammatory response and immune dysregulation.

Metaplasia of the Epithelium of Celomatic or Müllerian Origin

Ectopic EM can originate from mesothelial totipotent cells of the peritoneum through metaplasia. This notion is considerably sound due to the fact that the celomatic epithelium, from which the epithelial cells of the Müllerian ducts originate, also differs in pleural and peritoneal epithelial cells, as well as in cells of the ovarian surface. Novak was the first to suggest the possibility that metaplasia could be prompted by induction factors (11, 16), such as sexual hormones, tubal reflux of endometrial debris, and inflammatory processes.

Surgical Dissemination

Surgical dissemination seems likely to be responsible for endometrial tissue spreading to ectopic sites, for instance on laparotomy scars. The so-called "iatrogenic endometriosis" may occur after operations of the uterine cavity (myomectomy and metroplasty), or in the case of surgical interventions carried out on pelvic organs, which may account for localization at the vulvo-perineal level (17, 18).

Dysfunctional Immune System

Studies have also suggested that EM is due to an alteration in the immune system in terms of immune-cell recruitment, cell-adhesion, and upregulated inflammatory processes, which can facilitate the implantation and survival of endometriotic lesions (19, 20). A distinct epigenetic profile can be observed between eutopic and ectopic endometrial tissues. By analysing global promoter methylation patterns, researchers have demonstrated that differentially methylated genes are associated with immune surveillance, inflammatory response, cell adhesion and negative regulation of apoptosis (21).

There is a paramount role of immune cells in the pathogenesis of EM. Recently, it has been shown that the complement system is one of the most preponderant pathways impaired in the EM (20, 22, 23). In this review, we examine how immune cells and complement contribute to the development and maintenance of EM, and possible modalities available for complement-based therapy in the clinical practice.

ENDOMETRIOTIC IMMUNE MICROENVIRONMENT

Monocytes and Macrophages

Macrophages are in the protagonist immune cells in the pathogenesis of EM. In normal endometrium, the macrophages increase in number in secretory phase; their physiological role is the clearance of cell debris over the course of the menstrual period. In eutopic endometrium of EM patients, this increase in macrophage number does not happen, but a global augmentation (hormonal cycle-independent) of macrophages (in particular of M1 macrophages) has been observed, as compared to the endometrium of non-EM women. In ectopic tissue, a high number of angiogenesis-supportive M2 macrophages are found in the lesions. The presence of M2 macrophages is predominant in lesions, peritoneal cavity and fluid of women with EM compared to healthy women (24, 25). Blood monocytes, once differentiated into tissue macrophages, increase proliferation of endometrial cells isolated from women affected by EM, whereas monocytes derived from healthy women inhibit endometrial cell proliferation (26).

Uterine Natural Killer Cells

It is well known that uterine Natural Killer (uNK) cells, which are characterized by lower cytotoxicity ($CD16^{low}$, $CD56^{bright}$), increase in number during secretory and menstrual phases to establish a suitable environment for embryo implantation (27–29). In the uterine endometrium of EM patients, this fluctuation is maintained, although Giuliani et al. demonstrated a decreased uNK percentage and activity (30). The uNK cells present in the peritoneal fluid of women affected by EM showed a lower activity and, in the lesions, a lower capability to induce apoptosis of endometrial cells (31, 32). Subsequent studies confirmed a lower NK cell cytotoxic activity in EM; this reduction is associated with the severity of the disease (32).

Mast Cells

An augmented number and activity of mast cells (MCs) is usually associated with normal endometrial tissue during menstruation; however, this remains debatable although MC role in tissue angiogenesis and regeneration is well established. A high numbers of degranulated MCs are a common characteristic of endometriotic lesions (33–38). The MC "fingerprint" of their involvement in acute inflammation is an increase in the production of secreted mediators such as pro-inflammatory cytokines (such as TNF-α); tryptase is currently considered one of the main diagnostic markers for MC activation (39). Borelli et al. demonstrated that peritoneal fluid of EM patients was tryptase enriched and could affect sperm motility (40).

The involvement of MCs in the EM lesion formation has been investigated in a recent study that showed that numerous MCs with heightened activation level were present in endometriotic lesions in both animal models and humans. MC stabilizers and inhibitors may be successfully used to treat EM. The high number of increasingly activated and degranulated MCs in deeply infiltrating EM and an intimate histological connection between MCs and nerves, indicate that MCs could play a pivotal role in the occurrence of pain and hyperalgesia in EM, most likely exerting a direct effect on nerve endings (37, 38).

In EM, an abundant infiltration of MCs can be detected around the stromal lesions. These MCs exhibit degranulation; scattered granules are also commonly identified. MCs are hardly observed within eutopic endometrium and normal uterine serosa of both EM patients and healthy women (41). MCs are present in endometrial cyst tissues. The localization of cells in the endometrial stroma is very limited, while many MCs can be seen around blood vessels and fibrotic interstitia, i.e., the fibrotic interstitium of endometrial cysts. Thus, MCs likely take part in the development of EM. Localization of MCs leads to a particularly strong association with adhesion and fibrosis (35, 36, 41).

Eosinophils and Neutrophils

Although to a lesser extent compared to uNKs, eosinophil number increases normally during secretory and menstrual phases. A higher level of eotaxin (a chemoattractant for eosinophils), compared to normal endometrium, was described in both eutopic and ectopic endometrium of EM patients, as well as in peritoneal fluids of severe EM (42).

Neutrophil number increases only during the menstruation phase as well as in the endometrium of EM patient; but the neutrophils present in the eutopic tissue of EM patients, compared to those derived from healthy endometrium, present an increased activation state characterized by elevated reactive oxygen species production and CD11b expression (43, 44). The number of neutrophils are increased in the peritoneal cavity of EM patients; endometriotic neutrophils produce angiogenic factors and cytokines such as VEGF, IL-8, and CXCL10, and reactive oxygen species, which may support which may support the disease progression (45). In addition, Takamura et al. demonstrated a significant presence of neutrophils in ectopic endometrium, suggesting their role in the angiogenesis of the lesions (46).

Lymphocytes

Aberrant T lymphocyte response to autologous endometrial cells has been observed in EM. Co-cultures of autologous lymphocytes and endometrial cells allowed evaluation of lymphocyte proliferation in response to autologous endometrium in controls and to ectopic and eutopic endometrial cells from patients. The lymphocyte proliferative response to autologous endometrial cells appeared to be lower in women with EM and in animal models of spontaneous EM (47, 48). Furthermore, employing a ^{51}Cr microassay of lymphocytotoxicity to endometrial cell, Russel et al. demonstrated that T lymphocyte cytotoxicity against autologous endometrial cells is significantly decreased in women affected by EM (49–51). The defect in T-lymphocyte cytotoxicity, i.e. of $CD8^+$ cytotoxic T cells, was resolved by recombinant IL-2 stimulation of peripheral blood lymphocytes (52).

Fas ligand (FasL) is able to induce lymphocyte apoptosis by binding to its receptor, Fas, which is also expressed on lymphocytes. Therefore, cells expressing high levels of FasL may induce apoptosis of surrounding lymphocytes, thereby preventing lymphocyte response. Remarkably, FasL expression in endometrial stromal cells is stimulated by IL-8, and CCL2, CCL12, and CCL13 cytokines/chemokines, which are also increased in the peritoneal fluids and sera of the EM patients. Soluble FasL, which also induces apoptosis in Fas-expressing cells, showed reduced levels in the peritoneal fluid of women with advanced stages of EM. The CD4:CD8 ratio appeared to be decreased in endometriotic peritoneal fluid. Although the total number of $CD4^+$ T cells was found to be elevated, the activated status of $CD4^+$ as well as $CD8^+$ T cells, characterized by the expression of CD11, was decreased in endometriotic peritoneal fluid (49, 53).

The number of total and activated T lymphocytes is increased in ectopic endometrium in comparison with eutopic endometrium; IL-4 and IL-10 are upregulated in peripheral lymphocytes in women affected by EM. A higher IL-4 expression is also reported for lymphocytes present in endometriotic tissues and in peritoneal fluids. On the contrary, the production of IFN-γ is lower in peripheral lymphocytes in EM. T helper (Th)1/Th2 balance is shifted toward Th2 in EM (54). Hirata et al. recently demonstrated the presence of Th17 cells in peritoneal fluid of EM women. IL-17 stimulates EM stromal cell proliferation, and their expression of IL-8 and cyclooxygenase-2 (55). In eutopic endometrial tissues, the amount of regulatory T cells is significantly lower during the secretory phase in healthy women; this reduction was not present in EM women.

Studies have also focused on the role of B lymphocytes in the development of EM, considering in particular autoimmune responses. Wild and Shivers showed the presence of anti-endometrial antibodies in the sera of EM patients (56). Anti–nuclear antibodies, anti-DNA antibodies, and anti-phospholipid antibodies have also been detected in women with EM and it is likely that Th2 polarization in EM is the precipitating factor for the appearance of these autoantibodies (57). The relationship between autoantibody and EM may also explain EM-associated infertility, since these antibodies might bind not only to the endometrial tissue but also to embryos and sperms.

COMPLEMENT SYSTEM

The complement system plays a very important role in the recognition and clearance of pathogens, apoptotic and necrotic cells (58–61).

The complement system is represented by over 50 proteins, including soluble activation precursor components, regulators and cell surface receptors (62). The complement system is very efficient at tagging or flagging the non-self (pathogens), altered self (apoptotic/necrotic cells, and protein aggregates), and transformed self (tumor cells), which can result in lysis of target cells/pathogens, opsonization and subsequent enhanced uptake by phagocytic cells of the immune system *via* complement receptors, and generation of inflammatory mediators. In addition, the complement system can also modulate the adaptive immune response, and act as a link between innate and adaptive immunity (63).

Complement Classical Pathway

The complement system can be activated through three major pathways: classical, lectin, and alternative (**Figure 2**) (62, 64). The classical pathway is activated following the interaction of C1 complex with the antigen-antibody complex. C1 complex consists of three sub-components: C1q, C1r and C1s. Recognition of the Fc portion of cross-linked IgG1, IgG3 or IgM, fixed to a multivalent antigen, by C1q is the first step. The conformational change in the C1q molecule, induced by the bonding with immunoglobulins, activates the C1r subunit with serine-protease activity: this, in turn, triggers the proteolytic activity of the C1s molecule, which splits the subsequent protein of the complement cascade, the C4 molecule, in two

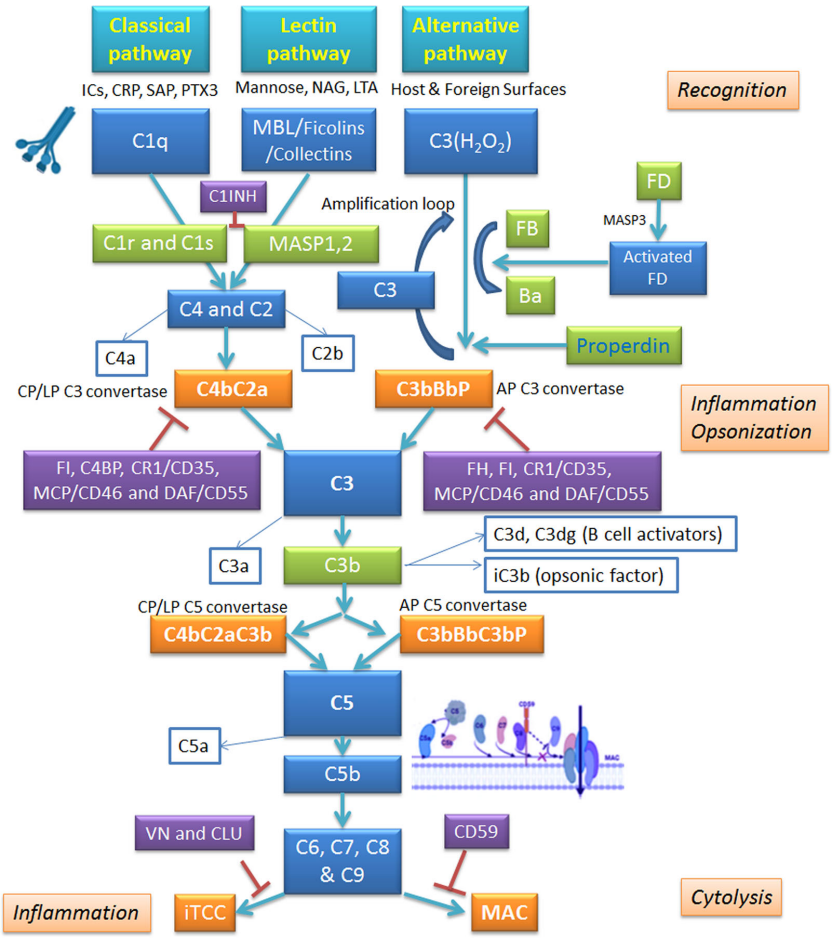

FIGURE 2 | Schematic overview of the complement system and its regulators. The complement system operates *via* three pathways: classical, alternative and lectin. Classical pathway is triggered by binding of C1q to antigen-antibody complex; alternative pathway involves autoactivation of C3, whereas lectin pathway is set in motion by Mannan-Binding Lectin (MBL) interaction with carbohydrate patterns on pathogen surface. All pathways converge on C3 convertase; from there, they follow identical routes of the cascade. The complement activation is kept in check by inhibitory regulators. AP, alternative pathway; CLU, clusterin; CP, classical pathway; CRP, C-reactive protein; CR1, complement receptor 1; C1INH, C1 inhibitor; DAF, decay-accelerating factor; FB, factor B; FD, factor B; FH, factor H; FI, factor I; ICs, immunocomplexes; iTCC, inactive terminal C complex; LP, lectin pathway; LTA, lipoteichoic acid; MAC, membrane attack complex; MCP, membrane cofactor protein; NAG, N-acetylglucosamine; PTX3, pentraxin 3; SAP, serum amyloid P component; VN, vitronectin.

fragments: C4a and C4b (65).The first fragment remains in circulation in the plasma, while the other binds covalently to membrane proteins and carbohydrates, ensuring that complement activity is maintained at a well-defined point. C4b, in the presence of Mg^{2+}, binds the C2 molecule and makes it susceptible to cleavage by the C1s subunit; following hydrolysis, the two fragments C2a and C2b are yielded: C2a binds to C4b giving rise to the complex C4b2a. The enzyme C4b2a, better known as C3 convertase of the classical pathway, remains attached to the surface of the pathogen/target and hydrolyzes the molecule C3 into C3a and C3b (66). C3a (anaphylatoxin) is a potent inflammatory molecule; C3b opsonizes target pathogen and brings about phagocytosis by macrophages and polymorphonuclear cells. In addition, C3b interacts with C4b2a complex, yielding C5 convertase of the classical pathway (C4b2a3b) (66).

The C5 convertase cleaves the C5 molecule into C5a and C5b; C5b, by binding to C6, forms a hydrophilic complex, which undergoes a conformational change following association with C7. This favors the exposure of lipophilic groups with which the β subunit of the C8 molecule makes contact, while the α subunit penetrates the lipid double layer of the membrane of the target cell, following the conformational changes of the complex. Finally, the association of C5b678 with C9 induces its polymerization, and therefore, the formation of stable, cylinder-shaped transmembrane porous channels, which promote an osmotic imbalance, i.e. they alter the flow of ions and the gradient of molecules and water, inducing cell lysis. The final components of the complement system are designated as the membrane attack complex (MAC) (62, 64). Recent studies have established that the classic pathway can be activated, regardless of the presence of antibodies, by damage signal

molecules such as C-reactive protein, viral proteins, amyloid β, polyanions (lipopolysaccharides, DNA and RNA), mitochondrial fragments, necrotic and apoptotic cells (60, 67).

Complement Lectin Pathway

The lectin pathway is initiated by the binding of mannan-binding lectin (MBL), ficolin (1, 2 or 3), or collectin 11 (CL-K1) to mannose residues and other carbohydrate patterns present on the cell surface of pathogenic microorganisms (68, 69). The binding promotes the association of MBL with the serine proteases, MASP (MBL-Associated Serine Protease): there are three MASPs which form complexes with MBL oligomers, MASP-1 (70), MASP-2 (71), and MASP- 3 (72), and two non-enzymatic associated proteins, Map44 (73) and Map19 (74). MASP-1 and MASP-2 activate the lectin pathway of the complement system (75, 76) *via* cleavage of C4 and C2, while MASP-3 is responsible for the activation of alternative pathway (75, 77). The MASPs are close homologs of C1r and C1s but they form only dimers, not tetramers. C1 has a fixed stoichiometry of one C1q, two C1r, and two C1s. The C1r binds directly to the C1q, and C1s then binds to C1r, thus yielding a hetero-tetramer. It has become clear that the MBL-MASPs complexes are not quite equivalent to C1: they are smaller and very heterogeneous. MBL forms homodimeric complexes with MASPs. MASP activation, and C4 and C2 cleavage, leads to the formation of the C3 convertase of the lectin pathway or C4b2a. This enzyme cleaves the C3 molecule to C3a and C3b, the resulting C4b2a3b complex degrades C5 to C5a and C5b; the subsequent phases are similar to those of the classical pathway. This pathway seems to be active especially during childhood and during the transition period from passive immunity, operated by maternal antibodies, to active immunity (67).

Complement Alternative Pathway

Unlike the classical and lectin pathways, the alternative pathway is independent of antigen-antibody complexes and can be directly induced by components of the cell wall of the bacteria and those present on the surface of the damaged host cells *via* C3. C3 consists of two polypeptide chains, α and β, linked by a disulfide bridge (78). Under normal physiological conditions, the C3 is subject to basal activation by spontaneous hydrolysis of its thioester residue (79). The product of the hydrolysis reaction is the C3 (H_2O) molecule, which is rapidly inactivated in circulation; when bound to the surfaces of target cells, for example bacteria, it can associate with factor B (FB). As soon as it binds to C3 (H_2O), FB loses a small fragment (Ba) by a protease called factor D (FD). The residual fragment, Bb, remains bound to C3 (H_2O) making up the complex C3 (H_2O) Bb. This enzyme complex is capable of splitting C3 into C3a and C3b, which analogously to C3 (H_2O), binds the FB on which the FD acts, causing the excision of the fragment Ba and the formation of the enzyme complex C3bBb or C3 convertase of the alternative pathway (80). The C3 convertase of the alternative pathway is capable of splitting large quantities of C3, thus acting as a rapid amplification loop where fixed C3b molecules generated by either the classical or lectin pathway can bind to FB, resulting in FB cleavage by FD and generation of the convertase C3bBb (81). On pathogen surface, the highly labile C3 convertase is stabilized by factor P or properdin, increasing its half-life by 10-fold (82). Properdin is a plasma protein and the only known up-regulator of the alternative pathway. The next phase of this pathway is represented by the binding of the C3b molecule to the C3 convertase yielding C5 convertase, which cleaves the molecule C5 into C5a and C5b; the latter by binding to the C6–9 molecules participates in the formation of the MAC (83).

C3b is an intermediate that reacts with water, with the hydroxyl groups present on carbohydrates on the cell surfaces, with complexes of the immune system, and with free IgG, in a radius of about 60 nm from the point of its generation. Thanks to these interactions, the C3b molecule ensures its protection against inactivation by complement regulators, such as factor H (FH) and factor I (FI) (84); conversely, the free form in the fluid phase has a half-life of less than 1 s. It has also been noted that the C3b reacts preferentially with IgG, the second most abundant protein present in the plasma. The resulting complex, (C3b)2-IgG, seems to be the best precursor in the formation of C3 convertase of the alternative pathway, being less vulnerable to inactivation by FH (85). All this translates into greater effectiveness in the assembly of the convertases, involving properdin, which stabilizes the bond with FB and reduces the dissociation of the Bb fragment. The step described creates a amplification loop that theoretically could go on indefinitely, generating increasing quantities of the converted C3 and C3b molecule. The regulation of this positive feedback circuit depends on the concentration of FB and C3b molecules. The alternative pathway, in addition to carrying out the primary task of quickly covering the bacterial surface with high quantities of the opsonizing fragment of the complement, C3b, acts on the altered tissues of the host, characterized by cells that undergo apoptosis or at the site of wounds and infection (81).

Regulators of Complement Activation

When an abnormal complement activation occurs, for instance in patients with dysfunctional regulatory proteins or affected by autoimmune pathologies, it can be responsible for a severe inflammatory response involving various organs (66). In some circumstances, C5b67 complexes can deposit on healthy neighboring host cells, causing their lysis. Clusterin, a regulatory molecule of the classical pathway, can bind to MAC and block the insertion of the complex in the membrane (86, 87). All host cells have CD59, a small 20kDa GPI-linked protein which binds C5b-8, and stops C9 binding. CD59 limits the incorporation of the C8 and C9 molecules, and therefore, the formation of the MAC (88). Furthermore, these complexes can elicit various metabolic and cellular pathways, in addition to the production of inflammatory mediators, such as prostaglandins and leukotrienes, inducing a diffuse inflammatory state. To ensure efficient regulation of the complement system, it is necessary to maintain the integrity of the regulatory proteins, since anomalies affecting them can lead to excessive activation of the complement and pathological states (66).

To overcome this, the host cells have defense systems to guarantee their own protection, i.e. soluble regulators in plasma or membrane-bound on their own cell surface. The first category

includes the serine protease inhibitor C1-INH, responsible for inhibiting the C1 complex of the classical pathway and MASP-1 and MASP-2 of the lectin pathway (89); FI (90), the protagonist of the cleavage of the α chain of the molecules C3b, mediated by the FH; and C4b-binding protein (C4bp), which represents the main cofactor of FI in C4b degradation. Membrane-bound regulatory proteins include the cofactors of FI: Complement Receptor 1 (CR1, CD35) (91) and Decay Accelerating Factor (DAF; also designated as CD55) (92), which participate in C3b and C4b degradation, and Membrane Cofactor Protein (MCP; also called CD46) (93), which is involved in the prevention of the formation of the C3- and C5-convertases and the acceleration of their decay. When C5b-8 or C5b-9 assemble in plasma, several plasma proteins can bind to them, preventing its insertion into a lipid bilayer. These proteins include vitronectin and clusterin (alternative names: S-protein, SP40.40).

The surface of the host cells is also protected from the action of C3 convertase, thanks to polyanionic molecules exposed on the membrane such as glycosaminoglycans, heparin and sialic acid, which by binding to FH facilitate its interaction with C3b, promoting its hydrolysis by FI (94) Mutations affecting the genes coding for regulatory proteins, present in heterozygosity (haploinsufficiency), predispose subjects to pathologies, such as atypical Hemolytic Uremic Syndrome (aHUS), type II Membranoproliferative Glomerulonephritis and Macular Degeneration related to age (95).

COMPLEMENT SYSTEM IN THE ENDOMETRIAL LESION

The presence of C3 in endometriotic tissue was first highlighted in 1980 by Weed and Arquembourg (96). Subsequently, Bartisik and co-workers (97) confirmed the presence of C3 and C4 in endometrial tissue of patients undergoing diagnostic laparoscopy. A number of studies have validated the presence of complement components in the EM lesions (98–103). Tao et al. estimated the gene expression of C3 distinguishing between human eutopic and ectopic endometrium; the expression of C3 mRNA and protein appeared to be significantly higher in human ectopic endometrium in comparison with matched eutopic one (104). Glandular epithelial cells present in endometriotic implants have been shown to secrete C3; its expression is up-regulated by estradiol (103, 105). A recent study showed an interesting association between a particular SNP involved in C3 gene upregulation and the increased risk for EM and EM-associated infertility (101). Despite evidence of the presence of complement components in EM, their contribution to EM pathogenesis is far from clear.

Endometrial tissue–specific complement activation is frequently observed in women affected by EM (105, 106). One of the likely causes of complement activation in the EM microenvironment is the triggering of the coagulation cascade due to periodic bleeding of EM tissue. Thrombin can be responsible for the cleavage of C3 to C3a and C3b; activated platelets are also implicated in C3 cleavage (107). Another activator of the C3 is heme that is released from hemoglobin during hemolysis: heme induces deposition of C3b on erythrocytes (108). Alternative pathway can be activated through properdin binding to activated platelets promoting C3 (H_2O) recruitment and complement activation. In addition, the treatment of endothelial cells with C3a or other factors promptly stimulate the expression of P-selectin, which through the binding to C3b induces the formation of C3 convertases (109).

In EM lesions, the complement regulatory protein expression seems to be altered too. DAF expression levels were significantly reduced in samples isolated from EM patients during mid secretory phase. A decreased DAF protein level was confirmed in cells dissected by laser micro dissection (110).

COMPLEMENT COMPONENTS IN ENDOMETRIOSIS-DERIVED CELLS

High-throughput studies have highlighted C3 and other complement genes as the most up-regulated genes in EM tissues in comparison with normal endometrium (98, 99, 111, 112). The gene expression profile of eutopic and ectopic endometrial stromal cells (98) revealed C3, C7 and SERPIN5 as highly expressed transcripts. Immortalized ectopic endometriotic stromal cells in EM have been shown to produce mainly C3 and PTX3 and display a differential regulation of iron metabolism (112).

In addition to estradiol, a potential factor for the upregulation of C3 expression by endometrial cells was the peritoneal fluid rich in pro-inflammatory factors (113); TNF-α and IL-1β levels appeared to be increased in the peritoneal fluid of patients with EM, and higher levels of TNF-α seemed to be associated with more advanced stages of the disease (113–116).

Studies by Suryawanshi et al. (99) and Edwards et al. (117) revealed that chronic inflammation in EM is dominated by the complement system, which remains active in EM-associated ovarian cancer (EAOC) but not tumors, further demonstrating heterogeneity in the inflammatory *milieu* within ovarian cancer. C7, FD, FB, FH, and MASP1 are differentially expressed in EM compared to normal tissue. They observed an increase in C7, FD, FB, FH and a decrease in MASP-1 levels. Furthermore, C3 and C4A were up-regulated in EM compared to normal tissues as well as EAOC (99).

It is clear that further investigation is required to identify the factors that are produced by the endometrial tissue disseminated within the abdominal cavity which impact on the release of C3 and other components by the uterine endometrium (102). Although the pertinent role of the complement system in EM has been repeatedly confirmed, studies using complement gene knock-out animals, offering important insights into the pathogenesis and therapeutic interventions have been missing. We have recently generated a murine model of EM *via* injection of minced uterine tissue from a donor mouse into the recipient mice peritoneum using wild type and C3 gene-deficient ($C3^{-/-}$) mice (118). We found that the C3-deficient mice showed a lower amount of EM cyst formation in the peritoneum than

the wild-type mice. Furthermore, peritoneal washing from the wild type mice with EM showed more degranulated MCs compared to $C3^{-/-}$ mice, consistent with higher C3a levels in the peritoneal fluid of EM patients. Thus, C3a participates in an auto-amplifying loop, leading to MCs infiltration and activation, which is pathogenic in EM (118).

COMPLEMENT IN ENDOMETRIOSIS PERITONEAL FLUID

Complement activation can generate C3a and C5a, two well-known anaphylatoxins, which are capable of stimulating the peritoneal MCs and macrophages to produce mediators such as histamine or cytokines, which in turn increases the endometrial vascular permeability (102), causing inflammation and pain. We observed increased levels of C3a in the peritoneal fluid of EM patients (118); Kabut et al. (119) have also reported increased levels of C3c, C4, and sC5b-9 in the peritoneal fluid and serum of EM patients in comparison with healthy women. A recent study reported significantly higher concentrations of C1q, MBL and C1-INH in the peritoneal fluids of EM women as compared to the control group (120). No difference in plasma C3a levels between women with and without EM was found (121).

POSSIBILITY OF ANTI-COMPLEMENT IMMUNOTHERAPY IN ENDOMETRIOSIS

All currently available treatments for EM are not curative but suppressive and are accountable just for a transitory relief of the symptoms. The prevalent therapeutic options for relieving EM-associated pain are represented by contraceptive rather than fertility-promoting treatments (122). Immunotherapy is beginning to be considered as an option for EM treatment.

The first drug that blocked the complement pathway and approved for clinical trials was Eculizumab; the other drug currently approved is used for the treatment of hereditary angioedema (HAE): C1INH (Berinert, Cinryze, Ruconest) (123, 124) (**Figure 3**). Food and Drug Administration (FDA) approved Eculizumab (anti-C5 antibody) for the treatment of paroxysmal nocturnal hemoglobinuria (PNH) in 2007 (125), 40 years after the demonstration that complement was the principal cause of this devastating disease (126, 127). The clinical use of eculizumab for PNH therapy demonstrated that blocking of complement could be relatively safe, bringing life-changing results (128).

FDA approval of eculizumab for treating the rare renal disease aHUS in 2011 has fueled development of new anti-complement drugs for clinical trials over the last few years (129–132); some have entered clinical development while others are in phase 3 trials. The use of Eculizumab may be promising in the treatment of EM, although blocking the complement activation at C5 level could leave uncovered all the effects induced by C3 activation (e.g. C3a formation), a pivotal step in the EM pathogenesis.

Most efforts to improve complement-targeting immunotherapy are aimed at improving the pharmacokinetic properties of these drugs: to reduce the dose. A next-generation "recycling" form of eculizumab, called ravulizumab (Ultomiris™) (133), has been approved by both FDA and European Medicines Agency for the treatment of PNH, and is currently under review for aHUS (Ultomiris™). "Recycling" or "pH-switched" antibodies are produced by changing the antigen-binding region (incorporating histidine residues) of existing antibodies, so that the antibody loses affinity in the acidic pH 6.0 environment of the endosome. After the internalization of the antibody into the cells, the acidic pH causes the release of the target and recycling of the "empty" antibody back to the circulation (134). Crovalimab (Roche; SKY59) is another recycling anti-C5 antibody that is currently in phase II clinical trial (135–137).

An additional approach to reduce drug dose is to develop an antibody that binds neoepitopes on complement proteins rather than using one directed against the native protein. Several drugs are currently undergoing clinical evaluation, such as IFX-1 (InflaRx), which targets the released C5a fragment (138), and BIVV020 (Sanofi), a preclinical antibody developed for binding to activated C1s. It is largely expected that these anti-complement drugs can be of great potential in setting up clinical trials in EM patients.

The current pandemic caused by severe acute respiratory syndrome coronavirus 2 (SARS-CoV-2) infection has led to the testing of some complement immunotherapy drugs as well. Compstatin-based C3 inhibitor AMY-101 was safely and successfully used for the treatment of a patient with COVID-19 pneumonia (139, 140). Narsoplimab, a lectin-pathway inhibitor, has been shown to prevent the initiation of the lectin pathway and endothelial cell damage induced by SARS-CoV-2, lowering the risk of thrombotic disorders; all patients who received narsoplimab treatment recovered and survived without exhibiting any drug-related adverse effect (141).

AMY-101 (and other C3 inhibitors) could be a promising treatment for relapsing EM as well, being able to block C3 activation (128, 142–145). It is anticipated that a MASP inhibitor such as Narsoplimab will not exert a massive therapeutic effect on the EM pathogenesis since no evidence is available so far that is suggestive of a key involvement of the complement lectin pathway in the EM lesion formation. Various prospective anti-complement inhibitors studied so far are listed in **Table 1** and **Figure 4** (128, 141–176).

ENDOMETRIOSIS AND IMMUNOTHERAPY

We have discussed a strong link between EM and alterations of local and systemic immune system. In the context of EM, NK cells may be exploited as a potential target for immunotherapy. A reduced NK cell activity in women with EM was first reported by Oosterlynck et al. (177); a lowered NK cell cytotoxic action against autologous endometrial cells, both in peripheral blood and peritoneal fluid, was noted correlating with the severity of the disease (177, 178). In fact, EM is characterized by a

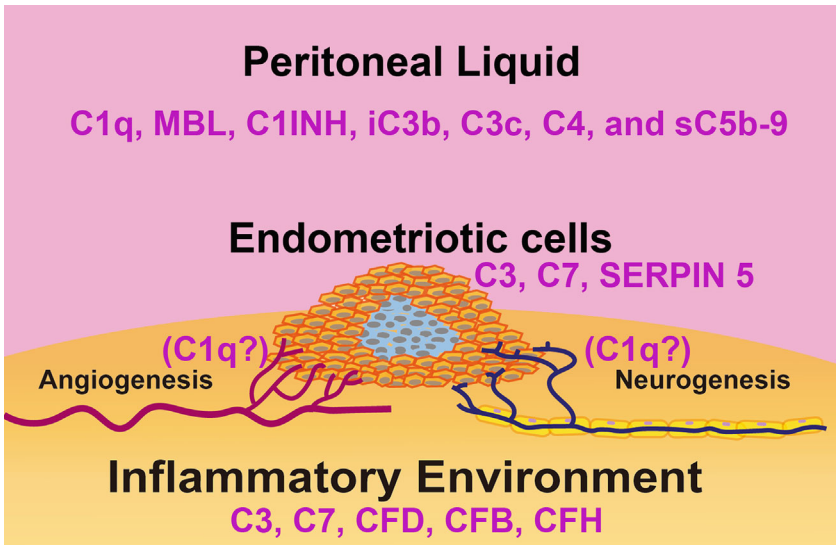

FIGURE 3 | Schematic representation of the complement system in the immune microenvironment of an endometriotic lesion. The lesions consist of epithelial, endothelial, stromal cells and leukocytes present in the tissue and surrounded by peritoneal liquid. Studies have linked disorders of the complement system activity/expression and pathogenesis of endometriosis. In the endometriotic lesions, high levels of C3, C7, factor D (FD), factor B (FB), and factor H (FH) have been detected. Isolated endometriotic cells express C3, C7 and SERPIN5. In the peritoneal liquid of EM patients, elevated levels of C1q, C4, Mannan-Binding Lectin (MBL), C1 Inhibitor (C1INH), inactivated C3b (iC3b), C3c and soluble C5b-9 (sC5b-9) have been reported.

downregulation of NK cell cytotoxicity (179, 180), probably due to the consistent amount of inhibitory cytokines in the peritoneal fluid of patients affected by EM, or to an augmented presence of several inhibitory NK cell receptors. It is reasonable to speculate that the incapacity of uNK cells, as well as macrophages, to recognize and eliminate endometriotic cells in the peritoneal cavity, can allow their survival and growth, leading to development and progression of EM (181).

In cancer, the activity of NK cells may depend on checkpoint molecules (182, 183). Thus, in EM, the activation of some checkpoint molecules could be involved in the reduced elimination of shed endometrial cells. For this reason, EM patients may benefit from suppressing NK cell negative control checkpoints, such as inhibitory NK cell receptors. Understanding checkpoints involved in the downregulation of NK cell activity in the progression of EM may be important for identifying new therapeutic targets (181).

A possible interaction between complement and impaired NK cell function has been demonstrated (184). In fact, Liu et al. hypothesized a role for the complement receptor, CR3, in imbalancing the tumor surveillance function of NK cells and suggested that the iC3b/CR3 signaling is a pivotal negative mediator of NK cell activity (184). Considering the consistent expression of CR3 on NK cells (185), negative regulatory roles of iC3b/CR3 axis and high level of iC3b in the peritoneal fluid of EM women (119), we can assume that iC3b/CR3 signaling is an important negative regulator of uNK cell function in EM, which possibly exerts a negative influence on cytotoxicity against autologous endometrial cells. Although high concentrations of C3c, C4, and sC5b-9 were found in the serum of patients with EM, iC3b levels were higher in the peritoneal fluid (119).

We consider that a complement C3 inhibitor could be used as a treatment for EM, exerting two potentially beneficial effects: on the one hand, one would attain an interruption from the beginning of the cascade of inflammatory signals that plays an important role in the pathogenesis of EM; on the other hand, a lower production of iC3b would result in a lower inhibition of the cytotoxic activity of the NK cells. The activation induced by C5a and C3a of macrophages and MCs in the endometriotic microenvironment could be partially blocked (or considerably reduced) by complement immune therapy; for instance, Danicopan could act to stop the auto-amplifying loop induced by C3a on MCs (118). Furthermore, C1q, present at high levels in the peritoneal fluid of the EM patients, can induce the differentiation of the tissue macrophages towards M2 phenotype (186, 187), and hence, promote the angiogenesis in EM lesions (188). Thus, an antibody able to block specifically the alternative functions of C1q could be interesting to test in the EM treatment, as well as in tumor development (189, 190).

In conclusion, EM is a devastating disease that has a range of social, personal and medical consequences for the women suffering from it. It has become apparent that immune dysregulation is a major factor that precipitates this pathological condition. While immune infiltration and constant inflammatory milieu foster the disease, the biggest pathological consequences arise from aberrant complement activation. There are a number of ways to suppress complement activation in EM patients. This therapeutic intervention needs careful pre-clinical and clinical trials, involving monotherapy or in combination with checkpoint inhibitors.

TABLE 1 | Principal anti-complement drugs.

Drug name	Target	References
ABP 959	C5	Chow et al. (146)
ACH-5448	FD	Zelek et al. (128)
ACH-5228	FD	Zelek et al. (128)
AMY101	C3	Mastellos et al. (142)
APL-2	C3	Zelek et al. (128); Wong et al. (143); Grossi et al. (144); Grossi et al. (145)
APL-9	C3	Zelek et al. (128)
AVACOPAN	C5aR1	Merkel et al. (147); Tesar et al. (148); Jayne et al. (149); Bekker et al. (150)
BERINERT	C1r/C1s, MASPs	Keating (151); Zanichelli et al. (152)
BIVV020	activated C1s	Zelek et al. (128)
CINRYZE	C1r/C1s, MASPs	Aygören-Pürsün et al. (153); Lyseng-Williamson (154); Bernstein (155)
CLG561	Properdin	Zelek et al. (128)
CP010	C6	Zelek et al. (128)
CROVALIMAB	C5	Röth et al. (156)
DANICOPAN	FD	Wiles et al. (157); Risitano et al. (158)
ECULIZUMAB	C5	Zelek et al. (128); Wijnsma et al. (159)
IFX-1	C5a	Zelek et al. (128); Giamarellos-Bourboulis et al. (160); Vlaar et al. (161)
IFX-2	C5a	Zelek et al. (128)
LNP023	FB	Zelek et al. (128)
MIROCOCEPT	CR1	Halstead et al. (162); Kassimatis et al. (163)
NOMACOPAN	C5	Schols et al. (164)
NARSOPLIMAB	MASP2	Rambaldi et al. (141); Elhadad et al. (165); Selvaskandan et al. (166)
OMS906	MASP3	Zelek et al. (128)
POZELIMAB	C5	Latuszek et al. (167)
PRO-02	C2	Zelek et al. (128)
RUCONEST	C1r/C1s, MASPs	Busse et al. (168); Cruz (169)
SOB ├005	C5	Zelek et al. (128)
SUTIMLIMAB	C1s	Freire et al. (170); Nikitin et al. (171); Bartko et al. (172); Jäger et al. (173)
TESIDOLUMAB	C5	Jordan et al. (174)
ZILUCOPLAN	C5	Albazli et al. (175); Wilkinson et al. (176)
ZILUCOPLAN-XR	C5	Zelek et al. (128)

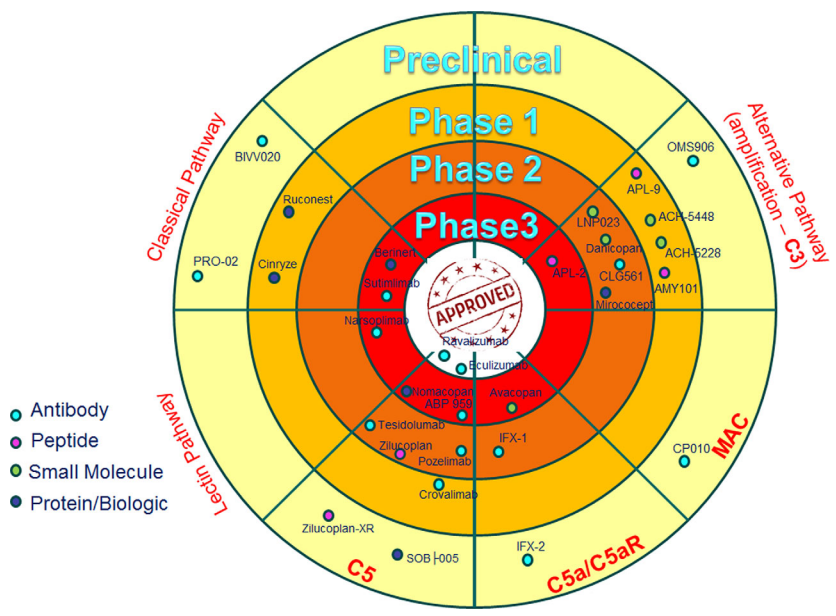

FIGURE 4 | Anti-complement drugs currently in clinical development. The dartboard with concentric rings indicates the different phases of clinical development, with "approved" in the centre. Only drugs currently in clinical development are shown and the most advanced stage of development for any indication is shown. The drugs are divided on the basis of the target (Classical, Lectin and Alternative Pathways), with the exception of some drugs that are directed to the common part of the three cascades (C5 and MAC), or drugs that are specifically blocking C5a activity (C5a/C5aR) (128).

AUTHOR CONTRIBUTIONS

CA, AB, AM, GZ, FR, GR, UK, and RB reviewed the literature and wrote sections of the review article. CA created figures. UK critically reviewed the entire manuscript. All authors contributed to the article and approved the submitted version.

FUNDING

The research was funded by the Italian Ministry of Health (RC 20/16, RC 23/18, RC 24/19 to GR and 5MILLE15D to CA – Institute for Maternal and Child Health IRCCS Burlo Garofolo, Trieste, Italy).

REFERENCES

1. Zondervan KT, Becker CM, Koga K, Missmer SA, Taylor RN, Vigano P. Endometriosis. *Nat Rev Dis Primers* (2018) 4(1):9. doi: 10.1038/s41572-018-0008-5
2. Zondervan KT, Becker CM, Missmer SA. Endometriosis. *N Engl J Med* (2020) 382(13):1244–56. doi: 10.1056/NEJMra1810764
3. Acien P, Velasco I. Endometriosis: a disease that remains enigmatic. *ISRN Obstet Gynecol* (2013) 2013:242149. doi: 10.1155/2013/242149
4. Shafrir AL, Farland LV, Shah DK, Harris HR, Kvaskoff M, Zondervan K, et al. Risk for and consequences of endometriosis: A critical epidemiologic review. *Best Pract Res Clin Obstet Gynaecol* (2018) 51:1–15. doi: 10.1016/j.bpobgyn.2018.06.001
5. Stuparich MA, Donnellan NM, Sanfilippo JS. Endometriosis in the Adolescent Patient. *Semin Reprod Med* (2017) 35(1):102–9. doi: 10.1055/s-0036-1597121
6. Rolla E. Endometriosis: advances and controversies in classification, pathogenesis, diagnosis, and treatment. *F1000Res* (2019) 8(F1000 Faculty Rev):529. doi: 10.12688/f1000research.14817.1
7. Agarwal N, Subramanian A. Endometriosis - morphology, clinical presentations and molecular pathology. *J Lab Phys* (2010) 2(1):1–9. doi: 10.4103/0974-2727.66699
8. Mehedintu C, Plotogea MN, Ionescu S, Antonovici M. Endometriosis still a challenge. *J Med Life* (2014) 7(3):349–57.
9. Wang Y, Nicholes K, Shih IM. The Origin and Pathogenesis of Endometriosis. *Annu Rev Pathol* (2020) 15:71–95. doi: 10.1146/annurev-pathmechdis-012419-032654
10. Dyson MT, Bulun SE. Cutting SRC-1 down to size in endometriosis. *Nat Med* (2012) 18(7):1016–8. doi: 10.1038/nm.2855
11. Lagana AS, Garzon S, Gotte M, Vigano P, Franchi M, Ghezzi F, et al. The Pathogenesis of Endometriosis: Molecular and Cell Biology Insights. *Int J Mol Sci* (2019) 20(22):5615. doi: 10.3390/ijms20225615
12. Liu H, Lang JH. Is abnormal eutopic endometrium the cause of endometriosis? The role of eutopic endometrium in pathogenesis of endometriosis. *Med Sci Monit* (2011) 17(4):RA92–9. doi: 10.12659/msm.881707
13. Li F, Alderman MH3rd, Tal A, Mamillapalli R, Coolidge A, Hufnagel D, et al. Hematogenous Dissemination of Mesenchymal Stem Cells from Endometriosis. *Stem Cells* (2018) 36(6):881–90. doi: 10.1002/stem.2804
14. Hey-Cunningham AJ, Fazleabas AT, Braundmeier AG, Markham R, Fraser IS, Berbic M. Endometrial stromal cells and immune cell populations within lymph nodes in a nonhuman primate model of endometriosis. *Reprod Sci* (2011) 18(8):747–54. doi: 10.1177/1933719110397210
15. Jerman LF, Hey-Cunningham AJ. The role of the lymphatic system in endometriosis: a comprehensive review of the literature. *Biol Reprod* (2015) 92(3):64. doi: 10.1095/biolreprod.114.124313
16. Suginami H. A reappraisal of the coelomic metaplasia theory by reviewing endometriosis occurring in unusual sites and instances. *Am J Obstet Gynecol* (1991) 165(1):214–8. doi: 10.1016/0002-9378(91)90254-o
17. Polyzos NP, Mauri D, Tsioras S, Messini CI, Valachis A, Messinis IE. Intraperitoneal dissemination of endometrial cancer cells after hysteroscopy: a systematic review and meta-analysis. *Int J Gynecol Cancer* (2010) 20(2):261–7. doi: 10.1111/igc.0b013e3181ca2290
18. Pathan ZA, Dinesh U, Rao R. Scar endometriosis. *J Cytol* (2010) 27(3):106–8. doi: 10.4103/0970-9371.71877
19. Herington JL, Bruner-Tran KL, Lucas JA, Osteen KG. Immune interactions in endometriosis. *Expert Rev Clin Immunol* (2011) 7(5):611–26. doi: 10.1586/eci.11.53
20. Symons LK, Miller JE, Kay VR, Marks RM, Liblik K, Koti M, et al. The Immunopathophysiology of Endometriosis. *Trends Mol Med* (2018) 24(9):748–62. doi: 10.1016/j.molmed.2018.07.004
21. Koninckx PR, Ussia A, Adamyan L, Wattiez A, Gomel V, Martin DC. Pathogenesis of endometriosis: the genetic/epigenetic theory. *Fertil Steril* (2019) 111(2):327–40. doi: 10.1016/j.fertnstert.2018.10.013
22. Miller JE, Ahn SH, Monsanto SP, Khalaj K, Koti M, Tayade C. Implications of immune dysfunction on endometriosis associated infertility. *Oncotarget* (2017) 8(4):7138–47. doi: 10.18632/oncotarget.12577
23. Ahn SH, Monsanto SP, Miller C, Singh SS, Thomas R, Tayade C. Pathophysiology and Immune Dysfunction in Endometriosis. *BioMed Res Int* (2015) 2015:795976. doi: 10.1155/2015/795976
24. Bacci M, Capobianco A, Monno A, Cottone L, Di Puppo F, Camisa B, et al. Macrophages are alternatively activated in patients with endometriosis and required for growth and vascularization of lesions in a mouse model of disease. *Am J Pathol* (2009) 175(2):547–56. doi: 10.2353/ajpath.2009.081011
25. Khan KN, Masuzaki H, Fujishita A, Kitajima M, Sekine I, Ishimaru T. Higher activity by opaque endometriotic lesions than nonopaque lesions. *Acta Obstet Gynecol Scand* (2004) 83(4):375–82. doi: 10.1111/j.0001-6349.2004.00229.x
26. Braun DP, Muriana A, Gebel H, Rotman C, Rana N, Dmowski WP. Monocyte-mediated enhancement of endometrial cell proliferation in women with endometriosis. *Fertil Steril* (1994) 61(1):78–84. doi: 10.1016/s0015-0282(16)56456-5
27. Stabile H, Carlino C, Mazza C, Giliani S, Morrone S, Notarangelo LD, et al. Impaired NK-cell migration in WAS/XLT patients: role of Cdc42/WASp pathway in the control of chemokine-induced beta2 integrin high-affinity state. *Blood* (2010) 115(14):2818–26. doi: 10.1182/blood-2009-07-235804
28. King AE, Critchley HO. Oestrogen and progesterone regulation of inflammatory processes in the human endometrium. *J Steroid Biochem Mol Biol* (2010) 120(2-3):116–26. doi: 10.1016/j.jsbmb.2010.01.003
29. King A. Uterine leukocytes and decidualization. *Hum Reprod Update* (2000) 6(1):28–36. doi: 10.1093/humupd/6.1.28
30. Giuliani E, Parkin KL, Lessey BA, Young SL, Fazleabas AT. Characterization of uterine NK cells in women with infertility or recurrent pregnancy loss and associated endometriosis. *Am J Reprod Immunol* (2014) 72(3):262–9. doi: 10.1111/aji.12259
31. Thiruchelvam U, Wingfield M, O'Farrelly C. Increased uNK Progenitor Cells in Women With Endometriosis and Infertility are Associated With Low Levels of Endometrial Stem Cell Factor. *Am J Reprod Immunol* (2016) 75(4):493–502. doi: 10.1111/aji.12486
32. Kikuchi Y, Ishikawa N, Hirata J, Imaizumi E, Sasa H, Nagata I. Changes of peripheral blood lymphocyte subsets before and after operation of patients with endometriosis. *Acta Obstet Gynecol Scand* (1993) 72(3):157–61. doi: 10.3109/00016349309013364
33. Kempuraj D, Papadopoulou N, Stanford EJ, Christodoulou S, Madhappan B, Sant GR, et al. Increased numbers of activated mast cells in endometriosis lesions positive for corticotropin-releasing hormone and urocortin. *Am J Reprod Immunol* (2004) 52(4):267–75. doi: 10.1111/j.1600-0897.2004.00224.x
34. Konno R, Yamada-Okabe H, Fujiwara H, Uchiide I, Shibahara H, Ohwada M, et al. Role of immunoreactions and mast cells in pathogenesis of human endometriosis–morphologic study and gene expression analysis. *Hum Cell* (2003) 16(3):141–9. doi: 10.1111/j.1749-0774.2003.tb00146.x
35. Sugamata M, Ihara T, Uchiide I. Increase of activated mast cells in human endometriosis. *Am J Reprod Immunol* (2005) 53(3):120–5. doi: 10.1111/j.1600-0897.2005.00254.x
36. Anaf V, Chapron C, El Nakadi I, De Moor V, Simonart T, Noel JC. Pain, mast cells, and nerves in peritoneal, ovarian, and deep infiltrating

endometriosis. *Fertil Steril* (2006) 86(5):1336–43. doi: 10.1016/j.fertnstert.2006.03.057
37. Kirchhoff D, Kaulfuss S, Fuhrmann U, Maurer M, Zollner TM. Mast cells in endometriosis: guilty or innocent bystanders? *Expert Opin Ther Targets* (2012) 16(3):237–41. doi: 10.1517/14728222.2012.661415
38. Paula R Jr, Oliani AH, Vaz-Oliani DC, D'Avila SC, Oliani SM, Gil CD. The intricate role of mast cell proteases and the annexin A1-FPR1 system in abdominal wall endometriosis. *J Mol Histol* (2015) 46(1):33–43. doi: 10.1007/s10735-014-9595-y
39. Butterfield JH, Ravi A, Pongdee T. Mast Cell Mediators of Significance in Clinical Practice in Mastocytosis. *Immunol Allergy Clin North Am* (2018) 38 (3):397–410. doi: 10.1016/j.iac.2018.04.011
40. Borelli V, Martinelli M, Luppi S, Vita F, Romano F, Fanfani F, et al. Mast Cells in Peritoneal Fluid From Women With Endometriosis and Their Possible Role in Modulating Sperm Function. *Front Physiol* (2019) 10:1543. doi: 10.3389/fphys.2019.01543
41. Matsuzaki S, Canis M, Darcha C, Fukaya T, Yajima A, Bruhat MA. Increased mast cell density in peritoneal endometriosis compared with eutopic endometrium with endometriosis. *Am J Reprod Immunol* (1998) 40 (4):291–4. doi: 10.1111/j.1600-0897.1998.tb00420.x
42. Hornung D, Dohrn K, Sotlar K, Greb RR, Wallwiener D, Kiesel L, et al. Localization in tissues and secretion of eotaxin by cells from normal endometrium and endometriosis. *J Clin Endocrinol Metab* (2000) 85 (7):2604–8. doi: 10.1210/jcem.85.7.6665
43. Arici A. Local cytokines in endometrial tissue: the role of interleukin-8 in the pathogenesis of endometriosis. *Ann N Y Acad Sci* (2002) 955:101–9. doi: 10.1111/j.1749-6632.2002.tb02770.x
44. Takehara M, Ueda M, Yamashita Y, Terai Y, Hung YC, Ueki M. Vascular endothelial growth factor A and C gene expression in endometriosis. *Hum Pathol* (2004) 35(11):1369–75. doi: 10.1016/j.humpath.2004.07.020
45. Izumi G, Koga K, Takamura M, Makabe T, Satake E, Takeuchi A, et al. Involvement of immune cells in the pathogenesis of endometriosis. *J Obstet Gynaecol Res* (2018) 44(2):191–8. doi: 10.1111/jog.13559
46. Takamura M, Koga K, Izumi G, Urata Y, Nagai M, Hasegawa A, et al. Neutrophil depletion reduces endometriotic lesion formation in mice. *Am J Reprod Immunol* (2016) 76(3):193–8. doi: 10.1111/aji.12540
47. Helvacioglu A, Aksel S, Peterson RD. Endometriosis and autologous lymphocyte activation by endometrial cells. Are lymphocytes or endometrial cell defects responsible? *J Reprod Med* (1997) 42(2):71–5.
48. Dmowski WP, Steele RW, Baker GF. Deficient cellular immunity in endometriosis. *Am J Obstet Gynecol* (1981) 141(4):377–83. doi: 10.1016/0002-9378(81)90598-6
49. Osuga Y, Koga K, Hirota Y, Hirata T, Yoshino O, Taketani Y. Lymphocytes in endometriosis. *Am J Reprod Immunol* (2011) 65(1):1–10. doi: 10.1111/j.1600-0897.2010.00887.x
50. Gilmore SM, Aksel S, Hoff C, Peterson RD. In vitro lymphocyte activity in women with endometriosis–an altered immune response? *Fertil Steril* (1992) 58(6):1148–52. doi: 10.1016/S0015-0282(16)55560-5
51. Steele RW, Dmowski WP, Marmer DJ. Immunologic aspects of human endometriosis. *Am J Reprod Immunol* (1984) 6(1):33–6. doi: 10.1111/j.1600-0897.1984.tb00106.x
52. Melioli G, Semino C, Semino A, Venturini PL, Ragni N. Recombinant interleukin-2 corrects in vitro the immunological defect of endometriosis. *Am J Reprod Immunol* (1993) 30(4):218–27. doi: 10.1111/j.1600-0897.1993.tb00623.x
53. Oosterlynck DJ, Meuleman C, Lacquet FA, Waer M, Koninckx PR. Flow cytometry analysis of lymphocyte subpopulations in peritoneal fluid of women with endometriosis. *Am J Reprod Immunol* (1994) 31(1):25–31. doi: 10.1111/j.1600-0897.1994.tb00843.x
54. Podgaec S, Abrao MS, Dias JA Jr, Rizzo LV, de Oliveira RM, Baracat EC. Endometriosis: an inflammatory disease with a Th2 immune response component. *Hum Reprod* (2007) 22(5):1373–9. doi: 10.1093/humrep/del516
55. Hirata T, Osuga Y, Hamasaki K, Yoshino O, Ito M, Hasegawa A, et al. Interleukin (IL)-17A stimulates IL-8 secretion, cyclooxygensase-2 expression, and cell proliferation of endometriotic stromal cells. *Endocrinology* (2008) 149(3):1260–7. doi: 10.1210/en.2007-0749
56. Wild RA, Shivers CA. Antiendometrial antibodies in patients with endometriosis. *Am J Reprod Immunol Microbiol* (1985) 8(3):84–6. doi: 10.1111/j.1600-0897.1985.tb00314.x
57. de Barros IBL, Malvezzi H, Gueuvoghlanian-Silva BY, Piccinato CA, Rizzo LV, Podgaec S. "What do we know about regulatory T cells and endometriosis? A systematic review". *J Reprod Immunol* (2017) 120:48–55. doi: 10.1016/j.jri.2017.04.003
58. Daha MR. Role of complement in innate immunity and infections. *Crit Rev Immunol* (2010) 30(1):47–52. doi: 10.1615/critrevimmunol.v30.i1.30
59. Conigliaro P, Triggianese P, Ballanti E, Perricone C, Perricone R, Chimenti MS. Complement, infection, and autoimmunity. *Curr Opin Rheumatol* (2019) 31(5):532–41. doi: 10.1097/BOR.0000000000000633
60. Trouw LA, Blom AM, Gasque P. Role of complement and complement regulators in the removal of apoptotic cells. *Mol Immunol* (2008) 45 (5):1199–207. doi: 10.1016/j.molimm.2007.09.008
61. Dunkelberger JR, Song WC. Complement and its role in innate and adaptive immune responses. *Cell Res* (2010) 20(1):34–50. doi: 10.1038/cr.2009.139
62. Walport MJ. Complement. First of two parts. *N Engl J Med* (2001) 344 (14):1058–66. doi: 10.1056/NEJM200104053441406
63. Hajishengallis G, Reis ES, Mastellos DC, Ricklin D, Lambris JD. Novel mechanisms and functions of complement. *Nat Immunol* (2017) 18 (12):1288–98. doi: 10.1038/ni.3858
64. Walport MJ. Complement. Second of two parts. *N Engl J Med* (2001) 344 (15):1140–4. doi: 10.1056/NEJM200104123441506
65. Lu J, Kishore U. C1 Complex: An Adaptable Proteolytic Module for Complement and Non-Complement Functions. *Front Immunol* (2017) 8:592. doi: 10.3389/fimmu.2017.00592
66. Noris M, Remuzzi G. Overview of complement activation and regulation. *Semin Nephrol* (2013) 33(6):479–92. doi: 10.1016/j.semnephrol.2013.08.001
67. Ehrnthaller C, Ignatius A, Gebhard F, Huber-Lang M. New insights of an old defense system: structure, function, and clinical relevance of the complement system. *Mol Med* (2011) 17(3-4):317–29. doi: 10.2119/molmed.2010.00149
68. Degn SE, Jensenius JC, Bjerre M. The lectin pathway and its implications in coagulation, infections and auto-immunity. *Curr Opin Organ Transplant* (2011) 16(1):21–7. doi: 10.1097/MOT.0b013e32834253df
69. Beltrame MH, Catarino SJ, Goeldner I, Boldt AB, de Messias-Reason IJ. The lectin pathway of complement and rheumatic heart disease. *Front Pediatr* (2014) 2:148. doi: 10.3389/fped.2014.00148
70. Matsushita M, Fujita T. Activation of the classical complement pathway by mannose-binding protein in association with a novel C1s-like serine protease. *J Exp Med* (1992) 176(6):1497–502. doi: 10.1084/jem.176.6.1497
71. Thiel S, Vorup-Jensen T, Stover CM, Schwaeble W, Laursen SB, Poulsen K, et al. A second serine protease associated with mannan-binding lectin that activates complement. *Nature* (1997) 386(6624):506–10. doi: 10.1038/386506a0
72. Dahl MR, Thiel S, Matsushita M, Fujita T, Willis AC, Christensen T, et al. MASP-3 and its association with distinct complexes of the mannan-binding lectin complement activation pathway. *Immunity* (2001) 15(1):127–35. doi: 10.1016/s1074-7613(01)00161-3
73. Degn SE, Hansen AG, Steffensen R, Jacobsen C, Jensenius JC, Thiel S. MAp44, a human protein associated with pattern recognition molecules of the complement system and regulating the lectin pathway of complement activation. *J Immunol* (2009) 183(11):7371–8. doi: 10.4049/jimmunol.0902388
74. Stover CM, Thiel S, Thelen M, Lynch NJ, Vorup-Jensen T, Jensenius JC, et al. Two constituents of the initiation complex of the mannan-binding lectin activation pathway of complement are encoded by a single structural gene. *J Immunol* (1999) 162(6):3481–90.
75. Heja D, Kocsis A, Dobo J, Szilagyi K, Szasz R, Zavodszky P, et al. Revised mechanism of complement lectin-pathway activation revealing the role of serine protease MASP-1 as the exclusive activator of MASP-2. *Proc Natl Acad Sci U S A* (2012) 109(26):10498–503. doi: 10.1073/pnas.1202588109
76. Schwaeble W, Dahl MR, Thiel S, Stover C, Jensenius JC. The mannan-binding lectin-associated serine proteases (MASPs) and MAp19: four components of the lectin pathway activation complex encoded by two genes. *Immunobiology* (2002) 205(4-5):455–66. doi: 10.1078/0171-2985-00146
77. Iwaki D, Kanno K, Takahashi M, Endo Y, Matsushita M, Fujita T. The role of mannose-binding lectin-associated serine protease-3 in activation of the alternative complement pathway. *J Immunol* (2011) 187(7):3751–8. doi: 10.4049/jimmunol.1100280

78. Fishelson Z, Muller-Eberhard HJ. Regulation of the alternative pathway of human complement by C1q. *Mol Immunol* (1987) 24(9):987–93. doi: 10.1016/0161-5890(87)90011-3
79. Fishelson Z, Pangburn MK, Muller-Eberhard HJ. Characterization of the initial C3 convertase of the alternative pathway of human complement. *J Immunol* (1984) 132(3):1430–4.
80. Fromell K, Adler A, Aman A, Manivel VA, Huang S, Duhrkop C, et al. Assessment of the Role of C3(H2O) in the Alternative Pathway. *Front Immunol* (2020) 11:530. doi: 10.3389/fimmu.2020.00530
81. Thurman JM, Holers VM. The central role of the alternative complement pathway in human disease. *J Immunol* (2006) 176(3):1305–10. doi: 10.4049/jimmunol.176.3.1305
82. Blatt AZ, Pathan S, Ferreira VP. Properdin: a tightly regulated critical inflammatory modulator. *Immunol Rev* (2016) 274(1):172–90. doi: 10.1111/imr.12466
83. Bayly-Jones C, Bubeck D, Dunstone MA. The mystery behind membrane insertion: a review of the complement membrane attack complex. *Philos Trans R Soc Lond B Biol Sci* (2017) 372(1726):20160221. doi: 10.1098/rstb.2016.0221
84. Schmidt CQ, Lambris JD, Ricklin D. Protection of host cells by complement regulators. *Immunol Rev* (2016) 274(1):152–71. doi: 10.1111/imr.12475
85. Skerka C, Chen Q, Fremeaux-Bacchi V, Roumenina LT. Complement factor H related proteins (CFHRs). *Mol Immunol* (2013) 56(3):170–80. doi: 10.1016/j.molimm.2013.06.001
86. Tschopp J, French LE. Clusterin: modulation of complement function. *Clin Exp Immunol* (1994) 97(Suppl 2):11–4. doi: 10.1111/j.1365-2249.1994.tb06256.x
87. Tschopp J, Chonn A, Hertig S, French LE. Clusterin, the human apolipoprotein and complement inhibitor, binds to complement C7, C8 beta, and the b domain of C9. *J Immunol* (1993) 151(4):2159–65.
88. Davies A, Simmons DL, Hale G, Harrison RA, Tighe H, Lachmann PJ, et al. CD59, an LY-6-like protein expressed in human lymphoid cells, regulates the action of the complement membrane attack complex on homologous cells. *J Exp Med* (1989) 170(3):637–54. doi: 10.1084/jem.170.3.637
89. Ratnoff OD, Lepow IH. Some properties of an esterase derived from preparations of the first component of complement. *J Exp Med* (1957) 106 (2):327–43. doi: 10.1084/jem.106.2.327
90. Nilsson SC, Sim RB, Lea SM, Fremeaux-Bacchi V, Blom AM. Complement factor I in health and disease. *Mol Immunol* (2011) 48(14):1611–20. doi: 10.1016/j.molimm.2011.04.004
91. Iida K, Nussenzweig V. Complement receptor is an inhibitor of the complement cascade. *J Exp Med* (1981) 153(5):1138–50. doi: 10.1084/jem.153.5.1138
92. Nicholson-Weller A, Wang CE. Structure and function of decay accelerating factor CD55. *J Lab Clin Med* (1994) 123(4):485–91.
93. Liszewski MK, Post TW, Atkinson JP. Membrane cofactor protein (MCP or CD46): newest member of the regulators of complement activation gene cluster. *Annu Rev Immunol* (1991) 9:431–55. doi: 10.1146/annurev.iy.09.040191.002243
94. Parente R, Clark SJ, Inforzato A, Day AJ. Complement factor H in host defense and immune evasion. *Cell Mol Life Sci* (2017) 74(9):1605–24. doi: 10.1007/s00018-016-2418-4
95. Wong EKS, Kavanagh D. Diseases of complement dysregulation-an overview. *Semin Immunopathol* (2018) 40(1):49–64. doi: 10.1007/s00281-017-0663-8
96. Weed JC, Arquembourg PC. Endometriosis: can it produce an autoimmune response resulting in infertility? *Clin Obstet Gynecol* (1980) 23(3):885–93. doi: 10.1097/00003081-198023030-00018
97. Bartosik D, Damjanov I, Viscarello RR, Riley JA. Immunoproteins in the endometrium: clinical correlates of the presence of complement fractions C3 and C4. *Am J Obstet Gynecol* (1987) 156(1):11–5. doi: 10.1016/0002-9378(87)90194-3
98. Rekker K, Saare M, Eriste E, Tasa T, Kukuskina V, Roost AM, et al. High-throughput mRNA sequencing of stromal cells from endometriomas and endometrium. *Reproduction* (2017) 154(1):93–100. doi: 10.1530/REP-17-0092
99. Suryawanshi S, Huang X, Elishaev E, Budiu RA, Zhang L, Kim S, et al. Complement pathway is frequently altered in endometriosis and endometriosis-associated ovarian cancer. *Clin Cancer Res* (2014) 20 (23):6163–74. doi: 10.1158/1078-0432.CCR-14-1338
100. Signorile PG, Baldi A. Serum biomarker for diagnosis of endometriosis. *J Cell Physiol* (2014) 229(11):1731–5. doi: 10.1002/jcp.24620
101. Ruiz LA, Dutil J, Ruiz A, Fourquet J, Abac S, Laboy J, et al. Single-nucleotide polymorphisms in the lysyl oxidase-like protein 4 and complement component 3 genes are associated with increased risk for endometriosis and endometriosis-associated infertility. *Fertil Steril* (2011) 96(2):512–5. doi: 10.1016/j.fertnstert.2011.06.001
102. Bischof P, Planas-Basset D, Meisser A, Campana A. Investigations on the cell type responsible for the endometrial secretion of complement component 3 (C3). *Hum Reprod* (1994) 9(9):1652–9. doi: 10.1093/oxfordjournals.humrep.a138768
103. Isaacson KB, Coutifaris C, Garcia CR, Lyttle CR. Production and secretion of complement component 3 by endometriotic tissue. *J Clin Endocrinol Metab* (1989) 69(5):1003–9. doi: 10.1210/jcem-69-5-1003
104. Tao XJ, Sayegh RA, Isaacson KB. Increased expression of complement component 3 in human ectopic endometrium compared with the matched eutopic endometrium. *Fertil Steril* (1997) 68(3):460–7. doi: 10.1016/s0015-0282(97)00254-9
105. Isaacson KB, Xu Q, Lyttle CR. The effect of estradiol on the production and secretion of complement component 3 by the rat uterus and surgically induced endometriotic tissue. *Fertil Steril* (1991) 55(2):395–402. doi: 10.1016/S0015-0282(16)54135-1
106. D'Cruz OJ, Wild RA. Evaluation of endometrial tissue specific complement activation in women with endometriosis. *Fertil Steril* (1992) 57(4):787–95. doi: 10.1016/S0015-0282(16)54960-7
107. Markiewski MM, Nilsson B, Ekdahl KN, Mollnes TE, Lambris JD. Complement and coagulation: strangers or partners in crime? *Trends Immunol* (2007) 28(4):184–92. doi: 10.1016/j.it.2007.02.006
108. Pawluczkowycz AW, Lindorfer MA, Waitumbi JN, Taylor RP. Hematin promotes complement alternative pathway-mediated deposition of C3 activation fragments on human erythrocytes: potential implications for the pathogenesis of anemia in malaria. *J Immunol* (2007) 179(8):5543–52. doi: 10.4049/jimmunol.179.8.5543
109. Harrison RA. The properdin pathway: an "alternative activation pathway" or a "critical amplification loop" for C3 and C5 activation? *Semin Immunopathol* (2018) 40(1):15–35. doi: 10.1007/s00281-017-0661-x
110. Palomino WA, Tayade C, Argandona F, Devoto L, Young SL, Lessey BA. The endometria of women with endometriosis exhibit dysfunctional expression of complement regulatory proteins during the mid secretory phase. *J Reprod Immunol* (2018) 125:1–7. doi: 10.1016/j.jri.2017.10.046
111. Ahn SH, Khalaj K, Young SL, Lessey BA, Koti M, Tayade C. Immune-inflammation gene signatures in endometriosis patients. *Fertil Steril* (2016) 106(6):1420–31 e7. doi: 10.1016/j.fertnstert.2016.07.005
112. Kobayashi H, Yamashita Y, Iwase A, Yoshikawa Y, Yasui H, Kawai Y, et al. The ferroimmunomodulatory role of ectopic endometriotic stromal cells in ovarian endometriosis. *Fertil Steril* (2012) 98(2):415–22 e1-12. doi: 10.1016/j.fertnstert.2012.04.047
113. Fassbender A, Burney RO, Dorien FO, D'Hooghe T, Giudice L. Update on Biomarkers for the Detection of Endometriosis. *BioMed Res Int* (2015) 2015:130854. doi: 10.1155/2015/130854
114. Eisermann J, Gast MJ, Pineda J, Odem RR, Collins JL. Tumor necrosis factor in peritoneal fluid of women undergoing laparoscopic surgery. *Fertil Steril* (1988) 50(4):573–9. doi: 10.1016/s0015-0282(16)60185-1
115. Bedaiwy MA, Falcone T. Peritoneal fluid environment in endometriosis. Clinicopathological implications. *Minerva Ginecol* (2003) 55 (4):333–45.
116. May KE, Conduit-Hulbert SA, Villar J, Kirtley S, Kennedy SH, Becker CM. Peripheral biomarkers of endometriosis: a systematic review. *Hum Reprod Update* (2010) 16(6):651–74. doi: 10.1093/humupd/dmq009
117. Edwards RP, Huang X, Vlad AM. Chronic inflammation in endometriosis and endometriosis-associated ovarian cancer: New roles for the "old" complement pathway. *Oncoimmunology* (2015) 4(5):e1002732. doi: 10.1080/2162402X.2014.1002732
118. Agostinis C, Zorzet S, Balduit A, Zito G, Mangogna A, Macor P, et al. Complement Component 3 expressed by the endometrial ectopic tissue is

involved in the endometriotic lesion formation through mast cell activation. *bioRxiv* (2020), 2020.11.19.389536. doi: 10.1101/2020.11.19.389536
119. Kabut J, Kondera-Anasz Z, Sikora J, Mielczarek-Palacz A. Levels of complement components iC3b, C3c, C4, and SC5b-9 in peritoneal fluid and serum of infertile women with endometriosis. *Fertil Steril* (2007) 88 (5):1298–303. doi: 10.1016/j.fertnstert.2006.12.061
120. Sikora J, Wroblewska-Czech A, Smycz-Kubanska M, Mielczarek-Palacz A, Cygal A, Witek A, et al. The role of complement components C1q, MBL and C1 inhibitor in pathogenesis of endometriosis. *Arch Gynecol Obstet* (2018) 297(6):1495–501. doi: 10.1007/s00404-018-4754-0
121. Fassbender A, D'Hooghe T, Mihalyi A, Kyama C, Simsa P, Lessey BA. Plasma C3a-des-Arg levels in women with and without endometriosis. *Am J Reprod Immunol* (2009) 62(3):187–95. doi: 10.1111/j.1600-0897.2009.00728.x
122. Zhang T, De Carolis C, Man GCW, Wang CC. The link between immunity, autoimmunity and endometriosis: a literature update. *Autoimmun Rev* (2018) 17(10):945–55. doi: 10.1016/j.autrev.2018.03.017
123. Csuka D, Veszeli N, Varga L, Prohaszka Z, Farkas H. The role of the complement system in hereditary angioedema. *Mol Immunol* (2017) 89:59–68. doi: 10.1016/j.molimm.2017.05.020
124. Morgan BP. Hereditary angioedema–therapies old and new. *N Engl J Med* (2010) 363(6):581–3. doi: 10.1056/NEJMe1006450
125. Rother RP, Rollins SA, Mojcik CF, Brodsky RA, Bell L. Discovery and development of the complement inhibitor eculizumab for the treatment of paroxysmal nocturnal hemoglobinuria. *Nat Biotechnol* (2007) 25(11):1256–64. doi: 10.1038/nbt1344
126. Rosse WF, Dacie JV. Immune lysis of normal human and paroxysmal nocturnal hemoglobinuria (PNH) red blood cells. I. The sensitivity of PNH red cells to lysis by complement and specific antibody. *J Clin Invest* (1966) 45(5):736–48. doi: 10.1172/JCI105388
127. Rosse WF, Dacie JV. Immune lysis of normal human and paroxysmal nocturnal hemoglobinuria (PNH) red blood cells. II. The role of complement components in the increased sensitivity of PNH red cells to immune lysis. *J Clin Invest* (1966) 45(5):749–57. doi: 10.1172/JCI105389
128. Zelek WM, Xie L, Morgan BP, Harris CL. Compendium of current complement therapeutics. *Mol Immunol* (2019) 114:341–52. doi: 10.1016/j.molimm.2019.07.030
129. Brodsky RA, Young NS, Antonioli E, Risitano AM, Schrezenmeier H, Schubert J, et al. Multicenter phase 3 study of the complement inhibitor eculizumab for the treatment of patients with paroxysmal nocturnal hemoglobinuria. *Blood* (2008) 111(4):1840–7. doi: 10.1182/blood-2007-06-094136
130. Harris CL, Pouw RB, Kavanagh D, Sun R, Ricklin D. Developments in anti-complement therapy; from disease to clinical trial. *Mol Immunol* (2018) 102:89–119. doi: 10.1016/j.molimm.2018.06.008
131. Morgan BP, Harris CL. Complement, a target for therapy in inflammatory and degenerative diseases. *Nat Rev Drug Discov* (2015) 14(12):857–77. doi: 10.1038/nrd4657
132. Ricklin D, Mastellos DC, Reis ES, Lambris JD. The renaissance of complement therapeutics. *Nat Rev Nephrol* (2018) 14(1):26–47. doi: 10.1038/nrneph.2017.156
133. Sheridan D, Yu ZX, Zhang Y, Patel R, Sun F, Lasaro MA, et al. Design and preclinical characterization of ALXN1210: A novel anti-C5 antibody with extended duration of action. *PLoS One* (2018) 13(4):e0195909. doi: 10.1371/journal.pone.0195909
134. Igawa T, Ishii S, Tachibana T, Maeda A, Higuchi Y, Shimaoka S, et al. Antibody recycling by engineered pH-dependent antigen binding improves the duration of antigen neutralization. *Nat Biotechnol* (2010) 28(11):1203–7. doi: 10.1038/nbt.1691
135. Fukuzawa T, Sampei Z, Haraya K, Ruike Y, Shida-Kawazoe M, Shimizu Y, et al. Long lasting neutralization of C5 by SKY59, a novel recycling antibody, is a potential therapy for complement-mediated diseases. *Sci Rep* (2017) 7 (1):1080. doi: 10.1038/s41598-017-01087-7
136. Sampei Z, Haraya K, Tachibana T, Fukuzawa T, Shida-Kawazoe M, Gan SW, et al. Antibody engineering to generate SKY59, a long-acting anti-C5 recycling antibody. *PLoS One* (2018) 13(12):e0209509. doi: 10.1371/journal.pone.0209509
137. Risitano AM, Marotta S, Ricci P, Marano L, Frieri C, Cacace F, et al. Anti-complement Treatment for Paroxysmal Nocturnal Hemoglobinuria: Time for Proximal Complement Inhibition? A Position Paper From the SAAWP of the EBMT. *Front Immunol* (2019) 10:1157. doi: 10.3389/fimmu.2019.01157
138. Riedemann NC, Habel M, Ziereisen J, Hermann M, Schneider C, Wehling C, et al. Controlling the anaphylatoxin C5a in diseases requires a specifically targeted inhibition. *Clin Immunol* (2017) 180:25–32. doi: 10.1016/j.clim.2017.03.012
139. Risitano AM, Mastellos DC, Huber-Lang M, Yancopoulou D, Garlanda C, Ciceri F, et al. Complement as a target in COVID-19? *Nat Rev Immunol* (2020) 20(6):343–4. doi: 10.1038/s41577-020-0320-7
140. Mastaglio S, Ruggeri A, Risitano AM, Angelillo P, Yancopoulou D, Mastellos DC, et al. The first case of COVID-19 treated with the complement C3 inhibitor AMY-101. *Clin Immunol* (2020) 215:108450. doi: 10.1016/j.clim.2020.108450
141. Rambaldi A, Gritti G, Micò MC, Frigeni M, Borleri G, Salvi A, et al. Endothelial Injury and Thrombotic Microangiopathy in COVID-19: Treatment with the Lectin-Pathway Inhibitor Narsoplimab. *Immunobiology* (2020) 225(6):152001. doi: 10.1016/j.imbio.2020.152001
142. Mastellos DC, Reis ES, Ricklin D, Smith RJ, Lambris JD. Complement C3-Targeted Therapy: Replacing Long-Held Assertions with Evidence-Based Discovery. *Trends Immunol* (2017) 38(6):383–94. doi: 10.1016/j.it.2017.03.003
143. Wong RS, Pullon HWH, Deschatelets P, Francois CG, Hamdani M, Issaragrisil S, et al. Inhibition of C3 with APL-2 Results in Normalisation of Markers of Intravascular and Extravascular Hemolysis in Patients with Paroxysmal Nocturnal Hemoglobinuria (PNH). *Blood* (2018) 132 (Supplement 1):2314–. doi: 10.1182/blood-2018-99-110827
144. Grossi F, Shum MK, Gertz MA, Roman E, Deschatelets P, Hamdani M, et al. Inhibition of C3 with APL-2 Results in Normalisation of Markers of Intravascular and Extravascular Hemolysis in Patients with Autoimmune Hemolytic Anemia (AIHA). *Blood* (2018) 132(Supplement 1):3623–. doi: 10.1182/blood-2018-99-119468
145. Grossi FV, Bedwell P, Deschatelets P, Edis L, Francois CG, Johnson PJ, et al. APL-2, a Complement C3 Inhibitor for the Potential Treatment of Paroxysmal Nocturnal Hemoglobinuria (PNH): Phase I Data from Two Completed Studies in Healthy Volunteers. *Blood* (2016) 128(22):1251–. doi: 10.1182/blood.V128.22.1251.1251
146. Chow V, Pan J, Chien D, Mytych DT, Hanes V. A randomized, double-blind, single-dose, three-arm, parallel group study to determine pharmacokinetic similarity of ABP 959 and eculizumab (Soliris((R))) in healthy male subjects. *Eur J Haematol* (2020) 105(1):66–74. doi: 10.1111/ejh.13411
147. Merkel PA, Jayne DR, Wang C, Hillson J, Bekker P. Evaluation of the Safety and Efficacy of Avacopan, a C5a Receptor Inhibitor, in Patients With Antineutrophil Cytoplasmic Antibody-Associated Vasculitis Treated Concomitantly With Rituximab or Cyclophosphamide/Azathioprine: Protocol for a Randomized, Double-Blind, Active-Controlled, Phase 3 Trial. *JMIR Res Protoc* (2020) 9(4):e16664. doi: 10.2196/16664
148. Tesar V, Hruskova Z. Avacopan in the treatment of ANCA-associated vasculitis. *Expert Opin Invest Drugs* (2018) 27(5):491–6. doi: 10.1080/13543784.2018.1472234
149. Jayne DRW, Bruchfeld AN, Harper L, Schaier M, Venning MC, Hamilton P, et al. Randomized Trial of C5a Receptor Inhibitor Avacopan in ANCA-Associated Vasculitis. *J Am Soc Nephrol* (2017) 28(9):2756–67. doi: 10.1681/ASN.2016111179
150. Bekker P, Dairaghi D, Seitz L, Leleti M, Wang Y, Ertl L, et al. Characterization of Pharmacologic and Pharmacokinetic Properties of CCX168, a Potent and Selective Orally Administered Complement 5a Receptor Inhibitor, Based on Preclinical Evaluation and Randomized Phase 1 Clinical Study. *PLoS One* (2016) 11(10):e0164646. doi: 10.1371/journal.pone.0164646
151. Keating GM. Human C1-esterase inhibitor concentrate (Berinert). *BioDrugs* (2009) 23(6):399–406. doi: 10.2165/11201100-000000000-00000
152. Zanichelli A, Azin GM, Cristina F, Vacchini R, Caballero T. Safety, effectiveness, and impact on quality of life of self-administration with plasma-derived nanofiltered C1 inhibitor (Berinert(R)) in patients with hereditary angioedema: the SABHA study. *Orphanet J Rare Dis* (2018) 13 (1):51. doi: 10.1186/s13023-018-0797-3

153. Aygoren-Pursun E, Soteres D, Moldovan D, Christensen J, Van Leerberghe A, Hao J, et al. Preventing Hereditary Angioedema Attacks in Children Using Cinryze(R): Interim Efficacy and Safety Phase 3 Findings. *Int Arch Allergy Immunol* (2017) 173(2):114–9. doi: 10.1159/000477541
154. Lyseng-Williamson KA. Nanofiltered human C1 inhibitor concentrate (Cinryze(R)): in hereditary angioedema. *BioDrugs* (2011) 25(5):317–27. doi: 10.2165/11208390-000000000-00000
155. Bernstein JA, Manning ME, Li H, White MV, Baker J, Lumry WR, et al. Escalating doses of C1 esterase inhibitor (CINRYZE) for prophylaxis in patients with hereditary angioedema. *J Allergy Clin Immunol Pract* (2014) 2 (1):77–84. doi: 10.1016/j.jaip.2013.09.008
156. Roth A, Nishimura JI, Nagy Z, Gaal-Weisinger J, Panse J, Yoon SS, et al. The complement C5 inhibitor crovalimab in paroxysmal nocturnal hemoglobinuria. *Blood* (2020) 135(12):912–20. doi: 10.1182/blood.2019003399
157. Wiles JA, Galvan MD, Podos SD, Geffner M, Huang M. Discovery and Development of the Oral Complement Factor D Inhibitor Danicopan (ACH-4471). *Curr Med Chem* (2020) 27(25):4165–80. doi: 10.2174/0929867326666191001130342
158. Risitano AM, Kulasekararaj AG, Lee JW, Maciejewski JP, Notaro R, Brodsky R, et al. Danicopan: an oral complement factor D inhibitor for paroxysmal nocturnal hemoglobinuria. *Haematologica* (2020). doi: 10.3324/haematol.2020.261826
159. Wijnsma KL, Ter Heine R, Moes D, Langemeijer S, Schols SEM, Volokhina EB, et al. Pharmacology, Pharmacokinetics and Pharmacodynamics of Eculizumab, and Possibilities for an Individualized Approach to Eculizumab. *Clin Pharmacokinet* (2019) 58(7):859–74. doi: 10.1007/s40262-019-00742-8
160. Giamarellos-Bourboulis EJ, Argyropoulou M, Kanni T, Spyridopoulos T, Otto I, Zenker O, et al. Clinical efficacy of complement C5a inhibition by IFX-1 in hidradenitis suppurativa: an open-label single-arm trial in patients not eligible for adalimumab. *Br J Dermatol* (2020) 183(1):176–8. doi: 10.1111/bjd.18877
161. Vlaar APJ, de Bruin S, Busch M, Timmermans S, van Zeggeren IE, Koning R, et al. Anti-C5a antibody IFX-1 (vilobelimab) treatment versus best supportive care for patients with severe COVID-19 (PANAMO): an exploratory, open-label, phase 2 randomised controlled trial. *Lancet Rheumatol* (2020) 2(12):e764–73. doi: 10.1016/S2665-9913(20)30341-6
162. Halstead SK, Humphreys PD, Goodfellow JA, Wagner ER, Smith RA, Willison HJ. Complement inhibition abrogates nerve terminal injury in Miller Fisher syndrome. *Ann Neurol* (2005) 58(2):203–10. doi: 10.1002/ana.20546
163. Kassimatis T, Qasem A, Douiri A, Ryan EG, Rebollo-Mesa I, Nichols LL, et al. A double-blind randomised controlled investigation into the efficacy of Mirococept (APT070) for preventing ischaemia reperfusion injury in the kidney allograft (EMPIRIKAL): study protocol for a randomised controlled trial. *Trials* (2017) 18(1):255. doi: 10.1186/s13063-017-1972-x
164. Schols S, Nunn MA, Mackie I, Weston-Davies W, Nishimura JI, Kanakura Y, et al. Successful treatment of a PNH patient non-responsive to eculizumab with the novel complement C5 inhibitor coversin (nomacopan). *Br J Haematol* (2020) 188(2):334–7. doi: 10.1111/bjh.16305
165. Elhadad S, Chapin J, Copertino D, Van Besien K, Ahamed J, Laurence J. MASP2 levels are elevated in thrombotic microangiopathies: association with microvascular endothelial cell injury and suppression by anti-MASP2 antibody narsoplimab. *Clin Exp Immunol* (2020). doi: 10.1111/cei.13497
166. Selvaskandan H, Kay Cheung C, Dormer J, Wimbury D, Martinez M, Xu G, et al. Inhibition of the Lectin Pathway of the Complement System as a Novel Approach in the Management of IgA Vasculitis-Associated Nephritis. *Nephron* (2020) 144(9):453–8. doi: 10.1159/000508841
167. Latuszek A, Liu Y, Olsen O, Foster R, Cao M, Lovric I, et al. Inhibition of complement pathway activation with Pozelimab, a fully human antibody to complement component C5. *PLoS One* (2020) 15(5):e0231892. doi: 10.1371/journal.pone.0231892
168. Busse PJ, Christiansen SC. Hereditary Angioedema. *N Engl J Med* (2020) 382 (12):1136–48. doi: 10.1056/NEJMra1808012
169. Cruz MP. Conestat alfa (ruconest): first recombinant c1 esterase inhibitor for the treatment of acute attacks in patients with hereditary angioedema. *P T* (2015) 40(2):109–14.
170. Freire PC, Munoz CH, Derhaschnig U, Schoergenhofer C, Firbas C, Parry GC, et al. Specific Inhibition of the Classical Complement Pathway Prevents C3 Deposition along the Dermal-Epidermal Junction in Bullous Pemphigoid. *J Invest Dermatol* (2019) 139(12):2417–24 e2. doi: 10.1016/j.jid.2019.04.025
171. Nikitin PA, Rose EL, Byun TS, Parry GC, Panicker S. C1s Inhibition by BIVV009 (Sutimlimab) Prevents Complement-Enhanced Activation of Autoimmune Human B Cells In Vitro. *J Immunol* (2019) 202(4):1200–9. doi: 10.4049/jimmunol.1800998
172. Bartko J, Schoergenhofer C, Schwameis M, Firbas C, Beliveau M, Chang C, et al. A Randomized, First-in-Human, Healthy Volunteer Trial of sutimlimab, a Humanized Antibody for the Specific Inhibition of the Classical Complement Pathway. *Clin Pharmacol Ther* (2018) 104(4):655–63. doi: 10.1002/cpt.1111
173. Jager U, D'Sa S, Schorgenhofer C, Bartko J, Derhaschnig U, Sillaber C, et al. Inhibition of complement C1s improves severe hemolytic anemia in cold agglutinin disease: a first-in-human trial. *Blood* (2019) 133(9):893–901. doi: 10.1182/blood-2018-06-856930
174. Jordan SC, Kucher K, Bagger M, Hockey HU, Wagner K, Ammerman N, et al. Intravenous immunoglobulin significantly reduces exposure of concomitantly administered anti-C5 monoclonal antibody tesidolumab. *Am J Transplant* (2020) 20(9):2581–8. doi: 10.1111/ajt.15922
175. Albazli K, Kaminski HJ, Howard JFJr. Complement Inhibitor Therapy for Myasthenia Gravis. *Front Immunol* (2020) 11:917. doi: 10.3389/fimmu.2020.00917
176. Wilkinson T, Dixon R, Page C, Carroll M, Griffiths G, Ho LP, et al. ACCORD: A Multicentre, Seamless, Phase 2 Adaptive Randomisation Platform Study to Assess the Efficacy and Safety of Multiple Candidate Agents for the Treatment of COVID-19 in Hospitalised Patients: A structured summary of a study protocol for a randomised controlled trial. *Trials* (2020) 21(1):691. doi: 10.1186/s13063-020-04584-9
177. Oosterlynck DJ, Meuleman C, Waer M, Vandeputte M, Koninckx PR. The natural killer activity of peritoneal fluid lymphocytes is decreased in women with endometriosis. *Fertil Steril* (1992) 58(2):290–5. doi: 10.1016/s0015-0282(16)55224-8
178. Oosterlynck DJ, Cornillie FJ, Waer M, Vandeputte M, Koninckx PR. Women with endometriosis show a defect in natural killer activity resulting in a decreased cytotoxicity to autologous endometrium. *Fertil Steril* (1991) 56 (1):45–51. doi: 10.1016/s0015-0282(16)54414-8
179. Thiruchelvam U, Wingfield M, O'Farrelly C. Natural Killer Cells: Key Players in Endometriosis. *Am J Reprod Immunol* (2015) 74(4):291–301. doi: 10.1111/aji.12408
180. Jeung I, Cheon K, Kim MR. Decreased Cytotoxicity of Peripheral and Peritoneal Natural Killer Cell in Endometriosis. *BioMed Res Int* (2016) 2016:2916070. doi: 10.1155/2016/2916070
181. Sciezynska A, Komorowski M, Soszynska M, Malejczyk J. NK Cells as Potential Targets for Immunotherapy in Endometriosis. *J Clin Med* (2019) 8(9):1468. doi: 10.3390/jcm8091468
182. Chen Z, Yang Y, Liu LL, Lundqvist A. Strategies to Augment Natural Killer (NK) Cell Activity against Solid Tumors. *Cancers (Basel)* (2019) 11(7):1040. doi: 10.3390/cancers11071040
183. Sivori S, Vacca P, Del Zotto G, Munari E, Mingari MC, Moretta L. Human NK cells: surface receptors, inhibitory checkpoints, and translational applications. *Cell Mol Immunol* (2019) 16(5):430–41. doi: 10.1038/s41423-019-0206-4
184. Liu CF, Min XY, Wang N, Wang JX, Ma N, Dong X, et al. Complement Receptor 3 Has Negative Impact on Tumor Surveillance through Suppression of Natural Killer Cell Function. *Front Immunol* (2017) 8:1602. doi: 10.3389/fimmu.2017.01602
185. Vivier E, Tomasello E, Baratin M, Walzer T, Ugolini S. Functions of natural killer cells. *Nat Immunol* (2008) 9(5):503–10. doi: 10.1038/ni1582
186. Son M, Porat A, He M, Suurmond J, Santiago-Schwarz F, Andersson U, et al. C1q and HMGB1 reciprocally regulate human macrophage polarization. *Blood* (2016) 128(18):2218–28. doi: 10.1182/blood-2016-05-719757
187. Spivia W, Magno PS, Le P, Fraser DA. Complement protein C1q promotes macrophage anti-inflammatory M2-like polarization during the clearance of atherogenic lipoproteins. *Inflammation Res* (2014) 63(10):885–93. doi: 10.1007/s00011-014-0762-0

188. Bossi F, Tripodo C, Rizzi L, Bulla R, Agostinis C, Guarnotta C, et al. C1q as a unique player in angiogenesis with therapeutic implication in wound healing. *Proc Natl Acad Sci USA* (2014) 111(11):4209–14. doi: 10.1073/pnas.1311968111
189. Bulla R, Tripodo C, Rami D, Ling GS, Agostinis C, Guarnotta C, et al. C1q acts in the tumour microenvironment as a cancer-promoting factor independently of complement activation. *Nat Commun* (2016) 7:10346. doi: 10.1038/ncomms10346
190. Mangogna A, Agostinis C, Bonazza D, Belmonte B, Zacchi P, Zito G, et al. Is the Complement Protein C1q a Pro- or Anti-tumorigenic Factor? Bioinformatics Analysis Involving Human Carcinomas. *Front Immunol* (2019) 10:865. doi: 10.3389/fimmu.2019.00865

Conflict of Interest: The authors declare that the research was conducted in the absence of any commercial or financial relationships that could be construed as a potential conflict of interest.

frontiers in Immunology

ORIGINAL RESEARCH
published: 11 January 2021
doi: 10.3389/fimmu.2020.609941

Complement-Dependent Activity of CD20-Specific IgG Correlates With Bivalent Antigen Binding and C1q Binding Strength

*Sina Bondza[1,2], Anita Marosan[3], Sibel Kara[3], Josephine Lösing[3], Matthias Peipp[4], Falk Nimmerjahn[3], Jos Buijs[1,2] and Anja Lux[3]**

[1] Department of Immunology, Genetics and Pathology, Uppsala University, Uppsala, Sweden, [2] Ridgeview Instruments AB, Uppsala, Sweden, [3] Department of Genetics, Friedrich-Alexander University, Erlangen, Germany, [4] Division of Stem Cell Transplantation and Immunotherapy, Department of Medicine II, UKSH, CAU Kiel, Kiel, Germany

OPEN ACCESS

Edited by:
Marcin Okrój,
Intercollegiate Faculty of Biotechnology of University of Gdańsk and Medical University of Gdańsk, Poland

Reviewed by:
Christian Klein,
Roche Innovation Center Zurich, Switzerland
Mark S. Cragg,
University of Southampton, United Kingdom

***Correspondence:**
Anja Lux
anja.lux@fau.de

Specialty section:
This article was submitted to Molecular Innate Immunity, a section of the journal Frontiers in Immunology

Received: 24 September 2020
Accepted: 19 November 2020
Published: 11 January 2021

Citation:
Bondza S, Marosan A, Kara S, Lösing J, Peipp M, Nimmerjahn F, Buijs J and Lux A (2021) Complement-Dependent Activity of CD20-Specific IgG Correlates With Bivalent Antigen Binding and C1q Binding Strength. Front. Immunol. 11:609941. doi: 10.3389/fimmu.2020.609941

Monoclonal antibodies directed against the CD20 surface antigen on B cells are widely used in the therapy of B cell malignancies. Upon administration, the antibodies bind to CD20 expressing B cells and induce their depletion *via* cell- and complement-dependent cytotoxicity or by induction of direct cell killing. The three antibodies currently most often used in the clinic are Rituximab (RTX), Ofatumumab (OFA) and Obinutuzumab (OBI). Even though these antibodies are all of the human IgG1 subclass, they have previously been described to vary considerably in the effector functions involved in therapeutic B cell depletion, especially in regards to complement activation. Whereas OFA is known to strongly induce complement-dependent cytotoxicity, OBI is described to be far less efficient. In contrast, the role of complement in RTX-induced B cell depletion is still under debate. Some of this dissent might come from the use of different *in vitro* systems for characterization of antibody effector functions. We therefore set out to systematically compare antibody as well as C1q binding and complement-activation by RTX, OFA and OBI on human B cell lines that differ in expression levels of CD20 and complement-regulatory proteins as well as human primary B cells. Applying real-time interaction analysis, we show that the overall strength of C1q binding to live target cells coated with antibodies positively correlated with the degree of bivalent binding for the antibodies to CD20. Kinetic analysis revealed that C1q exhibits two binding modes with distinct affinities and binding stabilities, with exact numbers varying both between antibodies and cell lines. Furthermore, complement-dependent cell killing by RTX and OBI was highly cell-line dependent, whereas the superior complement-dependent cytotoxicity by OFA was independent of the target B cells. All three antibodies were able to initiate deposition of C3b on the B cell surface, although to varying extent. This suggests that complement activation occurs but might not necessarily lead to induction of complement-dependent cytotoxicity. This activation could, however, initiate complement-dependent phagocytosis as an alternative mechanism of therapeutic B cell depletion.

Keywords: CD20, C1q, Rituximab, Ofatumumab, Obinutuzumab, CDC, B cells, interaction

INTRODUCTION

Monoclonal antibodies (mAb) applied in the treatment of malignant diseases employ different immune-mediated mechanisms that contribute to their efficacy such as antibody-dependent cellular cytotoxicity (ADCC) (1), antibody-dependent cellular phagocytosis (ADCP) (2), as well as activation of the complement system (3). While ADCC and ADCP are accepted as important mechanisms for successful monoclonal antibody (mAb) therapy, the importance of the complement system for mAb therapy is less clear. The Fc-terminus of antibodies harbors a binding site for the serum protein C1q (4) that activates the classical complement pathway which, through a series of proteolytic cleavage events, leads to deposition of the complement component 3b (C3b) on the surface of opsonized cells. If sufficient amounts of membrane bound C3b accumulate on the target cell, eventually pores, called membrane attack complexes (MAC), are formed by complement proteins C6 through C9 that mediate cell lysis; a process termed as complement-dependent cytotoxicity (CDC) (3). Moreover, membrane-bound complement cleavage products such as C3b or C4b also function as opsonins by interacting with complement receptors on effector cells which results in complement-dependent phagocytosis (CDCP) (5). Effective killing of tumor cells by CDC *in vitro* has been demonstrated, especially for certain anti-CD20 antibodies (6–8), but the contribution of complement to tumor killing *in vivo* is debated (9–15). To date, expression of negative regulators of the complement system (6, 16, 17) and exhaustion of complement components have been described to limit CDC efficacy in the clinic (11, 18).

Mechanistically, binding of C1q occurs preferably to a hexameric formation of IgG Fc-tails (19) and it has been shown that antibodies harboring mutations in the Fc-region that facilitate this arrangement can induce CDC more efficiently (20, 21). Depending on their capacity to cluster CD20 on the cell surface, anti-CD20 antibodies are grouped into type I and type II, the latter not having this ability (22, 23). Type I antibodies like Rituximab (RTX) or Ofatumumab (OFA) have been shown to efficiently activate complement, presumably because clustering facilitates the formation of hexameric IgG-Fc platforms suitable for C1q binding (19, 24). Platform formation could also be supported by type I mAbs acting as molecular seeds that locally increase antibody concentration. In contrast, recruitment of the type II mAb Obinutuzumab (OBI) prevented further binding of mAbs as well as complement components (25) providing an explanation for its reduced capacity to activate complement. With respect to their B cell depleting activity, both type I and type II antibodies are able to induce ADCC as well as ADCP (23). Type II antibodies are, however, more efficient at inducing direct cell death (26, 27). Type I and type II CD20-specific mAbs have also been shown to differ in their capacity to be internalized following interaction with FcγRIIb expressed on B cells (28, 29). The underlying molecular properties for the functional classification into type I and II are still debated but include the binding epitope (30), the elbow hinge angle (31, 32), as well as binding orientation (33) and binding stability of the antibody (34).

Recognition by C1q is the crucial step in activation of the classical pathway of complement and stronger binding of C1q to antibody opsonized cells has been correlated with more efficient target cell lysis (19, 35). However, the parameters involved in the formation of the optimal antibody platform for C1q binding are not completely understood yet. Contradicting observations have especially been made with respect to functionally monovalent antibodies inducing CDC more efficiently than their counterparts with bivalent binding capability (19, 36, 37). For C1q binding to antibody opsonized cells, affinity values in the low nM range have been reported without resolution of the kinetic binding parameters (38). Furthermore, the apparent binding affinity for C1q to monomeric IgG in solution is around 10 μM (39), whereas the binding to larger, clustered immune complexes is known to be in the nM range (40).

In a previous study, we analyzed the binding pattern of RTX, OBI and OFA to Daudi cells by real-time interaction analysis and showed that OFA displayed the highest degree of bivalent binding, followed by RTX and then OBI (41). Consequently, the OFA interaction was less dynamic, *i.e.* OFA showed a slower antibody exchange, possibly caused by a higher fraction of antibodies stabilized by bivalent binding. The degree of bivalent target engagement thus positively correlates with how efficiently these mAbs have been shown to induce CDC *in vitro*. As the notion that bivalent target engagement is beneficial for CDC stands in contrast to observations made with antibodies targeting EGFR (19) and HER2 (37), we set out to develop a real-time binding assay to investigate C1q capture on live cells opsonized with CD20 mAbs. We systematically compared CD20 mAb binding, C1q binding and complement-activation, as well as C3b deposition that can trigger target cell killing independently of MAC formation. Several human lymphoma B cell lines that differ in CD20 expression levels and complement-regulatory proteins as well as human primary B cells were included in our analysis to understand the influence of the model system in the context of complement activation by CD20 mAbs *in vitro*. Our data suggests that CD20 specific mAbs differ in their mode of binding which, in combination with the type of target cell, determines efficacy of CDC *in vitro*.

MATERIALS AND METHODS

Cell Culture and B Cell Isolation

Ramos (ATCC), Daudi (ATCC), P493.6, LCL1.11 (kindly provided by Georg Bornkamm, Helmholtz Zentrum, Munich, Germany) and K562 (kind gift from Dr. Stenerlöw, Uppsala University) were cultured in a humidified incubator at 37°C with 5% CO_2. For interaction analyses, Ramos and K562 cells were maintained in RPMI 1640 cell medium (Biochrom AG) supplemented with 10% heat-inactivated FBS (Sigma Life Science), 2 mM L-glutamine (Biochrom AG) and 100 μg/ml penicillin-streptomycin (Biochrom AG). Daudi and LCL1.11 cells were cultured in the same medium, but with additional sodium pyruvate (Sigma-Aldrich) added to a final concentration of 1 mM. P493.6 cells were cultured in RPMI 1640 without

phenol red (Biowest) with the same supplements as for Daudi cells and in addition 0.1 mM MEM non-essential amino acids (Invitrogen). B cell lines for functional assays were cultured in RPMI 1640 (Gibco) supplemented with 10% heat-inactivated FBS (Pan Biotech), 1 mM sodium pyruvate (Gibco), 100 µg/ml penicillin-streptomycin (C-C-Pro), 2 mM L-glutamine (C-C-Pro) and 0.1 mM MEM non-essential amino acids (Gibco). For isolation of human primary B cells, peripheral blood mononuclear cells were purified from blood cones by density gradient centrifugation. PBMCs were then subjected to MojoSort™ Human B Cell Isolation Kit (BioLegend) according to the manufacturer´s instructions. Healthy human and CLL patient PBMCs were isolated from peripheral blood by density gradient centrifugation and either used immediately or stored at −80°C in FBS containing 10% DMSO until usage.

Seeding for LigandTracer analysis

Cells were immobilized either on petri dishes (Nunc 263991, ThermoFisher Scientific) or LigandTracer MultiDishes 2x2 (Ridgeview Instruments) for real-time binding assays, essentially as previously published (42). In brief, a biomolecular anchor molecule (BAM) (SUNBRIGHT® OE-040CS, NOF Corporation) was dissolved to 2 mg/ml in ddH_2O water and circular drops of 400 µl were carefully placed onto the dishes and incubated for 1 h at room temperature. After carefully aspirating the BAM solution, cells suspended in PBS (due to differences in size $7.5*10^6$ cells/ml for Ramos, Daudi, P493.6 and LCL1.11, $2.5*10^6$ cells/ml for K562) were placed onto the BAM coated spots. Human primary B cells were resuspended in RPMI 1640 (supplemented with 1 mM sodium pyruvate, 100 µg/ml penicillin-streptomycin, 2 mM L-glutamine and 100 µM MEM non-essential amino acids) and $2*10^6$ cells and seeded on BAM coated spots. Cells were then incubated for 40 min at room temperature. Cells that did not attach were carefully removed and cell culture medium was added. Seeded cells were kept a humidified incubator at 37°C with 5% CO_2 and used for experiments the next day.

Antibodies and Protein Labeling

For real-time experiments Rituximab and Ofatumumab were purchased from Apoteket AB (Sweden) in clinical formulation, Rituximab and Ofatumumab for functional experiments, as well as Obinutuzumab were purchased from the pharmacy of the university hospital of Schleswig-Holstein (Kiel, Germany). Fab fragments were generated using the Pierce Fab Preparation Kit (Thermo Fisher Scientific) following the manufacturer's instructions, which essentially comprised enzymatic digestion with papain followed by removal of the Fc-part *via* a protein A column. Fab fragmentation was verified by running a non-reducing SDS-PAGE with subsequent Coomassie staining (**Supplementary Figure 1**). After Fab fragmentation, a buffer exchange to either PBS or borate buffer pH 9.2 (the latter if the Fab was to be labeled fluorescently) was performed using a Nap-5 Sephadex G-25 column (Illustra, GE Healthcare). Antibodies were diluted to 2 mg/ml in PBS and mixed with borate buffer pH 9.2 in 1:2 volume ratio for fluorescent labeling. Fluorescein isothiocyanate (FITC) was dissolved in DMSO and 100 ng FITC was added for every µg protein. After incubation at 37°C for 90 min, unconjugated FITC was removed by purification through a Nap-5 column (Illustra, GE Healthcare). Labeled antibodies and Fab fragments were kept at 4°C for short term and at −20°C for long storage. For labeling, human complement component C1q (Merck Millipore) was mixed 5:1 with 0.2 M sodium bicarbonate buffer pH 9. Atto488 was dissolved in DMSO and 0.5 µg for every µg protein was added and incubated for 1 h at room temperature. Excess fluorophore was removed through a Nap-5 column and C1q was stored at 4°C overnight and always used for experiments the following day. Protein concentrations after labeling were measured with NanoPhotometer (Implen P360). For C1q a molar extinction coefficient of $2.742*10^5$ $cm^{-1}M^{-1}$ was used.

Real-Time Cell-Binding Assay

LigandTracer Green (Ridgeview Instruments) was used to study molecular interactions on live cells. The instrument consists of an inclined cell dish holder that rotates during the measurement and a fluorescent detector mounted that records signals from the upper position of the cell dish, thereby avoiding fluorescence from the bulk liquid containing unbound ligand. For binding experiments with labeled antibodies or Fab fragments, at least two positions were measured during each rotation: CD20 expressing cells (Ramos, Daudi, P493.6, LCL1.11 or primary B cells) in the target position and K562 cells that lack CD20 or media only as control for subtraction of background fluorescence. Each full rotation takes 70 s and results in at least one background subtracted data point. Experiments were performed with the cell culture medium used for culturing the CD20 expressing cells. After recording a baseline, FITC-labeled protein was added to initiate the association phase. After recording an association phase, the incubation media was changed to either plain media not containing any ligand or media containing unlabeled ligand to monitor dissociation.

For binding experiments with labeled C1q and unlabeled antibodies, four positions were measured during each rotation with each half of the MultiDish 2x2 containing one spot of CD20 expressing cells and one spot with K562 cells for background correction, resulting in two background corrected binding curves with a data collection frequency of 0.86 min^{-1}. Cells were pre-incubated with unlabeled antibody in CO_2 independent RPMI medium at room temperature at a concentration and time that allowed for binding to reach equilibrium. This incubation solution was used as running buffer for LigandTracer experiments with C1q and, after recording a baseline, labeled C1q was added in three increasing concentrations (1.4 nM, 3.9 nM and 9.6 nM) for the association phase. For the dissociation phase, the incubation solution was exchanged to the same media containing unlabeled antibody to keep the antibody concentration constant during the entire experiment.

Real-Time Interaction Analysis

Real-time binding data for antibodies and Fab fragments was analyzed with TraceDrawer 1.9 (Ridgeview Instruments)

according to the 1:1 binding model. The 1:1 Langmuir model assumes that a reversible binding process between a ligand (L) and a target (T) receptor is characterized by a single association rate constant k_a and dissociation rate constant k_d (Eq. 1) also referred to as on- and off-rates.

$$[L] + [T] \underset{k_d}{\overset{k_a}{\rightleftarrows}} [LT] \quad [1]$$

The affinity K_D is calculated from the ratio of the rate constants (Eq. 2).

$$K_D = \frac{k_d}{k_a} \quad [2]$$

The interaction half-life $t_{1/2}$, *i.e.* the time until half of the bound ligands have dissociated, can be calculated from the off-rate (Eq. 2).

$$t_{1/2} = \frac{\ln(2)}{k_d} \quad [3]$$

In real-time interaction analysis, the kinetic parameters are extracted from the non-linearity of the binding signal, B, over time which needs to be proportional to the number of ligand-target complexes formed (Eq. 4).

$$^{\delta B}/_{\delta t} = k_a \cdot [L] \cdot (B_{max} - B) - k_d \cdot B \quad [4]$$

For this type of analysis, the number of targets needs to stay constant during the experiment and, in contrast to end-point measurements, target saturation is not required. Besides the interaction rate constants, also the theoretical signal at target saturation B_{max} is estimated from the binding curve.

Real-time binding data for C1q to antibody opsonized cells was also evaluated with InteractionMap (IM). This analysis searches for 1:1-like interactions in a defined k_a and k_d parameter space that correspond to the measured binding data when summed up (Eq. 5).

$$MeasuredCurve = \Sigma_{i=1}^{n} \Sigma_{j=1}^{m} [W_{ij} * \text{CurveComponent}(\text{conc}, k_a^i, k_d^j)] \quad [5]$$

Each interaction is depicted in an on-off plot and colors are assigned according the weighing factors W_{ij}: the more an individual interaction contributes to the measured curve, the warmer the color.

Human Samples

Human serum samples and peripheral blood for CDC assays were collected from healthy individuals with approved consent. Blood cones used to isolate B cells for interaction analysis were provided by the Department of Transfusion Medicine and Haemostaseology of the University Clinics Erlangen, Germany, with informed consent of the donor and the local ethical committee. PBMC from CLL patients were provided by the Department of Medicine II, Kiel, Germany with informed consent of the donors.

Complement Dependent Cytotoxicity (CDC) Assay

For analysis of CDC induction and complement C3b deposition $5*10^4$ Ramos, Daudi, P493.6 or LCL1.11 cells or $7.5*10^5$ human PBMCs were resuspended in RPMI 1640 supplemented with 10% FBS, 100 µg/ml penicillin-streptomycin, 2 mM L-glutamine, 1 mM sodium pyruvate and 0.1 mM MEM non-essential amino acids. CD20-specific antibodies (OFA, RTX, or OBI) were added at either 20 µg/ml or 2 µg/ml. Human serum was obtained, stored at −20°C and added to 20% of the reaction volume. Controls included serum heat inactivated at 56°C for 30 min or cells incubated with serum/heat-inactivated serum but no CD20-specific antibodies. Cells were then incubated for 30 min at 37°C. The reaction was stopped by addition of ice-cold PBS supplemented with 10% FBS and 0.05% sodium azide. Cells were then stained with DAPI and anti-C3b-FITC (clone 2C6, Cedarlane) for subsequent flow cytometry analysis. Human primary cells were in addition stained with anti-CD19-PE/Cyanine7 (clone HIB19, Biolegend) to label B cells. Samples were acquired on a FACSCantoII (BD Biosciences) and analyzed using FACSDiva and FlowJo Software.

Flow Cytometric Analysis

Expression of B cell surface markers was performed by flow cytometry. $1*10^5$ cells (B cell lines or human primary B cells) were stained with anti-CD19-PE/Cyanine7 (clone HIB19, BioLegend), anti-CD20-Alexa647 (Rituximab, labeled with ThermoFisher AlexaFluor647 Labeling Kit), anti-FcγRIIb-Alexa647 (clone 2B6, labeled with ThermoFisher AlexaFluor647 Labeling Kit), anti-CD55-PerCP/Cyanine5.5 (clone JS11, BioLegend) or anti-CD59-PE (clone H19, BioLegend). Dead cells were excluded by subsequent staining with DAPI. Samples were acquired on a FACSCantoII (BD Biosciences) and analyzed using FACSDiva and FlowJo Software.

C1q Binding ELISA

Interaction of CD20-specific mAbs with C1q was analyzed by enzyme-linked immunosorbent assay (ELISA). All incubation steps were performed at room temperature for 1 h. 100 µg/ml of mAbs were coated in 50 mM sodium bicarbonate buffer pH 9.6 (Sigma). After three washing steps with PBS 200 µl of blocking buffer (PBS containing 3% bovine serum albumin and 0.05% Tween-20) were added. After removal of blocking buffer increasing concentrations of native human C1q (Serotec) diluted in blocking buffer were added followed by three more washing steps. HRP-conjugated sheep anti human complement C1q (Serotec) was diluted 1:500 in blocking buffer. Plates were washed three times with PBS and TMB solution (Invitrogen) was added to detect anti-C1q-HRP. The reaction was stopped with 6% orthophosphoric acid.

Quantification of GM_1 Levels

Human B cells (Ramos, Daudi, P493.6, LCL1.11) or human peripheral blood leukocytes were incubated with AlexaFluor555-labeled cholera toxin subunit B (CT-B; ThermoFisher Scientific) diluted in RPMI 1640 medium for 10 min at 4°C. Bound CT-B

was crosslinked with anti-cholera toxin subunit B antibody (anti-CT-B, rabbit serum; ThermoFisher Scientific) for 15 min at 4°C and GM_1 levels were detected by flow cytometry on a FACSCytoFLEX S (Beckman Coulter Life Sciences). Human peripheral blood leukocytes were purified by RBC lysis and stained with anti-CD19-PE/Cyanine7 (clone HIB19; BioLegend) to detect GM_1 levels on primary B cells. Data was analyzed with Flow Cytometry Analysis Software (FlowJo).

Statistics

GraphPad Prism v8.3 was used for statistical analysis. Initially, shapiro-wilk test was used to determine Gaussian distribution of data sets. Subsequently, Kruskal-Wallis and Dunn´s multiple comparisons test (non-Gaussian distribution) or analysis of variance (ANOVA) followed by Sidak´s multiple comparisons *post hoc* test (Gaussian distribution) were performed. Alternatively, two-way RM ANOVA and multiple comparisons tests were applied. A detailed description of statistical tests used for individual experiments can be found in the respective figure legends.

RESULTS

A variety of B cell lines such as Raji (11, 23, 38, 43, 44), Ramos (44, 45), or Daudi (11, 38, 46) are routinely used to study

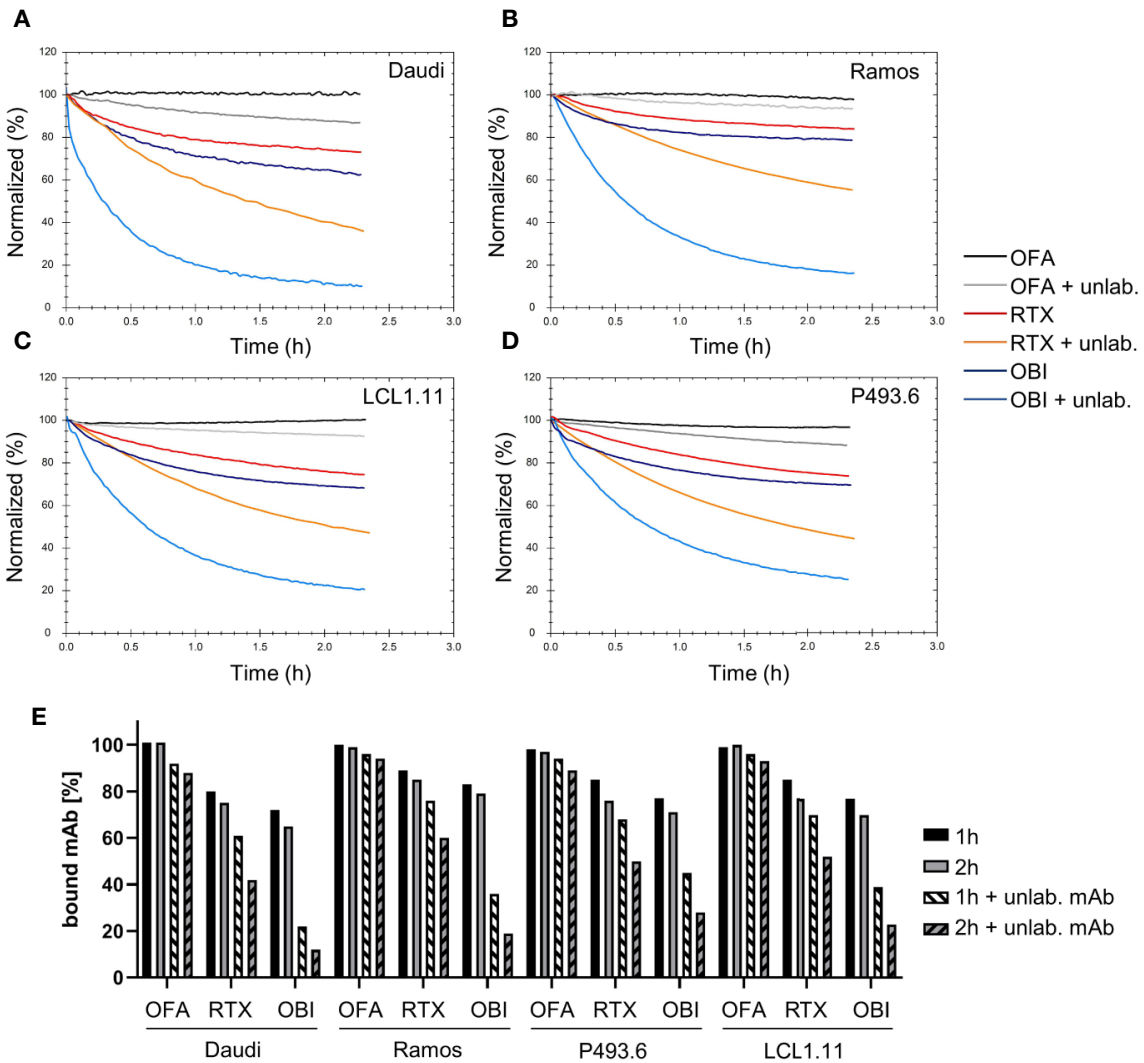

FIGURE 1 | Binding stability of CD20 mAbs to human lymphoma B cell lines. Binding of 60 nM Ofatumumab (OFA), Rituximab (RTX), or Obinutuzumab (OBI) to Daudi **(A)**, Ramos **(B)**, LCL1.11 **(C)**, or P493.6 **(D)** cells was recorded until equilibrium was approached (not shown) followed by measurement of mAb dissociation either in plain cell culture medium or in presence of 60 nM of the respective unlabeled (unlab.) antibody. For all cell lines the dissociation of OFA was measured in presence of 180 nM unlabeled OFA (instead of 60 nM) to enhance possible cell-line differences. **(E)** Signal intensities were normalized to 100% at the beginning of the dissociation. The remaining signal after 1 h (black) and 2 h (gray) dissociation both in plain media (solid) and in presence of unlabeled antibody (shaded) are plotted for human B cell lines.

cytotoxic IgG activity directed against CD20. When studying the interaction of CD20-specific mAbs, we previously found that binding to the Burkitt lymphoma cell line Daudi (47) is most stable for OFA, followed by RTX and least stable for OBI, due to the mAbs engaging in bivalent target binding to differing degrees (41). To extend our analyses, we evaluated the binding pattern of the three mAbs by real-time interaction analysis on additional human lymphoma B cell lines (the Burkitt lymphoma cell line Ramos (48) and the lymphoblastoid cell lines P493.6 (49) and LCL1.11) (**Figures 1A–D**), as well as primary human B cells (**Figure 2A**) purified from human peripheral blood (**Supplementary Figure 2**). Consistent with our previous data, OFA binding is most stable, followed by RTX, whereas OBI displayed the least stable binding (**Figures 1E** and **2B**). Also, in line with previous results, the number of cell-bound OFA molecules was barely influenced by the presence of free mAb in solution, whereas the number of cell-bound RTX and OBI molecules was clearly decreased by the presence of unbound mAb during the dissociation phase, implying more dynamic interactions, both on cell lines and on primary human B cells. Compared to RTX, the stability of bound OBI is even more strongly affected by the presence of free antibody in solution on all tested cell lines (**Figure 1E**), however this difference was less pronounced on primary human B cells (**Figure 2B**).

While confirming that the overall binding pattern of the CD20 mAbs is consistent across the tested cell lines as well as on primary human B cells, we also noticed differences in binding stability between the cell lines. On Ramos cells, RTX displayed most stable binding whereas the other three cell lines showed very similar dissociation patterns in plain cell culture medium (**Figure 3A**, solid lines). In the presence of free antibody in solution, the apparent off-rate for RTX was slowest for the dissociation from Ramos cells, followed by LCL1.11 cells, then P493.6 cells and lastly Daudi cells with the fastest apparent off-rate (**Figure 3A**, dashed lines, **Supplementary Table 1**). The stability of bound RTX further decreased with increasing concentrations for all cell lines (**Figure 3B**), with the half-life of bound RTX in the presence of free antibody in solution at 60 nM being roughly half compared to the half-life at 10 nM across all tested cell lines (**Table 1**). In contrast, the dissociation of RTX-Fab was neither influenced by the Fab concentration, nor by the presence of free ligand in solution (**Figures 3C, D**), which is a good indication for the interaction following a 1:1 behavior. Moreover, the stability of bound RTX-Fab did not significantly differ between the cell lines (**Figure 3D** and **Supplementary Table 2**), indicating that the differences in binding stability for RTX-IgG are due to secondary stabilizing effects, such as e.g. bivalency or Fc-interactions.

For OBI, the apparent off-rate as measured in plain medium was slowest for the dissociation from Ramos cells, followed by P493.6, LCL1.11 and lastly Daudi cells with the fastest apparent off-rate (**Figure 3E**, solid lines). This order changed when the stability of cell-bound OBI was studied in the presence of unlabeled antibody in solution: after 2 h the highest percentage of remaining OBI molecules was on P493.6 cells, followed by LCL1.11, Ramos and lastly Daudi cells (**Figure 3E**, dashed lines). In agreement with previously obtained data (41), the binding stability of OFA was not significantly influenced by the presence of equimolar amounts of free antibody in the 10-60 nM range (data not shown). Therefore, the stability of OFA was tested with 60 nM labeled antibody during the association, followed by three-fold molar excess of unlabeled antibody during the dissociation phase. OFA dissociated slowest from LCL1.11 cells, followed by Ramos and P493.6 cells and lastly Daudi cells with the fastest apparent off-rate (**Figures 3F, G**). Fitting a single exponential decay to the dissociation phase resulted in average half-lives of 26.7 h for LCL1.11, 17.8 h for Ramos, 12.2 h for P493.6 and 9.9 h for Daudi cells. For all three mAbs, both in absence and presence of unlabeled antibody, the apparent off-rate was fastest from Daudi cells.

The off-rate, which is a measure for the binding stability, as well as bivalent target engagement of mAbs have been discussed

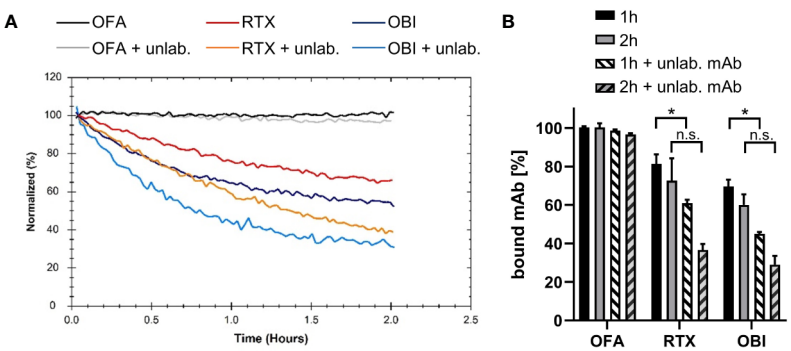

FIGURE 2 | Binding stability of CD20 mAbs to human primary B cells. Binding of 60 nM Ofatumumab (OFA), Rituximab (RTX) or Obinutuzumab (OBI) to primary human B cells isolated from blood of healthy donors was recorded until equilibrium was approached (not shown) and then mAb dissociation was measured either in plain cell culture medium or in presence of 60 nM of the respective unlabeled antibody. **(A)** One out of three independent measurements shown. **(B)** Signal intensities were normalized to 100% at the beginning of the dissociation. The remaining signal after 1 h (black) and 2 h (gray) dissociation both in plain media (solid) and in presence of unlabeled antibody (shaded) are plotted. Bars show mean ± standard deviation of n=3 experiments using cells from different donors. For statistical analysis of signal intensities in plain media and in presence of unlabeled antibody for individual time points, two-way ANOVA and Tukey's multiple comparison test were applied. *p<0.05, n.s. not significant.

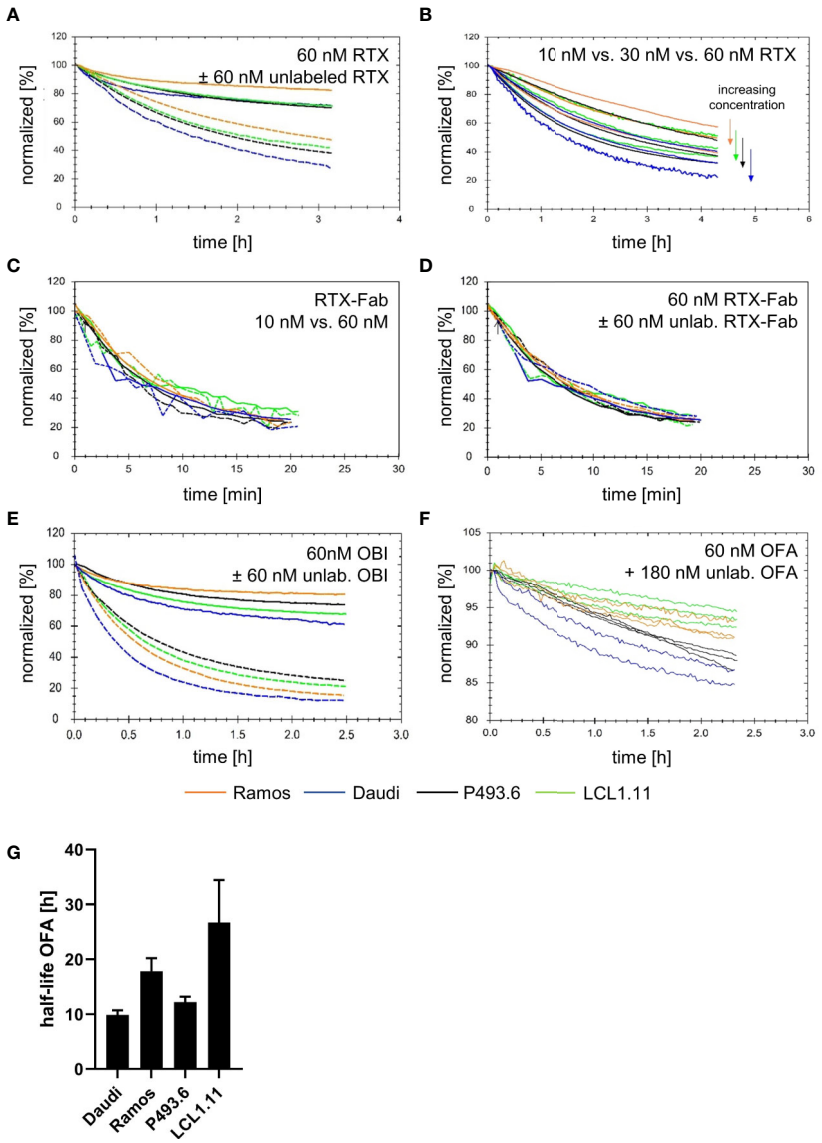

FIGURE 3 | Binding stability of CD20 mAbs across different lymphoma B cell lines. **(A)** Dissociation after incubation with 60 nM fluorescein isothiocyanate Rituximab (FITC-RTX) in either plain medium (solid lines) or in the presence of 60 nM unlabeled RTX (dashed lines). **(B)** Dissociation after incubation with 10 nM, 30 nM or 60 nM FITC-RTX in the presence of equimolar amounts of unlabeled RTX. **(C)** Dissociation in plain medium after incubation with either 10 nM (dashed lines) or 60 nM (solid lines) FITC-RTX-Fab. **(D)** Dissociation after incubation with 60 nM FITC-RTX-Fab in either plain medium (solid lines) or presence of 60 nM unlabeled RTX-Fab (dashed lines). **(E)** Dissociation after incubation with 60 nM FITC-Obinutuzumab (OBI) in either plain medium (solid lines) or in the presence of 60 nM unlabeled OBI (dashed lines). **(F)** Dissociation after incubation with 60 nM FITC-Ofatumumab (OFA) in the presence of 180 nM unlabeled OFA. Note the different y-axis scaling. **(G)** Average half-life for bound OFA calculated from data shown in **(F)**. Bars represent mean ± standard deviation of n=3–4 independent measurements.

as parameters that might influence the effectiveness of complement activation. We therefore set-up an assay to monitor C1q binding in real-time on living cells opsonized with CD20 antibodies to establish the kinetics of the C1q interaction. Binding to cells coated with either RTX or OFA clearly deviated from a 1:1 interaction which can be directly seen from the dissociation phase of the binding curves where a fraction of C1q quickly releases from the opsonized cells, whereas another fraction of C1q is more stably bound (**Figures 4A, B**). Data was evaluated with InteractionMap that depicts the number of 1:1-like interactions contributing to the overall binding pattern in an on-off plot. This type of analysis resulted in discovery of two distinct interaction components for all cell lines. These components primarily differed in their off-rates, which reflects the binding stability. The interaction of C1q to cells coated with OFA (**Figure 4B**) resulted in an over-all stronger and more stable interaction compared to cells coated with RTX (**Figure 4A**), whereas C1q binding to cells coated with OBI was too weak to give a clear signal above background (**Supplementary Figure 3**). Of note, C1q binding to OFA was

TABLE 1 | Rituximab (RTX) binding stability at 10 nM and 60 nM was studied in the presence of unlabeled mAb in solution.

Cell line	RTX conc	k_d (1/s)	Half-life (min)	Fold change half-life
Ramos	10 nM	3.32E-05	348	
	60 nM	7.54E-05	153	0.44
Daudi	10 nM	7.17E-05	161	
	60 nM	1.28E-04	90	0.56
P493.6	10 nM	4.97E-05	232	
	60 nM	1.03E-04	112	0.48
LCL1.11	10 nM	5.14E-05	225	
	60 nM	9.69E-05	119	0.53

The first 2 h of dissociation were used to calculate dissociation rate constants and corresponding half-lives.

not significantly superior to RTX or OBI in a cell-free enzyme-linked immunosorbent assay (ELISA), emphasizing the importance of a cellular model system for complex binding studies (**Supplementary Figure 4**).

Interaction analysis of C1q with Rituximab opsonized Daudi cells revealed affinity values in the range of 0.8-2.3 nM for the strong interaction and 32-70 nM for the weak interaction depending on the cell line (**Table 2**). The k_d value differed by more than 100-fold between the two interactions, resulting in half-lives above 2 h for the stable interaction (**Figure 4C**, peaks toward the left on the InteractionMaps) and 1-2 min for the transient interaction (**Figure 4C**, peaks toward the right on the InteractionMaps). For all cell-lines the strong interaction component contributed less to overall C1q binding, with an estimated strong binding site fraction of 0.13 for Daudi, 0.15 for Ramos 0.17 for LCL1.11 and 0.20 for P493.6 cells at the tested C1q concentrations (**Figure 4C**). The half-life for strongly bound C1q molecules was longest on LCL1.11 cells, followed by Ramos and P493.6 cells, whereas C1q displayed the shortest half-life on RTX-opsonized Daudi cells. Taking both half-life and fraction of binding sites into account, C1q binding was clearly least stable on Daudi cells, which corresponds with RTX also displaying least stable binding to these cells.

Depending on the cell line, the interaction with OFA opsonized cells resulted in affinities of 0.07-0.2 nM for the stable component and 5-20 nM for the weaker binding component. Half-lives for the weak C1q binding component were 1-3 min on OFA opsonized cells and thus very similar to those observed for the weak binding component on RTX opsonized cells. Half-lives for the strong C1q binding component were longer for OFA opsonized cells than for RTX opsonized cells. Concerning the cell-lines incubated with OFA, the half-life for strongly bound C1q was shortest on Daudi cells (9.3 h), followed by LCL1.11 cells (10.8 h) and very similar on Ramos and P493.6 cells (both 11.6 h) (**Table 2**). The fraction of strong C1q binding sites was similar on OFA-opsonized Daudi and P493.6 cells with 0.42 and 0.43 respectively, whereas it was higher with 0.77 for OFA-opsonized Ramos and highest on LCL1.11 cells with 0.85, which correlates with the OFA binding stability on these cell lines. Overall differences in C1q binding strength were more pronounced when comparing RTX and OFA than the differences between the cell lines.

Next, we analyzed the expression of selected cell surface proteins that might influence antibody binding stability and complement activation on these cell lines, as well as on primary human B cells to see if these could explain the observed differences (**Figure 5**). While Ramos and Daudi cells expressed CD20 to comparable degrees as primary B cells, CD20 expression on LCL1.11 cells was very low. In contrast to the other cell lines, P493.6 cells showed variable but elevated expression levels of CD20 and additionally high levels of inhibitory FcγRIIb that can potentially interact with the Fc portion of the antibodies (28). Daudi cells expressed FcγRIIb to comparable levels as primary B cells, whereas expression was higher on LCL1.11 cells and absent on Ramos cells. Consequently, a direct correlation for expression levels of CD20 and FcγRIIb did not become apparent in regards to antibody binding stability and subsequent C1q capture. The expression of the complement regulatory proteins CD55, an inhibitor of C3 and C5 convertases on the cell surface (50), and CD59 which blocks MAC formation (51) was also analyzed as these might have an impact on how C1q capture translates to complement activation. We found that CD55 expression was highest on P493.6 cells, LCL1.11 and primary B cells. CD59 expression was elevated on P493.6 and LCL1.11 cells in comparison to primary B cells. In contrast, Daudi and Ramos cells expressed only low levels or even completely lacked CD55 and CD59 confirming previous reports (52).

Given the remarkable differences observed for the lymphoma cell lines, we subsequently assessed the functional consequences of distinct CD20, CD55 and CD59 expression for induction of complement-dependent cell lysis (CDC) induced by the different CD20-specific IgG (**Figure 6**). Upon addition of surface-saturating doses of OFA (20μg/ml) normal human serum (NHS) was able to significantly induce cell death in all cell lines tested (**Figure 6A**, **Supplementary Figure 5**). At this dose, even OBI mediated CDC in Ramos and Daudi cells and RTX was in addition able to kill P493.6 cells. At lower antibody doses, CDC induction was overall decreased. Still, OFA retained its superior capacity to induce complement-dependent cell death, followed by RTX, while OBI was hardly able to induce CDC anymore (**Figure 6B**, **Supplementary Figure 6**). Of note, differences between the cell lines were not restricted to CDC induction. As OBI has previously been described to induce apoptosis (26) we also assessed the capacity of CD20-specific mAbs to induce direct killing of B cells. Indeed, following incubation of cells with anti-CD20 mAbs in absence of serum enhanced cell killing could only be observed for high-dose OBI treatment but was also restricted to P493.6 and LCL1.11 cells (**Supplementary Figures 7A, B**), the cell lines showing the highest or lowest CD20 expression levels, respectively. This suggests that other factors beyond CD20 expression are involved in this killing mechanism. In contrast to assays with human lymphoma cell lines where successful initiation of CDC resulted in an increase of $DAPI^+$ cells, it was not possible to detect dead B cells in primary human samples. Instead, primary B cells seemed to disintegrate during the incubation time. We therefore quantified living, *i.e.* $DAPI^-$, B cells instead and

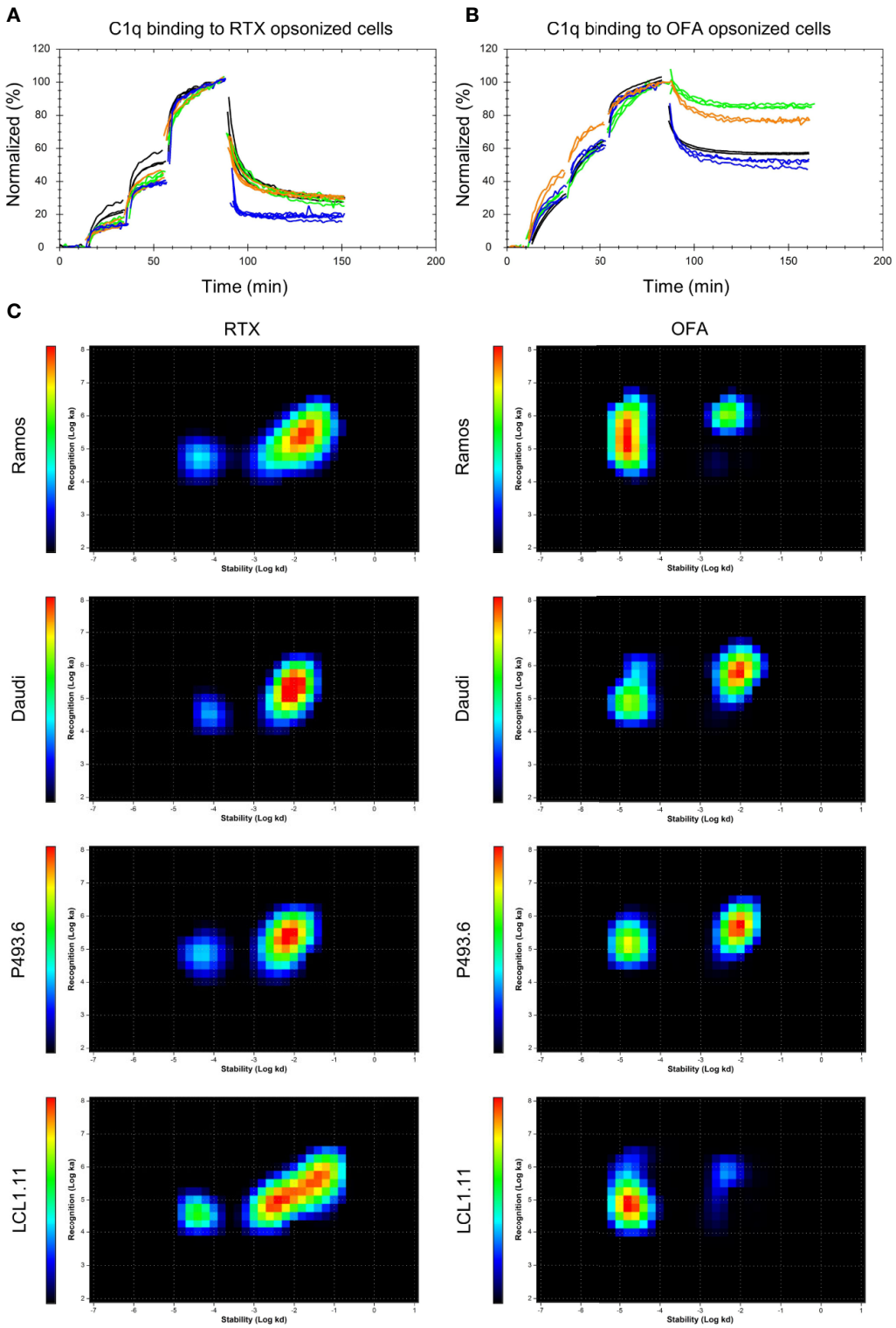

FIGURE 4 | Binding of C1q to antibody opsonized B cells. Binding of fluorescent C1q to mAb opsonized Ramos (orange), Daudi (blue), P493.6 (black) and LCL1.11 cells (green) at concentrations of 1.4 nM, 3.9 nM, and 9.6 nM followed by dissociation. Cells were pre-incubated with either 60 nM unlabeled Rituximab (RTX) **(A)** or Ofatumumab (OFA) **(B)** for 1 h at room temperature prior to C1q binding and the antibody concentration was kept constant during the entire experiment. **(C)** InteractionMap for C1q binding to mAb opsonized cells. InteractionMap (IM) is an on/off-plot with each pixel representing a unique k_a/k_d combination and heat-map coloration indicating how much each combination is contributing to the interaction analyzed. Per cell line n=3–4 replicates were calculated into one IM.

TABLE 2 | Kinetic values for C1q interaction components on mAb opsonized cells as extracted by global InteractionMap analysis for each condition.

Strong interaction component					
	k_{a1} (1/(M*s))	k_{d1} (1/s)	K_{D1} (M)	half-life (min)	fraction binding sites
RTX-Ramos	5.2E+04	4.8E-05	9.3E-10	240	0.15
RTX-Daudi	3.4E+04	7.8E-05	2.3E-09	147	0.13
RTX-P493.6	6.7E+04	5.6E-05	8.3E-10	208	0.20
RTX-LCL1.11	3.4E+04	4.0E-05	1.2E-09	286	0.17
OFA-Ramos	2.3E+05	1.7E-05	7.1E-11	694	0.77
OFA-Daudi	1.1E+05	2.1E-05	1.9E-10	558	0.42
OFA-P493.6	1.5E+05	1.7E-05	1.1E-10	700	0.43
OFA-LCL1.11	7.6E+04	1.8E-05	2.4E-10	649	0.85
Weak interaction component					
	k_{a2} (1/(M*s))	k_{d2} (1/s)	K_{D2} (M)	half-life (min)	fraction binding sites
RTX-Ramos	2.0E+05	1.4E-02	7.0E-08	1	0.85
RTX-Daudi	1.8E+05	9.1E-03	4.9E-08	1	0.87
RTX-P493.6	2.1E+05	6.7E-03	3.2E-08	2	0.80
RTX-LCL1.11	1.5E+05	9.8E-03	6.4E-08	1	0.83
OFA-Ramos	1.0E+06	5.3E-03	5.1E-09	2	0.23
OFA-Daudi	6.1E+05	8.8E-03	1.4E-08	1	0.58
OFA-P493.6	4.5E+05	8.8E-03	2.0E-08	1	0.57
OFA-LCL1.11	5.7E+05	4.3E-03	7.6E-09	3	0.15

observed that only OFA was able to cause a significant reduction in the presence of human serum (**Figures 7A, B**). With respect to direct cell killing by the mAbs, a non-significant reduction in viable B cells could be observed upon OBI addition (**Supplementary Figure 7C**).

Induction of CDC is the ultimate result of complement activation. One crucial step during the activation cascade is, however, deposition of complement C3 on the cell surface. In addition to its role in advancing the activation cascade the cleavage product C3b also poses as a ligand for complement receptors expressed on phagocytic cells thereby marking target cells for complement-dependent phagocytosis (CDCP) (5). Given that CDCP might therefore also be involved in complement-dependent effector functions of cytotoxic IgG *in vivo*, we also investigated deposition of C3b (and its inactivated form iC3b) upon treatment of B cells with anti-CD20 IgG. C3b could only be observed upon addition of anti-CD20 IgG and normal human serum, but not heat-inactivated serum (**Figures 6C, D**, and **7C**), and C3b levels were highest on P493.6 cells but surprisingly low on Ramos, Daudi and LCL1.11 cells. Potentially, sufficient complement activation (including C3b deposition) triggers lysis of cells so that C3b on these cells can no longer be detected. Consequently, only cells that are not killed by the complement system would still show elevated C3b levels. This might also explain higher C3b detection upon treatment with the lower antibody dose (**Figure 6D**) and the minor C3b deposition on primary human B cells (**Figure 7C**). Even though complement activation in this scenario might be insufficient to trigger direct cell killing *via* MAC formation one cannot exclude that the deposited C3b would be able to induce phagocytosis and thus contribute to target cell killing.

CD20-specific antibodies are used to treat a variety of B cell malignancies, however for chronic lymphocytic leukemia (CLL) a reduced therapeutic potential has been observed (52). This was previously attributed to the fact that CLL B cells have been shown to express lower levels of CD20 (53–55) that might in turn reduce effector functions by anti-CD20 IgG, especially those dependent on complement activation (56). Given that we noticed CD20 expression levels to not be the sole factor determining efficacy of complement activation we compared B cells from 9 different CLL patients with respect to B cell surface marker expression (**Figure 8A**). As previously described, CD20 was expressed at lower levels on most CLL B cell samples however two of the donors did show elevated expression. In comparison to B cells from healthy donors, CLL B cells were characterized by homogenous decreased CD55 expression. In contrast, CD59 expression varied largely between donors but was overall increased. This suggests a reduced susceptibility toward MAC formation and therefore CDC but potentially an accumulation of active C3b on the B cell surface. Within the CLL patient cohort we identified three samples with different profiles regarding CD20 and CD59 that were further submitted to our CDC assay. Upon treatment with anti-CD20 IgG and human serum, CD20 turned out to be the more prominent determinant of complement-induced cytotoxicity as the strongest reduction of living B cells ($CD19^+DAPI^-$) by OFA was observed in the $CD20^{++}$ sample. For this donor, RTX also caused a significant decrease in presence of NHS in comparison to HIS while no differences could be observed for OBI (**Figures 8B, C**). In addition, OFA and RTX, but not OBI, induced significant deposition of complement C3b (**Figure 8D**). Lower CD20 expression in the second and third CLL sample was associated with dampened OFA and abrogated RTX induced reduction of living B cells, irrespective of the CD59 expression level (**Figures 8B, C**). Surprisingly, we observed an increase in $CD19^-DAPI^-$ cells consistently upon treatment of CLL cells with OBI (**Figure 8B**, **Supplementary Figure 8**). Independent of cell killing this suggests that OBI might be able to induce CD19 loss on B cells as has previously only been described for RTX (57, 58). Accordingly, an increase of $CD19^-$ cells could also be noticed upon RTX addition for the

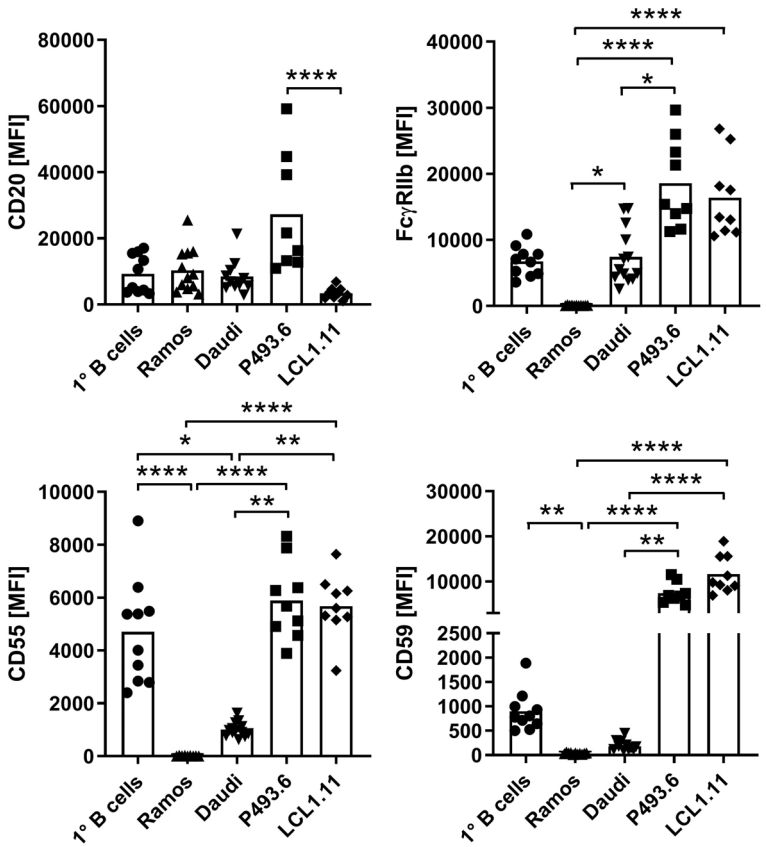

FIGURE 5 | Comparison of surface marker expression. Expression of CD20, inhibitory FcγRIIb and complement-regulatory proteins CD55 and CD59 was assessed by flow cytometry on various B cell lines in comparison to primary human peripheral blood B cells from healthy donors. Symbols indicate biological replicates of the median fluorescence intensity (MFI) of the respective marker. Bars show statistical mean. Kruskal-Wallis test and Dunn´s multiple comparisons *post-hoc* test were applied to calculate statistical significance. *p<0.05, **p<0.01, ****p<0.0001.

$CD20^{++}$ CLL sample (**Figure 8B**, **Supplementary Figure 8**). Of note, CLL PBMC samples were stored frozen before the assay. To exclude an impact of freezing on susceptibility for CDC we also performed the assays with healthy human PBMCs following frozen storage (**Supplementary Figure 9**). Indeed, cells previously frozen were much more sensitive toward anti-CD20 mAb induced CDC as OFA, RTX and even OBI caused significant cell death and C3b deposition not observed with fresh PBMCs.

DISCUSSION

By applying real-time interaction analysis, we have previously shown that the stability of bound mAbs relates to the fraction of molecules that engage in bivalent binding. Accordingly, the highest fraction of bivalently bound antibody and the least dynamic binding pattern can be seen for OFA, while OBI displays the most dynamic pattern least stabilized by bivalency. Even though the present study confirmed these observations for additional B cell lines as well as primary B cells, we also observed that binding stability of anti-CD20 IgGs varies between human B cell lines. For instance, the stability of RTX in the presence of unlabeled mAb in solution was roughly two-fold less on Daudi compared to Ramos cells during the first hour of dissociation while primary human B cells displayed less variation with apparent off-rates for RTX being similar to those observed on Daudi cells. Differences between cell types were, however, smaller than differences between the antibodies, with e.g. OFA having a 10-fold longer binding half-life than RTX on Daudi cells.

These differences further translate to specific kinetics of C1q capture by antibody opsonized cells: Whereas the overall binding stability of C1q seems to correlate with OFA binding stability, C1q binding to RTX-opsonized cells was overall quite similar, except for RTX-opsonized Daudi cells that exhibited the weakest C1q capture and in line with this also least stable RTX binding. Binding of C1q to OFA opsonized cells was thus clearly stronger than for RTX on all tested cell lines, whereas binding of C1q to OBI opsonized cells could not be detected. Bivalent target engagement therefore positively correlates with strong C1q capture for the investigated anti-CD20 IgGs and expanding

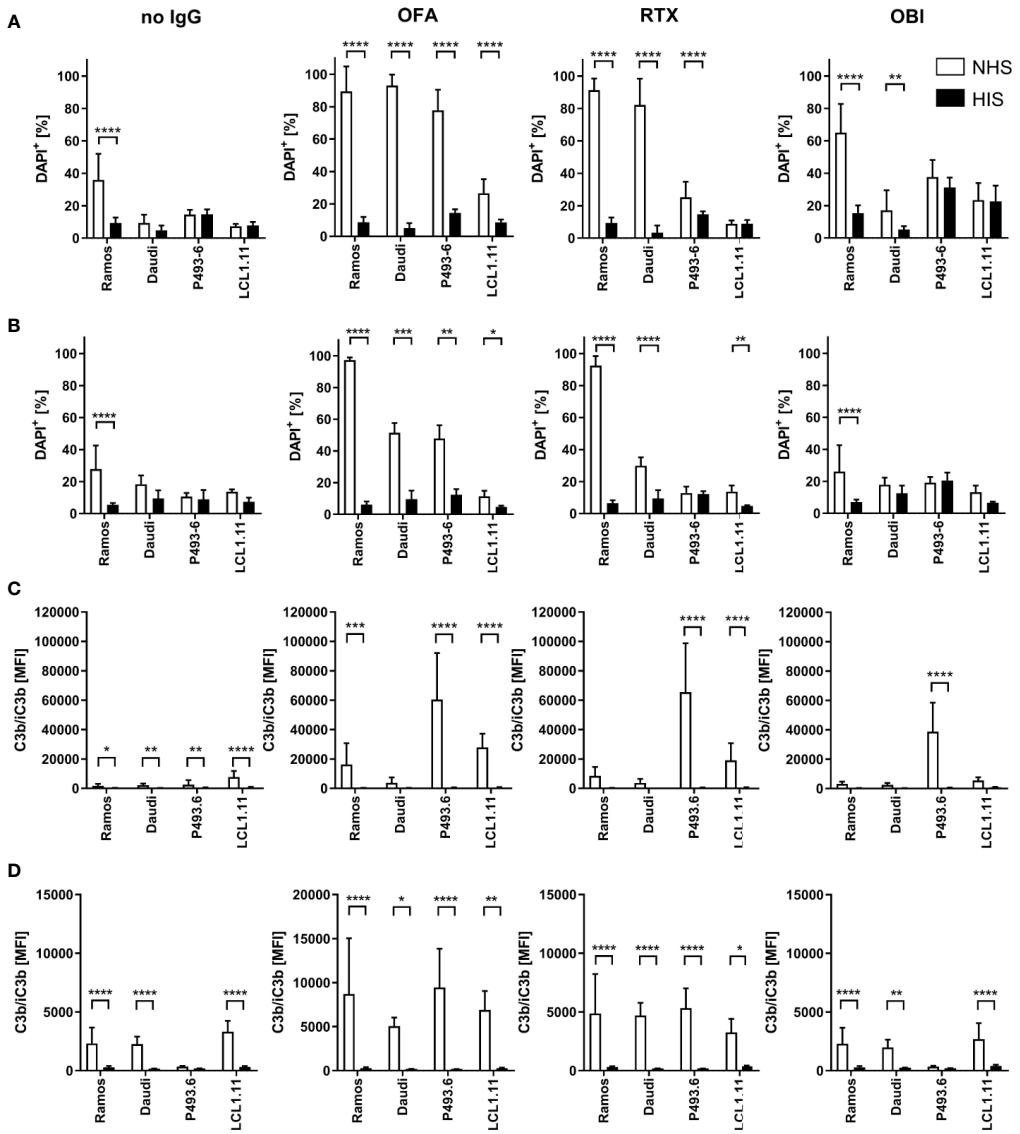

FIGURE 6 | Complement dependent lysis and C3b deposition on B cell lines. Ramos, Daudi, P493.6 and LCL1.11 B cell lines were treated with 20 µg/ml **(A, C)** or 2 µg/ml **(B, D)** anti-CD20 mAb and 20% human serum (white bars) for 30 min at 37°C. As controls, cells were treated with heat-inactivated serum (black bars) or with serum in absence of anti-CD20 mAb. **(A, B)** Dead cells were quantified by flow cytometry analysis of DAPI stained cells. **(C, D)** Quantification of C3b/iC3b deposition on B cells. Bars show statistical mean ± standard deviation of n=3–5 independent experiments each using three to seven human serum samples **(A, C)** or n=2–3 independent experiments each using three to four human serum samples **(B, D)** per cell line. For statistical analysis, two-way ANOVA and Tukey´s multiple comparison test were applied. *p<0.05, **p<0.01, ***p<0.001, ****p<0.0001.

this analysis to a larger panel of anti-CD20 IgGs would be of interest, as contrasting observations have been made for other antigens (19, 37). The real-time binding assay presented in this study also allowed to resolve the presence of two interactions, as well as their kinetic and affinity values for C1q binding to anti-CD20 IgG opsonized cells. The two interactions differed mainly with respect to their dissociation rate constant k_d, indicating that one fraction of C1q molecules is bound noticeably more stable than the remaining fraction. The interaction peaks of both C1q binding components as displayed in InteractionMaps were elongated in the y-axis direction, indicating heterogeneity in how C1q recognizes its binding partners, which is a sign of multivalent target engagement. As InteractionMap assumes that a binding curve can be explained by the weighted sum of individual 1:1 binding curves, multivalent binding becomes visible as a poorly defined k_a value that is seemingly changing during the interaction. This is due to the ratio of unbound receptors versus bound receptors decreasing faster than predicted as one ligand binds multiple targets, causing the rate of ligand-target complex formation to slow down more than what is expected according to a 1:1 model. This is especially noticeable for interaction peaks that represent a high percentage

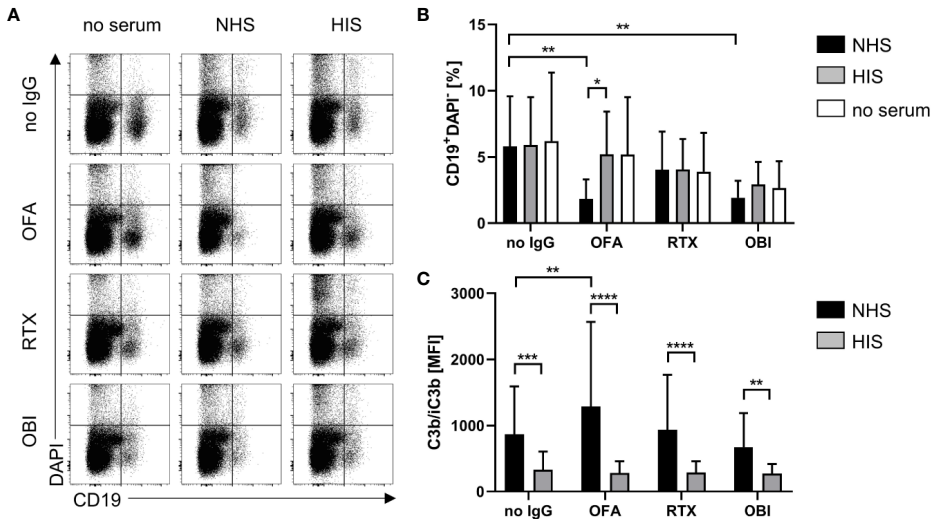

FIGURE 7 | Complement dependent lysis and C3b deposition on primary human B cells. CDC and C3b deposition were compared for primary human B cells derived from healthy donor blood upon treatment with 20 µg/ml Rituximab (RTX), Ofatumumab (OFA), or Obinutuzumab (OBI) in absence (white) or presence of 20% human serum (NHS, black bars) or heat-inactivated serum (HIS, gray bars) for 30 min at 37°C. **(A)** Exemplary dot plots of CD19 and DAPI staining. **(B)** Quantification of living $CD19^+DAPI^-$ cells. **(C)** Quantification of C3b/iC3b deposition on B cells. Bars show mean and standard deviation of n=4 independent experiments using PBMCs from different donors and treated with four human sera each. For statistical analysis, two-way ANOVA and Sidak´s multiple comparison test were applied. *p<0.05, **p<0.01, ***p<0.001, ****p<0.0001.

of binding sites such as the strong C1q binding component on OFA-opsonized Ramos cells. For interaction peaks that represent minor binding fractions this is less or not at all visible as the information contained in the binding traces is not sufficient to capture the exact shape of the interaction peak. Both InteractionMap peaks thus presumably represent multivalent binding of C1q to cell-bound IgG Fc-domains. The strong interaction component likely represents binding of C1q to IgG hexamers, whereas the less stable interaction component likely represents binding of C1q to IgG-Fc multimers that are smaller than hexamers, which have been shown to result in some CDC activity (24, 36). A general fast association for C1q is in agreement with previous reports and also explains the fast on-set of CDC, reaching maximum killing levels within 10 min even at C1q concentrations as low as 1 µg/ml (21, 38). The apparent affinity for C1q binding to OFA coated Daudi cells, as determined with an end-point assay, has been reported previously to be 16 nM (21, 38, 59), which is close to the value reported here for the less stable interaction component. Data resolution for end-point affinity measurements is typically not sufficient to discriminate between individual interaction components with different affinities. Of note, the C1q binding assay set-up in this study does not capture binding to IgG-Fc monomers, as binding is only detected if C1q concentrations are getting closer to the affinity value of the interaction, *i.e.*, around 10–100 µM for binding to Fc monomers (39) which might explain the lack of binding observed for OBI.

Regarding the functional consequences of C1q binding to mAb opsonized target B cells, we systematically compared complement mediated cell killing by RTX, OFA and OBI on human lymphoma cell lines and human primary B cells differing in expression levels of CD20 and complement regulatory proteins. Similar to what was previously reported (52), Ramos cells proved to be extremely sensitive in this assay as all three mAbs, and to a lesser extent serum in absence of anti-CD20 IgG, are able to significantly induce complement-dependent cell death. A potential explanation for Ramos cells being very sensitive to CDC is the strong C1q capture in combination with the absence of complement regulatory proteins. Even though LCL1.11 cells also display a strong C1q capture, CDC sensitivity is clearly reduced compared to Ramos cells, which might be explained by a lower expression of CD20 and the high expression of both CD55 and CD59. The low expression of both complement regulatory proteins might also account for the rather efficient CDC in Daudi cells, despite having the least strong C1q capture among the investigated cell lines. Surprisingly, P493.6 cells which strongly express CD20 and also nicely capture C1q were quite resistant to CDC induction supporting the notion that expression levels of complement regulatory proteins rather than CD20 determine the efficacy of complement-dependent killing of B cell lines. A decreased susceptibility for CDC and complement activation in general could also be observed for freshly isolated primary human B cells despite levels of CD20 and CD59 that are comparable to Ramos and Daudi. Elevated expression levels of CD55 on primary B cells might instead explain reduced complement activation. In fact, only OFA was able to consistently kill primary B cells as well as CLL B cells in a complement-dependent manner, again confirming the superior capacity of complement activation. In any case, the data presented here suggests that the choice of the *in vitro* model system and especially target B cell can dramatically impact conclusions about the extent of complement activation induced by CD20-specific mAbs. Given the contradictory literature (6, 56, 60–63), it therefore

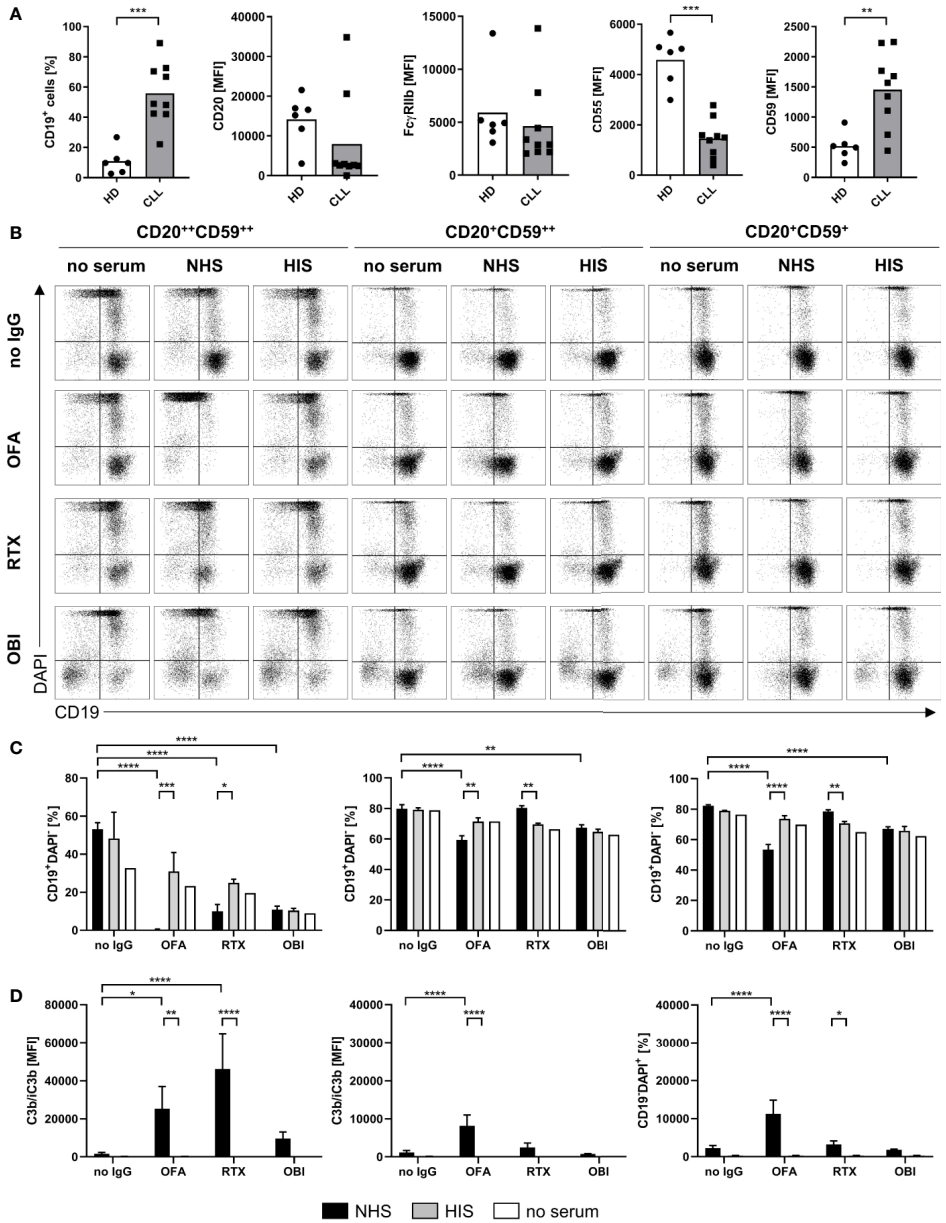

FIGURE 8 | Complement dependent lysis and C3b deposition on primary human chronic lymphocytic leukemia (CLL) B cells. Complement-dependent cytotoxicity (CDC) and C3b deposition were compared for primary human B cells derived from CLL patients with distinct expression profiles of CD20 and CD59 upon treatment with 20 µg/ml Rituximab (RTX), Ofatumumab (OFA), or Obinutuzumab (OBI) in absence (white) or presence of 20% normal (NHS, black) or heat-inactivated (HIS, gray) human serum for 30 min at 37°C. **(A)** Flow cytometry expression analysis of CD19 and CD20, FcγRIIb, CD55, and CD59 on $CD19^+$ cells of healthy (HD) or CLL B cells. **(B)** Exemplary dot plots of CD19 and DAPI staining. **(C)** Quantification of living $CD19^+DAPI^-$ cells for three to four sera. **(D)** Quantification of C3b/iC3b deposition on $CD19^+$ cells. Bars show mean ± standard deviation of three to four serum samples. For statistical analysis, Mann Whitney test **(A)** or two-way ANOVA and Sidak´s multiple comparison test **(C, D)** were applied. *p<0.05, **p<0.01, ****p<0.0001.

still remains to be seen whether CD20, complement regulator expression levels or a combination of both ultimately determine target cell susceptibility for complement dependent induction of cell death. Regarding the observed increase of $CD19^-$ cells in CLL samples upon OBI (and to a lesser extent RTX) treatment, we speculate that OBI might induce a down-regulation of CD19 as has been previously described for RTX (57, 58). To the best of our knowledge this has not been observed before for OBI but data by Reddy et al. suggest that this might indeed be the case (29). However, the specifics of this potential reduction in CD19 would need to be investigated in more detail. One factor affecting our observations could be the short incubation time of only 30 min in this study which might enable capturing transitional effects during OBI induced cell killing.

There is accumulating evidence that efficiency of CDC induction by mAbs is dependent on a range of factors, such as the binding epitope and binding orientation of the mAb, as well as the antibody elbow hinge angle (30–33). This complexity is difficult to mimic when measuring C1q binding in artificial, isolated protein systems, especially since antigen mobility in the membrane might play a role (36). For anti-EGFR mAbs it has been shown that monovalent target engagement results in higher CDC efficacy. This could be a consequence of monovalent binding resulting in a higher number of IgGs bound and this, in turn, might increase the likelihood for the formation of multimeric IgG-Fc platforms suitable for C1q binding (37). For anti-CD20 mAbs, on the other hand, bivalent binding might enhance crosslinking of CD20 and thus lead to more efficient clustering of CD20 and bound mAbs. This notion is supported by recent structural studies showing that for RTX and OFA two Fabs belonging to different antibody molecules can interact with the same CD20 dimer. In contrast, only one Fab of the type II mAb OBI can be bound per CD20 dimer due to sterical constraints. As a consequence, it was suggested that type I mAbs can act as molecular seeds that promote the concatenation of IgG and CD20 molecules into larger molecular assemblies (25, 64). In line with this, it was previously observed that binding of type I anti-CD20 mAbs causes segregation of CD20 into detergent-resistant membrane domains which facilitates CDC induction (22). One could therefore speculate that the differences observed between the lymphoma cell lines and primary B cells could be caused by specific plasma membrane compositions resulting in differential distribution and mobility of CD20 and subsequently enhanced or decreased capture by anti-CD20 mAbs. Indeed, we identified low levels of sphingomyelin GM_1, a typical component of organized membrane domains, in complement-resistant P493.6 cells while GM_1 was highly present in the membrane of highly susceptible Ramos cells (**Supplementary Figure 10**). This suggests that Ramos cells have more organized microdomains with potentially pre-clustered CD20. Consequently, bivalent target engagement, IgG crosslinking and thereby the formation of suitable platforms for C1q capture may be facilitated. It should also be noted that GM_1 levels in all tested cell lines were higher than in human primary cells.

One can further speculate that antibody induced clustering is more efficient in promoting IgG-Fc arrangements for C1q binding than increasing the total number of bound IgG that is not in clusters. This would explain why multivalent C1q binding to cells opsonized with the type I mAbs OFA and RTX, whose binding can act as molecular seeds and induces clustering of CD20, could be detected (22, 25). In contrast, no strong interaction of C1q was seen on cells opsonized with OBI, which binds CD20 dimers in a terminal conformation that does not allow the concatenation of several CD20 dimers into larger clusters (25). Differences in membrane mobility and mAb mediated clustering could also explain why type I anti-CD20 mAbs generally induce CDC more efficiently than anti-EGFR mAbs. Whether bivalent or monovalent target engagement is preferable for C1q binding might thus very well depend on the lateral receptor mobility in the cell membrane that may or may not be influenced by binding of the mAb. Interestingly, it has been reported that $(Fab)_2$ fragments of type I anti-CD20 mAbs can activate complement in a C1q dependent manner (65). This suggests that other factors than IgG-Fc arrangement contribute to cell lysis by CDC for B cells, further strengthening the notion that complement activation is complex and conditions for optimal CDC activity may vary between target surface molecules.

DATA AVAILABILITY STATEMENT

The raw data supporting the conclusions of this article will be made available by the authors, without undue reservation.

ETHICS STATEMENTS

The studies involving human participants were reviewed and approved by Ethics Committee CAU Kiel Head: Christine Glinicke, Schwanenweg 20, D-24105 Kiel, Germany. Ethics Committee FAU Erlangen. Head: Kerstin Amann, Krankenhausstr. 12, D-91054 Erlangen, Germany. The patients/participants provided their written informed consent to participate in this study.

AUTHOR CONTRIBUTIONS

SB, AL, and FN designed experiments. SB, AL, AM, SK, and JL performed experiments. SB, AL, and SK analyzed data. MP provided essential reagents (CD20-specific mAbs, B cell lines, CLL samples). SB and AL wrote the manuscript. MP, FN, and JB revised the manuscripts. All authors critically reviewed the manuscript. All authors contributed to the article and approved the submitted version.

FUNDING

This work was supported by the Deutsche Forschungsgemeinschaft (DFG) project grants DFG-TRR130-P13 and D-A-CH NI 711/9-1 to FN. FN was further supported by NIADS grant U01 AI-148119-01. AL was supported by Emerging Talents Initiative of the Friedrich-Alexander-University Erlangen-Nürnberg. AM was supported by Elitenetzwerk Bayern.

ACKNOWLEDGMENTS

We thank Bo Stenerlöw (Uppsala University, Uppsala, Sweden) and Georg Bornkamm (Helmholtz Centre Munich, Munich, Germany) for cell lines and Heike Albert and Heike Danzer (Friedrich-Alexander-University of Erlangen-Nürnberg) for expert technical assistance.

SUPPLEMENTARY MATERIAL

The Supplementary Material for this article can be found online at: https://www.frontiersin.org/articles/10.3389/fimmu.2020.609941/full#supplementary-material

REFERENCES

1. Wang W, Erbe AK, Hank JA, Morris ZS, Sondel PM. NK Cell-Mediated Antibody-Dependent Cellular Cytotoxicity in Cancer Immunotherapy. *Front Immunol* (2015) 6:368. doi: 10.3389/fimmu.2015.00368
2. Weiskopf K, Weissman IL. Macrophages are critical effectors of antibody therapies for cancer. *MAbs* (2015) 7(2):303–10. doi: 10.1080/19420862.2015.1011450
3. Meyer S, Leusen JH, Boross P. Regulation of complement and modulation of its activity in monoclonal antibody therapy of cancer. *MAbs* (2014) 6 (5):1133–44. doi: 10.4161/mabs.29670
4. Idusogie EE, Presta LG, Gazzano-Santoro H, Totpal K, Wong PY, Ultsch M, et al. Mapping of the C1q binding site on rituxan, a chimeric antibody with a human IgG1 Fc. *J Immunol* (2000) 164(8):4178–84. doi: 10.4049/jimmunol.164.8.4178
5. Reis ES, Mastellos DC, Ricklin D, Mantovani A, Lambris JD. Complement in cancer: untangling an intricate relationship. *Nat Rev Immunol* (2018) 18(1):5–18. doi: 10.1038/nri.2017.97
6. Golay J, Zaffaroni L, Vaccari T, Lazzari M, Borleri GM, Bernasconi S, et al. Biologic response of B lymphoma cells to anti-CD20 monoclonal antibody rituximab in vitro: CD55 and CD59 regulate complement-mediated cell lysis. *Blood* (2000) 95(12):3900–8. doi: 10.1182/blood.V95.12.3900.012k14_3900_3908
7. Kennedy AD, Solga MD, Schuman TA, Chi AW, Lindorfer MA, Sutherland WM, et al. An anti-C3b(i) mAb enhances complement activation, C3b(i) deposition, and killing of CD20+ cells by rituximab. *Blood* (2003) 101 (3):1071–9. doi: 10.1182/blood-2002-03-0876
8. Zent CS, Secreto CR, LaPlant BR, Bone ND, Call TG, Shanafelt TD, et al. Direct and complement dependent cytotoxicity in CLL cells from patients with high-risk early-intermediate stage chronic lymphocytic leukemia (CLL) treated with alemtuzumab and rituximab. *Leuk Res* (2008) 32(12):1849–56. doi: 10.1016/j.leukres.2008.05.014
9. Beers SA, Cragg MS, Glennie MJ. Complement: help or hindrance? *Blood* (2009) 114(27):5567–8; author reply 5568. doi: 10.1182/blood-2009-10-249466
10. Beers SA, French RR, Chan HT, Lim SH, Jarrett TC, Vidal RM, et al. Antigenic modulation limits the efficacy of anti-CD20 antibodies: implications for antibody selection. *Blood* (2010) 115(25):5191–201. doi: 10.1182/blood-2010-01-263533
11. Beurskens FJ, Lindorfer MA, Farooqui M, Beum PV, Engelberts P, Mackus WJ, et al. Exhaustion of cytotoxic effector systems may limit monoclonal antibody-based immunotherapy in cancer patients. *J Immunol* (2012) 188 (7):3532–41. doi: 10.4049/jimmunol.1103693
12. Boross P, Jansen JH, de Haij S, Beurskens FJ, van der Poel CE, Bevaart L, et al. The in vivo mechanism of action of CD20 monoclonal antibodies depends on local tumor burden. *Haematologica* (2011) 96(12):1822–30. doi: 10.3324/haematol.2011.047159
13. Golay J, Cittera E, Di Gaetano N, Manganini M, Mosca M, Nebuloni M, et al. The role of complement in the therapeutic activity of rituximab in a murine B lymphoma model homing in lymph nodes. *Haematologica* (2006) 91(2):176–83.
14. Uchida J, Hamaguchi Y, Oliver JA, Ravetch JV, Poe JC, Haas KM, et al. The innate mononuclear phagocyte network depletes B lymphocytes through Fc receptor-dependent mechanisms during anti-CD20 antibody immunotherapy. *J Exp Med* (2004) 199(12):1659–69. doi: 10.1084/jem.20040119
15. Lee CH, Romain G, Yan W, Watanabe M, Charab W, Todorova B, et al. IgG Fc domains that bind C1q but not effector Fcgamma receptors delineate the importance of complement-mediated effector functions. *Nat Immunol* (2017) 18(8):889–98. doi: 10.1038/ni.3770
16. Fishelson Z, Donin N, Zell S, Schultz S, Kirschfink M. Obstacles to cancer immunotherapy: expression of membrane complement regulatory proteins (mCRPs) in tumors. *Mol Immunol* (2003) 40(2-4):109–23. doi: 10.1016/s0161-5890(03)00112-3
17. Wang Y, Yang YJ, Wang Z, Liao J, Liu M, Zhong XR, et al. CD55 and CD59 expression protects HER2-overexpressing breast cancer cells from trastuzumab-induced complement-dependent cytotoxicity. *Oncol Lett* (2017) 14(3):2961–9. doi: 10.3892/ol.2017.6555
18. Kennedy AD, Beum PV, Solga MD, DiLillo DJ, Lindorfer MA, Hess CE, et al. Rituximab infusion promotes rapid complement depletion and acute CD20 loss in chronic lymphocytic leukemia. *J Immunol* (2004) 172(5):3280–8. doi: 10.4049/jimmunol.172.5.3280
19. Diebolder CA, Beurskens FJ, de Jong RN, Koning RI, Strumane K, Lindorfer MA, et al. Complement is activated by IgG hexamers assembled at the cell surface. *Science* (2014) 343(6176):1260–3. doi: 10.1126/science.1248943
20. de Jong RN, Beurskens FJ, Verploegen S, Strumane K, van Kampen MD, Voorhorst M, et al. A Novel Platform for the Potentiation of Therapeutic Antibodies Based on Antigen-Dependent Formation of IgG Hexamers at the Cell Surface. *PloS Biol* (2016) 14(1):e1002344. doi: 10.1371/journal.pbio.1002344
21. Lindorfer MA, Cook EM, Tupitza JC, Zent CS, Burack R, de Jong RN, et al. Real-time analysis of the detailed sequence of cellular events in mAb-mediated complement-dependent cytotoxicity of B-cell lines and of chronic lymphocytic leukemia B-cells. *Mol Immunol* (2016) 70:13–23. doi: 10.1016/j.molimm.2015.12.007
22. Cragg MS, Morgan SM, Chan HT, Morgan BP, Filatov AV, Johnson PW, et al. Complement-mediated lysis by anti-CD20 mAb correlates with segregation into lipid rafts. *Blood* (2003) 101(3):1045–52. doi: 10.1182/blood-2002-06-1761
23. Herter S, Herting F, Mundigl O, Waldhauer I, Weinzierl T, Fauti T, et al. Preclinical activity of the type II CD20 antibody GA101 (obinutuzumab) compared with rituximab and ofatumumab in vitro and in xenograft models. *Mol Cancer Ther* (2013) 12(10):2031–42. doi: 10.1158/1535-7163.MCT-12-1182
24. Ugurlar D, Howes SC, de Kreuk BJ, Koning RI, de Jong RN, Beurskens FJ, et al. Structures of C1-IgG1 provide insights into how danger pattern recognition activates complement. *Science* (2018) 359(6377):794–7. doi: 10.1126/science.aao4988
25. Kumar A, Planchais C, Fronzes R, Mouquet H, Reyes N. Binding mechanisms of therapeutic antibodies to human CD20. *Science* (2020) 369(6505):793–9. doi: 10.1126/science.abb8008
26. Alduaij W, Ivanov A, Honeychurch J, Cheadle EJ, Potluri S, Lim SH, et al. Novel type II anti-CD20 monoclonal antibody (GA101) evokes homotypic adhesion and actin-dependent, lysosome-mediated cell death in B-cell malignancies. *Blood* (2011) 117(17):4519–29. doi: 10.1182/blood-2010-07-296913
27. Reddy V, Klein C, Isenberg DA, Glennie MJ, Cambridge G, Cragg MS, et al. Obinutuzumab induces superior B-cell cytotoxicity to rituximab in rheumatoid arthritis and systemic lupus erythematosus patient samples. *Rheumatol (Oxford)* (2017) 56(7):1227–37. doi: 10.1093/rheumatology/kex067
28. Vaughan AT, Chan CH, Klein C, Glennie MJ, Beers SA, Cragg MS. Activatory and inhibitory Fcgamma receptors augment rituximab-mediated internalization of CD20 independent of signaling via the cytoplasmic domain. *J Biol Chem* (2015) 290(9):5424–37. doi: 10.1074/jbc.M114.593806
29. Reddy V, Cambridge G, Isenberg DA, Glennie MJ, Cragg MS, Leandro M. Internalization of rituximab and the efficiency of B Cell depletion in rheumatoid arthritis and systemic lupus erythematosus. *Arthritis Rheumatol* (2015) 67(8):2046–55. doi: 10.1002/art.39167
30. Teeling JL, Mackus WJ, Wiegman LJ, van den Brakel JH, Beers SA, French RR, et al. The biological activity of human CD20 monoclonal antibodies is linked to unique epitopes on CD20. *J Immunol* (2006) 177(1):362–71. doi: 10.4049/jimmunol.177.1.362
31. Mossner E, Brunker P, Moser S, Puntener U, Schmidt C, Herter S, et al. Increasing the efficacy of CD20 antibody therapy through the engineering of a new type II anti-CD20 antibody with enhanced direct and immune effector cell-mediated B-cell cytotoxicity. *Blood* (2010) 115(22):4393–402. doi: 10.1182/blood-2009-06-225979
32. Meyer S, Evers M, Jansen JHM, Buijs J, Broek B, Reitsma SE, et al. New insights in Type I and II CD20 antibody mechanisms-of-action with a panel of novel CD20 antibodies. *Br J Haematol* (2018) 180(6):808–20. doi: 10.1111/bjh.15132
33. Niederfellner G, Lammens A, Mundigl O, Georges GJ, Schaefer W, Schwaiger M, et al. Epitope characterization and crystal structure of GA101 provide insights into the molecular basis for type I/II distinction of CD20 antibodies. *Blood* (2011) 118 (2):358–67. doi: 10.1182/blood-2010-09-305847
34. Teeling JL, French RR, Cragg MS, van den Brakel J, Pluyter M, Huang H, et al. Characterization of new human CD20 monoclonal antibodies with potent

cytolytic activity against non-Hodgkin lymphomas. *Blood* (2004) 104 (6):1793–800. doi: 10.1182/blood-2004-01-0039
35. Moore GL, Chen H, Karki S, Lazar GA. Engineered Fc variant antibodies with enhanced ability to recruit complement and mediate effector functions. *MAbs* (2010) 2(2):181–9. doi: 10.4161/mabs.2.2.11158
36. Strasser J, de Jong RN, Beurskens FJ, Wang G, Heck AJR, Schuurman J, et al. Unraveling the Macromolecular Pathways of IgG Oligomerization and Complement Activation on Antigenic Surfaces. *Nano Lett* (2019) 19 (7):4787–96. doi: 10.1021/acs.nanolett.9b02220
37. Wang B, Yang C, Jin X, Du Q, Wu H, Dall'Acqua W, et al. Regulation of antibody-mediated complement-dependent cytotoxicity by modulating the intrinsic affinity and binding valency of IgG for target antigen. *MAbs* (2020) 12(1):1690959. doi: 10.1080/19420862.2019.1690959
38. Pawluczkowycz AW, Beurskens FJ, Beum PV, Lindorfer MA, van de Winkel JG, Parren PW, et al. Binding of submaximal C1q promotes complement-dependent cytotoxicity (CDC) of B cells opsonized with anti-CD20 mAbs ofatumumab (OFA) or rituximab (RTX): considerably higher levels of CDC are induced by OFA than by RTX. *J Immunol* (2009) 183(1):749–58. doi: 10.4049/jimmunol.0900632
39. Hughesjones NC, Gardner B. Reaction between the Isolation Globular Subunits of the Complement Component Clq and Igg-Complexes. *Mol Immunol* (1979) 16(9):697–701. doi: 10.1016/0161-5890(79)90010-5
40. Hughes-Jones NC, Gardner B. The reaction between the complement subcomponent C1q, IgG complexes and polyionic molecules. *Immunology* (1978) 34(3):459–63.
41. Bondza S, Ten Broeke T, Nestor M, Leusen JHW, Buijs J. Bivalent binding on cells varies between anti-CD20 antibodies and is dose-dependent. *MAbs* (2020) 12(1):1792673. doi: 10.1080/19420862.2020.1792673
42. Bondza S, Foy E, Brooks J, Andersson K, Robinson J, Richalet P, et al. Real-time Characterization of Antibody Binding to Receptors on Living Immune Cells. *Front Immunol* (2017) 8:455. doi: 10.3389/fimmu.2017.00455
43. Li Y, Huang K, Liu L, Qu Y, Huang Y, Wu Y, et al. Effects of complement and serum IgG on rituximab-dependent natural killer cell-mediated cytotoxicity against Raji cells. *Oncol Lett* (2019) 17(1):339–47. doi: 10.3892/ol.2018.9630
44. Barth MJ, Hernandez-Ilizaliturri FJ, Mavis C, Tsai PC, Gibbs JF, Deeb G, et al. Ofatumumab demonstrates activity against rituximab-sensitive and -resistant cell lines, lymphoma xenografts and primary tumour cells from patients with B-cell lymphoma. *Br J Haematol* (2012) 156(4):490–8. doi: 10.1111/j.1365-2141.2011.08966.x
45. Takei K, Yamazaki T, Sawada U, Ishizuka H, Aizawa S. Analysis of changes in CD20, CD55, and CD59 expression on established rituximab-resistant B-lymphoma cell lines. *Leuk Res* (2006) 30(5):625–31. doi: 10.1016/j.leukres.2005.09.008
46. Voso MT, Pantel G, Rutella S, Weis M, D'Alo F, Urbano R, et al. Rituximab reduces the number of peripheral blood B-cells in vitro mainly by effector cell-mediated mechanisms. *Haematologica* (2002) 87(9):918–25.
47. Klein E, Klein G, Nadkarni JS, Nadkarni JJ, Wigzell H, Clifford P. Surface IgM-kappa specificity on a Burkitt lymphoma cell in vivo and in derived culture lines. *Cancer Res* (1968) 28(7):1300–10.
48. Klein G, Giovanella B, Westman A, Stehlin JS, Mumford D. An EBV-genome-negative cell line established from an American Burkitt lymphoma; receptor characteristics. EBV infectibility and permanent conversion into EBV-positive sublines by in vitro infection. *Intervirology* (1975) 5(6):319–34. doi: 10.1159/000149930
49. Pajic A, Spitkovsky D, Christoph B, Kempkes B, Schuhmacher M, Staege MS, et al. Cell cycle activation by c-myc in a burkitt lymphoma model cell line. *Int J Cancer* (2000) 87(6):787–93. doi: 10.1002/1097-0215(20000915)87:6<787::aid-ijc4>3.0.co;2-6
50. Nicholson-Weller A, Wang CE. Structure and function of decay accelerating factor CD55. *J Lab Clin Med* (1994) 123(4):485–91.
51. Meri S, Morgan BP, Wing M, Jones J, Davies A, Podack E, et al. Human protectin (CD59), an 18-20-kD homologous complement restriction factor, does not restrict perforin-mediated lysis. *J Exp Med* (1990) 172(1):367–70. doi: 10.1084/jem.172.1.367
52. Okroj M, Eriksson I, Osterborg A, Blom AM. Killing of CLL and NHL cells by rituximab and ofatumumab under limited availability of complement. *Med Oncol* (2013) 30(4):759. doi: 10.1007/s12032-013-0759-5
53. Almasri NM, Duque RE, Iturraspe J, Everett E, Braylan RC. Reduced expression of CD20 antigen as a characteristic marker for chronic lymphocytic leukemia. *Am J Hematol* (1992) 40(4):259–63. doi: 10.1002/ajh.2830400404
54. Marti GE, Faguet G, Bertin P, Agee J, Washington G, Ruiz S, et al. CD20 and CD5 expression in B-chronic lymphocytic leukemia. *Ann N Y Acad Sci* (1992) 651:480–3. doi: 10.1111/j.1749-6632.1992.tb24651.x
55. Ginaldi L, De Martinis M, Matutes E, Farahat N, Morilla R, Catovsky D. Levels of expression of CD19 and CD20 in chronic B cell leukaemias. *J Clin Pathol* (1998) 51(5):364–9. doi: 10.1136/jcp.51.5.364
56. Golay J, Lazzari M, Facchinetti V, Bernasconi S, Borleri G, Barbui T, et al. CD20 levels determine the in vitro susceptibility to rituximab and complement of B-cell chronic lymphocytic leukemia: further regulation by CD55 and CD59. *Blood* (2001) 98(12):3383–9. doi: 10.1182/blood.v98.12.3383
57. Jones JD, Hamilton BJ, Rigby WF. Rituximab mediates loss of CD19 on B cells in the absence of cell death. *Arthritis Rheumatol* (2012) 64(10):3111–8. doi: 10.1002/art.34560
58. Kamburova EG, Koenen HJ, Joosten I, Hilbrands LB. CD19 is a useful B cell marker after treatment with rituximab: comment on the article by Jones et al. *Arthritis Rheumatol* (2013) 65(4):1130–1. doi: 10.1002/art.37871
59. Taylor RPA, Lindorfer MA. How Do mAbs Make Use of Complement to Kill Cancer Cells? The Role of Ca2+. *Antibodies* (2020) 9(3):45. doi: 10.3390/antib9030045
60. Weng WK, Levy R. Expression of complement inhibitors CD46, CD55, and CD59 on tumor cells does not predict clinical outcome after rituximab treatment in follicular non-Hodgkin lymphoma. *Blood* (2001) 98(5):1352–7. doi: 10.1182/blood.v98.5.1352
61. Ziller F, Macor P, Bulla R, Sblattero D, Marzari R, Tedesco F. Controlling complement resistance in cancer by using human monoclonal antibodies that neutralize complement-regulatory proteins CD55 and CD59. *Eur J Immunol* (2005) 35(7):2175–83. doi: 10.1002/eji.200425920
62. Macor P, Tripodo C, Zorzet S, Piovan E, Bossi F, Marzari R, et al. In vivo targeting of human neutralizing antibodies against CD55 and CD59 to lymphoma cells increases the antitumor activity of rituximab. *Cancer Res* (2007) 67(21):10556–63. doi: 10.1158/0008-5472.CAN-07-1811
63. Manches O, Lui G, Chaperot L, Gressin R, Molens JP, Jacob MC, et al. In vitro mechanisms of action of rituximab on primary non-Hodgkin lymphomas. *Blood* (2003) 101(3):949–54. doi: 10.1182/blood-2002-02-0469
64. Rouge L, Chiang N, Steffek M, Kugel C, Croll TI, Tam C, et al. Structure of CD20 in complex with the therapeutic monoclonal antibody rituximab. *Science* (2020) 367(6483):1224–30. doi: 10.1126/science.aaz9356
65. Engelberts PJ, Voorhorst M, Schuurman J, van Meerten T, Bakker JM, Vink T, et al. Type I CD20 Antibodies Recruit the B Cell Receptor for Complement-Dependent Lysis of Malignant B Cells. *J Immunol* (2016) 197(12):4829–37. doi: 10.4049/jimmunol.1600811

Conflict of Interest: SB is an employee and JB is an employee and shareholder of Ridgeview Instruments AB.

The remaining authors declare that the research was conducted in the absence of any commercial or financial relationships that could be construed as a potential conflict of interest.

frontiers in Immunology

CASE REPORT
published: 15 January 2021
doi: 10.3389/fimmu.2020.612706

Case Report: Variable Pharmacokinetic Profile of Eculizumab in an aHUS Patient

Romy N. Bouwmeester[1], Mendy Ter Avest[2], Kioa L. Wijnsma[1], Caroline Duineveld[3], Rob ter Heine[2], Elena B. Volokhina[1], Lambertus P. W. J. Van Den Heuvel[1], Jack F. M. Wetzels[3] and Nicole C. A. J. van de Kar[1]*

[1] Department of Pediatric Nephrology, Radboud Institute for Molecular Life Sciences, Amalia Children's Hospital, Radboud University Medical Center, Nijmegen, Netherlands, [2] Department of Pharmacy, Radboud University Medical Center, Nijmegen, Netherlands, [3] Department of Nephrology, Radboud Institute for Molecular Life Sciences, Radboud University Medical Center, Nijmegen, Netherlands

Background: With the introduction of eculizumab, a C5-inhibitor, morbidity and mortality improved significantly for patients with atypical hemolytic uremic syndrome (aHUS). In view of the high costs, actual needs of the drug, and increasing evidence in literature, aHUS patients can be treated according to a restrictive eculizumab regimen. We retrospectively analyzed the pharmacokinetic and dynamic parameters of eculizumab in one patient in time, emphasizing various factors which could be taken into account during tapering of treatment.

Case Presentation: A nowadays 18-year-old male with a severe, frequently relapsing form of atypical HUS due to a hybrid CFH/CFHR1 gene in combination with the homozygous factor H haplotype, required chronic plasma therapy (PT), including periods with plasma infusion, from the age of onset at 5 months until initiation of eculizumab at the age of 11 years. A mild but stable chronic kidney disease (CKD) and 9 years of disease remission enabled prolongation of eculizumab interval. At the age of 15 years, a sudden yet multifactorial progression of chronic kidney disease (CKD) was observed, without any signs of disease recurrence. However, an acquired glomerulocystic disease, a reduced left kidney function, and abnormal abdominal venous system of unknown etiology were found. In addition, after an aHUS relapse, an unexpected increase in intra-patient variability of eculizumab concentrations was seen. Retrospective pharmacokinetic analysis revealed a change in eculizumab clearance, associated with a simultaneous increase in proteinuria.

Conclusion: High intra-patient variability of eculizumab pharmacokinetics were observed over time, emphasizing the necessity for adequate and continuous therapeutic drug monitoring in aHUS patients. Eculizumab serum trough levels together with complement activation markers (CH50) should be frequently assessed, especially during tapering of drug therapy and/or changing clinical conditions in the patient. In addition, an increase in proteinuria could result in urinary eculizumab loss, indicating that urinary monitoring of eculizumab may be important in aHUS patients with an unexplained decline in serum concentrations.

Keywords: atypical hemolytic uremic syndrome, aHUS, eculizumab, therapeutic drug monitoring, pharmacokinetic, proteinuria

OPEN ACCESS

Edited by:
Mihály Józsi,
Eötvös Loránd University, Hungary

Reviewed by:
Michael Kirschfink,
Heidelberg University, Germany
Kevin James Marchbank,
Newcastle University, United Kingdom

****Correspondence:***
Romy N. Bouwmeester
Romy.Bouwmeester@radboudumc.nl

Specialty section:
This article was submitted to Molecular Innate Immunity, a section of the journal Frontiers in Immunology

Received: *30 September 2020*
Accepted: *01 December 2020*
Published: *15 January 2021*

Citation:
Bouwmeester RN, Ter Avest M, Wijnsma KL, Duineveld C, ter Heine R, Volokhina EB, Van Den Heuvel LPWJ, Wetzels JFM and van de Kar NCAJ (2021) Case Report: Variable Pharmacokinetic Profile of Eculizumab in an aHUS Patient. Front. Immunol. 11:612706. doi: 10.3389/fimmu.2020.612706

INTRODUCTION

The introduction of the complement therapeutic eculizumab led to a new era for patients with atypical hemolytic uremic syndrome (aHUS). aHUS is a rare and severe form of thrombotic microangiopathy (TMA) characterized by thrombocytopenia, microangiopathic hemolytic anemia (MAHA) and acute kidney failure (1). Dysregulation and overactivation of the alternative pathway (AP) of the complement system causes (glomerular) endothelial cell injury, ultimately leading to TMA (2). Currently, genetic mutations in complement factor and regulatory proteins are found in 50%–60% of patients with aHUS (3). The most frequent genetic alterations observed in aHUS are complement factor H (CFH) defects, including heterozygous mutations, or autoantibodies, all associated with a high risk of relapse and worse disease outcome (4–6). In 3%–5% of all aHUS cases, a genetic rearrangement between CFH and CFH related proteins (CFHR1-5) is found (7, 8). These CFH/CFHR hybrid proteins are associated with a structurally decreased complement regulatory function on the endothelial surface and a frequently relapsing form of aHUS (9, 10).

Before the implementation of complement therapeutics, plasma therapy (PT) was the only available treatment for patients with aHUS (11). In 2011, this changed dramatically with the introduction of eculizumab, the first monoclonal antibody targeting complement factor C5. By binding to C5, eculizumab prevents the splicing of C5 into C5a and C5b, and ultimately blocks the formation of the terminal membrane attack complex C5b-C9. With the introduction of eculizumab, morbidity and mortality improved significantly (12). The drug label advises a maintenance dose of 1200 mg biweekly in adult patients and pediatric patients with a body weight ≥40 kg. Treatment with eculizumab is very expensive, and dosing regimen as well as duration of treatment are topics of international debate. Moreover, multiple studies showed that it is safe and (cost-)efficient to taper and/or withdraw eculizumab therapy (6, 13, 14). During the maintenance phase, treatment with eculizumab at a reduced dose (through prolongation of the dose interval) while maintaining adequate complement blockade is now a common regimen in the Netherlands (6). Such personalized therapy is possible if therapeutic drug monitoring (TDM) is controlled by measuring eculizumab through levels and/or measuring of complement hemolytic activity (CH50) (15, 16). In aHUS, serum eculizumab concentrations of 50–100 μg/ml are recommended by the drug label for complete complement blockade (defined by CH50 <10%) (16, 17). Although various studies describe the utility of eculizumab TDM, adequate implementation in clinical care remains challenging. We retrospectively analyzed the pharmacokinetic and dynamic parameters of eculizumab in one patient during 4 years of eculizumab treatment, emphasizing various factors which could be taken into account during tapering of treatment.

CASE PRESENTATION

Here we report a nowadays 18-year-old male with a severe, frequently relapsing form of aHUS. At the age of 5 months, our patient presented with TMA and nephrotic range proteinuria (**Figure 1**). Genomic analysis using MLPA (multiplex ligation-dependent probe amplification) identified a heterozygous deletion of CFH Exon 23, CFHR3 and CFHR1 Exon 1-5, indicating a genomic rearrangement resulting in a CFH/CFHR1 hybrid gene (NC_000001.10: g.(196715130_196716240)_(196799813_196800926)del); LRG_47:p.(Ser119Leu) and LRG_47:p.(Val1197Ala)). In addition, the at-risk CFH-H3 haplotype was found in homozygosity (18). Mutations in complement factor I and B (CFI, CFB), C3, membrane cofactor protein (MCP/CD46), thrombomodulin (THBD), and diacylglycerol kinase epsilon (DGKe) were excluded. Patient was negative for autoantibodies against CFH (detection performed using an in-house enzyme-linked immunosorbent assay (ELISA) (19).

Paternal family history was positive for aHUS. Our patient's father is carrier of the same CFH/CFHR1 hybrid gene, however remained unaffected until present-day. Unfortunately, genetic analysis of the grandparents could not be performed, especially since two grandnieces of our patient developed aHUS over time: one fatal case more than 3 decades ago (age 32 years, no genetic analysis available) and one case, who presented with aHUS at the age of 47 years. Over time, she developed end stage kidney disease (ESKD) and recently presented with a first relapse after 14 years of disease remission. Genetic analysis confirmed a CFH/CFHR1 hybrid gene, identical to our patient's and his father's. The CFH-H3 risk haplotype was only found in heterozygous condition.

During follow-up of our patient, an unexpected yet unexplained chronic occlusion of the inferior vena cava (below renal veins) with substantial collateral formation was found. Furthermore, at the age of 15, imaging and biopsy revealed the remarkable presence of multiple, small medullary cysts, predominantly in the left kidney. Function of the left kidney was severely reduced (18%–28%) compared to the right kidney. Whole-exome sequencing (WES- kidney package, including cystic kidney diseases) did not provide any aberrations, and the etiology of the acquired glomerulocystic disease remained unknown. Only a few aHUS cases with an acquired cystic kidney disease (ACKD) of unknown (exact) pathogenesis have been described previously (20, 21).

Before the introduction of eculizumab, our patient required chronic PT. In his first four years, we attempted to withdraw PT on various occasions, yet this led to disease recurrence after (mostly infectious) triggering events. From the age of four until eleven years, disease remission was maintained with PT which, over the years, included plasma infusion (15–20 ml/kg) once weekly and plasma exchange (PE) once every 8th week. At the age of eleven years, eculizumab was initiated and PT was stopped. After two years of additional remission, the eculizumab dosing interval was extended from 2 to 4 weeks. To monitor therapy next to TMA parameters, eculizumab concentrations and complement activity were regularly analyzed. Eculizumab detection was performed using an in-house ELISA assay. Complement activity was accessed by determining the activity of classical complement route (CH50) using an ELISA method adapted from Roos et al. (22). Both methods have been described previously (15). During this 4 weekly dosing interval, eculizumab concentrations were adequate (70–84 μg/ml) and complement

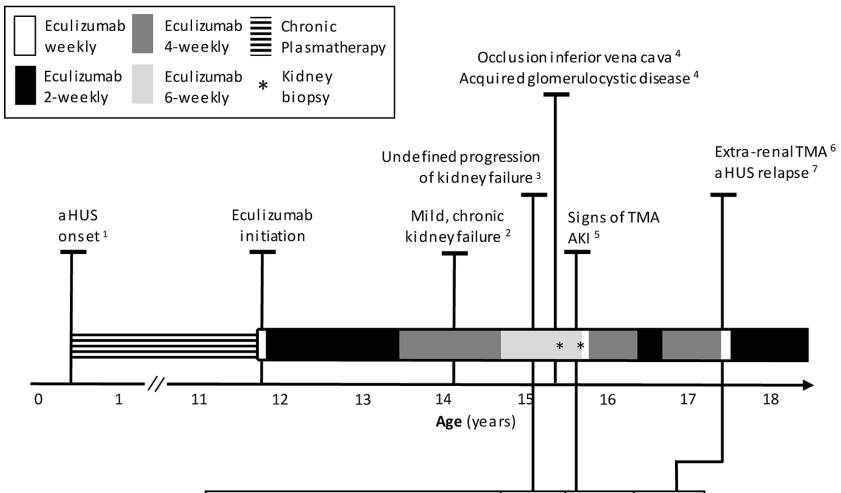

Thrombocytes	(150-400 10^09/l)	182	136	116
Hemoglobin	(8.4-10.8 mmol/l)	7.0	6.3	5.4
LDH	(<250 U/l)	273	346	332
Haptoglobin	(0.30-1.60 g/l)	0.86	0.52	0.26 [8]
Schistocytes	(absent, -)	-	-	-
eGFR	(>90 ml/min/1.73m^2)	43	18	14
UPCR	(<0.10 g/10mmol)	0.80	5.28	4.50
Eculizumab	(50-100 µg/ml)	<8	<8	171
CH50	(<10%)	94%	-	<10%
C3	(700-1500 mg/l)	927	1077	972
C3d	(<8.3 mg/l)	7.7	12.0	13.2
sC5b-9	(<0.50 CAU/ml)	0.37	0.50	-

FIGURE 1 | Timeline of treatment of aHUS in this patient, starting with the onset of disease at the age of 5 months until 18 years. Normal values of laboratory parameters indicated between parentheses. [1] After onset: chronic PT, including periods with plasma infusion. Every attempt to withdrawal in his first 4 years initiated a relapse. Number of relapses during PT period, n=7, [2] eGFR 65-70 ml/min/1.73m^2, UPCR 0.18–0.53 g/10 mmol, [3] No thrombocytopenia, no signs of hemolysis; kidney biopsy right kidney: chronic TMA, no signs of interstitial nephritis or acute TMA,25% IFTA but diffuse small cysts eci, [4] Date of onset unknown, [5] AKI defined by a sudden increase in proteinuria and serum creatinine; kidney biopsy; similar to previous biopsy, [6] A traumatically obtained, extremely painful, and non-healing ulceration was considered as a (trigger of) an extra-renal manifestation of TMA, [7] aHUS relapse defined by AKI, thrombocytopenia and signs of hemolysis. [8] Haptoglobin decreased from 1.89 to 0,26 g/L. aHUS, atypical Hemolytic Uremic Syndrome; AKI, Acute Kidney Injury; eGFR, estimated Glomerular Filtration Rate (Schwartz formula); IFTA interstitial fibrosis and tubular atrophy; PT, Plasmatherapy; TMA, Thrombotic Microangiopathy; UPCR, Urine Protein-to-Creatinine Ratio.

activity remained suppressed (CH50 <10%) (**Table 1**). Despite a mild, chronic kidney failure (eGFR 65–70 ml/min/1.73m^2, urine protein-to-creatinine ratio (UPCR) 0.18–0.53 g/10mmol), overall clinical situation remained stable (**Figure 1**). In addition, antihypertensive medications effectively regulated blood pressure.

Undefined Progression of Kidney Failure

After three years of eculizumab therapy, the dosing interval was further extended to every 6 weeks. As before, the patient was carefully monitored and instructed when to seek medical attention. Eculizumab serum trough levels decreased to subtherapeutic and undetectable concentrations (<8–10 µg/ml). An unblocked terminal complement system (CH50 94%–149%) was now observed and accepted due to a very stable clinical situation and taken into account that the patient was stable for years with only once weekly plasma-infusion (which suggested that full complement blockade over the entire treatment interval might not be necessary). After six months, an unexplained decrease in kidney function was observed (eGFR 43 ml/min/1.73m^2), with a mild increase in proteinuria (UPCR 0.80 g/10 mmol) (**Figure 2**). Hemoglobin-, thrombocytes, and haptoglobin levels were not decreased, LDH not elevated and schistocytes absent (**Figure 1**). In addition, blood pressure was normal (118/68 mmHg). Therefore, evident signs indicating aHUS disease recurrence were absent. Complement analysis showed no signs of (over)activation (C3 927 m g/L (normal range 700–1500), C3d 7.7 mg/L (<8.3), and sC5b-9 (0.37 CAU/ml (<0.50)). C3 levels were determined using ELISA, turbidometry (Cobas 8000 platform, F. Hoffman-La Roche Ltd, Basel, Switzerland) and C3d, sC5b-9, and C3bBbP levels by ELISA, as described before (23–25). While awaiting kidney biopsy in his best functioning right kidney, with the differential diagnosis of acute TMA or tubulointerstitial nephritis (TIN), an

TABLE 1 | Factors of potential influence to eculizumab clearance.

Age years normal value	Eculizumab serum 50–100 μg/ml	Eculizumab-C5 complex	C5 42–93 μg/ml	sC5b-9 <0.5 CAU/ml	Albumin serum 35-55 g/L	Total IgG serum 7.0–16.0 g/L	Urinary PCR <0.10 g/10 mmol
			2-weekly interval				
			Mild, chronic kidney failure				
12.4	598	199	38	0.37	34	8.67	0.27
12.7	558	234	87	0.55	34	9.52	0.28
			4-weekly interval				
			Mild, chronic kidney failure				
13.10	70	–	84	0.35	36	10.72	0.54
14.5	84	188	93	0.25	39	8.51	0.79
			4-weekly interval				
			Signs of TMA, AKI				
16.1	13	109	127	0.39	32	6.71	2.49
16.3	12	85	110	0.30	32	5.42	1.59
			2-weekly interval				
16.5	127	196	109	0.63	31	5.09	2.63
16.6	167	229	103	0.39	34	4.90	3.43
			4-weekly interval				
16.10	19	107	103	0.30	33	6.32	1.77
17.1	12	82	106	0.38	32	6.05	2.01

Relevant factors of potential influence to eculizumab clearance, i.e. eculizumab-C5, C5, sC5b-9, serum albumin levels, total serum IgG, and urinary protein to creatinine ratio measured in the different interval treatments of eculizumab. Target therapeutic ranges for eculizumab and normal reference ranges for C5, sC5b-9, albumin, total IgG, and urine protein-to-creatinine ratio (UPCR) are given.

extra dose of 1200 mg eculizumab was administered and temporary corticosteroid treatment initiated. The biopsy of the right kidney revealed only chronic TMA, without active (glomerular) thrombosis or tubule-interstitial infiltrate, but with the presence of interstitial fibrosis and tubular atrophy (25%) as well as the diffuse presence of small cysts eci. Eculizumab was continued on a 6-weekly interval. Despite a temporary improvement in kidney function (eGFR 61 ml/min/1.73m^2), an ongoing trend in CKD deterioration was observed (**Figure 2A**). Since pre-and post-renal explanatory causes could be excluded, it was suspected that the, possibly progressive, acquired glomerulocystic disease and reduced left kidney function contributed in some extent.

Signs of TMA During Incomplete Complement Blockade

Six months later, at the age of 15 years, a sudden increase in proteinuria (UPCR 5.28 g/10mmol) and decrease in kidney function (eGFR 18 ml/min/1.73m^2) were observed without a triggering event (**Figure 2**). Lactate dehydrogenase (LDH) was slightly elevated and thrombocytes and hemoglobin levels mildly decreased, whereas haptoglobin was normal and schistocytes were absent (**Figure 1**). In addition to these minimal signs of hematological TMA and decrease in eGFR, our patient noticed a facial edema and urticaria-like skin lesions, unrelated to eculizumab infusions, yet similar to dermatological features observed during an aHUS relapse twelve years prior. In suspicion of extra-renal TMA, skin biopsy was performed. However, only a superficial perivascular dermatitis was found, without any signs of microvascular changes. A kidney biopsy in the right kidney showed no other features than chronic TMA, similar to the previous biopsy. Complement analysis revealed signs of activation at the level of C3 (C3 1077 mg/L (700-1500), C3d 12.0 mg/L (<8.3), C3bBbP 16.8 CAU/ml (<12.0), however sC5b-9 levels were not elevated (0.50 CAU/ml). Blood pressure was elevated (129-144/78-87 mmHg), yet our patient had a variable compliance to antihypertensive medication and dietary restrictions. Since TMA could not be completely excluded, two doses of 1200 mg eculizumab were given on a weekly interval. Based on previous experience, 1200 mg of eculizumab administrations were continued on a 4-weekly interval while therapeutic eculizumab concentrations were expected. Although hematological values improved rapidly, kidney function and proteinuria only partly recovered and the gradual progression of CKD continued (**Figure 2**). Unexpectedly, low eculizumab concentrations (<8–21 μg/ml) and incomplete complement blockade (CH50 52%–122%) were observed during this 4-weekly interval period. Various factors were assessed to determine the cause of this intra-patient variability in eculizumab concentrations. Neutralizing human anti-human antibodies against eculizumab (in-house ELISA, unpublished) were not present and body weight was stable (67–70kg) during this period. C5 levels and eculizumab-C5 complexes were measured using ELISA, as described before (26, 27). Complement analysis revealed a persistent but mild elevation of C5 levels since this period, however this did not lead to an increase in eculizumab-C5 complexes (**Table 1**). In addition, sC5b-9 levels were not elevated (**Table 1**). Thorough retrospective evaluation revealed a (severe) progression in proteinuria simultaneous with the unexpectedly low eculizumab concentrations. Hence, increased urinary clearance of eculizumab was suspected. Since urine was not available for further analysis and eculizumab concentrations in our patient were only measured in plasma, we looked into the relation between eculizumab plasma concentrations and the UPCR. Empirical Bayes estimates for plasma pharmacokinetics were obtained by means of non-linear

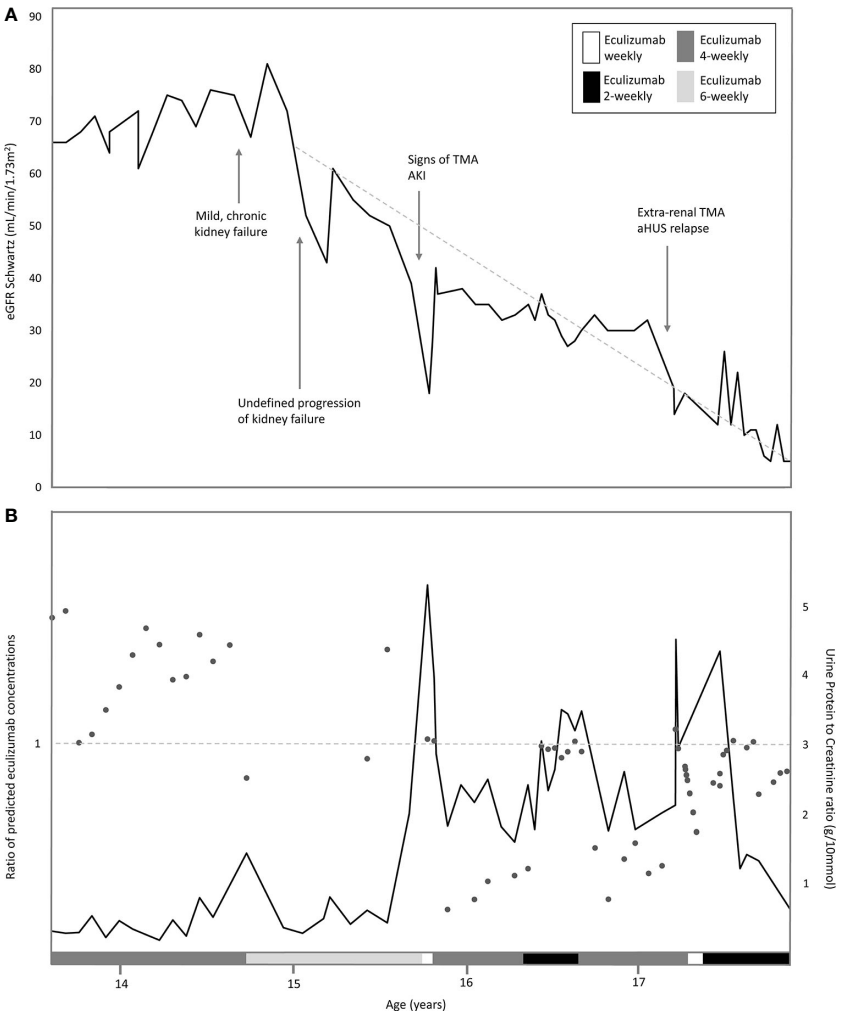

FIGURE 2 | Overview of eGFR, proteinuria and ratio of predicted eculizumab concentrations related to the eculizumab treatment in time. **(A)** Estimated eGFR (Schwartz formula) indicated with dark grey line, and the various interval treatment periods of eculizumab, indicated by the legends: white bar: eculizumab 1200 mg weekly middle grey colored bar: four-weekly 1200 mg eculizumab; light-grey colored bar 6-weekly 1200 mg eculizumab; dark grey colored bar: two-weekly 1200 mg eculizumab. Dotted line indicates the annual eGFR decline of 22.9 ml/min/1.73m^2 (baseline eGFR 68 ml/min/1.73m^2). **(B)** Urine Protein-to-Creatine ratio (g/10 mmol) in time indicated with dark grey line. Ratios of predicted eculizumab concentrations of our patient and a standardized patient of same weight indicated with dots. Ratio =1 (horizontal dotted line), normal clearance; Ratio >1, decreased clearance in our patient (eculizumab concentrations higher than expected); Ratio <1; increased clearance in our patient (eculizumab concentrations lower than expected.

mixed effects modeling. In short, the disposition of eculizumab was described with an one-compartment model with parallel first-order and Michaelis Menten elimination. The model was based on a wide range of ages and body weights. To account for differences in pharmacokinetics between children and adults, pharmacokinetics were allometrically scaled to total body weight. Using the established model, we predicted eculizumab concentrations for our patient as well as mean population concentrations for an individual with the same weight and calculated the ratio between these concentrations. A ratio >1 implies decreased clearance of eculizumab in our patient (eculizumab concentrations are higher than expected) and a ratio <1 implies increased clearance in our patient (eculizumab concentrations are lower than expected). **Figure 2B** shows that when the UPCR increases, the ratio of predicted eculizumab concentrations is lower than 1, implying faster clearance of eculizumab, probably due to urinary eculizumab loss. In addition, concurrent with the increase in UPCR, serum IgG levels decreased (**Table 1**).

Subsequently, in attempt to rescue kidney function and rule out any level of low-grade disease activity, eculizumab interval was intensified to biweekly for four months. With this schedule, adequate CH50 (<10%) and eculizumab concentrations (>100 μg/ml) were measured. However, no improvement in kidney function was observed, and administrations were continued on a 4-weekly interval (**Figure 2A**).

Extra-Renal TMA and Clinical aHUS Relapse

Seven months later, our patient presented with a traumatic and extremely painful ulceration. Although a skin biopsy was inconclusive for the presence of TMA, this ulcerative lesion was considered an extra-renal manifestation of TMA, especially taking into account the subsequent development of hematological signs of TMA several weeks later (**Figure 1**). In addition, kidney function and proteinuria severely worsened (eGFR 14 ml/min/1.73m^2, UCPR 4.50 g/10mmol), and hemodialysis was started for acute on chronic kidney injury (**Figure 2**). Eventually, TMA parameters improved after switching to a biweekly eculizumab interval (eculizumab concentrations >100 µg/ml, CH50 <10%). However, further deterioration of kidney function could not be haltered and continuation of hemodialysis was required. After bilateral nephrectomy to minimize the risk for aHUS recurrence after transplantation in this complex case with unexplained, acquired, bilateral ACKD, our patient successfully received a kidney transplant from a living- related donor while on eculizumab, biweekly 1200 mg.

DISCUSSION

There is variation in eculizumab pharmacokinetics between individuals. Therefore, optimal, individualized therapy requires therapeutic drug monitoring and measurement of eculizumab serum levels or complement inhibition (CH50). Our case clearly demonstrates that eculizumab pharmacokinetics can vary within a patient. Initially, a 4-weekly dosing schedule resulted in complement blockade and therapeutic drug levels. However, during follow-up in a period characterized by decreasing eGFR and increasing proteinuria, a similar dosing regimen proved insufficient. To determine the cause of this intra-patient variability, all factors that could increase eculizumab clearance were evaluated.

First, neutralizing human anti-human antibodies against eculizumab or a substantial change in body weight have been previously determined to potentially influence eculizumab pharmacokinetics, but could be excluded in our patient (16). Secondly, in aHUS patients, eculizumab concentrations can be decreased by the level of C5 in serum, for example during infectious events. Normally, free eculizumab can be recycled through the neonatal Fc receptor (FcRn). One eculizumab molecule can bind up to two C5 molecules. This eculizumab-C5 complex prevents eculizumab from being recycled. Hence, elevated levels of C5 and, consequently, of eculizumab-C5 complexes can increase the apparent clearance of eculizumab by decreasing eculizumab concentrations due to reduced recycling (16). In addition to C5, eculizumab can bind sC5b-9, albeit with lower affinity. Increased levels of sC5b-9 have been shown to influence eculizumab pharmacokinetics, potentially causing lower eculizumab concentrations in serum (28). Despite a mild but persistent elevation of C5 levels after the first aHUS relapse since the initiation of eculizumab, eculizumab-C5 complexes nor sC5b-9 levels were increased during the decrease in eculizumab through levels of our patient.

In our patient, increased eculizumab clearance could be confirmed by retrospective, non-linear mixed effects modeling of eculizumab concentrations. Since other factors causing increased clearance could be excluded, the remaining explanation could be the simultaneous progression in proteinuria. UPCR reflects urinary leakage of both intermediate molecular weight (MW) proteins (e.g. albumin) and high MW proteins (e.g. immunoglobulins (IgG)) (29). Eculizumab, an IgG, is usually not excreted *via* the kidneys due to its large size. However, previous studies have confirmed the loss of functionally active IgG, including eculizumab, in urine of patients with substantial proteinuria (30, 31). In our patient, in parallel to the increase in UPCR and drug clearance, total serum IgG levels remarkably declined below the lower limit of normal. Unfortunately, urinary samples were not available to confirm the correlation between IgG (including eculizumab) leakage and our patient's clearance.

In time, this aHUS patient developed end-stage kidney disease (ESKD) after 17-years of follow-up. One could argue that ESKD could have been delayed if the patient was treated with a biweekly eculizumab interval without therapy adjustment. However, progression of CKD started at the age of 15 years (annual eGFR decline 22.9 ml/min/1.73m^2), directly following growth-spurt, but without any other triggering event (including an aHUS relapse). It is suspected that especially in puberty, often associated with increased deterioration of CKD, a variable compliance to medication and dietary restrictions were also not favorable to the clinical course of our patient (32). Furthermore, various other factors contributed to both the pre-existence and progression of CKD in our complex patient, including chronic (endothelium) damage due to multiple aHUS relapses during infancy and PT for over a decade, the unexplained acquired glomerulocystic disease, abnormal abdominal venous system, and reduced left kidney function.

In conclusion, we retrospectively observed a high intra-patient variability of eculizumab serum concentrations over time, probably due to an increase in urinary drug loss by proteinuria. Consequently, former eculizumab trough levels are no assurance for future pharmacokinetics or therapy effectiveness. Eculizumab serum trough levels together with complement activation (CH50) should be frequently assessed, especially in patients with elongated treatment intervals as various clinical conditions can change the eculizumab availability and, consequently, the level of complement blockade. Future studies should provide information regarding the role of proteinuria in eculizumab pharmacokinetics and urinary eculizumab monitoring in aHUS patients.

PATIENT PERSPECTIVE

During the whole process, the patient and his parents were informed about treatment options, risk and possibility of relapse. They were aware of the complexity of his unusual case and the patient provided written informed consent for the publication of his case.

DATA AVAILABILITY STATEMENT

The original contributions presented in the study are included in the article/supplementary materials. Further inquiries can be directed to the corresponding author.

ETHICS STATEMENT

Written informed consent was obtained from the individual(s) for the publication of any potentially identifiable images or data included in this article.

AUTHOR CONTRIBUTIONS

Research idea and study design: RB, MT, RT, EV, NV. Data analysis/interpretation: RB, MT. Supervision: NV, EV, RT, JW, LV. Manuscript drafting: RB, KW, NK. Manuscript reviewing: MT, CD, EV, RT, JW, LV. All authors contributed to the article and approved the submitted version.

ACKNOWLEDGMENTS

LV, JW, and NV are members of the European Reference network for Rare Kidney Diseases (ERKNet-Project No. 739532).

REFERENCES

1. Fakhouri F, Zuber J, Fremeaux-Bacchi V, Loirat C. Haemolytic uraemic syndrome. *Lancet* (2017) 390(10095):681–96. doi: 10.1016/S0140-6736(17)30062-4
2. Westra D, Wetzels JF, Volokhina EB, van den Heuvel LP, van de Kar NC. A new era in the diagnosis and treatment of atypical haemolytic uraemic syndrome. *Neth J Med* (2012) 70(3):121–9.
3. Bresin E, Rurali E, Caprioli J, Sanchez-Corral P, Fremeaux-Bacchi V, Rodriguez de Cordoba S, et al. Combined complement gene mutations in atypical hemolytic uremic syndrome influence clinical phenotype. *J Am Soc Nephrol* (2013) 24(3):475–86. doi: 10.1681/ASN.2012090884
4. Jozsi M, Tortajada A, Uzonyi B, Goicoechea de Jorge E, Rodriguez de Cordoba S. Factor H-related proteins determine complement-activating surfaces. *Trends Immunol* (2015) 36(6):374–84. doi: 10.1016/j.it.2015.04.008
5. Fakhouri F, Fila M, Provot F, Delmas Y, Barbet C, Chatelet V, et al. Pathogenic Variants in Complement Genes and Risk of Atypical Hemolytic Uremic Syndrome Relapse after Eculizumab Discontinuation. *Clin J Am Soc Nephrol* (2017) 12(1):50–9. doi: 10.2215/CJN.06440616
6. Wijnsma KL, Duineveld C, Volokhina EB, van den Heuvel LP, van de Kar NCAJ, Wetzels JFM. Safety and effectiveness of restrictive eculizumab treatment in atypical haemolytic uremic syndrome. *Nephrol Dial Transplant* (2018) 33(4):635–45. doi: 10.1093/ndt/gfx196
7. Heinen S, Sanchez-Corral P, Jackson MS, Strain L, Goodship JA, Kemp EJ, et al. De novo gene conversion in the RCA gene cluster (1q32) causes mutations in complement factor H associated with atypical hemolytic uremic syndrome. *Hum Mutat* (2006) 27(3):292–3. doi: 10.1002/humu.9408
8. Venables JP, Strain L, Routledge D, Bourn D, Powell HM, Warwicker P, et al. Atypical haemolytic uraemic syndrome associated with a hybrid complement gene. *PLoS Med* (2006) 3(10):e431. doi: 10.1371/journal.pmed.0030431
9. Noris M, Remuzzi G. Atypical hemolytic-uremic syndrome. *N Engl J Med* (2009) 361(17):1676–87. doi: 10.1056/NEJMra0902814
10. Feitz WJC, van de Kar NCAJ, Orth-Holler D, van den Heuvel LPJW, Licht C. The genetics of atypical hemolytic uremic syndrome. *Med Genet* (2018) 30 (4):400–9. doi: 10.1007/s11825-018-0216-0
11. Johnson S, Stojanovic J, Ariceta G, Bitzan M, Besbas N, Frieling M, et al. An audit analysis of a guideline for the investigation and initial therapy of diarrhea negative (atypical) hemolytic uremic syndrome. *Pediatr Nephrol* (2014) 29(10):1967–78. doi: 10.1007/s00467-014-2817-4
12. Legendre CM, Licht C, Muus P, Greenbaum LA, Babu S, Bedrosian C, et al. Terminal complement inhibitor eculizumab in atypical hemolytic-uremic syndrome. *N Engl J Med* (2013) 368(23):2169–81. doi: 10.1056/NEJMoa1208981
13. Ardissino G, Possenti I, Tel F, Testa S, Salardi S, Ladisa V. Discontinuation of eculizumab treatment in atypical hemolytic uremic syndrome: an update. *Am J Kidney Dis* (2015) 66(1):172–3. doi: 10.1053/j.ajkd.2015.04.010
14. Merrill SA, Brittingham ZD, Yuan X, Moliterno AR, Sperati CJ, Brodsky RA. Eculizumab cessation in atypical hemolytic uremic syndrome. *Blood* (2017) 130(3):368–72. doi: 10.1182/blood-2017-02-770214
15. Volokhina E, Wijnsma K, van der Molen R, Roeleveld N, van der Velden T, Goertz J, et al. Eculizumab Dosing Regimen in Atypical HUS: Possibilities for Individualized Treatment. *Clin Pharmacol Ther* (2017) 102(4):671–8. doi: 10.1002/cpt.686
16. Wijnsma KL, Ter Heine R, Moes D, Langemeijer S, Schols SEM, Volokhina EB, et al. Pharmacology, Pharmacokinetics and Pharmacodynamics of Eculizumab, and Possibilities for an Individualized Approach to Eculizumab. *Clin Pharmacokinet* (2019) 58(7):859–74. doi: 10.1007/s40262-019-00742-8
17. Willrich MAV, Andreguetto BD, Sridharan M, Fervenza FC, Tostrud LJ, Ladwig PM, et al. The impact of eculizumab on routine complement assays. *J Immunol* (2018) 460:63–71. doi: 10.1016/j.jim.2018.06.010
18. Caprioli J, Castelletti F, Bucchioni S, Bettinaglio P, Bresin E, Pianetti G, et al. Complement factor H mutations and gene polymorphisms in haemolytic uraemic syndrome: the C-257T, the A2089G and the G2881T polymorphisms are strongly associated with the disease. *Hum Mol Genet* (2003) 12(24):3385–95. doi: 10.1093/hmg/ddg363
19. Dragon-Durey MA, Sethi SK, Bagga A, Blanc C, Blouin J, Ranchin B, et al. Clinical features of anti-factor H autoantibody-associated hemolytic uremic syndrome. *J Am Soc Nephrol* (2010) 21(12):2180–7. doi: 10.1681/ASN.2010030315
20. Roman-Ortiz E, Mendizabal Oteiza S, Pinto S, Lopez-Trascasa M, Sanchez-Corral P, Rodriguez de Cordoba S. Eculizumab long-term therapy for pediatric renal transplant in aHUS with CFH/CFHR1 hybrid gene. *Pediatr Nephrol* (2014) 29(1):149–53. doi: 10.1007/s00467-013-2591-8
21. Chan EYH, Warady BA. Acquired cystic kidney disease: an under-recognized condition in children with end-stage renal disease. *Pediatr Nephrol* (2018) 33 (1):41–51. doi: 10.1007/s00467-017-3649-9
22. Roos A, Bouwman LH, Munoz J, Zuiverloon T, Faber-Krol MC, Fallaux-van den Houten FC, et al. Functional characterization of the lectin pathway of complement in human serum. *Mol Immunol* (2003) 39(11):655–68. doi: 10.1016/S0161-5890(02)00254-7
23. Branten AJ, Kock-Jansen M, Klasen IS, Wetzels JF. Urinary excretion of complement C3d in patients with renal diseases. *Eur J Clin Invest* (2003) 33 (6):449–56. doi: 10.1046/j.1365-2362.2003.01153.x
24. Volokhina EB, Westra D, van der Velden TJ, van de Kar NC, Mollnes TE, van den Heuvel LP. Complement activation patterns in atypical haemolytic uraemic syndrome during acute phase and in remission. *Clin Exp Immunol* (2015) 181(2):306–13. doi: 10.1111/cei.12426
25. Bergseth G, Ludviksen JK, Kirschfink M, Giclas PC, Nilsson B, Mollnes TE. An international serum standard for application in assays to detect human complement activation products. *Mol Immunol* (2013) 56(3):232–9. doi: 10.1016/j.molimm.2013.05.221
26. van den Heuvel LP, van de Kar NCAJ, Duineveld C, Sarlea A, van der Velden TJAM, Liebrand WTB, et al. The complement component C5 is not responsible for the alternative pathway activity in rabbit erythrocyte hemolytic assays during eculizumab treatment. *Cell Mol Immunol* (2020) 17:653–5. doi: 10.1038/s41423-020-0406-y
27. Hallstensen RF, Bergseth G, Foss S, Jaeger S, Gedde-Dahl T, Holt J, et al. Eculizumab treatment during pregnancy does not affect the complement system activity of the newborn. *Immunobiology* (2015) 220(4):452–9. doi: 10.1016/j.imbio.2014.11.003
28. Jodele S, Fukuda T, Mizuno K, Vinks AA, Laskin BL, Goebel J, et al. Variable Eculizumab Clearance Requires Pharmacodynamic Monitoring to Optimize Therapy for Thrombotic Microangiopathy after Hematopoietic Stem Cell Transplantation. *Biol Blood Marrow Transplant* (2016) 22(2):307–15. doi: 10.1016/j.bbmt.2015.10.002

29. Ellam T, El Nahas M. Urinary albumin to protein ratio: more of the same or making a difference? *Nephrol Dial Transplant* (2012) 27(4):1293–6. doi: 10.1093/ndt/gfs029
30. Wehling C, Amon O, Bommer M, Hoppe B, Kentouche K, Schalk G, et al. Monitoring of complement activation biomarkers and eculizumab in complement-mediated renal disorders. *Clin Exp Immunol* (2017) 187 (2):304–15. doi: 10.1111/cei.12890
31. Roberts BV, Susano I, Gipson DS, Trachtman H, Joy MS. Contribution of renal and non-renal clearance on increased total clearance of adalimumab in glomerular disease. *J Clin Pharmacol* (2013) 53(9):919–24. doi: 10.1002/jcph.121
32. Ardissino G, Testa S, Dacco V, Paglialonga F, Vigano S, Felice-Civitillo C, et al. Puberty is associated with increased deterioration of renal function in patients with CKD: data from the ItalKid Project. *Arch Dis Child* (2012) 97 (10):885–8. doi: 10.1136/archdischild-2011-300685

Conflict of Interest: JFW is a member of the international advisory board of Alexion and also received a grant from Alexion.

The remaining authors declare that the research was conducted in the absence of any commercial or financial relationships that could be construed as a potential conflict of interest.

frontiers in Immunology

ORIGINAL RESEARCH
published: 11 February 2021
doi: 10.3389/fimmu.2020.603569

The Role of Alpha 2 Macroglobulin in IgG-Aggregation and Chronic Activation of the Complement System in Patients With Chronic Lymphocytic Leukemia

Naseba Naseraldeen[1,2†], Regina Michelis[1†], Masad Barhoum[2,3], Judith Chezar[3], Tamar Tadmor[4,5], Ariel Aviv[6], Lev Shvidel[7,8], Adi Litmanovich[2], Mona Shehadeh[9], Galia Stemer[6], Ety Shaoul[3] and Andrei Braester[2,3]*

[1] The Institute for Medical Research, Galilee Medical Center, Nahariya, Israel, [2] Azrieli Faculty of Medicine, Bar Ilan University, Safed, Israel, [3] Institute of Hematology, Galilee Medical Center, Nahariya, Israel, [4] Hematology Unit, Bnai Zion Medical Center, Haifa, Israel, [5] The Ruth and Bruce Rappaport Faculty of Medicine, Technion, Haifa, Israel, [6] Department of Hematology, Emek Medical Center, Afula, Israel, [7] Hematology Institute, Kaplan Medical Center, Rehovot, Israel, [8] Faculty of Medicine, Hebrew University, Jerusalem, Israel, [9] Biochemistry Laboratory, Galilee Medical Center, Nahariya, Israel

OPEN ACCESS

Edited by:
Marcin Okrój, Intercollegiate Faculty of Biotechnology of University of Gdańsk and Medical University of Gdańsk, Poland

Reviewed by:
Frank J. Beurskens, Genmab, Netherlands
Daniel Ajona, University of Navarra, Spain

***Correspondence:**
Regina Michelis
ReginaM@gmc.gov.il

†These authors have contributed equally to this work

Specialty section:
This article was submitted to Molecular Innate Immunity, a section of the journal Frontiers in Immunology

Received: *07 September 2020*
Accepted: *31 December 2020*
Published: *11 February 2021*

Citation:
Naseraldeen N, Michelis R, Barhoum M, Chezar J, Tadmor T, Aviv A, Shvidel L, Litmanovich A, Shehadeh M, Stemer G, Shaoul E and Braester A (2021) The Role of Alpha 2 Macroglobulin in IgG-Aggregation and Chronic Activation of the Complement System in Patients With Chronic Lymphocytic Leukemia. Front. Immunol. 11:603569. doi: 10.3389/fimmu.2020.603569

Chronic lymphocytic leukemia (CLL) is the most common leukemia in adults in the western world. One of the treatments offered for CLL is immunotherapy. These treatments activate various cellular and biochemical mechanisms, using the complement system. Recently it was shown that the complement system in CLL patients is persistently activated at a low level through the classical pathway (CP). The mechanism of chronic CP activation involves the formation of IgG-hexamers (IgG-aggregates). According to recent studies, formation of ordered IgG-hexamers occurs on cell surfaces *via* specific interactions between Fc regions of the IgG monomers, which occur after antigen binding. The present study investigated the formation of IgG-hexamers in CLL patients and normal (non-malignant) controls (NC), their ability to activate complement, their incidence as cell-free and cell-bound forms and the identity of the antigen causing their formation. Sera from 30 patients and 12 NC were used for separation of IgG- aggregates. The obtained IgG- aggregates were measured and used for assessment of CP activation. For evaluation of the presence of IgG- aggregates on blood cells, whole blood samples were stained and assessed by flow cytometry. Serum levels of IgG- aggregates were higher in CLL and they activated the complement system to a higher extent than in NC. Alpha 2 macroglobulin (A2M) was identified as the antigen causing the hexamerization/aggregation of IgG, and was found to be part of the hexamer structure by mass spectrometry, Western blot and flow cytometry analysis. The presence of A2M-IgG-hexamers on B-cells suggests that it may be formed on B cells surface and then be detached to become cell-free. Alternatively, it may form in the plasma and then attach to the cell surface. The exact time course of A2M-IgG-

hexamers formation in CLL should be further studied. The results in this study may be useful for improvement of current immunotherapy regimens.

Keywords: chronic lymphocytic leukemia, classical pathway, complement system, IgG-hexamers, alpha 2 macroglobulin

INTRODUCTION

Chronic lymphocytic leukemia (CLL) is the most common leukemia in adults in the western world. It affects the B-type lymphocytes in the bone marrow in 95% of the patients, and is characterized by increased numbers of monoclonal B-lymphocytes (>5 × 10^3/μl) that express specific antigens (CD5, CD19, CD20, CD23) on their surface (1).

One of the treatments offered for CLL patients is immunotherapy which allows the immune system to identify cancer cells or train the immune system to fight the malignant B cells (2). The mechanisms involved by the immunotherapeutic monoclonal antibodies are complement dependent cytotoxicity (CDC), antibody dependent cell-mediated cytotoxicity (ADCC), lysosomal membrane permeability (LMP) (3) and phagocytosis (4, 5). The complement system is an ancient defense mechanism preceding adaptive immunity (6). Three complement pathways utilize the nine central proteins of this system (C1–C9): the classical (CP), alternative (AP) and lectin pathways. The interaction of the first component in each pathway with an activator leads to an ordered cascade activation, typical for each pathway (7). All the complement pathways eventually produce the Membrane Attack Complex (MAC, C5b-9), a cytolytic end product, which causes osmotic lysis of the pathogen/target cell (8). The complement system in CLL patients shows decreased levels of complement components (9), decreased CP activity and chronic activation at a low level (10, 11). The CP is involved in this chronic activity, and the decrease in CP activity was assumed to be due to fatigue (10).

The CP is initiated by the binding of C1q to the Fc regions of antigen-bound immunoglobulins type G or M (IgG or IgM) (7). Conformational changes in C1q lead to the activation of C1r which, in turn, activates C1s (6, 12). All these proteins are serine proteases that combine C1, the first component of the CP (13). Clq shows weak binding to the Fc regions of monomeric, non-aggregated IgG, while in the presence of aggregated/hexamerized IgG, that occurs after antigen binding to the Fab domain, the strength of the binding increases and the CP is activated efficiently (14, 15). The formation of the IgG-hexamers is not entirely understood. According to some studies the binding of the antigen on cells causes specific non-covalent interactions between Fc segments of IgG which lead to the arrangement of hexamers (16), suggesting that IgG can form ordered hexamers only on cell surfaces (15). Recently we have demonstrated the presence of aggregates in plasma of CLL patients, which are not bound to cell surfaces (cell-free) (17). The antigen stimulating the formation of these IgG-hexamers may have great importance for the chronic CP activation in CLL, and is described in this study for the first time.

MATERIALS AND METHODS

Subjects

Blood samples were collected from 30 naïve CLL patients and 12 normal (non-malignant) controls (NC). Plasma and sera were separated and frozen at −80°C. The rest of the samples were analyzed in the biochemistry and hematology laboratories. Samples were carefully collected and handled as described (18) in order to avoid spontaneous complement activation. The study was approved by the Helsinki Committee (Institutional Review Board) of Galilee Medical Center, Nahariya, Israel. Patients were divided according to the detection of Ig-C5a (by Western blot analysis), a marker of chronic complement activity (10, 18).

Separation of IgG-hexamers

Affinity Purification of Total IgG

Cell-free IgG were separated from sera/plasma using a commercial kit for total IgG extraction, based on affinity chromatography, according to the manufacturer's instructions (Protein G HP SpinTrap™, GE Healthcare). The final stage of IgG separation included elution by a low pH (0.1 M glycine-HCl, pH 2.7), followed immediately by pH neutralization, according to the manufacturer's instructions. The IgG separated by this kit includes all IgG molecules, i.e. monomers and hexamers. According to the manufacturer, other immunoglobulins (IgM etc.) are not separated by the kit. Fractions of non-IgG proteins produced during the early stages of the purification procedure, were stored at 4°C for later use. Some of the IgG-hexamer separations were repeated using a different method, the Melon Gel IgG Purification Kit (Thermo Fisher Scientific), which does not include any exposure of the samples to acidic conditions.

Size Selection

The total IgG fraction separated using the protein G kit was transferred to a filtration column with a cutoff of 1000 kDa (Vivaspin, Sartorius), and centrifuged for 3 min at 4K g at 4°C. Due to the high molecular weight of IgG-hexamers, >1000 kDa, they are retained on top of the column while monomeric IgG move to the bottom. Protein concentrations of the samples remaining on top and at the bottom of the filtration column were measured by Nanodrop (Thermo scientific), and were used, with the sample volumes, for calculation of total protein amount. Monomeric IgG were also stored at 4°C for later use.

Protein Staining Methods

Silver Stain

To visualize the extracted IgG-hexamers, samples obtained after the filtration step were separated by SDS-PAGE and stained using a silver stain kit, (ProteoSilver™ Plus Silver Stain Kit-

SIGMA). Results were documented using a gel imaging system (G-BOX, Syngene). To assure that the amount of the silver-stained proteins is sufficient for sequencing/mass spectrometry, the gels were de-stained and stained again with Coomassie blue (CB).

Western Blot Analysis

Sera/plasma of CLL patients were tested to identify specific proteins related to the complement system (the Ig-C5a complex, C5, IgG, α-2 macroglobulin [A2M]). Proteins were separated by SDS-PAGE with or without denaturation, transferred to a nitrocellulose membrane, and the studied protein was identified with the appropriate primary [anti human IgG (Sigma), anti human C5 (Quidel), anti human A2M (Gentex)], and the appropriate secondary antibodies. Signals were developed using an ECL kit (Immobilon® Forte, Millipore) and documented using a gel imaging system (G-BOX, Syngene).

Complement Activity

Complement Activity Assay

In order to assess CP activity, IgG-hexamers or in-vitro aggregated IgG (19), were incubated with diluted (1:20) normal sera as described (10). The IgG-hexamers obtained from 10μl serum were used for the assay. Non-IgG and monomeric-IgG, obtained during the IgG-hexamers separation procedure, were acetone precipitated (due to their high volume) and incubated with diluted normal serum, C1q depleted serum (Quidel) or Factor B depleted serum (Quidel). The activity was measured by the levels of MAC/sC5b-9, quantified using ELISA.

ELISA

To quantify the complement activation product MAC, an ELISA kit (sC5b-9 PLUS EIA, Quidel) was used according to the manufacturer's instructions. The results were measured using an ELISA reader (CARIOSKAN LUX, Thermo scientific).

Cell Analysis

Flow Cytometry

Whole blood samples were diluted to 10^4/μl white blood cells (WBC), washed with PBS three times, and stained with fluorescent anti-CD19-PC7 (Beckman), anti CD45-APC (Beckman), anti-C1-FITC (Assaypro), anti A2M-PE (Assaypro), anti CD91-Per-CP-eF710 (Invitrogen, eBioscience), A2M-PerCP (Assaypro) and anti-GRP78 (anti-Bip, Cell Signaling Technology) antibodies. Anti-CD45 stains all the WBC while anti-CD19 marks B lymphocytes. C1 binds IgG only in its hexameric form and thus anti-C1 antibodies can detect cells to which IgG-hexamers and C1 are bound. Anti-CD91 and anti-78 kDa Glucose-Regulated Protein (GRP78) detect these A2M receptors on lymphocytes (20, 21). After incubation with the antibodies, the red blood cells were lysed with VersaLyse (Beckman). All incubations were performed at room temperature, in the dark, for 10 min. Cell staining was assessed by a Flow cytometer (NAVIOS, Beckman coulter).

Mass Spectrometry (Protein Sequencing)

The IgG-hexamers prepared from patients' sera were separated by SDS-PAGE and silver stained (with ProteoSilver™ plus, Sigma). The heavy (γ) and light chains were identified by their molecular mass and high abundance. All other protein bands were excised from the gels and subjected to mass spectrometry at the Smoler Protein Research Center (Technion – Israel Institute of Technology, Haifa, Israel).

Monomeric IgG-Aggregation with A2M

The samples used for these experiments were the monomeric IgG fractions, obtained after IgG affinity columns and size selection (i.e. the sample at the bottom of the 1000 kDa Vivaspin column). Monomeric IgG concentrations were measured by Nanodrop and 7.5 μg from each sample were incubated with 15.8μg of A2M. These protein amounts give a molar ratio of 1:1 for the IgG vs. the A2M dimer, namely one monomeric IgG molecule to one A2M dimer. As a control, monomeric IgG was incubated with human serum albumin (HSA) at a molar ratio of 1:1, or without any protein. All incubations were performed in 100μl PBS for 2hr at room temperature in glass test tubes (as A2M adsorps to non-glass surfaces) (22). After the incubation, samples were used for size selection using the 1,000 kDa Vivaspin columns (Sartorius). The volumes of the samples obtained on top and bottom of the columns were measured, and the IgG concentrations were quantified using a human-IgG ELISA kit (Invitrogen).

Statistical Analysis

Data were analyzed by Kolmogorov-Smirnov, Kruskal-Wallis and by Mann-Whitney tests, as appropriate. $P < 0.05$ was considered significant.

RESULTS

Characteristics of the Subjects' Groups

Clinical parameters of patients and NCs are shown in **Table 1**. WBC values were significantly higher in patients than in NC. Platelets were significantly higher in NC than in patients, although they were within the normal range. No significant differences were observed in all other parameters.

The Levels of Cell-Free IgG-Hexamers in Patients and NC

Protein G columns and 1,000 kDa filtration columns were used for separation of IgG-hexamers, and the percent of IgG-hexamers were calculated. The percent of IgG hexamers in the NC samples was 9.8 ± 5% of the total IgG while significantly higher percentage was observed in patients with and without chronic complement activation [according to the detection of Ig-C5a (10)], showing 19.53 ± 3% and 20.26 ± 4%, respectively (**Figure 1A**). The presence of IgG-hexamers was also verified by another separation method (The Melon Gel Kit), which does not include an elution step of the IgG by a low pH. The percentage of IgG-hexamers obtained by the Melon Gel Kit and the Protein G columns showed significant correlation (**Supplementary Data Sheet 1**). The identity of the separated IgG-hexamers was verified by Western blot using anti-human IgG antibodies (**Figure 1B**).

TABLE 1 | Characteristics of the subjects' groups.

Clinical Parameters (normal range)	CLL Patients	Normal Controls
n	30	12
Gender (male/female)	14/16	5/7
Age (years)	69.4 ± 10.9	59.7 ± 10.1
Serum C3 mg/dl (82–158)	109.7 ± 23.9	125.4 ± 21.5
Serum C4 mg/dl (15–35)	28.2 ± 8.8	29.3 ± 2.3
Cholesterol mg/dl (<200)	158.1 ± 35.2	203.6 ± 80.9
Triglycerides mg/dl (<150)	144.3 ± 78.5	177.1 ± 72.9
HDL mg/dl (>40)	37.8 ± 13.6	43.7 ± 9.6
LDL mg/dl (<100)	91.3 ± 38.7	112 ± 52.4
Non-HDL chol. mg/dl (<130)	120.1 ± 31.2	160.1 ± 80.5
Platlet X10e3/µl (130–400)	164.17 ± 75.9*	272.5 ± 98.3
WBC X10e3/µl (4–10)	33.3 ± 69.3*	7.4 ± 2.8
HGB g/dl (13–18)	13 ± 2.01	13.6 ± 1.1
Neutro abs X10e3/µl (1.5–8)	4.6 ± 2.1	4.7 ± 2.4

All values are given as mean ± SEM.
**indicates significant p value (p < 0.05).*

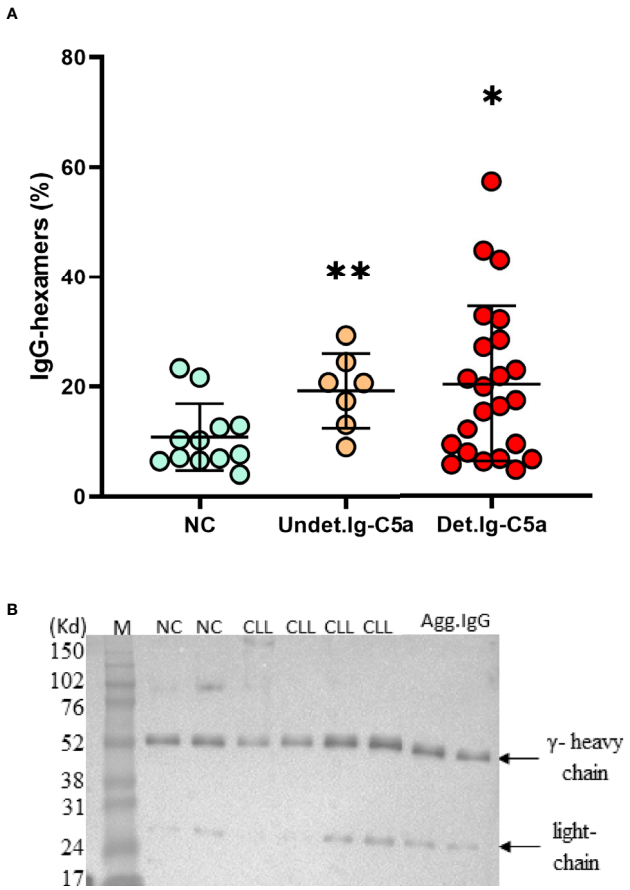

FIGURE 1 | Cell free IgG-hexamers patients and NC subjects. IgG-hexamers were purified from sera/plasma of CLL patients and NC subjects. **(A)** The percentage of IgG-hexamers were calculated. Detectable Ig-C5a (Det.Ig-C5a), n = 23, undetectable Ig-C5a (Undet.Ig-C5a) n = 7, NC n = 12. *, ** indicates significant p values (p < 0.04, 0.004, respectively) vs NC. **(B)** The samples were studied by Western blot using anti-IgG antibodies (representative results), equal protein amounts (10µg) were loaded in each lane. In vitro aggregated commercial IgG (Agg.IgG) was separated in parallel as a control. The heavy and light chains of the IgG are indicated by arrows.

IgG-Hexamers Contribute to the Chronic CP Activation in CLL Patients Serum

To assess the CP activation capacity of the IgG-hexamers, the CP was activated in normal serum by addition of the IgG-hexamers' preparations, and activity was assessed by the levels of the sC5b-9 produced (**Figure 2**). IgG-hexamers from patients with detectable Ig-C5a activated complement to a higher extent than those from NC plasma. IgG-hexamers from patients with undetectable Ig-C5a did not show similar results (**Figure 2A**). Non-IgG proteins (proteins that did not bind to the protein G columns) were able to activate complement in C1q-depleted serum (**Figure 2B**) suggesting activation *via* the AP. The data obtained using factor B depleted serum (**Figure 2C**) support AP activation. Non-hexameric (monomeric) IgG samples from patients or NC did not induce complement activation.

Cell-Bound IgG-Hexamers Are Detected on B Cells

Fresh blood samples from NC and CLL patients were stained with fluorescent antibodies against CD45, CD19 and C1 and tested in a flow cytometer in order to assess IgG-hexamers that are present on cells' surfaces. The results showed that the anti-C1 antibody stained WBC ($CD45^+$) and particularly B cells ($CD19^+$). In NC the C1+CD19+ staining was 20 ± 10% and 65 ± 8% in patients, when gated on WBC (**Figure 3A**, representative results and **Figure 3C**). In order to overcome the increase in B cell population in the patients, analysis was performed again after gating on lymphocytes. The percent of C1+CD19+ cells was significantly higher in patients, showing 95 ± 3%, compared to only 60 ± 20% in NC (**Figure 3B**, representative results and **Figure 3D**). The results were negatively correlated with the levels of cell-free IgG-hexamers ($p < 0.03$). This observation suggests that cell-free IgG-hexamers are in equilibrium with the cell-bound hexamers found on B-cell surfaces.

Identity of the Antigen That Is Causing the Hexamerization

Ten µg of the IgG-hexamer samples were used for SDS-PAGE and silver staining. The results showed additional proteins besides the heavy and light chains of the IgG (**Figure 4A**). These were excised from the gel and subjected to mass spectrometry. After elimination of all the IgG-related sequences, low molecular mass peptides, sequences with a total number of identified peptide sequences (peptide spectrum matches-#PSMs)<30, and sequences with coverage<25, the results indicated six proteins suspected as the antigens that may cause the IgG-hexamerization (**Figure 4B**). One of these candidates was found to be the A2M. The raw sequencing data of the A2M identified peptides can be accessed in the Dryad database under the accession number https://doi.org/10.5061/dryad.tmpg4f4xg. A2M was further studied by Western blot using anti-A2M antibody to verify the presence of A2M in the IgG-hexamer preparations. The Western blot results indicated A2M presence in IgG-hexamer samples of CLL patients (**Figure 5**) and very low or no A2M signal in NC samples, indicating its participation in the hexamer structure. A2M showed a MW of ~360 kDa, similar to that of the purified commercial A2M that was used as a positive control (**Figure 5**).

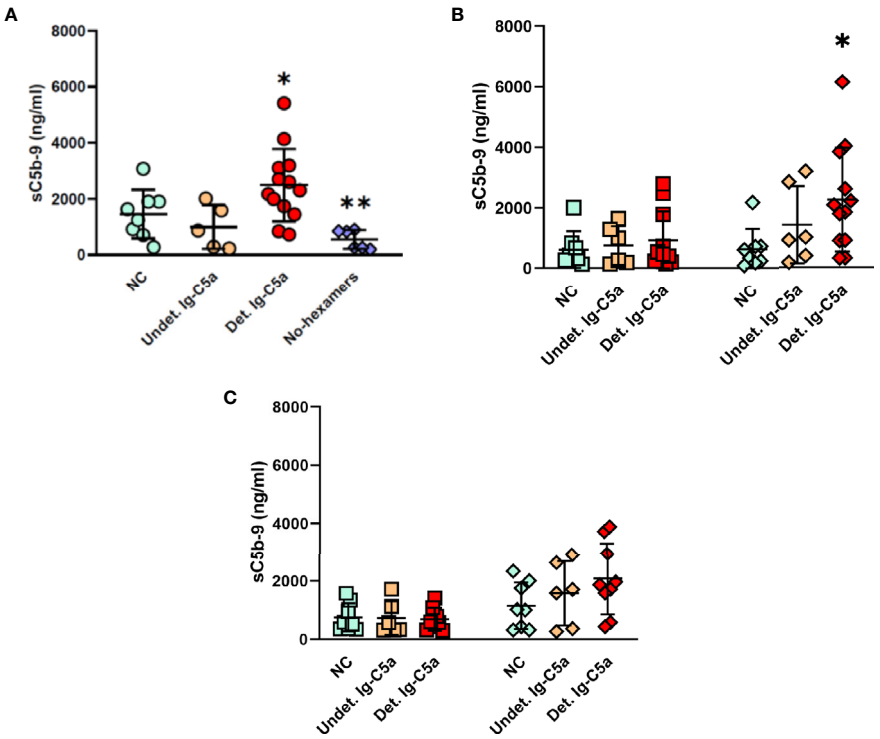

FIGURE 2 | Activation of the complement system by IgG-hexamers. Complement activity was measured in normal serum after incubation with IgG-hexamers from NC and patients **(A)**. Serum samples incubated with buffer were used as a negative control. Proteins that did not bind to the protein G columns (non-IgG proteins, ◊), and non-hexameric IgG (monomeric IgG, □) were used for complement activation in C1q depleted serum **(B)** and factor B depleted serum **(C)**. Activation was followed by the levels of sC5b-9. Detectable Ig-C5a (Det.Ig-C5a) n = 12, Undetectable Ig-C5a (Undet.Ig-C5a) n = 6, NC n = 8. *, ** indicates significant p values ($p < 0.05$, 0.005, respectively) compared to NC and No-hexamers.

The association of the A2M-IgG-hexamers with B lymphocytes was studied by flow cytometry. Fresh blood samples from NC and CLL patients were stained with fluorescent antibodies to A2M, C1 and two A2M receptors, the CD91 (data not shown) and GRP78. High A2M+GRP78+ staining in C1+CD19+ cells supports the presence of A2M-IgG-hexamers on B-cells in addition to the cell-free form (**Figure 6**). The data suggest that the A2M-IgG-hexamers are attached to B-cells by binding the GRP78 (**Figure 6**).

Monomeric IgG Form Hexamers *in-Vitro* After Incubation with A2M in a Cell-Free Environment

Our working assumption was that IgG molecules which bind A2M are those that form hexamers/aggregates. We assessed this assumption by incubation of total serum monomeric IgG with purified commercial A2M, followed by separation and measurement of the generated hexamers. The results shown in **Figure 7** indicate a significant increase in IgG-hexamer generation after incubation of A2M with monomeric IgG from patients with detectable Ig-C5a. Hexamer generation without addition of A2M was minimal, only 4.9% to 7.8% and without significant differences between the subject groups. A non-significant increase in IgG-hexamers was found in the NC group, and no increase was observed in patients with undetectable Ig-C5a (**Figure 7**). Also, no hexamerization was observed after incubation of IgG with a different protein, HSA. The results indicate the presence of anti-A2M antibodies in sera of patients with detectable Ig-C5a (chronic complement activation) and support the potential formation of hexamers in a cell-free environment, i.e. in the plasma.

DISCUSSION

Our study focused on characterization of the IgG-hexamers that are related to chronic CP activation in CLL. IgG-hexamers normally bind C1, the first component of the CP, and activate a cascade of complement proteins until C5b-9 is formed. The high level of these cell-free hexamers in patients has a key role in chronic CP activation, leading to the "weariness" of this pathway as well as to an increase in the formation of Ig-C5a complex and in the levels of other complement activation markers (17). IgG-hexamers are mainly formed after antigen binding that leads to non-covalent Fc-Fc interactions (23). We assumed that in CLL patients a particular antigen (or antigens) causes increased formation of IgG-hexamers, as shown by their high percentages in the patients' plasma. In this study, the antigen causing hexamerization was found to be A2M.

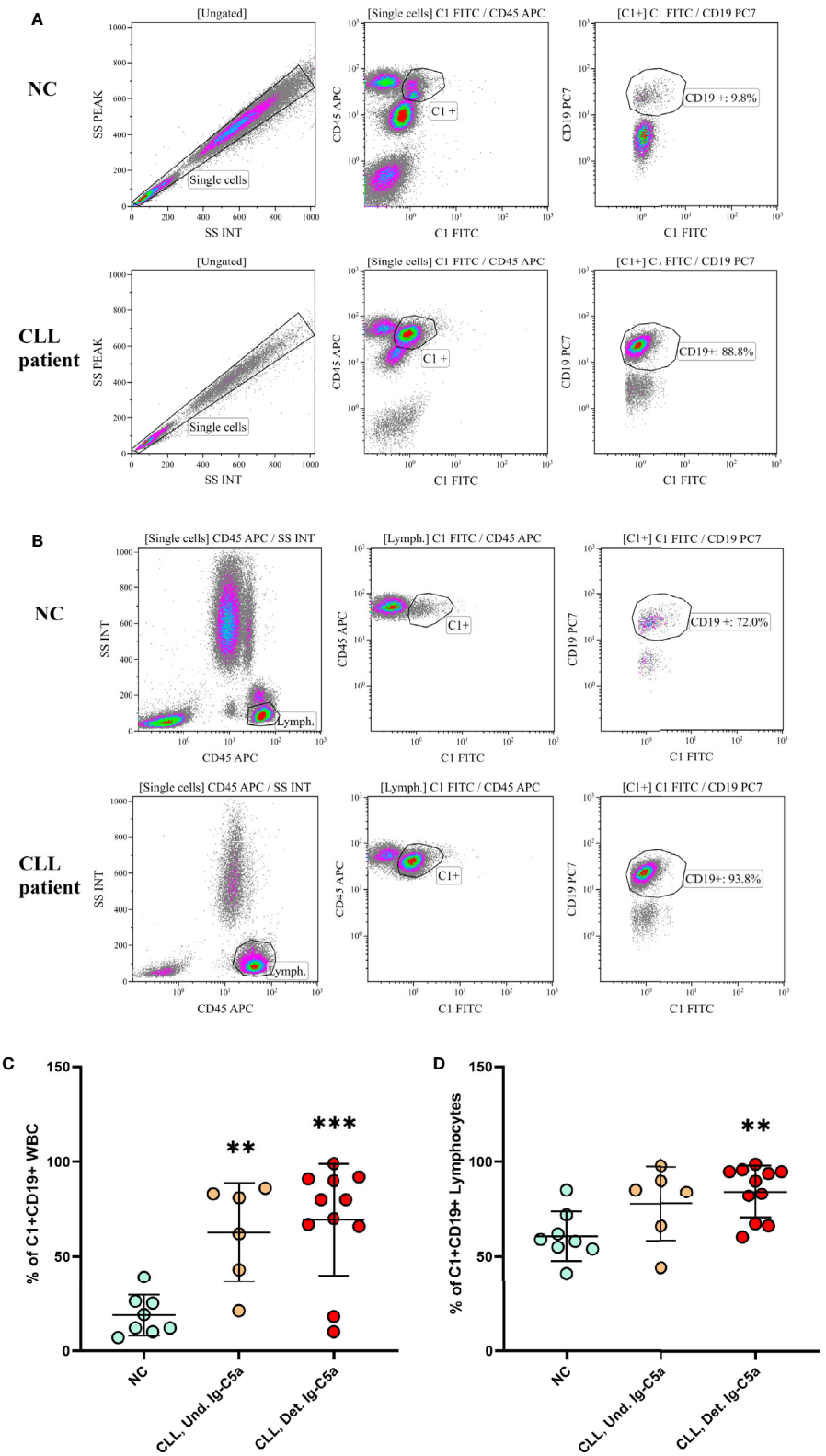

FIGURE 3 | IgG-hexamers on B cell surface. Blood samples from CLL patients and NC were stained with fluorescent antibodies against CD45, CD19 and C1, and tested in a flow cytometer. representative results are shown **(A, B)**. The results were gated on WBC **(A, C)** or on lymphocytes **(B, D)**. Detectable Ig-C5a n = 11; Undetectable Ig-C5a n = 6; NC n = 8. **, *** indicate significant p values ($p < 0.01$, 0.001, respectively) compared to NC.

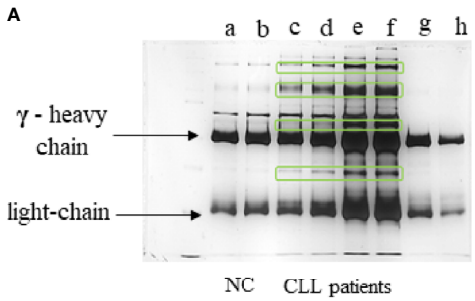

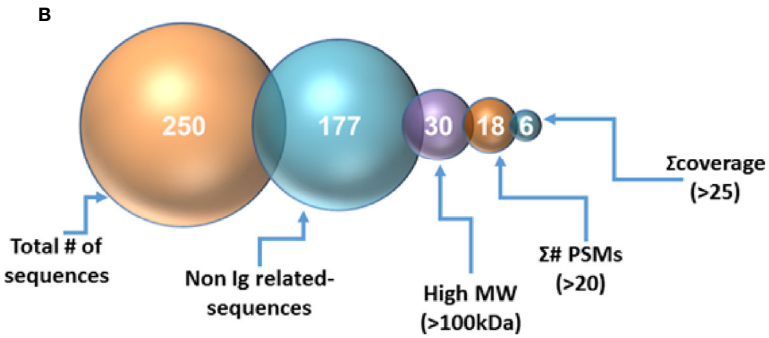

FIGURE 4 | Separation of the IgG-hexamer samples. **(A)** Samples of NC (a, b), CLL patients (c–f) and commercial IgG (g, h) were separated and silver stained. Heavy (γ) and light chain are indicated by arrows. Additional proteins besides heavy and light chains are marked in frames. **(B)** The process of selection of the resulting sequence data included elimination of all the IgG-related sequences, low molecular mass peptides, sequences with a total number of identified peptide sequences (peptide spectrum matches-#PSMs)<30, and sequences with coverage<25.

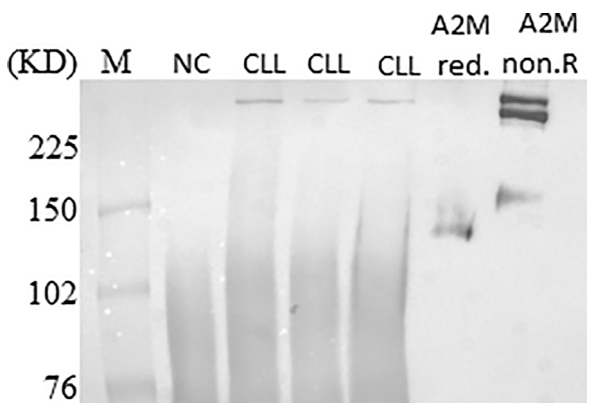

FIGURE 5 | A2M presence in IgG-hexamers samples. A2M was identified in IgG-hexamers samples by Western blot using anti-A2M antibodies (representative results). Purified commercial A2M, reduced (red.) and non-reduced (non.R) were used as a positive control.

The IgG-antigen aggregates (immune complexes) exist on the surface of malignant B cells and also as a detached, cell-free, form. The percentage of both cell-free and cell-bound IgG-hexamers is significantly higher in patients than in NC. The increased ability of these hexamers/aggregates to activate the CP supports their potential role in the chronic activation of the CP in CLL.

It is important to mention that in this study we show that natural IgG aggregates exist in complex with A2M, but we did not demonstrate the hexameric rings. Thus, the complexes formed between IgG and A2M may potentially involve Fab-mediated clustering of dimeric A2M, in addition to the known Fc : Fc interactions. In this case, large aggregated networks may be formed, and these aggregates may include complexes including more than six IgG molecules (17). These aggregates are very potent in complement activation and in depleting the complement system in CLL patients.

During normal physiological conditions, AP dominates activation of the complement system in plasma due to the spontaneous hydrolysis of complement component C3 (24). This hydrolysis can be hastened through some biological interfaces that include lipid complexes (8). Moreover, non-IgG proteins (from CLL patients with chronic complement activation) may also activate the AP, as suggested in this study by the data obtained using C1q depleted serum.

A previous study showed decreased expression of CD19 molecules on B-cells from CLL patients compared to normal B-cells (25). This information supports the significance of our findings on the differences in C1+CD19+ cell populations between patients and NCs and suggests that our findings are truly due to a higher presence of IgG-hexamers on B cell surface in the patients, rather than due to increased expression of CD19.

One or several of the additional non-IgG proteins that were found in the IgG-hexamer preparations was the antigen/s

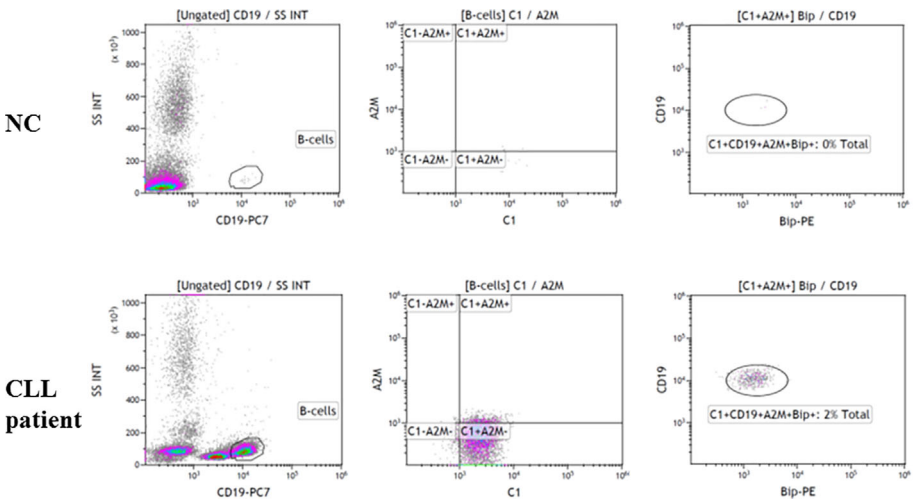

FIGURE 6 | Association of the A2M-IgG-hexamers with B lymphocytes. Blood samples from CLL patients and NC were stained with fluorescent antibodies against CD45, CD19, C1, A2M and GRP78 (Bip) and tested in a flow cytometer. Representative results are shown.

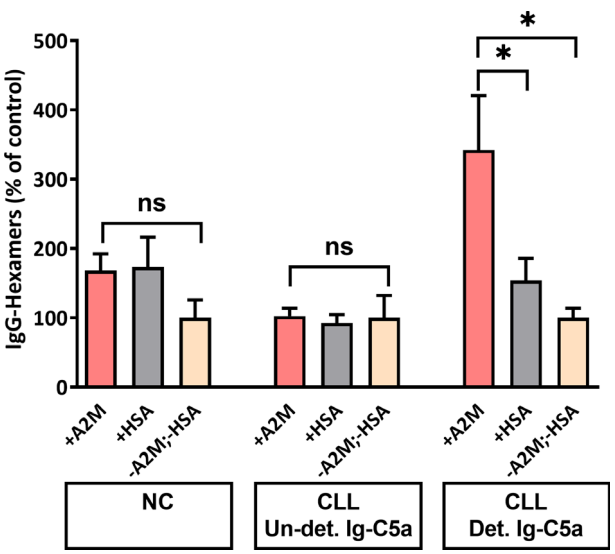

FIGURE 7 | IgG-hexamer formation after in-vitro incubation of monomeric IgG with A2M. Monomeric IgG were incubated with purified commercial A2M, HSA or PBS and the generated IgG-hexamers were separated. IgG were quantified by ELISA and the percent of IgG-hexamers was calculated.
*, ns indicate significant (< 0.05) and non-significant p values, respectively.

causing the hexamerization. Mass spectrometry (protein sequencing) analysis indicated that A2M could be the antigen. A2M is formed by the assembly of four 180-kDa subunits into two disulfide-linked dimers, which noncovalently associate to complete the tetrameric structure of A2M (26). However, several studies showed that A2M is present in the circulation in either a dimeric or tetrameric form (27, 28). A2M can bind through the CD91 receptor to T cells (20), and one study showed that A2M could also be expressed on B lymphocytes (29). Another receptor for A2M is GRP78, a member of the HSP70 gene family (30), whose levels are elevated in hypoxia and starvation conditions, allowing it to function as a shield for solid tumors in these cases (31). Studies have shown that GRP78 is mainly expressed on B cells compared to T cells and its levels are significantly higher in patients with CLL than in NC (32).

Both the Western blot and flow cytometry analyses confirmed that A2M was the antigen causing IgG hexamerization. The data suggest that A2M-IgG-hexamers do not necessarily form on the surface of B cells as they can also form in plasma before binding to the cells *via* A2M receptors. Antibodies that react against A2M may be part of a more general autoimmune phenomenon which is established occasionally in CLL patients (33, 34).

In hematologic malignancies, C activation can have both protective properties as well as tumor growth promoting effects, both direct and indirect (35). For example, hematological tumor cells show enhanced expression and surface binding of C regulators such as Factor H, Factor H like protein 1 (FHL-1), Factor H related protein 1 (CFHR1), FHR-4, FHR5, and C4b binding protein (C4BP). These C regulators further display the cofactor activity, which function together with factor I to block C activation at the level of C3 convertase, and lead to C evasion (35). Similarly to these soluble regulators, the membrane-bound C inhibitors CD46, CD55 and CD59 are up-regulated in various primary tumors and tumor lines to evade the C attack (35). Also, the soluble form of the C receptor 1 (CR1), expressed on most leukocytes membranes, is shed into the plasma, where it functions as a powerful C inhibitor. This represents another possible C evasion strategy utilized by leukemia cells (35).

Although our findings regarding the A2M-IgG-hexamers are novel, the factors that control the hexamerization process and the sequence of their formation in CLL plasma and on B-cells

have not yet been revealed and need further clarification. For the benefit of the patients, the results may be useful for improvement of current immunotherapy treatments, for example if A2M-IgG-hexamerization and the resulting chronic CP activation can be inhibited, and thus help the complement system attain maximal capacity. Alternatively, measurements of this protein or other complement activity markers can help physicians to identify patients who may be less responsive to immunotherapy. For these patients, other therapeutic options should be offered.

DATA AVAILABILITY STATEMENT

The raw sequencing data of the A2M identified peptides can be accessed in the Dryad database under the accession number https://doi.org/10.5061/dryad.tmpg4f4xg.

ETHICS STATEMENT

The studies involving human participants were reviewed and approved by Institutional Review Board of Galilee Medical Center, Nahariya, Israel. The patients/participants provided their written informed consent to participate in this study.

AUTHOR CONTRIBUTIONS

NN: data curation, methodology. RM: conceptualization, data curation, data analysis, methodology, project administration, supervision, validation, writing – original draft, writing – review and editing. MB: project administration, supervision. JC: data curation, data analysis, methodology. TT: conceptualization, resources. AA: resources. LS: resources. AL: resources. MS: methodology. GS: resources. ES: methodology. AB: supervision, resources, project administration, methodology, funding, conceptualization, review and editing. All authors contributed to the article and approved the submitted version.

FUNDING

The study was funded by the Health Corporation of Galilee Medical Center.

ACKNOWLEDGMENTS

The authors thank Mrs. Tobie Kuritsky and Prof. Chaim Putterman for their help in editing and proofreading of the manuscript, and Mr. Basem Hijazi, a professional statistician, for his help with the statistical analysis.

SUPPLEMENTARY MATERIAL

The Supplementary Material for this article can be found online at https://www.frontiersin.org/articles/10.3389/fimmu.2020.603569/full#supplementary-material

REFERENCES

1. Mohr A, Renaudineau Y, Bagacean C, Pers JO, Jamin C, Bordron A. Regulatory B lymphocyte functions should be considered in chronic lymphocytic leukemia. *Oncoimmunology* (2016) 5:e1132977. doi: 10.1080/2162402X.2015.1132977
2. Marabelle A, Tselikas L, de Baere T, Houot R. Intratumoral immunotherapy: using the tumor as the remedy. *Ann Oncol* (2017) 28:33–43. doi: 10.1093/annonc/mdx683
3. Chien WW, Niogret C, Jugé R, Lionnard L, Cornut-Thibaut A, Kucharczak J, et al. Unexpected cross-reactivity of anti-cathepsin B antibodies leads to uncertainties regarding the mechanism of action of anti-CD20 monoclonal antibody GA101. *Leuk Res* (2017) 55:41–8. doi: 10.1016/j.leukres.2017.01.010
4. Weiner LM, Surana R, Wang S. Monoclonal antibodies: versatile platforms for cancer immunotherapy. *Nat Rev Immunol* (2010) 10:317–27. doi: 10.1038/nri2744
5. Jaglowski SM, Alinari L, Lapalombella R, Muthusamy N, Byrd JC. Review article The clinical application of monoclonal antibodies in chronic lymphocytic leukemia. *Blood* (2010) 116:3705–14. doi: 10.1182/blood-2010-04-001230
6. Dunkelberger JR, Song WC. Complement and its role in innate and adaptive immune responses. *Cell Res* (2010) 20:34–50. doi: 10.1038/cr.2009.139
7. Pio R, Corrales L, Lambris JD. The role of complement in tumor growth.. *Adv Exp Med Biol* (2014) 772:229–62. doi: 10.1007/978-1-4614-5915-6_11
8. Merle NS, Church SE, Fremeaux-Bacchi V, Roumenina LT. Complement System Part I - Molecular Mechanisms of Activation and Regulation. *Front Immunol* (2015) 6:262. doi: 10.3389/fimmu.2015.00262
9. Schlesinger M, Broman I, Lugassy G. The complement system is defective in chronic lymphatic leukemia patients and in their healthy relatives. *Leukemia* (1996) 10:1509–13.
10. Michelis R, Tadmor T, Barhoum M, Shehadeh M, Shvidel L, Aviv A, et al. A C5a-Immunoglobulin complex in chronic lymphocytic leukemia patients is associated with decreased complement activity. *PloS One* (2019) 14:1–17. doi: 10.1371/journal.pone.0209024
11. Middleton O, Cosimo E, Dobbin E, McCaig AM, Clarke C, Brant AM, et al. Complement deficiencies limit CD20 monoclonal antibody treatment efficacy in CLL. *Leukemia* (2015) 29:107–14. doi: 10.1038/leu.2014.146
12. Arlaud GJ, Gaboriaud C, Thielens NM, Budayova-Spano M, Rossi V, Fontecilla-Camps JC. Structural biology of the C1 complex of complement unveils the mechanisms of its activation and proteolytic activity. *Mol Immunol* (2002) 39:383–94. doi: 10.1016/s0161-5890(02)00143-8
13. Mortensen SA, Sander B, Jensen RK, Pedersen JS, Golas MM, Jensenius JC, et al. Structure and activation of C1, the complex initiating the classical pathway of the complement cascade. *Proc Natl Acad Sci U S A* (2017) 114:986–91. doi: 10.1073/pnas.1616998114
14. Hansch RGOTGM. chapter 1.2.1, Classical Pathway of Activation. In: *Edition R. The Complement System. 2nd Revise*. Heidelberg Germany: Springer-Verlag Berlin Heidelberg New York (1998). p. 68–85.
15. Cook EM, Lindorfer MA, van der Horst H, Oostindie S, Beurskens FJ, Schuurman J, et al. Antibodies That Efficiently Form Hexamers upon Antigen Binding Can Induce Complement-Dependent Cytotoxicity under Complement-Limiting Conditions. *J Immunol* (2016) 197:1762–75. doi: 10.4049/jimmunol.1600648
16. Diebolder CA, Beurskens FJ, de Jong RN, Koning RI, Strumane K, Lindorfer MA, et al. Complement is activated by IgG hexamers assembled at the cell surface. *Science* (2014) 343:1260–3. doi: 10.1126/science.1248943

17. Michelis R, Tadmor T, Aviv A, Stemer G, Majdob R, Shvidel L, et al. Cell-free IgG-aggregates in plasma of patients with chronic lymphocytic leukemia cause chronic activation of the classical complement pathway. *PloS One* (2020) 15: e0230033. doi: 10.1371/journal.pone.0230033 Published 2020 Mar 9.
18. Mollnes TE, Garred P, Bergseth G. Effect of time, temperature and anticoagulants on in vitro complement activation: consequences for collection and preservation of samples to be examined for complement activation. *Clin Exp Immunol* (1988) 73:484–8.
19. Blom AM, Österborg A, Mollnes TE, Okroj M. Antibodies reactive to cleaved sites in complement proteins enable highly specific measurement of soluble markers of complement activation. *Mol Immunol* (2015) 66:164–70. doi: 10.1016/j.molimm.2015.02.029
20. Binder RJ, Karimeddini D, Srivastava PK. Adjuvanticity of alpha 2-macroglobulin, an independent ligand for the heat shock protein receptor CD91. *J Immunol* (2001) 166:4968–72. doi: 10.4049/jimmunol.166.8.4968
21. Zhang LH, Zhang X. Roles of GRP78 in physiology and cancer. *J Cell Biochem* (2010) 110:1299–305. doi: 10.1002/jcb.22679
22. Biltoft D, Gram JB, Larsen A, Münster AB, Sidelmann JJ, Skjoedt K, et al. Fast form alpha-2-macroglobulin - A marker for protease activation in plasma exposed to artificial surfaces. *Clin Biochem* (2017) 50:1203–8. doi: 10.1016/j.clinbiochem.2017.09.002
23. Strasser J, de Jong RN, Beurskens FJ, Wang G, Heck AJR, Schuurman J, et al. Unraveling the Macromolecular Pathways of IgG Oligomerization and Complement Activation on Antigenic Surfaces. *Nano Lett* (2019) 19:4787–96. doi: 10.1021/acs.nanolett.9b02220
24. Zhou X, Hu W, Qin X. The role of complement in the mechanism of action of rituximab for B-cell lymphoma: implications for therapy. *Oncologist* (2008) 13:954–66. doi: 10.1634/theoncologist.2008-0089
25. Ginaldi L, De Martinis M, Matutes E, Farahat N, Morilla R, Catovsky D. Levels of expression of CD19 and CD20 in chronic B cell leukaemias. *J Clin Pathol* (1998) 51:364–9. doi: 10.1136/jcp.51.5.364
26. Cater JH, Wilson MR, Wyatt AR. Alpha-2-Macroglobulin, a Hypochlorite-Regulated Chaperone and Immune System Modulator. *Oxid Med Cell Longev* (2019) 2019:5410657. doi: 10.1155/2019/5410657
27. Garcia-Ferrer I, Marrero A, Gomis-Rüth FX, Goulas T. α2-Macroglobulins: Structure and Function. *Subcell Biochem* (2017) 83:149–83. doi: 10.1007/978-3-319-46503-6_6
28. Pitekova B, Kupcova V, Uhlikova E, Mojto V, Turecky L. Alpha-2-macroglobulin and hyaluronic acid as fibromarkers in patients with chronic hepatitis C. *Bratisl Lek Listy* (2017) 118:658–61. doi: 10.4149/BLL_2017_125
29. James K, Tunstall AM, Parker AC, McCormick JN. The association of alpha2-macroglobulin with lymphocyte membranes in chronic lymphocytic leukaemia and other disorders. *Clin Exp Immunol* (1975) 19:237–49.
30. Ni M, Zhang Y, Lee AS. Beyond the endoplasmic reticulum: atypical GRP78 in cell viability, signalling and therapeutic targeting. *Biochem J* (2011) 434:181–8. doi: 10.1042/BJ20101569
31. Ijabi R, Roozehdar P, Afrisham R, Moradi-Sardareh H, Kaviani S, Ijabi J, et al. Association of GRP78, HIF-1α and BAG3 Expression with the Severity of Chronic Lymphocytic Leukemia. *Anticancer Agents Med Chem* (2020) 20:429–36. doi: 10.2174/1871520619666191211101357
32. Huergo-Zapico L, Gonzalez-Rodriguez AP, Contesti J, Gonzalez E, López-Soto A, Fernandez-Guizan A, et al. Expression of ERp5 and GRP78 on the membrane of chronic lymphocytic leukemia cells: association with soluble MICA shedding. *Cancer Immunol Immunother* (2012) 61:1201–10. doi: 10.1007/s00262-011-1195-z
33. Vitale C, Montalbano MC, Salvetti C, Boccellato E, Griggio V, Boccadoro M, et al. Autoimmune Complications in Chronic Lymphocytic Leukemia in the Era of Targeted Drugs. *Cancers (Basel)* (2020) 12:282. doi: 10.3390/cancers 12020282
34. Forconi F, Moss P. Perturbation of the normal immune system in patients with CLL. *Blood* (2015) 126:573–81. doi: 10.1182/blood-2015-03-567388
35. Luo S, Wang M, Wang H, Hu D, Zipfel PF, Hu Y. How Does Complement Affect Hematological Malignancies: From Basic Mechanisms to Clinical Application. *Front Immunol* (2020) 11:593610. doi: 10.3389/fimmu.2020.593610

Conflict of Interest: The authors declare that the research was conducted in the absence of any commercial or financial relationships that could be construed as a potential conflict of interest.

frontiers in Immunology

REVIEW
published: 11 February 2021
doi: 10.3389/fimmu.2020.599974

Deposition of the Membrane Attack Complex in Healthy and Diseased Human Kidneys

Jacob J. E. Koopman[1,2]*, *Mieke F. van Essen*[2], *Helmut G. Rennke*[3], *Aiko P. J. de Vries*[2] *and Cees van Kooten*[2]

[1] Division of Renal Medicine, Department of Medicine, Brigham and Women's Hospital, Harvard Medical School, Boston, MA, United States, [2] Division of Nephrology, Department of Internal Medicine, Leiden University Medical Center, Leiden, Netherlands, [3] Division of Renal Pathology, Department of Pathology, Brigham and Women's Hospital, Harvard Medical School, Boston, MA, United States

OPEN ACCESS

Edited by:
Marcin Okrój, Intercollegiate Faculty of Biotechnology of University of Gdańsk and Medical University of Gdańsk, Poland

Reviewed by:
Kevin James Marchbank, Newcastle University, United Kingdom
Lubka T. Roumenina, INSERM U1138 Centre de Recherche des Cordeliers (CRC), France

***Correspondence:**
Jacob J. E. Koopman
j.j.e.koopman@lumc.nl

Specialty section:
This article was submitted to Molecular Innate Immunity, a section of the journal Frontiers in Immunology

Received: 28 August 2020
Accepted: 21 December 2020
Published: 11 February 2021

Citation:
Koopman JJE, van Essen MF, Rennke HG, de Vries APJ and van Kooten C (2021) Deposition of the Membrane Attack Complex in Healthy and Diseased Human Kidneys. Front. Immunol. 11:599974. doi: 10.3389/fimmu.2020.599974

The membrane attack complex—also known as C5b-9—is the end-product of the classical, lectin, and alternative complement pathways. It is thought to play an important role in the pathogenesis of various kidney diseases by causing cellular injury and tissue inflammation, resulting in sclerosis and fibrosis. These deleterious effects are, consequently, targeted in the development of novel therapies that inhibit the formation of C5b-9, such as eculizumab. To clarify how C5b-9 contributes to kidney disease and to predict which patients benefit from such therapy, knowledge on deposition of C5b-9 in the kidney is essential. Because immunohistochemical staining of C5b-9 has not been routinely conducted and never been compared across studies, we provide a review of studies on deposition of C5b-9 in healthy and diseased human kidneys. We describe techniques to stain deposits and compare the occurrence of deposits in healthy kidneys and in a wide spectrum of kidney diseases, including hypertensive nephropathy, diabetic nephropathy, membranous nephropathy, IgA nephropathy, lupus nephritis, C3 glomerulopathy, and thrombotic microangiopathies such as the atypical hemolytic uremic syndrome, vasculitis, interstitial nephritis, acute tubular necrosis, kidney tumors, and rejection of kidney transplants. We summarize how these deposits are related with other histological lesions and clinical characteristics. We evaluate the prognostic relevance of these deposits in the light of possible treatment with complement inhibitors.

Keywords: biopsy, C5b-9 (membrane attack complex [MAC]), histopathology, immunofluorescence, immunohistochemistry, renal, clinicopathological correlation, glomerular disease

Abbreviations: aHUS, atypical hemolytic uremic syndrome; ANCA, antineutrophil cytoplasmic antibody; COVID19, coronavirus disease 2019; CR1, complement receptor 1; DAF, decay-accelerating factor; eGFR, estimated glomerular filtration rate; FB, complement factor B; FD, complement factor D; FHR, complement factor H related protein; FH, complement factor H; GFR, glomerular filtration rate; HBe, hepatitis B e antigen; HBs, hepatitis B surface antigen; HLA, human leukocyte antigens; MASP, mannose-associated serine protease; MBL, mannose-binding lectin; PLA2R, phospholipase A2 receptor; r, Pearson's correlation coefficient; ρ, Spearman's correlation coefficient; SLE, systemic lupus erythematosus; STEC-HUS, hemolytic uremic syndrome elicited by infection with Shiga toxin-producing enterohemorrhagic *Escherichia coli*; TTP, thrombotic thrombocytopenic purpura.

INTRODUCTION

The membrane attack complex is the end-product of the three complement pathways: the classical, lectin, and alternative pathway. Activation of these pathways leads to generation of C5 convertase, which cleaves C5 into C5a and C5b. While C5a functions as an anaphylatoxin, C5b binds to C6, C7, C8, and multiple copies of C9, constituting C5b-9, also known as the membrane attack complex. This complex forms a pore through a pathogen's or cell's membrane—structurally and functionally similar to perforin produced by cytotoxic T cells—and disrupts the pathogen's or cell's integrity. Formation of C5b-9 can cease incompletely without anchoring to a membrane, in which case it circulates as a soluble complex with vitronectin or clusterin, referred to as sC5b-9 (1, 2). Both C5b-9 and sC5b-9 promote inflammation and thrombosis.

Activation of the complement pathways plays an essential role in the pathogenesis of kidney diseases, but the pathways are involved to varying extents. Glomerular deposition of immune complexes predominantly activates the classical pathway in lupus nephritis, the lectin pathway in primary membranous nephropathy, and both the lectin and alternative pathway in IgA nephropathy (3). The extent to which C5b-9 is formed varies as well. The alternative pathway is activated in both C3 glomerulonephritis and dense deposit disease but leads to more C5b-9 in the former (4–6).

With the clinical development of targeted complement inhibitors (7–9), it is essential to know which parts of the complement pathways go awry in specific kidney diseases. Eculizumab, a monoclonal antibody binding C5, inhibiting its cleavage, and thus preventing formation of C5b-9, is used to treat aHUS and some cases of lupus nephritis, C3 glomerulonephritis, dense deposit disease, IgA nephropathy, and transplant rejection (10–17). Inhibitors of other complement factors are being developed (7–9). Although eculizumab seems to benefit particularly patients in whom much C5b-9 is formed (4, 11, 18, 19), it remains uncertain which patients benefit from which complement inhibitor.

Levels of sC5b-9 in blood and urine are elevated in various kidney diseases and associated with their activity and severity (4, 10–12, 20–33). Yet, measurement of sC5b-9 in blood or urine is cumbersome due to its easy formation *in vitro* and short half-life (34). Deposition of C5b-9 in kidneys is thought to better reflect the involvement of its formation in the pathogenesis of kidney diseases (35, 36). The membrane-bound form may more accurately indicate complement activation and disease activity than its circulating soluble form, as has been shown for other complement factors in SLE (10, 11, 37, 38). Deposition may also be associated with prognosis, similarly to deposition of C4d in IgA nephropathy and kidney transplants (15, 26, 39). Lastly, deposition indicates that C5a has been formed locally, which promotes inflammation and thrombosis through the C5a receptors. This is increasingly recognized as a pathogenetic process and possible treatment target in various kidney diseases and transplant rejection (10–12, 14, 15, 17, 26, 32, 40).

Since deposition of C5b-9 in human kidneys has never been compared across individual studies, it remains uncertain under which conditions, in which diseases, in which areas, and in which quantities it can be found (35). To aid in this understanding, we provide a review of studies on deposition of C5b-9 in healthy and diseased human kidneys. We describe our search strategy and methods, the methodological characteristics of the 141 included studies, and the findings of these studies in the **Supplementary Material**, which may be used as a reference for future research. We summarize the main findings derived from these studies in **Figure 1** and **Table 1**. We illustrate possible correlations between deposition of C5b-9 and histological lesions or clinical characteristics in the other figures. We detail the findings in the text, separately for healthy kidneys, nonimmunological kidney diseases, kidney diseases due to deposition of immune complexes, kidney diseases due to activation of the alternative pathway, vasculitis, general patterns of kidney injury, kidney tumors, and kidney transplantation. We discuss the findings in general in a closing discussion.

STAINING TECHNIQUES

Antibodies Against C5b-9

Around 1980, antibodies against C5b-9 were developed for immunofluorescent and immunoperoxidase staining. These antibodies recognize neoepitopes that arise when individual complement factors combine and change their conformation to form C5b-9 (1, 2). When C6 and C7 bind newly formed C5b, they expose a lipophilic tail that anchors to a membrane. C8 then binds this complex and reshapes to penetrate the membrane. Finally, eighteen copies of C9 integrate into the complex and penetrate the membrane to form an asymmetrical and flexible pore (41–43). The neoepitopes recognized by the antibodies are almost always exposed on polymerized C9 (44–49) and sometimes on incomplete forms lacking C9 (50–52). **Table 2** provides an overview of the antibodies that were used in the included studies to stain C5b-9 in kidneys.

Staining should be interpreted in the context of the selectivity of the antibodies, which is limited insofar they also bind incomplete forms of C5b-9, such as those lacking C9 or polymerized C9 lacking C5b, as shown in **Table 2**. These incomplete forms occur independently of C5b-9, both on membranes and in blood, and may have similar although smaller cytolytic or inflammatory effects (1, 2, 64). C5b-9 should, therefore, be stained with a monoclonal antibody that recognizes a neoepitope on C5b-9 but not its individual components and preferably not its incomplete forms.

Membrane-Bound Versus Soluble C5b-9

The antibodies cannot make a distinction between C5b-9 that has anchored a membrane or sC5b-9 that has remained circulating (65), as apparent from **Table 2**. Unlike membrane-bound C5b-9, the lipophilic parts of sC5b-9 are shielded from membranes as they are capped by vitronectin and clusterin (1, 66).

Several studies tried to distinguish both types of C5b-9 by costaining vitronectin, originally called S-protein. This

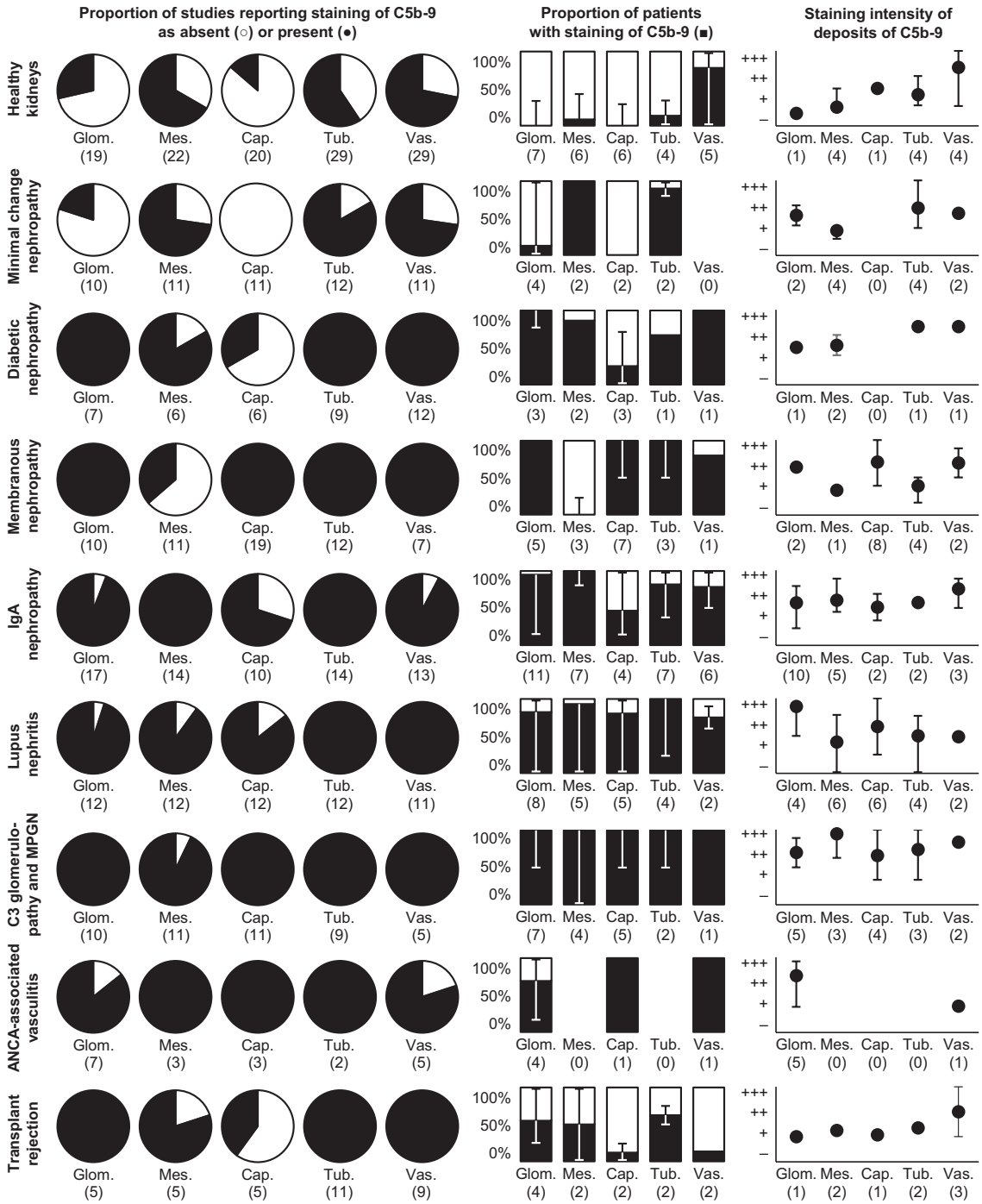

FIGURE 1 | Deposits of C5b-9 in healthy and diseased human kidneys. Pie charts show the proportion of studies that reported staining of C5b-9 as absent (light) or present (dark). Bar charts show the medians of the proportions of patients reported to exhibit staining. Scatter charts show the median staining intensities in these patients. All charts show data separately for staining in the glomerulus as a whole (glom.), in the mesangium (mes.), along the glomerular capillary wall (cap.), along the tubular basement membrane (tub.), or in the extraglomerular vascular wall (vas.). Error bars show the lowest and highest reported values. Numbers of studies are indicated between brackets. Some studies reported only part of the data shown, explaining differences in the numbers of studies between pie, bar, and scatter charts. Nothing is indicated if the data were never reported. Detailed data per study are listed in **Supplementary Table 2**. Membranous nephropathy excludes studies conducted specifically on secondary membranous nephropathy. IgA nephropathy excludes studies conducted specifically on IgA vasculitis with nephritis. Data on these diseases and on glomerular basement membrane diseases, hypertensive nephropathy, interstitial nephritis, acute tubular necrosis, and kidney tumors are only listed in **Supplementary Table 2** because of a paucity of data. ANCA: antineutrophil cytoplasmic antibody; MPGN: membranoproliferative glomerulonephritis.

TABLE 1 | Histological lesions and clinical characteristics correlated with deposits of C5b-9 in diseased human kidneys.

	Localization of deposits		
	Glomerulus	**Tubules**	**Vascular wall**
Hypertensive nephropathy	Glomerulosclerosis		Loss of vascular smooth muscle cells; arteriosclerosis
Diabetic nephropathy	Mesangial expansion; glomerulosclerosis; IFTA; severity of nephropathy; type of diabetes; creatinine; albuminuria	Interstitial inflammation; IFTA; urine biomarkers of tubular injury; creatinine; albuminuria	Loss of vascular smooth muscle cells; vascular AGEs; arteriosclerosis; severity of nephropathy; creatinine; albuminuria
Minimal change nephropathy	Glomerulosclerosis	IFTA	Arteriosclerosis
Membranous nephropathy	Mesangial hypercellularity; capsular adhesions; glomerulosclerosis; proteinuria; disease progression	Interstitial inflammation; interstitial fibrosis; creatinine	Arteriosclerosis
IgA nephropathy	Mesangial expansion and hypercellularity; endocapillary hypercellularity; capsular adhesion; crescents; thrombotic microangiopathy; glomerulosclerosis; interstitial inflammation; IFTA; age; creatinine; proteinuria; nephrotic syndrome; disease progression	Interstitial inflammation; IFTA; creatinine; proteinuria; nephrotic syndrome; disease progression	Thrombotic microangiopathy; arteriosclerosis
Lupus nephritis	Histological activity and chronicity indices; glomerulosclerosis; blood pressure; proteinuria; serum C3 and C4; lack of treatment effect	Interstitial inflammation; interstitial fibrosis	Arteriosclerosis
C3 glomerulopathy	eGFR		
Membranoproliferative glomerulonephritis type I	Glomerulosclerosis; serum sC5b-9; disease progression	Interstitial fibrosis; disease progression	Arteriosclerosis
Hypertension-associated thrombotic microangiopathy	Proteinuria; plasma complement activity		
ANCA-associated vasculitis	Mesangial expansion; creatinine; proteinuria	Interstitial inflammation; interstitial fibrosis; creatinine; lack of treatment effect	
Interstitial nephritis		Interstitial inflammation; IFTA	Interstitial inflammation; IFTA; arteriosclerosis
Acute tubular necrosis		IFTA; degenerative abnormalities of the tubular basement membrane	
Kidney transplant rejection	eGFR; Banff score; transplant survival	IFTA; anti-ABO antibodies; transplant survival	Arteriosclerosis

Histological lesions and clinical characteristics found to correlate with deposits of C5b-9 in different localizations in the kidney are indicated separately for different kidney diseases, as discussed in more detail in the text. Characteristics found not to correlate are only discussed in the text.
AGEs, advanced glycation end-products; ANCA, antineutrophil cytoplasmic antibody; eGFR, estimated glomerular filtration rate; IFTA, interstitial fibrosis and tubular atrophy.

circulating protein binds incomplete forms of C5b-9, interrupts its complete formation, and prevents membrane binding (1, 2). Colocalization was therefore thought to identify soluble sC5b-9 that had deposited in the kidney without anchoring to a membrane (67–71). Indeed, deposits of vitronectin were seldomly seen in the absence of C5b-9 (70, 72, 73). However, vitronectin can also bind complete membrane-bound C5b-9 (60, 64, 65, 74), had a similar distribution as the membrane-bound regulatory factor CD59 (58), was found without C5b-9 in healthy kidneys (72, 75), did not always colocalize with C5b-9 in diseased kidneys (61, 67, 72, 73, 76, 77), colocalized with immune deposits in diseased kidneys when C5b-9 was deficient (78), was associated with the extracellular matrix (75), and was localized in the subepithelial space which it cannot reach when bound to soluble sC5b-9 (67, 73, 75, 79). Therefore, costaining of vitronectin cannot be used as an indicator of sC5b-9.

Clusterin, a protein with a similar function as vitronectin (1, 2), was less often studied. It was present in the vascular wall in healthy kidneys and both the glomerulus and vascular wall in diseased kidneys, colocalized with C5b-9 according to some but not to other studies (58, 69, 70, 73, 80). By contrast, CD59, also known as protectin, is a membrane-bound protein that binds and inhibits membrane-bound C5b-9 only (1, 2). It can bind the lipophilic parts of C8 or C9 in incomplete forms of C5b-9, preventing their penetration of the membrane and integration of other copies of C9 into the complex (2, 41–43). Reports on its presence in healthy and diseased kidneys were inconclusive (58, 81–87).

Apart from protective factors like CD59, cells can resist the cytolytic effects of C5b-9 by shedding parts of their membranes to which C5b-9 has bound as extracellular vesicles. Extracellular vesicles are also shed in various other pathological and physiological processes and can subsequently be targeted by C5b-9. Extracellular vesicles are present in blood, urine, and kidney tissue (88, 89). Antibodies cannot distinguish C5b-9 on extracellular vesicles from C5b-9 bound to cells or circulating sC5b-9.

TABLE 2 | Selective antibodies used to stain C5b-9 in human kidneys.

Name	Clonality	Source	Binding									
			C5	C6	C7	C8	C9	Poly-C9	Incomplete C5b-9[a]	Soluble C5b-9	Membrane-bound C5b-9	Ref.
ab55811	Polyclonal	Rabbit	Unkn.	Unkn.	Unkn.	Unkn.	Unkn.	Unkn.	Unkn.	Unkn.	Unkn.	(53, 54)
aE11 or M0777	Monoclonal	Mouse	–	–	–	–	±	+	+	+	+	(46, 51)
Anti-C5b-9(m)	Polyclonal	Rabbit	–	–	–	–	–	Unkn.	Unkn.	+	+	(55, 56)
Anti-MAC	Polyclonal	Rabbit	–	–	–	–	–	Unkn.	Unkn.	+	+	(57)
Anti-MAC-neo	Polyclonal	Rabbit	–	–	–	–	–	Unkn.	+	+	+	(52)
bC5 or A239	Monoclonal	Mouse	–	–	–	–	±	+	±	+	+	(46)
B7	Monoclonal	Mouse	–	–	–	–	±	+	Unkn.	+	+	(58, 59)
Kolb 1975[b]	Polyclonal	Rabbit	–	–	–	–	–	Unkn.	+	+	+	(50)
PolyC9-MA	Monoclonal	Mouse	–	–	Unkn.	–	–	+	–	Unkn.	+	(44)
WU-7,2	Monoclonal	Mouse	–	–	–	–	±	–	Unkn.	+	+	(48, 60)
WU-13,15	Monoclonal	Mouse	Unkn.	–	–	Unkn.	±	–	–	+	+	(48, 60)
X197	Monoclonal	Mouse	Unkn.	Unkn.	Unkn.	–	+	+	–	Unkn.	+	(47, 49)
Xia 1988[b]	Monoclonal	Mouse	–	–	–	–	–	Unkn.	Unkn.	+	+	(61, 62)
3B1	Monoclonal	Mouse	–	–	–	–	–	+	–	+	+	(45)
1B4	Monoclonal	Unkn.	Unkn.	Unkn.	Unkn.	Unkn.	–	+	Unkn.	+	+	(63)

All antibodies against C5b-9 used for staining of C5b-9 in the included original studies, as specified per study in ***Supplementary Table 1****, are indicated. References to studies on their binding selectivity are given.*

[a]*Incomplete forms of C5b-9 without C9, either soluble or membrane-bound, commonly referred to as C5b-6, C5b-7, and C5b-8.*

[b]*Names used in* ***Supplementary Tables 1*** *and* ***2*** *for antibodies without a specific name.*

–, no binding; ±, weak binding; +, strong binding; poly-C9, polymerized C9; unkn., unknown.

Comparisons of Different Staining Techniques

Some studies used a combination of antibodies against individual components, such as C6 and C9, instead of a selective antibody to stain deposits of C5b-9 (**Supplementary Table 1**). These complement factors are, in contrast to C5b-9, ever-present in blood (45, 46, 55, 60). Some of them—notably C5, C6, and C9—may be present in the glomerulus when others are not (90–92). As a result, individual complement factors could stain when C5b-9 did not (44, 52, 57, 78) and could stain with varying intensities (44, 52, 57, 67, 76, 93, 94), as illustrated in **Figures 3A, B**. Staining intensities of C6 and C7 were generally lowest (44, 52, 94), while that of C9 often resembled that of C5b-9 (18, 44, 94–97).

Only one study compared different selective antibodies against C5b-9—among which aE11, anti-C5b-9(m), and B7—and found identical glomerular staining (58). Results obtained with different antibodies in included studies might vary slightly, but we could not discern a relation with their selectivities, though comparisons were hampered by a paucity of data (**Supplementary Tables 2** and **3** and **Supplementary Figures 1** and **2**).

Different staining techniques were rarely compared directly. Two studies found similar immunofluorescent and immunoperoxidase staining using anti-C5b-9(m) or anti-MAC in various kidney diseases (57, 98). One study mentioned that aE11 did not stain well in paraffin-fixed tissue (28). Direct immunofluorescent staining of C5b-9 was not, in contrast to IgG and C3, affected by acidity, denaturation, or proteolysis (95). Comparisons of staining techniques between included studies were hampered by a paucity of data. Antigen retrieval and blocking, secondary antibodies, antibody concentrations, and detection techniques remained mostly unspecified, yet these techniques determine whether, how intensely, and how selectively staining is perceived. We provide an example of a complete description of staining techniques in the legend of **Figure 2**. We could not discern differences in results of included studies depending on staining techniques (**Supplementary Tables 2** and **3**), except for a possibly higher frequency of tubular deposits based on immunofluorescent as compared with immunoperoxidase staining (**Supplementary Figures 3** and **4**).

Staining of C5b-9 was similar in tissue obtained with autopsy or biopsy in studies on diabetic nephropathy and lupus nephritis (27, 95). In a study on healthy kidneys, it was more often present in tissue obtained with autopsy than biopsy (27), possibly because the latter were healthy living donors. Also in included studies, autopsies might reveal more frequent staining in healthy but not diseased kidneys (**Supplementary Figures 5** and **6**).

Clearance of C5b-9

Membrane-bound C5b-9 is stable and cleared slowy. Indeed, glomerular staining of C5b-9 was equal in patients with active or chronic lupus nephritis, while that of C3 disappeared from the latter (18). It was present in biopsies taken both shorter and longer than twenty weeks after the onset of IgA vasculitis, whereas C3 and MBL were present in only the former (99). It remained present with unchanged intensity in patients with C3 glomerulopathy or thrombotic microangiopathy after one or two weeks (100), after three months (101), after four months (102), and after a year (103) of treatment with eculizumab. Yet, in other reports on various kidney diseases, its staining resolved within three days after administration of eculizumab (104), after three months to 3 years of treatment with eculizumab (105–108), and after half a year of treatment with other immunosuppressive medication (18, 109), as illustrated in **Figure 3C**. Resolution over short periods may reflect active shedding of C5b-9 from cells,

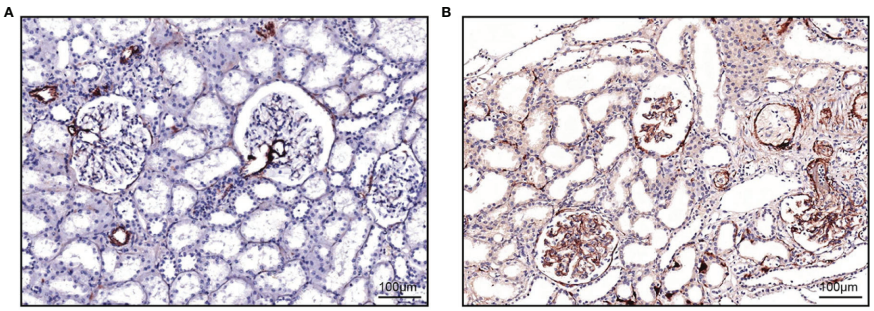

FIGURE 2 | Staining of C5b-9 in a healthy and a diseased kidney. Examples of staining of C5b-9 from our laboratory are shown. **(A)** In a healthy kidney, staining was present in the vascular pole of the glomerulus and the vascular wall of extraglomerular arteries and focally with less intensity along Bowman's membrane and the tubular basement membrane. This tissue was obtained with a biopsy from a living donor before kidney transplantation. **(B)** In a kidney of a patient with aHUS, staining was present along the glomerular capillary wall, in the vascular wall of extraglomerular arteries and focally along Bowman's membrane and the tubular basement membrane. This tissue was obtained with a clinically indicated biopsy. Both tissues were fixed, paraffin-embedded, and sectioned. After deparaffinization (xylol and ethanol) and antigen retrieval (PBS-0.1% Proteinase XXIV, P8038, Sigma), sections were washed and endogenous peroxidase was blocked (PBS, 0.1% NaN_3, 1% H_2O_2) for 30 min at room temperature. Sections were washed (PBS) and incubated with mouse anti-human C5b-9 (2 µg/ml, aE11, HM2167, Hycult Biotech, Uden, the Netherlands) or an isotype control (mouse IgG2a, 2 µg/ml, X0943, Dako, Jena, Germany) in PBS with 1% BSA over night at room temperature. Next day, slides were washed and incubated with goat anti-mouse horseradish peroxidase (HRP, 5 µg/ml, P0447, Dako) for 30 min at room temperature. Slides were washed and incubated with rabbit anti-goat HRP (2.5 µg/ml, P0449, Dako) for 30 min at room temperature. Slides were washed and developed using NovaRED following protocol (Vector Labs, Peterborough, UK) and counterstained (Mayer's hematoxylin, 1.09249.0500, Merck, Darmstadt, Germany) for 25 s. Slides were not counterstained with eosin, which explains why tubules may seem dilated. Slides were dried overnight at room temperature before being covered using entellan (1.07961, Merck).

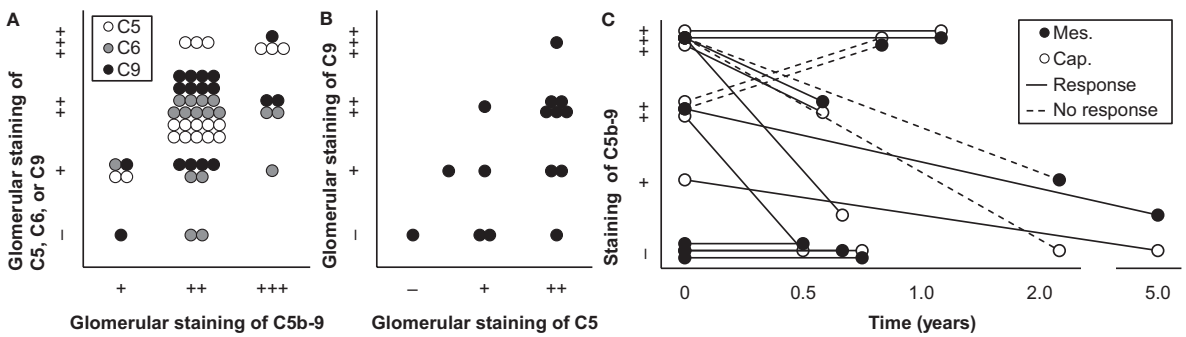

FIGURE 3 | Technical aspects of staining of C5b-9. **(A)** Glomerular staining intensity of C5b-9 is shown in relation with those of its individual components C5, C6, and C9 in kidney biopsies of patients with IgA nephropathy (n = 18). Antibody anti-MAC-neo was used for staining of C5b-9. We plotted previously published individual data (52). **(B)** Glomerular staining intensities of C5 and C9 are compared in kidney biopsies of patients with IgA nephropathy (n = 15). We plotted previously published individual data (76). **(C)** Staining intensities of C5b-9 in the mesangium (mes.) and along the capillary wall (cap.) are shown for first and repeat biopsies with the time between both biopsies in patients with lupus nephritis (n = 8) who responded or did not respond to immunosuppressive treatment. Antibody aE11 was used for staining. We plotted previously published individual data (18).

initial staining of C5b-9 on extracellular vesicles, initial staining of circulating sC5b-9, or variability of the staining technique; resolution over longer periods may reflect a true effect of complement inhibition.

HEALTHY KIDNEYS

Knowledge on deposition of C5b-9 in healthy kidneys is crucial to understand its relevance in kidney diseases. Tissue from healthy kidneys is, however, generally unavailable for research. Deposition was, consequently, explored infrequently and only in small, ill-defined, and sometimes heterogeneous groups. These groups mostly served as controls in studies on patients with kidney diseases, yet might themselves not always have healthy kidneys. For example, in a rare study providing such details, controls were biopsied because of proteinuria, hematuria, edema, hypertension, or an elevated creatinine up to 522 µmol/l and sometimes had lesions consistent with a mesangioproliferative glomerulonephritis (52). Other sources of tissue included autopsies, biopsies of kidney transplants before, during, or after transplantation, biopsies without histological lesions

conducted in most cases because of microscopic hematuria, unaffected parts of kidneys nephrectomized because of a kidney tumor, and unclear sources.

In these presumably healthy kidneys, deposits of C5b-9 were absent (31, 52, 70, 76, 90, 92, 95, 102, 110–125) or sparse and granular in the mesangium (18, 28, 44, 67, 72, 75, 77, 96, 97, 102, 103, 111, 126–133) and vascular pole (18, 44, 126, 132, 134). Deposits were variably reported to be present or absent in the capillary wall (18, 27, 28, 44, 52, 67, 70, 75, 97, 103, 111, 112, 123, 126, 127, 129, 132, 134). Deposits were furthermore reported occasionally along Bowman's capsule (28, 96, 103, 111, 128, 129) and segmentally and granularly along the tubular basement membrane (18, 28, 46, 67, 70, 72, 75, 83, 94, 96, 97, 103, 118, 127, 129, 135, 136). Deposits were more prominent in the vascular wall (18, 27, 28, 44, 67, 70, 72, 75, 77, 84, 94, 96, 97, 103, 111, 124, 126, 127, 130, 131, 134, 135, 137–139) but absent from peritubular capillaries (83, 130). In the vascular wall, staining covered on average 6% of the media (84). We provide an example of sparse mesangial staining and more prominent vascular staining in a living donor before kidney transplantation —probably the closest representation of a healthy kidney—in **Figure 2A**.

Immunoelectron microscopy revealed C5b-9 granularly along extracellular striated membranous structures—thought to be cell membrane fragments—in the mesangium, glomerular basement membrane, tubular basement membrane, and adjacent to myocytes in the vascular wall but not on cells themselves. This was similar for autopsies (126), nephrectomized kidneys (96), biopsies (72), and kidney tissue of unclear source (44, 97).

Formation and deposition of C5b-9 is physiologically expected to be negligible in healthy kidneys, as confirmed by several studies. Sparse and segmental deposition, as described in other studies and as shown in **Figure 2A**, may be explained by localized cellular injury acquired during aging, due to subclinical or unrecognized kidney disease, or as a result of tissue sampling. This explanation fits observations of deposits of C5b-9 being accompanied by deposits of C1q, C3, C4, or FH in the glomerulus (18, 27, 44, 83, 96, 103, 131) and by deposits of C3, C4, or FH along the tubular basement membrane and in the vascular wall (44, 67, 70, 75, 94, 96, 103, 134, 138). This explanation suggests that deposition of C5b-9 is more likely in tissue obtained from older individuals, in the presence of a kidney tumor, or with autopsy.

In one comparative study, staining of C5b-9 was absent from the kidney of a fetus, sparse in the mesangium and vascular wall in a newborn but stronger in the mesangium and in the vascular wall and additionally appearing along the capillary wall and tubular basement membrane in two adults aged 55 and 65 years (44, 126). In two individuals with unknown ages, glomerular staining was independent of age (137). Although only a limited number of other studies reported ages, glomerular staining seemed more common and more intense in those that included older individuals (**Supplementary Table 2**).

Deposition of C5b-9 might be more frequent in kidney tissues obtained with autopsy than biopsy or nephrectomy, as discussed in the previous section.

Staining of C5b-9 in the vascular wall is recognized as a positive control (19, 134). Staining in the vascular pole of the glomerulus was similarly common (**Figure 2A**). In addition to the explanation above, staining in association with the vasculature may reflect the recently discovered ability of renin to cleave C3 and activate the alternative pathway (101, 140).

Apart from the vasculature, deposition of C5b-9 in presumably healthy kidneys was less common and less intense than in most kidneys diseases, as shown in **Figures 1** and **2** and discussed hereafter.

NON-IMMUNOLOGICAL KIDNEY DISEASES

Minimal Change Nephropathy

In minimal change nephropathy, complement activation is not known to play a pathogenetic role. Complement factors and immunoglobulins are usually absent from the kidney. In line with this, deposition of C5b-9 was similar as in healthy kidneys, being absent from the glomerulus or weakly present as fine granules in the mesangium but not in the capillary wall, and more intense in the vascular wall, predominantly in areas of vascular hyalinosis and sclerosis (57, 61, 67, 70, 72, 75, 79, 81, 85–87, 96, 98, 113, 121, 128, 139, 141–143). Few studies reported slightly more frequent and intense staining in the glomerulus as compared with healthy kidneys (18, 116, 117). One study reported prominent deposits along Bowman's capsule (79). Deposits were furthermore focally present along the tubular basement membrane, concentrated in areas of tubulointerstitial injury (18, 57, 67, 70, 72, 75, 79, 96, 142, 143). Immunoelectron microscopy revealed that deposits were associated with striated membranous structures or cell remnants in the glomerular basement membrane, mesangium, podocyte foot processes, tubules, and vascular wall (72, 79).

Glomerular Basement Membrane Diseases

Patients with glomerular basement membrane disease, like Alport's syndrome, were used as negative controls. They had no or only traces of deposits of C5b-9 or other complement factors in the glomerulus (18, 85–87, 130, 139, 143), except for areas of glomerulosclerosis (96, 143). Reports were inconsistent as to whether they had deposits along the tubular basement membrane and in the vascular wall (18, 96, 130, 143).

Hypertensive Nephropathy

Hypertension can be regarded as a chronic smoldering inflammatory disease. It is associated—through unclear mechanisms—with activation of complement and formation of C5b-9, which contribute to vascular injury and end-organ dysfunction in animal models (40).

Glomerular deposits of C5b-9 were more common and extensive in patients with hypertensive nephropathy than in young women with hypertension or healthy individuals (44, 131), while deposits of C3 were absent (44, 67, 144). C5b-9

was found extensively in the mesangium, including the juxtaglomerular region, in a coarse granular pattern along Bowman's capsule but not or only focally along the capillary wall (44, 67) and sometimes along the tubular basement membrane (44, 67, 95, 143). It was predominant in glomerular and vascular areas of expansion, sclerosis, and hyalinization (44, 67, 143). Vascular staining was moderately intense and covered 10% of the arterial media, similar to hypertension without nephropathy but more intense and extensive than in healthy kidneys (44, 67, 84). The extent of staining in the media correlated with loss of smooth muscle cells in hypertension with or without nephropathy (r = 0.82 and r = 0.79, respectively) (84).

Preeclampsia

Preeclampsia, characterized by hypertension and proteinuria in pregnancy, is partly attributable to activation of complement in the placenta and along the endothelium elsewhere. It is associated with elevated levels of C5a and sC5b-9 in blood and urine, which explains why treatment with eculizumab has beneficial effects (32). The only study on deposits of C5b-9 found them rarely and segmentally in the glomerulus, mostly in areas of glomerulosclerosis. Other localizations were not evaluated (131).

Diabetic Nephropathy

Chronic hyperglycemia leads to glycation of proteins, referred to as advanced glycation end-products. These proteins may expose neoepitopes that are recognized by C1q and MBL, which activate the classical and lectin pathways. Glycation of factors that normally inhibit complement activation, like CD59, may enhance complement activation or directly induce formation of C5b-9. As a result, sC5b-9 circulates at higher levels in diabetes, is excreted in urine in diabetic nephropathy, and deposits in various organs affected by diabetes (27, 28, 30, 113, 145).

Glomerular deposits of C5b-9 were more common in patients with diabetic nephropathy than in healthy individuals (27, 28, 44, 72, 96, 113, 126, 139, 143). Deposits were found ubiquitously and granularly in the mesangium, coarsly along Bowman's capsule, and focally along the capillary wall (28, 44, 67, 70, 96, 126), although more along the capillary wall than in the mesangium in one study (113). Deposits were coarsely present along the tubular basement membrane with MBL and MASPs (28, 44, 67, 70, 72, 96, 126, 142) and in the vascular wall (28, 44, 67, 70, 72, 84, 96, 126), also with higher staining intensity than in healthy kidneys (28, 84). Intense staining in the glomerulus and vascular wall was likewise observed in a case of recurrent diabetic nephropathy after transplantation (113). Deposits were most extensive in glomerular, tubular, and vascular areas of expansion, sclerosis, hyalinization, and amyloidosis (28, 44, 67, 70, 72, 96, 126, 143) but absent from crescents (72, 96). Glomerular and vascular deposits were only slightly more frequent in diabetic nephropathy than in diabetes without kidney disease (27), as reproduced in **Figure 4A**.

Immunoelectron microscopy revealed that C5b-9 colocalized with cell membrane fragments in areas of glomerulosclerosis, in the glomerular basement membrane, tubular basement membrane, and vascular wall but not bound to epithelial, mesangial, or tubular cells (96, 126).

Histological Correlates

As reproduced in **Figure 4B**, glomerular deposits of C5b-9 were increasingly common in more severe cases of diabetic nephropathy (27). The extent to which staining covered the arterial media likewise increased from 10% in mild to 28% in severe diabetic nephropathy (84).

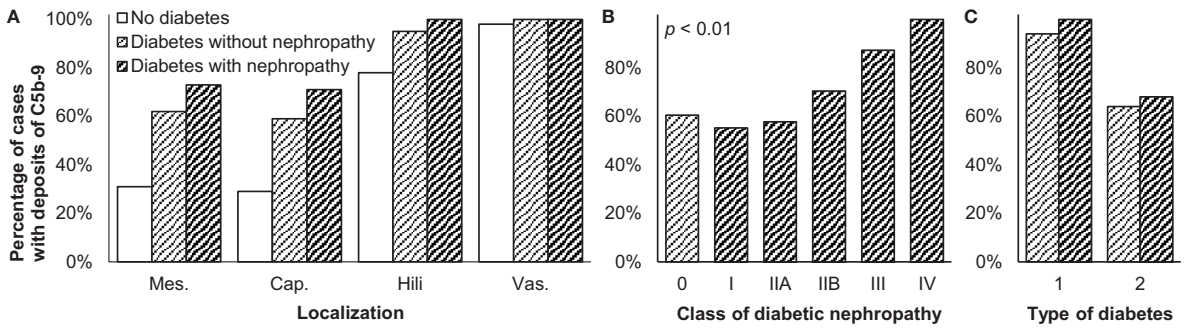

FIGURE 4 | Deposits of C5b-9 in diabetic nephropathy. **(A)** Presence of C5b-9 in the mesangium (mes.), along the glomerular capillary wall (cap.), in glomerular hili, and in the extraglomerular vascular wall (vas.) is compared between patients without diabetes or kidney disease (n = 41), patients with diabetes who had no nephropathy (n = 58), and patients with diabetic nephropathy (n = 101). **(B)** Presence of C5b-9 in the glomerulus is compared between patients with different classes of diabetic nephropathy (n = 101) according to the classification of the Renal Pathology Society (146). Patients with diabetes but without diabetic nephropathy (n = 58) are indicated as class 0. Differences between classes were tested with Spearman's correlation. We reproduced both panels without adaptations from their previous publication under the CC BY-NC-ND license (27), © International Society of Nephrology. **(C)** Presence of C5b-9 in the glomerulus is compared between patients with diabetes type 1 (n = 17) and type 2 (n = 120). It was different between diabetes types 1 and 2, both among patients without and with diabetic nephropathy, as tested with Fisher's exact test (both $p < 0.05$). The antibody used for staining in these three panels was unspecified. We plotted previously published data (27).

Staining intensity of C5b-9 was reported to correlate with the severity of histological lesions. In the glomerulus, it correlated with the degree of mesangial expansion; in both the glomerulus and tubules, it correlated with the degree of tubular injury and atrophy (27, 28, 96, 143). In the tubules and interstitium combined, it correlated with the number of interstitial infiltrating cells (ρ = 0.53, p < 0.01), interstitial volume (ρ = 0.56, p < 0.01), and the degree of tubular and interstitial inflammation and injury (ρ = 0.52, p < 0.01) (28). In the vascular wall, C5b-9 colocalized with glycated CD59 (113) and other advanced glycation end-products and apoptotic smooth muscle cells (84).

Clinical Correlates

Staining intensity of C5b-9 throughout the kidney was higher in patients with higher creatinine and more albuminuria. Staining intensity in the tubules and interstitium combined correlated weakly with levels of urine markers reflecting tubular injury. Staining did not correlate with the plasma level of sC5b-9 (28). One study found glomerular deposits more often in patients with diabetes type 1 than type 2, as shown in **Figure 4C**, possibly due to a longer disease duration (27).

KIDNEY DISEASES DUE TO IMMUNE COMPLEX DEPOSITION

Primary Membranous Nephropathy

Primary—formerly idiopathic—membranous nephropathy is caused by autoantibodies that bind antigens expressed by podocytes, in most cases PLA2R. These autoantibodies are predominantly of the IgG4 class, which cannot bind C1q and thus cannot activate the classical pathway. Rather, the lectin and alternative pathways are activated, given that C3, C4, FH, FB, and MBL, but not C1q, affect the risk of membranous nephropathy and are generally present in the subepithelial immune deposits. However, the pathways may be variably activated due to variation in the characteristics of the autoantibodies and their antigens, even during the disease's course. Autoantibodies of the IgG1 class directed against exostosin or neutral endopeptidase activate the classical pathway (24, 25).

Formation of C5b-9 is regarded essential for the development of kidney injury and proteinuria (24, 25). It disrupts proteins of organelles, the cytoskeleton, and slit diaphragm of podocytes. The urine level of sC5b-9—probably shed by podocytes—correlates with disease activity. In animal models, deficiency or inhibition of C5, C6, or C8 prevents deposition of C5b-9 and proteinuria (24, 25, 79, 123).

In line with this, staining of C5b-9 was more intense and extensive in membranous nephropathy than in healthy kidneys (18, 44, 67, 72, 75, 82, 96, 123, 139), also when recurring in a transplant (147). It was intense in the glomerulus (57, 81, 82, 139, 143, 148–151), always along the capillary wall, but not or hardly in the mesangium (18, 44, 67, 72, 75, 77, 79, 87, 98, 112, 123, 141, 147, 152–155), in a granular (77, 82, 112, 154), linear (123), or mixed pattern (79). It was furthermore focally found along Bowman's capsule (79, 152), as coarse granules along the tubular basement membrane (18, 44, 57, 67, 70, 72, 75, 79, 96, 112, 142), occasionally on tubular cells (79, 112), in the vascular wall (18, 57, 67, 72, 96, 112), in capsular adhesions, crescents, and glomerular and vascular areas of hyalinosis and sclerosis (44, 57, 67, 70, 72, 77, 96, 143). The extent of tubular staining varied widely between 10 and 88% (112). Not all studies specified included cases as specifically primary membranous nephropathy.

Immunoelectron microscopy revealed that C5b-9 was associated with striated membranous structures in immune deposits, basal membranes of adjacent podocyte foot processes, the glomerular basement membrane, and the mesangium, more often so in stage IV than I or II (72, 79, 152).

Histological Correlates

C5b-9 colocalized with immune deposits containing IgG, C3, and sometimes C1q and C4 in the capillary wall in all stages of primary membranous nephropathy (44, 67, 70, 72, 75, 77, 81, 82, 87, 96, 112, 139, 143, 147–149, 152, 154–156), except for stage I according to one report (72). It colocalized with causative autoantibodies in subepithelial immune deposits (150, 155, 156). By contrast, it was absent from the glomerulus where its inhibitors clusterin and CD59 were present (80, 82). Staining along the capillary wall correlated with mesangial hypercellularity (87), as illustrated in **Figure 5A**. Staining was more frequent in glomeruli with than without capsular adhesions (83 vs. 17%) (77). The extent of glomerular staining correlated with neither the stage of disease nor the extent of tubular staining (112). Tubular staining was concentrated in areas of interstitial inflammation and fibrosis and tubular atrophy (57, 70, 72, 96, 112), as reproduced in **Figure 5B**.

Clinical Correlates

Glomerular staining intensity correlated with the amount of proteinuria (57); patients with glomerular staining had more proteinuria than those without (3.6 vs. 2.3 g/d) (77). The extent of tubular staining correlated with creatinine (112), as reproduced in **Figure 5C**. Glomerular and tubular staining intensities of C5b-9 did not correlate with blood pressure, the nephrotic syndrome, hematuria, or serum levels of C4 or C3 (87, 112).

As illustrated in **Figure 5D**, glomerular staining intensity seemed associated with the outcome during treatment among children (87). In a case of lupus-like membranous nephropathy, however, staining remained unchanged despite decreased proteinuria after 40 weeks of treatment with intraveneus immunoglobulins (149).

Secondary Membranous Nephropathy

Secondary membranous nephropathy is caused by autoantibodies that circulate due to infections, autoimmune diseases, malignancies, or medication. They deposit in the subepithelial and often also the subendothelial space and activate the classical or lectin pathway (24, 25). Only few studies reported on deposition of C5b-9 in secondary membranous nephropathy. It was present in immune deposits in medication-induced membranous nephropathy stages II and III but not I (96, 157). It was

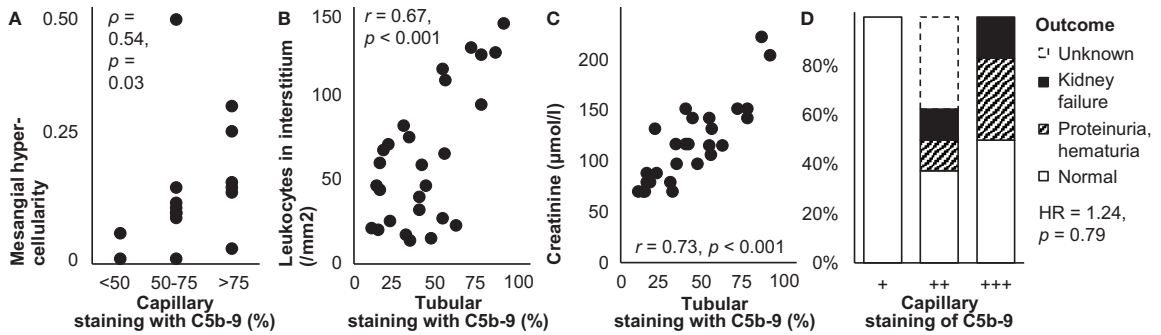

FIGURE 5 | Deposits of C5b-9 in primary membranous nephropathy: examples of correlations with histological lesions and clinical characteristics. **(A)** The extent of staining of C5b-9 in the capillary wall is shown in relation with mesangial hypercellularity scored on scale from 0–3 in children with idiopathic membranous nephropathy (n = 16). The antibody used for staining was unspecified. Relations were tested with Spearman's correlation (ρ). We plotted previously published individual data (87). **(B)** The extent of staining of C5b-9 in tubules is shown in relation with the number of leukocytes in the interstitium in patients with idiopathic membranous nephropathy (n = 27). **(C)** The extent of staining of C5b-9 in tubules is shown in relation with serum creatinine at the time of biopsy in patients with idiopathic membranous nephropathy (n = 27). Antibody aE11 was used for staining in both panels. Relations were tested with Pearson's correlation (r). We reproduced both panels without adaptations from their previous publication with permission (112), © European Renal Association–European Dialysis and Transplant Association. **(D)** The extent of staining of C5b-9 in the capillary wall is shown in relation with the clinical outcome after 14-171 months of treatment in children with idiopathic membranous nephropathy (n = 16). The antibody used for staining was unspecified. The hazard ratio (HR) for kidney failure, proteinuria, or hematuria as compared with normal outcomes is given as estimated with Cox's regression. We plotted previously published individual data (87).

similarly found in immune deposits along the capillary wall in membranous nephropathy due to hepatitis B (152)—although not in all cases (77)—where it colocalized with HBe and sometimes HBs (152).

IgA Nephropathy

In IgA nephropathy, galactose-deficient IgA due to aberrant glycosylation is bound by autoantibodies and deposits as immune complexes in the mesangium. There, it causes mesangial expansion and inflammation with widely varying histological and clinical presentations (15, 17).

Circulating and deposited IgA–containing immune complexes can activate the alternative and lectin pathways but not the classical pathway. C3, FH, and properdin of the alternative pathway and sometimes C4d, MBL, and MASPs of the lectin pathway deposit in the mesangium too. C1q of the classical pathway is only infrequently present. Whether only the alternative or also the lectin pathway is activated probably varies between patients (15, 17, 158). As their end-product, the urine level of sC5b-9 is elevated and associates with disease severity. Inhibiting the formation of C5b-9 with eculizumab has inconsistent beneficial effects in patients (15, 17, 21, 158, 159).

In small comparative studies, all or almost all patients with IgA nephropathy had deposits of C5b-9 in the glomerulus that were more intense, more diffuse, and more coarse than in healthy individuals (44, 52, 67, 72, 75, 81, 96, 97, 124, 128, 139). All individual components of C5b-9 were two to four times more abundant in the glomerulus in patients with stable IgA nephropathy than in healthy individuals as quantified with mass spectrometry (124).

Mostly small descriptive studies found C5b-9 as coarse granules in the glomerulus (57, 58, 72, 76, 81, 137, 139, 143, 158, 160, 161)—always in the mesangium, sometimes also along the capillary wall (19, 44, 52, 67, 75, 96, 97, 110, 115, 124, 128, 162–166), in one case report only along the capillary wall (159)—, along Bowman's capsule (52, 162, 163), as coarse granules (19, 44, 52, 57, 70, 72, 75, 96, 97, 110, 115, 163) or linearly (110, 115) along the tubular basement membrane and occasionally on tubular cells (110), and in the vascular wall (19, 52, 57, 67, 72, 96, 110, 115, 137, 162). Deposits along the capillary wall were localized in the subepithelial space (97, 164). The extent of staining in tubules varied widely between 19 and 87% (110, 115). Deposits were furthermore present in areas of mesangial expansion and in glomerular and vascular areas of amyloidosis, hyalinosis, and sclerosis (19, 44, 57, 67, 72, 75, 96, 97, 143) but not in crescents (19, 72, 96, 97). Among patients with IgA nephropathy or IgA vasculitis with nephritis together, deposits were less frequent in the mesangium and vascular wall (19, 167). One case of IgA nephropathy with thrombotic microangiopathy exhibited no deposits (130).

Immunoelectron microscopy revealed deposits of C5b-9 in various patterns: as homogeneous fine granules along the glomerular basement membrane in the paramesangial region, as rings or ribbons associated with striated membranous structures or cell remnants in the glomerular basement membrane, subepithelial space, mesangium, tubular basement membrane, and vascular wall, and as patches in electron-dense deposits in the mesangium (72, 97).

Histological Correlates

Glomerular deposits of C5b-9 colocalized with IgA and C3–containing immune complexes (44, 52, 57, 67, 70, 72, 75, 76, 81, 96, 97, 110, 128, 137, 143, 158, 160, 161, 165). Their staining was less intense than that of IgA (52, 76, 137). The localization and intensity of their staining correlated with those of C3 mRNA expression (128).

Various studies reported a relation between staining of C5b-9 and histological lesions. Glomerular staining intensity

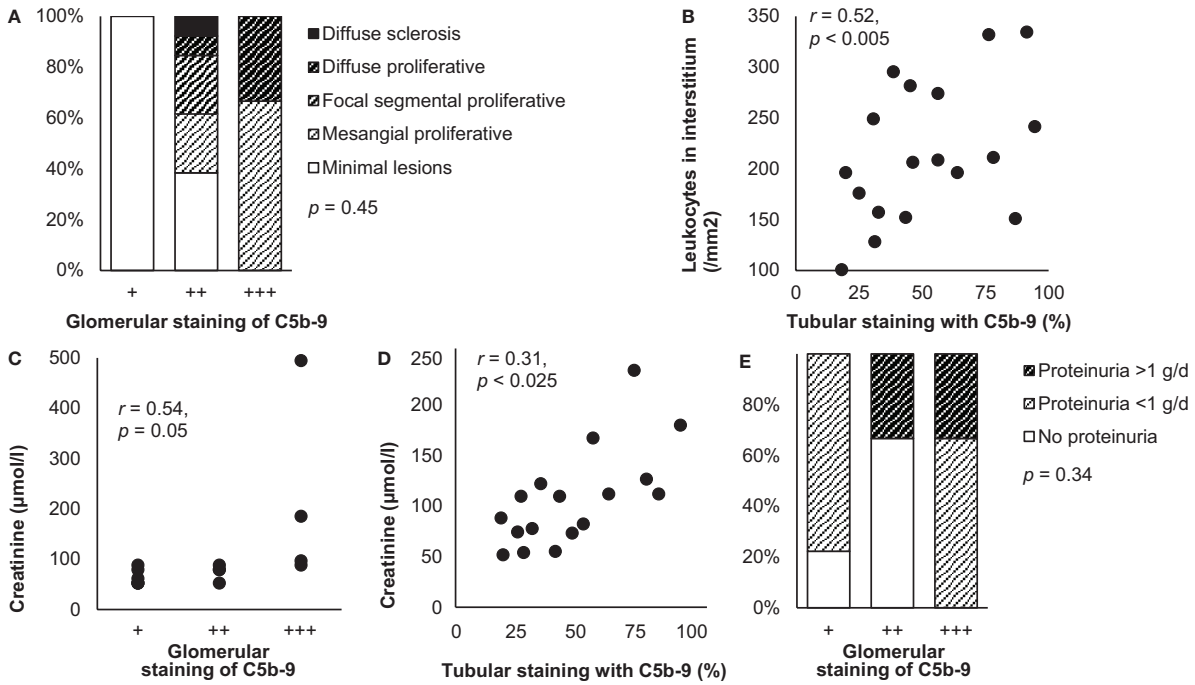

FIGURE 6 | Deposits of C5b-9 in IgA nephropathy: examples of correlations with histological lesions and clinical characteristics. **(A)** Staining intensity of C5b-9 in the glomerulus is shown in relation with histological patterns in patients with IgA nephropathy (n = 18). Antibody anti-MAC-neo was used for staining. Differences between staining intensities were tested with Fisher's exact test. We plotted previously published individual data (52). **(B)** The extent of staining of C5b-9 in tubules is shown in relation with the number of interstitial monocytes and macrophages in patients with IgA nephropathy (n = 18). Antibody aE11 was used for staining. We reproduced this panel without adaptations from its previous publication with permission (110), © European Renal Association–European Dialysis and Transplant Association. **(C)** Staining intensity of C5b-9 in the glomerulus is shown in relation with serum creatinine at the time of biopsy in patients with IgA nephropathy (n = 14). Antibody aE11 was used for staining. We plotted previously published individual data (128). **(D)** The extent of staining of C5b-9 in tubules is shown in relation with serum creatinine at the time of biopsy in patients with IgA nephropathy (n = 18). Antibody aE11 was used for staining. We reproduced this panel without adaptations from its previous publication with permission (110), © European Renal Association–European Dialysis and Transplant Association. Relations were tested with Pearson's correlation (r). **(E)** Staining intensity of C5b-9 in the glomerulus is shown in relation with proteinuria at the time of biopsy in patients with IgA nephropathy (n = 18). Antibody anti-MAC-neo was used for staining. Differences between staining intensities were tested with Fisher's exact test. The relatively small number of patients may explain why proteinuria <1 g/d was not observed in the group with a staining intensity of ++. We plotted previously published individual data (52).

correlated with the extents of mesangial expansion and hypercellularity, glomerulosclerosis, interstitial inflammation, interstitial fibrosis, and tubular atrophy (57, 115, 128, 137, 139, 163). It also seemed correlated with the extent of proliferative glomerulonephritis (52), as illustrated in **Figure 6A**. Individual components of C5b-9 were two times more abundant in patients with than without global mesangial hypercellularity, endocapillary hypercellularity, or moderate to extensive interstitial fibrosis or tubular atrophy but equally abundant in patients with or without glomerulosclerosis (124). Glomerular deposits were more frequent when capsular adhesion and crescents were present (76), while those with cellular or fibrocellular crescents had more intense staining (166). Deposits seemed also more frequent in the glomerulus (27 vs. 12%, p = 0.06) and vascular wall (68 vs. 46%, p = 0.06) when thrombotic microangiopathy was present (167). Global glomerular staining was associated with loss of podocytes (r^2 = 0.18, $p < 0.05$), perhaps due to their lower expression of CR1 (r^2 = 0.45, $p < 0.05$), which antagonizes complement activation (164). Tubular staining intensity correlated with the extents of interstitial inflammation and fibrosis and tubular atrophy (57, 72, 96, 110, 115), as reproduced in **Figure 6B**.

Although the aforementioned studies included children, two studies including only children did not find any correlation between glomerular or tubular staining and histological lesions (19, 97).

Clinical Correlates

Various studies also reported a relation between staining of C5b-9 and clinical outcomes. Glomerular and tubular staining intensities of C5b-9 correlated with creatinine (110, 115, 128), as shown in **Figures 6C, D**. They were also higher in patients with heavy proteinuria or the nephrotic syndrome (19, 52, 163), as illustrated in **Figure 6E**, although these correlations did not hold in sensitivity analyses (19). Amounts of its individual components in microdissected glomeruli were higher when blood pressure was higher or when eGFR was lower but not related to proteinuria (124). A correlation between glomerular staining intensity and age was reported without further details (137). Otherwise, staining was not related with age, sex,

hematuria, serum levels of immunoglobulins, C3, or C4, or disease duration (19, 52, 76, 97, 110, 128, 137).

Glomerular deposits of C5b-9 were more often present (41 vs. 89%, unadjusted odds ratio 12, $p = 0.004$) and stained more intensely in progressive as compared with stable IgA nephropathy (158). Amounts of C5 through C9 were about twice as high in the former as compared with the latter, which was among the largest difference of all studied proteins (124).

Among children with IgA nephropathy or IgA vasculitis with nephritis, those with deposits of C5b-9 in the glomerulus or tubules received immunosuppressive medication more often than those without deposits (89 vs. 62%, $p = 0.02$) and had, probably as a result, a shorter time to recovery (unadjusted hazard rate 0.17, $p = 0.02$) (19). In adults who had C5b-9 in more than half of the tubules, creatinine increased from 150 to 248 μmol/l during a mean follow-up of 30 months, while it remained stable around 88 μmol/l in those who had less tubular deposits (110). An undefined relation between glomerular and tubular staining intensities and creatinine after a longer follow-up was reported too (115).

IgA Nephropathy With Complement Factor Deficiency

Mild forms of IgA nephropathy were reported in patients with complement factor deficiencies limiting formation of C5b-9, in whom disease could arise from sublytic effects of incomplete C5b-9. Two children with a congenital C9 deficiency developed IgA nephropathy with mesangial deposits of C3, C5, and C8 but not C9 or C5b-9. Their histological lesions were only mild, eGFR remained normal, and proteinuria resolved spontaneously (78). An adolescent with IgA nephropathy and homozygous C3 deficiency exhibited weak mesangial staining of C5b-9 together with immunoglobulins, C1q, C4, and properdin but not C3. He too had only mild histological abnormalities (93). An adult man with C9 deficiency suffered from progressive IgA nephropathy without deposition of C5b-9 (151).

IgA Vasculitis With Nephritis

IgA vasculitis—or Henoch-Schönlein purpura—can present with a nephritis that closely resembles IgA nephropathy, so that some regard it as a systemic form of IgA nephropathy. Activation of the alternative and lectin pathways are similarly thought to underlie the nephritis (168, 169). In the few studies conducted specifically on patients who had IgA vasculitis with nephritis, deposits of C5b-9 were present in the mesangium and capillary wall, colocalized with IgA and C3–containing immune complexes (52, 61, 75, 85, 99, 139), along the tubular basement membrane, and in the vascular wall (75, 96). Mesangial deposits of C5b-9 were less common in patients with mesangial deposits of IgA1 only, in whom the alternative pathway was activated, than in those with deposits of both IgA1 and IgA2, in whom the lectin pathway was also activated (73 vs. 100%). Four patients without deposits of C5b-9 had less intense staining of IgA and C3 but paradoxically more proteinuria than 27 with deposits (median 210 vs. 80 mg/dl) (85). Deposits of C5b-9 were not different between children with IgA vasculitis or IgA nephropathy but were less clearly associated with prognosis in the former (19).

Lupus Nephritis

Autoantibodies that circulate in SLE give rise to lupus nephritis when they form or deposit as immune complexes in the glomerulus. They activate the classical pathway, reflected in most patients by specific full-house deposition of IgG, IgA, IgM, C1q, and C3. Activation of the alternative pathway, seems essential too, given that more C3 than C4 deposits, that deficiencies of factors of the alternative pathway, like FB and FD, ameliorate lupus nephritis, and that deficiencies of its inhibitory factors, like FH, promote lupus nephritis in animal models (10, 11).

Formation of C5b-9 may be both a cause and consequence of deposition of immune complexes and cellular injury (11, 119). Levels of sC5b-9 are elevated in blood and urine of patients and correlate with disease activity. Pointing to a causative role, inhibition of C5 reduces histological lesions, proteinuria, and mortality in animal models, while eculizumab exerts beneficial effects in patients (10, 11).

In line with such a role, glomerular and tubular deposits of C5b-9 were more common in patients with lupus nephritis than healthy individuals (18, 44, 46, 67, 72, 75, 81, 96, 111, 119, 133, 139). Descriptive studies on mostly small numbers of patients reported ubiquitous deposits in the glomerulus (18, 46, 58, 72, 77, 81, 95, 96, 111, 119, 133, 139, 143, 170, 171)—both in the mesangium and along the capillary wall (18, 44, 57, 67, 75, 111, 172–174) and sometimes along Bowman's capsule (119, 171) —, linearly or granularly along the tubular basement membrane (18, 44, 57, 67, 70, 72, 75, 95, 96, 119, 142, 151, 171), and in the vascular wall (18, 57, 67, 72, 95, 96, 119, 171). Deposits were also present in glomerular and vascular areas of hyalinization, sclerosis, and fibrinoid necrosis (44, 57, 67, 70, 95, 96, 143) but not in crescents (72, 96, 171).

Deposits of C5b-9 were mainly located in the mesangium in lupus nephritis class II, III, or IV and granularly along the subepithelial side of the capillary wall in class V, although mesangial deposits often extended into the capillary walls and vice versa (18, 77, 95, 111, 152, 172). They colocalized with immune deposits containing immunoglobulins and other complement factors in all classes (44, 46, 57, 67, 70, 72, 75, 77, 81, 95, 96, 143, 152, 172, 173). Glomerular, but not tubular, staining of C5b-9 was more intense in more severe classes, increasing from I and II to III and V and being strongest in class IV (18, 95, 111, 119, 139, 171, 174). In lupus nephritis with thrombotic microangiopathy, staining intensity was variable in the glomerulus and strong in the vascular wall (100, 130, 175).

Immunoelectron microscopy revealed that C5b-9 was associated with immune deposits, striated membranous structures, and partly shedded cell membrane extensions or with cell membrane fragments in the mesangium, the capillary wall, and glomerular basement membrane without signs of cellular lysis (95, 96, 152, 172). Some cell membrane fragments in the glomerular basement membrane appeared to be infolding degraded parts of podocytes (170, 172). C5b-9 was furthermore

associated with structural defects of the tubular basement membrane (95).

Histological Correlates

Staining intensity of C5b-9 correlated with those of immunoglobulins and C3 (70) and with loss of podocytic expression of CR1 (111). Glomerular staining intensity of C5b-9 did not consistently correlate with histological signs of active or chronic nephritis. In a small study, it correlated with the activity index (111), but in other studies it rather correlated with the chronicity index, although weakly (174), or with neither index (18, 171). It did not correlate with the number of macrophages in the glomerulus (18). Tubular staining colocalized with interstitial inflammation (70, 95) and correlated with interstitial fibrosis (18, 57, 72, 96), as reproduced in **Figure 7**. The extents of glomerular and tubular staining of C5b-9 did not correlate mutually (95, 171).

Clinical Correlates

Correlations between deposits of C5b-9 and clinical characteristics were studied little. Patients with lupus nephritis class V and other types of membranous nephropathy had more proteinuria if they had deposits in the capillary wall (3.6 vs. 2.3 g/l, $p < 0.02$) (77). Patients with various classes of lupus nephritis were more often men (39 vs. 6%, $p = 0.06$), had higher blood pressure (133/82 vs. 117/70 mmHg, $p < 0.03$) and seemed more frequently to have low serum levels of C3 (92 vs. 65%, $p = 0.10$) (171) and C4 (57) if they had deposits in the glomerulus. There were no correlations with age, race, symptoms of SLE, medication, creatinine, hematuria, hemoglobin, albumin, or serum level of anti-dsDNA autoantibodies (18, 77, 171).

Glomerular deposits of C5b-9 seemed to predict treatment effect: patients with deposits responded less often, with an unadjusted odds ratio of 0.60 ($p = 0.58$) for any response after a year of treatment (18) and a multivariate-adjusted odds ratio of 0.22 for any response after six months of treatment (171). Their staining intensity seemed to correlate with treatment effect too, although the change in intensity in biopsies repeated after treatment did not (18), as illustrated in **Figure 3C**. In a case of recurrent lupus nephritis class II, mesangial staining was similar as in a first biopsy taken 5 years earlier, while staining of immunoglobulins and other complement factors had increased (170).

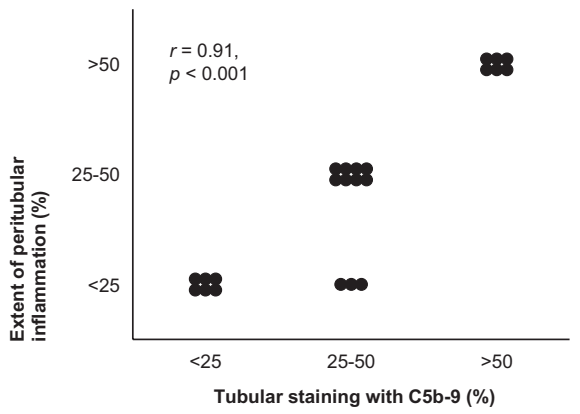

FIGURE 7 | Deposits of C5b-9 in lupus nephritis: examples of correlations with histological lesions and clinical characteristics. The extent of staining of C5b-9 in tubules is shown in relation with the extent of peritubular inflammation in patients with lupus nephritis class II, III, IV, or V ($n = 22$). The antibody indicated as Kolb 1975 in **Table 2** was used for staining. The relation was tested with Pearson's correlation (r). We reproduced this panel without adaptations from its previous publication with permission (95), © Rockefeller University Press.

Lectin Pathway

The lectin pathway has recently been suspected to contribute to the pathogenesis of lupus nephritis. Polymorphisms of MBL increase the risk of lupus, its circulating level is high in patients with lupus nephritis, and it frequently deposits in their kidneys (18, 24, 176). Glomerular deposits of C5b-9 and MBL concurred in 82% and their staining intensities correlated well in eleven patients with lupus nephritis. C5b-9 and MBL were also deposited in Bowman's capsule, tubules, and the vascular wall (119).

Membranoproliferative Glomerulonephritis

Immune complex-mediated membranoproliferative glomerulonephritis is regarded a disease of an activated classical pathway, elicited by deposition of immunoglobulins and subsequently leading to codeposition of complement factors. Deposits of C5b-9 were present with immune complexes along the capillary wall (108), although C5 through C9 were only rarely detected with mass spectrometry of microdissected glomeruli (90). In two teenagers treated with eculizumab, the extent of glomerular staining decreased slightly and histological inflammation improved, but GFR and proteinuria improved in only one of both. With similar clinical characteristics and serum complement levels, the successfully treated case differed only by exhibiting histological thrombotic microangiopathy (108).

KIDNEY DISEASES DUE TO ALTERNATIVE PATHWAY ACTIVATION

C3 Glomerulopathy

C3 glomerulopathy is regarded a disease of an activated alternative pathway, characterized by deposition of C3 but no or scarce deposition of immunoglobulins or other complement factors. Before this pathogenetic distinction, C3 glomerulopathy and immune complex-mediated membranoproliferative glomerulonephritis were together classified into membranoproliferative glomerulonephritis types I, II, and III according to the localization of immune deposits. An essential role of C5 has been demonstrated in animal models of membranoproliferative glomerulonephritis and C3 glomerulopathy, but rather through effects of C5a on its receptor than formation of C5b-9. Deficiency or inhibition of C5 or the C5a receptor, reduces histological lesions, creatinine, proteinuria, and mortality, whereas deficiency of C6—preventing

deposition of C5b-9—does not (177, 178). Correspondingly, inhibition of C5 with eculizumab has beneficial effects in only a subset of patients (4, 5, 7–9).

C3 glomerulopathy is subdivided into C3 glomerulonephritis and dense deposit disease according to the microscopic appearance of electron-dense immune deposits in the glomerular basement membrane (4, 5). As a possible difference in pathogenesis, formation of C5b-9 is presumed to be more pronounced in C3 glomerulonephritis than dense deposit disease (4–6). Individual components of C5b-9 were indeed more abundant in microdissected glomeruli in the former when quantified with mass spectrometry (5, 91, 92), although immunofluorescence staining of C5b-9 was similar in both disease subtypes (103). Staining intensity in both was higher than in healthy kidneys (103) and correlated with those of C3 and FHR5 (102).

In C3 glomerulonephritis, C5b-9 was found in the mesangium, along the capillary wall, Bowman's capsule, most of the tubular basement membrane, and in the vascular wall (102, 103, 107, 179, 180). Serial biopsies revealed that glomerular staining of C5b-9 and other complement factors increased as the disease progressed (102, 106, 107), regressed during three months to 3 years of treatment with eculizumab along with histological and clinical improvement in three patients (106, 107) but remained unchanged during four months to a year of treatment with eculizumab despite varying histological and clinical responses in three other patients (102, 103).

In dense deposit disease, staining of C5b-9 was intense in the glomerulus (57, 75, 101, 103, 105, 181), similarly when recurring after kidney transplantation (102, 182). They surrounded immune deposits in the mesangium, along the capillary wall, and diffusely along the tubular basement membrane and additionally formed granules along the interstitial side of the tubular basement membrane (44, 103, 126, 181). Treatment with eculizumab resulted in disappearance of their staining after 13 to 18 months in two patients, but unaltered staining after three months to a year in three other patients, with histological and clinical improvement in all five (101, 103, 105, 106).

In a study on patients with C3 glomerulonephritis or dense deposit disease together, median eGFR was 15 ml/min/1.73 m^2 lower ($p = 0.03$) if glomerular staining of C5b-9 was maximally intense than less intense (102).

Deposition of C5b-9 was reported to be similar in membranoproliferative glomerulonephritis types I, II, and III (75). In membranoproliferative glomerulonephritis type I, deposits of C5b-9 were practically always present in the glomerulus—both in the mesangium and capillary wall similarly to immune deposits —, frequently along the tubular basement membrane (44, 57, 67, 72, 75, 96, 114, 139, 143), and in the vascular wall (57, 67, 72, 96) with variable but higher staining intensity than in healthy kidneys. They surrounded immune deposits in the mesangium, along the capillary wall, and along the tubular basement membrane (44, 72, 96). Immunoelectron microscopy revealed that they were also associated with striated membranous structures in extracellular matrix and with partly shedded cell membrane extensions of mesangial, endothelial, and epithelial cells without signs of cellular lysis (96). Glomerular, tubular, and vascular deposits were concentrated in areas of sclerosis (44, 57, 67, 72, 96). Glomerular staining intensity correlated with the serum level of sC5b-9 (114). In two children with unspecified types of membranoproliferative glomerulonephritis, of whom only one had deposits of C5b-9 in the glomerulus and along the tubular basement membrane, frequent relapses despite treatment occurred in the one with deposits, whereas the one without deposits reached complete remission after seven months (98, 141).

Postinfectious Glomerulonephritis

Postinfectious glomerulonephritis is often clinically indistinguishable from C3 glomerulopathy and may be regarded an acute variant of a similar pathogenesis (4, 5). Deposits of C5b-9 were found along with immune deposits in the mesangium, along the capillary wall, the tubular basement membrane, and in the vascular wall with higher intensities than in healthy kidneys (67, 86, 143, 183, 184). Staining was restricted to the capillary wall in cases biopsied two weeks after the disease's onset but increasingly extended into the mesangium after three weeks (183). Glomerular staining intensity was not correlated with age, disease duration, blood pressure, creatinine, proteinuria, hematuria, endocapillary hypercellularity, or crescents, but the number of subepithelial hump-like immune deposits—considered characteristic of postinfectious glomerulonephritis—was higher when staining was intenser (median 0.2 vs. 0.5 per glomerulus, $p = 0.002$) (86).

Thrombotic Microangiopathy

aHUS is a thrombotic microangiopathy caused by genetic mutations or autoantibodies that activate the alternative pathway, eventually leading to formation of C5b-9 on endothelial cells. In animal models of aHUS, deficiency or inhibition of C5 reduces the thrombotic microangiopathy and histological lesions, creatinine, kidney failure, and mortality. Contrary to C3 glomerulopathy, these effects are brought about through formation of C5b-9 rather than C5a. Deficiency of C6 or C9—preventing deposition of C5b-9—has similar effects as deficiency or inhibition of C5, whereas deficiency of the C5a receptor does not (185, 186). In patients, inhibition of C5 with eculizumab has become standard treatment (12, 187). Regarded a typical finding (12), intense staining of C5b-9 was present in almost all biopsies, in the mesangium, along the capillary wall, along the tubular basement membrane, and predominantly in the vascular wall (75, 103, 130, 188) but not in peritubular capillaries (130). An example is shown in **Figure 2B**. In a late-stage case, staining was weak in the mesangium, absent from the capillary wall, and intense in the vascular wall (100). Staining in recurrent aHUS after transplantation was similar to that in native kidneys (130). Despite its beneficial effects, staining of C5b-9 remained unchanged after treatment with eculizumab (103).

In STEC-HUS, the alternative pathway is activated by direct and indirect effects of the Shiga toxin (189). Although deposition

of C5b-9 was found granularly along the capillary wall, in the vascular pole, and in the vascular wall of peritubular capillaries in a child (122) and diffusely in the glomerulus in an adult (190), it was not found in the kidney in eleven other adult patients (130, 153). In line with this, treatment with eculizumab has only exerted beneficial effects in a few children (122, 153).

The alternative pathway is also activated in TTP (120). Deposition of C5b-9 was found along the capillary wall in few glomeruli, in few tubules, in the vascular wall but not in peritubular capillaries, without clear clinical or histological correlates (120, 132).

Thrombotic microangiopathy after hematopoietic stem cell transplantation is characterized by variable complement activation (191). C5b-9 stained moderately in the mesangium and capillary wall in one case, weakly in only the mesangium in another case, and strongly in the vascular wall in both cases. Similar staining was found before and after treatment with eculizumab in one of them (100).

Thrombotic microangiopathy elicited by hypertension has been postulated as often attributable to genetic mutations or autoantibodies that activate the alternative pathway. Supporting this postulation, C5b-9 was often deposited together with C3 and C4d along the capillary wall, segmentally in the vascular pole, and always in the vascular wall in patients with hypertension-associated thrombotic microangiopathy. Staining was intense, though weaker in recurrent cases after transplantation. Staining intensity did not correlate with age, sex, blood pressure, the plasma level of sC5b-9, or disease severity but seemed to correlate with proteinuria and correlated with complement activity, as illustrated in **Figure 8**. Treatment with eculizumab prevented progression to end-stage kidney disease and recurrence after transplantation (144, 192, 193).

In a heterogenous group of patients with thrombotic microangiopathy, the localization and intensity of staining of C5b-9 did not correlate with the presence of immunoglobulins or histological signs of active thrombotic microangiopathy (100).

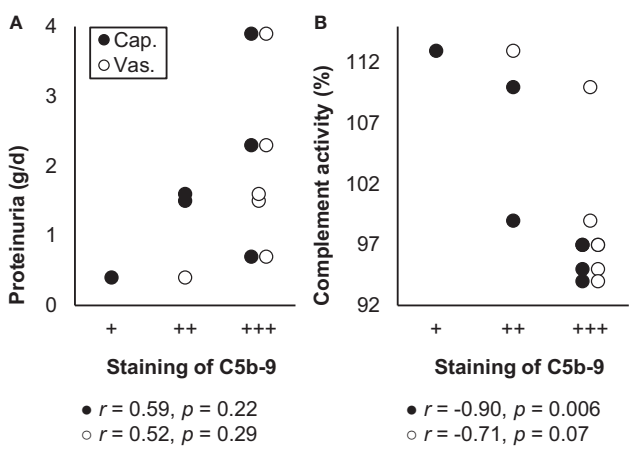

FIGURE 8 | Deposits of C5b-9 in hypertension-associated thrombotic microangiopathy: examples of correlations with histological lesions and clinical characteristics. Staining intensity of C5b-9 along the glomerular capillary wall (cap.) and in the extraglomerular vascular wall (vas.) is shown in relation with **(A)** proteinuria and **(B)** plasma complement activity (CH50) at the time of biopsy in patients with hypertension-associated thrombotic microangiopathy (n = 6). The antibody used for staining was unspecified. Relations were tested with Pearson's correlation (r). We plotted previously published individual data (192).

VASCULITIS

ANCA-associated vasculitis manifests as a crescentic and necrotizing glomerulonephritis with scarce deposits of immunoglobulins or complement factors, referred to as pauci-immune. Nonetheless, factors of the alternative pathway, including C3, FB, and properdin, can be found in the glomerulus. Activation of the alternative pathway and the subsequent formation of C5a are essential in its pathogenesis, while their inhibition attenuates the development of kidney injury in both animal models and human patients (14, 22, 23).

Staining of C5b-9 was more frequent and more intense in patients with ANCA-associated vasculitis than in healthy individuals (22, 116, 139). It was found in the glomerulus (53, 116, 139, 143, 194), both in the mesangium and along the capillary wall (22, 116), in a patchy and granular pattern, colocalized with C3d, FB, and properdin (22, 116, 143, 194). Staining was predominant in glomeruli with crescents (116, 194). It was furthermore seen granularly in the vascular wall (22, 116). No glomerular or vascular staining was found in one case with thrombotic microangiopathy (130).

Glomerular staining intensity of C5b-9 was lower in glomeruli that were normal, mildly hypercellular (116), or focally affected (53), as illustrated in **Figures 9A, B**. It correlated with proteinuria (r = 0.63, p < 0.001) in one (22) but not another study (53). The frequency, extent, and intensity of glomerular staining of C5b-9 did not correlate with the type of ANCA, clinical vasculitis activity, eGFR, serum and urine levels of sC5b-9 or C3, the presence of glomerulosclerosis, crescents, thrombotic microangiopathy, interstitial fibrosis, or tubular atrophy, or the occurrence of end-stage renal disease or death (22, 53, 116, 194), except for a trend toward higher creatinine in patients with more intense staining (116), as illustrated in **Figure 9C**.

Similar findings were reported for patients with ANCA-negative pauci-immune crescentic glomerulonephritis. They had granular deposits of C5b-9 in the mesangium, along the capillary wall, and in the vascular wall, more often and more intense than in healthy kidneys. Deposits were predominant in crescents. They colocalized well with C3d and, if present, C4d and FB. Glomerular staining intensity did not correlate with age, sex, hemoglobin, proteinuria, or dependence on dialysis but correlated with creatinine (117), as shown in **Figure 9D**.

Among patients with idiopathic rapidly progressive glomerulonephritis, of whom three-quarters were ANCA-positive, deposits of C5b-9 were present in the glomerulus, the vascular wall, and a third of the tubules and prominent in fibrocellular and fibrous crescents. Staining was independent of presence and type of ANCA. Tubular, but not glomerular,

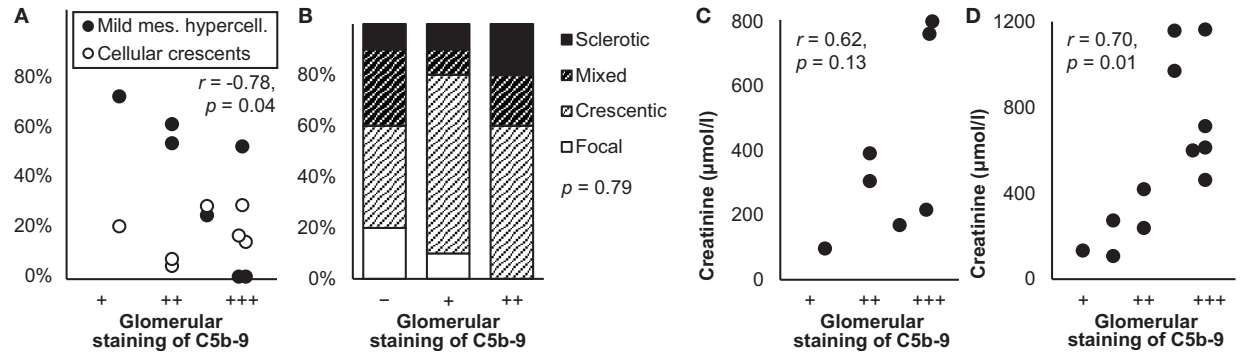

FIGURE 9 | Deposits of C5b-9 in ANCA-associated vasculitis: examples of correlations with histological lesions and clinical characteristics. **(A)** The average staining intensity of C5b-9 in glomeruli is shown in relation with the percentage of glomeruli with mild mesangial hypercellularity and that with cellular crescents in patients with myeloperoxidase antineutrophil cytoplasmic antibody (ANCA)-associated vasculitis (n = 7). The antibody used for staining was unspecified. The correlation coefficient for mild mesangial hypercellularity is given; that for cellular crescents was nonsignificant. We plotted previously published individual data (116). **(B)** Staining intensity of C5b-9 in the glomerulus is shown in relation with histological patterns in patients with renal ANCA-associated vasculitis (n = 25). Antibody ab55811 was used for staining. Differences between staining intensities were tested with Fisher's exact test. We plotted previously published individual data (53). **(C)** The average staining intensity of C5b-9 in glomeruli is shown in relation with serum creatinine at the time of biopsy in patients with myeloperoxidase antineutrophil cytoplasmic antibody (ANCA)-associated vasculitis (n = 7). The antibody used for staining was unspecified. We plotted previously published individual data (116). **(D)** The average staining intensity of C5b-9 in glomeruli is shown in relation with serum creatinine at the time of biopsy in patients with ANCA-negative pauci-immune crescentic glomerulonephritis (n = 12). The antibody used for staining was unspecified. We plotted previously published individual data (117). Relations were tested with Pearson's correlation (r).

staining of C5b-9 correlated with markers of inflammation and fibrosis, creatinine, and a lack of treatment effect (195, 196).

GENERAL PATTERNS OF KIDNEY INJURY

Interstitial Nephritis

Formation of C5b-9 participates in the development of interstitial inflammation and fibrosis, but the mechanisms are unclear (197). As one explanation, the alterative pathway may be activated in the tubules and peritubular interstitium due to modification of C3 by ammonia, produced as a result of proteinuria (198). The C5b-9 formed there is partly excreted in the urine, more so in severe forms of acute tubulointerstitial nephritis (31).

In patients with acute tubulointerstitial nephritis, staining of C5b-9 was weak in the glomerulus and vascular wall, similar to healthy kidneys (70, 96, 143, 199) but more intense in the interstitium and along the tubular basement membrane as compared with healthy kidneys or kidneys with acute tubular necrosis (31, 70, 199). It covered 39% of tubules (31). Tubular and vascular staining were most diffuse and intense in areas of interstitial inflammation and fibrosis (70, 96, 139, 143). Across various underlying glomerulopathies, the extent and intensity of tubular staining correlated with the severity of interstitial inflammation (r = 0.84, $p < 0.001$) and interstitial volume (r = 0.79, $p < 0.001$) (139).

Patients with juvenile nephronophthisis, a congenital ciliopathy with chronic tubulointerstitial nephritis and tubular cysts, also had more frequent and more intense tubular staining than healthy individuals. Staining was associated with signs of apoptosis and striated membranous structures (118).

Acute Tubular Necrosis

Deposition of C5b-9 in tubules—and elsewhere in the kidney—has been proposed as a physiological mechanism for removal of cell remnants (94), but it is also a pathogenic mechanism by which activation of the alternative pathway causes kidney injury after ischemia and reperfusion, a common cause of acute tubular necrosis (136, 197, 200), or during proteinuria (20, 198, 201). In animal models of ischemia and reperfusion injury and of proteinuria, deficiency of C5 or C6 protects against tubular deposition of C5b-9 and acute tubular necrosis (198, 201, 202).

Patients with acute tubular necrosis had segmental thick linear deposits of C5b-9 along the tubular basement membrane, primarily in proximal tubules and atrophic tubules and similarly to C3 (94, 135, 136, 200). Tubular, but not glomerular or vascular, deposits were more frequent, widespread, and intense than in patients without tubular atrophy and necrosis or without kidney disease (94, 136). Deposits were not seen in or on tubular cells (136). They covered 15% of tubules in acute tubular necrosis due to medication or autoimmune disease (31), but the majority of tubules in most cases of acute tubular necrosis due to medication, sepsis, or ischemia-reperfusion after kidney transplantation (136).

Six autopsy cases of COVID19 with acute loss of eGFR exhibited common acute tubular necrosis, variable interstitial inflammation, and minimal glomerular lesions. All had deposits of C5b-9 on tubular cells, together with viral antigens, while two had sparse deposits in the glomerulus and in the vascular wall (125).

One case of adenovirus-associated hemorrhagic cystitis, characterized by severe tubular degeneration and necrosis, but

minimal interstitial inflammation or glomerular lesions, had coarse granular deposits of C5b-9 along the tubular basement membrane and, with less intensity, along Bowman's capsule. They colocalized with C3 and adenoviral antigens (203).

Across various glomerulopathies, the extent and intensity of tubular staining of C5b-9 correlated with the extents of degenerative lesions of the tubular basement membrane, including thickening (r = 0.51, $p < 0.05$), lysis (r = 0.77, $p < 0.05$), detachment of tubular cells (r = 0.46, $p < 0.05$), and membranous structures to which C5b-9 was bound (r = 0.75, $p < 0.05$) (142).

Reflux Nephropathy

Chronic urolithiasis, chronic vesicoureteral reflux, and chronic pyelonephritis, which characterize reflux nephropathy, expose the kidney to bacterial pathogens that activate the classical and alternative complement pathways. Inhibition of their activation prevents kidney injury in animal models (204–206). In three small studies on reflux nephropathy, deposits of C5b-9 were not or scarcely found in histologically normal glomeruli—similarly to healthy kidneys—but as intense coarse granules in areas of glomerulosclerosis together with C3 and properdin. Podocytes had regressed in these areas. Deposits were furthermore found along the tubular basement membrane without C3 (44, 75, 127) and extensively in the vascular wall (44).

KIDNEY TUMORS

In clear cell renal cell carcinomas, no deposits of C5b-9, but abundant deposits of C1q and pentraxin-3 were present (207), the latter of which can activate the complement pathways in various ways (208). In various types of renal cell carcinomas, staining of C5b-9 was similarly absent or weakly present in only a sixth to a tenth of tumors, covering not more than half of each tumor (138, 209). Enhanced expression of CD59 and other inhibitory factors might explain the absence of C5b-9 (138, 207, 209). Yet, in another study on various types of renal cell carcinomas, staining of C5b-9 was weak in 55% and moderate in 27% of tumors, despite enhanced expression of inhibitory factors. The tumors could be partitioned into those with deposits of only C3 due to activation of the alternative pathway—with much necrosis as a cause or consequence —, those with deposits of IgG and C1q due to activation of the classical pathway, and those without immune deposits. Although present in all three groups, stainings of C5b-9 and inflammatory markers were most intense in tumors with activation of either pathway (210).

KIDNEY TRANSPLANTATION

During kidney transplantation, the donor's death and the transplant's surgical excision, transportation, and reperfusion all contribute to activate the complement pathways. The extent of complement activation influences the function of the kidney transplant. The serum level of sC5b-9 is elevated in deceased donors and predicts the risk of acute rejection and chronic graft failure after transplantation. Deposits of C5b-9 in transplants are not taken into account—contrary to the routine assessment of deposits of C4d, especially in peritubular capillaries—as a diagnostic criterion for antibody-mediated rejection as part of the Banff classification (16, 26, 29). Complicating the interpretation of their relevance, deposits of C5b-9 in kidney transplants may result from physiological deposition in the donor as in healthy kidneys, from kidney disease in the donor, from the transplantation itself, from rejection in the recipient, as well as from *de novo* or recurrent kidney disease in the recipient.

Ischemia and Reperfusion Injury

Ischemia and reperfusion—inevitable consequences of transplantation—induce acidosis and reactive oxygen species, which both lead to activation of the lectin and alternative pathways and subsequent inflammation, especially in the tubulointerstitium. Inhibition of C5b-9 formation ameliorates the inflammation (13, 16, 26). Nonetheless, in human kidney transplants, deposits of C5b-9 were absent from the tubules and vascular wall both before and shortly after reperfusion, despite a transient elevation of sC5b-9 in arteriovenous samples in between (211). This may explain why eculizumab does not prevent delayed transplant function (13, 16, 26). On the other hand, once kidney transplants suffered from delayed function, C5b-9 appeared in the glomerulus and tubules (54).

Kidney Transplant Rejection

Antibodies against donor antigens on the transplant's endothelium activate the classical pathway (13, 16, 26). As a result, in acutely rejected transplants, deposits of C5b-9 were present in the glomerulus and vascular wall with higher staining intensities than in healthy kidneys and with variable staining intensity along the tubular basement membrane (54, 67, 70, 83, 100, 104, 130, 143, 211, 212). The proportion of glomeruli that contained deposits varied widely between 8 and 77% (54). In the glomerulus, deposition was restricted to the mesangium (67, 96, 212), extended along the capillary wall (70, 100), or was restricted to the capillary wall (143). Tubular and vascular deposits were concentrated in areas of sclerosis (67, 70, 143). C5b-9 was absent from peritubular capillaries, despite the presence of C4d, which was explained by concurrent presence of CD59 (83, 130, 212). In one group of patients biopsied a week after transplantation according to protocol, of whom the majority experienced acute rejection, no deposits were found other than those found at the time of transplantation (129). Glomerular and tubular depositions did not correlate with each other or with age, sex, creatinine, proteinuria, HLA mismatch, or the severity of rejection (54, 83). Depositions throughout the kidney diminished strikingly in three days after acute antibody-mediated rejection was successfully treated with eculizumab in one (104) but not another case (100). The efficacy of eculizumab to prevent or treat rejection remains uncertain (13, 16).

Chronically rejected transplants had similar deposition of C5b-9 as acutely rejected transplants (54). In a group of

patients with acute or chronic antibody-mediated rejection together, weak, granular, and subendothelial staining along the capillary wall was found in 24% and staining in the peritubular capillaries in 2%, whereas staining of C4d was present in both localizations in almost all patients. Those with global and diffuse glomerular staining of C5b-9 had a lower eGFR (26 vs. 34 ml/min/1.73 m^2, $p = 0.04$), more often double contours (100 vs. 40%, $p = 0.01$), and a higher Banff score (1.7 vs. 0.8, $p = 0.01$). They also had a shorter transplant survival (median 6 vs. 41–44 months, $p = 0.02$), though not after adjustment for other risk factors (134).

One study compared deposition of C5b-9 in biopsies conducted because of a clinical suspicion of rejection and biopsies conducted according to protocol in patients with ABO-incompatible transplants. Almost all rejections were acute T-cell mediated; the numbers of confirmed rejections were not reported. Deposition of C5b-9 was more common in the glomerulus, tubules, and peritubular capillaries in the clinically indicated biopsies, whereas depositions of C1q, C3c, and C4d were similar. Peritubular C5b-9 in these biopsies correlated with titers of anti-ABO antibodies before transplantation ($r = 0.72$, $p = 0.002$) and with the occurrence of rejection ($r = 0.52$, $p = 0.02$) (213).

De Novo Kidney Disease After Transplantation

Deposition of C5b-9 in kidney diseases arising after kidney transplantation was similar as in native kidneys. Among patients who developed *de novo* membranous nephropathy, deposits were restricted to the mesangium as fine granules in those with stage I and were localized along the capillary wall together with immune deposits in stage II (214). Cases who developed thrombotic microangiopathy without rejection—a common phenomenon, often without a clear cause (26)—had few deposits in the mesangium, but many deposits in the vascular wall, similar to cases without thrombotic microangiopathy (100).

DISCUSSION

This review is the first to provide an overview of studies on deposition of C5b-9 in healthy and diseased human kidneys. Other reviews have summarized the various mechanisms through which C5b-9 exerts its lytic and sublytic effects on kidney cells (43, 64, 88, 101, 187, 197, 215–217).

In healthy kidneys, staining of C5b-9 was absent, weak in the mesangium, or more prominent in the glomerular vascular pole and the extraglomerular vascular wall, for which we discuss possible explanations in the section on healthy kidneys. Across a wide spectrum of kidney diseases—excluding minimal change nephropathy and glomerular basement membrane diseases—staining of C5b-9 was more frequent, extensive, and intense, as outlined in **Figure 1** and detailed in **Supplementary Table 2**.

In kidney diseases due to deposition of immune complexes and kidney diseases due to activation of the alternative pathway, glomerular deposits of C5b-9 colocalized with immune deposits containing immunoglobulins or other complement factors (44, 57, 67, 73, 75, 81, 96, 126, 143, 218). Correspondingly, glomerular staining of C5b-9 was more frequent, diffuse, and intense than in healthy kidneys and kidney diseases without immune deposits (44, 67, 75, 96, 126, 143), was found along the capillary wall in membranous nephropathy and lupus nephritis class V, in the mesangium in IgA nephropathy and lupus nephritis classes III and IV, and throughout the glomerulus in C3 glomerulopathy, thrombotic microangiopathies, and vasculitis. Studies generally regarded these deposits of C5b-9 as most likely locally formed along with the immune deposits as part of the cause of disease.

In all kidney diseases, deposits of C5b-9 were prominent in areas of glomerulosclerosis, tubulointerstitial injury, and vascular hyalinosis and sclerosis. This finding was clearest in hypertensive and diabetic nephropathy, interstitial nephritis, and acute tubular necrosis. These deposits did not consistently colocalize with immunoglobulins or other complement factors (19, 27, 44, 54, 67, 70, 72, 73, 75, 94–97, 103, 118, 127, 134, 139, 141, 175, 200), although C5b-9 and C3 colocalized more often in areas of glomerulosclerosis when immune deposits were present in other areas of the glomerulus (44, 67, 143) and both C5b-9 and C3 were more prominent in tubules and arteries in areas of tubulointerstitial injury (44, 57, 67, 75, 94, 96, 135, 139, 143, 200). These deposits may either be formed locally when complement pathways are activated by cellular injury or originate in urine or blood when sC5b-9 passes the tubular or vascular wall. sC5b-9 can be formed in or excreted into the tubular lumen, particularly in presence of proteinuria (20, 33, 198, 201). The observation that C5b-9 resided on both sides of the tubular basement membrane, but C3 only on the interstitial side (44), fits with an origin in the tubular lumen. Studies generally regarded these deposits of C5b-9 as a nonspecific consequence of kidney injury rather than a cause of kidney disease.

Across kidney diseases, deposits of C5b-9 seemed associated with cell membrane fragments rather than bound to cells themselves, as revealed by immunoelectron microscopy. Cells may have shed these fragments after C5b-9 has bound the cells or C5b-9 may have bound these fragments after having been shed by cells, as discussed in the section on staining techniques. Both processes, though, contribute to cellular activation, proliferation, inflammation, sclerosis, and fibrosis.

Studies using immunohistochemical staining cannot unravel whether deposits of C5b-9 are a cause of kidney disease or a consequence of kidney injury and cannot distinguish between C5b-9 that has bound cells, has been shed by cells, has bound extracellular vesicles, or has remained soluble. **Table 3** summarizes these and other inherent limitations.

Whether C5b-9 is a cause of kidney disease or a consequence of kidney injury does not affect its potential as a prognostic marker. Deposition of C5b-9 indicates that complement activity has resulted in formation of both C5a and C5b-9, both of which may participate in the causation of disease and the response to tissue injury. Indeed, the presence and intensity of staining of C5b-9 correlated with histological lesions, clinical characteristics, prognosis, and treatment effects in various kidney diseases, as

TABLE 3 | Summary of the limitations and remaining questions of immunohistochemical studies on deposition of C5b-9 in human kidneys.

Inherent limitations of current studies in general
• They cannot unravel whether deposits of C5b-9 are a cause of kidney disease or a consequence of kidney injury.
• They cannot distinguish between locally formed C5b-9 bound to cells, C5b-9 bound to or shedded as extracellular vesicles, and sC5b-9 originating in urine or blood.
• They cannot assess when deposits have arisen, so that, given their slow clearance, deposits may have chronically accumulated.
• They evaluate staining subjectively and semiquantitatively.
Specific limitations of current included studies
• Included patients were generally ill-characterized.
• Staining techniques were often described very concisely.
• Different staining techniques and antibodies were seldomly compared.
• The method of evaluating staining was mostly undefined.
• The method of evaluating staining was variable. As examples, traces of staining were usually considered negligible but sometimes counted as positive (18) and scoring systems were used incidentally and incomparably (19, 31, 52, 83, 84, 87, 94, 116, 117, 135, 136, 139, 142, 209).
• Variability of staining among individual patients with the same kidney disease was rarely documented, while it might be large (57).
• Staining across different kidney diseases was directly compared in only few studies (44, 57, 67, 70, 72, 75, 79, 84, 96, 98, 126, 141–143).
• Colocalization with immunoglobulins and other complement factors, especially in tubules and vessels, was reported only briefly.
• Correlations between deposits and histological lesions or clinical characteristics were not studied systematically.
• Changes in staining were uncommonly tracked through time or treatment.
Remaining questions for future studies
• Does staining of C5b-9 differ when directly comparing staining techniques and antibodies?
• Is staining more common in tissue obtained with autopsy than biopsy or nephrectomy? And can this be explained by a different selection of patients?
• How do deposits of C5b-9 differ between kidney diseases due to deposition of immune complexes, due to activation of the alternative pathway, and due to other mechanisms?
• How do deposits vary among patients with the same kidney disease?
• Are deposits dependent on the age and sex of patients?
• With which immunoglobulins and other complement factors do deposits colocalize in various localizations and in various kidney diseases?
• What structures are associated with deposits on immunoelectron microscopy?
• How fast are deposits cleared in various kidney diseases and across individual patients with the same kidney disease?
• How do deposits change through time and treatment? And how does the change relate to variable activation of complement pathways, for example in membranous nephropathy?
• Do deposits consistently predict prognosis and treatment effect? And how does this depend on their localizations and on the underlying kidney disease?

summarized in **Table 1**. Illustrations of such correlations are given in the figures, while a complete discussion of possible correlations is given in the text.

Further analytical comparisons and firm conclusions were hampered by a lack of detailed data and descriptions of methods and results in the included studies, as summarized in **Table 3**. As a consequence, we could not precisely specify differences in deposition of C5b-9 as dependent on staining techniques and between kidney diseases due to deposition of immune complexes, kidney diseases due to activation of the alternative pathway, and kidney diseases due to other mechanisms.

Future studies are necessary to overcome the limitations of current studies, to confirm our findings, and to answer remaining questions as proposed in **Table 3**. To facilitate analytical comparisons, future studies should systematically study deposition of C5b-9 in well-described populations and tissues with detailed data and descriptions of their methods and results. Immunohistochemical studies may be strengthened by a combination with other techniques, such as immunoelectron microscopy or mass spectrometry of microdissected glomeruli, which are more objective, sensitive, and quantitative (90–92, 124, 180).

In this review, we aim to motivate and guide future studies on deposition of C5b-9 in human kidneys by summarizing the available data and by identifying the data that still lack. We describe when deposition of C5b-9 in kidneys may be regarded a cause of kidney disease and when a consequence of kidney injury. We substantiate that staining of C5b-9 in kidneys, although not yet routinely conducted, promises to be valuable for evaluating activation of complement pathways, estimating prognosis, and identifying possible treatment targets.

AUTHOR CONTRIBUTIONS

JK and HR conceived and designed this review. JK and ME collected literature. JK drafted the manuscript, designed the tables, and drew the figures. ME contributed to the drafting of the manuscript and to the design of tables. All authors contributed to the article and approved the submitted version.

FUNDING

JK was supported with a Niels Stensen Fellowship and with a travel grant of the NVLE Fund. ME was supported with a grant from the Dutch Kidney Foundation (COMBAT grant 130CA27).

SUPPLEMENTARY MATERIAL

The Supplementary Material for this article can be found online at: https://www.frontiersin.org/articles/10.3389/fimmu.2020.599974/full#supplementary-material

REFERENCES

1. Bayly-Jones C, Bubeck D, Dunstone MA. The mystery behind membrane insertion: a review of the complement membrane attack complex. *Philos Trans R Soc Lond B Biol Sci* (2017) 372:20160221. doi: 10.1098/rstb.2016.0221
2. Morgan BP, Boyd C, Bubeck D. Molecular cell biology of complement membrane attack. *Semin Cell Dev Biol* (2017) 72:124–32. doi: 10.1016/j.semcdb.2017.06.009
3. Bomback AS, Markowitz GS, Appel GB. Complement-mediated glomerular diseases: a tale of 3 pathways. *Kidney Int Rep* (2016) 1:148–55. doi: 10.1016/j.ekir.2016.06.005
4. Koopman JJE, Teng YKO, Boon CJF, Van den Heuvel LP, Rabelink TJ, Van Kooten C, et al. Diagnosis and treatment of C3 glomerulopathy in a center of expertise. *Neth J Med* (2019) 77:10–8.
5. Smith RJH, Appel GB, Blom AM, Cook HT, D'Agati VD, Fakhouri F, et al. C3 glomerulopathy: understanding a rare complement-driven renal disease. *Nat Rev Nephrol* (2019) 15:129–43. doi: 10.1038/s41581-018-0107-2
6. Corvillo F, Okrój M, Nozal P, Melgosa M, Sánchez-Corral P, López-Trascasa M. Nephritic factors: an overview of classification, diagnostic tools and clinical associations. *Front Immunol* (2019) 10:886. doi: 10.3389/fimmu.2019.00886
7. Andrighetto S, Leventhal J, Zaza G, Cravedi P. Complement and complement targeting therapies in glomerular diseases. *Int J Mol Sci* (2019) 20:6336. doi: 10.3390/ijms20246336
8. Mastellos DC, Ricklin D, Lambris JD. Clinical promise of next-generation complement therapeutics. *Nat Rev Drug Discovery* (2019) 18:707–29. doi: 10.1038/s41573-019-0031-6
9. Zipfel PF, Wiech T, Rudnick R, Afonso S, Person F, Skerka C. Complement inhibitors in clinical trials for glomerular diseases. *Front Immunol* (2020) 10:2166. doi: 10.3389/fimmu.2019.02166
10. Bao L, Cunningham PN, Quigg RJ. Complement in lupus nephritis: new perspectives. *Kidney Dis (Basel)* (2015) 1:91–9. doi: 10.1159/000431278
11. Birmingham DJ, Hebert LA. The complement system in lupus nephritis. *Semin Nephrol* (2015) 35:444–54. doi: 10.1016/j.semnephrol.2015.08.006
12. Laurence J, Haller H, Mannucci PM, Nangaku M, Praga M, Rodriguez de Cordoba S. Atypical hemolytic uremic syndrome (aHUS): essential aspects of an accurate diagnosis. *Clin Adv Hematol Oncol* (2016) 14 Suppl 11:2–15.
13. Biglarnia AR, Huber-Lang M, Mohlin C, Ekdahl KN, Nilsson B. The multifaceted role of complement in kidney transplantation. *Nat Rev Nephrol* (2018) 14:767–81. doi: 10.1038/s41581-018-0071-x
14. Nakazawa D, Masuda S, Tomaru U, Ishizu A. Pathogenesis and therapeutic interventions for ANCA-associated vasculitis. *Nat Rev Rheumatol* (2019) 15:91–101. doi: 10.1038/s41584-018-0145-y
15. Rizk DV, Maillard N, Julian BA, Knoppova B, Green TJ, Novak J, et al. The emerging role of complement proteins as a target for therapy of IgA nephropathy. *Front Immunol* (2019) 10:504. doi: 10.3389/fimmu.2019.00504
16. Grafals M, Thurman JM. The role of complement in organ transplantation. *Front Immunol* (2019) 10:2380. doi: 10.3389/fimmu.2019.02380
17. Tortajada A, Gutierrez E, Pickering MC, Praga Terente M, Medjeral-Thomas N. The role of complement in IgA nephropathy. *Mol Immunol* (2019) 114:123–32. doi: 10.1016/j.molimm.2019.07.017
18. Wilson HR, Medjeral-Thomas NR, Gilmore AC, Trivedi P, Seyb K, Farzaneh-Far R, et al. Glomerular membrane attack complex is not a reliable marker of ongoing C5 activation in lupus nephritis. *Kidney Int* (2019) 95:655–65. doi: 10.1016/j.kint.2018.09.027
19. Dumont C, Mérouani A, Ducruet T, Benoit G, Clermont MJ, Lapeyraque AL, et al. Clinical relevance of membrane attack complex deposition in children with IgA nephropathy and Henoch-Schönlein purpura. *Pediatr Nephrol* (2020) 35:843–50. doi: 10.1007/s00467-019-04445-x
20. Morita Y, Ikeguchi H, Nakamura J, Hotta N, Yuzawa Y, Matsuo S. Complement activation products in the urine from proteinuric patients. *J Am Soc Nephrol* (2000) 11:700–7.
21. Onda K, Ohsawa I, Ohi H, Tamano M, Mano S, Wakabayashi M, et al. Excretion of complement proteins and its activation marker C5b-9 in IgA nephropathy in relation to renal function. *BMC Nephrol* (2011) 12:64. doi: 10.1186/1471-2369-12-64
22. Gou SJ, Yuan J, Wang C, Zhao MH, Chen M. Alternative complement pathway activation products in urine and kidneys of patients with ANCA-associated GN. *Clin J Am Soc Nephrol* (2013) 8:1884–91. doi: 10.2215/CJN.02790313
23. Gou SJ, Yuan J, Chen M, Yu F, Zhao MH. Circulating complement activation in patients with anti-neutrophil cytoplasmic antibody-associated vasculitis. *Kidney Int* (2013) 83:129–37. doi: 10.1038/ki.2012.313
24. Ma H, Sandor DG, Beck LH Jr. The role of complement in membranous nephropathy. *Semin Nephrol* (2013) 33:531–42. doi: 10.1016/j.semnephrol.2013.08.004
25. Borza DB. Alternative pathway dysregulation and the conundrum of complement activation by IgG4 immune complexes in membranous nephropathy. *Front Immunol* (2016) 7:157. doi: 10.3389/fimmu.2016.00157
26. Cernoch M, Viklicky O. Complement in kidney transplantation. *Front Med* (2017) 4:66. doi: 10.3389/fmed.2017.00066
27. Bus P, Chua JS, Klessens CQF, Zandbergen M, Wolterbeek R, Van Kooten C, et al. Complement activation in patients with diabetic nephropathy. *Kidney Int Rep* (2018) 3:302–13. doi: 10.1016/j.ekir.2017.10.005
28. Zheng JM, Ren XG, Jiang ZH, Chen DJ, Zhao WJ, Li LJ. Lectin-induced renal local complement activation is involved in tubular interstitial injury in diabetic nephropathy. *Clin Chim Acta* (2018) 482:65–73. doi: 10.1016/j.cca.2018.03.033
29. Lammerts RGM, Eisenga MF, Alyami M, Daha MR, Seelen MA, Pol RA, et al. Urinary properdin and sC5b-9 are independently associated with increased risk for graft failure in renal transplant recipients. *Front Immunol* (2019) 10:2511. doi: 10.3389/fimmu.2019.02511
30. Li XQ, Chang DY, Chen M, Zhao MH. Complement activation in patients with diabetic nephropathy. *Diabetes Metab* (2019) 45:248–53. doi: 10.1016/j.diabet.2018.04.001
31. Zhao WT, Huang JW, Sun PP, Su T, Tang JW, Wang SX, et al. Diagnostic roles of urinary kidney injury molecule 1 and soluble C5b-9 in acute tubulointerstitial nephritis. *Am J Physiol Renal Physiol* (2019) 317:F584–92. doi: 10.1152/ajprenal.00176.2019
32. Pierik E, Prins JR, Van Goor H, Dekker GA, Daha MR, Seelen MAJ, et al. Dysregulation of complement activation and placental dysfunction: a potential target to treat preeclampsia? *Front Immunol* (2020) 10:3098. doi: 10.3389/fimmu.2019.03098
33. Khalili M, Bonnefoy A, Genest DS, Quadri J, Rioux JP, Troyanov S. Clinical use of complement, inflammation and fibrosis biomarkers in autoimmune glomerulonephritis. *Kidney Int Rep* (2020) 5:1690–9. doi: 10.1016/j.ekir.2020.07.018
34. Van der Pol P, De Vries DK, Van Gijlswijk DJ, Van Anken GE, Schlagwein N, Daha MR, et al. Pitfalls in urinary complement measurements. *Transpl Immunol* (2012) 27:55–8. doi: 10.1016/j.trim.2012.06.001
35. Le Quintrec M, Lapeyraque AL, Lionet A, Sellier-Leclerc AL, Delmas Y, Baudouin V, et al. Patterns of clinical response to eculizumab in patients with C3 glomerulopathy. *Am J Kidney Dis* (2018) 72:84–92. doi: 10.1053/j.ajkd.2017.11.019
36. Mohebnasab M, Eriksson O, Persson B, Sandholm K, Mohlin C, Huber-Lang M, et al. Current and future approaches for monitoring responses to anti-complement therapeutics. *Front Immunol* (2019) 10:2539. doi: 10.3389/fimmu.2019.02539
37. Wallace DJ, Alexander RV, O'Malley T, Khosroshahi A, Hojjati M, Loupasakis K, et al. Randomised prospective trial to assess the clinical utility of multianalyte assay panel with complement activation products for the diagnosis of SLE. *Lupus Sci Med* (2019) 6:e000349. doi: 10.1136/lupus-2019-000349
38. Ramsey-Goldman R, Alexander RV, Massarotti EM, Wallace DJ, Narain S, Arriens C, et al. Complement activation in patients with probable systemic lupus erythematosus and ability to predict progression to American College of Rheumatology-classified systemic lupus erythematosus. *Arthritis Rheumatol* (2020) 72:78–88. doi: 10.1002/art.41093
39. Espinosa M, Ortega R, Sánchez M, Segarra A, Salcedo MT, González F, et al. Association of C4d deposition with clinical outcomes in IgA nephropathy. *Clin J Am Soc Nephrol* (2014) 9:897–904. doi: 10.2215/CJN.09710913
40. Ruan CC, Gao PJ. Role of complement-related inflammation and vascular dysfunction in hypertension. *Hypertension* (2019) 73:965–71. doi: 10.1161/HYPERTENSIONAHA.118.11210

41. Menny A, Serna M, Boyd CM, Gardner S, Joseph AP, Morgan BP, et al. CryoEM reveals how the complement membrane attack complex ruptures lipid bilayers. *Nat Commun* (2018) 9:5316. doi: 10.1038/s41467-018-07653-5
42. Parsons ES, Stanley GJ, Pyne ALB, Hodel AW, Nievergelt AP, Menny A, et al. Single-molecule kinetics of pore assembly by the membrane attack complex. *Nat Commun* (2019) 10:2066. doi: 10.1038/s41467-019-10058-7
43. Xie CB, Jane-Wit D, Pober JS. Complement membrane attack complex: new roles, mechanisms of action, and therapeutic targets. *Am J Pathol* (2020) 190:1138–50. doi: 10.1016/j.ajpath.2020.02.006
44. Falk RJ, Dalmasso AP, Kim Y, Tsai CH, Scheinman JI, Gewurz H, et al. Neoantigen of the polymerized ninth component of complement: characterization of a monoclonal antibody and immunohistochemical localization in renal disease. *J Clin Invest* (1983) 72:560–73. doi: 10.1172/JCI111004
45. Hugo F, Jenne D, Bhakdi S. Monoclonal antibodies against neoantigens of the terminal C5b-9 complex of human complement. *Biosci Rep* (1985) 5:649–58. doi: 10.1007/BF01116996
46. Mollnes TE, Lea T, Harboe M, Tschopp J. Monoclonal antibodies recognizing a neoantigen of poly(C9) detect the human terminal complement complex in tissue and plasma. *Scand J Immunol* (1985) 22:183–95. doi: 10.1111/j.1365-3083.1985.tb01870.x
47. Yoden A, Moriyama T, Inoue K, Inai S. The role of the C9b domain in the binding of C9 molecules to EAC1-8 defined by monoclonal antibodies to C9. *J Immunol* (1988) 140:2317–21.
48. Würzner R, Xu H, Franzke A, Schulze M, Peters JH, Götze O. Blood dendritic cells carry terminal complement complexes on their cell surface as detected by newly developed neoepitope-specific monoclonal antibodies. *Immunology* (1991) 74:132–8.
49. Hatanaka M, Seya T, Yoden A, Fukamoto K, Semba T, Inai S. Analysis of C5b-8 binding sites in the C9 molecule using monoclonal antibodies: participation of two separate epitopes of C9 in C5b-8 binding. *Mol Immunol* (1992) 29:911–6. doi: 10.1016/0161-5890(92)90129-l
50. Kolb WP, Müller-Eberhard HJ. Neoantigens of the membrane attack complex of human complement. *Proc Natl Acad Sci USA* (1975) 72:1687–9. doi: 10.1073/pnas.72.5.1687
51. Tschopp J, Mollnes TE. Antigenic crossreactivity of the alpha subunit of complement component C8 with the cysteine-rich domain shared by complement component C9 and low density lipoprotein receptor. *Proc Natl Acad Sci USA* (1986) 83:4223–7. doi: 10.1073/pnas.83.12.4223
52. Rauterberg EW, Lieberknecht HM, Wingen AM, Ritz E. Complement membrane attack (MAC) in idiopathic IgA-glomerulonephritis. *Kidney Int* (1987) 31:820–9. doi: 10.1038/ki.1987.72
53. Manenti L, Vaglio A, Gnappi E, Maggiore U, Allegri L, Allinovi M, et al. Association of serum C3 concentration and histologic signs of thrombotic microangiopathy with outcomes among patients with ANCA-associated renal vasculitis. *Clin J Am Soc Nephrol* (2015) 10:2143–51. doi: 10.2215/CJN.00120115
54. Hu C, Li L, Ding P, Li L, Ge X, Zheng L, et al. Complement inhibitor CRIg/FH ameliorates renal ischemia reperfusion injury via activation of PI3K/AKT signaling. *J Immunol* (2018) 201:3717–30. doi: 10.4049/jimmunol.1800987
55. Bhakdi S, Muhly M. A simple immunoradiometric assay for the terminal SC5b-9 complex of human complement. *J Immunol Methods* (1983) 57:283–9. doi: 10.1016/0022-1759(83)90088-1
56. Bhakdi S, Bjerrum OJ, Bhakdi-Lehnen B, Tranum-Jensen J. Complement lysis: evidence for an amphiphilic nature of the terminal membrane C5b-9 complex of human complement. *J Immunol* (1978) 121:2526–32.
57. Ootaka T, Suzuki M, Sudo K, Sato H, Seino J, Saito T, et al. Histologic localization of terminal complement complexes in renal diseases: an immunohistochemical study. *Am J Clin Pathol* (1989) 91:144–51. doi: 10.1093/ajcp/91.2.144
58. Veerhuis R, van der Valk P, Janssen I, Zhan SS, Van Nostrand WE, Eikelenboom P. Complement activation in amyloid plaques in Alzheimer's disease brains does not proceed further than C3. *Virchows Arch* (1995) 426:603–10. doi: 10.1007/BF00192116
59. Kemp PA, Spragg JH, Brown JC, Morgan BP, Gunn CA, Taylor PW. Immunohistochemical determination of complement activation in joint tissues of patients with rheumatoid arthritis and osteoarthritis using neoantigen-specific monoclonal antibodies. *J Clin Lab Immunol* (1992) 37:147–62.
60. Würzner R, Schulze M, Happe L, Franzke A, Bieber FA, Oppermann M, et al. Inhibition of terminal complement complex formation and cell lysis by monoclonal antibodies. *Complement Inflamm* (1991) 8:328–40. doi: 10.1159/000463204
61. Kawana S, Shen GH, Kobayashi Y, Nishiyama S. Membrane attack complex of complement in Henoch-Schönlein purpura skin and nephritis. *Arch Dermatol Res* (1990) 282:183–7. doi: 10.1007/BF00372620
62. Xia P, Jordon RE, Geoghegan WD. Complement fixation by pemphigus antibody: assembly of the membrane attack complex on cultured human keratinocytes. *J Clin Invest* (1988) 82:1939–47. doi: 10.1172/JCI113813
63. Kusunoki Y, Takekoshi Y, Nagasawa S. Using polymerized C9 to produce a monoclonal antibody against a neoantigen of the human terminal complement complex. *J Pharmacobiodyn* (1990) 13:454–60. doi: 10.1248/bpb1978.13.454
64. Nicholson-Weller A, Halperin JA. Membrane signaling by complement C5b-9, the membrane attack complex. *Immunol Res* (1993) 12:244–57. doi: 10.1007/BF02918256
65. Würzner R. Immunochemical measurement of complement components and activation products. *Methods Mol Biol* (2000) 150:103–12. doi: 10.1385/1-59259-056-X:103
66. Hadders MA, Bubeck D, Roversi P, Hakobyan S, Forneris F, Morgan BP, et al. Assembly and regulation of the membrane attack complex based on structures of C5b6 and sC5b9. *Cell Rep* (2012) 1:200–7. doi: 10.1016/j.celrep.2012.02.003
67. Falk RJ, Podack E, Dalmasso AP, Jennette JC. Localization of S protein and its relationship to the membrane attack complex of complement in renal tissue. *Am J Pathol* (1987) 127:182–90.
68. Mollnes TE, Harboe M. Immunohistochemical detection of the membrane and fluid-phase terminal complement complexes C5b-9(m) and SC5b-9: consequences for interpretation and terminology. *Scand J Immunol* (1987) 26:381–6. doi: 10.1111/j.1365-3083.1987.tb02270.x
69. Murphy BF, Kirszbaum L, Walker ID, d'Apice AJ. SP-40,40, a newly identified normal human serum protein found in the SC5b-9 complex of complement and in the immune deposits in glomerulonephritis. *J Clin Invest* (1988) 81:1858–64. doi: 10.1172/JCI113531
70. Murphy BF, Davies DJ, Morrow W, d'Apice AJ. Localization of terminal complement components S-protein and SP-40,40 in renal biopsies. *Pathology* (1989) 21:275–8. doi: 10.3109/00313028909061073
71. Tschopp J, French LE. Clusterin: modulation of complement function. *Clin Exp Immunol* (1994) 97 Suppl 2:11–4. doi: 10.1111/j.1365-2249.1994.tb06256.x
72. Bariety J, Hinglais N, Bhakdi S, Mandet C, Rouchon M, Kazatchkine MD. Immunohistochemical study of complement S protein (vitronectin) in normal and diseased human kidneys: relationship to neoantigens of the C5b-9 terminal complex. *Clin Exp Immunol* (1989) 75:76–81.
73. French LE, Tschopp J, Schifferli JA. Clusterin in renal tissue: preferential localization with the terminal complement complex and immunoglobulin deposits in glomeruli. *Clin Exp Immunol* (1992) 88:389–93. doi: 10.1111/j.1365-2249.1992.tb06459.x
74. Bhakdi S, Käflein R, Halstensen TS, Hugo F, Preissner KT, Mollnes TE. Complement S-protein (vitronectin) is associated with cytolytic membrane-bound C5b-9 complexes. *Clin Exp Immunol* (1988) 74:459–64.
75. Okada M, Yoshioka K, Takemura T, Akano N, Aya N, Murakami K, et al. Immunohistochemical localization of C3d fragment of complement and S-protein (vitronectin) in normal and diseased human kidneys: association with the C5b-9 complex and vitronectin receptor. *Virchows Arch A Pathol Anat Histopathol* (1993) 422:367–73. doi: 10.1007/BF01605455
76. Tomino Y, Yagame M, Eguchi K, Nomoto Y, Sakai H. Immunofluorescent studies on S-protein in glomeruli from patients with IgA nephropathy. *Am J Pathol* (1987) 129:402–6.
77. Lai KN, Lo ST, Lai FM. Immunohistochemical study of the membrane attack complex of complement and S-protein in idiopathic and secondary membranous nephropathy. *Am J Pathol* (1989) 135:469–76.
78. Yoshioka K, Takemura T, Akano N, Okada M, Yagi K, Maki S, et al. IgA nephropathy in patients with congenital C9 deficiency. *Kidney Int* (1992) 42:1253–8. doi: 10.1038/ki.1992.412

79. Ogawa T, Yorioka N, Yamakido M. Immunohistochemical studies of vitronectin, C5b-9, and vitronectin receptor in membranous nephropathy. *Nephron* (1994) 68:87–96. doi: 10.1159/000188225
80. Rastaldi MP, Candiano G, Musante L, Bruschi M, Armelloni S, Rimoldi L, et al. Glomerular clusterin is associated with PKC-alpha/beta regulation and good outcome of membranous glomerulonephritis in humans. *Kidney Int* (2006) 70:477–85. doi: 10.1038/sj.ki.5001563
81. Tamai H, Matsuo S, Fukatsu A, Nishikawa K, Sakamoto N, Yoshioka K, et al. Localization of 20-kD homologous restriction factor (HRF20) in diseased human glomeruli: an immunofluorescence study. *Clin Exp Immunol* (1991) 84:256–62. doi: 10.1111/j.1365-2249.1991.tb08158.x
82. Lehto T, Honkanen E, Teppo AM, Meri S. Urinary excretion of protectin (CD59), complement SC5b-9 and cytokines in membranous glomerulonephritis. *Kidney Int* (1995) 47:1403–11. doi: 10.1038/ki.1995.197
83. Nishi S, Imai N, Ito Y, Ueno M, Fukase S, Mori H, et al. Pathological study on the relationship between C4d, CD59 and C5b-9 in acute renal allograft rejection. *Clin Transplant* (2004) 18 Suppl 11:18–23. doi: 10.1111/j.1399-0012.2004.00242
84. Uesugi N, Sakata N, Nangaku M, Abe M, Horiuchi S, Hisano S, et al. Possible mechanism for medial smooth muscle cell injury in diabetic nephropathy: glycoxidation-mediated local complement activation. *Am J Kidney Dis* (2004) 44:224–38. doi: 10.1053/j.ajkd.2004.04.027
85. Hisano S, Matsushita M, Fujita T, Iwasaki H. Activation of the lectin complement pathway in Henoch-Schönlein purpura nephritis. *Am J Kidney Dis* (2005) 45:295–302. doi: 10.1053/j.ajkd.2004.10.020
86. Hisano S, Matsushita M, Fujita T, Takeshita M, Iwasaki H. Activation of the lectin complement pathway in post-streptococcal acute glomerulonephritis. *Pathol Int* (2007) 57:351–7. doi: 10.1111/j.1440-1827.2007.02107.x
87. Segawa Y, Hisano S, Matsushita M, Fujita T, Hirose S, Takeshita M, et al. IgG subclasses and complement pathway in segmental and global membranous nephropathy. *Pediatr Nephrol* (2010) 25:1091–9. doi: 10.1007/s00467-009-1439-8
88. Karpman D, Ståhl A, Arvidsson I. Extracellular vesicles in renal disease. *Nat Rev Nephrol* (2017) 13:545–62. doi: 10.1038/nrneph.2017.98
89. Karasu E, Eisenhardt SU, Harant J, Huber-Lang M. Extracellular vesicles: packages sent with complement. *Front Immunol* (2018) 9:721. doi: 10.3389/fimmu.2018.00721
90. Sethi S, Gamez JD, Vrana JA, Theis JD, Bergen HR, Zipfel PF, et al. Glomeruli of dense deposit disease contain components of the alternative and terminal complement pathway. *Kidney Int* (2009) 75:952–60. doi: 10.1038/ki.2008.657
91. Sethi S, Fervenza FC, Zhang Y, Zand L, Vrana JA, Nasr SH, et al. C3 glomerulonephritis: clinicopathological findings, complement abnormalities, glomerular proteomic profile, treatment, and follow-up. *Kidney Int* (2012) 82:465–73. doi: 10.1038/ki.2012.212
92. Sethi S, Vrana JA, Fervenza FC, Theis JD, Sethi A, Kurtin PJ, et al. Characterization of C3 in C3 glomerulopathy. *Nephrol Dial Transplant* (2017) 32:459–65. doi: 10.1093/ndt/gfw290
93. Imai K, Nakajima K, Eguchi K, Miyazaki M, Endoh M, Tomino Y, et al. Homozygous C3 deficiency associated with IgA nephropathy. *Nephron* (1991) 59:148–52. doi: 10.1159/000186535
94. Khan TN, Sinniah R. Role of complement in renal tubular damage. *Histopathology* (1995) 26:351–6. doi: 10.1111/j.1365-2559.1995.tb00197.x
95. Biesecker G, Katz S, Koffler D. Renal localization of the membrane attack complex in systemic lupus erythematosus nephritis. *J Exp Med* (1981) 154:1779–94. doi: 10.1084/jem.154.6.1779
96. Hinglais N, Kazatchkine MD, Bhakdi S, Appay MD, Mandet C, Grossetete J, et al. Immunohistochemical study of the C5b-9 complex of complement in human kidneys. *Kidney Int* (1986) 30:399–410. doi: 10.1038/ki.1986.198
97. Miyamoto H, Yoshioka K, Takemura T, Akano N, Maki S. Immunohistochemical study of the membrane attack complex of complement in IgA nephropathy. *Virchows Arch A Pathol Anat Histopathol* (1988) 413:77–86. doi: 10.1007/BF00844284
98. Nanulescu M, Rus HG, Niculescu F, Cristea A, Florescu P. C5b-9 deposition in children with glomerular diseases. *Med Interne* (1987) 25:99–104.
99. Endo M, Ohi H, Ohsawa I, Fujita T, Matsushita M. Complement activation through the lectin pathway in patients with Henoch-Schönlein purpura nephritis. *Am J Kidney Dis* (2000) 35:401–7. doi: 10.1016/s0272-6386(00)70192-2
100. Cassol CA, Brodsky SV, Satoskar AA, Blissett AR, Cataland S, Nadasdy T. Eculizumab deposits in vessel walls in thrombotic microangiopathy. *Kidney Int* (2019) 96:761–8. doi: 10.1016/j.kint.2019.05.008
101. Békássy ZD, Kristoffersson AC, Rebetz J, Tati R, Olin AI, Karpman D. Aliskiren inhibits renin-mediated complement activation. *Kidney Int* (2018) 94:689–700. doi: 10.1016/j.kint.2018.04.004
102. Medjeral-Thomas NR, Moffitt H, Lomax-Browne HJ, Constantinou N, Cairns T, Cook HT, et al. Glomerular complement H-related protein 5 (FHR5) is highly prevalent in C3 glomerulopathy and associated with renal impairment. *Kidney Int Rep* (2019) 4:1387–400. doi: 10.1016/j.ekir.2019.06.008
103. Herlitz LC, Bomback AS, Markowitz GS, Stokes MB, Smith RN, Colvin RB, et al. Pathology after eculizumab in dense deposit disease and C3 GN. *J Am Soc Nephrol* (2012) 23:1229–37. doi: 10.1681/ASN.2011121186
104. Locke JE, Magro CM, Singer AL, Segev DL, Haas M, Hillel AT, et al. The use of antibody to complement protein C5 for salvage treatment of severe antibody-mediated rejection. *Am J Transplant* (2009) 9:231–5. doi: 10.1111/j.1600-6143.2008.02451.x
105. Vivarelli M, Pasini A, Emma F. Eculizumab for the treatment of dense-deposit disease. *N Engl J Med* (2012) 366:1163–5. doi: 10.1056/NEJMc1111953
106. Le Quintrec M, Lionet A, Kandel C, Bourdon F, Gnemmi V, Colombat M, et al. Eculizumab for treatment of rapidly progressive C3 glomerulopathy. *Am J Kidney Dis* (2015) 65:484–9. doi: 10.1053/j.ajkd.2014.09.025
107. Payette A, Patey N, Dragon-Durey MA, Frémeaux-Bacchi V, Le Deist F. Lapeyraque AL. A case of C3 glomerulonephritis successfully treated with eculizumab. *Pediatr Nephrol* (2015) 30:1033–7. doi: 10.1007/s00467-015-3061-2
108. Carrara C, Podestà MA, Abbate M, Rizzo P, Piras R, Alberti M, et al. Morphofunctional effects of C5 convertase blockade in immune complex-mediated membranoproliferative glomerulonephritis: report of two cases with evidence of terminal complement activation. *Nephron* (2020) 144:195–203. doi: 10.1159/000505403
109. Pickering MC, Ismajli M, Condon MB, McKenna N, Hall AE, Lightstone L, et al. Eculizumab as rescue therapy in severe resistant lupus nephritis. *Rheumatol (Oxford)* (2015) 54:2286–8. doi: 10.1093/rheumatology/kev307
110. Alexopoulos E, Papaghianni A, Papadimitriou M. The pathogenetic significance of C5b-9 in IgA nephropathy. *Nephrol Dial Transplant* (1995) 10:1166–72.
111. Teixeira JE, Costa RS, Lachmann PJ, Würzner R, Barbosa JE. CR1 stump peptide and terminal complement complexes are found in the glomeruli of lupus nephritis patients. *Clin Exp Immunol* (1996) 105:497–503. doi: 10.1046/j.1365-2249.1996.d01-776.x
112. Papagianni AA, Alexopoulos E, Leontsini M, Papadimitriou M. C5b-9 and adhesion molecules in human idiopathic membranous nephropathy. *Nephrol Dial Transplant* (2002) 17:57–63. doi: 10.1093/ndt/17.1.57
113. Qin X, Goldfine A, Krumrei N, Grubissich L, Acosta J, Chorev M, et al. Glycation inactivation of the complement regulatory protein CD59: a possible role in the pathogenesis of the vascular complications of human diabetes. *Diabetes* (2004) 53:2653–61. doi: 10.2337/diabetes.53.10.2653
114. Kobayashi Y, Hasegawa O, Honda M. Terminal complement complexes in childhood type I membranoproliferative glomerulonephritis. *J Nephrol* (2006) 19:746–50.
115. Stangou M, Alexopoulos E, Pantzaki A, Leonstini M, Memmos D. C5b-9 glomerular deposition and tubular α3β1-integrin expression are implicated in the development of chronic lesions and predict renal function outcome in immunoglobulin A nephropathy. *Scand J Urol Nephrol* (2008) 42:373–80. doi: 10.1080/00365590801943241
116. Xing GQ, Chen M, Liu G, Heeringa P, Zhang JJ, Zheng X, et al. Complement activation is involved in renal damage in human antineutrophil cytoplasmic autoantibody associated pauci-immune vasculitis. *J Clin Immunol* (2009) 29:282–91. doi: 10.1007/s10875-008-9268-2
117. Xing GQ, Chen M, Liu G, Zheng X, Jie E, Zhao MH. Differential deposition of C4d and MBL in glomeruli of patients with ANCA-negative pauci-immune crescentic glomerulonephritis. *J Clin Immunol* (2010) 30:144–56. doi: 10.1007/s10875-009-9344-2

118. Sugimoto K, Takemura Y, Yanagida H, Fujita S, Miyazawa T, Sakata N, et al. Renal tubular dysgenesis and tubulointerstitial nephritis antigen in juvenile nephronophthisis. *Nephrol (Carlton)* (2011) 16:495–501. doi: 10.1111/j.1440-1797.2011.01442.x
119. Nisihara RM, Magrini F, Mocelin V, Messias-Reason IJ. Deposition of the lectin pathway of complement in renal biopsies of lupus nephritis patients. *Hum Immunol* (2013) 74:907–10. doi: 10.1016/j.humimm.2013.04.030
120. Tati R, Kristoffersson AC, Ståhl AL, Rebetz J, Wang L, Licht C, et al. Complement activation associated with ADAMTS13 deficiency in human and murine thrombotic microangiopathy. *J Immunol* (2013) 191:2184–93. doi: 10.4049/jimmunol.1301221
121. Ma R, Cui Z, Hu SY, Jia XY, Yang R, Zheng X, et al. The alternative pathway of complement activation may be involved in the renal damage of human anti-glomerular basement membrane disease. *PloS One* (2014) 9:e91250. doi: 10.1371/journal.pone.0091250
122. Arvidsson I, Rebetz J, Loos S, Herthelius M, Kristoffersson AC, Englund E, et al. Early terminal complement blockade and C6 deficiency are protective in enterohemorrhagic *Escherichia coli*-infected mice. *J Immunol* (2016) 197:1276–86. doi: 10.4049/jimmunol.1502377
123. Liu WJ, Li ZH, Chen XC, Zhao XL, Zhong Z, Yang C, et al. Blockage of the lysosome-dependent autophagic pathway contributes to complement membrane attack complex-induced podocyte injury in idiopathic membranous nephropathy. *Sci Rep* (2017) 7:8643. doi: 10.1038/s41598-017-07889-z
124. Paunas TIF, Finne K, Leh S, Marti HP, Mollnes TE, Berven F, et al. Glomerular abundance of complement proteins characterized by proteomic analysis of laser-captured microdissected glomeruli associates with progressive disease in IgA nephropathy. *Clin Proteom* (2017) 14:30. doi: 10.1186/s12014-017-9165-x
125. Diao B, Wang C, Wang R, Feng Z, Tan Y, Wang H, et al. Human kidney is a target for novel severe acute respiratory syndrome coronavirus 2 (SARS-CoV-2) infection. *MedRxiv [preprint]* (2020). doi: 10.1101/2020.03.04.20031120
126. Falk RJ, Sisson SP, Dalmasso AP, Kim Y, Michael AF, Vernier RL. Ultrastructural localization of the membrane attack complex of complement in human renal tissues. *Am J Kidney Dis* (1987) 9:121–8. doi: 10.1016/s0272-6386(87)80089-6
127. Yoshioka K, Takemura T, Matsubara K, Miyamoto H, Akano N, Maki S. Immunohistochemical studies of reflux nephropathy: the role of extracellular matrix, membrane attack complex, and immune cells in glomerular sclerosis. *Am J Pathol* (1987) 129:223–31.
128. Abe K, Miyazaki M, Koji T, Furusu A, Shioshita K, Tsukasaki S, et al. Intraglomerular synthesis of complement C3 and its activation products in IgA nephropathy. *Nephron* (2001) 87:231–9. doi: 10.1159/000045920
129. Sund S, Hovig T, Reisaeter AV, Scott H, Bentdal Ø, Mollnes TE. Complement activation in early protocol kidney graft biopsies after living-donor transplantation. *Transplantation* (2003) 75:1204–13. doi: 10.1097/01.TP.0000062835.30165.2C
130. Chua JS, Baelde HJ, Zandbergen M, Wilhelmus S, van Es LA, de Fijter JW, et al. Complement factor C4d is a common denominator in thrombotic microangiopathy. *J Am Soc Nephrol* (2015) 26:2239–47. doi: 10.1681/ASN.2014050429
131. Penning M, Chua JS, Van Kooten C, Zandbergen M, Buurma A, Schutte J, et al. Classical complement pathway activation in the kidneys of women with preeclampsia. *Hypertension* (2015) 66:117–25. doi: 10.1161/HYPERTENSIONAHA.115.05484
132. Itami H, Hara S, Matsumoto M, Imamura S, Kanai R, Nishiyama K, et al. Complement activation associated with ADAMTS13 deficiency may contribute to the characteristic glomerular manifestations in Upshaw-Schulman syndrome. *Thromb Res* (2018) 170:148–55. doi: 10.1016/j.thromres.2018.08.020
133. Tseng MH, Lin SH, Wu CY, Chien HP, Yang HY, Chen YC, et al. Serum complement factor I is associated with disease activity of systemic lupus erythematosus. *Oncotarget* (2018) 9:8502–11. doi: 10.18632/oncotarget.23907
134. Goutaudier V, Perrochia H, Mucha S, Bonnet M, Delmas S, Garo F, et al. C5b9 deposition in glomerular capillaries is associated with poor kidney allograft survival in antibody-mediated rejection. *Front Immunol* (2019) 10:235. doi: 10.3389/fimmu.2019.00235
135. Khan TN, Sinniah R. Renal tubular antiproteinase (alpha-1-antitrypsin and alpha-1-antichymotrypsin) response in tubulo-interstitial damage. *Nephron* (1993) 65:232–9. doi: 10.1159/000187480
136. Rodríguez E, Gimeno J, Arias-Cabrales C, Barrios C, Redondo-Pachón D, Soler MJ, et al. Membrane attack complex and H in humans with acute kidney injury. *Kidney Blood Press Res* (2018) 43:1655–65. doi: 10.1159/000494680
137. Eguchi K, Tomino Y, Yagame M, Miyazaki M, Takiura F, Miura M, et al. Double immunofluorescence studies of IgA and poly C9 (MAC) in glomeruli from patients with IgA nephropathy. *Tokai J Exp Clin Med* (1987) 12:331–5.
138. Niehans GA, Cherwitz DL, Staley NA, Knapp DJ, Dalmasso AP. Human carcinomas variably express the complement inhibitory proteins CD46 (membrane cofactor protein), CD55 (decay-accelerating factor), and CD59 (protectin). *Am J Pathol* (1996) 149:129–42.
139. Mosolits S, Magyarlaki T, Nagy J. Membrane attack complex and membrane cofactor protein are related to tubulointerstitial inflammation in various human glomerulopathies. *Nephron* (1997) 75:179–87. doi: 10.1159/000189529
140. Nakano D, Nishiyama A. A novel role of renin inhibitor in the complement cascade. *Kidney Int* (2018) 94:650–2. doi: 10.1016/j.kint.2018.05.025
141. Rus HG, Niculescu F, Nanulescu M, Cristea A, Florescu P. Immunohistochemical detection of the terminal C5b-9 complement complex in children with glomerular diseases. *Clin Exp Immunol* (1986) 65:66–72.
142. Sinniah R, Khan TN. Renal tubular basement membrane changes in tubulointerstitial damage in patients with glomerular diseases. *Ultrastruct Pathol* (1999) 23:359–68. doi: 10.1080/019131299281329
143. Murphy B, Georgiou T, Machet D, Hill P, McRae J. H-related protein-5: a novel component of human glomerular immune deposits. *Am J Kidney Dis* (2002) 39:24–7. doi: 10.1053/ajkd.2002.29873
144. Timmermans SAMEG, Abdul-Hamid MA, Potjewijd J, Theunissen ROMFIH, Damoiseaux JGMC, Reutelingsperger CP, et al. C5b9 formation on endothelial cells reflects complement defects among patients with renal thrombotic microangiopathy and severe hypertension. *J Am Soc Nephrol* (2018) 29:2234–43. doi: 10.1681/ASN.2018020184
145. Flyvbjerg A. The role of the complement system in diabetic nephropathy. *Nat Rev Nephrol* (2017) 13:311–8. doi: 10.1038/nrneph.2017.31
146. Cohen Tervaert TW, Mooyaart AL, Amann K, Cohen AH, Cook HT, Drachenberg CB, et al. Pathologic classification of diabetic nephropathy. *J Am Soc Nephrol* (2010) 21:556–63. doi: 10.1681/ASN.2010010010
147. Debiec H, Hanoy M, Francois A, Guerrot D, Ferlicot S, Johanet C, et al. Recurrent membranous nephropathy in an allograft caused by IgG3κ targeting the PLA2 receptor. *J Am Soc Nephrol* (2012) 23:1949–54. doi: 10.1681/ASN.2012060577
148. Endo M, Fuke Y, Tamano M, Hidaka M, Ohsawa I, Fujita T, et al. Glomerular deposition and urinary excretion of complement H in idiopathic membranous nephropathy. *Nephron Clin Pract* (2004) 97:c147–53. doi: 10.1159/000079174
149. Lhotta K, Würzner R, Rumpelt HJ, Eder P, Mayer G. Membranous nephropathy in a patient with hereditary complete complement C4 deficiency. *Nephrol Dial Transplant* (2004) 19:990–3. doi: 10.1093/ndt/gfh008
150. Bruschi M, Carnevali ML, Murtas C, Candiano G, Petretto A, Prunotto M, et al. Direct characterization of target podocyte antigens and auto-antibodies in human membranous glomerulonephritis: alfa-enolase and borderline antigens. *J Proteom* (2011) 74:2008–17. doi: 10.1016/j.jprot.2011.05.021
151. Miura T, Goto S, Iguchi S, Shimada H, Ueno M, Nishi S, et al. Membranoproliferative pattern of glomerular injury associated with complement component 9 deficiency due to Arg95Stop mutation. *Clin Exp Nephrol* (2011) 15:86–91. doi: 10.1007/s10157-010-0358-0
152. Akano N, Yoshioka K, Aya N, Miyamoto H, Takemura T, Tohda M, et al. Immunoelectron microscopic localization of membrane attack complex and hepatitis Be antigen in membranous nephropathy. *Virchows Arch A Pathol Anat Histopathol* (1989) 414:325–30. doi: 10.1007/BF00734087

153. Porubsky S, Federico G, Müthing J, Jennemann R, Gretz N, Büttner S, et al. Direct acute tubular damage contributes to Shigatoxin-mediated kidney failure. *J Pathol* (2014) 234:120–33. doi: 10.1002/path.4388
154. Vivarelli M, Emma F, Pellé T, Gerken C, Pedicelli S, Diomedi-Camassei F, et al. Genetic homogeneity but IgG subclass-dependent clinical variability of alloimmune membranous nephropathy with anti-neutral endopeptidase antibodies. *Kidney Int* (2015) 87:602–9. doi: 10.1038/ki.2014.381
155. Bally S, Debiec H, Ponard D, Dijoud F, Rendu J, Fauré J, et al. Phospholipase A2 receptor-related membranous nephropathy and mannan-binding lectin deficiency. *J Am Soc Nephrol* (2016) 27:3539–44. doi: 10.1681/ASN.2015101155
156. Prunotto M, Carnevali ML, Candiano G, Murtas C, Bruschi M, Corradini E, et al. Autoimmunity in membranous nephropathy targets aldose reductase and SOD2. *J Am Soc Nephrol* (2010) 21:507–19. doi: 10.1681/ASN.2008121259
157. Debiec H, Valayannopoulos V, Boyer O, Nöel LH, Callard P, Sarda H, et al. Allo-immune membranous nephropathy and recombinant aryl sulfatase replacement therapy: a need for tolerance induction therapy. *J Am Soc Nephrol* (2014) 25:675–80. doi: 10.1681/ASN.2013030290
158. Medjeral-Thomas NR, Troldborg A, Constantinou N, Lomax-Browne HJ, Hansen AG, Willicombe M, et al. Progressive IgA nephropathy is associated with low circulating mannan-binding lectin-associated serine protease-3 (MASP-3) and increased glomerular H-related protein-5 (FHR5) deposition. *Kidney Int Rep* (2018) 3:426–38. doi: 10.1016/j.ekir.2017.11.015
159. Rosenblad T, Rebetz J, Johansson M, Békássy Z, Sartz L, Karpman D. Eculizumab treatment for rescue of renal function in IgA nephropathy. *Pediatr Nephrol* (2014) 29:2225–8. doi: 10.1007/s00467-014-2863-y
160. Endo M, Ohi H, Ohsawa I, Fujita T, Matsushita M, Fujita T. Glomerular deposition of mannose-binding lectin (MBL) indicates a novel mechanism of complement activation in IgA nephropathy. *Nephrol Dial Transplant* (1998) 13:1984–90. doi: 10.1093/ndt/13.8.1984
161. Ootaka T, Saito T, Soma J, Yusa A, Abe K. Mechanism of infiltration and activation of glomerular monocytes/macrophages in IgA nephropathy. *Am J Nephrol* (1997) 17:137–45. doi: 10.1159/000169087
162. Chen HC, Tomino Y, Yaguchi Y, Fukui M, Koide H. Detection of polymorphonuclear cells, superoxide dismutase and poly C9 in glomeruli of patients with IgA nephropathy. *Nephron* (1991) 59:338. doi: 10.1159/000186583
163. Takahashi T, Inaba S, Okada T. Vitronectin in children with renal disease 1: immunofluorescence study of vitronectin and C5b-9 in childhood IgA nephropathy. *Nihon Jinzo Gakkai Shi* (1995) 37:213–23.
164. Xu L, Yang HC, Hao CM, Lin ST, Gu Y, Ma J. Podocyte number predicts progression of proteinuria in IgA nephropathy. *Mod Pathol* (2010) 23:1241–50. doi: 10.1038/modpathol.2010.110
165. Segarra-Medrano A, Carnicer-Caceres C, Valtierra-Carmeno N, Agraz-Pamplona I, Ramos-Terrades N, Jatem Escalante E, et al. Study of the variables associated with local complement activation in IgA nephropathy. *Nefrologia* (2017) 37:320–9. doi: 10.1016/j.nefro.2016.11.019
166. Itami H, Hara S, Samejima K, Tsushima H, Morimoto K, Okamoto K, et al. Complement activation is associated with crescent formation in IgA nephropathy. *Virchows Arch* (2020) 477:565–72. doi: 10.1007/s00428-020-02800-0
167. Chua JS, Zandbergen M, Wolterbeek R, Baelde HJ, Van Es LA, De Fijter JW, et al. Complement-mediated microangiopathy in IgA nephropathy and IgA vasculitis with nephritis. *Mod Pathol* (2019) 32:1147–57. doi: 10.1038/s41379-019-0259-z
168. Davin JC, Ten Berge IJ, Weening JJ. What is the difference between IgA nephropathy and Henoch-Schönlein purpura nephritis? *Kidney Int* (2001) 59:823–34. doi: 10.1046/j.1523-1755.2001.059003823.x
169. Heineke MH, Ballering AV, Jamin A, Ben Mkaddem S, Monteiro RC, Van Egmond M. New insights in the pathogenesis of immunoglobulin A vasculitis (Henoch-Schönlein purpura). *Autoimmun Rev* (2017) 16:1246–53. doi: 10.1016/j.autrev.2017.10.009
170. Sato M, Kogure T, Kanemitsu M. A case of systemic lupus erythematosus showing invagination of the podocyte into the glomerular basement membrane: an electron microscopic observation of a repeated-renal biopsy. *Clin Exp Nephrol* (2008) 12:455–61. doi: 10.1007/s10157-008-0091-0
171. Wang S, Wu M, Chiriboga L, Zeck B, Belmont HM. Membrane attack complex (MAC) deposition in lupus nephritis is associated with hypertension and poor clinical response to treatment. *Semin Arthritis Rheumatol* (2018) 48:256–62. doi: 10.1016/j.semarthrit.2018.01.004
172. Fujigaki Y, Muranaka Y, Sakakima M, Ohta I, Sakao Y, Fujikura T, et al. Analysis of intra-GBM microstructures in a SLE case with glomerulopathy associated with podocytic infolding. *Clin Exp Nephrol* (2008) 12:432–9. doi: 10.1007/s10157-008-0095-9
173. Song D, Guo WY, Wang FM, Li YZ, Song Y, Yu F, et al. Complement alternative pathway's activation in patients with lupus nephritis. *Am J Med Sci* (2017) 353:247–57. doi: 10.1016/j.amjms.2017.01.005
174. Ma H, Liu C, Shi B, Zhang Z, Feng R, Guo M, et al. Mesenchymal stem cells control complement C5 activation by H in lupus nephritis. *EBioMedicine* (2018) 32:21–30. doi: 10.1016/j.ebiom.2018.05.034
175. Hadaya K, Ferrari-Lacraz S, Fumeaux D, Boehlen F, Toso C, Moll S, et al. Eculizumab in acute recurrence of thrombotic microangiopathy after renal transplantation. *Am J Transplant* (2011) 11:2523–7. doi: 10.1111/j.1600-6143.2011.03696.x
176. Machida T, Sakamoto N, Ishida Y, Takahashi M, Fujita T, Sekine H. Essential roles for mannose-binding lectin-associated serine protease-1/3 in the development of lupus-like glomerulonephritis in MRL/lpr mice. *Front Immunol* (2018) 9:1191. doi: 10.3389/fimmu.2018.01191
177. Pickering MC, Warren J, Rose KL, Carlucci F, Wang Y, Walport MJ, et al. Prevention of C5 activation ameliorates spontaneous and experimental glomerulonephritis in factor H-deficient mice. *Proc Natl Acad Sci USA* (2006) 103:9649–54. doi: 10.1073/pnas.0601094103
178. Williams AL, Gullipalli D, Ueda Y, Sato S, Zhou L, Miwa T, et al. C5 inhibition prevents renal failure in a mouse model of lethal C3 glomerulopathy. *Kidney Int* (2017) 91:1386–97. doi: 10.1016/j.kint.2016.11.018
179. Habbig S, Mihatsch MJ, Heinen S, Beck B, Emmel M, Skerka C, et al. C3 deposition glomerulopathy due to a functional factor H defect. *Kidney Int* (2009) 75:1230–4. doi: 10.1038/ki.2008.354
180. Sethi S, Fervenza FC, Zhang Y, Nasr SH, Leung N, Vrana J, et al. Proliferative glomerulonephritis secondary to dysfunction of the alternative pathway of complement. *Clin J Am Soc Nephrol* (2011) 6:1009–17. doi: 10.2215/CJN.07110810
181. Figuères ML, Frémeaux-Bacchi V, Rabant M, Galmiche L, Marinozzi MC, Grünfeld JP, et al. Heterogeneous histologic and clinical evolution in 3 cases of dense deposit disease with long-term follow-up. *Hum Pathol* (2014) 45:2326–33. doi: 10.1016/j.humpath.2014.07.021
182. Chen Q, Manzke M, Hartmann A, Büttner M, Amann K, Pauly D, et al. Complement H-related 5-hybrid proteins anchor properdin and activate complement at self-surfaces. *J Am Soc Nephrol* (2016) 27:1413–25. doi: 10.1681/ASN.2015020212
183. Parra G, Platt JL, Falk RJ, Rodriguez-Iturbe B, Michael AF. Cell populations and membrane attack complex in glomeruli of patients with post-streptococcal glomerulonephritis: identification using monoclonal antibodies by indirect immunofluorescence. *Clin Immunol Immunopathol* (1984) 33:324–32. doi: 10.1016/0090-1229(84)90303-9
184. Matsell DG, Wyatt RJ, Gaber LW. Terminal complement complexes in acute poststreptococcal glomerulonephritis. *Pediatr Nephrol* (1994) 8:671–6. doi: 10.1007/BF00869086
185. Smith-Jackson K, Yang Y, Denton H, Pappworth IY, Cooke K, Barlow PN. Hyperfunctional complement C3 promotes C5-dependent atypical hemolytic uremic syndrome in mice. *J Clin Invest* (2019) 129:1061–75. doi: 10.1172/JCI99296
186. Ueda Y, Miwa T, Ito D, Kim H, Sato S, Gullipalli D. Differential contribution of C5aR and C5b-9 pathways to renal thrombic microangiopathy and macrovascular thrombosis in mice carrying an atypical hemolytic syndrome–related factor H mutation. *Kidney Int* (2019) 96:67–79. doi: 10.1016/j.kint.2019.01.009
187. Noris M, Remuzzi G. Terminal complement effectors in atypical hemolytic uremic syndrome: C5a, C5b-9, or a bit of both? *Kidney Int* (2019) 96:13–5. doi: 10.1016/j.kint.2019.02.038
188. Webb TN, Griffiths H, Miyashita Y, Bhatt R, Jaffe R, Moritz M, et al. Atypical hemolytic uremic syndrome and chronic ulcerative colitis treated with

eculizumab. *Int J Med Pharm Case Rep* (2015) 4:105–12. doi: 10.9734/IJMPCR/2015/18771
189. Orth-Höller D, Würzner R. Role of complement in enterohemorrhagic Escherichia coli-Induced hemolytic uremic syndrome. *Semin Thromb Hemost* (2014) 40:503–7. doi: 10.1055/s-0034-1375295
190. Alberti M, Valoti E, Piras R, Bresin E, Galbusera M, Tripodo C, et al. Two patients with history of STEC-HUS, posttransplant recurrence and complement gene mutations. *Am J Transplant* (2013) 13:2201–6. doi: 10.1111/ajt.12297
191. Wanchoo R, Bayer RL, Bassil C, Jhaveri KD. Emerging concepts in hematopoietic stem cell transplantation-associated renal thrombotic microangiopathy and prospects for new treatments. *Am J Kidney Dis* (2018) 72:857–65. doi: 10.1053/j.ajkd.2018.06.013
192. Timmermans SAMEG, Abdul-Hamid MA, Vanderlocht J, Damoiseaux JGMC, Reutelingsperger CP, Van Paassen P. Patients with hypertension-associated thrombotic microangiopathy may present with complement abnormalities. *Kidney Int* (2017) 91:1420–5. doi: 10.1016/j.kint.2016.12.009
193. Timmermans SAMEG, Wérion A, Damoiseaux JGMC, Morelle J, Reutelingsperger CP, Van Paassen P. Diagnostic and risk factors for complement defects in hypertensive emergency and thrombotic microangiopathy. *Hypertension* (2020) 75:422–30. doi: 10.1161/HYPERTENSIONAHA.119.13714
194. Hilhorst M, Van Paassen P, Van Rie H, Bijnens N, Heerings-Rewinkel P, Van Breda Vriesman P, et al. Complement in ANCA-associated glomerulonephritis. *Nephrol Dial Transplant* (2017) 32:1302–13. doi: 10.1093/ndt/gfv288
195. Alexopoulos E, Gionanlis L, Papayianni E, Kokolina E, Leontsini M, Memmos D. Predictors of outcome in idiopathic rapidly progressive glomerulonephritis (IRPGN). *BMC Nephrol* (2006) 7:16. doi: 10.1186/1471-2369-7-16
196. Gionanlis L, Alexopoulos E, Papagianni A, Leontsini M, Memmos D. Fibrotic mechanisms in idiopathic rapidly progressive glomerulonephritis: the role of TGF-beta1 and C5b-9. *Ren Fail* (2008) 30:239–46. doi: 10.1080/08860220701804979
197. Takano T, Elimam H, Cybulsky AV. Complement-mediated cellular injury. *Semin Nephrol* (2013) 33:586–601. doi: 10.1016/j.semnephrol.2013.08.009
198. Nangaku M. Mechanisms of tubulointerstitial injury in the kidney: final common pathways to end-stage renal failure. *Intern Med* (2004) 43:9–17. doi: 10.2169/internalmedicine.43.9
199. Nagamachi S, Ohsawa I, Sato N, Ishii M, Kusaba G, Kobayashi T, et al. Immune complex-mediated complement activation in a patient with IgG4-related tubulointerstitial nephritis. *Case Rep Nephrol Urol* (2011) 1:7–14. doi: 10.1159/000330664
200. Thurman JM, Lucia MS, Ljubanovic D, Holers MV. Acute tubular necrosis is characterized by activation of the alternative pathway of complement. *Kidney Int* (2005) 67:524–30. doi: 10.1111/j.1523-1755.2005.67109.x
201. Hsu SIH, Couser WG. Chronic progression of tubulointerstitial damage in proteinuric renal disease is mediated by complement activation: a therapeutic role for complement inhibitors? *J Am Soc Nephrol* (2003) 14:S186–91. doi: 10.1097/01.asn.0000070032.58017.20
202. Zhou W, Farrar CA, Abe K, Pratt JR, Marsh JE, Wang Y, et al. Predominant role for C5b-9 in renal ischemia/reperfusion injury. *J Clin Invest* (2000) 105:1363–71. doi: 10.1172/JCI8621
203. Yuzawa Y, Aoi N, Fukatsu A, Ichida S, Yoshida F, Akatsuka Y, et al. Acute renal failure and degenerative tubular lesions associated with in situ formation of adenovirus immune complexes in a patient with allogeneic bone marrow transplantation. *Transplantation* (1993) 55:67–72. doi: 10.1097/00007890-199301000-00013
204. Schena FP, Selvaggi FP, Salvatore C, Barbuti S, Marzullo F, Tallarigo A, et al. Immunological and bacteriological studies in chronic pyelonephritis associated with kidney stones. *Nephron* (1979) 23:162–8. doi: 10.1159/000181628
205. Roberts JA. Etiology and pathophysiology of pyelonephritis. *Am J Kidney Dis* (1991) 17:1–9. doi: 10.1016/s0272-6386(12)80242-3
206. Choudhry N, Li K, Zhang T, Wu KY, Song Y, Farrar CA, et al. The complement factor 5a receptor 1 has a pathogenic role in chronic inflammation and renal fibrosis in a murine model of chronic pyelonephritis. *Kidney Int* (2016) 90:540–54. doi: 10.1016/j.kint.2016.04.023
207. Netti GS, Lucarelli G, Spadaccino F, Castellano G, Gigante M, Divella C, et al. PTX3 modulates the immunoflogosis in tumor microenvironment and is a prognostic factor for patients with clear cell renal cell carcinoma. *Aging (Albany NY)* (2020) 12:7585–602. doi: 10.18632/aging.103169
208. Ma YJ, Garred P. Pentraxins in complement activation and regulation. *Front Immunol* (2018) 19:3046. doi: 10.3389/fimmu.2018.03046
209. Blok VT, Daha MR, Tijsma OM, Weissglas MG, van den Broek LJ, Gorter A. A possible role of CD46 for the protection in vivo of human renal tumor cells from complement-mediated damage. *Lab Invest* (2000) 80:335–44. doi: 10.1038/labinvest.3780038
210. Magyarlaki T, Mosolits S, Baranyay F, Buzogány I. Immunohistochemistry of complement response on human renal cell carcinoma biopsies. *Tumori* (1996) 82:473–9.
211. De Vries DK, Van der Pol P, Van Anken GE, Van Gijlswijk DJ, Damman J, Lindeman JH, et al. Acute but transient release of terminal complement complex after reperfusion in clinical kidney transplantation. *Transplantation* (2013) 95:816–20. doi: 10.1097/TP.0b013e31827e31c9
212. Noone D, Al-Matrafi J, Tinckam K, Zipfel PF, Herzenberg AM, Thorner PS, et al. Antibody mediated rejection associated with complement factor H-related protein 3/1 deficiency successfully treated with eculizumab. *Am J Transplant* (2012) 12:2546–53. doi: 10.1111/j.1600-6143.2012.04124.x
213. Van Sandwijk MS, Klooster A, Ten Berge IJ, Diepstra A, Florquin S, Hoelbeek JJ, et al. Complement activation and long-term graft function in ABO-incompatible kidney transplantation. *World J Nephrol* (2019) 8:95–108. doi: 10.5527/wjn.v8.i6.95
214. Cosyns JP, Kazatchkine MD, Bhakdi S, Mandet C, Grossetete J, Hinglais N, et al. Immunohistochemical analysis of C3 cleavage fragments, H, and the C5b-9 terminal complex of complement in de novo membranous glomerulonephritis occurring in patients with renal transplant. *Clin Nephrol* (1986) 26:203–8.
215. Bentzel CJ. The filtered complement hypothesis. *Kidney Int* (2000) 58:2597–8. doi: 10.1046/j.1523-1755.2000.00449.x
216. Morgan BP. The membrane attack complex as an inflammatory trigger. *Immunobiology* (2016) 221:747–51. doi: 10.1016/j.imbio.2015.04.006
217. Fishelson Z, Kirschfink M. Complement C5b-9 and cancer: mechanisms of cell damage, cancer counteractions, and approaches for intervention. *Front Immunol* (2019) 10:752. doi: 10.3389/fimmu.2019.00752
218. Lhotta K, Würzner R, König P. Glomerular deposition of mannose-binding lectin in human glomerulonephritis. *Nephrol Dial Transplant* (1999) 14:881–6. doi: 10.1093/ndt/14.4.881
219. Ito Y, Fukatsu A, Baba M, Mizuno M, Ichida S, Sado Y, et al. Pathogenic significance of interleukin-6 in a patient with antiglomerular basement membrane antibody-induced glomerulonephritis with multinucleated giant cells. *Am J Kidney Dis* (1995) 26:72–9. doi: 10.1016/0272-6386(95)90157-4
220. Alexopoulos E, Stangou M, Papagianni A, Pantzaki A, Papadimitriou M. Factors influencing the course and the response to treatment in primary focal segmental glomerulosclerosis. *Nephrol Dial Transplant* (2000) 15:1348–56. doi: 10.1007/BF02918256
221. Hagiwara S, Ohi H, Eishi Y, Kodama F, Tashiro K, Makita Y, et al. A case of renal sarcoidosis with complement activation via the lectin pathway. *Am J Kidney Dis* (2005) 45:580–7. doi: 10.1053/j.ajkd.2004.11.020
222. Hirt-Minkowski P, Trendelenburg M, Gröschl I, Fischer A, Heijnen I, Schifferli JA. A trial of complement inhibition in a patient with cryoglobulin-induced glomerulonephritis. *Case Rep Nephrol Urol* (2012) 2:38–45. doi: 10.1159/000339403
223. Devresse A, Aydin S, Le Quintrec M, Demoulin N, Stordeur P, Lambert C, et al. Complement activation and effect of eculizumab in scleroderma renal crisis. *Med (Baltimore)* (2016) 95:e4459. doi: 10.1097/MD.0000000000004459
224. Merle NS, Grunenwald A, Rajaratnam H, Gnemmi V, Frimat M, Figuères ML, et al. Intravascular hemolysis activates complement via cell-free heme and heme-loaded microvesicles. *JCI Insight* (2018) 3:e96910. doi: 10.1172/jci.insight.96910
225. Tao J, Lieberman J, Lafayette RA, Kambham N. A rare case of Alport syndrome, atypical hemolytic uremic syndrome and pauci-immune crescentic glomerulonephritis. *BMC Nephrol* (2018) 19:355. doi: 10.1186/s12882-018-1170-4

226. Boudhabhay I, Poillerat V, Grunenwald A, Torset C, Leon J, Daugan MV, et al. Complement activation is a crucial driver of acute kidney injury in rhabdomyolysis. *Kidney Int* (2020). doi: 10.1016/j.kint.2020.09.033

Conflict of Interest: The authors declare that the research was conducted in the absence of any commercial or financial relationships that could be construed as a potential conflict of interest.

Advantages of publishing in Frontiers

OPEN ACCESS
Articles are free to read for greatest visibility and readership

FAST PUBLICATION
Around 90 days from submission to decision

HIGH QUALITY PEER-REVIEW
Rigorous, collaborative, and constructive peer-review

TRANSPARENT PEER-REVIEW
Editors and reviewers acknowledged by name on published articles

Frontiers
Avenue du Tribunal-Fédéral 34
1005 Lausanne | Switzerland

Visit us: www.frontiersin.org
Contact us: frontiersin.org/about/contact

REPRODUCIBILITY OF RESEARCH
Support open data and methods to enhance research reproducibility

DIGITAL PUBLISHING
Articles designed for optimal readership across devices

FOLLOW US
@frontiersin

IMPACT METRICS
Advanced article metrics track visibility across digital media

EXTENSIVE PROMOTION
Marketing and promotion of impactful research

LOOP RESEARCH NETWORK
Our network increases your article's readership